

**Chemotaxonomic Investigations on Resins of the Frankincense  
Species *Boswellia papyrifera*, *Boswellia serrata* and *Boswellia  
sacra*, respectively, *Boswellia carterii***

A Qualitative and Quantitative Approach by Chromatographic and  
Spectroscopic Methodology

**Dissertation**

zur Erlangung des Grades  
des Doktors der Naturwissenschaften  
der Naturwissenschaftlich-Technischen Fakultät III  
Chemie, Pharmazie, Bio- und Werkstoffwissenschaften der



UNIVERSITÄT  
DES  
SAARLANDES

Michael Paul

Saarland University  
Saarbrücken, Saarland, Germany  
2012

Tag des Kolloquiums:	09.11.2012
Dekan:	Prof. Dr. V. Helms
1. Berichterstatter:	Prof. Dr. J. Jauch
2. Berichterstatter:	Prof. Dr. A. Speicher
Vorsitz:	Prof. Dr. M. Springborg
Akad. Mitarbeiter:	Dr. J. Zapp

The research project described here was carried out from March 2009 until December 2011 at the Department of Organic Chemistry II, Faculty 8.1, of the Saarland University under supervision of Prof. Dr. Johann Jauch.

Special thanks to Prof. Dr. Johann Jauch for giving me the possibility of pure and applied scientific work in an academically free environment.

Parts of the dissertation have been already published:

**Qualitative and Quantitative Analysis of 17 Different Types of Tetra- and Pentacyclic Triterpenic Acids in *Boswellia papyrifera* by a Semi-Automatic Homomodal 2D HPLC method**

Michael Paul, Gerit Brüning, Joachim Wehrather and Johann Jauch; *Chromatographia* 74, 2011, Vol 1-2, pages 29-40.

DOI: 10.1007/s10337-011-2041-3

**A Thin-Layer-Chromatography Method for the Identification of Three Different Olibanum Species (*Boswellia papyrifera*, *Boswellia serrata* and *Boswellia sacra*, respectively, *Boswellia carterii*)**

Michael Paul, Gerit Brüning, Jochen Bergmann and Johann Jauch; *Phytochemical Analysis* 23, 2012, 2, pages 184-189.

DOI: 10.1002/pca.1341

**Efficient Preparation of Incensole and Incensole Acetate, and Quantification of These Bioactive Diterpenes in *Boswellia papyrifera* by a RP-DAD-HPLC Method**

Michael Paul and Johann Jauch; *Natural Product Communications* 7, 2012, 3, pages 283-288.

<http://www.naturalproduct.us/>

To whom it may concern

*"It seemed to me that a careful examination of the room and the lawn might possibly reveal some traces of this mysterious individual. You know my methods, Watson. There was not one of them which I did not apply to the enquiry. And it ended by my discovering traces, but very different ones from those which I had expected."*

Sherlock Holmes in "The Crooked Man"

From *The Memoirs of Sherlock Holmes* (1893) by Sir Arthur Conan Doyle (Writer, 1859-1930)

## Danksagung

Ganz spezieller Dank gilt Herrn Prof. Dr. Johann Jauch, der mir überhaupt erst die Möglichkeit zur Promotion an der UdS eröffnete – Besten Dank dafür.

Des Weiteren bedanke ich mich für das gute Arbeitsklima und die ständige Unterstützung bei allen Mitarbeitern (z. B. Heike Röser, Thomas Scherer, Joachim Kriesamer, Matthias Großer und Rudolf Thomes, etc.), Studenten (alle, die ich kennen lernte, etc.) und Doktoranden- bzw. AK-Kollegen (Sabine Caspar-Klär, Gerit Brüning, Eva Feidt, Steffi Schmitt, David Hartmann, Hans Müller, Daniel Rawer, Marcus Hans, Joachim Wehrather et Mael Charpentier), insbesondere auch unseren Stockwerkskollegen vom AK Prof. Dr. Andreas Speicher (Petra Schmitz, Judith Holz, Lisa Dejon, Markus Malter, Daniel Meidlinger und Matthias Groh), respektive, Herrn Prof. Dr. Andreas Speicher selbst, selbstverständlich.

Herrn Dr. Josef Zapp gilt besonderer Dank für die unkomplizierte und schnelle Aufnahme der NMR-Spektren, speziell mittels Mikroprobenkopf.

Vielen Dank auch an das gesamte Team der *AureliaSan GmbH*, wobei hier noch einmal Daniela Müller, Moritz Verhoff (Uni Tübingen), Dr. Martin Deeg (Uni Tübingen) und Johannes Ertelt, die mir gute Freunde geworden, gesondert zu nennen sind. Den weiteren Mitgliedern des AK Prof. Dr. Oliver Werz in Tübingen (jetzt Uni Jena), respektive, Herrn Prof. Dr. Oliver Werz selbst natürlich, sei an dieser Stelle auch noch einmal besonderer Dank mitgeteilt.

Ganz großer Dank an meine Familie, hier speziell meinen Eltern, die mich immer voll unterstützt haben, unabhängig von meinen zwischenzeitlichen und teilweise recht seltsamen Lebensentwurfsmodellen (z. B. Marssonde, Panzergeneral oder Geisterjäger, etc.).

Nicht zu vergessen, vielen Dank auch an den Industrie-Beamten Herrn Norbert R. sowie an das seltsame Haus von Poseidon unweit dieses geheimnisvollen und sagenumwobenen Baggersees. Auch nicht zu vergessen: Meine Laufschuhe, Kopfhörer, die Musikkapelle *Modest Mouse* („*And we'll all float on any way, well*“) und der Wald neben der Bildungsanstalt, die mich an „*Tagen des Wahnsinns*“ vor genau diesem bewahrt und wieder geerdet haben – Vielen Dank.

Einige Freunde seien hier nochmals explizit erwähnt, da sie mir in den Saarbrücker Tagen auch eine wichtige abwechselnde Stütze zum wissenschaftlichen Alltag waren: Stefan S. (für die regelmäßigen Fernseh- und Fußballabende sowie guten Gespräche über den Superhelden „*Lethargo et Le Demi Poulet*“), Arne T. (für gute intellektuelle Konversation am Rande der Vernunft), Britta M. (für immer ein offenes Ohr), Gaby K. (für immer ein offenes Ohr), Franziska B. (für immer ein offenes Ohr), Tom F. (für die Bombenveranstaltung und ein offenes Ohr jederzeit) sowie die Stuttgarter (Welf R., Jan Z., Nico M., etc.) und Berliner (Marko L., etc.) für die mittlerweile langjährigen Freundschaften und, und, und...

PS: Additional thanks are due to the whole „*Friends of Nekhen*“ team, archaeologists and supporters who gave me the possibility of testing my acquired knowledge on ancient materials from Hierakonpolis, Egypt. Here especially to mention are Tanja Pommering (Uni Mainz, Germany), Elena Marinova-Wolff (KU Leuven, Belgium), Renee Friedman (British Museum, London, UK), Margaret Serpico (Petrie Museum, University College London, UK), Jan Baeten (KU Leuven, Belgium), Peter Schönborn (Principality of Monaco), Wim van Neer (KU Leuven, Belgium) and Stan Hendrickx (MAD-Faculty, Hasselt, Belgium).

## Contents

<b><i>Abstract of the Dissertation</i></b> .....	<b>1</b>
<b><i>Zusammenfassung der Dissertation</i></b> .....	<b>2</b>
<b><i>Explanatory Notes</i></b> .....	<b>3</b>
<b><i>Major Symbols and Abbreviations</i></b> .....	<b>3</b>
<b>1 Introduction</b> .....	<b>7</b>
<b>1.1 Anecdotes of the Early History of Frankincense</b> .....	<b>8</b>
<b>1.2 Biological, Botanical and Geographical Facts</b> .....	<b>9</b>
<b>1.3 Biosynthesis of Terpenes</b> .....	<b>12</b>
<b>1.4 Chemistry</b> .....	<b>19</b>
<b>1.4.1 Boswellic Acids</b> .....	<b>19</b>
<b>1.4.2 Lupeolic Acids</b> .....	<b>25</b>
<b>1.4.3 Tirucallic Acids</b> .....	<b>26</b>
<b>1.4.4 Roburic Acids</b> .....	<b>28</b>
<b>1.4.5 Neutral Terpenic Compounds</b> .....	<b>28</b>
<b>1.5 Pharmacology</b> .....	<b>32</b>
<b>1.5.1 Inflammatory Processes in General</b> .....	<b>32</b>
<b>1.5.2 Pharmacology of Frankincense Extracts and their Single Compounds</b> .....	<b>36</b>
<b>1.6 Aim of the Study</b> .....	<b>41</b>
<b>2. Experimental Part</b> .....	<b>43</b>
<b>2.1 Material and Methods</b> .....	<b>43</b>
<b>2.1.1 Resin Material</b> .....	<b>43</b>
<b>2.1.2 Solvents and Chemicals</b> .....	<b>44</b>
<b>2.2 Extraction Procedures</b> .....	<b>44</b>
<b>2.2.1 Preparative Extraction Scale (Soxhlet Apparatus)</b> .....	<b>44</b>
<b>2.2.2 Discontinuous Extraction (Separation Funnel)</b> .....	<b>44</b>
<b>2.2.3 Continuous Extraction (Kutscher-Stuedel Perforator)</b> .....	<b>44</b>
<b>2.2.4 Analytical Extraction Scale (TLC, HPLC)</b> .....	<b>45</b>
<b>2.2.5 Steam Distillation (For GC analysis)</b> .....	<b>45</b>
<b>2.3 Chromatographic Techniques</b> .....	<b>46</b>
<b>2.3.1 Thin-Layer Chromatography (TLC)</b> .....	<b>46</b>
<b>2.3.2 Flash-Column-Chromatography</b> .....	<b>46</b>
<b>2.3.3 Preparative High Performance Liquid Chromatography</b> .....	<b>47</b>
<b>2.3.4 Analytical High Performance Liquid Chromatography (HPLC)</b> .....	<b>47</b>
<b>2.3.4.1 General Remarks concerning the Method Development</b> .....	<b>48</b>
<b>2.3.4.2 Standard Quantitation Conditions (1D chromatography)</b> .....	<b>49</b>
<b>2.3.4.3 Fraction Collection Conditions 2D Analysis</b> .....	<b>50</b>

## Contents

---

2.3.4.4 Standard 2D Quantitation Conditions ( $\alpha$ - and $\beta$ -boswellic acid) .....	50
2.3.5 Validation Parameters (1D chromatography) .....	52
2.3.6 Validation Parameters (2D chromatography) .....	54
2.3.7 Statistical Analysis of the Quantitative HPLC Data .....	55
2.3.8 Principal Component Analysis (PCA) .....	57
2.3.9 HPLC Method (EUROPEAN PHARMACOPOEIA 6.0) .....	58
2.3.10 Gas Chromatography – Flame Ionisation Detector (GC-FID) .....	59
2.4 Spectroscopy .....	60
2.4.1 Mass Spectrometry (MS) .....	60
2.4.2 Nuclear Magnetic Resonance Spectroscopy (NMR) .....	60
2.5 Pharmacological Assays .....	61
2.5.1 Purification of A549 Microsomes .....	61
2.5.2 Determination of PGE2 Synthase Activity in Microsomes of A549 Cells .....	61
2.6 Stability Tests and Estimation of Decomposition Kinetics .....	62
2.6.1 Decomposition Tests with Inc-Ac (room temperature and 60 °C) .....	62
2.6.2 Kinetic Study of the Decomposition of Inc-Ac .....	63
2.7 Partial- and Semi-Synthetic Procedures .....	63
2.7.1 Semi Synthesis of Compound 19 from Compound 15 .....	63
2.7.2 Isolation and Semi-Synthesis of Inc and Inc-Ac .....	64
<b>3. Results and Discussion .....</b>	<b>66</b>
3.1 Isolation of Biomarker Compounds .....	66
3.1.1 Isolation of Compounds from <i>Boswellia papyrifera</i> (Bpap) .....	66
3.1.1.1 Isolation of Incensole (22) and Incensole Acetate (23) .....	66
3.1.1.2 Isolation of Verticillia-4(20),7,11-triene (24) .....	66
3.1.1.3 Isolation of 3 $\alpha$ -O-Acetyl-7,24-dien-tirucallic acid (18) and 3 $\beta$ -O-Acetyl-8,24-dien-tirucallic acid (19) .....	67
3.1.2 Isolation of Compounds from <i>Boswellia carterii</i> (Bcar) .....	70
3.1.2.1 Isolation of $\beta$ -Caryophyllene oxide (28) and Serratol (21) .....	70
3.1.2.2 Isolation of $\tau$ -Cadinol (25) and Iso-Serratol (20) .....	70
3.1.2.4 Isolation of Incensole (22) and 3- $\beta$ -OH-Tirucalol (29) .....	71
3.1.2.5 Isolation of 3- $\alpha$ -OH-11-Keto-12-ursen (30) .....	71
3.2 Spectroscopic Data .....	72
3.2.1 Incensole (22) .....	72
3.2.2 Incensole Acetate (23) .....	77
3.2.3 3 $\alpha$ -O-Acetyl-7,24-dien-tirucallic acid (18) .....	81
3.2.4 3 $\beta$ -O-Acetyl-8,24-dien-tirucallic acid (19) .....	85
3.2.5 Verticillia-4(20),7,11-triene (24) .....	90
3.2.6 Serratol (21) .....	94
3.2.7 Iso-Serratol (20) .....	97
3.2.8 $\beta$ -Caryophyllene oxide (28) .....	102
3.2.9 $\tau$ -Cadinol (25) .....	108

## Contents

---

3.2.10 3- $\beta$ -OH-Tirucalol (29)	111
3.2.11 3- $\alpha$ -OH-11-Keto-12-ursen (30)	116
3.3 Extraction and Separation (Acid Fraction and Neutral Fraction)	122
3.3.1 Analytical Extraction Scale (Bpap, Bser, Bsac/Bcar)	122
3.4 TLC data (Bpap, Bser, Bsac/Bcar)	124
3.5 GC data (Qualitative Analysis of Essential Oils from Bpap, Bser and Bcar)	128
3.6 Validation Results (1D and 2D HPLC)	134
3.6.1 Validation Parameters (1D chromatography)	134
3.6.2 Validation Parameters (2D chromatography)	138
3.6.2.1 General Remarks on the 2D Method Sample Preparation	140
3.6.3 General Discussion and Statistical Evaluation of the HPLC Calibration	141
3.6.3.1 HPLC Calibration Data	141
3.6.3.2 General Calibration Issue (Example of Compound 12, AcLA)	144
3.7 HPLC Analysis (Qualitative Consideration)	149
3.7.1 <i>Boswellia papyrifera</i> (RE, NB, RS)	149
3.7.2 <i>Boswellia serrata</i> (RE, NB, RS)	153
3.7.3 <i>Boswellia sacra</i> (RE, NB, RS)	157
3.7.4 <i>Boswellia carterii</i> (RE, NB, RS)	161
3.7.5 Qualitative Comparison 2D HPLC Data	165
3.7.6 Comparison of Specific Wavelengths for Bpap, Bser and Bsac/Bcar	168
3.8 HPLC Data (Quantitative Consideration)	171
3.9 Comparison with Literature Results (HPLC)	176
3.10 Summary (Analytics)	178
3.11 Experiments with Incensole and its Acetate	179
3.11.1 Semisynthesis of Inc-Ac (NB-fraction of Bpap)	179
3.11.2 Decomposition Results for Incensole Acetate	182
3.11.3 Reaction Kinetic Model for the Decomposition of Incensole Acetate	185
3.11.4 Qualitative TLC Analysis of the Decomposition Products	187
3.12 Pharmacological Results	188
3.12.1 mPGES-1-Results for Incensole Acetate and its Decomposition Products	188
3.12.2 mPGES-1-Results for Compound 18 and 19 in Differing Compositions	192
3.13 Biosynthetic Pathway Proposal	194
3.13.1 Proposal of the Specific Biosynthesis Pathways	195
3.13.1.1 Sesquiterpenes	195
3.13.1.2 Diterpenes	196
3.13.1.3 Tetra- and Pentacyclic Triterpenes	198
3.14 Validation of Biosynthesis Hypothesis by PCA	203
<b>Conclusion and Outlook</b>	<b>209</b>
<b>Zusammenfassung und Ausblick</b>	<b>216</b>
<b>Bibliography</b>	<b>223</b>

## Abstract of the Dissertation

Extracts from the resin exudates of the frankincense tree again returned into the focus of pharmacological research within the last 20 years. So far, several research groups reported on promising anti-inflammatory, anti-microbial and even anti-tumour effects (*in vitro* and *in vivo*). The Boswellic acids are regarded as one of the most potent active agents thereof. However, the resins still contain innumerable amounts of terpenoid compounds. Their interactions, when administered as an extract, are not really understood hitherto. In addition, the information given in literature as to which molecular entity refers to which species has not been clearly verified in several publications.

Thus, this work reports on qualitative and quantitative analytical methods (LC, GC, TLC, MS and NMR), which enable the unequivocal identification of the common incense species *Boswellia papyrifera* (Eritrea, Ethiopia), *Boswellia serrata* (India) and *Boswellia sacra* (Oman, Yemen), respectively, *Boswellia carterii* (Somalia). Based on these results, a general, though not yet empirically verified, hypothesis on the biosynthetic routes has been postulated. Besides, a partial-synthetic method for the enrichment of one compound (Incensole acetate) was developed. In cooperation with Prof. Werz (Jena) a few of the isolated compounds were tested to evaluate their pharmacological potential. The results delivered evidence on possible synergistic effects which were partly based on decompositions of single molecules.

### Zusammenfassung der Dissertation

Weihrauchharzbaumextrakte sind innerhalb der letzten 20 Jahre wieder verstärkt in den Fokus der pharmakologischen Forschung gerückt. So wurden bis dato verschiedenste *in vitro* und *in vivo* Arbeiten mit Hinweisen auf anti-inflammatorische, anti-mikrobielle und sogar zytostatische Wirkung veröffentlicht. Als potenteste Wirkstoffklasse werden die Boswelliasäuren angesehen. Jedoch beinhalten diese Harze noch eine unzählbare Menge an terpenoiden Verbindungen, deren Zusammenspiel, wenn als Extrakt verabreicht, bisher noch gänzlich unbekannt ist. Hinzu kommt, dass die Angaben in der Literatur, welche molekulare Entität von welcher Harzsorte stammt, oft noch divergieren.

Diese Arbeit liefert qualitative und quantitative analytische Methoden (LC, GC, DC, MS und NMR), die eine eindeutige Identifizierung der drei weitverbreiteten Weihrauchspezies *Boswellia papyrifera* (Eritrea, Äthiopien), *Boswellia serrata* (Indien) und *Boswellia sacra* (Oman, Yemen) bzw. *Boswellia carterii* (Somalia) ermöglichen. Auf Basis dieser Ergebnisse ist eine Hypothese zur Biosynthese aufgestellt worden. Außerdem wurde eine partialsynthetische Methode zur Anreicherung eines potentiellen Wirkstoffkandidaten (Incensol-Acetat) entwickelt. In Zusammenarbeit mit Prof. Werz (Jena) wurden einige der hier isolierten Verbindungen auf ihre pharmakologische Wirkung hin untersucht. Die Resultate lieferten Hinweise auf mögliche synergistische Effekte, die zum Teil auf Zersetzungsprodukten der Moleküle beruhen.

### Explanatory Notes

It should be noted that some “awkwardly” sounding abbreviations, such as RE for raw extract, NB for neutral fraction and RS for acid fraction, are based on the German terms and are kept as the author has become too familiar with them [e.g. RE = Rohextrakt (Ger.), basically the same as in English, NB = Neutralbestandteile (Ger.), RS = Rohsäure (Ger.)].

In this work, merely the most important molecules (biomarkers for qualitative and quantitative analysis by TLC, HPLC, GC, MS and NMR) were indicated by a representative number (**1** to **30**). Other molecules are discussed but not explicitly addressed by an abbreviation.

The abbreviations Ser-OH and Iso-Ser, used in this work, are representative for the diterpenes serratol and its isomer iso-serratol, and do not refer to the amino acids serine and iso-serine, respectively.

### Major Symbols and Abbreviations

°C	Degrees (Celsius scale)
µg	Micro gram
µl	Micro litre
µM	Micro mol
11-OH-β-ABA	3α-O-Acetyl-11-OH-β-boswellic acid ( <b>7</b> )
11-OMe-β-ABA	3α-O-Acetyl-11-OMe-β-boswellic acid ( <b>8</b> )
1D	One-Dimensional
2D	Two-Dimensional
3-O-TA	3-Oxo-8,24-dien-tirucallic acid ( <b>13</b> )
3β-OH-Tir	3β-OH-Tirucallol ( <b>29</b> )
3α-OH-KU	3α-OH-11-keto-urs-12-en ( <b>30</b> )
9,11-dehydro-β-ABA	3α-O-Acetyl-9,11-dehydro-β-boswellic acid ( <b>10</b> )
9,11-dehydro-β-BA	3α-OH-9,11-dehydro-β-boswellic acid ( <b>9</b> )
AA	Arachidonic Acid
ABAs	Acetylated Boswellic acids (including here compound <b>2</b> and <b>4</b> )
AcLA	Acetyl-lupeolic acid ( <b>12</b> )
ACN	Acetonitrile
AD	Anno domini (when Christ was born)
BAAs	Boswellic acids (including here compound <b>1</b> and <b>3</b> )
BC	Before Christ
Bcar	<i>Boswellia carterii</i>
Bpap	<i>Boswellia papyrifera</i>
br s	(abbrev. Broad singlet etc.)
BSA	Bovine Serum Albumine
Bsac	<i>Boswellia sacra</i>
Bser	<i>Boswellia serrata</i>
c	Concentration
C.V.	Coefficient of Variation (S.D./Mean * 100 %)
C.V.s	Plural of CV (Coefficient of Variation)
CI	Chemical Ionisation
conc.	Concentrated
CYP	Cytochrome P 450 Oxygenase (Enzyme)
d	Dublet
DAD	Diode Array Detector, respectively, Detection
DCM	Dichloromethane
dd	dublet of dublets (ddd, dddd, etc)

## Explanatory Notes and Abbreviations

---

Delta ( $\delta$ )	Chemical shift (in NMR spectroscopy)
DEPT 135	Distortionless Enhancement by Polarization Transfer 135
DEPT 90	Distortionless Enhancement by Polarization Transfer 90
DMEM	Dulbecco's Modified Eagle Medium
DXP	1-Deoxy-Pentulose-5-Phosphate Pathway
ec	End capped (HPLC columns)
EC	Eppendorf Cup
EDTA	Ethylene diamine tetra acetic acid
et al.	and co-workers
FCS	Fetal Calf Serum
FID (GC)	Flame Ionisation Detection
FID (NMR)	Free Induction Decay
FPP	Farnesyldiphosphate
Fr.	Fraction (isolation and preparative chromatography)
g	Gravity (term in centrifugation; synonym: rpm)
GC-FID	Gas Chromatography with Flame Ionisation Detection
gem.	Geminal
GGPP	Geranylgeranyldiphosphate
GPP	Geranyldiphosphate
GSH	2.5 mM Glutathione and 250 mM Sucrose
HH-COSY	Proton-Correlated Spectroscopy (2D NMR technique)
HMBC	Heteronuclear Multiple Bond Correlation
HMQC	Heteronuclear Multiple Quantum Correlation
HOAc	Acetic Acid
HPLC	High Performance Liquid Chromatography
HRMS	High Resolution Mass Spectrometry
HSQC	Heteronuclear Single Quantum Coherence
I.D.	Inner Diameter
IC <sub>50</sub>	Inhibitory Concentration, where the enzymatic activity is only 50 % of the activity without inhibitor
IL-1 $\beta$	Interleukin 1 $\beta$
Inc	Incensole ( <b>22</b> )
Inc-Ac	Incensole acetate ( <b>23</b> )
IPP	Isopentenylidiphosphate
Iso-Ser	Iso-Serratol ( <b>20</b> )
IUPAC	International Union of Pure and Applied Chemistry
<i>J</i>	Coupling Constant (in NMR technology)
k	Capacity Factor (HPLC; elution volume of an analyte)
KI	Kovats Indices (synonym: RI)
KPi (KPI)	Potassium phosphate buffer (pH 7.4)
LA	Lupeolic acid ( <b>11</b> )
Lambda ( $\lambda$ )	Wavelength [nm]
LAs	Lupeolic acids (including here compound <b>11</b> and <b>12</b> )
LC	Liquid Chromatography
m	Mass (e.g. mg)
m/m	Mass percent (e.g. mg / mg in %)
MeOH	Methanol
MevA	Mevalonat-Acetate Pathway
MHz	Megahertz
min	Minutes (time unit)
MK8886	Control-Inhibitor (mPGES-1)
mol peak	Molecular Peak (important for mass spectrometry)
MS	Mass Spectrometry
MU	Measurement Uncertainty
NB	Neutral Fraction (After separation from the acid fraction)

## Explanatory Notes and Abbreviations

---

nm	Nanometer
NMR	Nuclear Magnetic Resonance
NOESY	Nuclear Overhauser Enhancement Spectroscopy
NP	Normal Phase (term in chromatography)
P	Penicillin
$p$	Significance level (e.g. $p = 0.99$ gives a 99 % security that the expected value lies within this distribution).
PgH <sub>2</sub>	Prostaglandin H <sub>2</sub>
PI	Prediction interval
PMNL	Polymorphonuclear Leukocytes
PMSF	Phenylmethanesulfonylfluoride
ppm	Part per million (chemical shift in NMR)
prep	Preparative (HPLC-column)
ps tr	Pseudo triplet etc., means that it is normally a multiplet or dd which appears as a triplet etc.
Psi	Pounds per square inch
$R$	Resolution (Chromatography)
RE	Raw Extract (Lipophilic Olibanum Extract)
$R_f$	Retention Factor (Thin Layer Chromatography, TLC)
RI	Retention Indices (synonym: KI)
RP	Reversed Phase
rpm	Rounds per minute (in Centrifugation)
RS	Raw Acid Extract (Raw Acid after separation of the neutral compounds)
RSD	Residual Standard Deviation
$R_t$	Retention Time (HPLC)
RT	Room Temperature
s	Second (time unit)
S	Streptomycin
S.D.	Standard Deviation (of a random sample)
S/N	Signal to Noise Ratio
Ser-OH	Serratol ( <b>21</b> )
SIM	Selected Ion Monitoring
SPE	Solid Phase Extraction
$\beta$	beta (position of an atom above the paper plane)
$\beta$ -ABA	$\beta$ -Acetyl-boswellic acid ( <b>4</b> )
$\beta$ -Ac-8,24-dien-TA	3 $\beta$ -O-Acetyl-8,24-dien-tirucallic acid ( <b>19</b> )
$\beta$ -AKBA	3 $\alpha$ -O-Acetyl-11-keto- $\beta$ -boswellic acid ( <b>6</b> )
$\beta$ -BA	$\beta$ -Boswellic acid ( <b>3</b> )
$\beta$ -Car	$\beta$ -Caryophyllene ( <b>27</b> )
$\beta$ -Car-Ox	$\beta$ -Caryophyllene oxide ( <b>28</b> )
$\beta$ -KBA	3 $\alpha$ -OH-11-keto- $\beta$ -boswellic acid ( <b>5</b> )
$\beta$ -PgE <sub>2</sub>	Prostaglandin E <sub>2</sub>
$\beta$ -TA	3 $\beta$ -OH-8,24-dien-tirucallic acid ( <b>15</b> )
STI	Soybean Trypsin Inhibitor
T	Temperature
T/E	Trypsin/EDTA
$t_0$	Dead retention time (chromatography)
TAs	Tirucallic acid (including here compound <b>13</b> – <b>19</b> )
TIC	Total Ion Current
TLC	Thin Layer Chromatography
$t_r$	Retention Time (chromatography)
UHPLC	Ultra-High Performance Liquid Chromatography
UV	Ultra Violet
v/v	Volume percent
Vert-4(20),7,11-triene	Verticillia-4(20),7,11-triene ( <b>24</b> )

## Explanatory Notes and Abbreviations

---

VIS	Visual Spectral Area
VVK	Coefficient of Variation referring to the linear calibration model
w	Peak width (peak width: peak end minus peak start)
$\alpha$	Alpha (position of an atom under the paper plane)
$\alpha$ -7,24-dien-TA	3 $\alpha$ -OH-7,24-dien-tirucallic acid ( <b>17</b> )
$\alpha$ -ABA	$\alpha$ -Acetyl-boswellic acid ( <b>2</b> )
$\alpha$ -Ac-7,24-dien-TA	3 $\alpha$ -O-Acetyl-7,24-dien-tirucallic acid ( <b>18</b> )
$\alpha$ -Ac-TA	3 $\alpha$ -O-Acetyl-8,24-dien-tirucallic acid ( <b>16</b> )
$\alpha$ -AKBA	3 $\alpha$ -O-Acetyl-11-keto- $\alpha$ -boswellic acid
$\alpha$ -BA	$\alpha$ -Boswellic acid ( <b>1</b> )
$\alpha$ -Hum	$\alpha$ -Humulene ( <b>26</b> )
$\alpha$ -KBA	3 $\alpha$ -OH-11-keto- $\alpha$ -boswellic acid
$\alpha$ -TA	3 $\alpha$ -OH-8,24-dien-tirucallic acid ( <b>14</b> )
$\tau$ -Cad-OH	$\tau$ -Cadinol ( <b>25</b> )

### 1 Introduction

The first what someone may associate with the word frankincense or incense in our modern western civilisation is probably the word “catholic church”. There, it is burned on coal during the mass and emits a more or less pleasant odour, which certainly is dependent on the personal preference on how to define an agreeable scent. Additionally, it is described in several chapters of the bible, where it for example is mentioned 22 times (see also the *Handbook of Medicinal Plants in the Bible* by J. A. Duke et al. [1]).

A very famous quotation, in connection with frankincense and even myrrh, may be thus the following one (Matthew 2, 10-11, English Standard Version): *“When they saw the star, they rejoiced exceedingly with great joy. And going into the house they saw the child with Mary his mother, and they fell down and worshiped him. Then, opening their treasures, they offered him gifts, gold and frankincense and myrrh.”* Another one, likely to be less known, is that a mixture of myrrh and wine was offered to Jesus Christ on the cross to soothe his pain (Mark 15:23, King James Bible): *“And they gave Him to drink wine mingled with myrrh; but he received it not.”* Finally, myrrh was also used to embalm the body of Jesus Christ (John 19:39): *“And there came also Nicodemus, which at first came to Jesus by night, and brought a mixture of myrrh and aloes, about a hundred pound weight.”* Thus, it is somehow quite astonishing how valuable these materials might had been during the time of Christ when His life began and even ended with them (e.g. at His birth to worship Him, and in His end to soothe His pain and lastly to embalm Him). Surely, frankincense and myrrh do not have the same esteem as they had ca. two thousand years before, and according to the paper of Thieret [2] it may be really quite interesting what the Wise Men would bring to Christ today (to quote Thieret: *“Perhaps gold, dates and oil.”*).

However, what probably is nowadays not known among many western community citizens is the fact that frankincense and also myrrh had an inestimable value for many older and especially ancient civilisations (e. g. the Egyptian, Greek and even the Roman cultures). At that time, it was not only used for religious and spiritual purposes but also for pharmacological applications. Most probably, the property of frankincense and myrrh, used as scents and for embalming, was a sign of great prosperity during these ancient times. By trading these goods, the early South Arabian cultures of the areas called Hadramaut and Dhofar (today Yemen, respectively, Oman) generated a prosperous welfare, perhaps comparable with the current welfare of Saudi Arabia established on the production of oil [3]. These days, frankincense still is important for the fragrance industry since its resins contain innumerable amounts of volatile and odorous molecules [4].

Additionally, since Safayhi et al. [5] have coincidentally discovered anti-inflammatory actions of an Indian frankincense extract in the early nineties of the last century, the pharmacological interest in extracts and single isolated compounds thereof, as an alternative herbal treatment, has been growing enormously to the present day. Even though, there is more and more encouraging proof that extracts of frankincense may be an effective therapy against several diseases (e.g. asthma, rheumatoid arthritis and Crohn’s disease etc.), the evidence thus far is not absolutely compelling [6]. One advantage of frankincense preparations seems to be the comparably low occurrence of side-effects when used as medication. However, to quote E. Ernst, absence of evidence is not the same as evidence of absence [6]. The hitherto administered medication in cases of inflammatory diseases, the so-called Non-Steroidal Anti-

inflammatory Drugs (NSAIDs), such as acetylsalicylic acid or ibuprofen, and the corticosteroids, such as cortisol, are reported to have several more severe side-effects instead, if taken over a longer period of time.

Furthermore, patients with an interest and a demand of medical frankincense preparations mainly have to trust in nutritional supplements, as they are accredited by the *European Food Safety Authority* (EFSA) for such an application, though there is nothing established about a certain frankincense metabolism in the human body - *Do we need frankincense resins to survive? Like air, sugar, proteins and water? Has anybody ever heard of a human being suffering and/or starving because of a lack of frankincense dietary supplements?* These supplements are offered by several distributors, most probably with an unknown and hence not analytically guaranteed composition of active ingredients. How these multiple compound containing extracts interact in the human body is so far still elusive. Whether or not it will be possible to understand their interactions - in a synergistic or antagonistic manner - in the human body in the near future may also be questioned.

However, these are just a few points which are currently highly discussed about the benefits and drawbacks of herbal preparations. If extracts of frankincense will eventually achieve the status of a declared and by clinical studies validated herbal remedy can not be surely predicted to date. It will depend on an investor being courageous enough to take a risk in the enormously expensive conduction of a sufficiently representative clinical trial. Thus far, the risk seems far too big.

In the following introducing chapters on this topic the history, the biology and botany, some geographical facts, the biosynthesis of terpenes, the chemistry and the pharmacology for resins of *Boswellia*, which finally will lead to the aim of the study presented here, are described.

### 1.1 Anecdotes of the Early History of Frankincense

Beside the reports on frankincense given in the bible (see chapter 1. Introduction), there are several other sources witnessing the trade and application of frankincense for different purposes. The first reliable reports about border-crossing drug trade have been concluded for the old Babylonians, where the caravan roads from India, Arabia and Syria crossed each other, and additionally for the old Egyptians. Thus, in the old-Babylonian settlement Sippar (ca. 2250 BC) the drug merchants already bartered with several natural products, probably including frankincense and myrrh [3].

However, the greatest insight in the cultures of pre-Christian times is granted for the early Egyptians. For them the historians and archaeologists revealed many indications and evidence for the application of resins for fumigation (Olibanum; synonym of frankincense) and embalmment (myrrh). Very early in time (ca. 2470-2350 BC) the old Egyptians already sailed with huge merchant fleets to the legendary country of Punt, which exact location is even hitherto not definitely known by modern historians (it is assumed around the Horn of Africa, today: Somalia, and even on the other shore of the Red Sea and Gulf of Aden, today the areas of Yemen and Oman). The Greek historian Herodot (ca. 484-425 BC) mentioned merely Arabia, "*the outermost land of the world in the far south*", as origin for these goods. The most famous travel to the fabulous land of Punt was the expedition of the female

Egyptian pharaoh Hatshepsut (ca. 1478-1457 BC). Several wall drawings found in the great temple of Deir el-Bahari in Egypt witness the great expeditions of hers to this secret land. On these drawings depictions of frankincense and myrrh trees are shown, which were transported in baskets back to Egypt for cultivations. However, these claims of cultivation did not succeed [3,7].

Furthermore, one of the oldest ancient trading routes is the so called *Incense Road*. This path led from Dhofar (Oman) via Yemen, the Asir Province (Saudi-Arabia) and the landscape of Hedjas (western Saudi-Arabia) to the Mediterranean ports of Gaza (today Palestinian territory) and Damaskus (today Syria), from where these goods were further transported to the then prosperous Mediteranean states. The booming years of the trade along the *Incense Road* were about 800 BC, when the ancient South Arabian kingdoms of Sheba, Qataban, Hadhramaut and the Minaeans controlled the trade with frankincense. Therefore, these kingdoms generated a great prosperity during that time. However, through the resumed rise of the sea maritime trade (ca. 100 BC) the *Incense Road* lost more and more its relevance and the South Arabian welfare, based on the trade with frankincense, declined. There may be still a lot to report on these quite interesting ancient times, about the rise and fall of certain kingdoms, and for this purpose the corresponding literature may be consulted [3].

Another source for the pharmacological use of frankincense can be found in India, connected to the philosophy of Ayurveda, a kind of traditional medicine native there. *Boswellia serrata* (Abbr.: Bser; synonym: *salai gugal* or *salai gugul*), the Indian Frankincense, is described in Ayurvedic text books (Charaka Samhita, 1<sup>st</sup> – 2<sup>nd</sup> century AD and in Astangahrdya Samhita, 7<sup>th</sup> century AD) to treat a variety of diseases [8]. Furthermore, the oldest pharmacological note, the papyrus Ebers (received by Moritz Fritz Ebers in 1873 from an Arabian businessman), already mentions frankincense as a drug. The papyrus itself contains information for medical doctors concerning diagnosis and treatment of several diseases. The age of the papyrus Ebers is dated to the time of Pharaoh Amenophis I and was thus probably written around 1500 BC [3].

Interestingly, the use of frankincense has continued, even until our modern age of technology. Though it is today in the common sense mainly abstracted with its smell in catholic churches, in a pharmacological point of view it regained a strong interest over the last two decades [8,9].

### 1.2 Biological, Botanical and Geographical Facts

Botanically, the frankincense tree belongs to the family of the *Burseracea*. Its genus is denoted as *Boswellia*, whereas the myrrh trees, another similar commonly known plant, also belonging to the *Burseracea* family, are denoted as *Commiphora* (genus). Both are historical important resin providing plants. The genus of *Boswellia* (named after Johann Boswell, who wrote a paper on ambergris in 1735) contains hitherto 25 species, whereby it is not clearly verified if some of the species are doubly counted. It is mainly distributed in the dry areas of the Horn of Africa (Somalia, Sudan, Ethiopia, and Eritrea), the Arabian Peninsula (Oman and Yemen) and in India. There are rather differing indications in literature on the specific names and spreading of the single species. A few representative species are given in Table 1.1 [3,10].

## Introduction

---

The term *Boswellia carterii* is adopted for the Somalian tree and the term *Boswellia sacra* for the South-Arabian (Oman, Yemen) plant, although both species can be regarded as the same, at least on a chemotaxonomic and a botanical point of view [11-13]. The Indian tree is called *Boswellia serrata* [14]. The quite common species *Boswellia papyrifera* is primarily growing in Sudan, Eritrea and Ethiopia [15,16], and is often mistaken with the species *Boswellia carterii* from Somalia (see also chapter 1.4.5 on neutral terpenic compounds). Interestingly, these four species seem to be the only ones thus far which definitely have been described to contain the boswellic acids in great quantities, the class of pentacyclic triterpene acids specific for the *Boswellia* trees (see also chapter 1.4.1 on chemistry).

The *Boswellia* plants are deciduous trees and can reach a height of up to 5 m and even more, dependent on the species and the growing area. They have bald stems and branches with a peeling bark and appear bush or tree like. The branches have compound leaves and an odd number of leaflets. They bloom in spring, mostly in April.

**Tab. 1.1** A few representative *Boswellia* species and their geographical distribution. The trees of *Boswellia carterii* Birdw. and *Boswellia sacra* Flück. can be regarded as the same species, according to the chemotaxonomic and biological evaluations [11-13]. They are just differing because of their geographical origin.

Species	Geographical Distribution
<i>Boswellia carterii</i> Birdw.	Somalia, Nubia
<i>Boswellia sacra</i> Flück.	Oman, Yemen
<i>Boswellia frereana</i> Birdw.	Somalia
<i>Boswellia papyrifera</i> Hochst.	Ethiopia, Eritrea, Sudan
<i>Boswellia serrata</i> Roxb.	India
<i>Boswellia neglecta</i> S. Moore	Somalia
<i>Boswellia odorata</i> Hutch.	Tropical Africa
<i>Boswellia dalzielli</i> Hutch.	Tropical Africa
<i>Boswellia ameero</i> Balf. Fils.	Socotra
<i>Boswellia elongata</i> Balf. Fils.	Socotra
<i>Boswellia socotrana</i> Balf. Fils.	Socotra

The term *Burseraceae* means that these plants produce balms and resins in special tissue canals. A resin is generally a mixture of several organic compounds (e.g. terpenes, terpenoids and polysaccharides) which has an amorphous shape. When cold, these resins appear often as a viscous and glassy solid. When heated they start to liquefy, and when cooled again, they once more become an amorphous solid without any crystallisation. Resins are quite robust materials, staying inert towards chemical and environmental influences [17]. Plant resins are products of the secondary metabolism, which basically means that neither energy nor material for the growth of the plant is generated thereby. On the contrary, the primary metabolism serves for the decomposition (catabolism, delivering mostly energy) and composition (anabolism, for the functional cell construction) of biologically important molecules [18]. The biological benefit of the secondary metabolism is not completely understood hitherto. A sensible reason may be the protection against hazardous environmental influences (e.g. against microorganisms, if the bark gets injured etc.). Furthermore, certain volatile compounds may serve for communication interactions between specific plants and insects (e.g. linalool, a monoterpene, produced by flowers often attracts

moth pollinators during the night, while other plant species, not producing linalool, attract other insects like bees and butterflies during daytime [19]).

The harvesting of the *Boswellia* resins begins in spring with start of the yearly hot period (end of March in Somalia and April in Dhofar, Oman). Therefore, the stem and the thicker branches are cut with a special knife. During this process the resin containing excretion vessels in the bark are injured. The gum resin exudates can thus emerge. Due to the air exposure the viscous material solidifies to a gum resin. Gum resins are resins which contain besides ethereal essential oils and further non-polar terpenoids a greater amount of polysaccharides (ca. 25-30 %). The congealed resin is then harvested during the whole summer period. The first cut and drying process delivers a resin of inferior quality. The second cut, ca. three weeks later, delivers the yellow dyed and resinous material in greater quality and quantity, forming teardrop like solids when congealed. These are finally scraped off for the first time after one or two weeks. Dependent on the age, height and condition of the tree, its exploitation is executed for three consecutive years. Afterwards, a several year taking period of rest begins. The yield of one tree is about 3 - 10 kg, depending on the health and growth of the tapped tree [3].

Another point to be discussed may be the sustainability of the frankincense production in the present and even its future tendencies. Many frankincense accommodating countries are considered as politically unstable states with low educational levels and a poorly economical strength (e.g. Somalia, Sudan, Eritrea and Ethiopia), not to mention randomly happening existential crisis such as starvation or violent conflicts.

The situation in India may be more promising, since most of the clinical studies have been implemented with extracts of *Boswellia serrata*, the Indian frankincense tree [6]. Therefore, especially the Sallaki-TABLETS<sup>®</sup> (formerly known as H15 Gufic) from the GUFIC BIOSCIENCES LIMITED in Karnataka, India, have been evaluated. Additionally, the Indian frankincense is monographed as *Olibanum Indicum* in the European Pharmacopeia 6.0, respectively, 7.0 [20,21], and a comprehensive article on its clinical particularities and pharmacological properties is published in the ESCOP (*European Scientific Cooperative on Phytotherapy*) Monographs [22]. Hence, there may be precautions met in India to preserve this highly valuable plant.

In Oman the situation may be different, since the frankincense trade does definitely not have the same importance as it had in its early history [3]. The reason therefore may be the modern economical development, especially the oil export, which binds most of the workforce of the country. Furthermore, the harvest of frankincense is tedious under the harsh conditions such as heat and dry climate [23]. In addition to that, the agricultural economy will also decrease more and more in the country of Oman, if frankincense is not considered as a highly valuable resource anymore.

For the country of Yemen, which also accommodates the *Boswellia sacra* tree, the same problems as reported for the Oman may be recognisable. Furthermore, Yemen, one of the poorest Arabian countries, accommodates forces of the terror network *al-Qaeda*, and another problem may be the addiction of the farmers to the production of the drug khat (*Catha edulis*), which is strongly consumed among the locals [24]. Thus, the country has definitely a lot of other worries and problems to overcome. And if the value of its indigenous *Olibanum* trees is understood there, is also questionable.

The situation at the Horn of Africa may be even worse than for the countries mentioned above. Particularly Somalia, a country without any real government since 1991 and thus characterised as a “failed state”, suffers regularly from food crises and terrorism. Well known may be the regularly reported piracy in the Gulf of Aden [25]. How the situation is going to develop in this region can not be really predicted. Hitherto, *Somalian Olibanum* is still available on the market.

The situation in Ethiopia, Eritrea and Djibouti may be not really much better, since several border conflicts are reported (e.g. violent conflict over the border region Badme between Ethiopia and Eritrea; between 1998 and 2002, 100.000 people died in a war there [25]). Thus, there may exist still great resentments between these two countries. Additionally, the real value of frankincense, as a possible economical resource, is probably also not realised.

In 2006, Ogbazghi et al. published their results of a field study on the distribution of the frankincense tree *Boswellia papyrifera* in Eritrea depending on environmental influences and land use [16]. They concluded that the distribution of this tree has decreased during the past decades, mainly due to an increasing human population, resulting in the conversion of woodlands into agricultural fields and increasing livestock pressure hindering natural regeneration.

The temporary most reliable predictions on the future of frankincense have been made for the species *Boswellia papyrifera* in Eritrea and Ethiopia by Groenendijk et al. [26], recently published in 2011. The authors studied twelve populations of *Boswellia papyrifera* in northern Ethiopia and compared tapped (for resin harvesting used) and untapped populations in order to develop a matrix based model to predict the population dynamics. The studies took place from 2007 to 2009. Their outcomes are quite serious. It is concluded that under “business as usual” conditions (e.g. exploitation of the trees for firewood, grazing material for livestock and other environmental influences like beetle attacks etc.) 90 % of both populations, tapped and untapped, are going to decline within the next 50 years. Furthermore, a 50 % decline in frankincense yield within the next 15 years has been stated. Model simulations for restoration scenarios conclude that populations and frankincense production could only be sustained with intensive efforts leading to full sapling recruitment and a 50-75 % reduction in adult mortality. This is hitherto the first large-scale study on population dynamics of a frankincense-producing tree. The results also suggest that a lack of regeneration and high adult mortality (6-7 % per year), independent from resin tapping, is causing strong declines in the *Boswellia papyrifera* population. These findings may also be projectable to the situation in the other frankincense producing countries of Africa and Arabia (e.g. Somalia, Yemen).

### 1.3 Biosynthesis of Terpenes

Though natural products, many of them derived from plants, have been used throughout the history of mankind for several different purposes, the scientific evaluation of their active ingredients became firstly possible in the 19<sup>th</sup> century when chemistry as a science had its major ascendancy (During that time the rise of chemistry as a science may be comparable with the developments in biotechnology or information sciences nowadays).

One great class of natural products are the terpenes or terpenoids (terpenes with differing functional groups such as hydroxyl-, aldehyde-, ketone-, carboxylate-, etc.). The term

## Introduction

“Terpenes” has been derived from Turpentine products (e.g. the first diterpene resin acid, abietic acid from rosin, a by-product of turpentine oil industry was isolated although in impure form in 1824 [27]). They universally occur in all living organisms but especially are referred to the class of plants where they can be found in great quantities in special extra-cellular compartments. One example of a great terpene and terpenoid source are the *Boswellia* species, whose resinous material, obtained by incision of the stems of the trees, consists of several different terpenic compounds [3]. As universal metabolites, terpenes have several biological functions, and for many of them the specific function is thus far not completely understood. They function, for example, as pheromones for many plant and insect species and serve hence for the interactive communication system of these beings [19].

Besides, they play an important role for the flavour, fragrance and pharmaceutical industries. Smaller volatile terpenes (e.g. citral from lemongrass oil, *Cymbopogon citratus*; or linalool from the oil of lavender, *Lavandula angustifolia*) are very interesting compounds for the fragrance industry as they reveal, dependent on their molecular structures, specific scents. Others are used as spices and several more are interesting candidates for drugs with promising applications (e.g. the boswellic acids as anti-inflammatory agents from *Boswellia* species; or Paclitaxel, known as Taxol<sup>®</sup>, firstly isolated in minimal amounts from the pacific yew, syn. *Taxus brevifolia*, which is applied as an anti-tumour agent). Thus far, up to 30.000 terpenes are known in literature, and still, there may be every day new derivatives or chemical entities described.

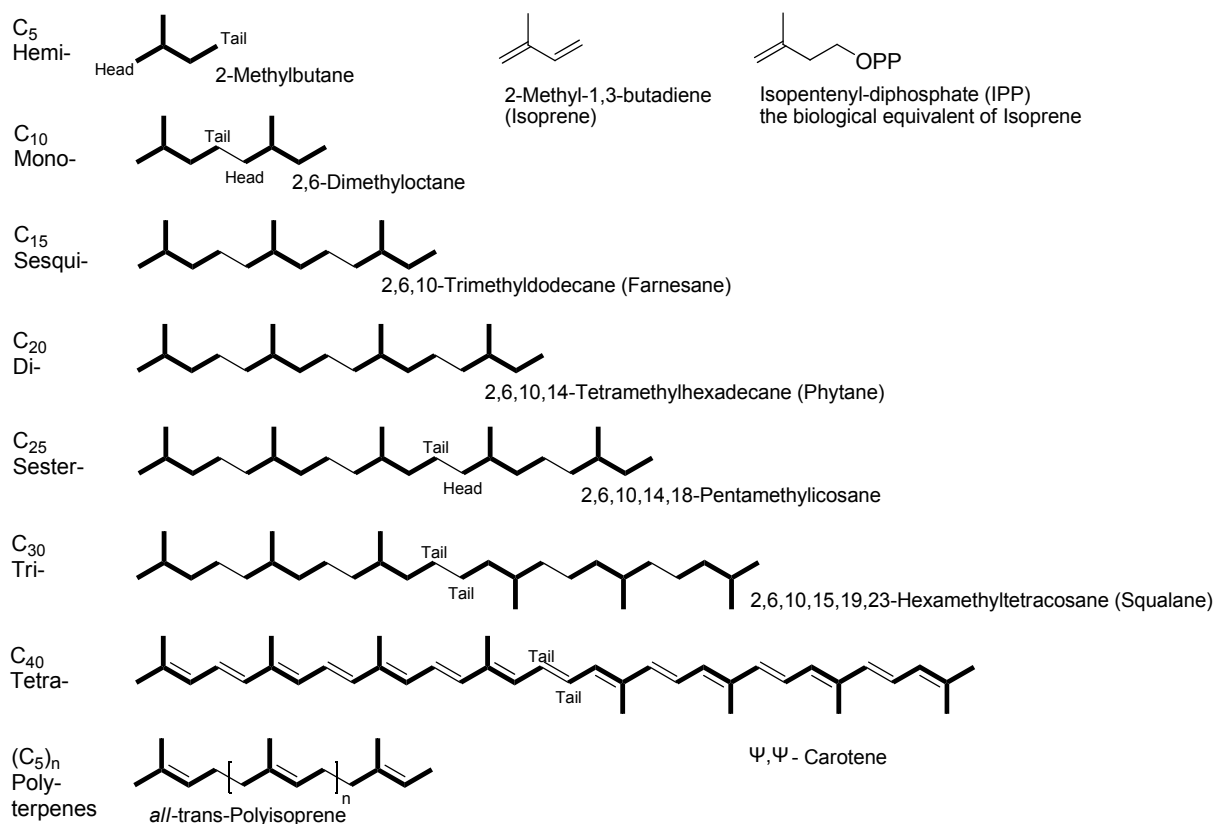


**Fig. 1.1** The basic hydrocarbons of the terpenes (isoprenoids).

The greatest impacts on terpene chemistry were accomplished by Wallach (Nobel Prize in Chemistry 1910) in the 19<sup>th</sup> century and by Ruzicka (Nobel Prize in Chemistry 1939) in the

20<sup>th</sup> century, two chemists whose lifework consisted of the research and structural elucidation of many naturally occurring terpenes. Based on their experimental observations they developed the so-called *Isoprene Rule*. This is a general principle that every terpene consists of C<sub>5</sub>-units (2-methyl-1,3-butadiene or *isoprene* units) which build up the carbon skeleton of the class of terpenoids. Hence, they are also denoted as *isoprenoids* [28-30]. Predominately, they can be found as hydrocarbons with several functionalities in nature (e.g. as alcohols and their glycosides, ethers, aldehydes, ketones, carboxylic acids and esters). The basic structures are shown in Fig. 1.1. It is differentiated between hemi- (C<sub>5</sub>), mono- (C<sub>10</sub>), sesqui- (C<sub>15</sub>), di- (C<sub>20</sub>), sester- (C<sub>25</sub>), tri- (C<sub>30</sub>), tetraterpenes (C<sub>40</sub>) and polyterpenes (C<sub>5</sub>)<sub>n</sub> with n > 8 [31]. It should be emphasised that it is rather astonishing that the basic pathways for terpene synthesis are universally occurring in all kind of living organisms. This means that every organism, more or less, uses the same tools for the production of certain metabolites, if the specific pathway exists. Just another impressive example of how systematically “Mother Nature” works. As depicted in Fig. 1.1, the isopropyl part of 2-methylbutane is defined as *Head*. The ethyl part of it is denoted as *Tail*. The combinations for each isoprenoid class differ. For mono-, sesqui-, di- and sesterterpenes the units are connected to each other from *Head-to-Tail*. The tri- and tetraterpenes are linked to each other by one *Tail-to-Tail* connection in the centre [31].

In the middle of the last century the theory by Wallach and Ruzicka was finally experimentally proved by Lynen and Bloch (Both together obtained the Nobel Prize in Physiology or Medicine in 1964) [32,33]. They revealed that acetyl-coenzyme A, known as *activated acetic acid*, is the biogenetic precursor of terpenes. This classical pathway is called *acetate-mevalonate pathway* (MevA). There, two equivalents of acetyl-CoA are linked to acetoacetyl-CoA, which reaction mechanism is similar to a classical *Claisen* condensation. Acetoacetyl-CoA is the biological analogue of acetoacetate. Subsequently, acetoacetyl-CoA reacts with another equivalent of acetyl-CoA, similar to an aldol reaction, leading to β-hydroxy-β-methylglutaryl-CoA. By reduction with dihydronicotinamide adenine dinucleotide (NADPH + H<sup>+</sup>), a universal co-factor in enzymatic redox reactions [18], (*R*)-mevalonic acid is obtained (see Fig. 1.2). Adenosine triphosphate (ATP), another universal co-factor and the universal biological energy source on this planet [18], donates the pyro-phosphate leading to the diphosphate of mevalonic acid which is transformed into isopentenylpyrophosphate (syn. isopentenylidiphosphate, IPP) by decarboxylation and dehydration. Isomerisation of the latter gives dimethylallylpyrophosphate [31]. Further reaction steps lead to monoterpenes or sesquiterpenes (e.g. dimethylallylpyrophosphate reacts with IPP to geranylpyrophosphate, GPP, and thus monoterpenes, and the subsequent reaction of geranylpyrophosphate with another equivalent IPP leads to farnesylidiphosphate, FPP, and hence sesquiterpenes). The here described reaction steps are shown in Fig. 1.2. The next higher terpenes, the diterpenes (C<sub>20</sub>), are synthesised by the nucleophilic head attachment of IPP (C<sub>5</sub>) to the electrophilic tail of FPP (C<sub>15</sub>) leading to geranylgeranylpyrophosphate (GGPP). A further linkage of IPP (C<sub>5</sub>) with GGPP (C<sub>20</sub>), *Head- to-Tail*, gives the sesterterpenes (C<sub>25</sub>). The combination of two molecules FPP, *Tail-to-Tail*, leads to the triterpene squalene (C<sub>30</sub>). In the same way the *Tail-to-Tail* connection of two equivalents of GGPP results in the tetraterpenes (C<sub>40</sub>) such as 16-*trans*-phytoene [31]. The basic reaction schemes are presented in Fig. 1.3.

## Introduction

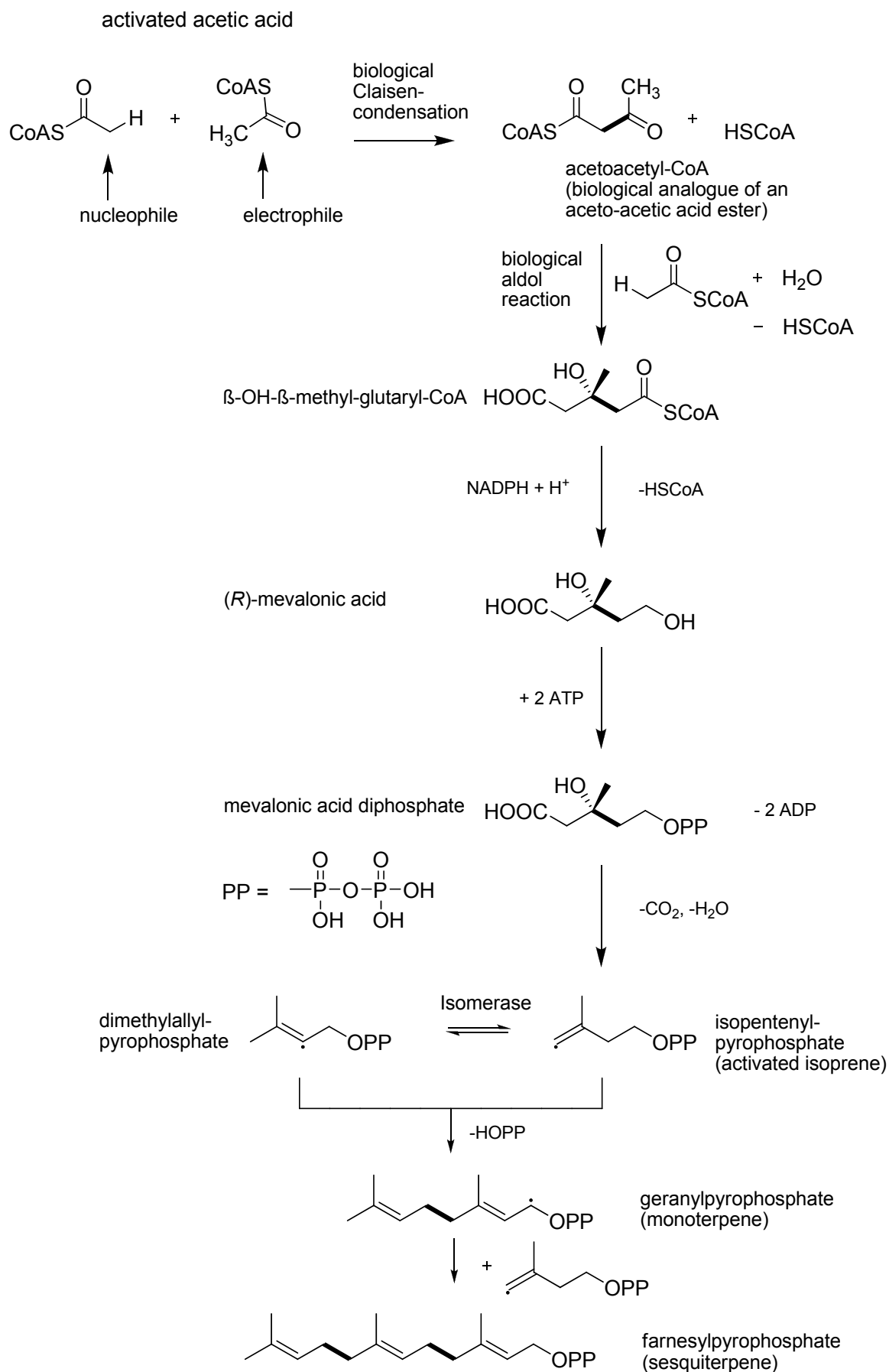


**Fig. 1.2** Reaction scheme (MevA-pathway) of the biogenesis of mono- and sesquiterpenes. For further details see text or the book of Breitmaier [31].

## Introduction

The MevA terpene pathway had been considered as the universal biosynthetic pathway until the end of the 1980s. Though, there had been detected a few contradictory outcomes (e.g. isotopically labelled MevA and acetate were usually not well incorporated into carotenoids and monoterpenes in plant systems while they were incorporated quite well into other isoprenoids such as steroids; from the review of Barkovich and Liao [34]). These facts have been also shortly discussed in the dissertation of Basar [35].

Experiments by Rohmer et al. [36], published in 1993, with incorporation of  $^{13}\text{C}$ -labelled glucose, acetate, pyruvate or erythrose allowed to detect the origin of carbon atoms of triterpenoids of the hopane series and of the ubiquinones from several bacteria (e.g., *Escherichia coli*, *Alicyclobacillus acidoterrestris* etc.). They figured out, by failed incorporations of  $^{13}\text{C}$ -labeled acetate and successful incorporations of  $^{13}\text{C}$ -labeled glycerol and pyruvate in hopanes and ubiquinones, that there exists another pathway different from the known *acetate mevalonate pathway*. The finding by Rohmer et al. showed that isopentenyl diphosphate (IPP) originates also from activated acetaldehyde ( $\text{C}_2$ , by reaction of pyruvate and thiamine diphosphate) and glyceraldehyde-3-phosphate ( $\text{C}_3$ ). Thus, the so-called *1-deoxy-pentulose-5-phosphate* is generated delivering the first unbranched  $\text{C}_5$  precursor of IPP. This pathway, the *deoxyxylulose phosphate pathway* (DXP), is depicted in Fig. 1.4.

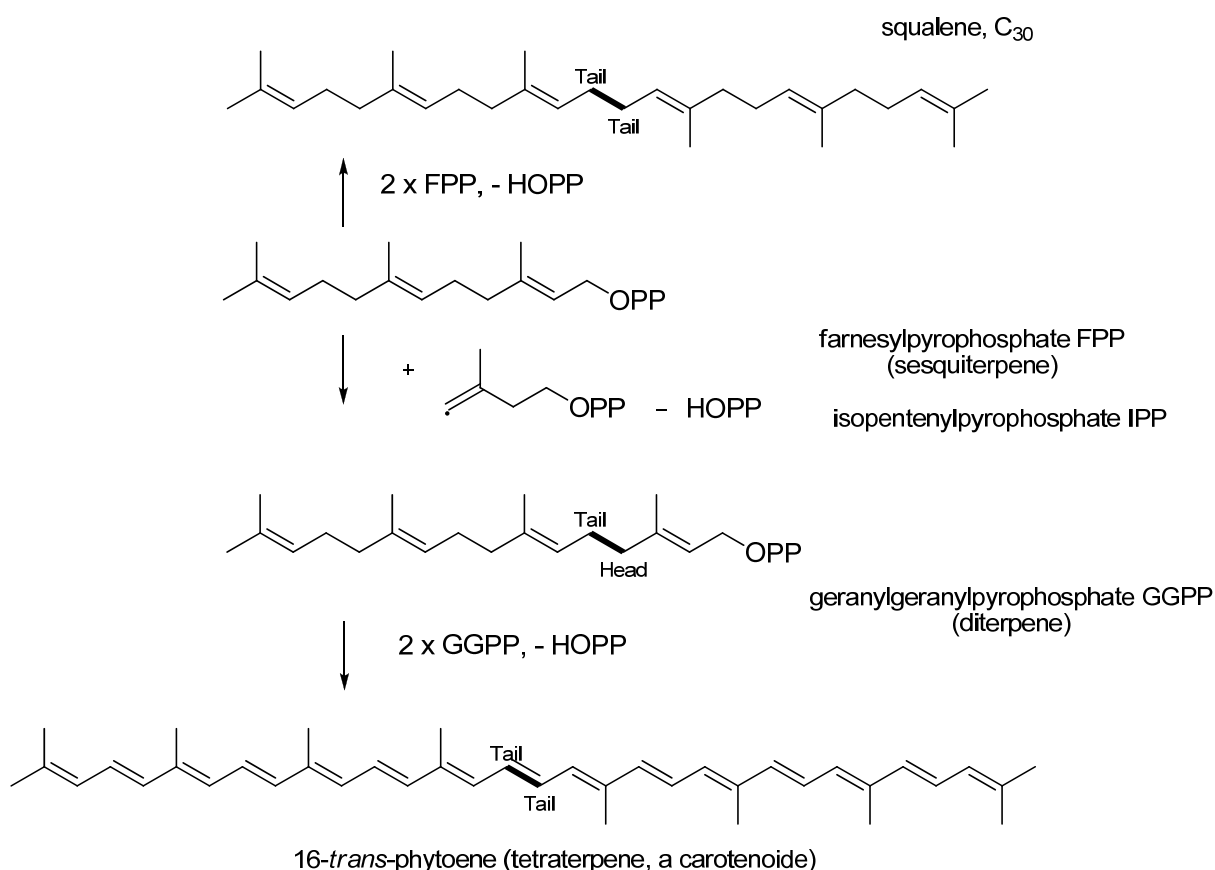


**Fig. 1.3** Basic reaction scheme for the biogenesis of di-, tri- and tetraterpenes. For further details see text or the book of Breitmaier [31].

So far, fungi and yeast merely use the MevA-pathway. Bacteria reveal both metabolic pathways. In higher plants both pathways are used, whereas the products of the cytosol (sterols, triterpenes) are produced via MevA and products from the chloroplasts (phytol, caretenoides, plastochinone and other small terpenes) are synthesised via the DXP pathway. Between both pathways intermediates are exchangeable (IPP, GPP, FPP, GGPP). The specific pathway can be identified by genes, encoding specific enzymes, or by inhibitors blocking these enzymes (e.g. Lovastatin for MevA or Fosmidomycin for DXP [34]). Hence, especially the DXP pathway is an interesting target for drugs (e.g. Fosmidomycin as an antibiotic [37]).

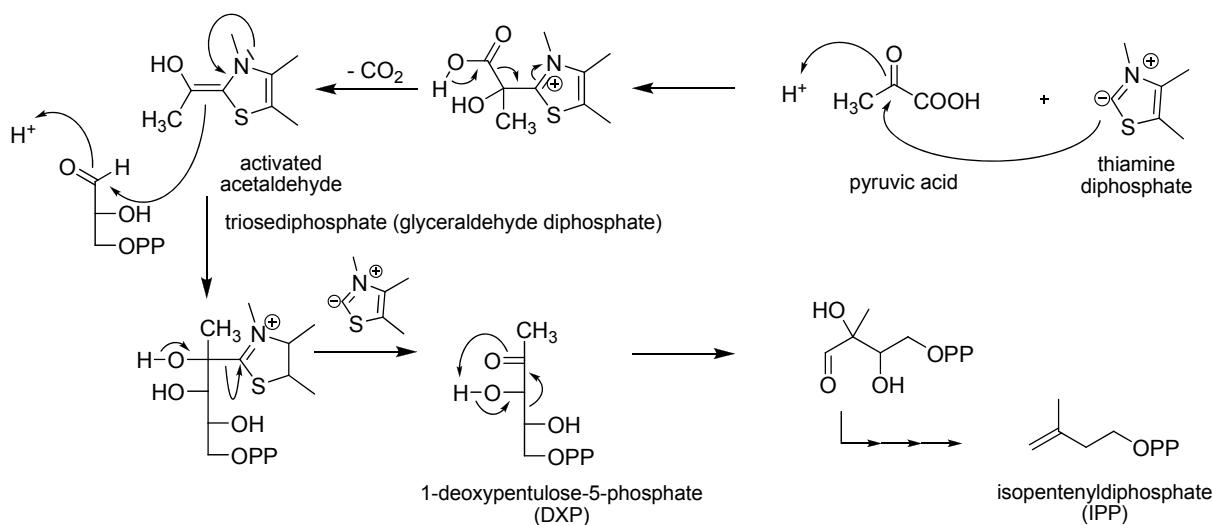


**Fig. 1.4** Reaction scheme (DXP-pathway) of the alternative precursor synthesis of IPP. For further details see text or the book of Breitmaier and the dissertation of Basar [31,35].

For the biosynthesis of further cyclic and polycyclic terpenes the participation of intermediate carbenium ions is assumed. However, evidence for this *in vivo* was given only in some cases. One simple example of the synthesis of limonene, a monocyclic monoterpene, is given in Fig. 1.5. Through an intra-molecular reaction of the allylic cation with the spatially near double-bond, the GPP-cation cyclises to give a cyclohexyl cation then transformed into (*R*)- or (*S*)-limonene by deprotonation. The biogenesis of other terpenes is obtained by similar reactions steps, additionally including 1,2-hydride and 1,2-alkyl shifts (Wagner-Meerwein rearrangements) and sigmatropic reactions (Cope rearrangements), most probably stereosepecifically guided by enzymes. Further examples are given in the book of Breitmaier or in the review of Rucker on sesquiterpenes [31,38].

A few assumed biogenesis pathways of some particular terpenes, found in frankincense resins, are depicted in chapter 3.13 as a proposal. These are based on the results obtained by the qualitative and quantitative HPLC experiments presented in chapter 3.7 and 3.8.

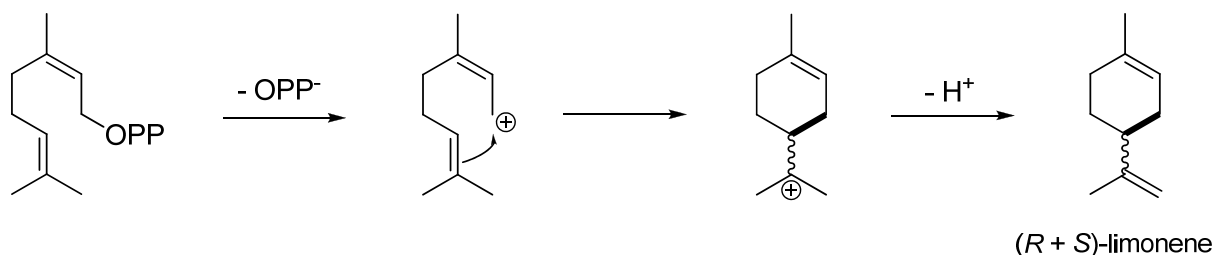


**Fig. 1.5** The biosynthesis of (*R* + *S*)-limonene via an assumed carbo-cation intermediate stage. For further details see text or the book of Breitmaier [31].

Another class of tetracyclic triterpenes with a gonane or sterane carbon skeleton are the steroids. They are derived from tetracyclic triterpenes obtained by the biosynthesis reported here and only differ in the amount of C-atoms, thus, not following the classical Isoprene rule (multiple of  $C_5$ ) anymore. The structure of its mostly known representative is cholesterol ( $C_{27}$ ) which is the precursor for several other steroids with specific biological functions of each. The overview scheme on the biogenetic origins of tetracyclic triterpenes and steroids is given in Fig. 1.6, and in Fig. 1.7 the structure of cholesterol, including the basic skeleton of steroids, is shown.

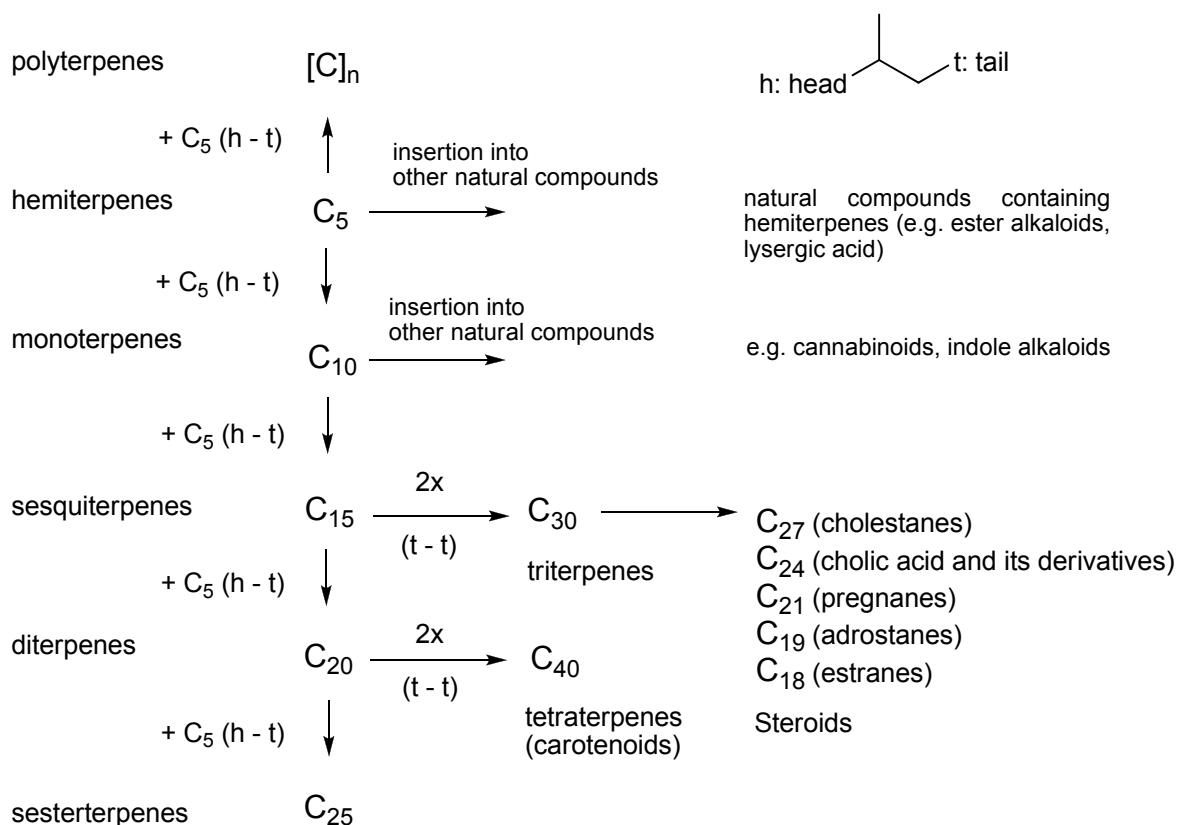


**Fig. 1.6** Overview on the specific origins of tetracyclic triterpenes and steroids. For further details see text or the book of Breitmaier [31].

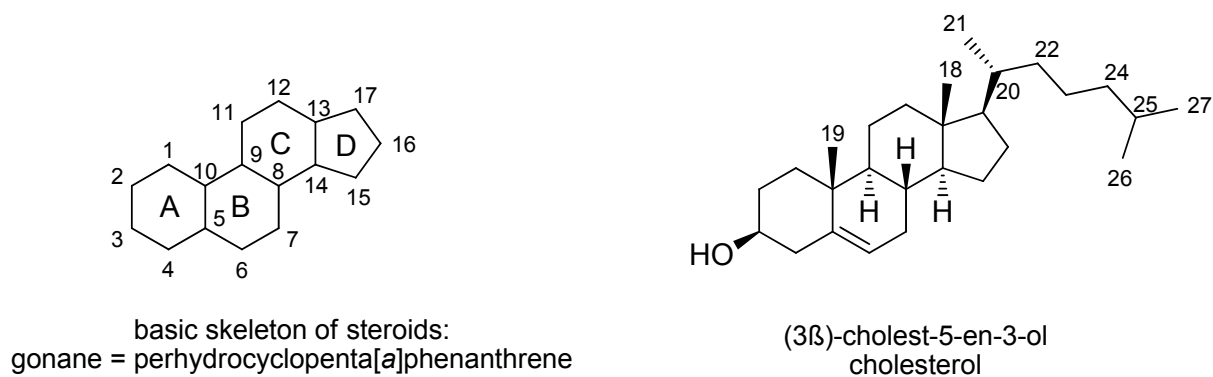


**Fig. 1.7** The basic structure of the gonane-type steroids and its mostly known representative cholesterol. For further details see text.

Cholesterol is correlated with high blood pressure and cardiovascular diseases in humans. Furthermore, it is the predecessor of the female and male sex hormones (oestrogens with C<sub>18</sub>, respectively, testosterone with C<sub>19</sub>) and several other types of functional steroids. For the explicit clarification of the biosynthesis routes, mechanisms and functionalities the corresponding literature may be consulted [18]. A good short overview is additionally summarised in the dissertation of Basar [35].

## 1.4 Chemistry

In the following chapters a few specific classes of terpenic compounds found in *Boswellia* resins are presented. Principally, the most common classes are described. Thus far, merely the species *Boswellia papyrifera* (Bpap), *Boswellia serrata* (Bser), *Boswellia sacra* (Bsa), respectively, *Boswellia carterii* (Bcar) seem to definitely contain the boswellic acids in high quantities. These findings have been already clarified in the dissertation of Jochen Bergmann (2004) [17]. He analytically compared the species *B. ameero*, *B. frereana*, *B. papyrifera*, *B. sacra*, *B. carterii*, *B. serrata* and *B. socotrana* and only detected for the species Bpap, Bser, Bsa/Bcar the specific boswellic acids. *B. frereana* for example consisted mainly of neutral compounds, revealing almost no quantity of acids. Furthermore, the analysis of *Boswellia neglecta*, *Boswellia riviae* and again *Boswellia frereana* in the dissertation of Basar (2005) revealed boswellic acids merely in traces [35]. Consequently, the species Bpap, Bser and Bsa/Bcar may be the most important classes of *Boswellia* species, if the pharmacological activity, based on triterpenic acids, is regarded.

### 1.4.1 Boswellic Acids

The first comprehensive and reliable investigations on resins of frankincense were realised by Alexander Tschirch and Oscar Halbey during the years from 1892 to 1899. Their results are published in several writings and publications [39-41]. Basically, they separated the alcoholic extract into its neutral and acidic fraction by solvent extraction with diethyl ether (Et<sub>2</sub>O) and an alkaline soda solution, a method still used today. After several reprecipitation steps they isolated a mono-basic raw product, which they denominated as “Boswellinsäure”

(Note: The expression *Säure* means acid in German). For this raw product they suggested the chemical formula  $C_{32}H_{52}O_4$ . About the chemical structure was nothing exactly known then (Note: The compound most probably had been a mixture of 3-O-acetyl- $\beta$ -boswellic acid and its  $\alpha$ -isomer; compounds **2** and **4** in Fig. 1.8).

During the research of Halbey and Tschirch, the terpene chemistry had become increasingly important by development of the so called *isoprene rule*. This rule was proposed by Otto Wallach [28] who wrote more than 100 papers on the chemistry of terpenes, and who finally obtained the Chemistry Nobel Prize in 1910 therefore. His oeuvre on terpenes and especially the *isoprene rule* led to a rise of the natural product and terpenoid chemistry [29,35].

In 1932 two other researchers on *Boswellia* resins, Winterstein and Stein, revealed that the raw product isolated by Tschirch and Halbey is a mixture of four specific boswellic acids, namely the  $\alpha$ - and  $\beta$ -boswellic acids (compound **1** and **3**) and their acetylated derivatives (compound **2** and **4**) as shown in Fig 1.8. They achieved to isolate the four compounds as pure substances and finally suggested the correct chemical formula  $C_{32}H_{50}O_4$  [42]. Though, they did not have any clue about the correct chemical structures.

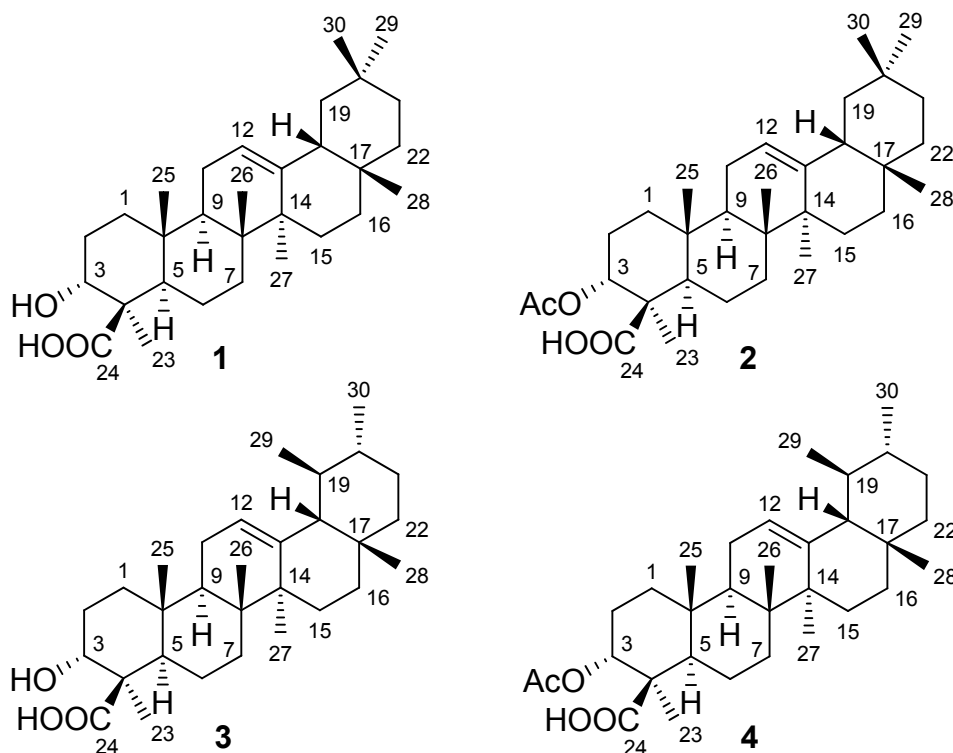


**Fig. 1.8** The structures of  $\alpha$ -BA (**1**),  $\alpha$ -ABA (**2**),  $\beta$ -BA (**3**) and  $\beta$ -ABA (**4**). Thus far, the boswellic acid compounds are highly specific biomarkers for the species from *Boswellia*.

Simpson, in 1937, published his experiments about  $\beta$ -boswellic acid (**3**) and classified it as  $\beta$ -hydroxy-acid (Note that in this case only the position of the hydroxyl group at C-3, neighbouring to the carboxyl group, is meant, not the configuration; compare also with Fig. 1.10 later in the text). He deduced this fact from reactions of chrom(VI)oxid ( $CrO_3$ ) with the free acid giving a mono-ketone by decarboxylation, and with the methyl ester which instead delivered the stable keto-ester [43].

Ruzicka and Wirz published in 1939 and 1949 their own experiments, where they finally correlated a relationship between the boswellic acids and the triterpenes  $\alpha$ - and  $\beta$ -amyrine [44,45]. This was achieved by transformation of the  $\alpha$ - and  $\beta$ -boswellic acids into their corresponding amyrynes (see also Fig. 1.9). By this relationship many attributes of the amyryne-derivates could be conveniently transferred to the boswellic acids. Ruzicka has been also the chemist who thoroughly developed the *isoprene rule* from 1921-1953 [30], based on the proposal by Wallach. Furthermore, for his merits on the chemistry of terpenes he obtained together with Butenandt the Chemistry Nobel Prize in 1939. Thus, he had also a major impact on the structural elucidation of the boswellic acids found in incense resins. In the 1950s of the last century Beton et al. elucidated finally the configuration of the OH- and COOH-group in  $\beta$ -boswellic acid. Their results were published in 1956, and as it is depicted in Fig. 1.10 the configuration of the OH-group is  $\alpha$  (meaning under the ring) and the configuration of the COOH-group is  $\beta$  (meaning above the ring) [46].

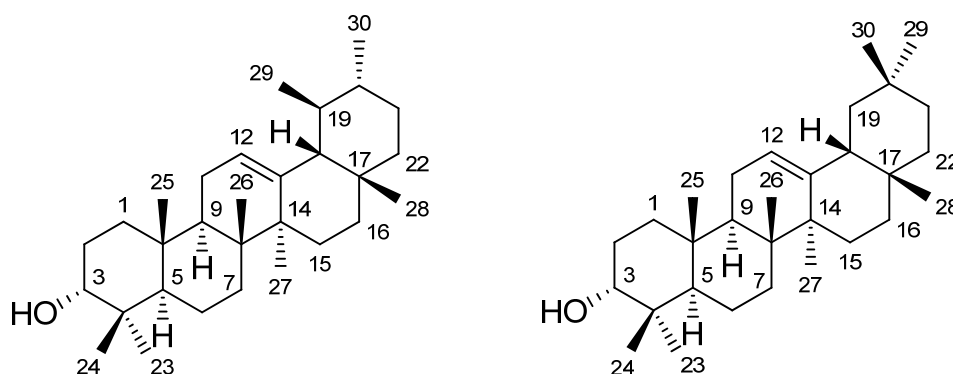


**Fig. 1.9** The structures of  $\alpha$ -amyryne (left, ursane-type skeleton) and  $\beta$ -amyryne (right, oleanane-type skeleton). Confusingly, the structures of  $\beta$ -BA (**3**) and  $\beta$ -ABA (**4**) refer to the  $\alpha$ -amyryne, vice versa, for  $\alpha$ -BA (**1**) and  $\alpha$ -ABA (**3**), which refer to  $\beta$ -amyryne. This has unfortunately historical reasons.

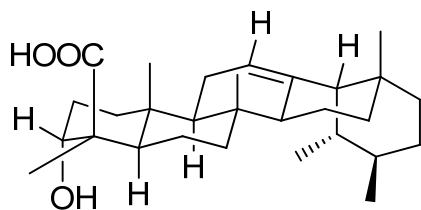


**Fig. 1.10** The configuration of the OH- and COOH-function in  $\beta$ -BA. The OH-group is  $\alpha$ -configured (under the plain) and the COOH-group is  $\beta$ -configured (above the plain).

The elucidation of organic molecules in the following two decades became increasingly easier. The reason therefore was the development and establishment of more precise techniques such as mass spectrometry (MS) and nuclear magnetic resonance spectroscopy (NMR). Both are instrumental measurement tools which made the work of organic chemists tremendously more convenient, especially concerning questions on unknown chemical structures.

Hence, in the year 1963 Budzikiewicz et al. published the first mass spectrometric data base on amyryne derivates [47]. These data is even nowadays used for the characterisation of the molecular framework of unknown triterpenes. In 1978, Pardhy and Bhattacharyya, delivered

first mass spectrometric and  $^1\text{H}$ -NMR data for the  $\beta$ -boswellic acids (compound **3** and **4**) [48]. Furthermore, they presented spectroscopic data for two other very specific incense resin compounds, 11-keto- $\beta$ -boswellic acid (**5**,  $\beta$ -KBA) and 3-O-acetyl-11-keto- $\beta$ -boswellic acid (**6**,  $\beta$ -AKBA) shown in Fig. 1.11. The structure of compound **5** was firstly described by Snatzke and Vertesy in 1966 [49]. In the year 2000 the working group of Ammon published the crystal structure of  $\beta$ -AKBA (**6**) [50], and in 2001 Gupta et al. published the crystal structure of  $\beta$ -ABA (**4**) [51]. However, it took over 20 years until Culioli et al. and Belsner et al. published in 2003 the first complete NMR data sets ( $^1\text{H}$  and  $^{13}\text{C}$ ) for  $\alpha/\beta$ -BA (**1** and **3**),  $\alpha/\beta$ -ABA (**2** and **4**), the  $\beta$ -BA-9,11-dehydro derivatives (**9** and **10**) and  $\beta$ -AKBA (**6**) [52,53]. Before, merely the chemical shifts of H-3 and H-12 were certainly assigned.

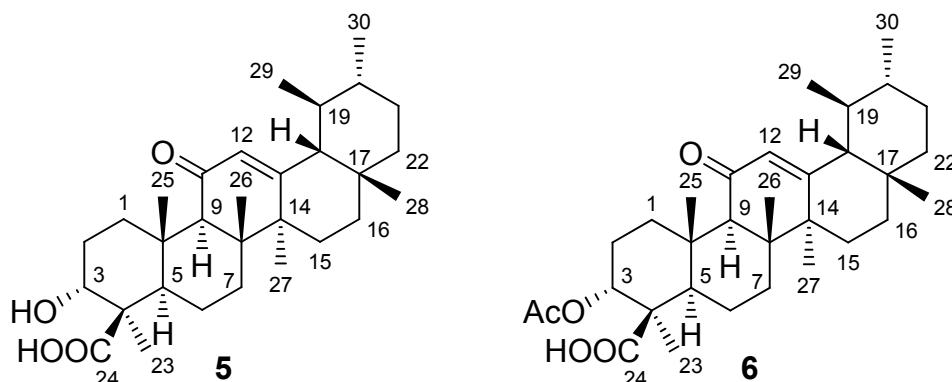


**Fig. 1.11** The structures of  $\beta$ -KBA (**5**) and  $\beta$ -AKBA (**6**).

In 1964, Corsano and Iavarone isolated from the acid fraction of *Olibanum* the methyl ester of 3-O-acetyl-11-OH- $\beta$ -boswellic acid (**7**, 11-OH- $\beta$ -ABA) [54]. The compound, shown in Fig. 1.12, is known to be rather unstable. The working group of Ammon was able to figure out in the 1990s the reaction pathway of compound **7**, leading to 3-O-acetyl-9,11-dehydro- $\beta$ -boswellic acid (**10**; 9,11-dehydro- $\beta$ -ABA) via its methoxy derivative, 3-O-acetyl-11-OMe- $\beta$ -boswellic acid (**8**; 11-OMe- $\beta$ -ABA) [55]. The structures are altogether presented in Fig. 1.12. Seitz firstly isolated compound **7** purely without any decomposition and defined the position of the 11-OH-group as  $\alpha$ -configured [56]. Furthermore, 3-OH-9,11-dehydro- $\beta$ -boswellic acid (**9**; 9,11-dehydro- $\beta$ -BA) was additionally described by Büchele et al. and quantified in the resin matrix by a RP-DAD-HPLC method (see also Fig. 1.12) [57].

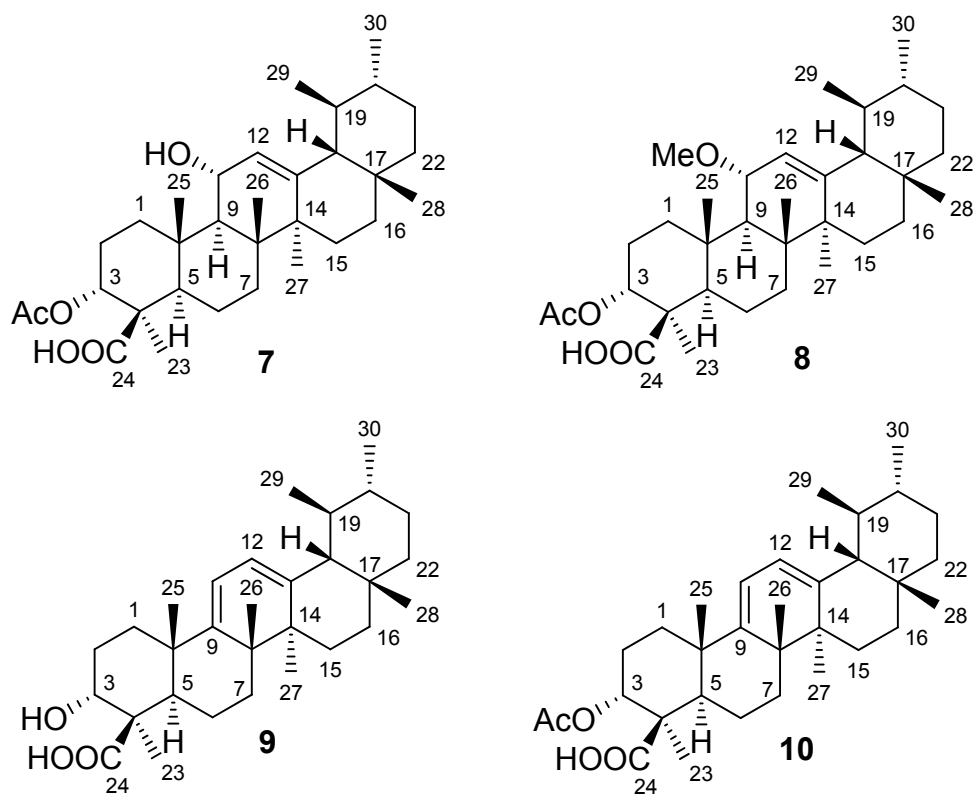


**Fig. 1.12** The structures of 11-OH- $\beta$ -ABA (**7**); 11-OMe- $\beta$ -ABA (**8**); 9,11-dehydro- $\beta$ -BA (**9**) and 9,11-dehydro- $\beta$ -ABA (**10**).

Büchle et al. also isolated the corresponding 9,11-dehydro derivatives of the  $\alpha$ -boswellic acids (**1** and **3**) and quantified them by the HPLC method mentioned before. Their structures are shown in Fig. 1.13.

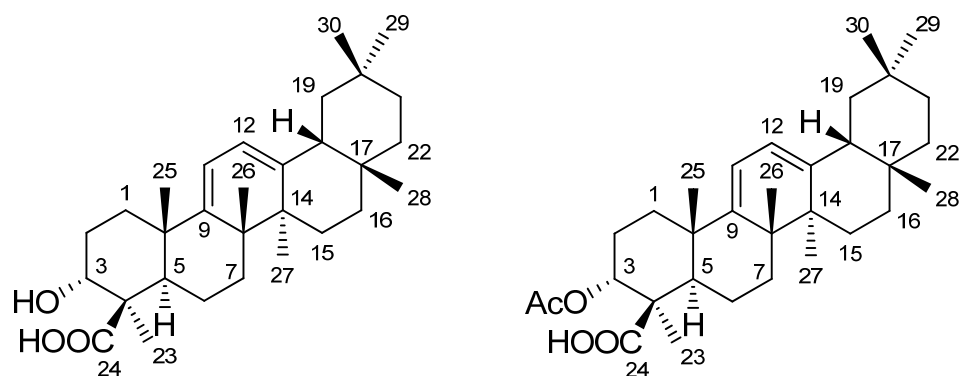


**Fig. 1.13** The structures of 9,11-dehydro- $\alpha$ -BA (left) and 9,11-dehydro- $\alpha$ -ABA (right).

In accordance, Büchle et al. synthesised the 11-keto-derivative from  $\alpha$ -ABA (**3**),  $\alpha$ -AKBA (see Fig. 1.14), and separated it from  $\beta$ -AKBA (**6**) by application of a fluorinated HPLC stationary phase. Thus, revealing also the difficulty of separating  $\alpha$ -AKBA from  $\beta$ -AKBA (**6**) by application of conventional reversed phase stationary phases, normally, the separation system of choice for HPLC separations of boswellic acids [58]. Additionally,  $\alpha$ -KBA (see also Fig. 1.14) and  $\alpha$ -AKBA may occur naturally in minor amounts, but are just not easily resolvable. The hypothesis may be correct as shown in the HPLC publication of Paul et al.

[59]. There, for each peak signal ( $\beta$ -KBA, **5**, and  $\beta$ -AKBA, **6**) at 250 nm detection wavelength, a minor fronting inhomogeneity is visible, which might refer to  $\alpha$ -KBA and  $\alpha$ -AKBA, respectively.

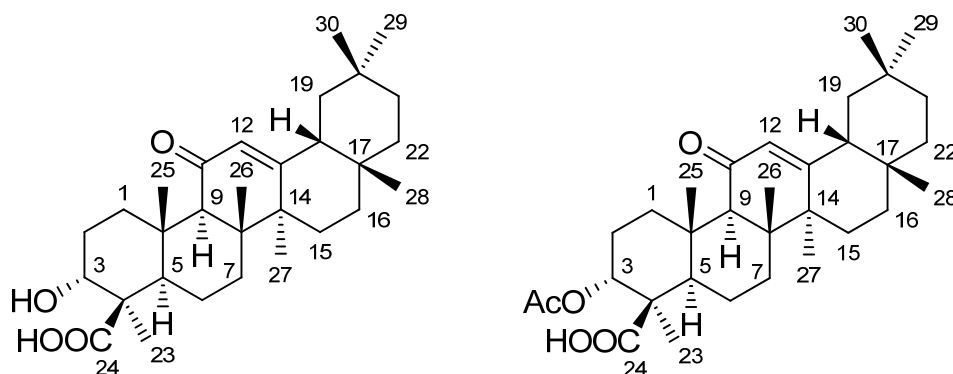


**Fig. 1.14** The structures of 11-keto- $\alpha$ -BA (syn.  $\alpha$ -KBA, left) and 11-keto- $\alpha$ -ABA (syn.  $\alpha$ -AKBA, right). Both structures have yet not been isolated from a naturally source. For further details see text.

Moreover, the existence of several oleanane-type boswellic acids (e.g.  $\alpha$ -BA/ $\alpha$ -ABA), similar to already known ursane-type boswellic acids (e.g.  $\beta$ -BA/ $\beta$ -ABA), has been postulated by the working group of Simmet in Ulm, Germany [57]. Their structures are shown in Fig. 1.15. The molecules depicted there (11-OH- $\alpha$ -BA and 11-OH- $\alpha$ -ABA) seem to be the predecessors of 9,11-dehydro- $\alpha$ -BA and 9,11-dehydro- $\alpha$ -ABA shown in Fig. 1.13, following basically the identical discussion about reaction pathways already given for Fig. 1.12.

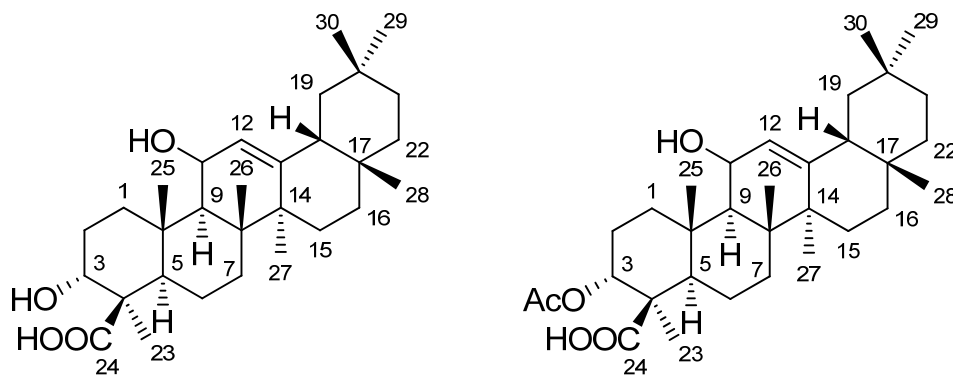


**Fig. 1.15** The structures of 11-OH- $\alpha$ -BA (left) and 11-OH- $\alpha$ -ABA (right). Both structures have yet not been isolated from a naturally source. For further details see text.

Furthermore, Seitz firstly isolated another  $\beta$ -boswellic acid where the OH-function at position 3 is  $\beta$ -configured, namely 3- $\beta$ -OH- $\beta$ -boswellic acid [56]. The structure, which was found in the species *Boswellia carterii*, is depicted in Fig. 1.16.

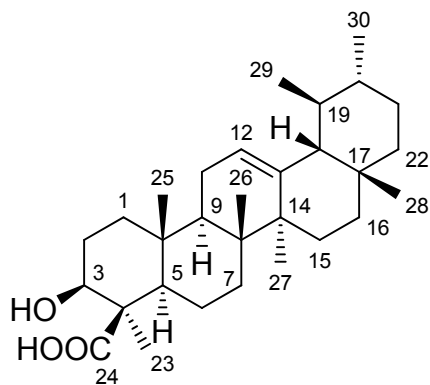


**Fig. 1.16** The structure of 3-β-OH-β-boswellic acid.

Chemically, the boswellic acids refer to the class of pentacyclic triterpenic acids. There can be a vast amount of naturally occurring triterpenic acids found in several different plant species, with only a few single functional differences in their molecular framework [31]. Hitherto, the boswellic acids have been merely isolated from resins of the genus *Boswellia*. Therefore, they can be regarded as genus specific thus far.

#### 1.4.2 Lupeolic Acids

Another class of pentacyclic triterpenic acids found in the resins of *Boswellia* species are the lupeolic acids. These triterpenic acids are not specific for the genus of *Boswellia* and as well have been isolated from other plant material sources [31]. Culioli et al. isolated in 2003 the lupeolic acid (**11**, LA) from a methanolic extract of a gum resin called “Erytrean-type” [52]. Shortly thereafter in 2003, the working group of Simmet published the isolation and structural elucidation of 3-α-O-acetyl-lupeolic acid (**12**, Ac-LA) from *Boswellia serrata* [60]. The group of Choudray reported in 2005 on another lupeolic acid type derivative from the bark of *Boswellia papyrifera*. It revealed instead of a methyl group at C-27 a primary alcohol function and was denoted as 3-α-O-acetyl-27-OH-lupeolic acid (**12a**) [61]. Furthermore, Seitz reported on the isolation of 3-α-O-acetyl-28β-OH-lupeolic acid (**12b**) from *Boswellia carterii* [56]. The structures of all here discussed lupeolic acids are depicted in Fig. 1.17.

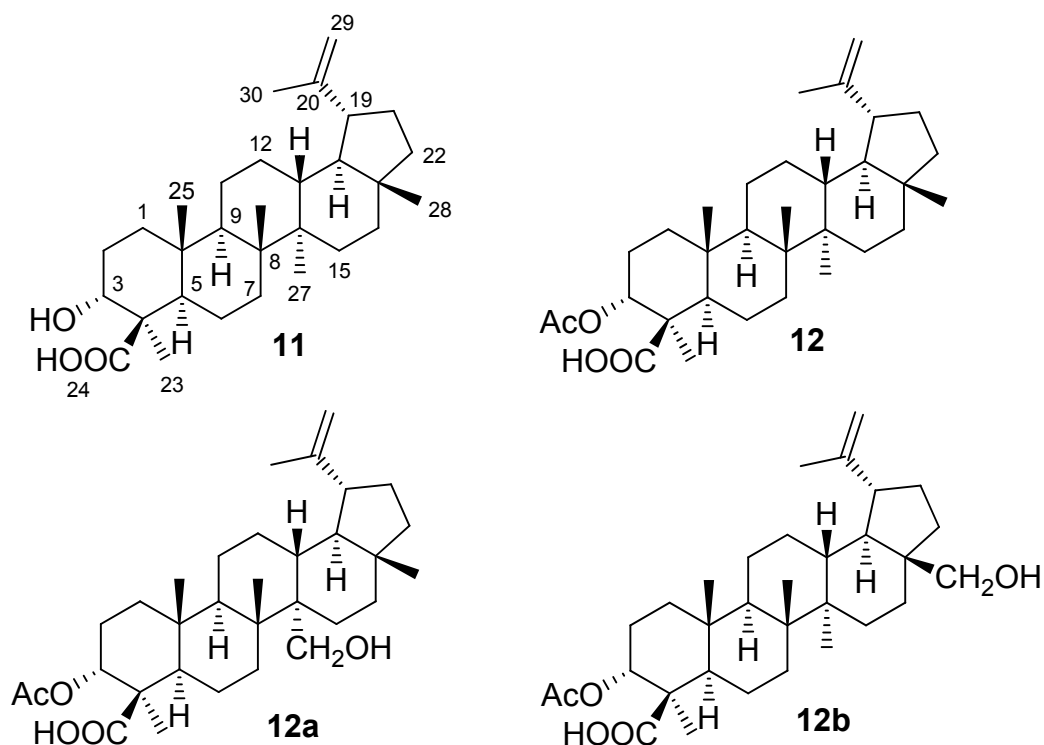


**Fig. 1.17** The structures of compound **11** (LA), **12** (Ac-LA), **12a** and **12b**. For further details see text.

### 1.4.3 Tirucallic Acids

The tirucallic acids represent another class of tetracyclic triterpenic acids that have been isolated from *Boswellia* resins. They are not genus specific for the *Boswellia* species, since they were additionally found in other plants [62-64]. In 1962, Corsano and Picconi isolated 3-Oxo-elema-8,24-dien-21-oic-acid from an incense extract [65]. A synonym for this compound is also 3-oxo-8,24-dien-tirucallic-acid (**13**, 3-Oxo-TA), as the COOH-function can be normally always found at position C-21 for the class of tirucallic acids (see also Fig. 1.18).

Similar compounds have been isolated from the resin of *Boswellia serrata* by Pardhy and Bhattacharyya in 1978 [66]. Beside the isolation of compound **13**, they also reported on the isolation of 3- $\alpha$ -OH-8,24-dien-tirucallic acid (**14**,  $\alpha$ -TA), 3- $\beta$ -OH-8,24-dien-tirucallic acid (**15**,  $\beta$ -TA) and 3- $\alpha$ -O-acetyl-8,24-dien-tirucallic acid (**16**,  $\alpha$ -Ac-TA). Additionally, Akihisa and Banno et al. [67,68] reported on the isolation of 3- $\alpha$ -OH-7,24-dien-tirucallic acid (**17**,  $\alpha$ -7,24-dien-TA) from *Boswellia carterii* in 2006, though the resin identity in their work had probably not been definitely verified. The crystal structure of compound **17** was published by Mora et al. in 2001 [69]. All tirucallic acids discussed hitherto (**13-17**) had been also isolated by Seitz from the resin of *Boswellia papyrifera* [56].

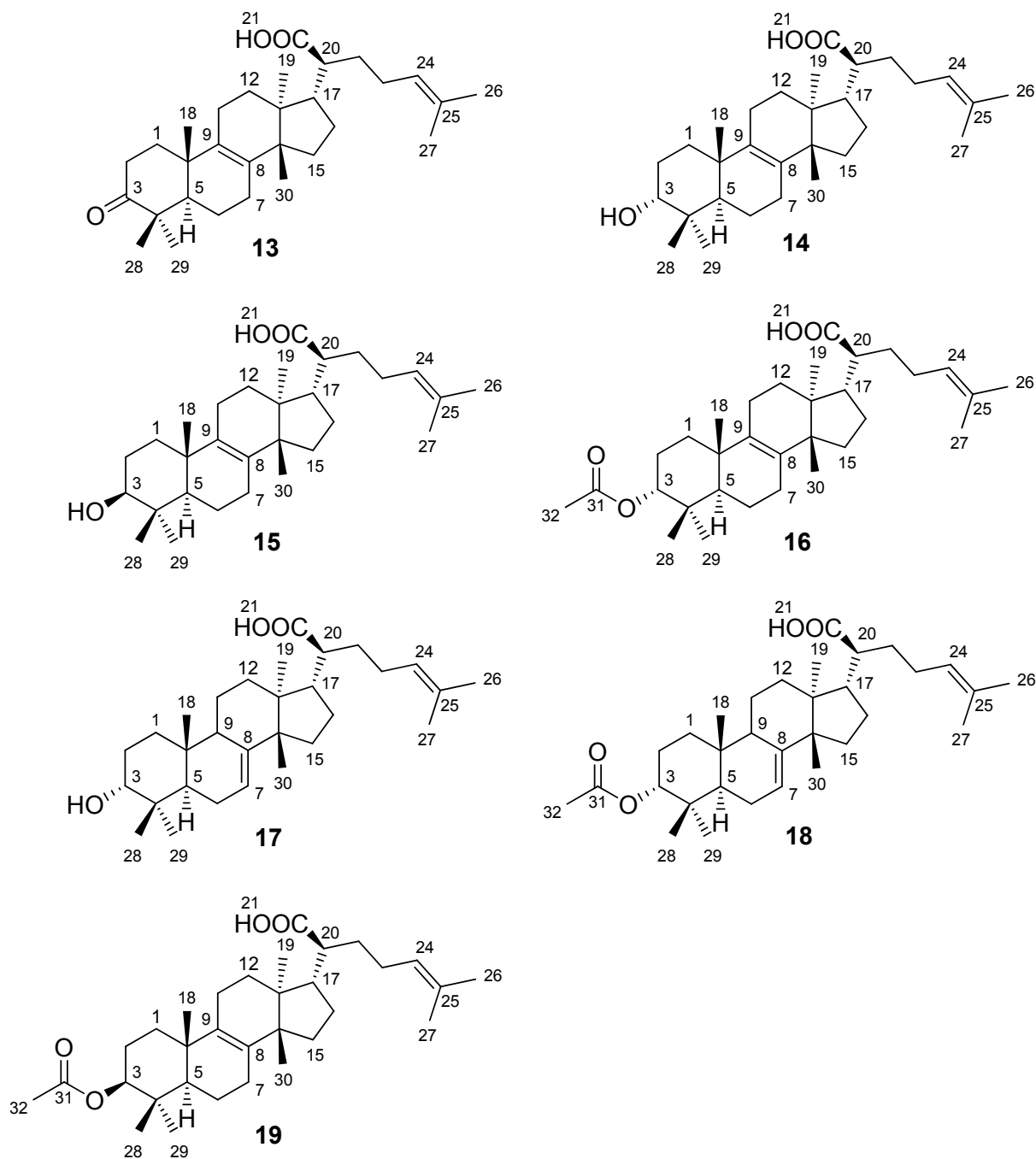


**Fig. 1.18** The structures of the tirucallic acids (**13-19**). For further details see text.

Two further tirucallic acid structures were reported by Estrada et al. in 2010, namely 3- $\alpha$ -O-acetyl-7,24-dien-tirucallic acid (**18**,  $\alpha$ -Ac-7,24-dien-TA) and 3- $\beta$ -O-acetyl-8,24-dien-tirucallic acid (**19**,  $\beta$ -Ac-8,24-dien-TA) [70]. Their chemical structures are also presented in Fig. 1.18. The authors claim that they isolated **18** and **19** from *Boswellia carterii*. However, about the isolation is nothing specific mentioned in their publication. Further on, the quoted reference [57], which should report on the isolation of **18** and **19**, does not reveal anything about these two tirucallic acids in detail. As it will be later on concluded in this work, it was more likely the species *Boswellia papyrifera* instead, where these compounds (**18** and **19**) naturally originate from (see especially chapter 3.7.5).

#### 1.4.4 Roburic Acids

The roburic acids represent a class of tetracyclic triterpenic acids rarely found in natural sources. They are not considered to be specific for *Boswellia* resins, as they were also isolated from other plant sources (e.g. roburic acid from *Gentiana macrophylla* by Jong et al. in 1994 [71]). Fattorusso et al., in 1983, have been the first research group who found a representative molecule of this class in the acid fraction of *Boswellia carterii* [72]. The isolated compound was 4(23)-dihydro-roburic acid and was regarded by them as a probable degradation product, caused by geochemical processes. Seitz had also isolated the 4(23)-dihydro-roburic acid and additionally three more roburic acids from the acid fraction of the resin *Boswellia socotrana* (Note: Since this species did not reveal any boswellic acids, expectably typical for them, it may be doubtful if it really is a *Boswellia* resin, according to the comments given in the dissertation by Seitz [56]). Thus, she elucidated the structures of roburic acid, 11-keto-roburic acid and 4(23)-dihydro-11-keto-roburic acid. The latter two keto-roburic acids have been firstly described by her. The structures are shown in Fig. 1.19.

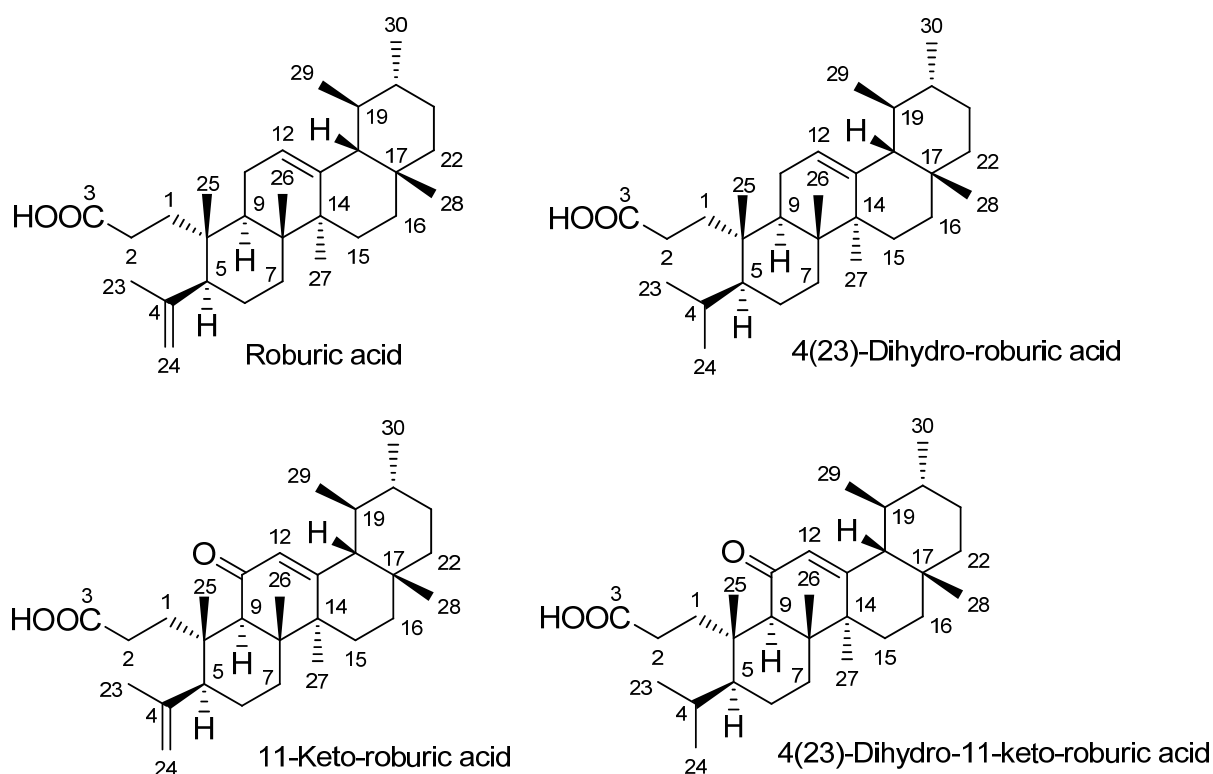


**Fig. 1.19** The structures of the different roburic acids. For further details see text.

#### 1.4.5 Neutral Terpenic Compounds

The neutral compounds from resins of frankincense have been evaluated thoroughly because of their significant odour intensities. Generally, these resins contain an innumerable amount of monoterpenes, sesquiterpenes, diterpenes and triterpenes. Many of them are ubiquitously occurring in nature [31]. They can not be regarded as specific biomarkers for a certain species in general. However, in combination with other compounds they may be helpful for classification in some cases.

A good overview on the great volatile amounts of mono-, sesqui- and diterpenes, occurring in these resins, is given by Hamm et al. [13], who published their results (GC-MS) in 2005. In the author's opinion, this paper can be regarded as highly important and reliable, since they used voucher specimens of these resins in order to evaluate the specific biomarker differences. Another paper by Mathe et al. [73], published in 2004, gives a good overview on typical neutral triterpenic compounds, mainly amyrine and lupeol derivatives, occurring in these resins. Some exemplary terpenic compounds are shown in Fig. 1.20.

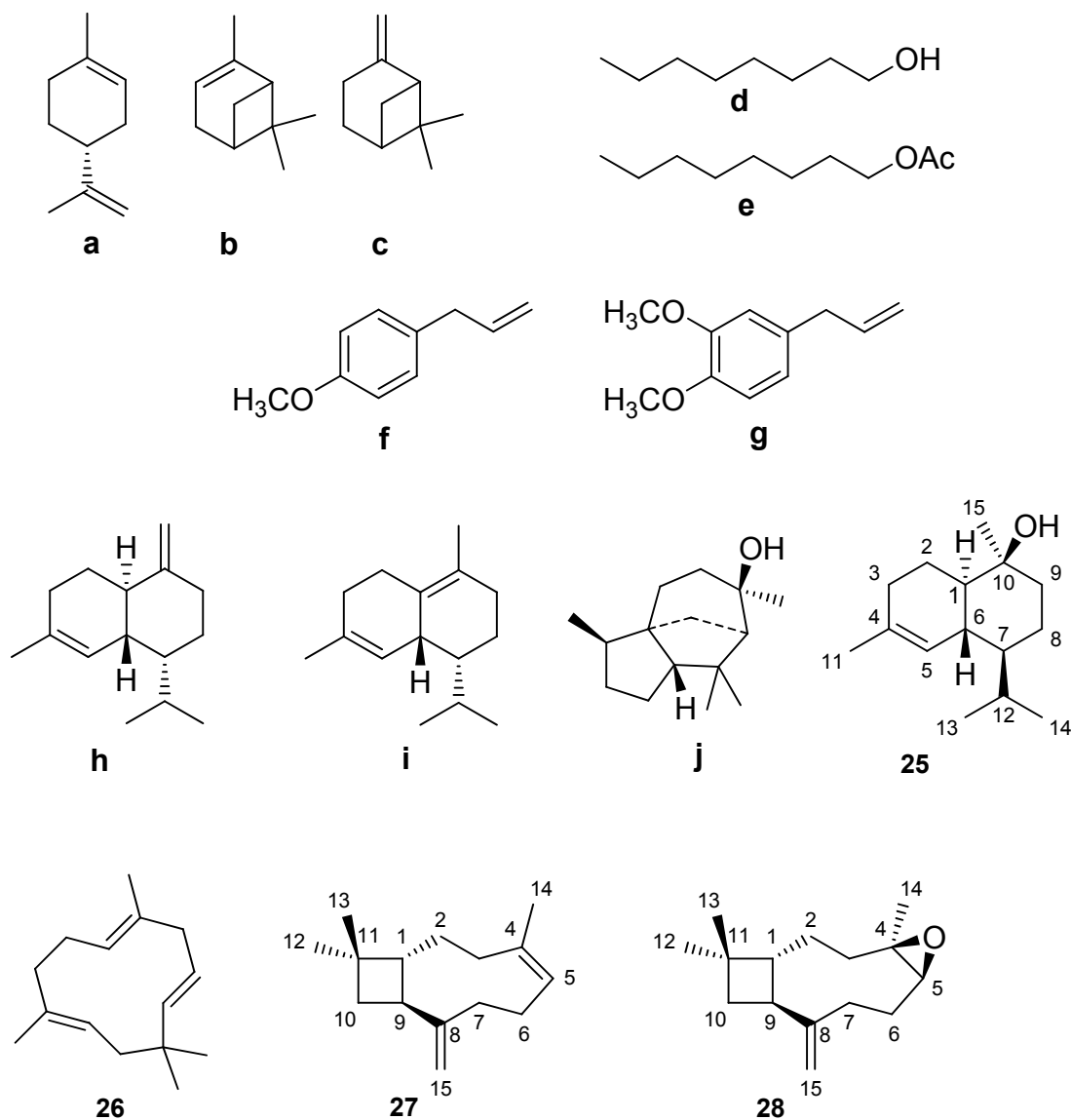


**Fig. 1.20** A few examples of terpenes found in the essential oils of *Olibanum* resins. Monoterpenes: limonene (**a**),  $\alpha$ -pinene (**b**),  $\beta$ -pinene (**c**). Sesquiterpenes:  $\gamma$ -cadinene (**h**),  $\delta$ -cadinene (**i**), cedrol (**j**),  $\tau$ -cadinol (**25**,  $\tau$ -Cad-OH),  $\alpha$ -humulene (**26**,  $\alpha$ -Hum),  $\beta$ -caryophyllene (**27**,  $\beta$ -Car),  $\beta$ -caryophyllene-oxide (**28**,  $\beta$ -Car-Ox). Additionally, quite specific for some species are the following molecules (no real classical terpenic compounds): n-octanol (**d**) and n-octyl-acetate (**e**), which both are detectable in huge quantities in the species *Boswellia papyrifera*; and methyl chavicol (**f**) and methyl eugenol (**g**), which both seem to be specific for the species *Boswellia serrata*. See also the publications of Hamm et al. and Camarda et al. [13,74].

## Introduction

A few specific neutral terpenes isolated from *Olibanum* are discussed here. In 1967 Corsano and Nicoletti described the structure of a new diterpene alcohol, isolated from frankincense, and denoted it as incensole (**22**, Inc) [75]. Furthermore, they described two different incensole derivatives, incensole-oxide (**22a**) and iso-incensole-oxide (**22b**), in the shortly following years (1972 and 1973) [76,77]. In Fig. 1.21 their structures are depicted. The authors claimed that these molecules were isolated from the species *Boswellia carterii*.

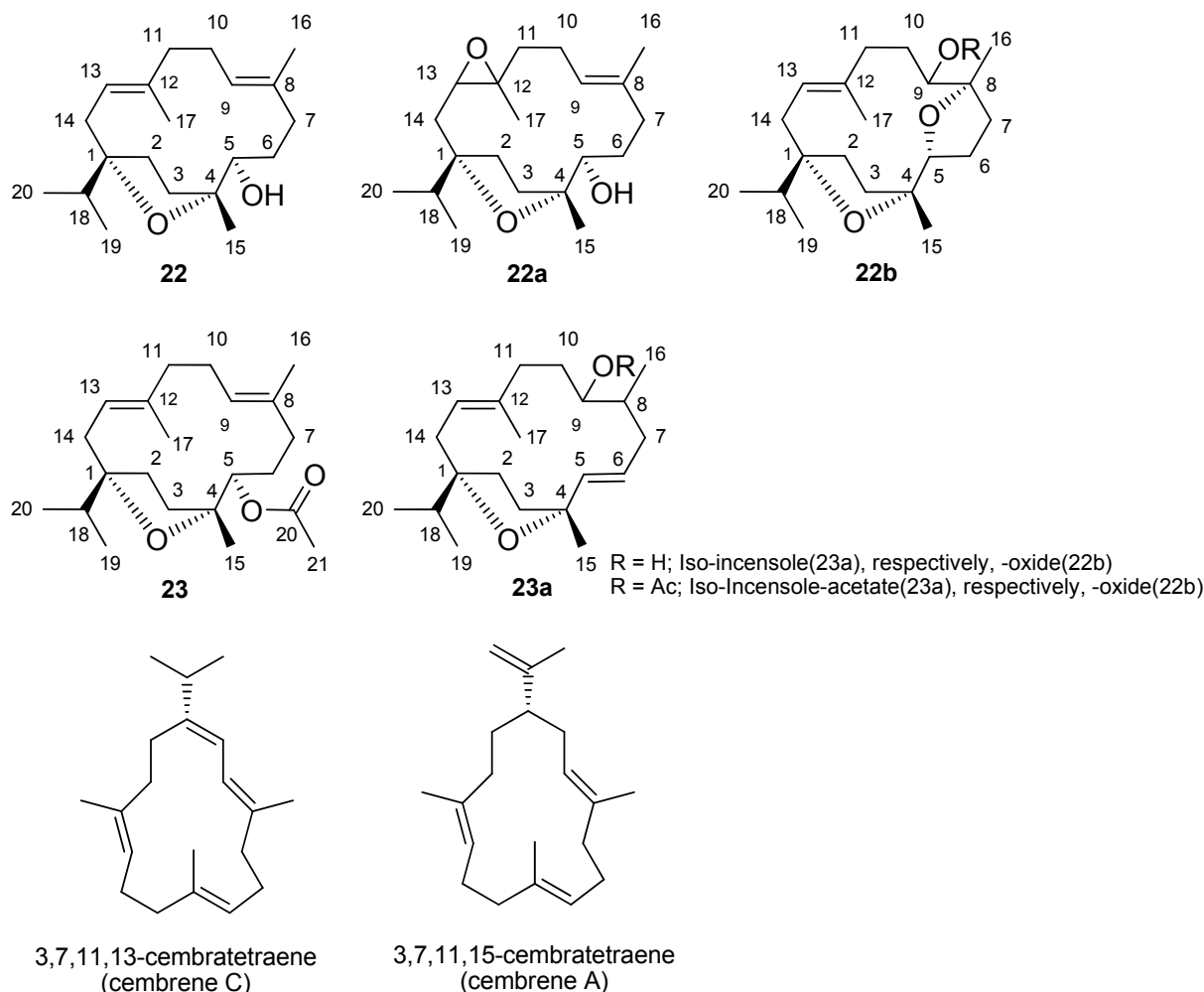


**Fig. 1.21** The structures of specific diterpenes found in incense: Incensole (**22**), incensole-oxide (**22a**), iso-incensole-oxide (**22b**, R = H) and its acetate (**22b**, R = Ac), incensole acetate (**23**) and iso-incensole (**23a**, R = H) and its acetate (**23a**, R = Ac). Iso-incensole and its acetate seem to be specific biomarkers for *Boswellia carterii* [13,78]. Furthermore the probable predecessor molecules, where these compounds originate from, are shown: cembrene A and cembrene C.

However, the research, concerning the oils from *Olibanum*, by Obermann and his co-workers at the DRAGOCO Company, Holzminden, Germany (now *Symrise GmbH & Co. KG*) in the end of the 1970s gave differing results compared with the ones of Nicoletti and his team. Oberman analysed two different *Olibanum* oils, one was denoted as “Aden” and the other as “Eritrea”, by TLC and GC-MS and published his results in 1977 [79]. His final statement had been that the sort “Aden” mainly contains neutral triterpenes as it was already described by Snatzke and Vertesy in 1966 [49]. Incensole (**22**), the compound described by Corsano and Nicoletti in 1967 for *Boswellia carterii* [75], was merely found in traces by GC-MS in the

“Aden”-type. On the contrary, for the sort “Eritrea” he could detect incensole (**22**) and additionally its acetate (**23**, Inc-Ac) in great quantities, comparable with the quantities given by Corsano and Nicoletti. Furthermore, Obermann realised that the commercial grades *Somalia* and *Indian Frankincense* were olfactorily similar to the commercial grade “Aden”, whereas “Eritrea” had a significantly different odour. The same conclusions have been made by the author of this dissertation and are proved chemotaxonomically based on voucher specimens and reliable literature results (see experimental part of the dissertation; e.g. chapter 3.4). Thus, the sample “Aden” refers to the species *Boswellia carterii*, respectively, *Boswellia sacra*, since both species are chemotaxonomically identical. Moreover, the commercial brand “Aden” usually refers to the Somalian Olibanum, most likely to be *Boswellia carterii*, as it is transported from Somalia to the port of Aden, Yemen, and then internationally traded as “Aden”-type [80]. The sort “Eritrea” had been the species *Boswellia papyrifera*, since the specific biomarkers were found for it. Therefore, the publications of Obermann, Hamm et al. and Camarda et al. may be comparably consulted for clarification [13,74,79]. Additionally, Gacs-Baitz et al. published in 1978 the first complete  $^{13}\text{C}$ -NMR datasets on the fourteen-membered macrocyclic diterpene class of the incensole family [81]. The chemical structures of all molecules discussed up to here are depicted in Fig. 1.21. In the same year, 1978, Klein and Obermann in Germany, and, Pardhy and Bhattacharyya in India, reported on another new type of diterpenic alcohol of the cembrane type [82,83]. Pardhy and Bhattacharyya, who isolated the compound from *Boswellia serrata*, denominated it as serratol (**21**, Ser-OH). Klein and Obermann isolated the compound from the species *Boswellia carterii* (“Aden”) together with incensole (**22**). They also deduced already that serratol (**21**) is most probably the predecessor molecule of incensole (see also chapter 3.13 on biosynthesis, where the probable mechanism is depicted). The structure is presented in Fig. 1.22. In addition, Seitz isolated serratol (**21**) from the resin of *Boswellia carterii* [56], and Schmidt et al. firstly published its complete NMR dataset in 2011, including the evaluation of its antiprotozoal activity [84].

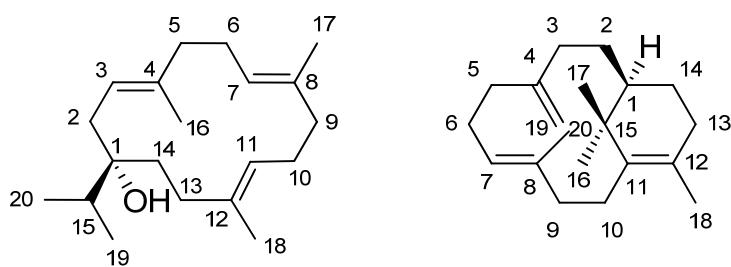


**Fig. 1.22** The structures of serratol (**20**, Ser-OH; left) and verticilla-4(20),7,11-triene (**24**, Vert-4(20),7,11-triene; right).

In 2001, Basar et al. reported on a new verticillane diterpene from the essential oil of *Boswellia carterii* (see also Fig. 1.22) [85]. The compound was termed as verticilla-4(20),7,11-triene (**24**, Vert-4(20),7,11-triene). Interestingly, this compound has been merely found in the essential oils from *Boswellia papyrifera* by the groups of Hamm and Camarda [13,74]. Thus, the sample of Basar was quite probably unfortunately mistaken as *Boswellia carterii*, while it had been indeed the species *Boswellia papyrifera* instead. This fact may be additionally clarified by the data presented in this dissertation (see results and discussion;

e.g. chapter 3.4-3.7). Nevertheless, the species *Boswellia papyrifera* has been most likely in many publications mistaken as *Boswellia carterii* (e.g. [67,68,86-88]).

Three recent papers from Japan (Yoshikawa et al. [89] and Morikawa et al. [90,91]), published in 2009, 2010 and 2011, report on several new minorly occurring compounds, so called "Olibanumols", from the species *Boswellia carterii*. All these compounds are different terpenic alcohols (e.g. monoterpenes, tetra- and pentacyclic triterpenes with OH-functions at different positions). Additionally, the newly isolated compounds are only in quite minimal amounts present (e.g. Olibanumol A = 0.037 % to Olibanumol I = 0.00074 % from [89]) and though they show in some cases pharmacological activity, the concentrations are far too low to play a significant role for the major actions of anti-inflammatory Olibanum extract medications. However, particularly with regard to the finding of new bio-active compounds the research is definitely not unnecessary.

Hitherto, it seems that the major compounds, which may play an important role for the pharmacological activities of *Boswellia* species, have been almost completely isolated and structurally elucidated, at least for the species Bpap, Bser and Bpac/Bcar.

### 1.5 Pharmacology

About the use of frankincense resins in older and ancient times, there is of course no real scientific data obtainable. Merely, the Papyrus Ebers and old scripts of the Ayurvedic communities in India giving witness on the use as a therapy [3]. Though frankincense was still mentioned in older monographs of pharmacy, the knowledge about as a herbal remedy became obsolete within the 20<sup>th</sup> century [8]. The reason therefore had been the ascendancy of modern science and the pharmaceutical industry. For example, the accidental discovery of penicillin by A. Fleming in 1928 or the industrial production of Aspirin<sup>®</sup> by the German company Bayer [92,93]. So far, these single dosage preparations are the classical drug administrations of conventional medicinal treatment [94]. However, this way does not seem to be the final solution for the treatment of several diseases. Antibiotics loose more and more its efficacy since several bacterial strains are reported to show resistances against them [95]. The search for new molecular entities, useful as antibiotics, is difficult. Additionally, many medications show severe side effects when long-term used. Acetyl salicylic acid, for example, can cause ulcers since several homeostatic mediators are inhibited, and corticoids can lead to osteoporosis [94]. Therefore, the research on alternative treatments, showing fewer side effects, is still ongoing.

#### 1.5.1 Inflammatory Processes in General

Invasive foreign matters and/or pathogens which infiltrate the organism have to be swiftly eliminated and repelled to avoid serious damages. Normally, the defence is responded by a locally delimited inflammation reaction of the organism. This inflammatory response is initiated by pathogens, physical and chemical noxins or the overreaction of the immune system (e.g. allergens). Symptomatically, these reactions are usually characterised by swellings and reddening of the tissue, including pain and local heating. The defence reaction is initiated by different immune cells releasing several classes of biological messenger

substances, the so called inflammatory mediators, coordinating and enhancing the immunological response. Two important mediator classes represent the prostaglandins and the leukotrienes, both members of the eicosanoid family, which originate from the so called *arachidonic acid cascade* [56,94,96]. The first step of this cascade is depicted in Fig. 1.23. Currently, acute inflammations are treated with substances inhibiting the synthesis of prostaglandins. These molecular entities are denoted as non-steroidal anti-inflammatory drugs (NSAIDs), such as acetyl salicylic acid or ibuprofen. Their effect is based on the inhibition of the cyclooxygenases 1 and 2 (COX-1, COX-2) preventing the synthesis of prostaglandins involved in inflammatory processes.

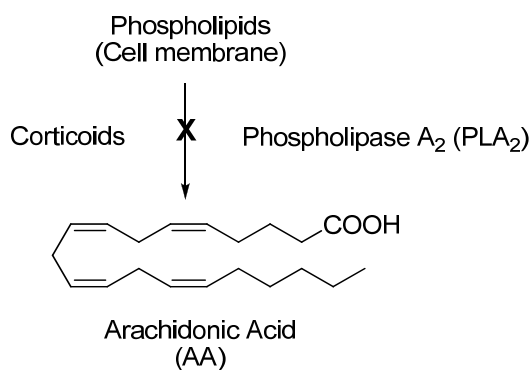


**Fig. 1.23** The first step with the release of AA from the phospholipids of the cell membrane by the enzyme PLA<sub>2</sub>. This step can be inhibited by the class of corticoids (e.g. cortisol). For further details see text.

In contrast to acute inflammations, in a chronic inflammatory process the immune system is not able anymore to maintain its defence reactions locally and timely limited. The inflammatory process sustains continuously, though actually no immune response is necessary. Chronic diseases, revealing this phenomenon, are for example asthma, rheumatism, chronic bronchitis, psoriasis, neurodermatitis, Crohn's disease and ulcerative colitis. All these diseases are correlated with high levels of leukotrienes, especially leukotriene B<sub>4</sub> [97], and prostaglandins, particularly PGE<sub>2</sub> [98], maintaining the inflammatory process at a constant level. The leukotriene pathway and the synthesis of PGH<sub>2</sub>, the precursor molecule of PGE<sub>2</sub>, are depicted in Fig. 1.24.

Leukotrienes originate from arachidonic acid by lipoxygenases (5-, 11-, 12- and 15-LO; the number refers to the position where the AA is oxidised), via hydroperoxyeicosatetraenic acid (5-, 11-, 12- and 15-HpETE) intermediates, which are subsequently transformed into the leukotrienes (LTB<sub>4</sub>, LTA<sub>4</sub>, LTC<sub>4</sub>, LTD<sub>4</sub>, and LTE<sub>4</sub>) [99]. They are preferably synthesised by inflammatory cells like polymorphonuclear leukocytes, macrophages and mast cells. Especially the 5-LO of the classes of lipoxygenases is considered to be involved in the maintenance of chronic diseases (e.g. asthma) by production of leukotrienes [100].

The prostaglandins formed by most cells in the human body are immediately and locally signalling mediators acting to their site of synthesis. They are synthesised *de novo* from membrane-released arachidonic acid (AA) when the immune response is activated (e.g. mechanical trauma, chemical stimulus etc.). The enzymes involved in this process, receiving their substrates from COX-1 and COX-2, are the so called prostaglandin synthases (e.g.

PGI, PGD, PGF, PGE and  $\text{TXA}_2$  etc.) depicted in Fig. 1.25. Here especially the mPGES-1 seems to be a promising target for inhibition, as it is assumed to be involved in inflammatory processes [101-103]. One problem of COX-inhibitors (NSAIDs) and COX-2 specific inhibitors (denoted as coxibs) is that the synthesis of several other and essential mediator compounds is inhibited, thus, causing side-effects (e.g. thromboxanes,  $\text{TXA}_2$  and  $\text{TXB}_2$ , necessary for platelet aggregation, or gastrointestinal injury and renal irritations, apparently due to impaired biosynthesis of other physiologically relevant prostanoids [98]). Additionally, COX-1 is the enzyme constitutively expressed to synthesise prostaglandins useful for homeostasis (syn. maintenance) of the organism (e.g. protection of the gastric mucosa etc.); whereas, on the other hand, COX-2 is most likely involved in the synthesis of prostaglandins when the immune system is offended by exogenous toxicants, and thus is increasingly expressed [101] (It should be noted that this is merely a short simplification of rather complex mechanisms and interactions which are hitherto not nearly completely understood). Therefore, it was tried to develop COX-2 selective inhibitors which show reduced gastrointestinal complications. However, recent clinical trials indicated a significantly increased cardiovascular risk, if COX-2 is inhibited [98,101]. These facts have been leading to the currently research on mPGES-1 inhibitive compounds not affecting COX enzymes [104].

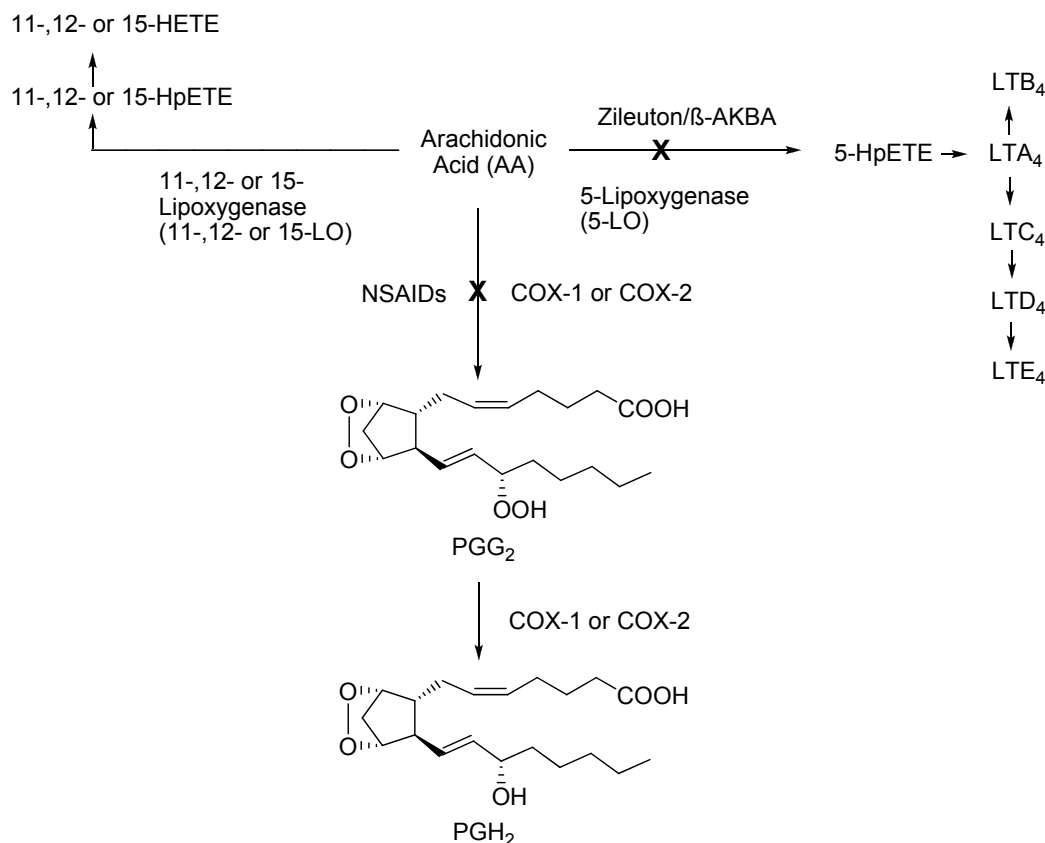


**Fig. 1.24** The enzymatic steps of COX-1 and COX-2 giving finally  $\text{PGH}_2$ . The biosynthesis steps for the 5-LO, respectively, the 11-, 12- and 15-LOX giving lastly the class of leukotrienes are also depicted. COX-1 and COX-2 can be inhibited by NSAIDs. For 5-LO inhibition merely the redox inhibitor Zileuton is approved (Asthma).  $\beta$ -AKBA (**6**), according to the results of Ammon et al. [105,106] is regarded as a non-redox inhibitor of 5-LOX, though the evidence *in vivo* is not absolutely compelling so far. For further details see text.

In the present, severe chronic diseases are conventionally treated with glucocorticoids such as cortisol. These inhibit the enzyme phospholipase A<sub>2</sub> (PLA<sub>2</sub>) and consequently stop the production of leukotrienes and prostaglandins as it is shown in Fig 1.23. The problem with these treatments of chronic diseases by NSAIDs and/or glucocorticoids is the occurrence of partly severe side-effects, as explained before, particularly when they are used over a greater period of time.

Thus, the research on alternative treatments is still ongoing. One approach is to find selective redox- and non-redox lipoxygenase inhibitors. However, most of them revealed strong side effects during clinical trials or are less efficient *in vivo* than *in vitro* [107].

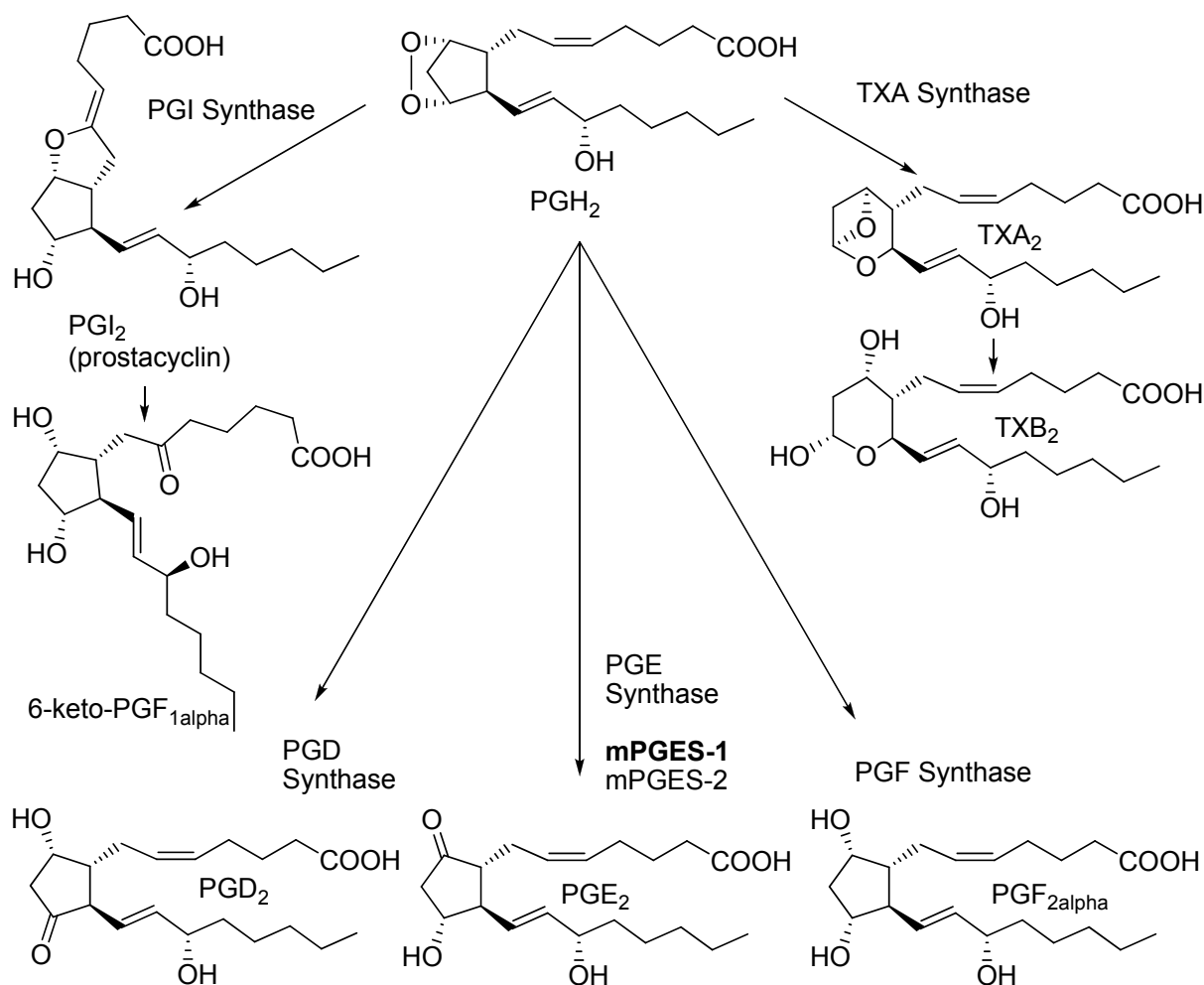


**Fig. 1.25** The further reaction steps leading to different classes of prostaglandins and the thromboxanes (TXA<sub>2</sub> and TXB<sub>2</sub>). Especially the formation of PGE<sub>2</sub>, via COX-2 and mPGES-1 enzymes, is involved in several inflammatory activities [101]. Therefore, the selective inhibition of mPGES-1 is a target of major interest since fewer side effects are assumed, if only this enzyme is blocked. For further details see text.

Currently, the selective suppression of microsomal prostaglandin E<sub>2</sub> synthase-1 (mPGES-1) seems to be a promising target to achieve anti-inflammatory effects without interfering other enzymes (e.g. COX-1 and 2) necessary for homeostatic processes [98].

Finally, the aim is to find and/or develop a therapeutic agent which is similar efficient as the NSAIDs and/or glucocorticoids, and additionally almost free from severe side effects. This

would be an improvement for many patients suffering from the temporary situation, the chronic disease and the side effects of conventional therapies. Therefore, extracts of frankincense resins may be a promising alternative [8,108].

### 1.5.2 Pharmacology of Frankincense Extracts and their Single Compounds

Extracts from frankincense resins have been used in traditional medicine in India and African countries for the treatment of a variety of diseases [3]. In the Indian folk medicine Ayurveda, it was mainly applied to cure chronic arthritis and bronchitis [8]. Thus far, a methanolic extract from the Indian frankincense, *Boswellia serrata* (salai gugal), is distributed under the brand name Sallaki<sup>®</sup> (from the company GUFIC-BIOSCIENCES LIMITED, Karnataka, India). This medication is only authorised as treatment for chronic arthritis in the Swiss canton Appenzell-Außerrhoden, at least until the end of 2013 [109]. Thus far, there is no - on unequivocal clinical evidence based - medication available.

In recent years the interest in preparations, based on frankincense resins as a treatment for several diseases, ascended again. The first scientific evidence on the anti-inflammatory effects of a *Boswellia* extract *in vivo* (rat- and mice model) was published by Singh et al. in India in 1986 [110]. Further *in vivo* studies (animal- and human models) revealed encouraging activities of these extracts in the treatment of several inflammatory diseases and even malignant tumours [111-119]. Though the evidence for the effectiveness of *Boswellia serrata* is hitherto encouraging but not convincing, the existing data do warrant further investigation of this herbal medicine, according to the review of E. Ernst in 2008 [6].

The first investigations on the anti-inflammatory properties of Olibanum preparations, under a pharmacological point of view, were conducted by the working group of Ammon in Tübingen, Germany, in 1991 [5,97]. They observed the specific inhibition of the leukotriene B<sub>4</sub> (LTB<sub>4</sub>, see also Fig. 1.24) synthesis through an extract of *Boswellia serrata*. With identification of the boswellic acids β-BA (3), β-ABA (4), β-KBA (5) and β-AKBA (6), they elucidated the compounds which have been held responsible for the inhibition of the enzyme 5-lipoxygenase (5-LO, see also Fig. 1.24). Furthermore, Ammon et al. revealed that boswellic acids are specific non-redox/non-competitive inhibitors of 5-LO interacting at an allosteric position distant from the active centre of the enzyme [105,106,120]. They also figured out the importance of a hydrophilic group (e.g. -COOH or -CH<sub>2</sub>-OH) at C-4 and a keto-function at C-11 for an effective inhibition [120]. Their investigations led to the conclusion that β-AKBA (6) is the most effective 5-LO inhibitor (IC<sub>50</sub> = 1.5 μM), followed by β-KBA (5) and β-BA (3), each IC<sub>50</sub> = 4.5 μM, and β-ABA (4) with an IC<sub>50</sub> = 7 μM [56,120]. It should be noted that these tests were implemented with collected peritoneal exudate leukocytes (PMNL) from Wistar rats [5]. Evaluations of other cell systems and species gave differing results. The group of Ammon et al. obtained an IC<sub>50</sub>-value of 16 μM for β-AKBA (6) with purified human 5-LO [121]. Werz et al., who used a cytosolic fraction of human cells of purified 5-LO instead, determined an IC<sub>50</sub>-value of 50 μM for β-AKBA (6) [122]. Furthermore, at a defined concentration range of β-KBA (5) and β-AKBA (6) even a stimulatory effect on 5-LO was observed [123,124].

However, the data generated and especially the findings of rather low β-KBA (5) and β-AKBA (6) plasma concentration levels in human blood samples [125-127] suggested that not only 5-LO may be a target enzyme for the ingredients of *Boswellia* extracts [128].

Furthermore, there may be other, hitherto unknown targets, responsible for the anti-inflammatory properties of frankincense resins. The research groups of Jauch and Werz carried out so called target-fishing experiments, where  $\beta$ -BA (**3**) and  $\beta$ -KBA (**5**) were immobilised on a sepharose gel [96]. There, the interaction of  $\beta$ -KBA (**5**) with 12-lipoxygenase (12-LO; see also Fig. 1.24) in a cell lysate from human leukocytes was observed. This interaction had been excluded before then, since **5** was regarded together with  $\beta$ -AKBA (**6**) as a specific 5-LO inhibitor [5]. A specific interaction of the  $\beta$ -KBA (**5**), bound to sepharose, with 5-LO was not detectable. Nevertheless, this may be arbitrary as the sepharose- $\beta$ -KBA (**5**) complex may be not similar to free  $\beta$ -KBA (**5**) in the cell. Thus, interpretations of *in vitro* findings have to be extrapolated carefully to *in vivo* situations. For COX-1 and COX-2 were additionally interactions determined, whereas COX-1 was stronger bound [129]. These targets, COX-1 and COX-2, had been also excluded by then [130]. The group of Werz determined thereupon the IC<sub>50</sub>-values for  $\beta$ -AKBA (**6**) and the new enzymatic targets [56,96,129] as shown in Tab 1.2.

**Tab. 1.2** IC<sub>50</sub>-values of  $\beta$ -AKBA (**6**) upon 12-LO, COX-1 and COX-2.

	IC <sub>50</sub> $\beta$ -AKBA ( <b>6</b> ) [ $\mu$ M]	Test System
12-LO	15	cell-free
COX-1	6 - 23	whole cells
COX-1	28	isolated enzyme
COX-2	100	isolated enzyme

A comparison of the IC<sub>50</sub>-values from  $\beta$ -AKBA (**6**) upon 12-LO and COX-1 with the values for the inhibition of 5-LO revealed a certain similarity [96]. Comparative studies by Werz et al. with known COX-1 inhibitors such as ibuprofen and Aspirin<sup>®</sup> showed that the action of  $\beta$ -AKBA (**6**) in the cell-free systems is analogue ibuprofen and even better than Aspirin<sup>®</sup>. It was further approved that the inhibition of COX-1 is reversible and occurs in the active centre [96,129]. These investigations prove that several enzymes of the *arachidonic acid cascade* are influenced by  $\beta$ -AKBA (**6**), and, besides the inhibition of leukotriene biosynthesis, the prostaglandin synthesis may be equally affected. Finally, Werz and Jauch concluded that  $\beta$ -AKBA (**6**) can not be regarded as selective 5-LO inhibitor anymore [96]. How these findings may be correlated with anti-inflammatory actions *in vivo* is thus far not clarified. The IC<sub>50</sub>-values for inhibition of 12-LO and COX-1 have been far above the determined plasma concentrations of  $\beta$ -AKBA (0.10 – 0.56  $\mu$ M) [125-127,131].

In addition to the newly discovered targets of the *arachidonic acid cascade*, the target-fishing tests by Werz and Jauch identified cathepsin G as a before unknown enzyme in correlation with anti-inflammation of boswellic acids [96,132]. Cathepsin G belongs to the family of peptidases or proteases, which are included in lysosomes and after release contribute to phagocytosis of exogenous microorganisms. They additionally serve for the activation of specific receptors participating in different inflammatory processes [56,96,132]. The determined IC<sub>50</sub>-values for different boswellic acids lay in the range of the ascertained  $\beta$ -AKBA (**6**) plasma concentrations (see Tab 1.3). Based on these findings, cathepsin G could play a pivotal role for the antiphlogistic action of  $\beta$ -AKBA (**6**) *in vivo* [96,132].

**Tab. 1.3** IC<sub>50</sub>-values of boswellic acids upon cathepsin G.

	IC <sub>50</sub> cathepsin G [μM]	Test System
β-AKBA ( <b>6</b> )	0.6	cell-free
β-BA ( <b>3</b> )	0.8	cell-free
β-ABA ( <b>4</b> )	1.2	cell-free
β-KBA ( <b>5</b> )	3.7	cell-free

Furthermore, the working group of Ammon et al. evaluated the 5-LO activity of the artefacts 11-OMe-β-ABA (**8**) and 9,11-dehydro-β-ABA (**10**) originating from the decomposition of 11-OH-β-ABA (**7**). Their findings concluded that **8** is an incomplete inhibitor, whereas **10** almost totally suppressed the 5-LO activity. They could not isolate **7** due to its fast decomposition [55]. In contrast, Seitz (dissertation, 2008 [56]) has been the first person reporting on the successful isolation of compound **7**. Moreover, newly isolated compounds showed an interesting pharmacological behaviour. In collaboration with the group of Werz, the activity of 3-α-O-acetyl-28β-OH-lupeolic acid (see Fig. 1.17, compound **12b**), purified from *Boswellia carterii*, for inhibition of 5-LO was comparable with β-AKBA (**6**), and for inhibition of cathepsin G it showed similar activity as β-ABA (**4**). Further examples can be found in her dissertation [56].

Another interesting behaviour was observed for the class of tirucallic acids (see Fig. 1.18). Boden et al. showed in 2001 that 3-Oxo-TA (**13**) even stimulates the leukotriene synthesis in intact polymorphonuclear cells [133]. However, by exceeding a certain concentration level the leukotriene synthesis was suppressed again revealing a quite contradictory behaviour. In cell-free systems 3-Oxo-TA (**13**) merely decreased the 5-LO product formation, demonstrating the pivotal role of an intact cell structure for its activating property.

In context to that, the work of Estrada et al. [70], recently published in 2009, revealed significant anti-tumour activities for the tirucallic acids α-Ac-7,24-dien-TA (**18**) and β-Ac-8,24-dien-TA (**19**). Their results showed that these compounds, **18** and **19**, induce apoptosis in prostate cancer cell lines, but not in nontumorigenic cells. Thus, the tirucallic acids may also play a crucial role for the bioactivity of multi-compound containing frankincense extracts.

In two further publications by Büchele et al. in 2005 and 2006, respectively, the apoptosis inducing property of the partially synthesised compound α-AKBA (see Fig. 1.14) has been demonstrated [58,134].

In context to anti-tumour actions, several papers have been published hitherto, revealing inhibition of human topoisomerases I and IIa and apoptosis in HL60- and CCRF-CEM cells by application of boswellic acids [135,136]. There are several more publications giving evidence on the anti-proliferative action upon cancer cell lines [137-139], the inhibition of implant rejection [140] and the inhibition of elastase in human leukocytes [141].

Furthermore, based on positive data on the treatment of peritumoral brain edema accompanying gliomas [142], the European Medicines Agency designated an *orphan drug* status to *Boswellia serrata* resin extracts in 2002 [143].

Metabolic studies revealed that a concomitant high-fat food intake during the orally consumption of *Boswellia serrata* preparations significantly increased the plasma levels of

boswellic acids (**1-6**). The control group (fastened state) showed lower plasma concentration levels. Interestingly,  $\beta$ -BA (**3**) revealed the highest plasma concentration levels [125].

Another *in vitro* and *in vivo* study by Krüger et al. [143], published in 2008, gives evidence that  $\beta$ -KBA (**5**) but not  $\beta$ -AKBA (**6**) undergoes extensive phase I metabolism, and that  $\beta$ -AKBA (**6**) is not deacetylated to  $\beta$ -KBA (**5**).

Recent studies, measuring the plasma concentration levels of boswellic acids, additionally showed that  $\beta$ -BA (**3**) seems to be the boswellic acid with the throughout highest plasma concentration levels [126,144]. Thus, this compound ( $\beta$ -BA, **3**) could be an interesting candidate responsible for the major pharmacological actions in *Boswellia* preparations.

Therefore, the research group of Werz tested recently boswellic acids and derivatives thereof upon the inhibition of microsomal prostaglandin E<sub>2</sub> synthase-1 (mPGES1; see also Fig. 1.25), in order to evaluate a further molecular basis for the anti-inflammatory actions of *Boswellia* extracts [104]. After evaluation of defined boswellic acids in cell-free and cell-based assays as well as carrageenan-induced mouse paw oedema and rat pleurisy models, their key-findings suggest that especially  $\beta$ -BA (**3**) may contribute to the overall anti-inflammatory activity *in vivo*. Thus, the decrease in PGE<sub>2</sub>-product formation may occur through selective mPGES1-inhibition. Furthermore,  $\beta$ -BA (**3**) did not significantly affect the 6-keto PGF<sub>1 $\alpha$</sub> -formation (see also Fig. 1.25) in the rat model, whereas indomethacin (a NSAID) did. Hence, revealing a benefit for  $\beta$ -BA (**3**) in selectivity by not significantly affecting other *arachidonic acid cascade* enzymes (e.g. COX-1 and COX-2).

Other compounds which recently gained some attention are incensole (Inc, **22**; see also Fig. 1.21) and its acetate (Inc-Ac, **23**; see also Fig. 1.21). Moussaieff et al. published three papers on these compounds in the years 2007 and 2008 [87,145,146]. Their key-findings suggested that incensole (**22**) and especially incensole acetate (**23**) are two novel anti-inflammatory compounds inhibiting the nuclear Factor- $\kappa$ B activation which also may contribute to inflammatory processes. According to them, the boswellic acids did not reveal any influence in this assay, though the concentrations of Inc-Ac (**23**) for inhibition were rather high (140 – 560  $\mu$ M) [87]. In another paper they reported on the agonistic effect of Inc-Ac (**23**) upon the transient-receptor-potential-vanilloid-3 (TRPV3), an ion channel implicated in the perception of warmth in the skin. The role of TRPV3 channels remains unknown hitherto. They showed that Inc-Ac (**23**) agonised the TRPV3 channel, causing anxiolytic-like and anti-depressive-like behavioural effects in wild-type mice [145]. Additionally, in a further mouse model, they investigated the potential of Inc-Ac (**23**) as novel neuroprotective agent. In this head injury model, Inc-Ac (**23**) reduced glial activation, inhibited the expression of interleukin-1b and tumor necrosis factor- $\alpha$ -mRNAs, and induced cell death in macrophages at the area of trauma [146]. These results revealed another molecular entity, isolated from *Boswellia* resins, with an interesting and perhaps promising pharmacological potential. In 2012, Moussaieff et al. reported also on a protective effect of Inc-Ac (**23**) on cerebral ischemic injury in a mouse model [147].

Furthermore, anti-microbial actions of the essential oils from frankincense resins against *Gram-positive* and *Gram-negative* bacteria have been described [74].

Generally, a good overview on important publications on all medical topics concerning *Boswellia* can be gained, if in the online PubMed library the term "*boswellia OR boswellic acid*" is entered as a key-word [148].

Thus far, it is still absolutely elusive how the uncountable amounts of compounds, occurring in frankincense resins, influence pharmacological activities *in vivo*. Possibly, these substances interact in a synergistic and/or antagonistic manner. It is also still unclear how these target enzymes (e.g. cathepsin G, mPGES-1, COX-1 and COX-2 or 5-LO) react with different combinations of these single compounds.

The proposal of synergistic and antagonistic effects was established on a scientific basis by Berenbaum in 1989 [149]. Basically, the results of Berenbaum conclude that if two or more bioactive substances are evaluated in a biological assay, these substances can be enhancing each other in their bioactivity, thus, leading to a more effective inhibition of the target (synergism); or, they could deteriorate the bioactivity of each other, hence, giving a less effective inhibition of the target enzyme (antagonism). A third case is possible, which is the so-called zero-interaction, when neither a synergistic nor an antagonistic effect can be detected. Thus, the compounds do not interact in any way with each other and just the single activities of each are added. A review on this interesting field, especially concerning phytotherapeutics like frankincense resins, has been published by Wagner and Ulrich-Merzenich in 2009 [150]. In addition to that, the multi-compound containing frankincense preparations may reveal a still unknown great potential, if a synergistic effect of the single compounds can be approved by scientific evidence. Unfortunately, convincing experiments with frankincense extract preparations, revealing such phenomena, are so far still lacking.

### 1.6 Aim of the Study

It was shown in chapter 1 (Introduction) that extracts of resins from frankincense and isolated compounds thereof reveal several pharmacological activities. Beside the primarily observed anti-inflammatory actions, there have been also publications on the anti-tumour and anti-microbial potential of this natural product. The main constituents, held responsible for the pharmacological actions, are the boswellic acids (see Fig. 1.8). However, these extracts contain still an innumerable amount of several different types of terpenes and hence these may contribute to the overall anti-inflammatory activity in a synergistic and/or antagonistic manner [150].

Especially the tirucallic acids (see Fig. 1.18) showed a concentration-dependent contradictory behaviour. At certain concentrations they stimulated the leukotriene biosynthesis in intact polymorphonuclear cells, and after exceeding a defined concentration the inhibition of 5-LO was again observed [133]. Thus, one aim of the study presented here has been the development of a HPLC-method capable of quantifying the amounts of tirucallic acids in frankincense extracts, since no analytical work hitherto has published any detailed quantitative results on the tirucallic acid content in *Boswellia* preparations. Therefore, prepared resins from *Boswellia papyrifera*, *Boswellia serrata* and *Boswellia sacra*, respectively, *Boswellia carterii*, were evaluated by different analytical tools (TLC, HPLC and GC).

Furthermore, since the literature reported in some cases contradictory results on the biomarker compositions of *Boswellia carterii* and *Boswellia papyrifera*, it had been tried to clarify these misinterpretations by investigation of certified sample material (voucher specimen). As both species are considered as African frankincense, it has been most likely that the species *Boswellia papyrifera* (Eritrea, Ethiopia and Sudan) had been purchased in many cases as *Boswellia carterii* (Somalia) instead, leading to falsely reported facts [35,67,68,70,75,85,86,88,146]. The clarification was additionally carried out by analysis of the three common species *Boswellia papyrifera*, *Boswellia serrata* and *Boswellia sacra*, respectively, *Boswellia carterii*, with the afore mentioned tools (TLC, HPLC and GC).

To achieve this, already known, as external standards for HPLC-quantitation, and even new substances had to be isolated and purified from the extracts of *Boswellia papyrifera* and *Boswellia carterii* by conventional extraction (liquid-liquid) and separation methods (liquid chromatography). Their structures had to be elucidated by a combination of mass spectrometric (MS) and 1D and 2D-nuclear magnetic resonance experiments (NMR). Finally, the combination of all techniques (TLC, HPLC and GC) should give methods which definitely could clarify the identity of an unknown frankincense resin species being questioned. In addition, the HPLC method should be feasible to quantify as much major compounds as possible in order to gain a better knowledge on the overall composition of these resins. Through quantification of certain molecules, some evidence on the biosynthesis preferences of each species should be elucidated.

In cooperation with the working group of Prof. Dr. Oliver Werz (Tübingen, Germany; now Jena, Germany) some of the isolated compounds and multi-compound containing extracts had to be tested to reveal their pharmacological potential.

## Introduction

---

To summarise, this work should give an intellectual tool on how to distinguish the resins of the three mostly distributed *Boswellia* species (*Boswellia papyrifera*, *Boswellia serrata* and *Boswellia sacra*, respectively, *Boswellia carterii*) in a chemotaxonomic point of view. In addition, it was tried to establish a HPLC-method capable of quantifying as many compounds as possible in the resin matrix, but particularly the class of tirucallic acids since no analytical method before has been revealing something about their quantities in detail. Furthermore, some characteristics on the biosynthesis differences of each species may be obtained. And the pharmacological potential of newly isolated chemical entities, structurally defined by MS and NMR experiments, should be investigated.

## 2. Experimental Part

### 2.1 Material and Methods

#### 2.1.1 Resin Material

Most of the resin material used for the investigations reported here was obtained from the distributor *Gerhard Eggebrecht Vegetabilien und Harze*, Doppelreihe 1a, D-25361, Germany. The material was already correctly assigned as authentic frankincense resin material in the PhD thesis of Dr. Jochen Bergmann [17] by comparison with voucher specimens. Furthermore, the data basis presented in this thesis guaranteed authenticity of the material purchased. Resins, obtained from other distributors and analysed, are stated explicitly in the corresponding chapters. A table of all analysed samples is shown in chapter 3.14 (Table 3.37).

#### *Boswellia papyrifera* (Bpap)

Distributor: Eggebrecht; Denomination: Gum olibanum (Frankincense) Eritrea 1. Choice; Origin: Eritrea (Manufacturer information).

#### *Boswellia serrata* (Bser)

Distributor: Eggebrecht; Denomination: Gum olibanum (Frankincense) Indian Siftings or Gummi Olibanum indisch No. 1; Origin: India (Manufacturer information).

#### *Boswellia carterii* (Bcar)

Distributor: Eggebrecht; Denomination: Gum olibanum (Frankincense) Aden 1. Choice and Somalia 1. Choice; Origin: Somalia (Manufacturer information).

#### *Boswellia sacra* (Bsac)

Distributor: Eggebrecht; Denomination: Gum olibanum (Frankincense) Oman white No. 1; Origin: Oman (Manufacturer information).

Article numbers of each of the resins (Bpap, Bser and Bsac, respectively, Bcar) are indicated in the corresponding experimental chapters.

#### Voucher Specimen

Certified resin samples from Bpap and Bsac were obtained from the Royal Botanic Gardens, Kew Gardens in England, UK, donated by Mrs. J. Steele. Additional samples of Bsac and Bcar were received by Dr. Jochen Bergmann from Dr. M. Al-Amri (Ministry of Agriculture, Rumais Research Station, Muscat, Oman) during his visit to Oman in 2004-2005 and from Mr. Giama, Bremerhaven, Germany. Original Gufic tablets (Bser, Sallaki Tablets®) from India and Bser-siccum 96% ethanolic extracts were obtained from AureliaSan GmbH, Bisingen, Germany.

### 2.1.2 Solvents and Chemicals

All chemicals and solvents were obtained from Sigma Aldrich (Steinheim, Germany) or VWR (Darmstadt, Germany) and of analytical reagent grade unless stated otherwise. Solvents for extraction, thin-layer and flash chromatography (e.g. DCM, Et<sub>2</sub>O, pentane, etc.) were distilled prior to application. HPLC solvents (ACN, MeOH and H<sub>2</sub>O) were of appropriate "HPLC grade" purity. NMR spectra were normally recorded in deuterated chloroform (CDCl<sub>3</sub>; 99.8 % D) if not stated otherwise. HPLC quantitation standards (see also chapter 3.6.3.1) were isolated from Bpap by flash column chromatography and purified by preparative HPLC (purity > 99 % by HPLC) and the identity of each molecule was verified by co-injection HPLC tests, MS and NMR evaluation (see also [56]). Any peculiarities and differences from the descriptions given here are mentioned in the corresponding experimental chapters.

## 2.2 Extraction Procedures

### 2.2.1 Preparative Extraction Scale (Soxhlet Apparatus)

The extraction procedures generally followed the descriptions already given in the work of Bergmann and Seitz [17,56]. The isolation of huge amounts of resinous materials (> 100 g) is also described in the paper of Paul et al. [59]. A briefly general description is given here. The respective resin (e.g. 200 g) was cooled in a freezer (for 1-2 h) and powdered in an electrical mixer. The powder was filled into an extraction thimble, covered with wed and extracted with 1.5 l DCM or Et<sub>2</sub>O in a Soxhlet apparatus overnight. The solvent was removed under vacuum at 40 °C and a crude yellow and fragrant solidus material was obtained (lipophilic raw extract = RE, yield: ca. 50-70 %).

### 2.2.2 Discontinuous Extraction (Separation Funnel)

The discontinuous extraction was implemented in a separation funnel. The crude extract (Soxhlet Apparatus) was dissolved again in ca. 250 ml Et<sub>2</sub>O and extracted with 100 ml 5 % (m/m) KOH solution. The alkaline aqueous solution was then extracted with Et<sub>2</sub>O again (3 x 30 ml). The combined organic phases were washed with brine (saturated NaCl), dried (MgSO<sub>4</sub>) and evaporated in vacuo. The neutral fraction was obtained (fragrant and yellow orange oil, neutral fraction = NB; yield: 30–40 %). The alkaline aqueous phase was acidified with cooling to pH 2-3 (conc. HCl) and extracted with Et<sub>2</sub>O (3 x 50 ml). After combination of the organic phases, it was washed with brine, dried (MgSO<sub>4</sub>) and evaporated to dryness in vacuo. A less fragrant yellowish solid material was obtained (acid fraction = RS; yield: ca. 20–30 %).

### 2.2.3 Continuous Extraction (Kutscher-Steudel Perforator)

The continuous extraction was carried out in a Kutscher-Steudel Perforator. The crude extract (Soxhlet Apparatus) was dissolved in ca. 250 ml Et<sub>2</sub>O, treated with 3 – 4 litres of 5 % (m/m) KOH and equilibrated with Et<sub>2</sub>O overnight. The organic phase was separated, dried (MgSO<sub>4</sub>) and concentrated under vacuum to give fragrant and yellow oil (neutral compounds = NB; yield: 30–40 %). The alkaline aqueous phase was acidified with cooling to pH 2-3

(conc. HCl) and extracted with Et<sub>2</sub>O in the Kutscher-Steudel apparatus overnight. After separation, the organic phase was dried (MgSO<sub>4</sub>) and the solvent was removed under reduced pressure, leading to a less fragrant yellowish light brown powder (acid fraction = RS; yield: 20-30 %).

### 2.2.4 Analytical Extraction Scale (TLC, HPLC)

Minor amounts of resins for analytical evaluations (TLC, HPLC) were extracted using the following standard operation procedure: The resinous material (5-10 g; great sample population as even within the same sample batch great differences may occur) was put in a freezer (- 30 °C) for ca. 1 h. Afterwards, the resin chunks were powdered using an electrical mixer or a mortar and pestle. Approximately 300 – 600 mg from this powder were dissolved in 10 ml Et<sub>2</sub>O and sonicated for 15 min (ultra-sonic bath). The colloidal solution was then filtered (0.2 µm; Filtropur S, Sarstedt, Nürnbrecht, Germany) and the filtrate was evaporated in vacuo. The amount of raw extract (RE) was determined (yield ca. 50-60 %) and an aliquot (ca. 10 mg) for further HPLC analysis was saved. The rest was dissolved in 4 ml Et<sub>2</sub>O and 12 ml KOH (1 M) were added, and the RE was extracted in a separation funnel (V = 50 ml) with 3 x 4 ml Et<sub>2</sub>O. The organic phases were combined (ca. 10 – 12 ml) and re-extracted with 5 ml KOH (1 M). Afterwards, the organic phase was dried (MgSO<sub>4</sub>), filtered and evaporated in vacuo, leading to the neutral fraction (NB) with a yield of ca. 20-30 % referring to the overall weighed sample amount. The combined KOH-phases (ca. 15–17 ml) were acidified with HCl (1 M) until precipitation (white solid) occurred (pH ca. 1-3). Subsequently, it was extracted with 3 x 8 ml Et<sub>2</sub>O and the combined organic phases were dried (MgSO<sub>4</sub>), filtered and evaporated in vacuo, giving the acid fraction (RS) with a yield of ca. 20-30 % referring to the overall weighed sample amount. Note that in some cases, especially experienced for samples of Bsac/Bcar (expectably high contents of BAs, **1** and **3**, and ABAs, **2** and **4**), the phase separation (alkaline – organic) can be difficult (formation of an emulsion). To avoid this disturbing phenomenon, it is helpful to increase the difference in density between the phases by addition of brine or organic phase, respectively.

### 2.2.5 Steam Distillation (For GC analysis)

A certain amount of the oily neutral compounds from Bpap, Bser and Bcar (ca. 1 g; see chapter 3.5) was dissolved in a bit of acetone (ca. 3 ml) in a 250 ml flask and 100 ml of H<sub>2</sub>O were added (milky white emulsion). The apparatus for steam distillation is shown in Fig. 2.1 The mixture (oil and water) was stirred under heating (oil bath) and a slight vacuum (boiling temperature: 55 – 60 °C). The distillate (Liebig condenser) was collected in a cooled receiving flask (ice bath) and the process was stopped when almost all of the water was distilled. The aromatically aqueous phase (a few drops of oil were visible) was extracted with 2 x 20 ml Et<sub>2</sub>O. The combined organic phases were dried (MgSO<sub>4</sub>) and evaporated in vacuo, giving a colourless very aromatic essential oil (yield: 1.5 – 6.7 % of the weighed neutral compounds; see also chapter 3.5). The samples were stored at 4 °C and used for further GC-FID analysis.

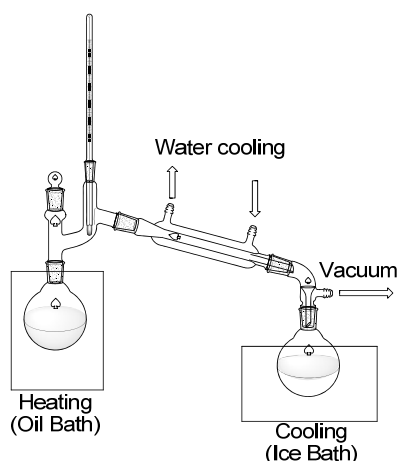


**Fig. 2.1** The apparatus for steam distillation (see also text).

## 2.3 Chromatographic Techniques

### 2.3.1 Thin-Layer Chromatography (TLC)

TLC Silica gel 60 F<sub>254</sub> Multifomat prescored to 5 x 10 cm glass plates (stationary phase) were purchased from Merck (Darmstadt, Germany). The mobile phase standardly consisted of a mixture of two parts of pentane and one part of Et<sub>2</sub>O plus 1 % (v/v) of HOAc (unless stated otherwise). TLC plate start lines were drawn (pencil) at 1.5 cm; giving an elution distance of maximal 8.5 cm. Spots were put on with a small capillary. UV detection (254 nm) was carried out by a conventional UV light source (Duo – UV – Source for Thin-layer and Column chromatography, Desaga, Heidelberg, Germany). Chromatograms were further developed by an unspecific dyeing reagent (0.5 ml anisaldehyde in 50 ml HOAc plus 1 ml conc. H<sub>2</sub>SO<sub>4</sub>). After development of the chromatograms, the TLC plate was completely immersed into a solution of this dyeing reagent and heated with a heat gun until the coloured spots appeared. The spots were visually detectable after colour development at room temperature (ca. 15 – 30 min). The standard sample preparation procedure, if not stated otherwise, was as follows: The different olibanum resins were cooled in a freezer to –30 °C (1–2 h) and powdered in an electrical mixer. The powder (1 g) was dissolved in 80 ml methanol or diethyl ether (MeOH and Et<sub>2</sub>O as solvents for extraction of the powdered resins give identical TLC chromatograms) in a 100 ml volumetric flask and sonicated for 20 min (the resin will not be completely dissolved). Afterwards, 20 mL MeOH (or Et<sub>2</sub>O) were added (final volume = 100 ml). Aliquots (1 ml) were taken from the filtered solution (0.2 µm; Filtropur S; Sarstedt, Nürnberg, Germany) for further TLC analysis. See also the paper on TLC analysis of Bpap, Bser, Bpac/Bcar of Paul et al. [11].

### 2.3.2 Flash-Column-Chromatography

Normal phase (NP) silica gel (stationary phase) with particle size 40–60 µm was purchased from Merck (Darmstadt, Germany). The mobile phase standardly used was a mixture of pentane/Et<sub>2</sub>O plus 1 % (v/v) HOAc (Note: HOAc was only added when the acid fraction was separated. For the separation of neutral fraction compounds the addition of HOAc is

unnecessary). A step gradient, each step 500 ml, of increasing polarity for raw material (neutral and acid fraction) separations was applied. The chromatography itself followed basically the instructions of Still et al. [151]. Silica gel was suspended with the eluent, shortly degassed in vacuo and filled into the column. The sample was dissolved, dependent on the sample size, in a bit of eluent or DCM and evenly added on top of the column bed. After the sample was adsorbed inside the silica gel, fine sand was put on top of the column bed to keep the silicagel area even when additional solvent was transferred from the reservoir during the chromatographic separation. Separation itself was carried out by action of a middle strong air-pressure (1-1.3 bar) and fractions were collected using an automatic fraction collector (LKB-Bromma 2211 SUPERRAC; 180 fractions, 20 ml test tubes). Fractions were monitored by TLC and combined to overall fractions due to their chromatographic analogies. Different application conditions for flash chromatography, otherwise than stated here, are described in the appropriate chapter.

### **2.3.3 Preparative High Performance Liquid Chromatography**

The preparative HPLC system consisted of a S 1521 Solvent Delivery System and a S 3210 UV/VIS Diode Array Detector (all components from Sykam, Fürstfeldbruck, Germany). For sample injection a 3725-038 Valve Bracket Injector (Rheodyne) with a 10 ml loop and a 1 ml syringe (Hamilton, Bonaduz, Switzerland) were used. Basically, isolation and separation of target analytes was achieved by usage of MeOH and H<sub>2</sub>O mixtures (MeOH content always greater than 90 %) and is stated in detail in the corresponding chapter (see chapter 3.1.1 and 3.1.2). As separation columns a NUCLEODUR 100-5 C18 ec, 250 x 21 mm I.D. (Machery & Nagel, Düren, Germany) and an YMC-Pack Pro C18 RS, 250 x 20 mm I.D. S-5 µm, 8 nm (YMC-Europe, Dinslaken, Germany) served. Pre-runs were carried out on the analytical HPLC device with the corresponding analytical columns (NUCLEODUR analogue prep column, only with 250 x 4 mm I.D.; YMC analogue prep column, only with 250 x 4.6 mm I.D.), following basically the descriptions in the book of Meyer [152] for column scale up. The chromatographic data was recorded with Chromstar DAD software, Version 6.2 (SCPA, Weyhe-Leeste, Germany). Detection was done at three different wavelengths (210, 250 and 280 nm) simultaneously and the UV spectrum was recorded from 200-400 nm.

### **2.3.4 Analytical High Performance Liquid Chromatography (HPLC)**

The analytical HPLC device consisted of a S 7121 Reagent Organizer, a S 1122 Solvent Delivery System, a S 8111 Low Pressure Gradient Mixer and a S 3210 UV/VIS Diode Array Detector (all components from Sykam, Fürstfeldbruck, Germany). A Jetstream 2 Series column oven (Techlab, Erkerode, Germany) was used for temperature control. Samples were injected by a S 5111 Valve Bracket Injector (Rheodyne) with a 20 µl loop (100 µl were injected for quantitative determinations, overfilling) and a 250 µl syringe (Hamilton, Bonaduz, Switzerland). Solvent reservoirs were degassed with Helium (He) and kept constantly under He-pressure during analysis.

Injected sample concentrations depended on the linearity range of the target analytes of interest and are in detail mentioned in the corresponding chapters (see chapter 3.6.3.1). Usually, the sample concentration was 5 mg/ml for RS fraction samples and 1.25 mg/ml for

NB fraction samples (quantitation of compound **20**, **21**, **22** and **23**). If one of the analytes revealed contents above the linearity range (e.g. compound **6** in Bpap, respectively, Bsac/Bcar, and compound **10** as an artefact, see also [55]), a minor concentration was injected ( $c = 2$  mg/ml). Compound **3** ( $\beta$ -BA) was evaluated to elute as inhomogeneous peak (co-elution with compound **18**) in samples of Bpap and Bser. If further 2D analysis was applied (Bpap- and Bser-RS), normally a minimum concentration of 5 mg/ml had been necessary to generate 2D chromatograms less susceptible to integration errors (see also chapter 3.6.2).

Every sample was injected twice unless stated otherwise. After each injection, the injector was purged with 500  $\mu$ l MeOH and the injection syringe was purged twice with 250  $\mu$ l MeOH. The chromatographic data was recorded for 1D and 2D chromatograms with Chromstar DAD software, Version 6.3 (SCPA, Weyhe-Leeste, Germany). Detection was simultaneously carried out at three different wavelengths (210, 250 and 280 nm) and the UV spectrum was recorded from 200-400 nm. Peak Integration was manually implemented by comparison of the baseline with blank runs. Minor inhomogeneities at peak edges were separated by the perpendicular drop function of the integration software. Further statistical calculations were achieved by application of Microsoft Excel<sup>®</sup> 2003 software.

### 2.3.4.1 General Remarks concerning the Method Development

The method development was generally based on the descriptions given in the book of Dolan and Snyder [153]. Accurate quantitation of frankincense species samples has been revealed to be highly intricate, since these resin materials contain numerous amounts of several terpenic compounds. It was finally achieved to develop a HPLC method for the separation of almost all significant triterpenic acid peak signals in the acid fraction of the species Bpap, Bser and Bsac/Bcar.

The method fulfilled the requirements for an adequate operation procedure. Interestingly, the boswellic and lupeolic acids follow a classical so called "*regular-sample-elution pattern*" ( $\log k$ , with  $k$  = capacity factor, is linear with gradient time and no isotherm-crossing occurs; meaning that if  $\log k$  is plotted against two different gradient times or two isocratic mixtures, e.g. 10 min and 20 min, while keeping all other parameters constant, the regular sample peaks become - theoretically - better resolved, linear in the same direction. For a detailed explanation see [153]).

However, the co-existence of tirucallic acids with boswellic and lupeolic acids in these species made the method development more complicated and a so called "*irregular-sample-elution pattern*" has been obtained ( $\log k$  linearities tend to cross each other by different gradient times or isocratic mixtures, meaning that samples do not move in parallel in the same direction, as for a regular sample, and thus co-elution may occur; see again [153] for further details). A graphical explanation of the linear solvent strength model for a simple problem is demonstrated in Fig. 2.2.

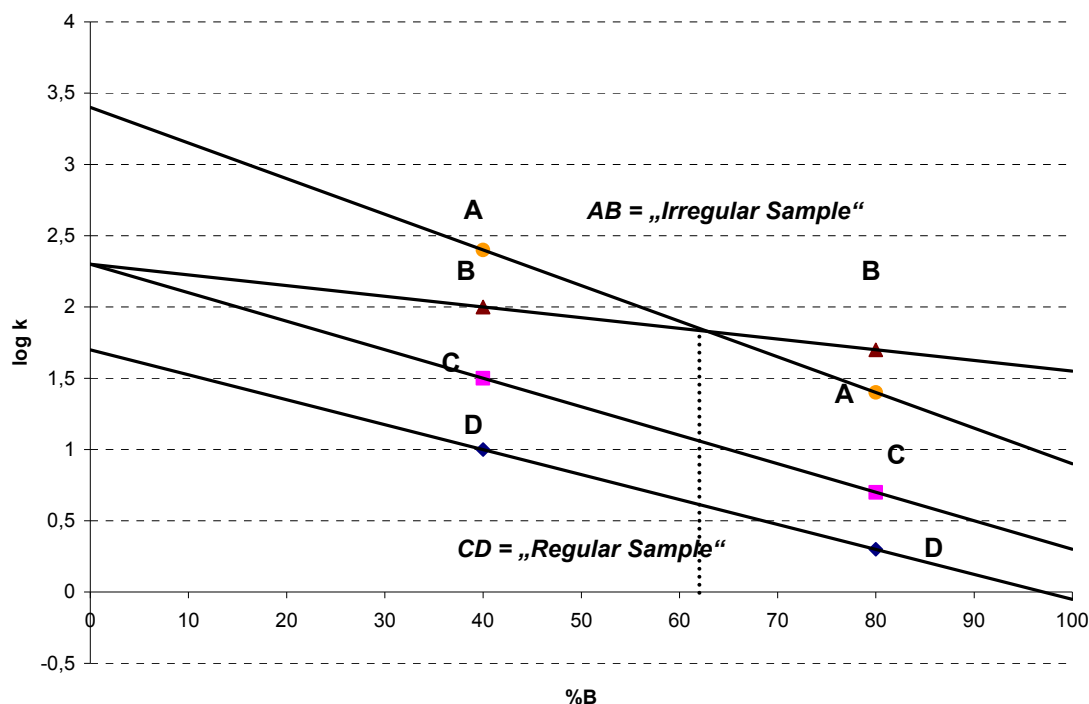


**Fig. 2.2** Graphical explanation of the Linear-Solvent-Strength model. Log  $k$  ( $k$  = retention factor) plotted against %B (stronger elution solvent). Minimum requirement: All parameters constant (temperature, column-type, flow rate, etc.) and two experiments with two different isocratic runs, respectively, gradient times (then  $\log k^*$ , see also [153]). Here: Isocratic example (run 1 = 40 % and run 2 = 80 % B). As can be seen, the regular sample (CD) elutes parallel with increasing %B, whereas the irregular sample (AB) shows different sensitivities to the change in %B and thus has similar  $k$ -values (co-elutes) at ca. 64 % B (denoted by the vertical line). It is obvious that with an increasing number of compounds to be separated, the model can become extremely complicated. For further details see text.

### 2.3.4.2 Standard Quantitation Conditions (1D chromatography)

All quantitation experiments for the acid and neutral fractions were carried out using the following standard setting: Analytical HPLC device as described as in 2.3.4; guard-column: GROM Saphir 110 C18, 5  $\mu$ m 20 x 4 mm I.D. (GROM, Rottenburg, Germany) for column protection; separation-columns: 2 x YMC-Pack Pro C18 RS 250 x 4.6 mm I.D. S-5  $\mu$ m, 8 nm (YMC-Europe, Dinslaken, Germany) in series connected; flow rate = 0.85 ml/min;  $T$  = 45 °C. The mobile phase consisted of MeOH (A) and H<sub>2</sub>O plus 0.1 % TFA (B); gradient profile: Isocratic elution with 85 % A for 2 min, then a linear gradient to 100 % A in 13 min, followed by an isocratic elution with 100 % A for additional 45 min and an isocratic period with 85 % A for 15 min to equilibrate the columns again (Total time: 75 min each run). Data recording was carried out as described in point 2.3.4. Note that with only one YMC column a similar resolution can be obtained if the flow rate is set to 0.43 ml/min and the gradient delay to 1 min (isocratic), followed by a gradient to 100 % MeOH in 6.5 min while keeping all other parameters constant (see also [153]). However, the method with two columns in series connected has been giving slightly better resolution values (narrower peaks). For quantitation experiments the method of external calibration has been applied (Peak area plotted against

concentration in mg/ml). All external quantitation standards were isolated from Bpap (acid fraction standards and compounds **22** and **23**) as it is already reported in the dissertation of Seitz [56] or the paper of Paul and Jauch [154]. Compounds **20** and **21** were isolated from Bcar, as it is reported in chapter 3.1.2. Routinely, each analyte (compounds **1-8** and **10-16** for RS samples; compounds **20**, **21**, **22** and **23** for NB samples) was dissolved in MeOH due to its corresponding linearity range (see also Tab. 3.23 - 3.25 in chapter 3.6.3.1). Normally, a complete master mix, containing all target analytes of interest in one solution (see also [59] for acid fractions and [154] for neutral fractions), was prepared. Samples were dissolved in 8 ml MeOH in a 10 ml volumetric flask and sonicated (approximately 15-30 min). At last, the final volume was adjusted to 10 ml with additional MeOH. From the stem solution, 5 to 6 standards with decreasing concentrations levels of factor two were generated (10 ml volumetric flasks or by calibration qualified automatic pipette systems). Prior to injections each solution was filtered (0.2  $\mu\text{m}$  syringe filter). The expected peak area was determined by preliminary tests. The analyte concentration range was adjusted to the expectation value in the pure resin sample (see also chapter 3.8). Any peculiarities and differences from the descriptions given here are mentioned in the corresponding experimental chapters.

### 2.3.4.3 Fraction Collection Conditions 2D Analysis

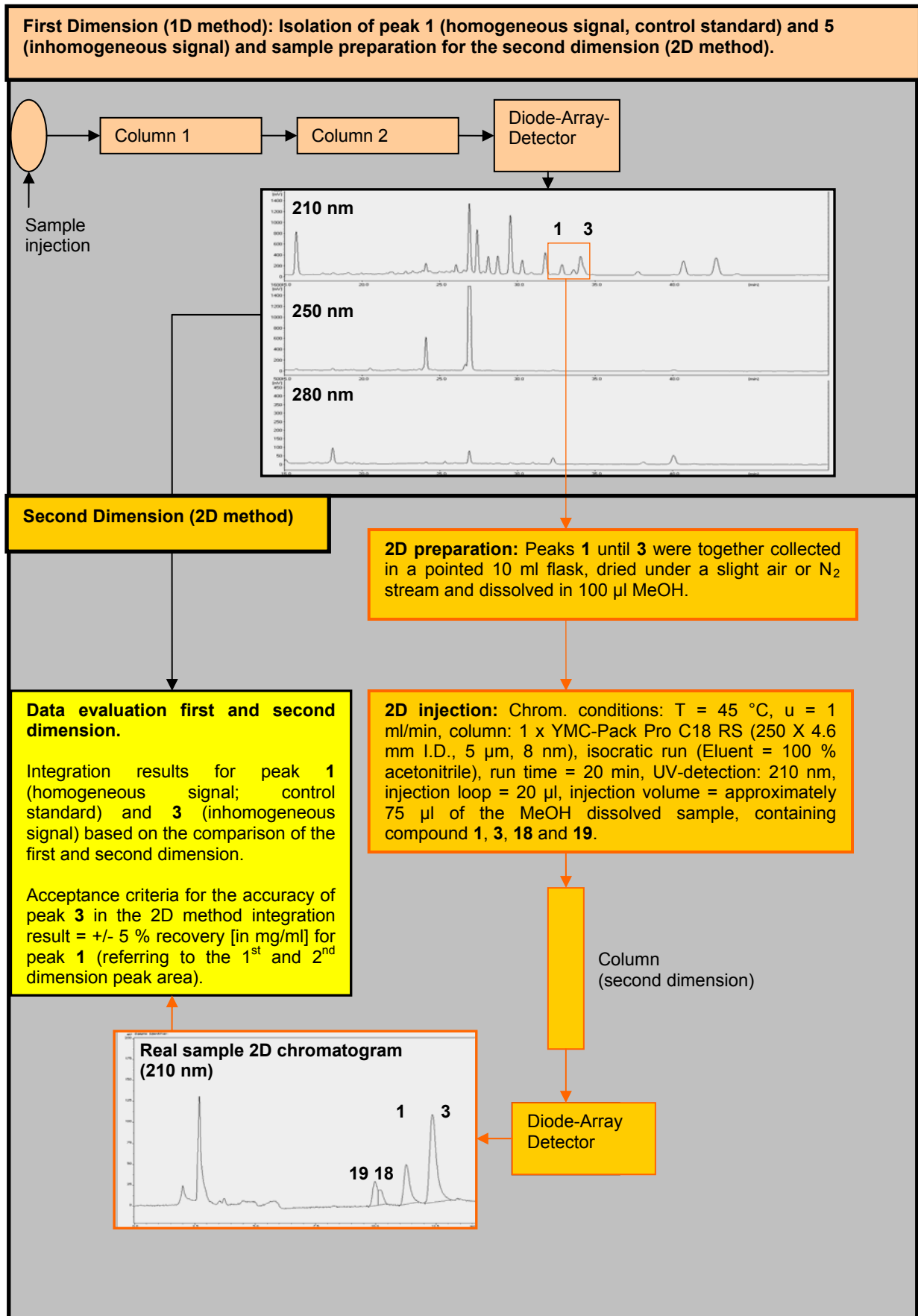
During the method development it was figured out that compound **18** co-elutes with compound **3** (significantly in Bpap RS samples and as well in Bser RS samples). Since resolution of these two peak signals within one chromatography dimension was not achievable without sacrificing resolution of other signals (Irregular elution sample; see [153]), a second dimension was introduced.

Therefore, peaks of  $\alpha$ - and  $\beta$ -boswellic acid (**1** and **3**) and 11-OMe- $\beta$ -ABA (**8**) and also the inhomogeneities (compound **18**, co-eluting with compound **3** in Bpap and Bser, and compound **19** in real samples) were collected due to their retention time area in a pointed 10 ml flask, subsequently dried under a light  $\text{N}_2$ - or air-stream and stored at room temperature for further 2D Analysis. A short graphical overview on the complete method is presented in Scheme 2.1. Significant co-elution of compound **18** and **3** has been only observed for the species Bpap and Bser. Normally, for Bpac, respectively Bcar, the second dimension is not necessary (see also chapter 3.7.5).

### 2.3.4.4 Standard 2D Quantitation Conditions ( $\alpha$ - and $\beta$ -boswellic acid)

Quantitation results for  $\alpha$ - and  $\beta$ -boswellic acid ( $\beta$ -BA, **3**, inhomogeneous peak in Bpap and Bser; see also chapter 3.7.5) were corrected using the following standard adjustment: Analytical HPLC device as described; guard-column: GROM Saphir 110 C18, 5  $\mu\text{m}$  20 x 4 mm I.D. (GROM, Rottenburg, Germany) for column protection; separation-column: 1 x YMC-Pack Pro C18 RS 250 x 4.6 mm I.D. S-5  $\mu\text{m}$ , 8 nm (YMC-Europe, Dinslaken, Germany); flow rate = 1.00 ml/min; T = 45  $^\circ\text{C}$ . The mobile phase consisted of 100 % ACN (isocratic run). Each run was recorded for 20 min. Data recording conditions were as described in point 2.3.4. The prepared sample (see chapter 2.3.4.3) was carefully dissolved in 100  $\mu\text{l}$  MeOH (using a calibrated 250  $\mu\text{l}$  Hamilton microliter injection syringe [155]), shortly sonicated and immediately injected after sample preparation. The injection volume contented of

## Experimental Part



Sch. 2.1 Graphical explanation of the offline 2D chromatography method.

approximately 75  $\mu$ l to guarantee sample loop overfilling (sample loop volume: 20  $\mu$ l). The corresponding peak area in the second dimension was plotted against its associated concentration value (in mg/ml) in the first chromatography dimension. Compound **1** (homogeneous peak signal) served as internal control standard for the recovery of compound **3** (co-elution with compound **18**). The graphical overview is presented in Scheme 2.1.

### 2.3.5 Validation Parameters (1D chromatography)

#### Determination of Precision, Selectivity, Peak Homogeneity, Robustness and Accuracy

For an explicit declaration of validation parameter terms, the corresponding literature may be consulted (e.g. [152,156-158]). All quantitation experiments for the acid and neutral fractions were carried out using the standard quantitation method described in chapter 2.3.4.2. A Gradient System Performance Test was implemented before each quantitation experiment as demonstrated in the book of Snyder and Dolan [153] (chapter 4, page 145). The dwell volume of the low pressure gradient system has been determined to be 2.8 ml. Prior to larger series of quantitation sets (Bpap, Bser and B<sub>ac</sub>/B<sub>car</sub>) the external calibration was carried out with the isolated standards (see also chapter 3.6.3.1). Generation of calibration curves was realised by plotting the resulting peak area against the corresponding mass of analyte (in mg/ml) and accepted when the correlation coefficient condition ( $R^2 > 0.999$ ) was satisfied. Operating ranges for the quantified compounds are given in chapter 3.6.3.1, Tab. 3.23 and Tab 3.24 for the RS fractions and in Tab. 3.25 for the NB fractions. The curves itself were generated by three injections of each of the six standards and accepted when the coefficient of variation (C.V.) for peak areas was  $< 2\%$  (system repeatability conditions) for each standard concentration level. At the limit of quantification (LOQ) and limit of detection (LOD) higher C.V. values than stated ( $< 2\%$ ) were observed. Every calibration curve consisted at least of six points. Different linear regression models were applied (unweighted and weighted linear regression). In dependence on the experimental result (target analyte concentration in the sample), the decision, which of the regression models has been used, was made individually (see also chapter 3.6.3). Hence, system repeatability and thus precision of the external standardisation method was granted, if the requirements were met (correlation coefficient  $> 0.999$  and C.V.  $< 2\%$ , peak area for three injections - above the LOQ).

Detection specificity was evaluated for compounds additionally detectable at 250 (compound **5** and **6**) and 280 nm (compound **9** and **10**), since at these wavelengths the chromatograms appear less complex compared with chromatograms at 210 nm detection.

Method selectivity for compounds, merely absorbing at 210 nm, has been evaluated by resolution values of up to  $R = 1.5$  (definition of peak baseline separation). Peak signals with  $R < 1.5$  were separated by the perpendicular drop function of the integration software and generally accepted when the linearity for the specific analyte was ensured.

Peak identity was verified by exact comparison of retention times, relative resolutions of neighbouring peaks, comparison of UV spectra and additionally by co-injection of all isolated standards. Peak homogeneity was analysed by comparing first and second derivatives of peaks and by comparing the ratio plot (peak height and area) at two different wavelengths if

necessitated [157]. Minor inhomogeneities appearing in the crude sample at the target analytes edges were separated by the perpendicular drop function of the integration software. Compound **3** (co-elution with compound **18**) has been determined as inhomogeneous peak signal in the real samples for Bpap and Bser incense species (see also chapter 3.7.5).

During the method development several parameters (solvents, temperature, stationary phase and gradient time) were changed to find the best resolution within the system. Basically, the method development followed the descriptions given in the book of Dolan and Snyder (chapter 3, Method Development) by application of the linear solvent strength model [153]. Thus, the logarithmic retention factors ( $\log k^*$ ) of each target analyte at different gradient times were compared and optimised to give an acceptable value for the resolution  $R$  (see also chapter 2.3.4.1). Compounds **14** and **15** were defined as the most critical peak pair, appearing as one single peak signal at the beginning of the method development under already known gradient elution conditions (see for example [56,133]). The system was optimised for their resolution. Therefore, as a most significant parameter, the stationary phase was ascertained.

Robustness of the method was evaluated by changing following parameters slightly at two different levels and the resulting differences in retention time, relative resolution, peak-height and -area were compared:

- Temperature: +/- 2 °C (One run at 43 °C and one run at 47 °C)
- Flow rate: +/- 0.5 ml/min (One run at 0.80 ml/min and one run at 0.90 ml/min)
- Gradient time: +/- 0.5 min (One run at 12.5 min gradient from 85 to 100 % A and one run at 13.5 min from 85 to 100 % A)

Accuracy has been evaluated by comparison of the external quantitation results for the method described here with another HPLC method, comprising less sample preparation steps, described in the European Pharmacopoeia 6.0 [20] (analysis on specifically detectable compounds **5** and **6** in the crude extract without separation of acid and neutral fraction). Furthermore, the accuracy for the separation of NB- from RS-fractions has been controlled by comparison of the corresponding chromatograms (NB overview chromatogram compared with corresponding RS overview chromatogram), where no significant peak signals should be observable for a definition of quantitative extraction.

A general remark is that at 210 nm detection wavelength the standard solution chromatograms were considered as ideal chromatograms, the “real sample” chromatograms were supposed to be similar to, to guarantee accurate quantitation results.

Determination of peak areas in the real sample chromatogram with minor peak inhomogeneities at the edges could be verified by statistical analysis (in general, a greater confidence interval is given; see also [159]). Comparison of an “ideal” standard chromatogram with a “real” sample chromatogram at 210 nm detection wavelength is presented in Fig. 2.3.

## Experimental Part

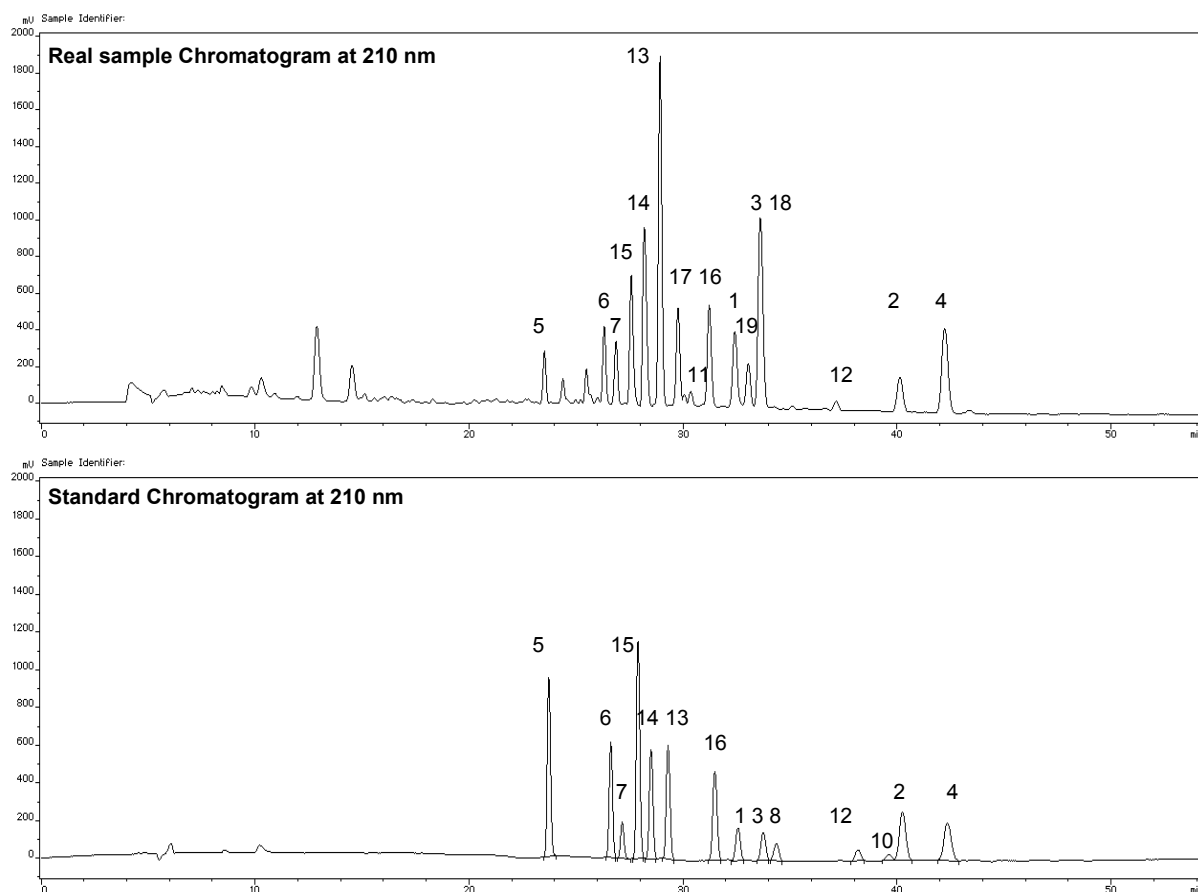


**Fig. 2.3** Comparison of a real sample RS fraction chromatogram (upper chromatogram; Bser, c = 5 mg/ml) with a standard chromatogram (lower chromatogram) at 210 nm detection wavelength. Ideally, the real sample should be as similar as possible to the standard chromatogram for accurate and precise quantitation results. Compound **18** co-elutes under compound **3**. Compound **8** has never been detectable in the "real sample" chromatograms. For further details see text.

### 2.3.6 Validation Parameters (2D chromatography)

#### Determination of Precision, Recovery and Accuracy (compared with 1D results)

Quantitation of  $\alpha$ - and  $\beta$ -boswellic acid ( $\beta$ -BA, **3**, eluted as inhomogeneous peak in Bpap and Bser, see chapter 3.7.5) was additionally achieved by implementation of a homomodal [160] second chromatography dimension, using the same column type with a different eluent (ACN, isocratic elution). Since  $\beta$ -BA (**3**) was proved to elute as inhomogeneous peak in the first chromatography dimension, the second dimension was introduced to resolve this probably highly important boswellic acid compound from its inhomogeneity (Note that according to recent findings,  $\beta$ -BA, **3**, shows the highest *in vivo* plasma levels of all investigated boswellic acids hitherto and thus seems to be a promising candidate responsible for the anti-inflammatory actions in the human body [125,144,161]). Therefore, the whole eluting area of compound **1** to **8** (in case of real samples compound **18** and **19** are included) was collected (see also chapter 2.3.4.3).  $\alpha$ -BA (**1**) served as control standard for the recovery of  $\beta$ -BA (**3**).

Second dimension calibration curves for compound **1** and **3** were generated with the prepared solutions from the 1D chromatograms for every injection of all six standard

concentrations and accepted when the coefficient of variation did not exceed 3 % (system repeatability condition; note that near the limit of quantitation, LOQ, greater C.V.s of up to 10 % are possible) for each concentration level. Obtained peak areas of the second dimension were plotted against the contents (in mg/ml) referring to the first dimension. The two calibration curves were generated by classical and weighted linear regression models [162] consisting of at least five points. The values for real sample chromatograms in the second dimension were accepted, when the value for the control standard  $\alpha$ -BA (**1**, homogenous peak signal in the first dimension) delivered the same content in mg/ml, within a  $\pm 5$  % confidence interval (quantitative control), as determined in the first dimension, and when the peaks of compound **18** and **19** eluted in front of  $\alpha$ -BA (qualitative control). The quantitative control value of  $\pm 5$  % had been based on empirical results and is within the theoretical estimated error propagation of the system (Theory:  $\pm 1$  % failure during the slight  $N_2$ -drying of the fraction;  $\pm 2$  % failure by resolving in 100  $\mu$ l MeOH;  $\pm 2$  % failure by injection and integration; see also the review of Meyer on measurement uncertainty [163]).

### 2.3.7 Statistical Analysis of the Quantitative HPLC Data

Quantitation results were obtained by external linear regression. Confidence and prediction intervals for the coefficient of regression were given analogous to the descriptions in the book of Sachs and Hedderich (page 336-347) [159].

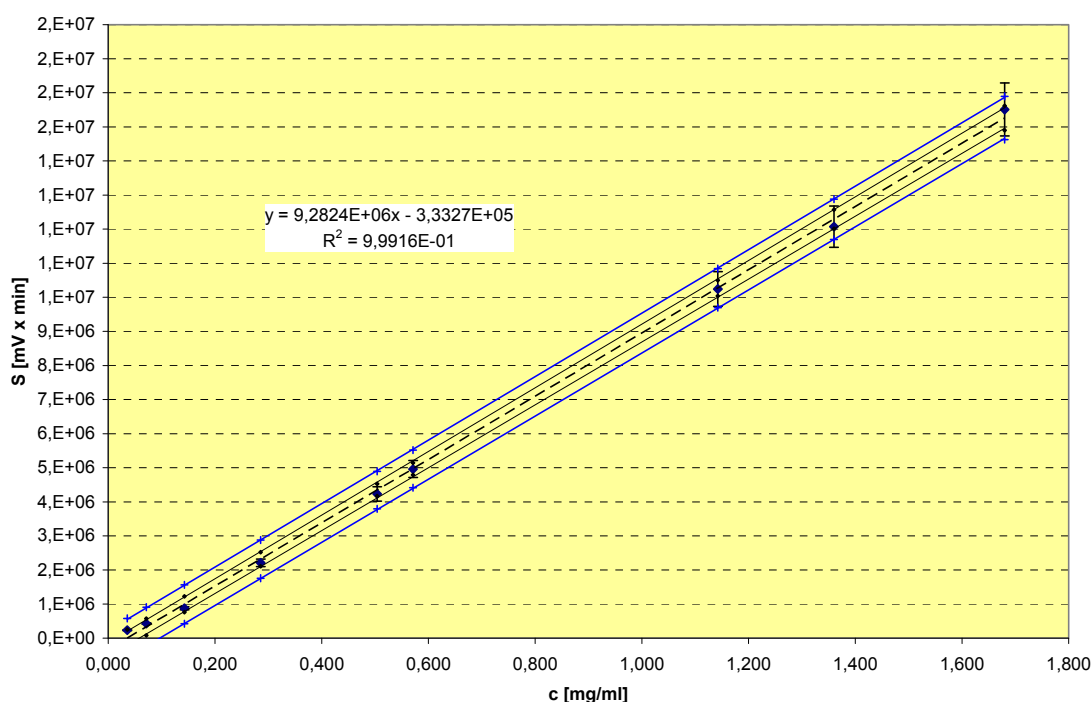


**Fig. 2.4** Linear Regression Model for compound **4** ( $\beta$ -ABA), obtained as described in [159] with Microsoft Excel<sup>®</sup> 2003. Peak Area plotted against concentration [mg/ml]. Linear Regression: Dashed line (- - -). Confidence Interval: Continuous inner lines (----). Prediction Interval: Blue outer lines (----). For further details see text.

In addition to the experimental data evaluation by the Chromstar DAD software 6.3 (SCPA, Weyhe-Leeste, Germany), the Microsoft Excel® 2003 software was used for further statistical calculations. For determination of the confidence and prediction intervals, the quantile of the Student t-distribution [159] was chosen at 99 % probability certainty ( $p = 0.99$ ). An exemplary graphical depiction is given for compound  $\beta$ -ABA (**4**) in Fig 2.4.

Furthermore, the programmed excel working sheet from the book of Kromidas and Kuss [162] was used for comparison of the linear regression with the weighted linear regression.

It should be noted that depending on the analyte concentration each regression model had its advantages and even disadvantages (see discussion in chapter 3.6.3). However, most important had been the knowledge of the specific error of the regression model, particularly, concerning the extreme values (lowest and highest concentration value of the curve of the analyte being questioned). On the one hand, for a sample containing only minimal amounts of the analyte, the weighted linear regression model expectably gave a more accurate result; whereas on the other hand, for a sample containing the analyte in greater quantities, the conventional linear regression model had been delivering a better fit in some cases. Content approximation models, based on the here evaluated sample population, were as follows:

- For Bpap great contents of  $\beta$ -AKBA (**6**) and TAs (**13-19**) were expected, whereas LAs (**11** and **12**) and BAs (**1-4**) occurred in lower contents in this species.
- For Bser great contents of BAs (**1-4**) and TAs (**13-19**) were expected, whereas LAs (**11** and **12**) and  $\beta$ -KBA (**5**), respectively,  $\beta$ -AKBA (**6**) occurred in lower contents in this species.
- For Bsac/Bcar great contents of BAs (**1-4**) and LAs (**11** and **12**) were expected, whereas TAs (**13-19**) occurred in lower contents.  $\beta$ -KBA (**5**), respectively,  $\beta$ -AKBA (**6**) had not been reliably predictable (strong extreme values for high and low contents).

Finally, a careful evaluation of every chromatogram and target analyte of interest has been hitherto unavoidable, as thus far the pattern recognition of a human mind is still sovereign over a simple programmed computer algorithm (personal evaluation and experience of the author with chromatography software in general).

The residual standard deviation (*RSD*) and the coefficient of variation of the applied linearity model (*VVK*) deliver a descriptive value for the scattering of measured points around the straight regression line (see also [162]). These two values give information on the quality and reliability of the generated regression model.

$$RSD = \sqrt{\frac{[y - y(x)]^2}{n - 2}}$$

*RSD* = Residual Standard Deviation (Difference between measured and calculated *y*-values)

*y* = Measured Signal Value

*y(x)* = Signal Value as function of the regression model

*n* = Number of measuring points (concentration levels)

$$VVK = \frac{RSD}{b \times x_M}$$

VVK = Coefficient of Variation of the applied regression model referred to the mean x-value (c in mg/ml) of the linearity range (e.g.  $x_1 = 1$ ,  $x_2 = 2$ ,  $x_3 = 3$ ; thus,  $x_2 = 2 = x_M$ ).

RSD = Residual Standard Deviation (Difference between measured and calculated y-values)

b = Slope-Factor for the corresponding linear regression model ( $y = bx + a$ ; a = Ordinate Intercept)

$x_M$  = Mean value of the concentration range, see also VVK

Furthermore, the here in this work additionally used equations for the prediction interval (PI; referring to the y-deviation) and the measurement uncertainty (MU; referring to the x-deviation) have been calculated as follows (see also [162,163]):

$$PI = t \times RSD \times \sqrt{\frac{1}{w_k} + \frac{1}{\sum w} + \frac{(x_k - x_w)^2}{\sum (x_k - x_w)^2}}$$

t = Student t factor (see also [159]). Here with  $p = 95 \%$  and  $n - 2$ .

RSD = Residual Standard Deviation

$w_k$  = individual weighting factor at the corresponding concentration level

w = weighting factor

$x_k$  = concentration level referring to  $w_k$

$x_w$  = arithmetic mean value over all measured x (centre of the calibration curve).

$$MU = \frac{t \times RSD}{b} \times \sqrt{\frac{1}{w_a} + \frac{1}{\sum w} + \frac{(y_a - y_w)^2}{b^2 \sum (x_a - y_w)^2}}$$

t = Student t factor (see also [159]). Here with  $p = 99 \%$  and  $n - 2$ .

RSD = Residual Standard Deviation

b = slope of the calibration curve ( $y = b * x + a$ ; with a as ordinate intercept)

$w_a$  = individual weighting factor at the corresponding concentration level

w = weighting factor

$y_a$  = signal response at corresponding concentration level

$y_w$  = arithmetic mean value over all obtained signal responses y (centre of the calibration curve)

$x_a$  = concentration level referring to  $w_a$

### 2.3.8 Principal Component Analysis (PCA)

For the qualitative evaluation of all samples analysed by HPLC and TLC the statistical method of principal component analysis (PCA) was used. This approach should lead to a graphical separation of all samples into certain clusters (e.g. expectably, clusters for Bser,

Bpap, Bsac and Bcar, if distinguishable among their HPLC/TLC results) on a two-dimensional plot, corresponding to their specific HPLC and/or TLC results.

PCA itself is a tool in multivariate data analysis to reduce the multidimensionality of complex data matrices and thus to better understand the variability structure of the data being questioned. Briefly, the aim of PCA is to reduce the variables ( $m$ , here the quantitative HPLC and qualitative TLC results of all analytes for each sample) of a data matrix through a lower number ( $h < m$ ) of mutual correlating factors (so called principal components or latent variables) in order to keep their original information preserved. The results of PCA give a simple graphical tool which enables by usage of a two dimensional plot the understanding of complex data sets qualitatively (e.g. here, correlation of analytes with a specific frankincense resin). However, for a thorough understanding of PCA methodology the corresponding literature may be consulted [164-166]. The technique is more and more used in the elucidation of significant parameters in complex biological matrices [167] and even to understand HPLC column systems for example [168]. Here it was used to graphically show the differences and commonalities for the species being investigated (Bpap, Bser and Bsac/Bcar).

The calculation itself was processed with the statistiXL software Add-In-tool for Microsoft Excel<sup>®</sup> 2003 from *statistiXL*, 3302 Broadway-Nedlands, Western Australia, 6009 (<http://www.statistixl.com/>). The following matrix parameters were used: The columns (variables) consisted of the compounds **1-6**, **11-16** (acid fraction compounds) and of **20-24** (neutral terpenic compounds) and of **28** ( $\beta$ -caryophyllene-oxide). Compounds **1-6**, **11-16** and **20-23** were quantified by HPLC analysis. Thus the found contents (% in g/g referring to the acid and neutral fraction, respectively) have been used for calculation. For compound **24** (verticillia-4(20),7,11-triene) and **28** ( $\beta$ -caryophyllene-oxide), which both were not quantified by HPLC, the column values were set to 0 = not detectable and 1 = detectable. This nominal scale has been chosen since both were only specifically found for Bpap (compound **24**, by GC and HPLC) and for Bsac/Bcar (compound **28**, by GC and TLC) in all here analysed samples. Though, if quantified (GC or HPLC), both also could be used metrically. However, the nominal scale (0 or 1) delivers, in a good approximation, the same solution for the PCA applied here (see table 3.37 in chapter 3.14). The matrix rows consisted of the samples Bpap ( $n = 10$ ), Bser ( $n = 14$ ), Bcar ( $n = 6$ ) and Bsac ( $n = 4$ ) as shown in table 3.37 in chapter 3.14. Descriptive Statistics, the Correlation Matrix standardized to S.D. = 1 (for strong deviating variances), the Scree-Plot, the Scatter Plot, the Casewise Scores and the Coefficients were included into the major plot. Some of the calculation data is presented in chapter 3.14.

### 2.3.9 HPLC Method (EUROPEAN PHARMACOPOEIA 6.0)

For comparison of the standard quantitation method described in chapter 2.3.4.2 the validated HPLC method described in the EUROPEAN PHARMACOPOEIA 6.0 for Indian Frankincense [20] (*Olibanum Indicum*, page 2128-2129) was implemented. This method does not require a separation of acid- and neutral fractions as  $\beta$ -KBA (**5**) and  $\beta$ -AKBA (**6**) are specifically detectable due to their good absorption at 250 nm wavelength. The method had been almost adapted; only TFA was used as mobile phase additive instead of phosphoric

acid. Importantly, it is based on a one-point calibration. Thus, there may be a rather significant uncertainty in the determined quantities, if the amounts of  $\beta$ -KBA (**5**) and  $\beta$ -AKBA (**6**) in the sample differ greatly from the amounts weighed in the test solution. However, the method has been thus far approved to be sufficient for its main purpose, at least for the species Bser.

HPLC-System: As described in chapter 2.3.4. Column: 1 x YMC-Pack Pro C18 RS, 250 x 4.6 mm I.D. S-5  $\mu$ m, 8 nm (YMC-Europe, Dinslaken, Germany). Mobile phase A: H<sub>2</sub>O + 0.1 % TFA. Mobile phase B: ACN + 0.1 % TFA. Flow rate: 1.0 ml/min. Detection: 250 nm. Injection: 100  $\mu$ L (20  $\mu$ L loop, overfilling). Gradient profile: From 84 % B to 94 % B in 12.5 min, then to 100 % B in 1 min, isocratic run at 100 % B for another 14.5 min and finally re-equilibration of the column for 15 min at 84 % B.

Test solution: To 1.0 g of the powdered sample 90 ml of MeOH were added and it was sonicated for 10 min. It was diluted to 100 ml with MeOH. After settling of the undissolved material, the colloidal solution was filtered (0.2  $\mu$ m, syringe filter) and 1 ml of the clear solution was diluted with 10 ml of a mixture of 16 volumes of mobile phase A and 84 volumes of mobile phase B. Reference solution:  $\beta$ -KBA (1.0 mg) and  $\beta$ -AKBA (1.0 mg) were dissolved in 20 ml MeOH and 1 ml of this solution was given to 10 ml of mobile phase A. Every sample was injected twice (test and reference solution) and values were accepted when the coefficient of correlation was less than 1 % (repeatability condition).

The percentage contents of  $\beta$ -KBA (**5**), respectively,  $\beta$ -AKBA (**6**) in the sample (test solution) were calculated using the following equation (one point calibration):

$$(\%KBA / AKBA) = \frac{A_1 \times m_1 \times 5 \times p_1}{A_2 \times m}$$

$A_1$  = area of the peak due to  $\beta$ -KBA, respectively,  $\beta$ -AKBA in the chromatogram obtained with the test solution;

$A_2$  = area of the peak due to  $\beta$ -KBA, respectively,  $\beta$ -AKBA in the chromatogram obtained with the reference solution;

$m$  = mass of the substance to be examined, in grams;

$m_1$  = mass of  $\beta$ -KBA, respectively,  $\beta$ -AKBA in the reference solution, in grams;

$p_1$  = percentage content of  $\beta$ -KBA, respectively,  $\beta$ -AKBA in the reference material of  $\beta$ -KBA, respectively,  $\beta$ -AKBA.

### 2.3.10 Gas Chromatography – Flame Ionisation Detector (GC-FID)

The gas chromatography device consisted of a GC 9000 series (9130, EL 980, VIC 900, FISOONS Instruments) system. Detection was realised by flame ionisation technique (FID). Clarity Lite software (DataApex, Prague, Czech Republic; version. 2.6.04.402) was used for data recording and processing. The injector temperature was adjusted to 250 °C and He was used as carrier gas (pressure: 14 psi). An Optima capillary column (1 : 0.25  $\mu$ m, 25 m x 0.25 mm, 340-360 °C max. Temp., Machery & Nagel, Düren, Germany) was applied as stationary phase. Samples were injected with a 1  $\mu$ L syringe (Hamilton, Bonaduz, Switzerland) by split and splitless injection. The following temperature gradient was used: 40 °C for 1 min, then 9

°C/min for 10 min to 130 °C, then 4 °C/min for 20 min to 210 °C, then 2 °C/min for 20 min to 250 °C, then constantly at 250 °C for another 10 min (Total time: 61 min) and afterwards cooling to 40 °C again. Kovats retention indices (*KI* or *RI*) [169] were obtained by injection of corresponding C<sub>8</sub> to C<sub>22</sub> homologue n-alkanes. The van den Dool variant of the Kovats equation had been used since a temperature gradient was performed [170], as given in the following equation:

$$RI_x = 100n + 100 \frac{t_x - t_n}{t_{x+1} - t_n}$$

*RI<sub>x</sub>* = Retention index (or Kovats index, *KI*)

*n* = number of C atoms (e.g. for C<sub>9</sub>, *n* = 9; for C<sub>10</sub>, *n* = 10, etc.)

*t<sub>n</sub>* = retention time of n-alkane with *n* C atoms, eluting in front of compound *x* (*x* = unknown peak signal)

*t<sub>x+1</sub>* = retention time of n-alkane with *n*+1 C atoms, eluting after compound *x* (*x* = unknown peak signal)

*t<sub>x</sub>* = retention time of unknown peak signal *x*

## 2.4 Spectroscopy

### 2.4.1 Mass Spectrometry (MS)

Mass spectrometric data was recorded on a Finnigan MAT 95S spectrometer (CI mode; HRMS) and a ZQ 4000-ESI-Mass spectrometer (ESI; Single quadrupol) from Waters (Eschborn, Germany) at the Department of Organic Chemistry at the Saarland University. The LC-MS conditions for the detection of compound **18** and **19** in the isolated mixture (see chapter 3.2.3 and 3.2.4) were as follows: ZQ 4000-ESI-MS (Single quadrupol); isocratic elution with solvent A (MeOH + 0.1 % HCOOH); flow rate (0.3 ml/min); run time (60 min); column (YMC-Pack-Pro C18 RS, 250 x 4.6 mm I.D., S-5 μm, 8 nm); UV detection (210 nm); ESI negative mode for molecular ion detection. The chromatograms are shown in chapter 3.2.3, respectively, 3.2.4.

### 2.4.2 Nuclear Magnetic Resonance Spectroscopy (NMR)

NMR experiments were carried out on 400 MHz (AV 400) and 500 MHz (AV 500) NMR spectrometers from Bruker (Rheinstetten, Germany). CDCl<sub>3</sub> was purchased from Sigma Aldrich (Steinheim, Germany). For structural assignment of the isolated compounds <sup>1</sup>H, <sup>13</sup>C, HH-COSY, HSQC, HMBC, 2D-NOESY, DEPT 90 and DEPT 135 spectra were recorded in CDCl<sub>3</sub>. The data was processed with MestReC software, version 4.9.9.6 (Mestrelab Research S.L.). NMR spectra were calibrated against the residual solvent peak δ<sub>C</sub>(CDCl<sub>3</sub>) = 77.0 ppm and δ<sub>H</sub>(CDCl<sub>3</sub>) = 7.26 ppm.

### 2.5 Pharmacological Assays

The pharmacological investigations were carried out at the University of Tübingen, Germany, in the Department of Biopharmaceutical Analytics under supervision of Prof. Dr. Oliver Werz (now Professor at the University of Jena, Germany). The experiments were conducted by Moritz Verhoff and/or Daniela Müller. A few of the here isolated compounds were sent there to evaluate their actions on the microsomal prostaglandin E2 synthase-1 (mPGES-1) in a cell-free assay with the microsomal preparations of Interleukin 1 $\beta$  (IL-1 $\beta$ ) stimulated A549 cells [102]. In the corresponding discussion (chapter 3.12), the results from compound **23** (Inc-Ac) and its decomposition products (chapter 3.11.2) and the data of the isolated peak mixture, including compound **18** and **19**, from Fraction 9 (see chapter 3.1.1.3) are presented.

#### 2.5.1 Purification of A549 Microsomes

A549 cells were cultured in DMEM/high glucose (4.5 g/ml) medium supplemented with heat-inactivated fetal calf serum (10 %, v/v), penicillin (100 U/ml) and streptomycin (100 lg/ml) at 37 °C in a 5 % CO<sub>2</sub> incubator.

After 20 h, the medium was changed to DMEM/high glucose (4.5 g/ml) medium supplemented with heat-inactivated fetal calf serum (2 %, v/v), penicillin (100 U/ml) and streptomycin (100 lg/ml), and cells were stimulated with 2 ng/ml IL-1 $\beta$  for 72 h. After 72 h, the cells were detached using 1 x trypsin/EDTA. After a wash step with PBS, pH 7.4, the pellet was frozen in liquid N<sub>2</sub> and re-suspended in ice-cold homogenisation buffer (0.1 M potassium buffer, 250 mM sacharose, 1 mM PMSF, 60  $\mu$ g/ml STI, 1  $\mu$ g/ml Leupeptin, 2.5 mM GSH) and sonicated at low density (3 x 20 s).

The homogenate was first centrifuged at 10000 g for 10 min and then the supernatant was centrifuged at 174000 g for 1 h. The pellet (microsomal fraction) was then re-suspended in 1 ml homogenisation buffer. The total protein concentration was determined by the Coomassie protein assay [171]. The microsomal fraction can be stored at -80 °C for several months [102,103,172].

#### 2.5.2 Determination of PGE<sub>2</sub> Synthase Activity in Microsomes of A549 Cells

Microsomal membranes of A549 cells were diluted in 0.1 M potassium phosphate buffer, pH 7.4, containing 2.5 mM glutathione (total volume, 100  $\mu$ l), and test compounds or vehicle (DMSO) were added. After 15 min, PGE<sub>2</sub> formation was initiated by addition of PGH<sub>2</sub> (final concentration, 20  $\mu$ M). After 1 min at 4°C, the reaction was terminated with 100  $\mu$ l of stop solution (40 mM FeCl<sub>2</sub>, 80 mM citric acid, and 10  $\mu$ M 11 $\beta$ -PGE<sub>2</sub>), and PGE<sub>2</sub> was separated by solid-phase extraction on reversed phase (RP)-C18 material using acetonitrile (200  $\mu$ l) as eluent and analysed by RP-HPLC [30% aqueous acetonitrile + 0.007% trifluoroacetic acid (v/v); Nova-Pak C18 column, 5 x 100 mm, 4- $\mu$ m particle size, flow rate 1 ml/min], with UV detection at 195 nm. 11 $\beta$ -PGE<sub>2</sub> was used as internal standard to quantify PGE<sub>2</sub> product formation by integration of the area under the peaks [102,103,172].

## 2.6 Stability Tests and Estimation of Decomposition Kinetics

### 2.6.1 Decomposition Tests with Inc-Ac (room temperature and 60 °C)

Decomposition tests were carried out with the purified compound **23** (see chapter 3.1.1). This was done, since it was realised that not compound **23** (Inc-Ac) had been responsible for the firstly observed inhibitory effects in the mPGES1-Assay; instead a great amount of decomposition compounds, originating from **23**, have been responsible for the inhibition. The same discussion is basically valid for compound **22** (Inc), where a similar behaviour was noticed (data not shown). Thus, these compounds, even if stable for a long time in the NB fraction and at low temperatures (4 °C or -30 °C), are vulnerable to oxidation at higher temperatures (air exposure effects and thus kinetics are temperature dependent) when purified as single compounds. Aliquots (EC) of the isolated compounds were therefore tested under air-exposition for a certain time at room temperature and in a compartment drier at 60 °C to test their stability. The following experiments were carried out with an aliquot of compound **23** (Note that for Test 1-4 the same sample was used):

**Test 1:** Stability test for 7 days at room temperature. The sample of compound **23** (2.5 mg) was stored in an EC (with lid open for air exposure). After 7 days it was analysed by HPLC (Standard Quantitation Method as described in chapter 2.3.4.2). Therefore, the sample was dissolved in 1 ml MeOH ( $c = 2.5 \text{ mg/ml}$ ) and 100  $\mu\text{l}$  thereof were used for injection (HPLC). The remaining 900  $\mu\text{l}$  were dried (slight  $\text{N}_2$ -stream at room temperature) and used for the next test (Test 2).

**Test 2:** Stability test for 16 h at 60 °C in a compartment drier. The sample of compound **23** (2.3 mg, from Test 1) was stored in an EC (with lid open for air exposure). After 16 h it was analysed by HPLC (Standard Quantitation Method as described in chapter 2.3.4.2). The sample was dissolved in 1 ml MeOH ( $c = 2.3 \text{ mg/ml}$ ) and 100  $\mu\text{l}$  thereof were used for injection (HPLC). An Aliquot (400  $\mu\text{l}$ ) was saved and stored at 4 °C in a refrigerator. The remaining 500  $\mu\text{l}$  were dried (slight  $\text{N}_2$ -stream at room temperature) and used for the next test (Test 3).

**Test 3:** Stability test for another 15 h at 60 °C in a compartment drier. The sample of compound **23** (1.2 mg, from Test 2) was stored in an EC (with lid open for air exposure). After 15 h it was analysed by HPLC (Standard Quantitation Method as described in chapter 2.3.4.2). The sample was dissolved in 1 ml MeOH ( $c = 1.2 \text{ mg/ml}$ ) and 100  $\mu\text{l}$  thereof were used for injection (HPLC). No Aliquot was saved. The remaining 900  $\mu\text{l}$  were dried (slight  $\text{N}_2$ -stream at room temperature) and used for the next test (Test 4).

**Test 4:** Stability test for another 16 h at 60 °C in a compartment drier. The sample of compound **23** (1.0 mg, from Test 3) was stored in an EC (with lid open for air exposition). After 16 h it was analysed by HPLC (Standard Quantitation Method as described in chapter 2.3.4.2). The sample was dissolved in 1 ml MeOH ( $c = 1.0 \text{ mg/ml}$ ) and 100  $\mu\text{l}$  thereof were used for injection (HPLC). The remaining 900  $\mu\text{l}$  were dried (slight  $\text{N}_2$ -stream at room temperature) and stored at 4 °C in a refrigerator.

Finally, the decomposed samples from Test 2, Test 4 and an intact sample of Inc-Ac (**23**, purity > 99 %, HPLC) were sent to the laboratory of the University of Tübingen for mPGES-1 testing. Hence, to prove the theory that only the decomposition products of Inc-Ac (+/- Inc-Ac itself) are responsible for the enzyme inhibition (see also chapter 3.12). The results of the decomposition tests are presented in chapter 3.11.2.

### 2.6.2 Kinetic Study of the Decomposition of Inc-Ac

Since purified Inc (**22**) and Inc-Ac (**23**) revealed a low stability under air-exposure and room or higher temperatures, the quantitative HPLC results (see chapter 2.6.1) were used to give an estimation of the reaction kinetics underlying their decomposition. For basic explanations on reaction kinetics in chemistry please view the literature (e.g. [173,174]). The reaction order of the decomposition of Inc-Ac (**23**) obeys most probably a first order reaction kinetic (Note: Probably, the decomposition is pseudo first order due to the excess of oxygen in the air), leading to the following reaction rate law:

$$v(A) = -\frac{dc(A)}{dt} = k \times c(A) \quad \text{or} \quad \frac{dc(A)}{c(A)} = -k \times dt$$

Integration of this expression leads to the linear and exponential function terms:

$$\ln c(A) = -k \times t + \ln c_0(A) \quad \text{or} \quad c(A) = c_0(A) \times e^{-kt}$$

$v(A)$  = reaction rate (here first order kinetics)

$c(A)$  = concentration of compound A

$c_0(A)$  = concentration of compound A at the beginning of the reaction

$dc(A)$  = change of concentration of compound A dependent on time

$t$  = time

$dt$  = change of time

$k$  = reaction rate constant

## 2.7 Partial- and Semi-Synthetic Procedures

### 2.7.1 Semi Synthesis of Compound 19 from Compound 15

3 $\beta$ -OH-8,24-dien-tirucallic acid (compound **15**; 21.5 mg, 0.047 mmol) was dissolved in DCM (5 ml). Pyridine (0.015 ml, 0.188 mmol), acetic anhydride (0.011 ml, 0.118 mmol) and DMAP (2.59 mg, 0.021 mmol) were successively added. The reaction mixture was refluxed for ca. 4 h. After cooling to room temperature, the reaction was quenched with 10 ml ice-cold 1M HCl and the organic phase was separated. The aqueous phase was extracted with 3 x Et<sub>2</sub>O and the combined organic phases were dried with MgSO<sub>4</sub>, filtered and evaporated to give the final product (white solid; ca. 19 mg; yield: ca. 81 %). Optional: Purification by liquid column chromatography or preparative HPLC. The product was used as co-injection standard for the structure verification of compound **19** (see also chapter 3.2.4).

### 2.7.2 Isolation and Semi-Synthesis of Inc and Inc-Ac

*Acetylation of the Neutral fraction from Boswellia papyrifera:* 25 g of the orange coloured neutral compounds were dissolved in 30 ml dichloromethane in a 500 ml three-necked flask. 18 ml of pyridine (17.4 g, 0.22 mol), 20.4 ml of acetic anhydride (20.4 g, 0.2 mol) and 3 g DMAP (0.025 mol) were added successively. The temperature was raised till the reaction mixture started gently to reflux. It was stirred for 4 hours. After the reaction was complete, the mixture was quenched with 300 ml 1 N HCl. Phases were separated and the aqueous phase was extracted with diethyl ether (3 x ca. 100 ml). The combined organic phases were dried with MgSO<sub>4</sub> and after filtration and evaporation in vacuo orange oil was obtained (yield: 28.7 g).

*Isolation of Incensole acetate (flash and instrumental preparative chromatography):* The orange oil (28.7 g) was dissolved in 30 ml DCM. Normal phase silica gel flash chromatography (column diameter: 10 cm) was performed by using an eluent consisting of 6 parts petroleum ether and one part diethyl ether (6:1). 14 fractions were collected. All fractions were evaporated in vacuo. Each fraction contained yellow oil. Fraction 2 (3.1 g, 43 % **23**), 3 (6.9 g, 85 % **23**) and 4 (2.2 g, 61 % **23**) contained incensole acetate in large quantities. Fraction 3, as the purest fraction (85 % by HPLC control), was further purified by preparative HPLC. The whole amount of fraction 3 (6.9 g) was dissolved in 100 ml methanol, sonicated and 30 mL (2.07 g) of this solution were filtered (0.2 µm) and used for preparative HPLC (The remaining 70 ml, 4.83 g, were evaporated again and stored at – 30 °C). The following HPLC conditions were used: As preparative column a YMC-Pack Pro C18 RS (250 x 20 mm I.D. S-5 µm, 8 nm; YMC, Dinslaken, Germany) served; flow rate = 19 ml/min; T = room temperature (ca. 25 °C); eluent: 100 % methanol, injection volume = 3 mL, total injections = 10 (30 ml, c = 69 mg/ml); three fractions were collected (see chapter 3.11.1). The middle fraction contained 1.28 g (yield: 62 % of total 2.07 g) referring to compound **23** with a purity higher 99 %. The remaining fraction 3 (4.8 g) is stable at -30 °C (at least for 12 month, probably even longer, not tested anymore). For further details see chapter 3.11.

Note: Alternative preparation conditions on a NUCLEODUR 100-5 C18 ec, 250 x 21 mm I.D., Machery & Nagel, Düren, Germany, preparative column: flow rate = 27.6 ml/min; T = room temperature, ca. 25 °C; eluent: methanol 96 % and water 4 %. These conditions gave similar resolution for purifying incensole acetate.

*Deacetylation of Incensole acetate:* The isolated incensole-acetate (350 mg, 1 mmol) was dissolved in 10 ml 1 N KOH in *i*PrOH. The reaction mixture was refluxed for 3 hours. After cooling to room temperature, the *i*PrOH was mostly removed in vacuo. The remaining residue was acidified with 20 ml 1 N HCl and extracted with dichloromethane (3 x 10 ml). The combined organic extracts were dried with MgSO<sub>4</sub>. After filtration, the solvent was evaporated in vacuo to give colourless oil (yield: 268 mg, 0.87 mmol, ca. 90 %; purity: > 99 %). Optional: purification by column chromatography or preparative HPLC.

*Acetylation of Incensole:* Incensole (25.0 mg, 82 µmol) was dissolved in 5 ml DCM, 30 µL of pyridine (30 µg, 372 µmol), 33 µL of acetic anhydride (32 µg, 326 µmol) and 6 mg of DMAP

## Experimental Part

---

(49  $\mu\text{mol}$ ) were added successively. The reaction mixture was heated until it started gently to reflux. It was stirred for 4 hours at that temperature. After the reaction was complete, the mixture was cooled to room temperature and quenched with 40 ml 1 N HCl. The organic phase was saved and the aqueous phase was extracted with diethyl ether (3 x ca. 10 ml). The combined organic phases were dried with  $\text{MgSO}_4$  and after filtration and evaporation in vacuo colourless oil was obtained (yield: 26.6 mg, 76  $\mu\text{mol}$ , ca. 93 %; purity: > 98 %).  
Optional: Purification by column chromatography or preparative HPLC.

### 3. Results and Discussion

#### 3.1 Isolation of Biomarker Compounds

##### 3.1.1 Isolation of Compounds from *Boswellia papyrifera* (Bpap)

###### 3.1.1.1 Isolation of Incensole (22) and Incensole Acetate (23)

An extract of Bpap (AS-050509-E2h) from the AureliaSan GmbH, Bisingen (Germany), which is used for an ointment formulation, was investigated in order to find pharmacologically interesting ingredients. Therefore 4 g, dissolved in 3 ml DCM, of the yellow powder were subjected on a normal phase silica gel column (diameter: 5 cm) and fractionated using the standard step gradient and fraction collection method as described in chapter 2.3.2. The chromatography was monitored by TLC and 13 fractions were combined. All fractions were evaporated in vacuo. Fr. 2 (90 mg; clear oil and minor particles) and Fr. 7 (170 mg; clear oil) were further purified by preparative HPLC. Fr. 2 contained incensole acetate (23). The purifying conditions were: NUCLEODUR C18 prep column; T = 25 °C; eluent = MeOH : H<sub>2</sub>O (98 : 2); flow rate = 25 ml/min; c = 6.7 mg/ml in MeOH; 4 ml each injection; yield: 26.9 mg; purity > 99 % (HPLC). Fr. 7 contained incensole (22). The purifying conditions were: NUCLEODUR C18 prep column; T = 25 °C; eluent = MeOH : H<sub>2</sub>O (95 : 5); flow rate = 25 ml/min; c = 13.8 mg/ml in MeOH; 5 ml each injection; yield: 23.0 mg; purity > 99 % (HPLC). The structures are presented in Fig. 3.1.

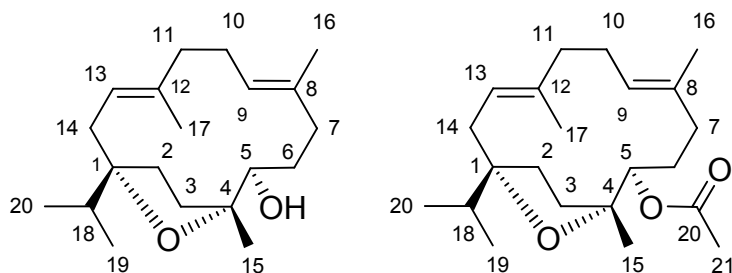


**Fig. 3.1** Structures of incensole **22** (left) and incensole acetate **23** (right).

###### 3.1.1.2 Isolation of Verticillia-4(20),7,11-triene (24)

Verticillia-4(20),7,11-triene (24) was isolated from the neutral compounds of Bpap described in chapter 3.11.1. Fr. 1 (500 mg) of the by column chromatography separated fractions contained this compound. It was further purified through following preparative HPLC conditions: NUCLEODUR C18 prep column; T = 25 °C; eluent = MeOH (100 %); flow rate = 25 ml/min; c = 10 mg/ml in MeOH; 4 ml each injection; yield: 31.6 mg; purity > 98 % (HPLC). The structure is shown in Fig. 3.2.

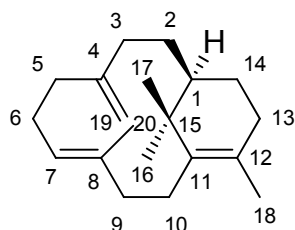


**Fig. 3.2** Structure of verticillia-4(20),7,11-triene (**24**).

### 3.1.1.3 Isolation of 3 $\alpha$ -O-Acetyl-7,24-dien-tirucallic acid (18) and 3 $\beta$ -O-Acetyl-8,24-dien-tirucallic acid (19)

The compounds 3 $\alpha$ -Ac-7,24-dien-TA (18) and 3 $\beta$ -Ac-8,24-dien-TA (19) were firstly found in the Bpap extract (AS-050509-E2h; AureliaSan GmbH) described in section 3.1.1.1. Fr. 9 (429 mg) of this extract (AS-050509-E2h) contained a not verified peak signal, which revealed an interesting chromatographic behaviour. In Figures 3.3 and 3.4 this behaviour is depicted. Interestingly, the presumed homogenous peak signal was separable into three further signals when a column with a higher carbon load density had been used. Conditions for the isolation (prep HPLC) of the peak signal shown in Fig. 3.3 and 3.4: NUCLEODUR C18 prep column; T = 25 °C; eluent = MeOH : H<sub>2</sub>O (97 : 3); flow rate = 25 ml/min; c = 6.6 mg/ml in MeOH; 5 ml each injection; 9 sub fractions were collected; fraction 6 contained the peak signal with a overall yield of 25.1 mg.

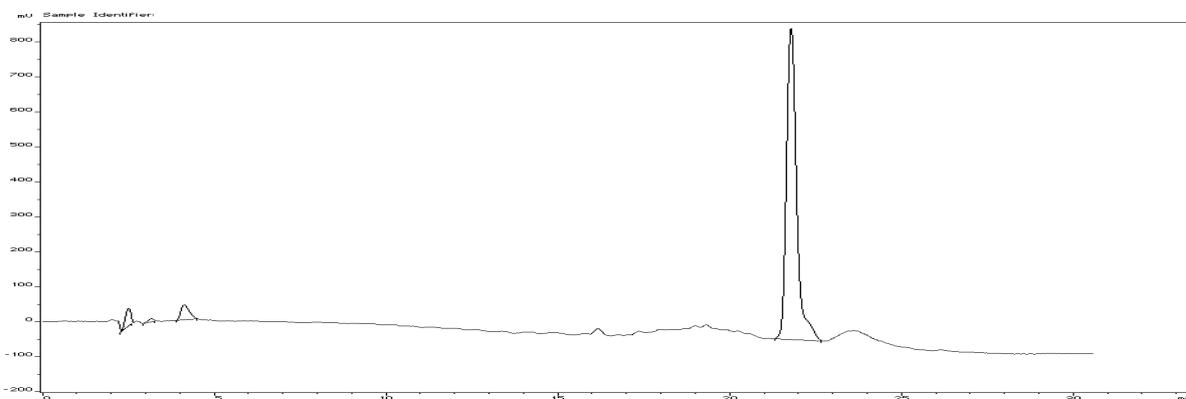


**Fig. 3.3** Qualitative standard gradient chromatogram (210 nm) of the isolated compound from Fr. 9 on a NUCLEODUR C18 analytical column (250 x 4 mm I.D., 100-5 ec). The peak appears as an almost homogenous signal ( $R_t$  = ca. 22 min). HPLC conditions: T = 25 °C; u = 0.85 ml/min; Solvent A = MeOH; Solvent B = H<sub>2</sub>O + 0.1 % TFA; Gradient: 0-1 min at 15 % B, 1-13 min gradient to 0 % B, 13-45 min 0 % B (isocratic).

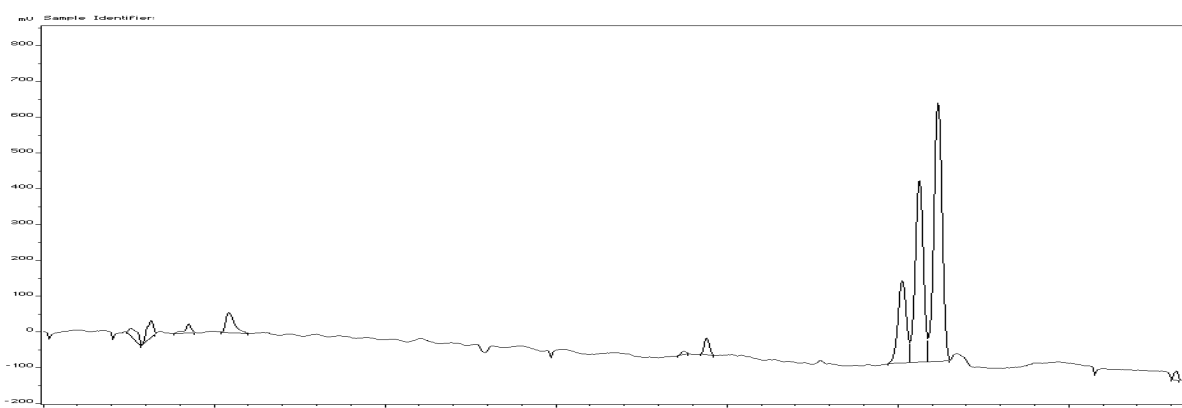


**Fig. 3.4** Qualitative standard gradient chromatogram (210 nm) of the isolated compound from Fr. 9 on a YMC-Pack Pro C18 RS analytical column (250 x 4.6 mm I.D.; S-5  $\mu$ m, 8 nm). The peak resolves into three signals ( $R_t$  = 25.2, 25.5 and 26.3 min). Peak 2 and 3 are 3 $\alpha$ -Ac-7,24-dien-TA (Peak 3;  $R_t$  = 26.3 min; rel. peak area: 46 %) and 3 $\beta$ -Ac-8,24-dien-TA (Peak 2;  $R_t$  = 25.5 min; rel. peak area: 32 %). Peak 1 is unknown (rel. peak area: 16 %). HPLC conditions as described in Fig. 3.3 above.

## Results and Discussion

Since the yield (only 25 mg) of these three compounds isolated from Fr. 9 was too low for an adequate isolation of single compounds, a new extract with more resin material from Bpap was made.

Therefore 19 g, dissolved in 50 ml DCM, of the Bpap acid fraction of a newly made extract were subjected on a normal phase silica gel column (diameter: 10 cm) and fractionated using the standard step gradient and fraction collection method as described in chapter 2.3.2. The chromatography was monitored by TLC and 12 fractions were combined. All fractions were evaporated in vacuo. Fr. 5 (2 g, white solid) contained the target compounds. However, only peak 2 and 3 were found again as shown in Fig. 3.5. The first minor peak was not detectable anymore in this extract (proved by co-injection of both fractions; compare also with Fig. 3.4). Fr. 5 was further purified by preparative HPLC. The purifying conditions were: NUCLEODUR C18 prep column; T = 25 °C; eluent = MeOH : H<sub>2</sub>O (98 : 2); flow rate = 25 ml/min; c = 17.9 mg/ml in MeOH; 5 ml each injection; 4 further fractions were collected (Nr. 1 – 4); Nr. 2 was the target compound containing peak 2 and 3 eluting as one peak on a NUCLEODUR C18 prep/analytical column; yield: 92.0 mg; purity > 99 % (HPLC).

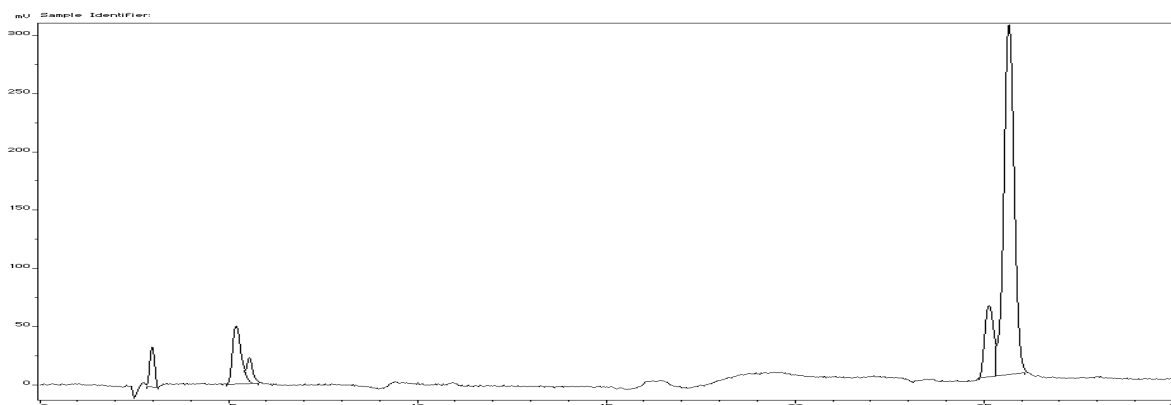


**Fig. 3.5** Qualitative standard gradient chromatogram (210 nm) of the isolated compounds from Fr. 5 on a YMC-Pack Pro C18 RS analytical column (250 x 4.6 mm I.D.; S-5  $\mu$ m, 8 nm). The peak resolves into two signals. The minor peak eluting at front refers to 3 $\beta$ -Ac-8,24-dien-TA (rel. peak area: 19 %) and the main peak to 3 $\alpha$ -Ac-7,24-dien-TA (rel. peak area: 80 %). HPLC conditions as described in Fig. 3.3.

Fraction Nr. 2 was thus further purified with following conditions: YMC-Pack Pro C18 RS prep column; T = 25 °C; eluent = MeOH (100 %); flow rate = 19 ml/min; c = 3.7 mg/ml in MeOH; 3 ml each injection; 3 fractions were obtained of which the third fraction contained compound  $\alpha$ -Ac-7,24-dien-TA (**18**); yield: 17.0 mg; purity > 95 % (HPLC). Note that the peak was not baseline separated and thus only the last fraction, fraction 3, could be purified sufficiently enough for an unequivocal NMR structure elucidation. Fraction 1 and 2 were a combination of compound **18** and **19** in differing percentages, whereas the material of Fr. 1 was negligible and Fr. 2 delivered 41 mg. The structure is presented in Fig. 3.6.

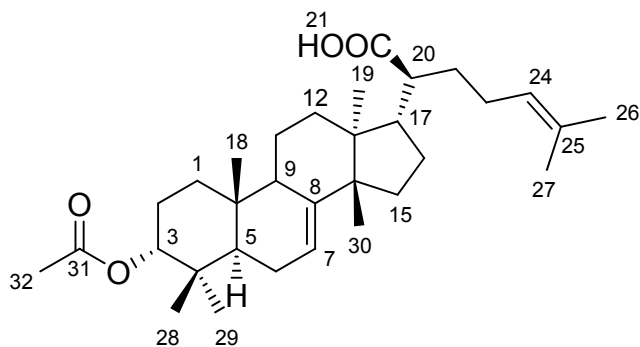


**Fig. 3.6** Structure of 3 $\alpha$ -O-acetyl-7,24-dien-tirucallic acid (**18**).

The separation of 3 $\beta$ -Ac-8,24-dien-TA (**19**) from 3 $\alpha$ -Ac-7,24-dien-TA (**18**) was more difficult and appeared to be infeasible on a conventional preparative HPLC column (20 mm I.D.). However, since the resolution on the preparative scale was not implementable, it was realised by preparative chromatography on the analytical HPLC device. Therefore the 20  $\mu$ l injection loop was replaced by a self-made injection loop (PEEK Tubing; 0.75 mm I.D.; length = 32 cm) with a thus resulting injection volume of approximately 140  $\mu$ l.

Following conditions were used: 2 x YMC-Pack Pro RS C18 analytical in row; T = 30  $^{\circ}$ C; eluent = MeOH (100 %); flow rate = 1.0 ml/min; c = 1.3 mg/ml in MeOH (Fr. 2, 41 mg, from the first separation was therefore used); 100  $\mu$ l per injection; yield of compound  $\beta$ -Ac-8,24-dien-TA (**19**) = 1.2 mg; purity > 99 % (HPLC). An example chromatogram is shown in Fig. 3.7 and the structure is presented in Fig. 3.8.

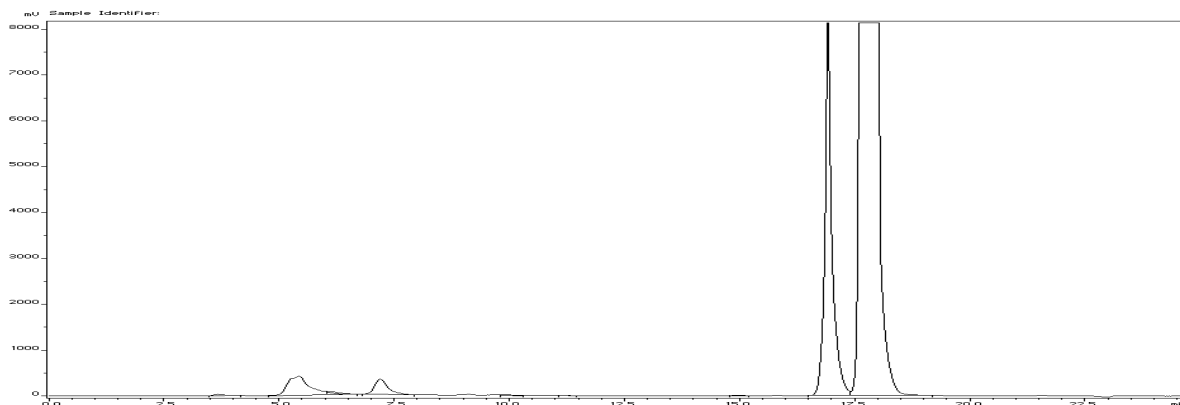


**Fig. 3.7** Preparative chromatogram (210 nm) on the analytical HPLC device. Peak 1 ( $R_t$  = 16.9 min) = 3 $\beta$ -O-acetyl-8,24-dien-tirucallic acid and Peak 2 ( $R_t$  = 18.0 min) = Structure of 3 $\alpha$ -O-acetyl-7,24-dien-tirucallic acid. For further details see text.

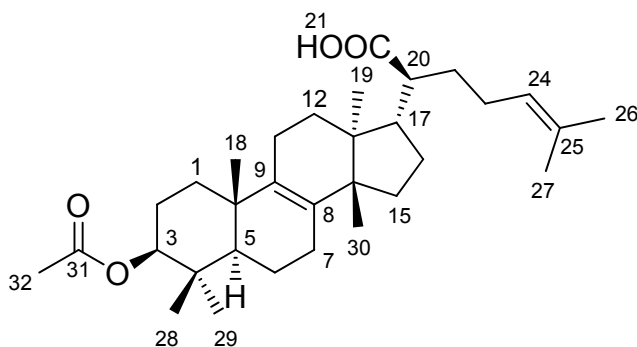


**Fig. 3.8** Structure of 3 $\beta$ -O-acetyl-8,24-dien-tirucallic acid (**19**).

### 3.1.2 Isolation of Compounds from *Boswellia carterii* (Bcar)

#### 3.1.2.1 Isolation of $\beta$ -Caryophyllene oxide (**28**) and Serratol (**21**)

The yellow-orange oil (5 g, neutral compounds) of Bcar was dissolved in 5 ml DCM, subjected on a normal phase silica gel column (diameter: 5 cm) and fractionated using the standard step gradient and fraction collection method as described in chapter 2.3.2. The chromatography was monitored by TLC and 14 fractions were combined. All fractions were evaporated in vacuo. Fr. 5 (325 mg) contained  $\beta$ -Car-Ox (**28**) and Ser-OH (**21**) and was further purified by preparative HPLC. Conditions for the isolation of  $\beta$ -Car-Ox (**28**) and Ser-OH (**21**): NUCLEODUR C18 prep column; T = 25 °C; eluent = MeOH (100 %); flow rate = 25 ml/min; c = 16.3 mg/ml in MeOH; 5 ml each injection; yield: 200 mg, containing  $\beta$ -Car-Ox (**28**) and Ser-OH (**21**). Pure  $\beta$ -Car-Ox (**28**) and Ser-OH (**21**) were obtained by following chromatographic conditions: YMC-Pack Pro C18 RS prep column; T = 25 °C; eluent = MeOH : H<sub>2</sub>O (98 : 2); flow rate = 19 ml/min; c = 13.3 mg/ml; 5 ml each injection; three fractions were collected: Fr. 1 = 58 mg of  $\beta$ -Car-Ox (**28**) with a purity > 98 %; Fr. 3 = 82 mg of Ser-OH (**21**) with a purity > 99 %. The structures are shown in Fig. 3.9.

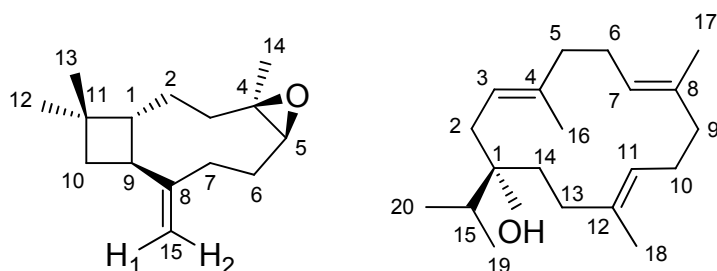


**Fig. 3.9** Structures of  $\beta$ -caryophyllene oxide **28** (left) and serratol **21** (right).

#### 3.1.2.2 Isolation of $\tau$ -Cadinol (**25**) and Iso-Serratol (**20**)

Fr. 10 (417 mg) of the separated Bcar extract contained  $\tau$ -cadinol (**25**) and iso-serratol (**20**). The purifying conditions were as follows: NUCLEODUR C18 prep column; T = 25 °C; eluent = MeOH (100 %); flow rate = 25 ml/min; c = 13.9 mg/ml in MeOH; 5 ml per injection; yield: 94 mg, containing  $\tau$ -cadinol (**25**) and iso-serratol (**20**). Purification was achieved by following conditions: YMC-Pack Pro C18 RS prep column; T = 25 °C; eluent = MeOH : H<sub>2</sub>O (98 : 2); flow rate = 19 ml/min; c = 6 mg/ml; 5 ml each injection; two fractions were collected: Fr. 1 = 36 mg of  $\tau$ -cadinol (**25**) with a purity > 97 %; Fr. 2 = 40 mg of iso-serratol (**20**) with a purity > 99 %. The structures are shown in Fig. 3.10.

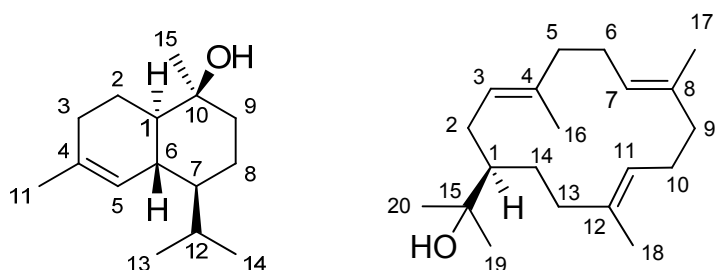


**Fig. 3.10** Structures of  $\tau$ -cadinol **25** (left) and iso-serratol **20** (right).

### 3.1.2.4 Isolation of Incensole (22) and 3- $\beta$ -OH-Tirucallol (29)

Fr. 12 (185 mg) of the separated Bcar extract contained incensole (22) already isolated from Bpap and 3- $\beta$ -OH-tirucallol (29). The purifying conditions were as follows: NUCLEODUR C18 prep column; T = 25 °C; eluent = MeOH (100 %); flow rate = 25 ml/min; c = 9.3 mg/ml in MeOH; 5 ml per injection; two fractions were collected: Fr. 1 = 66.5 mg (containing incensole) and Fr. 2 = 10.5 mg (3- $\beta$ -OH-tirucallol) with a purity > 93 %. Incensole was further purified with following conditions: YMC-Pack Pro C18 RS prep column; T = 25 °C; eluent = MeOH : H<sub>2</sub>O (98 : 2); flow rate = 19 ml/min; c = 4.4 mg/ml; 5 ml each injection; yield: 11 mg with a purity > 98 %. The structure of 3- $\beta$ -OH-tirucallol is shown in Fig. 3.11 and the structure of incensole is already presented in section 3.1.1.1.

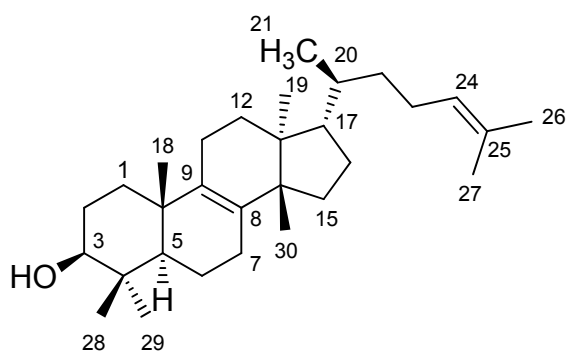
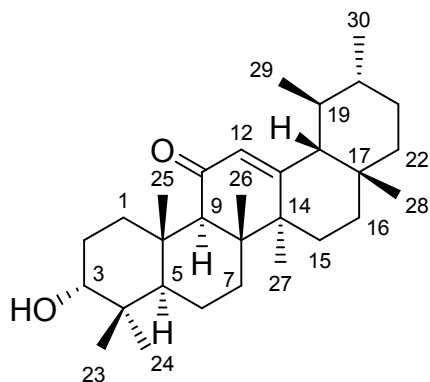


Fig. 3.11 Structure of 3- $\beta$ -OH-tirucallol (29).

### 3.1.2.5 Isolation of 3- $\alpha$ -OH-11-Keto-12-ursen (30)

3- $\alpha$ -OH-11-Keto-12-ursen (30) was isolated from another Bcar neutral compound extract. Therefore, 3 g from the neutral compounds were separated on a normal phase silica gel column (diameter: 2.5 cm) using the standard step gradient and fraction collection method as described in chapter 2.3.2. The chromatography was monitored by TLC and combined to 8 fractions. All fractions were evaporated in vacuo. Fr. 8 (805 mg) contained 3- $\alpha$ -OH-11-keto-12-ursen (30) and was further purified by preparative HPLC. The following conditions were implemented: NUCLEODUR C18 prep column; T = 25 °C; eluent = MeOH : H<sub>2</sub>O (98 : 2); flow rate = 25 ml/min; c = 16.0 mg/ml in MeOH; 5 ml each injection; two fractions were collected; Fr. 2 contained 3- $\alpha$ -OH-11-keto-12-ursen (30); yield: 42.8 mg. This fraction was further purified. Conditions: YMC-Pack Pro C18 RS prep column; T = 25 °C; eluent = MeOH : H<sub>2</sub>O (98 : 2); flow rate = 19 ml/min; c = 4.3 mg/ml; 3 ml each injection; yield: 10 mg with a purity > 92 %. The structure of 3- $\alpha$ -OH-11-Keto-12-ursen is shown in Fig. 3.12.



**Fig. 3.12** Structure of 3- $\alpha$ -OH-11-keto-12-ursen (**30**).

## 3.2 Spectroscopic Data

### 3.2.1 Incensole (**22**)

Incensole was isolated as colourless viscous oil. The structure is shown in Fig. 3.13. Analysis by TLC (Pentane/Et<sub>2</sub>O 2:1 and 1 % HOAc) showed a strong brown spot after dyeing and heating with anisaldehyde reagent at  $R_f = 0.27$ . Detection by DAD-RP-HPLC was only possible at 210 nm and the compound eluted at a  $R_t$  value of ca. 25.9 min under standard HPLC conditions (2.3.4.2). Mass spectrometric detection (CI-MS; low resolution) delivered the following significant fragmentation pattern:  $m/z$  (%): 306.4 [M]<sup>+</sup> (43); 289.2 (10); 155.1 (35); 125.1 (70); 83.9 (100); 71.0 (50). The <sup>13</sup>C-NMR spectrum revealed 20 carbon atom signals as presented in Fig. 3.14. DEPT 90/135 spectra divided these 20 C-atoms into 4 quaternary, 4 CH-, 7 CH<sub>2</sub>- and 5 methyl carbon atoms. The <sup>1</sup>H-spectrum is shown in Fig. 3.15 and the further structural elucidation by conventional 2D-NMR techniques (HSQC, COSY, NOESY, and HMBC) is basically presented in Tab. 3.1.

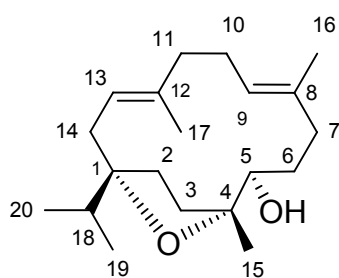


**Fig. 3.13** Structure of incensole (**22**).

## Results and Discussion

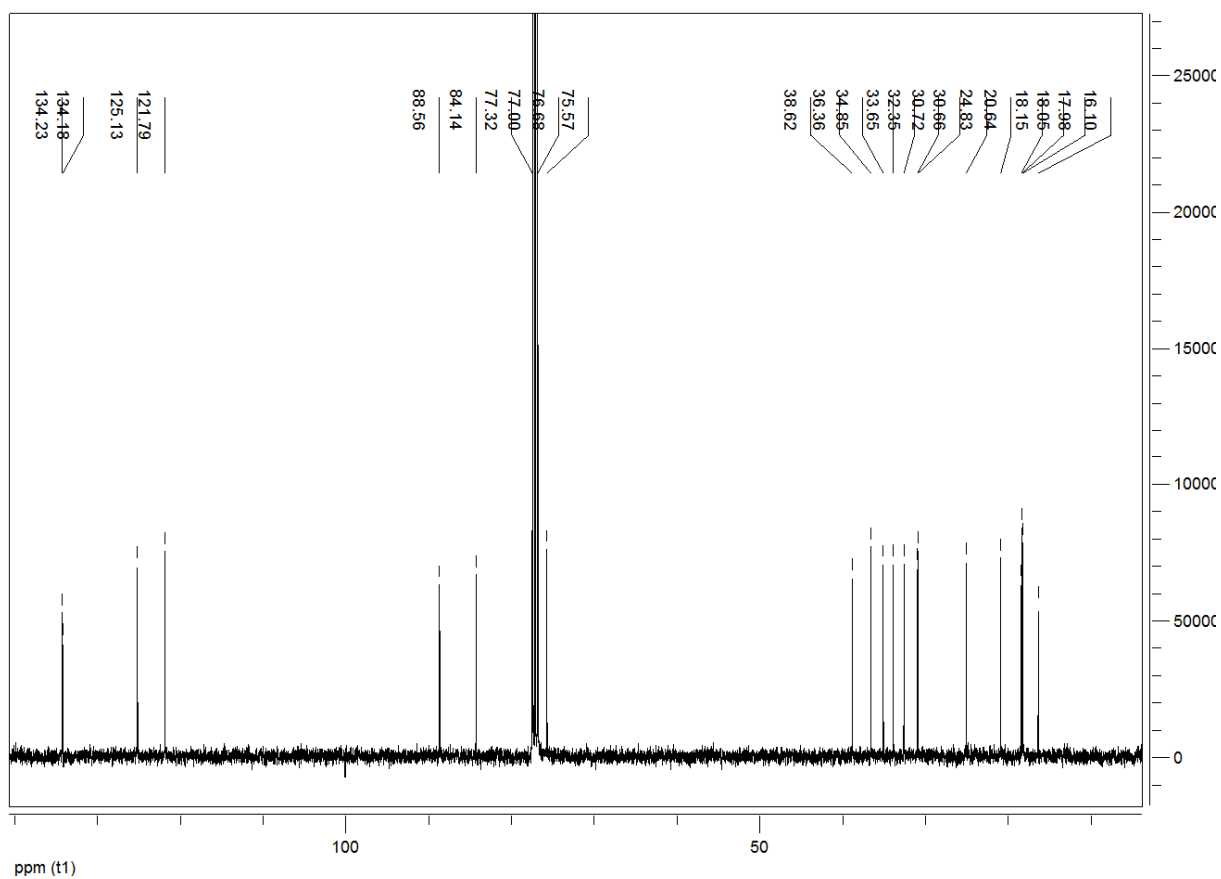


**Fig. 3.14** <sup>13</sup>C-NMR spectrum of incensole (22).

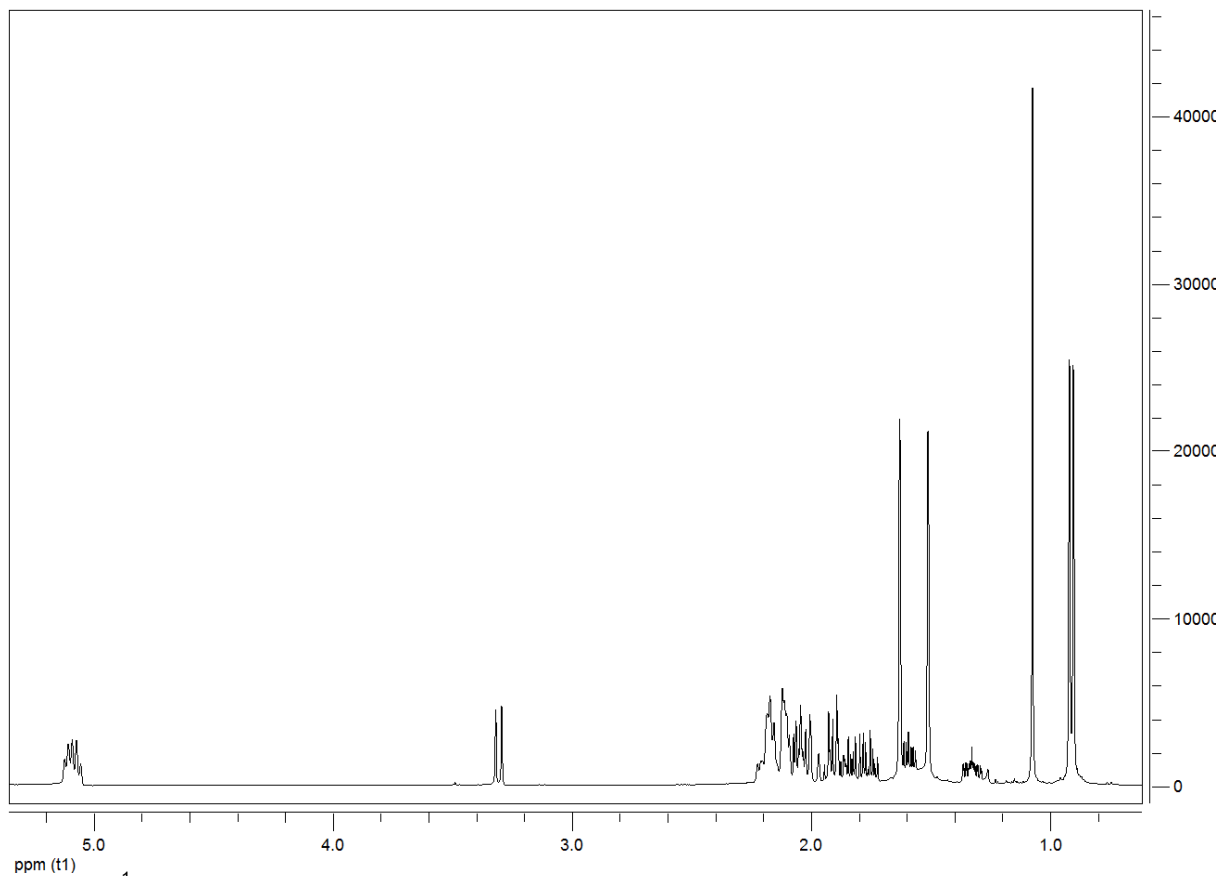


**Fig. 3.15** <sup>1</sup>H-NMR spectrum of incensole (22).

## Results and Discussion

**Tab. 3.1**  $^1\text{H}$  and  $^{13}\text{C}$  NMR assignments (400 MHz) for incensole (**22**).

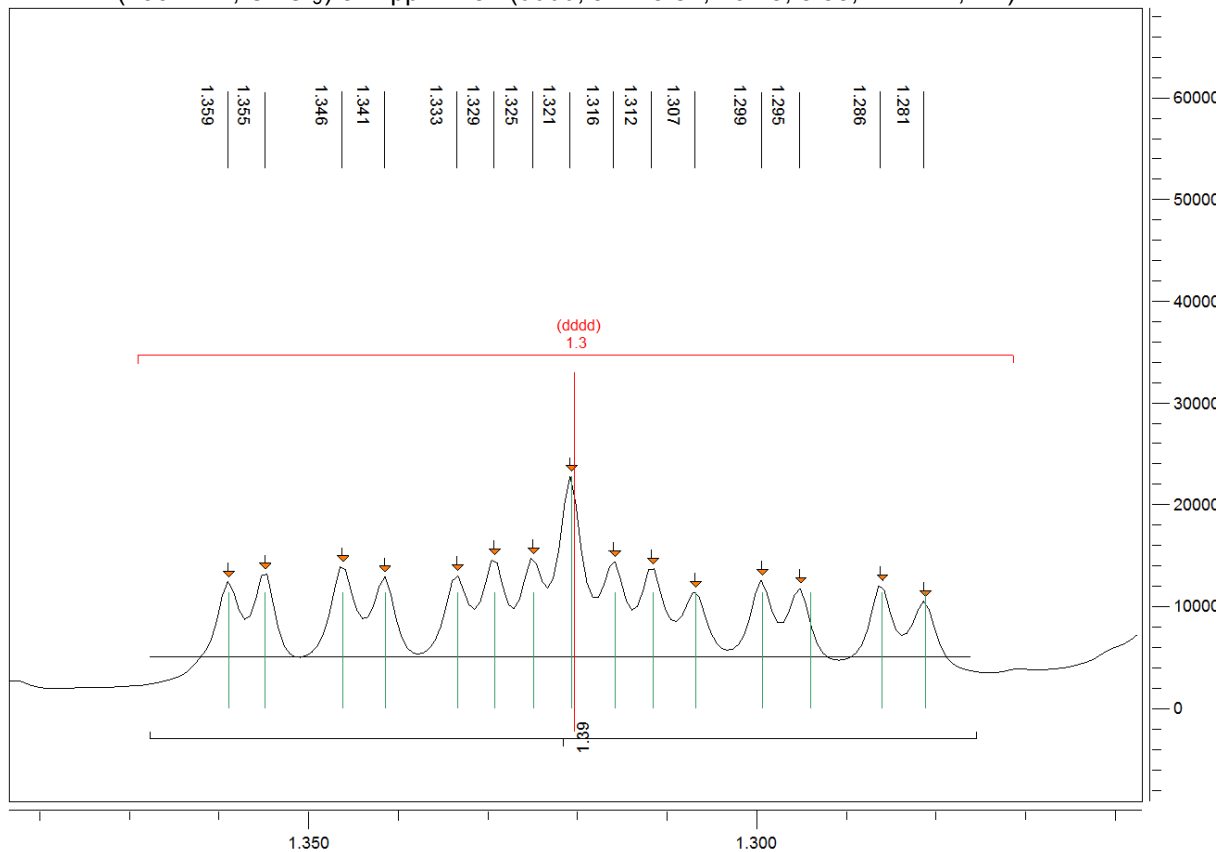
Atom Nr.	$^{13}\text{C}$ $\delta$ [ppm]	$^1\text{H}$ $\delta$ [ppm], $J$ [Hz]	HMBC ( $^2J$ in Hz)	HMBC ( $^3J$ in Hz)	HH-COSY	NOESY
1	88.56		$2\alpha/\beta$ , $14\alpha/\beta$ , 18	$3\alpha/\beta$ , 13, 19, 20		
2	30.66	1.84 1.59 ( $\beta$ , ddd, $J = 11.6, 7.6, 4$ )	$3\alpha/\beta$	$14\alpha/\beta$ , 18	2 ( <i>gem.</i> ), $3\alpha/\beta$	18
3	36.36	2.06 1.74	$2\alpha/\beta$	$5\beta$ , 15	$2\alpha/\beta$	
4	84.14		$3\alpha/\beta$ , $5\beta$ , 15	$2\alpha/\beta$		
5	75.57	3.30 (dd, $J = 10, 0.8$ )	4, $6\alpha/\beta$	$3\alpha/\beta$ , $7\alpha/\beta$ , 15	$6\alpha/\beta$ , 15	$2\beta$ , $3\beta$ , $6\alpha/\beta$ , 9, 13, 14, 15
6	30.72	1.89 ( $\alpha$ , m) 1.32 ( $\beta$ , dddd, $J = 14.0, 10.0, 5.6, 1.6$ )	$5\beta$ , $7\alpha/\beta$		$7\alpha/\beta$ , 6( <i>gem.</i> ) $5\beta$	15, (6 <i>gem.</i> )
7	33.65	2.12 (dd, $J = 14.0, 5.6$ ) 1.99 (m)	$6\alpha/\beta$	$5\beta$ , 9, 16		
8	134.18		$7\alpha/\beta$ , 16	$6\alpha/\beta$ , $10\alpha/\beta$		
9	125.13	5.08 (m)	$10\alpha/\beta$	$7\alpha/\beta$ , $11\alpha/\beta$ , 16	$10\alpha/\beta$ , 16	$5\beta$
10	24.83	2.11-2.18 (m, 2H)	9, $11\alpha/\beta$			
11	38.62	2.11-2.16 (m, 2H)	$10\alpha/\beta$	9, 13, 17		
12	134.23		$11\alpha/\beta$ , 17	$10\alpha/\beta$ , $14\alpha/\beta$		
13	121.79	5.12 (m)	$14\alpha/\beta$	17	$14\alpha/\beta$ , 17	$2\beta$ , $5\beta$ , 14, 18, 19, 20
14	32.35	2.04 2.17	13	$2\alpha/\beta$ , 18		
15	20.64	1.07 (s)		$5\beta$ , $3\alpha/\beta$	$5\beta$	$6\beta$
16	18.15	1.62 (m)	8	$7\alpha/\beta$ , 9	9	
17	16.10	1.50 (m)	12	$11\alpha/\beta$ , 13	$11\alpha/\beta$ , 13	
18	34.85	1.90 (sep, $J = 6.8$ Hz)	19, 20	$2\alpha/\beta$ , $14\alpha/\beta$	19,20	$2\beta$ , $6\beta$
19	17.98	0.89 (d, $J = 6.8$ Hz)	18	1, 20	18	15
20	18.05	0.91 (d, $J = 6.8$ Hz)	18	1, 19	18	15

Evaluation of the spectral data and comparison with data found in the literature [81,87] confirmed the isolated compound as incensole. The compound itself was firstly described by Corsano and Nicoletti in 1966 [75]. Obermann [79] described in the year 1977 incensole as one of the main constituents of the neutral fraction of the *Boswellia* species termed as "Eritrea", thus, referring to the species *Boswellia papyrifera*.

Furthermore a few special spectral characteristics from the  $^1\text{H}$ -NMR spectrum of incensole are described. The H6 $\beta$  atom shows a specific multiplet structure which is the product of a dddd coupling to its four neighbours (H5, H6 $\alpha$  and H7 $\alpha/\beta$ ) as it shown in Fig. 3.16.

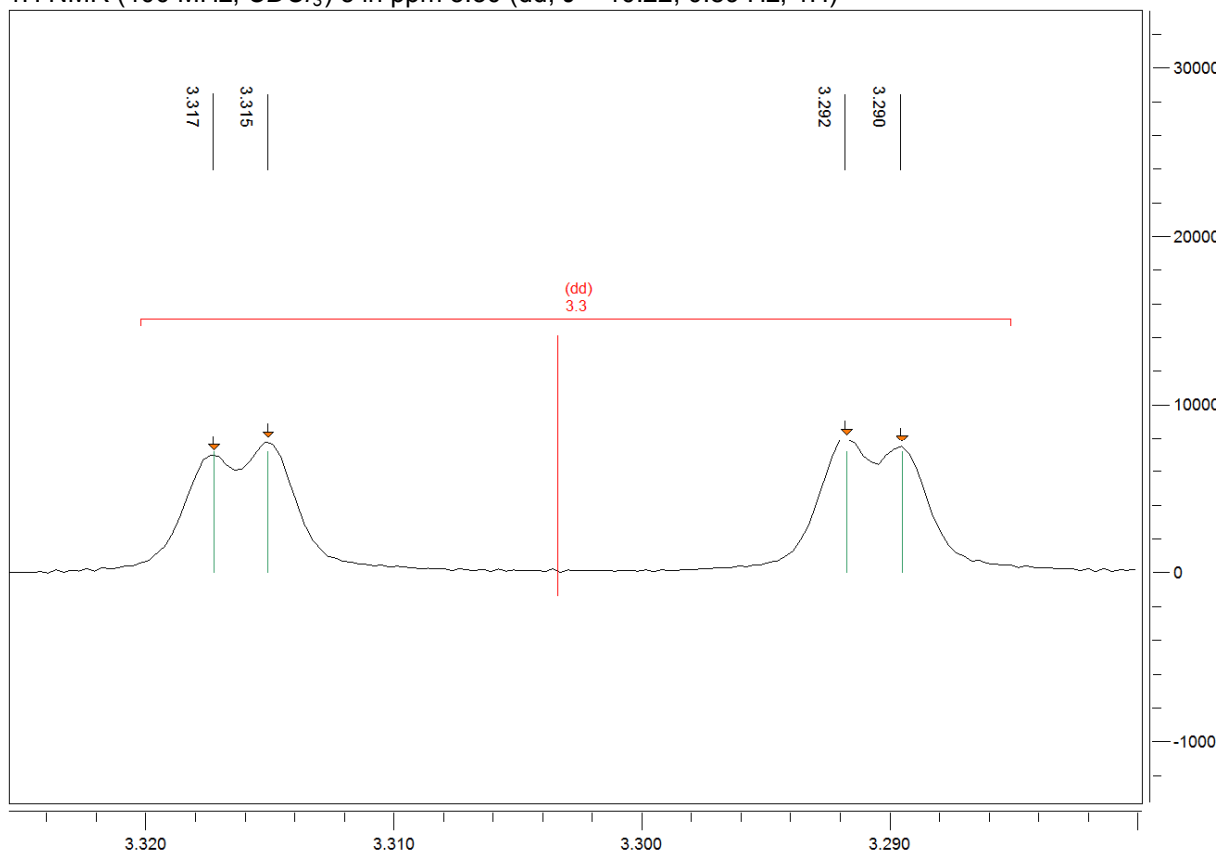
## Results and Discussion

$^1\text{H}$  NMR (400 MHz,  $\text{CDCl}_3$ )  $\delta$  in ppm 1.32 (dddd,  $J = 13.87, 10.25, 5.33, 1.77$  Hz, 1H)



ppm (t1)  
**Fig. 3.16** The  $^1\text{H}$ -NMR fine structure of the  $\text{H}_{6\beta}$  signal at 1.32 ppm.

$^1\text{H}$  NMR (400 MHz,  $\text{CDCl}_3$ )  $\delta$  in ppm 3.30 (dd,  $J = 10.22, 0.89$  Hz, 1H)



ppm (t1)  
**Fig. 3.17** The  $^1\text{H}$ -NMR fine structure of the  $\text{H}_{5\beta}$  signal at 3.30 ppm.

$^1\text{H}$  NMR (400 MHz,  $\text{CDCl}_3$ )  $\delta$  in ppm 1.59 (ddd,  $J = 12, 8, 4$  Hz, 1H)

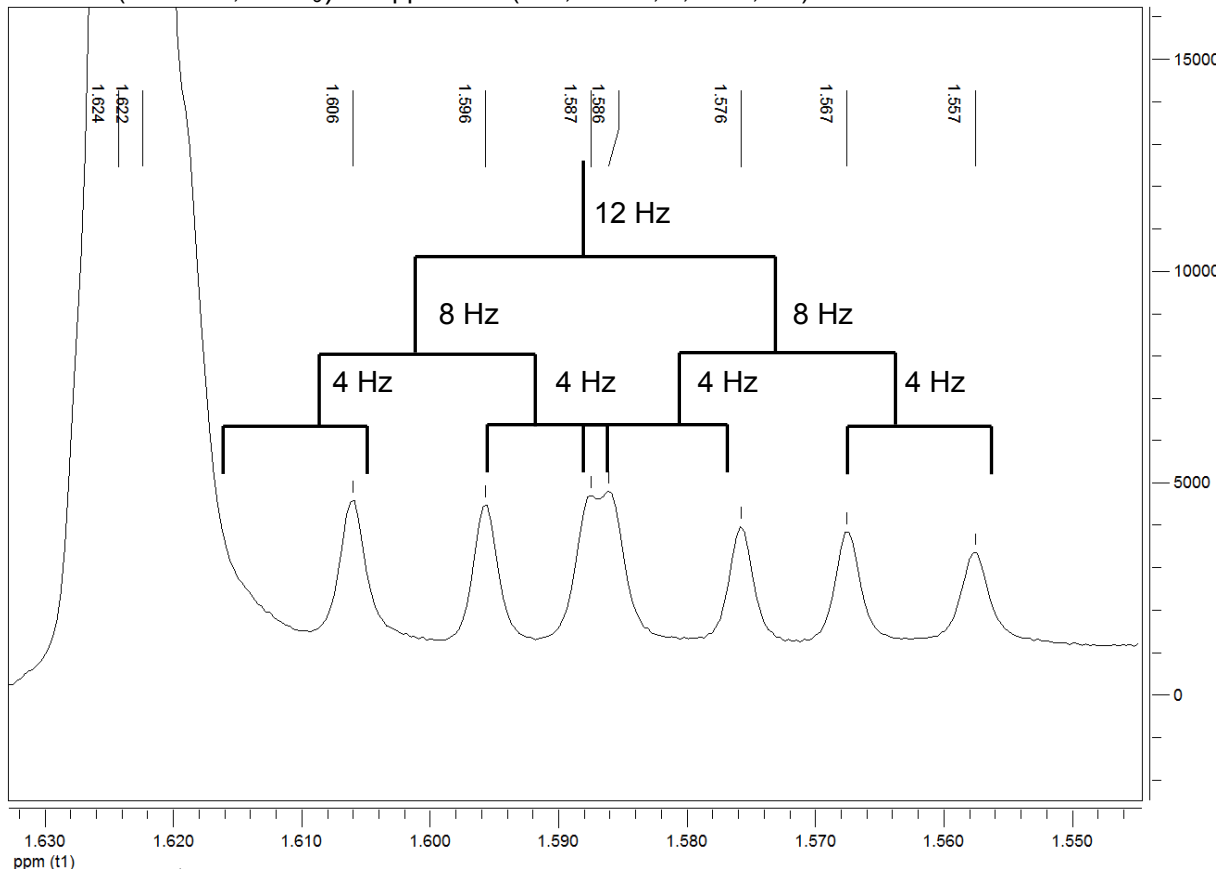


**Fig. 3.18** The  $^1\text{H}$ -NMR fine structure of the  $\text{H}_{2\beta}$  signal at 1.59 ppm. One signal is overlapped by the methyl signal of  $\text{C}_{16}$  (1.62 ppm).

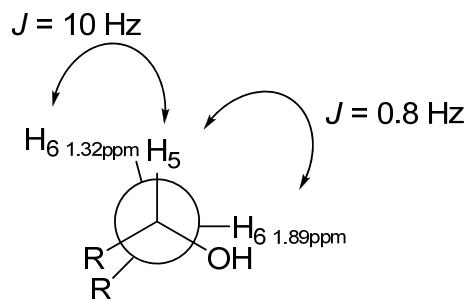


**Fig. 3.19** Newman projection of the assumed spatial orientation of the  $\text{H}_{6\alpha/\beta}$  atoms relative to  $\text{H}_{5\beta}$ .

Exact assignment of the other coupling  $^1\text{H}$  neighbour atoms ( $\text{H}_{6\alpha}$  and  $\text{H}_{7\alpha/\beta}$ ) was unfortunately not possible as these signals have not been clearly resolved and showed overlapping with other signals (area: 1.85-2.25 ppm).

In Fig. 3.17 the coupling of the  $\text{H}_{5\beta}$  with the  $\text{H}_{6\beta}$  atom is presented. Additionally, there is a weak coupling of about 0.8 Hz (exponential apodization with MestRec software) with  $\text{H}_{6\alpha}$  which concludes, according to the Karplus rule [175] that the  $\text{H}_{6\alpha}$  is preferably positioned about  $90^\circ$  to the  $\text{H}_{5\beta}$  signal; whereas the  $\text{H}_{6\beta}$  signal is ca.  $0^\circ$  next to the  $\text{H}_{5\beta}$  signal. The  $\text{H}_{6\beta}$  signal shows a strong interaction with the  $\text{C}_{15}$  methyl group (2D-NOESY), which leads to this deduction (see also the Newman projection for clarification in Fig. 3.19). The signal of  $\text{H}_{2\beta}$  at 1.59 ppm shows also a relatively good resolved fine structure as can be seen in Fig.

3.18. It gives a vicinal coupling with H3 $\alpha$ / $\beta$  and a geminal coupling with H2 $\alpha$  (ddd,  $J = 12, 8$  and 4 Hz). Again, the other coupling partner signals (H2 $\alpha$  and H3 $\alpha$ / $\beta$ ) can not be certainly assigned since their fine structures are covered by additional signals.

### 3.2.2 Incensole Acetate (23)

Incensole Acetate was isolated as colourless viscous oil. The structure is shown in Fig. 3.20. Analysis by TLC (Pentane/Et<sub>2</sub>O 2:1 and 1 % HOAc) showed a strong brown spot after dyeing and heating with anisaldehyde reagent at  $R_f = 0.68$ . Detection by DAD-RP-HPLC was only possible at 210 nm and the compound eluted at a  $R_t$  value of ca. 33.5 min under standard HPLC conditions (2.3.4.2). Mass spectrometric detection (CI-MS; low resolution) delivered the following significant fragmentation pattern:  $m/z$  (%): 348.3 [M]<sup>+</sup> (57); 305.2 (10) [M - C<sub>3</sub>H<sub>7</sub>]<sup>+</sup>; 289.2 (100) [M - CH<sub>3</sub>-COO]<sup>+</sup>; 271.2 (29); 149.1 (40); 135.1 (47); 127.1 (65); 81.1 (62). The <sup>13</sup>C-NMR spectrum revealed 22 carbon atom signals as presented in Fig. 3.21. DEPT 90/135 spectra divided these 20 C-atoms into 5 quaternary, 4 CH-, 7 CH<sub>2</sub>- and 6 methyl carbon atoms. The <sup>1</sup>H-spectrum is shown in Fig. 3.22 and the further structural elucidation by conventional 2D-NMR techniques (HSQC, COSY, NOESY, and HMBC) is basically presented in Tab. 3.2.

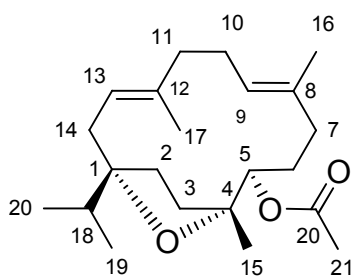
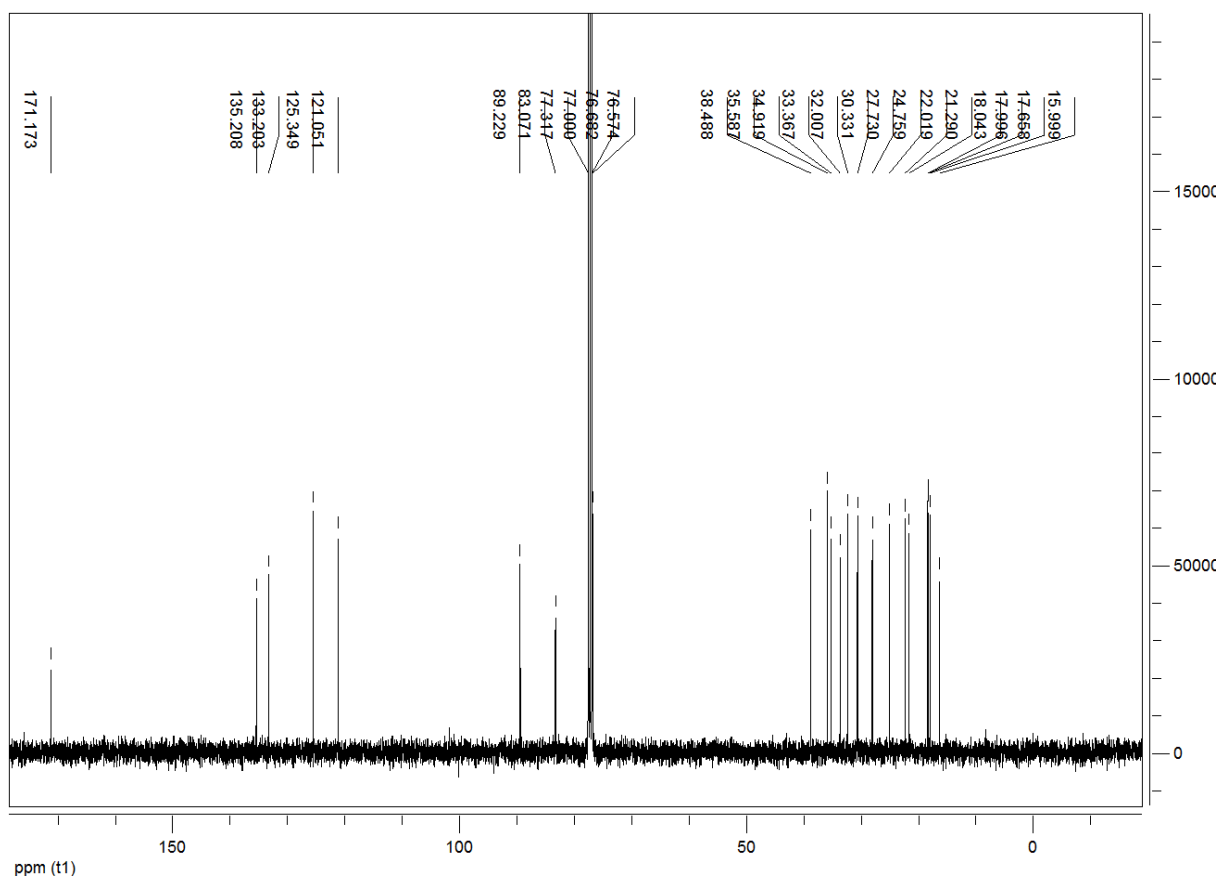
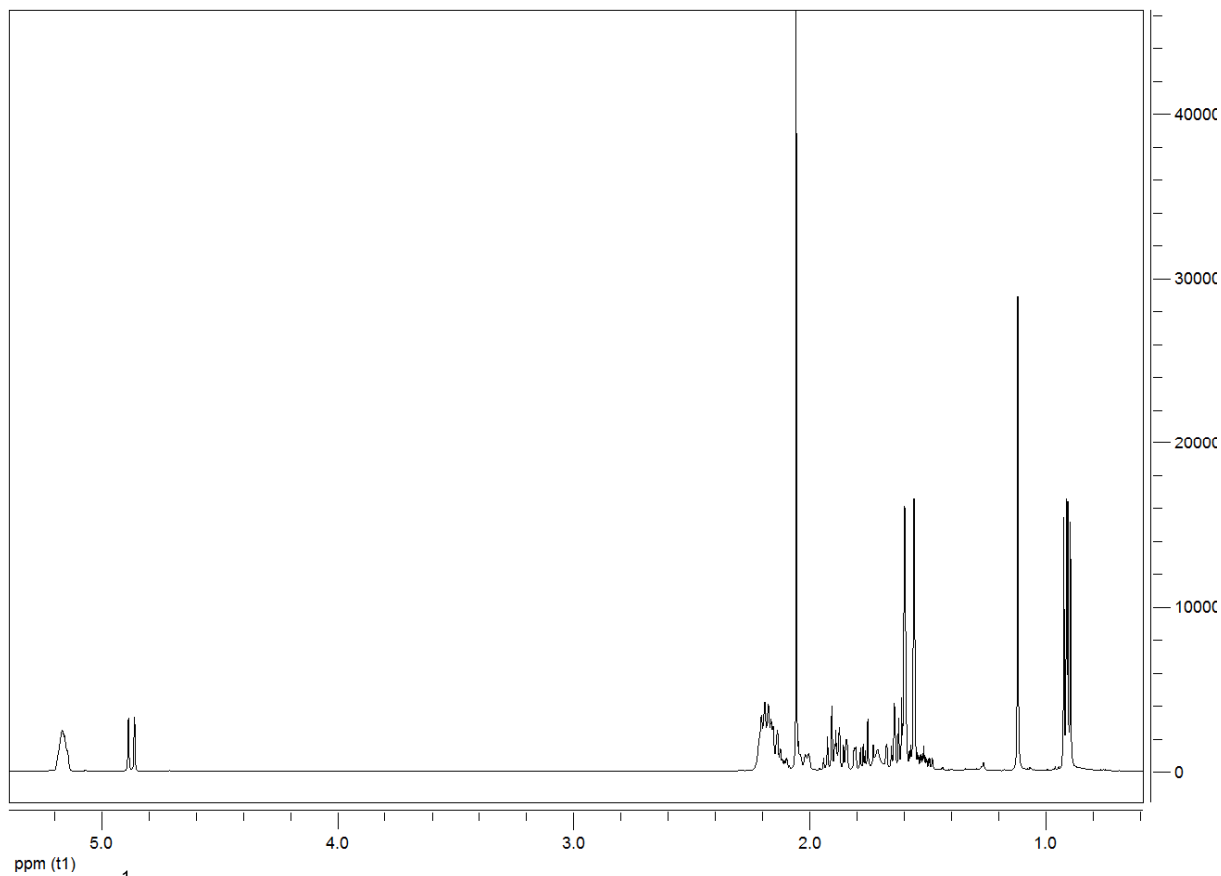


Fig. 3.20 Structure of incensole acetate (23).

## Results and Discussion



**Fig. 3.21**  $^{13}\text{C}$ -NMR spectrum of incensole acetate (**23**).



**Fig. 3.22**  $^1\text{H}$ -NMR spectrum of incensole acetate (**23**).

## Results and Discussion

**Tab. 3.2**  $^1\text{H}$  and  $^{13}\text{C}$  NMR assignments (400 MHz) for incensole acetate (**23**).

Atom Nr.	$^{13}\text{C}$ $\delta$ [ppm]	$^1\text{H}$ $\delta$ [ppm], $J$ [Hz]	HMBC ( $^2J$ in Hz)	HMBC ( $^3J$ in Hz)	HH-COSY	NOESY
1	89.23		2 $\alpha/\beta$ , 14 $\alpha/\beta$ , 18	3 $\alpha/\beta$ , 13, 19, 20		
2	30.33	1.78 1.61	3 $\alpha/\beta$	14 $\alpha/\beta$ , 18		
3	35.59	1.89 1.59	2 $\alpha/\beta$	5 $\beta$ , 15		
4	83.07		3 $\alpha/\beta$ , 5 $\beta$ , 15	2 $\alpha/\beta$		
5	76.57	4.87 (dd, $J = 10, 0.8$ )	4, 6 $\alpha/\beta$	3 $\alpha/\beta$ , 7 $\alpha/\beta$ , 15, 21	6 $\alpha/\beta$ , 15	2 $\beta$ , 3 $\beta$ , 6 $\alpha/\beta$ , 7 $\alpha/\beta$ , 9, 13, 14, 15 (6gem.)
6	27.73	1.85 ( $\alpha$ , m) 1.51 ( $\beta$ , dddd, $J = 14.0, 10.0, 5.6, 1.6$ )	5 $\beta$ , 7 $\alpha/\beta$			
7	33.37	2.02 (dd, $J = 14.0, 5.6$ ) 1.63 (m)	6 $\alpha/\beta$	5 $\beta$ , 9, 16	6 $\alpha/\beta$ , 7(gem.)	
8	133.20		7 $\alpha/\beta$ , 16	6 $\alpha/\beta$ , 10 $\alpha/\beta$		
9	125.35	5.18 (m)	10 $\alpha/\beta$	7 $\alpha/\beta$ , 11 $\alpha/\beta$ , 16	10 $\alpha/\beta$ , 16	5 $\beta$
10	24.76	2.19 (m, 2H)	9, 11 $\alpha/\beta$			
11	38.49	2.15 (m, 2H)	10 $\alpha/\beta$	9, 13, 17		
12	135.21		11 $\alpha/\beta$ , 17	10 $\alpha/\beta$ , 14 $\alpha/\beta$		
13	121.05	5.16 (m)	14 $\alpha/\beta$	17	14 $\alpha/\beta$ , 17	2 $\beta$ , 5 $\beta$ , 14, 18, 19, 20
14	32.01	2.17 (m, 2H)	13	2 $\alpha/\beta$ , 18		
15	22.02	1.11 (s)		5 $\beta$ , 3 $\alpha/\beta$	5 $\beta$	6 $\beta$
16	17.66	1.59 (m)	8	7 $\alpha/\beta$ , 9	9	6 $\alpha$
17	16.00	1.55 (m)	12	11 $\alpha/\beta$ , 13	11 $\alpha/\beta$ , 13	11 $\alpha/\beta$
18	34.92	1.90 (sep, $J = 6.8$ Hz)	19, 20	2 $\alpha/\beta$ , 14 $\alpha/\beta$	19,20	
19	18.00	0.89 (d, $J = 6.8$ Hz)	18	1, 20	18	2 $\alpha/\beta$ , 3 $\alpha$ , 14, 15, 18
20	18.04	0.91 (d, $J = 6.8$ Hz)	18	1, 19	18	2 $\alpha/\beta$ , 3 $\alpha$ , 14, 15, 18
21	171.17		22	5 $\beta$		
22	21.29	2.05 (s)	21			2 $\beta$ , 3 $\beta$

Evaluation of the spectral data and comparison with data found in the literature [35,81,87] confirmed the isolated compound as incensole acetate. The compound itself was firstly described by Obermann [79]. The first one-dimensional NMR data were obtained by Gacs-Baitz et al. [81] and the first two-dimensional NMR assignments by Basar [35].

In Fig. 3.23 the  $^1\text{H}$ -NMR spectral fine structure of H6 $\beta$  is shown. It is principally the same fine structure as already described for incensole (view chapter 3.2.1), only downfield shifted (from 1.32 to 1.51 ppm) by the appearance of the carbonyl group in its acetate derivate. A part of the fine structure is covered by the methyl signal of C17 (1.55 ppm).

## Results and Discussion

1H NMR (400 MHz,  $CDCl_3$ )  $\delta$  in ppm 1.51 (dddd,  $J = 13.87, 10.25, 5.33, 1.77$  Hz, 1H)

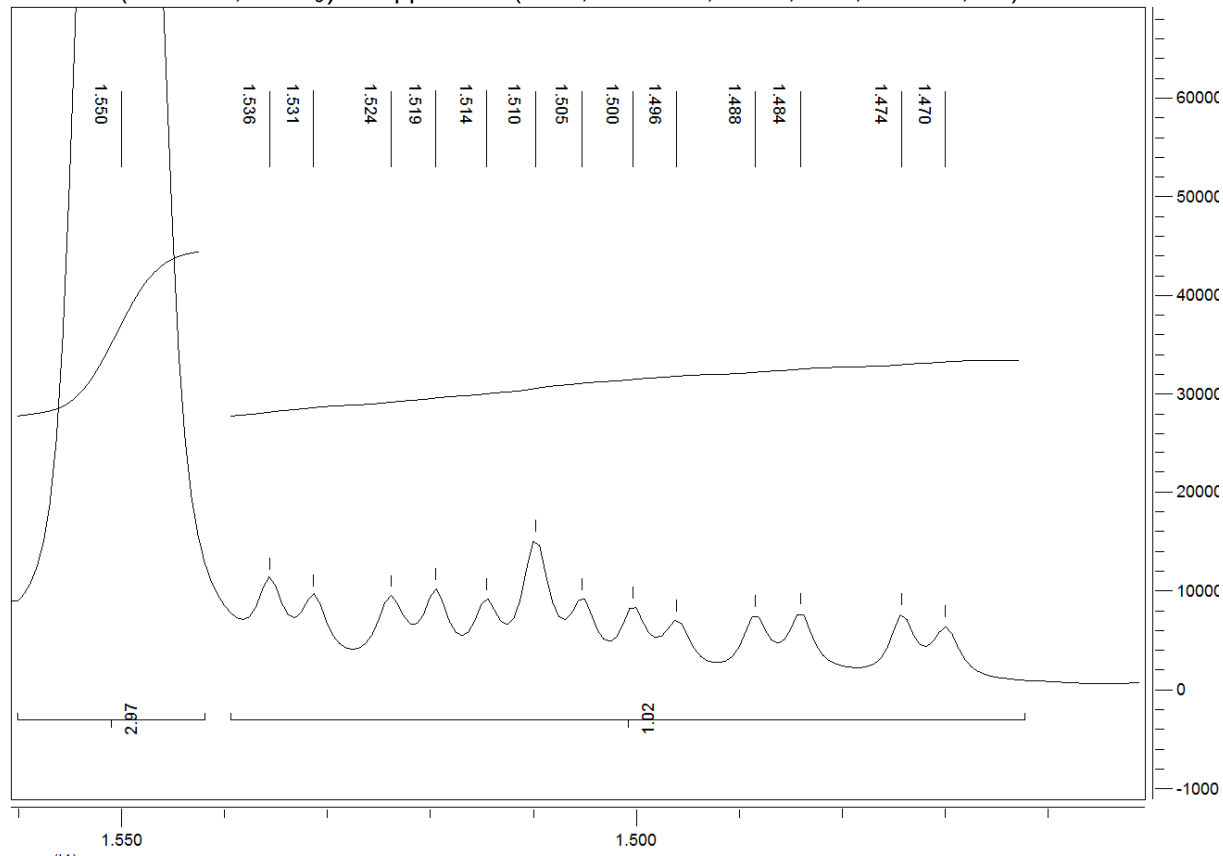


**Fig. 3.23** The  $^1H$ -NMR fine structure of the  $H_{6\beta}$  signal at 1.51 ppm.

In Fig. 3.24 the coupling of the  $H_{5\beta}$  with the  $H_{6\beta}$  atom is presented. It represents the same fine structure pattern as already shown for incensole (chapter 3.2.1). Likewise the signal of  $H_{6\beta}$ , the  $H_{5\beta}$  signal is also downfield shifted (from 3.30 ppm in incensole to 4.87 ppm in incensole acetate) by occurrence of the carbonyl group. The relatively big acetyl substituent is in an equatorial position as demonstrated in Fig. 3.24 and thus leads to the same relative stereochemistry as already shown for incensole. The fine structure of  $H_{5\beta}$  is presented in Fig. 3.25.

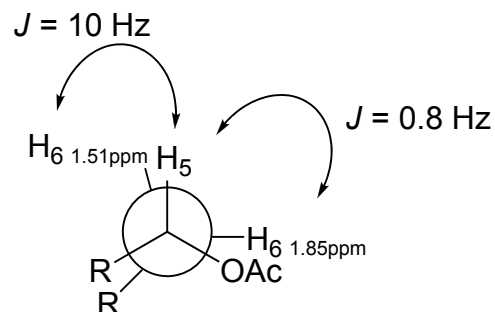


**Fig. 3.24** Newman projection of the assumed spatial orientation of the  $H_{6\alpha/\beta}$  atoms relatively to  $H_{5\beta}$ .

$^1\text{H NMR}$  (400 MHz,  $\text{CDCl}_3$ )  $\delta$  in ppm 4.87 (dd,  $J = 10.43, 0.79$  Hz, 1H)

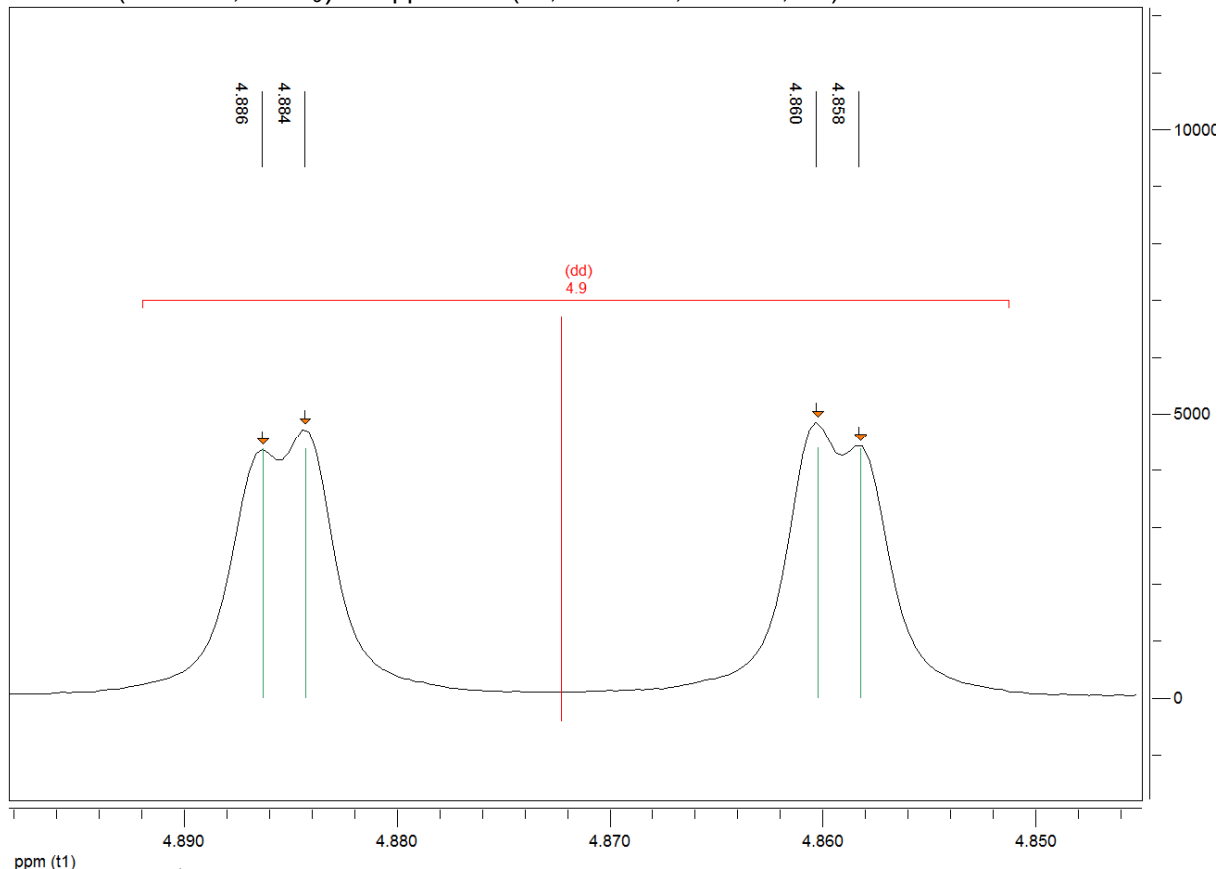


**Fig. 3.25** The  $^1\text{H-NMR}$  fine structure of the H5 $\beta$  signal at 4.87 ppm.

### 3.2.3 3 $\alpha$ -O-Acetyl-7,24-dien-tirucallic acid (**18**)

The compound was isolated as a white solid. The structure is shown in Fig. 3.26. Analysis by TLC (Pentane/ $\text{Et}_2\text{O}$  2:1 and 1 % HOAc) showed a strong blue spot after dyeing and heating with anisaldehyde reagent at  $R_f = 0.26$ , eluting between incensole and the  $\alpha/\beta$ -ABAs (see also section 3.4). Detection by DAD-RP-HPLC was only possible at 210 nm and the  $R_t$  value was ca. 33.7 min under standard HPLC conditions (2.3.4.2). Thus, the compound co-eluted with compound **3** ( $\beta$ -BA). Mass spectrometric detection (LC-ESI-MS; negative mode, low resolution) gave a mol peak of 497.6 g/mol ( $[\text{M} - \text{H}]^-$ ; for LC-ESI-conditions see section 2.4.1). The mass spectroscopic data is presented in Fig. 3.27.

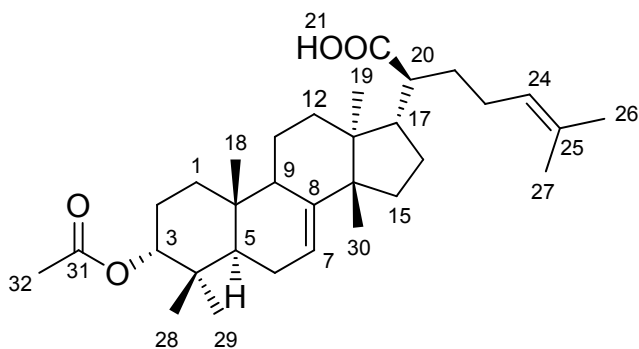


**Fig. 3.26** Structure of 3 $\alpha$ -O-acetyl-7,24-dien-tirucallic acid (**18**).

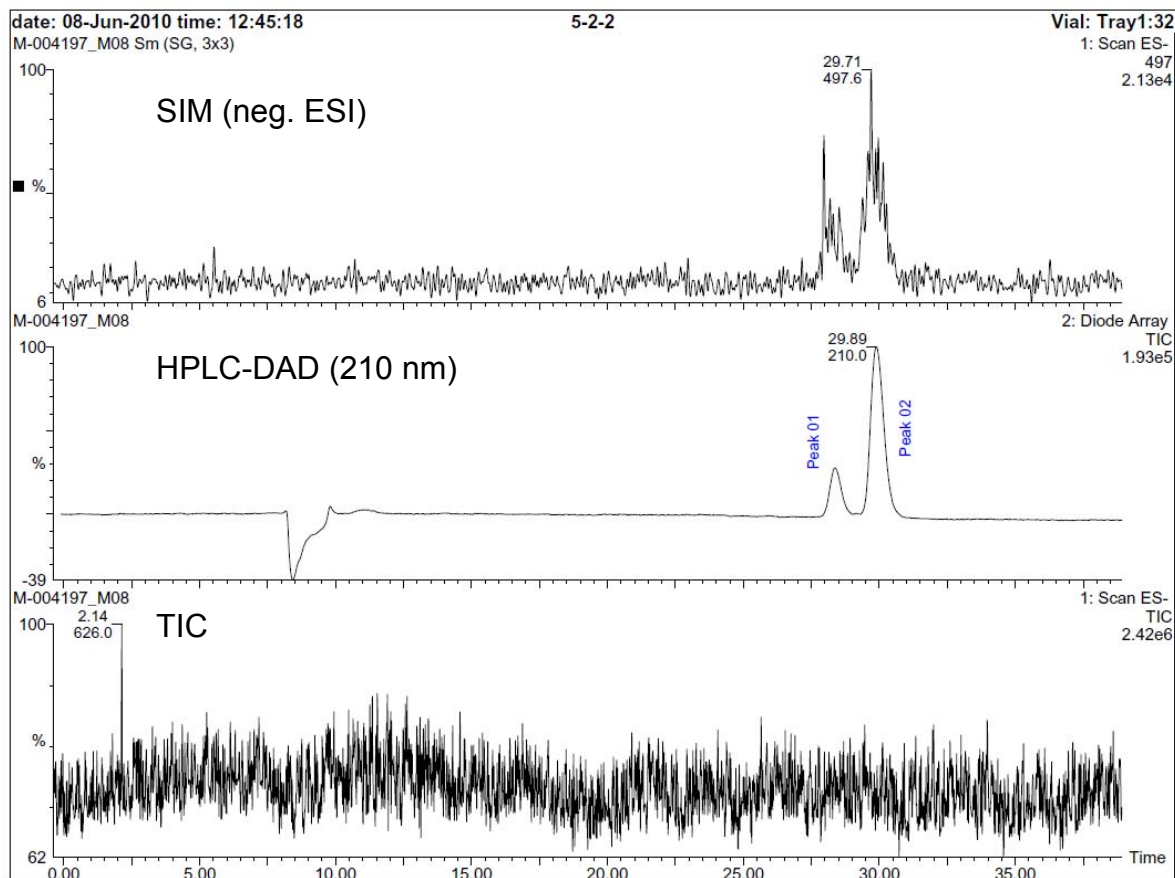


**Fig. 3.27** Mass spectroscopic data (ESI neg. mode) of compound **18** (Peak 2). Peak 1 refers to 3 $\beta$ -O-acetyl-8,24-dien-tirucallic acid (**19**). For further details see text.

The  $^{13}\text{C}$ -NMR spectrum revealed 32 carbon signals as presented in Fig. 3.28. The DEPT 90 and DEPT 135 spectra divided these 32 C-atoms into 8 quaternary, 7 CH-, 9 CH<sub>2</sub>- and 8 methyl carbon atoms. At 183.0 ppm, the downfield signal referred to a carboxyl group (C-21) and the signal at 170.8 ppm to a carbonyl group (C-31). Four further signals between 145.6 and 118.2 ppm correspond to two tri-substituted double bonds. One double bond (C-24 with 123.6 ppm; C-25 with 132.3 ppm) was characterised by a vinyl proton at 5.09 ppm (H-24, t,  $J = 7$  Hz) and by an isopropylidene group with two methyl groups at 1.67 ppm (H-26, s) and 1.58 ppm (H-27, s). The second double bond (C-7 with 118.2 ppm; C-8 with 145.6 ppm) revealed a quaternary carbon atom (C-8) and showed a vinyl proton at 5.26 ppm (H-7, m). The chemical shift signal of 78.3 ppm referred to the acetyl group substituted carbon atom (C-3) and also showed a significant downfield proton signal at 4.67 ppm (H-3, brs). The  $^1\text{H}$ -spectrum is shown in Fig. 3.29 and the further structural elucidation by conventional 2D-NMR techniques (HSQC, COSY, NOESY, and HMBC) is basically presented in Tab. 3.3. Pardhy and Bhattacharyya [66] described how to easily distinguish between 3- $\alpha$ -OH- and 3- $\beta$ -OH-tirucallic acids, only based on 1D- $^1\text{H}$ -NMR spectra according to the Karplus theory [175]. Therefore, the equatorial H at C-3 gives for the 3- $\alpha$ -OH-tirucallic compound a broad singlet, respectively, for the 3- $\alpha$ -OAc-group in compound **18**. And the axial H at C-3 gives for the 3- $\beta$ -OH-tirucallic molecule a duplet of duplets, respectively, for the 3- $\beta$ -OAc group in compound **19**. Hence, even without NOESY correlations the relative configuration of H atoms at position C-3 can be assigned in these classes of molecules.

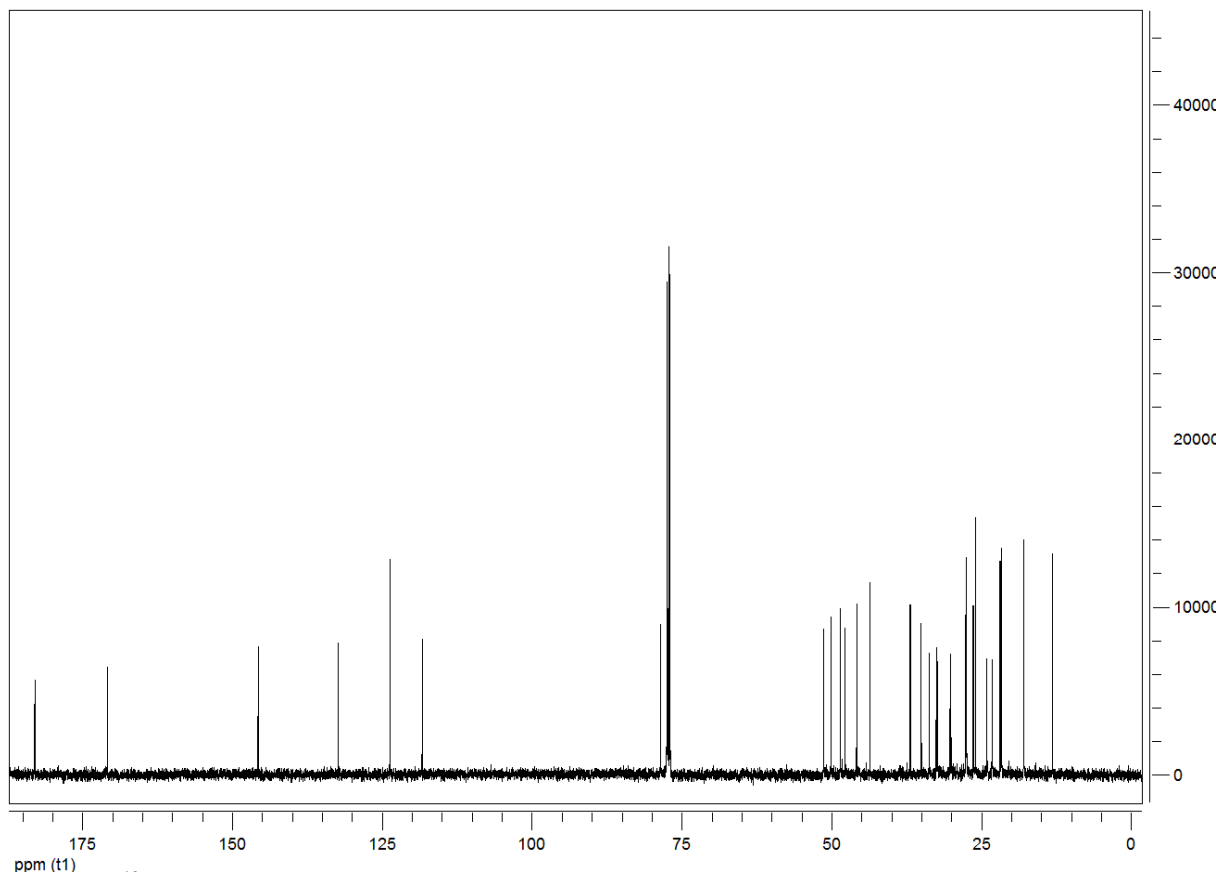


**Fig. 3.28**  $^{13}\text{C}$ -NMR of  $3\alpha\text{-O-acetyl-7,24-dien-tirucallic acid (18)}$ .

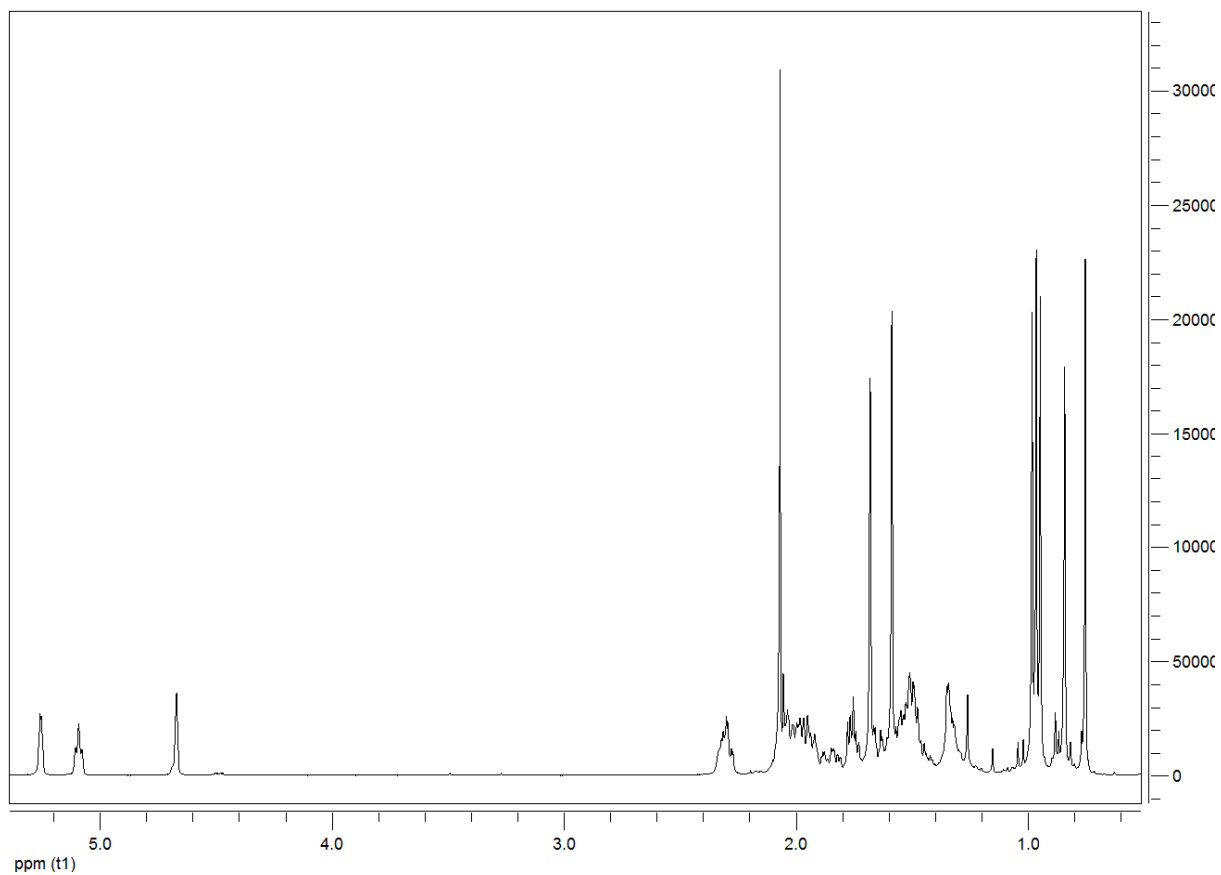


**Fig. 3.29**  $^1\text{H}$ -NMR of  $3\alpha\text{-O-acetyl-7,24-dien-tirucallic acid (18)}$ .

## Results and Discussion

**Tab. 3.3**  $^1\text{H}$  and  $^{13}\text{C}$  NMR assignments (500 MHz) for 3 $\alpha$ -O-acetyl-7,24-dien-tirucallic acid (**18**).

Atom Nr.	$^{13}\text{C}$ $\delta$ [ppm]	$^1\text{H}$ $\delta$ [ppm], $J$ [Hz]	HMBC ( $^2J$ in Hz)	HMBC ( $^3J$ in Hz)	HH-COSY	NOESY
1	32.03	1.33 1.33	2 $\alpha/\beta$	3, 5, 18	2 $\alpha/\beta$	9, 18
2	22.86	1.64 ( $\alpha$ ) 1.83 ( $\beta$ )	1 $\alpha/\beta$	3	1 $\alpha/\beta$ , 2( <i>gem.</i> )	2( <i>gem.</i> )
3	78.33	4.67 (br s)	2 $\alpha$ , 4	5, 28, 29, 31, 32(4J)	2 $\alpha/\beta$	2 $\alpha/\beta$ , 28, 29, 32
4	36.58		3, 5, 28, 29	2 $\alpha$ , 6 $\beta$		
5	45.55	1.75	6 $\alpha/\beta$	1 $\alpha/\beta$ , 9, 18 28, 29	6 $\alpha/\beta$	9, 29
6	23.76	1.91 ( $\beta$ ) 2.06 ( $\alpha$ )	5, 7	4	5	
7	118.18	5.26 (m)	6	5, 9, 14	6 $\alpha/\beta$ , 5, 9	5, 6 $\alpha/\beta$ , 15 $\alpha/\beta$ , 18, 30
8	145.62			11 $\alpha/\beta$ , 30		
9	48.30	2.31	11	1, 5, 12, 18	11 $\alpha/\beta$	5, 19
10	34.74		1 $\alpha/\beta$ , 5, 18	2 $\alpha$ , 6 $\alpha$		
11	17.64	1.42 ( $\alpha$ ) 1.48 ( $\beta$ )	9, 12	8, 13	9	18
12	29.92	1.48 ( $\alpha$ ) 1.74 ( $\beta$ )	11 $\alpha/\beta$	17, 19	12( <i>gem.</i> ), 19(4J)	
13	43.34		12 $\alpha/\beta$ , 17, 19	11 $\alpha/\beta$ , 20, 30		
14	51.05		15, 30	19		
15	33.43	1.48 1.51	16	30	30(4J)	
16	27.17	1.31 ( $\alpha$ ) 1.97 ( $\beta$ )	15, 17	20	15 $\alpha/\beta$ , 17 16( <i>gem.</i> )	16( <i>gem.</i> ), 20
17	49.85	2.03	16, 20	12, 15, 19	20	
18	12.84	0.74 (s)	10	1, 5, 9	1(4J), 5(4J)	1, 2 $\beta$ , 9, 11, 28
19	21.56	0.94 (s)	13	12, 14, 17	12(4J)	12 $\alpha$ , 20
20	47.48	2.29	17, 21, 22	13, 16, 23	17, 22 $\alpha/\beta$	16 $\alpha/\beta$ , 19, 22
21	182.96	11.83 (br s, COOH)	20	22		
22	32.23	1.54 1.59	21, 23 $\alpha/\beta$	17	20	20
23	26.06	1.94 1.98	22	25		27
24	123.55	5.09 (tr, $J = 7$ Hz) <sup>*</sup>	23 $\alpha/\beta$	26, 27	23 $\alpha/\beta$ , 26, 27	22 $\alpha/\beta$ , 23 $\alpha/\beta$ , 20, 26
25	132.25		26, 27	23 $\alpha/\beta$		
26	25.67	1.67 (s)	25	24, 27	27	24
27	17.62	1.58 (s)	25	24, 26	26	23
28	21.39	0.96 (s)	4	3, 29	29(4J)	2 $\beta$ , 6 $\beta$ , 18, 29
29	27.24	0.83 (s)	4	3, 28	28(4J)	5, 6 $\alpha$ , 28
30	27.37	0.97 (s)	14	13, 15	15 $\alpha/\beta$ (4J)	11 $\beta$ , 12 $\beta$ , 16 $\beta$ , 17
31	170.81		32	3		
32	21.29	2.06 (s)	31	3(4J)		

\* actually the signal represents an unresolved multiplet fine structure within the triplet structure

Evaluation of the spectral data confirmed the isolated compound as 3 $\alpha$ -O-acetyl-7,24-dien-tirucallic acid. The deacetylated derivative (3 $\alpha$ -OH-7,24-dien-tirucallic acid, **17**) was isolated by Seitz [56] from Bpap and by Mora et al. [69] from the resin of *Protium crenatum* (Burseraceae). Additionally, Banno et al. [68] and Akihisa et al. [67] report of compound **18** from Bcar, which they obtained by acetylation of 3 $\alpha$ -OH-7,24-dien-tirucallic acid (**17**). However, according to the data presented here the resin was more likely to be the species Bpap than Bcar, as tirucallic acids are generally less expressed in Bcar (see chapter 3.8) and as compound **23** (Inc-Ac, thus far a specific biomarker for Bpap) had been isolated in both works [67,68]. Finally, Estrada et al. [70] report on the isolation of compound **18** from Bcar (though again it is more likely that the resin was Bpap instead) and refer to the paper of Büchele et al. [57] for its isolation, although it is nothing mentioned about compound **18** in this paper. Thus, the NMR data presented here is the first thoroughly published description of this molecule, including data of its isolation (see chapter 3.1.1).

### 3.2.4 3 $\beta$ -O-Acetyl-8,24-dien-tirucallic acid (**19**)

The compound (**19**) was isolated as a white solid. The structure is shown in Fig. 3.30. Analysis by TLC (Pentane/Et<sub>2</sub>O 2:1 and 1 % HOAc) showed a strong blue spot after dyeing and heating with anisaldehyde reagent at  $R_f = 0.26$ , eluting between incensole and the  $\alpha/\beta$ -ABAs (see also section 3.4) and thus co-eluting with 3 $\alpha$ -O-acetyl-7,24-dien-tirucallic acid (**18**) and 3 $\alpha$ -O-Acetyl-8,24-dien-tirucallic acid (**16**). Detection by DAD-RP-HPLC was only possible at 210 nm and the compound eluted at a  $R_t$  of ca. 33.4 min between compound **1** ( $\alpha$ -BA) and **3** ( $\beta$ -BA) under standard HPLC conditions (2.3.4.2). Mass spectrometric detection (LC-ESI-MS; negative mode, low resolution) gave a mol peak of 497.6 g/mol ( $[M - H]^-$ ; for LC-ESI-conditions see section 2.4.1). The mass spectroscopic data is presented in Fig. 3.31.

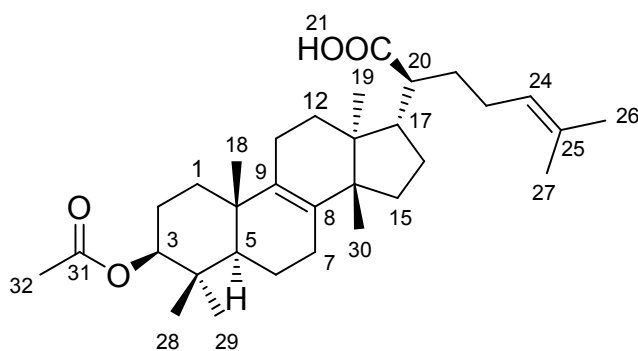


**Fig. 3.30** Structure of 3 $\beta$ -O-Acetyl-8,24-dien-tirucallic acid (**19**).

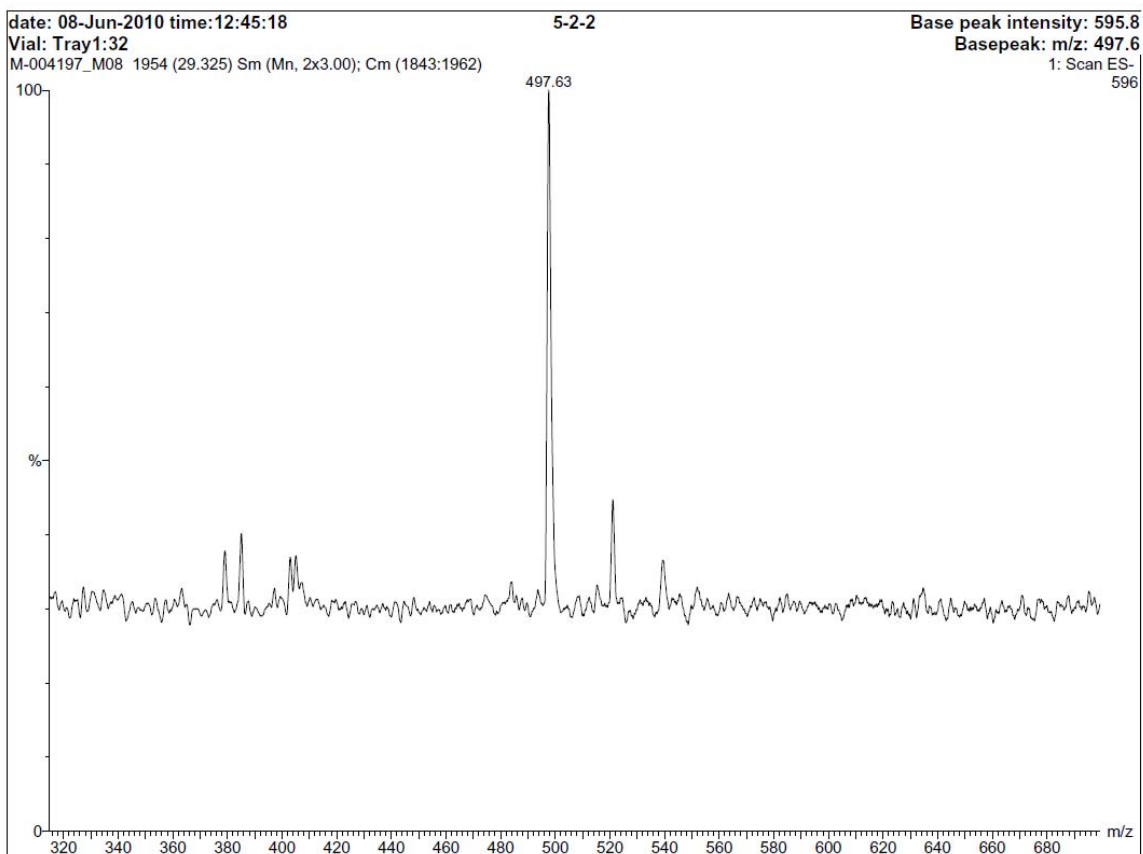


**Fig. 3.31** Mass spectroscopic data (ESI neg. mode; Scan-Range: ca. 320-700 m/z) of compound **19**. The minor peak next to at  $m/z$  ca. 520 refers to the compound +  $\text{Na}^+$  (sodium).

The  $^{13}\text{C}$ -NMR (125 Hz, micro probe head) spectrum revealed only 31 carbon atom signals as presented in Fig. 3.32. The DEPT 90 and DEPT 135 spectra divided these 31 C-atoms into 8 quaternary, 5 CH-, 10  $\text{CH}_2$ - and 8 methyl carbon atoms. At 182.3 ppm, the downfield signal of the carboxyl group (C-21) diminishes inside the noise (probable reason: micro probe head and a low sample concentration). However, as demonstrated in Fig. 3.33 the HMBC spectrum reveals the  $2J$  coupling of C-21 with H-20 and the  $3J$  coupling of H $\alpha/\beta$ -20 (stronger signal). Furthermore, the correct molecule identity was validated by acetylation of 3 $\beta$ -OH-8,24-dien-tirucallic acid (**15**) (see chapter 2.7.1) and co-injection by the standard RP-HPLC-DAD method (2 x YMC column in row). The signal at 171.0 ppm belongs to a carbonyl group (C-31). Signals between 133.9 and 123.6 ppm correspond to a tri-substituted and a tetra-substituted double bond. One double bond (C-24 with 123.6 ppm; C-25 with 132.2 ppm) was characterised by a vinyl proton at 5.09 ppm (H-24, t,  $J = 7$  Hz) and by an isopropylidene group with two methyl groups at 1.68 ppm (H-26, s) and 1.58 ppm (H-27, s). The second double bond (C-8 with 133.3 ppm; C-9 with 133.9 ppm) revealed two quaternary carbon atoms. The chemical shift signal of 80.9 ppm referred to the acetyl group substituted carbon atom (C-3) and also showed a significant downfield proton signal at 4.50 ppm (H-3, dd,  $J = 11.8$  and 4.5 Hz; see also Fig. 3.35). The  $^1\text{H}$ -spectrum is shown in Fig. 3.34 and the impurity signals (only 1.2 mg of the compound were isolated, thus even minor proton impurities gave significant signal levels) are tagged (frame). The structural elucidation data by conventional 2D-NMR techniques (HSQC, COSY, NOESY, and HMBC) is basically presented in Tab. 3.4.

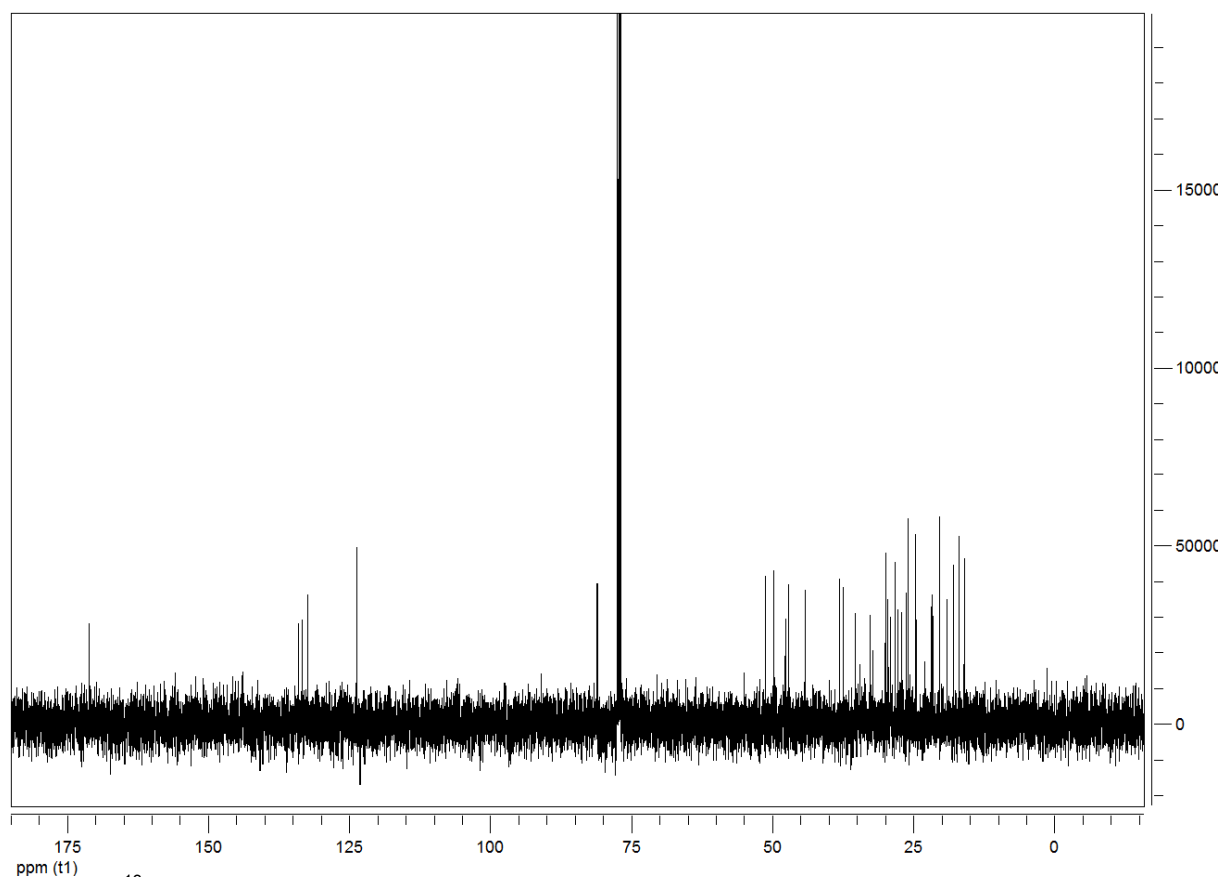


**Fig. 3.32**  $^{13}\text{C}$ -NMR (125 Hz, micro probe head) of  $3\beta$ -O-acetyl-8,24-dien-tirucallic acid (**19**).

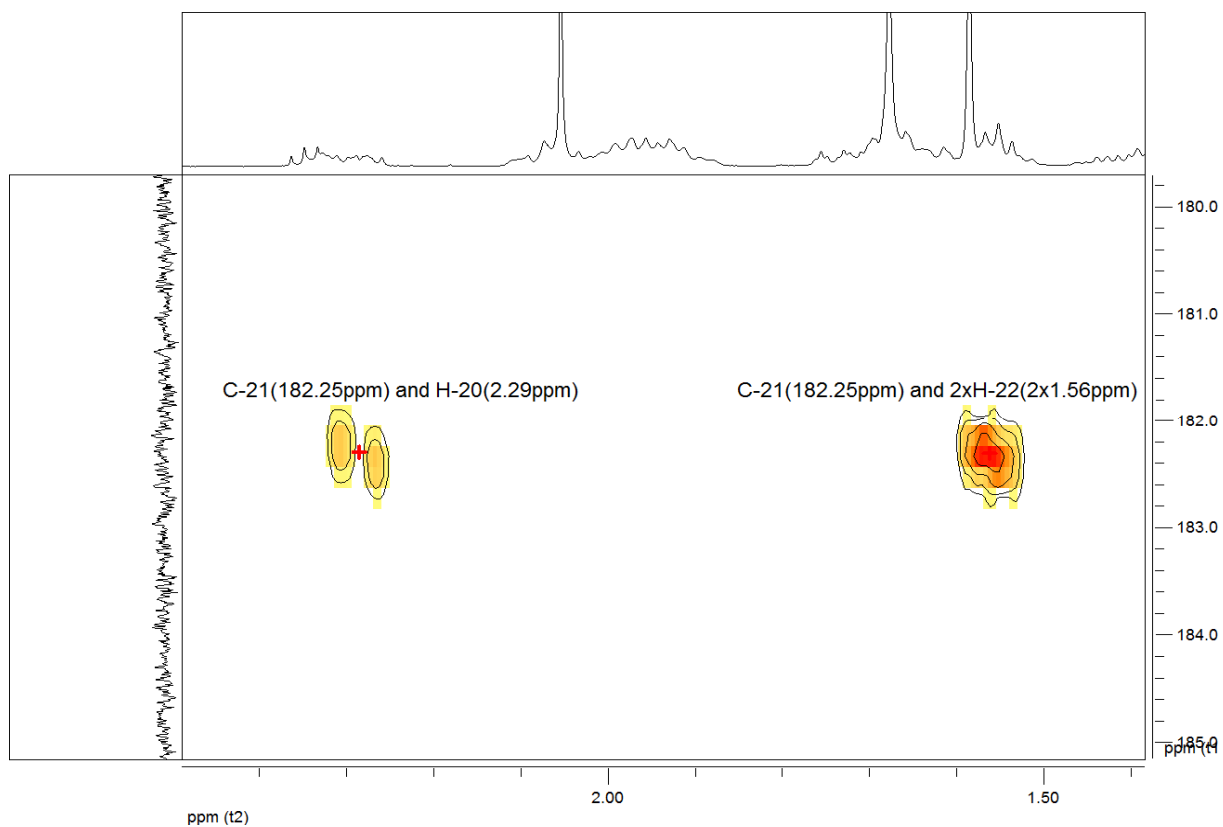


**Fig. 3.33** HMBC of  $3\beta$ -O-acetyl-8,24-dien-tirucallic acid (**19**), declaring the existence of C-21 (not detectable in the  $^{13}\text{C}$ -NMR spectrum). For further details see text.

## Results and Discussion

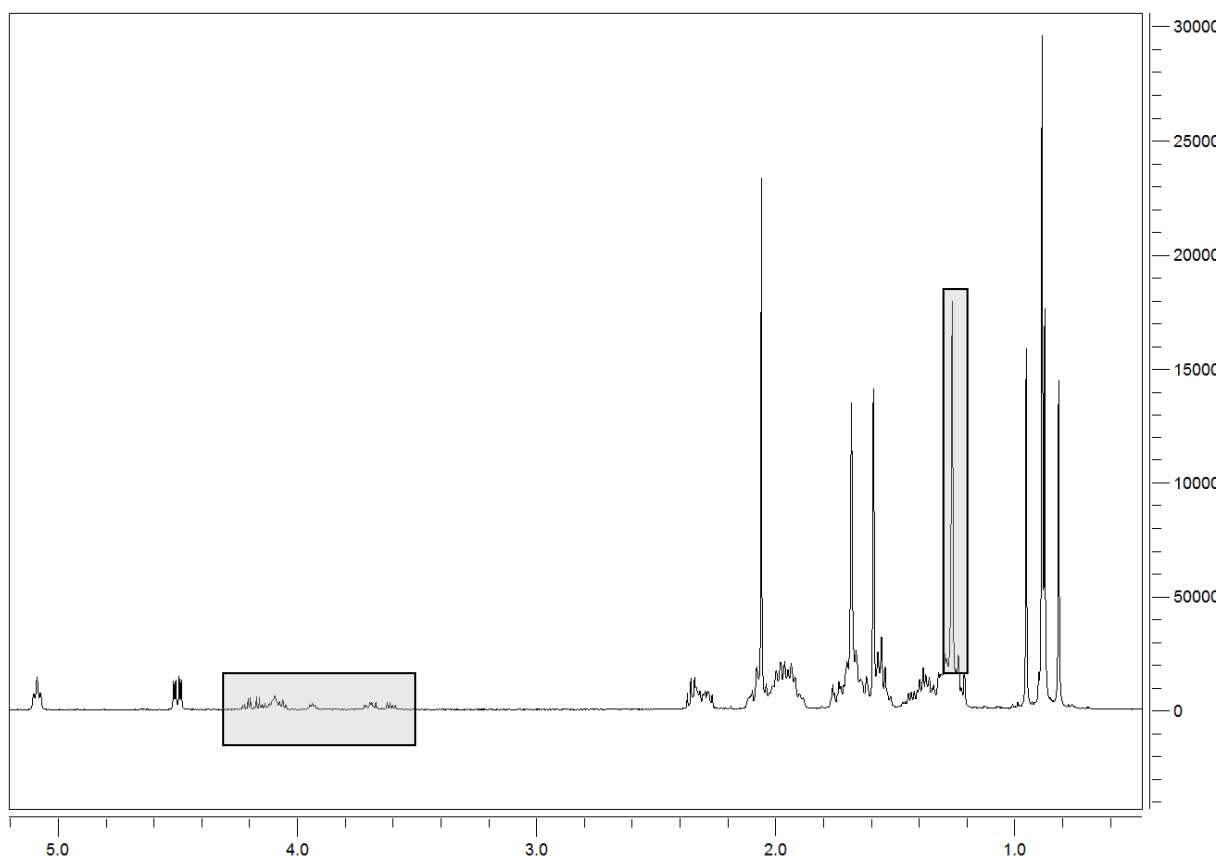


**Fig. 3.34** <sup>1</sup>H-NMR (500 MHz, micro probe head) of 3 $\beta$ -O-acetyl-8,24-dien-tirucallic acid (**19**). The impurities are marked by the grey rectangles.

<sup>1</sup>H NMR (500 MHz, CDCl<sub>3</sub>)  $\delta$  in ppm 4.50 (dd,  $J = 11.76, 4.47$  Hz, 1H)

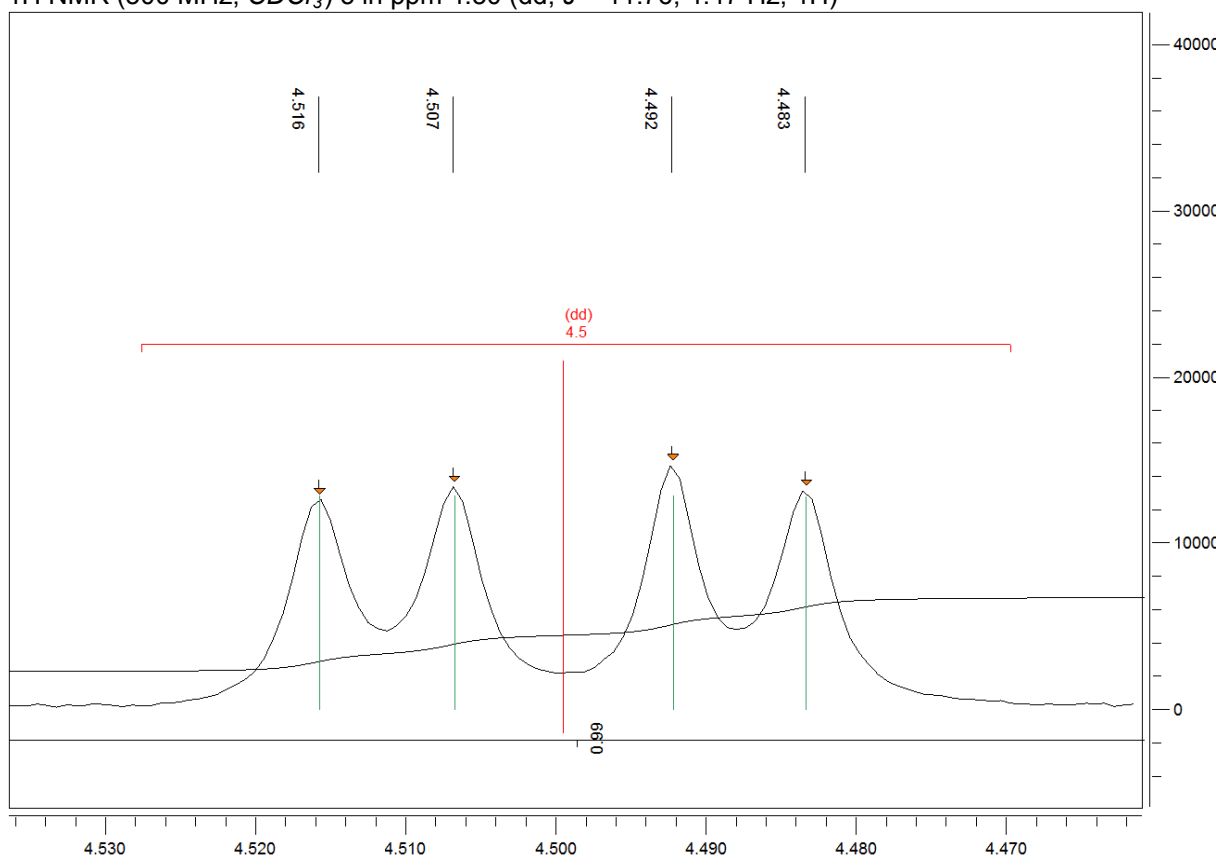


**Fig. 3.35** The dd at 4.5 ppm in the <sup>1</sup>H-NMR-spectrum declaring the  $\alpha$ -position (axial) of the proton at C-3.

## Results and Discussion

**Tab. 3.4**  $^1\text{H}$  and  $^{13}\text{C}$  NMR assignments (500 MHz; Micro probe head) for 3 $\beta$ -O-acetyl-8,24-dien-tirucallic acid (**19**).

Atom Nr.	$^{13}\text{C}$ $\delta$ [ppm]	$^1\text{H}$ $\delta$ [ppm], $J$ [Hz]	HMBC ( $^2J$ in Hz)	HMBC ( $^3J$ in Hz)	HH-COSY	NOESY
1	34.98	1.28 ( $\alpha$ ) 1.74 ( $\beta$ )	2 $\beta$	5, 18	1( <i>gem.</i> ), 2 $\alpha/\beta$	1( <i>gem.</i> )
2	24.17	1.60 ( $\beta$ ) 1.68 ( $\alpha$ )	1 $\alpha/\beta$		1 $\alpha/\beta$	
3	80.85	4.50 (dd, $J = 11.8, 4.5$ )	2, 4	1 $\beta$ , 5, 28, 29, 31	2 $\alpha/\beta$	1 $\alpha$ , 2 $\alpha/\beta$ , 5, 29, 32
4	37.87		3, 5, 28, 29			
5	51.03	1.22	6 $\alpha/\beta$ , 10	7 $\alpha$ , 18, 28, 29	6 $\alpha/\beta$ , 28, 29	1 $\alpha$ , 3, 29
6	18.74	1.42 ( $\beta$ ) 1.68 ( $\alpha$ )	5		5	
7	27.46	1.93 ( $\beta$ ) 2.08 ( $\alpha$ )	6 $\alpha/\beta$	5	6 $\beta$ (7 $\alpha$ )	
8	133.30			6 $\alpha$ , 30		
9	133.90		11 $\beta$	12 $\alpha$ , 18		
10	37.15		1 $\alpha/\beta$ , 5, 18	2 $\beta$ , 6 $\alpha/\beta$		
11	21.52	1.91 ( $\beta$ ) 2.01 ( $\alpha$ )	12 $\alpha/\beta$			
12	28.75	1.37 ( $\alpha$ ) 1.66 ( $\beta$ )		19	12( <i>gem.</i> )	12( <i>gem.</i> )
13	43.88		17, 19	11 $\beta$ , 12 $\alpha/\beta$ , 30		
14	49.59		15 $\alpha$ , 30	12 $\alpha$ , 19		
15	29.33	1.30 ( $\beta$ ) 1.55 ( $\alpha$ )		30		
16	26.86	1.34 ( $\alpha$ ) 1.95 ( $\beta$ )	17		17	16( <i>gem.</i> )
17	46.92	2.07	20	19, 22	16 $\alpha/\beta$ , 20	17, 21 $\alpha/\beta$ , 30
18	20.09	0.94 (s)		1 $\alpha/\beta$ , 5		1 $\beta$ , 2 $\beta$ , 6 $\beta$ , 11 $\beta$ , 28
19	15.70	0.81 (s)		12 $\alpha/\beta$ , 17		17, 12 $\alpha$ , 21 $\alpha/\beta$
20	47.45	2.29	17, 21		17, 22 $\alpha/\beta$	19, 16 $\alpha/\beta$ , 21 $\alpha/\beta$
21	182.09 <sup>†</sup>		20	22		
22	32.45	1.56 1.56	20, 21	17	20	
23	25.94	1.93 2.00	24	25	23 $\alpha/\beta$	
24	123.59	5.09 (tr, $J = 7.1$ Hz)*	23 $\alpha/\beta$	26, 27	23, 26 27	20, 22 $\alpha/\beta$ , 23 $\alpha/\beta$ , 26
25	132.24		26, 27	23 $\alpha/\beta$		
26	25.68	1.68 (s)	25	24, 27	23 $\alpha/\beta$ , 24	27
27	17.64	1.58 (s)	25	24, 26	24	16 $\beta$ , 26
28	16.62	0.87 (s)		3, 5, 29	5	6 $\beta$ , 18
29	27.96	0.88 (s)		3, 5, 28	5	3, 5, 32
30	24.41	0.88 (s)		15	15 $\alpha$	16 $\beta$
31	171.05		32	3		
32	21.32	2.05 (s)	31			29

<sup>†</sup> actually the signal represents an unresolved multiplet fine structure within the triplet structure

Evaluation of the spectral data confirmed the isolated compound as 3 $\beta$ -O-acetyl-8,24-dien-tirucallic acid. The deacetylated derivative (3 $\beta$ -OH-8,24-dien-tirucallic acid, **15**) was isolated by Pardhy and Bhattacharya [66] from Bser and by Seitz [56] from Bpap. Banno et al. [68] and Akihisa et al. [67] reported it (**15**) from Bcar, though the species was more likely to be a sample of Bpap instead (same discussion as in chapter 3.2.3). The compound itself, as acetylated variety, has been firstly reported by Estrada et al. [70], isolated from Bcar (see also chapter 3.2.3). The isolation of it is referred by Estrada et al. [70] to the paper of Büchele et al. [57]. However, neither the compound itself nor something about its isolation are mentioned in that publication [57]. Hence, the NMR data shown here delivers the first thoroughly published description of this molecule, concerning as well as the isolation (see chapter 3.1.1.3) and the analytical evaluation.

### 3.2.5 Verticillia-4(20),7,11-triene (**24**)

This compound was isolated as colourless viscous oil. The structure is shown in Fig. 3.37. Analysis by TLC (Pentane/Et<sub>2</sub>O 2:1 and 1 % HOAc) showed a violet spot after dyeing and heating with anisaldehyde reagent at  $R_f = 0.80$ . Detection by DAD-RP-HPLC was only possible at 210 nm and the compound eluted at a  $R_t$  value of ca. 53.9 min under standard HPLC conditions (2.3.4.2). The <sup>13</sup>C-NMR spectrum revealed 20 carbon signals as presented in Fig. 3.36. DEPT 90/135 spectra divided these 20 C-atoms into 5 quarternary, 2 CH-, 9 CH<sub>2</sub>- and 4 methyl carbon atoms. The <sup>1</sup>H-spectrum is shown in Fig. 3.38 and the further structural elucidation by conventional 2D-NMR techniques (HSQC, COSY, NOESY, and HMBC) is basically presented in Tab. 3.5.

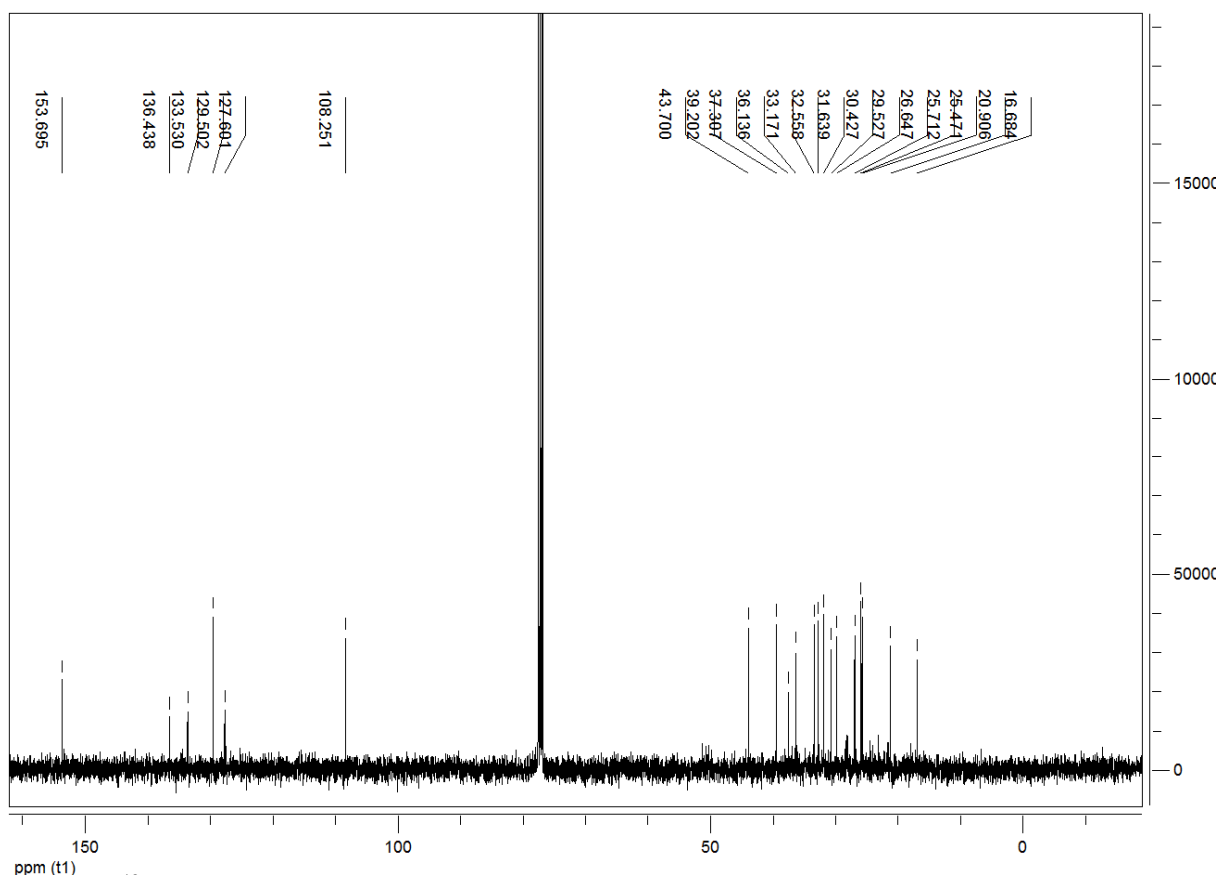
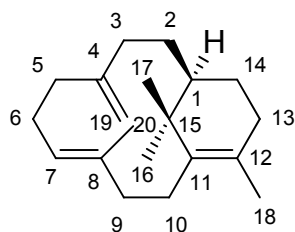
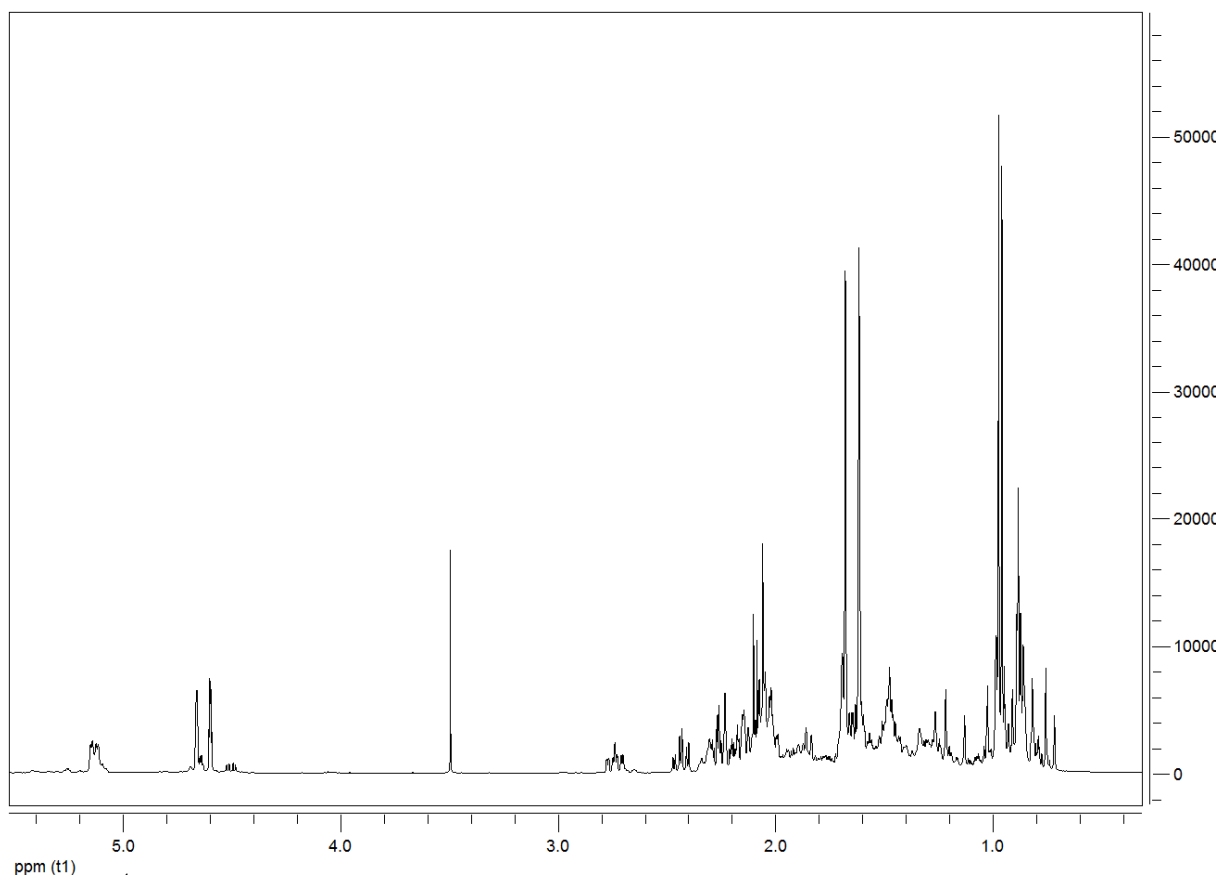


Fig. 3.36 <sup>13</sup>C-NMR spectrum of verticillia-4(20),7,11-triene (**24**).



**Fig. 3.37** Structure of verticillia-4(20),7,11-triene (**24**).



**Fig. 3.38**  $^1\text{H-NMR}$  spectrum of verticillia-4(20),7,11-triene (**24**).

Evaluation of the spectral data and comparison with data found in the literature [85] confirmed the isolated compound as verticillia-4(20),7,11-triene. The compound was described by Basar [35] for the first time. However, Basar noted that it was isolated from the essential oil of Bcar. Referring to the data presented here (see chapter 3.7.1), the compound originates from the frankincense species Bpap and thus is a significant marker for it.

## Results and Discussion

**Tab. 3.5**  $^1\text{H}$  and  $^{13}\text{C}$  NMR assignments (400 MHz) for verticillia-4(20),7,11-triene (**24**).

Atom Nr.	$^{13}\text{C}$ $\delta$ [ppm]	$^1\text{H}$ $\delta$ [ppm], J [Hz]	HMBC ( $^2J$ in Hz)	HMBC ( $^3J$ in Hz)	HH-COSY	NOESY
1	43.70	1.47	2 $\alpha/\beta$ , 15	3( $\beta$ ), 11, 13 $\alpha/\beta$ , 16, 17	2 $\alpha/\beta$ , 14 $\alpha/\beta$	2 $\alpha$ , 13 $\alpha$ , 14 $\alpha$ , 16
2	31.64	1.58 ( $\beta$ ) 1.66 ( $\alpha$ )	1, 3( $\beta$ )		1, 3 $\alpha/\beta$	1
3	32.60	2.01 ( $\alpha$ ) 2.73 ( $\beta$ , ddd, J = 14.6, 7.1, 2.7)		20	3( <i>gem.</i> ), 2 $\alpha/\beta$	3( <i>gem.</i> ), 5 $\beta$ , 17, 20( $H_2$ )
4	153.70		3 $\alpha/\beta$ , 5 $\alpha/\beta$			
5	36.14	2.01 ( $\beta$ ) 2.25 ( $\alpha$ )		20	6 $\alpha/\beta$	20( $H_1$ ), 5( <i>gem.</i> )
6	29.53	2.05 ( $\alpha$ ) 2.18 ( $\beta$ )			5 $\alpha/\beta$ , 7	
7	129.50	5.13 (dd, J = 10.6, 3.5)	6 $\alpha/\beta$	5 $\alpha/\beta$ , 9 $\alpha/\beta$ , 19	6 $\alpha/\beta$ , 9 $\alpha/\beta$ , 19	3 $\beta$ , 5 $\beta$ , 6 $\beta$ , 9 $\alpha/\beta$
8	133.53		9 $\alpha/\beta$ , 19			
9	39.20	2.03 ( $\beta$ ) 2.42 ( $\alpha$ , dtr, J = 12.4, 4.3)	8	7, 11, 19	7, 9( <i>gem.</i> ), 10 $\alpha/\beta$	9( <i>gem.</i> ), 18
10	25.47	2.24 ( $\beta$ ) 2.30 ( $\alpha$ )	9 $\alpha/\beta$		9 $\alpha/\beta$ , 10( <i>gem.</i> )	18
11	136.44			1, 9 $\alpha/\beta$ , 13 $\alpha$ , 16, 17, 18		
12	127.60		13 $\alpha/\beta$ , 18			
13	30.43	1.83 ( $\beta$ ) 2.12 ( $\alpha$ )	12	1, 18	13( <i>gem.</i> ), 14 $\alpha/\beta$	13( <i>gem.</i> ), 18
14	25.71	1.45 ( $\beta$ ) 2.13 ( $\alpha$ )	1, 13 $\alpha/\beta$		1, 14( <i>gem.</i> ), 13 $\alpha/\beta$	1
15	37.31		1, 16, 17	2 $\alpha/\beta$		
16	33.17	0.97 (s)	15	1, 11, 17		1
17	26.65	0.95 (s)	15	1, 11, 16		3 $\beta$ , 5 $\beta$ , 10 $\beta$ , 19
18	20.91	1.67 (br s)	12	11, 13		9 $\alpha$ , 10 $\alpha/\beta$ , 13 $\alpha/\beta$
19	16.68	1.61 (br s)	8	9 $\alpha/\beta$		17
20	108.25	4.66 $H_1$ (m)		3 $\alpha/\beta$ , 5 $\alpha/\beta$	3 $\alpha/\beta$ , 5 $\alpha/\beta$	5 $\alpha$
		4.60 $H_2$ (m)			3 $\beta$ , 5 $\alpha/\beta$	3 $\beta$

In Fig. 3.39-3.41 the fine structures of three relatively good resolved  $^1\text{H}$ -NMR signals are presented. Basically, they represent the same data already published by Basar [35]. A few minor differences in the resolution of signals, compared with the publications of Basar [35,85] (in [85]  $\text{C}_6\text{D}_6$  was used as deuterated solvent), may refer to magnetic field inhomogeneities (not optimal shimming time etc.) and different NMR device conditions in common. Furthermore, the compound is rather unstable showing already strong decomposition within a few days when purified (even when stored at 4 °C).

One significant difference may be found, compared with Basars data: C10 and C14 seem to be vice versa assigned in the publications of Basar. Both signals are near to each other in the  $^{13}\text{C}$ -Spectrum. Basar declared them vice versa than reported here. However, the HH-COSY and HMBC data obtained leads to a different conclusion (see Tab. 3.5): C10 highfield shifted and C14 downfield shifted.

## Results and Discussion

$^1\text{H}$  NMR (400 MHz,  $\text{CDCl}_3$ )  $\delta$  in ppm 5.13 (dd,  $J = 10.57, 3.50$  Hz, 1H)

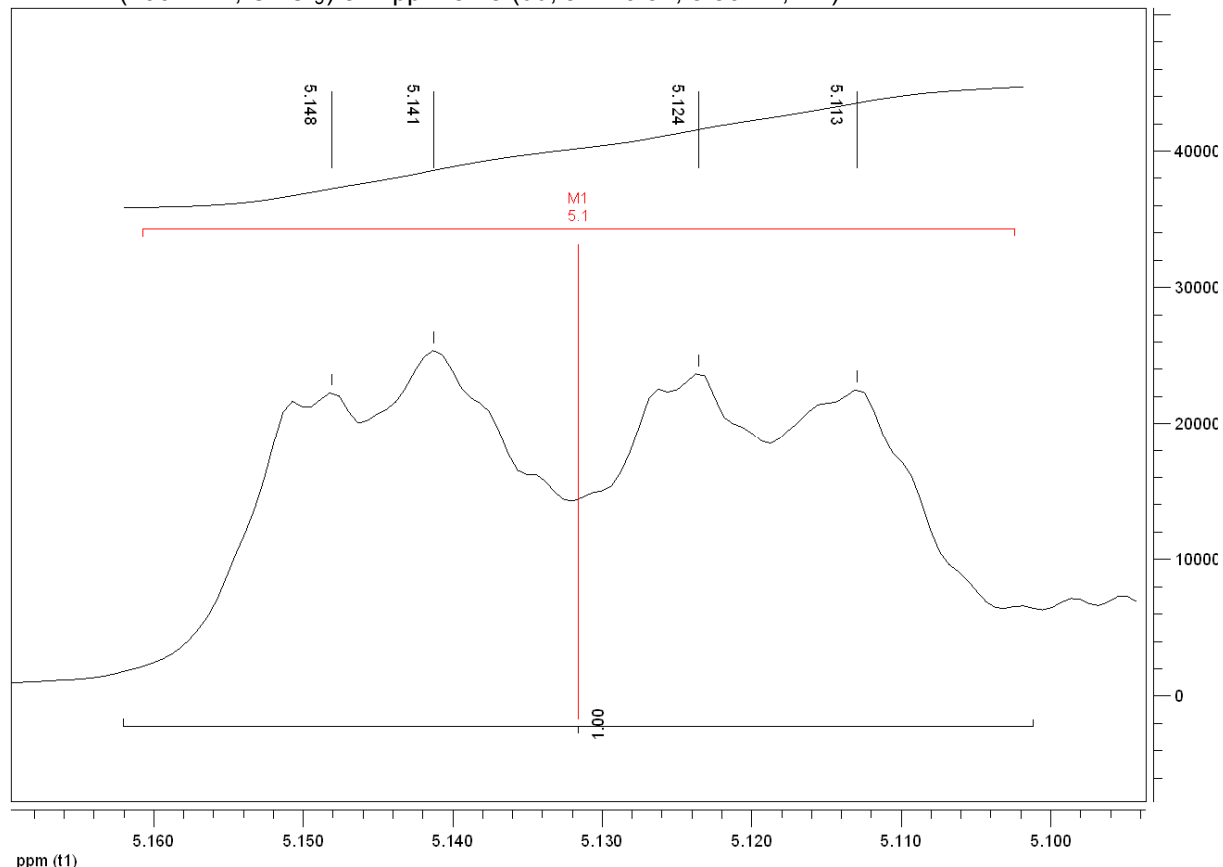


**Fig. 3.39** The  $^1\text{H}$ -NMR fine structure of the H7 signal at 5.13 ppm.

$^1\text{H}$  NMR (400 MHz,  $\text{CDCl}_3$ )  $\delta$  in ppm 2.74 (ddd,  $J = 14.64, 7.14, 2.68$  Hz, 1H)

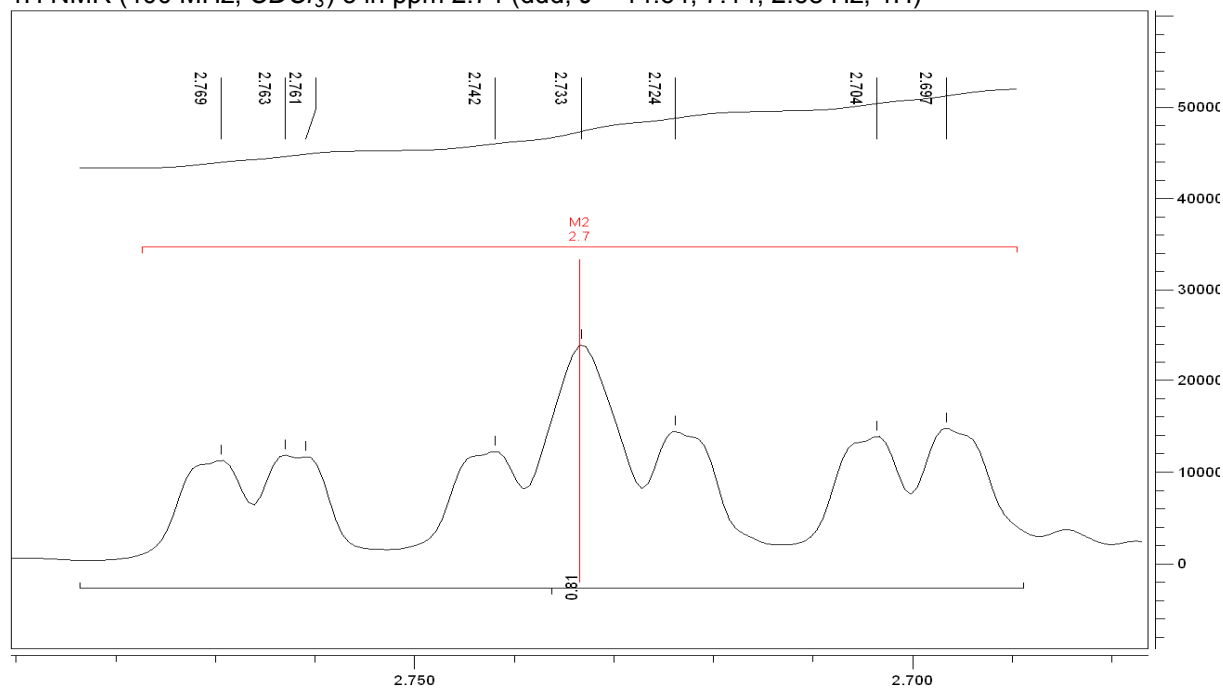


**Fig. 3.40** The  $^1\text{H}$ -NMR fine structure of the H3 $\beta$  signal at 2.74 ppm.

$^1\text{H}$  NMR (400 MHz,  $\text{CDCl}_3$ )  $\delta$  in ppm 2.43 (dt,  $J = 12.40, 4.31$  Hz, 1H)

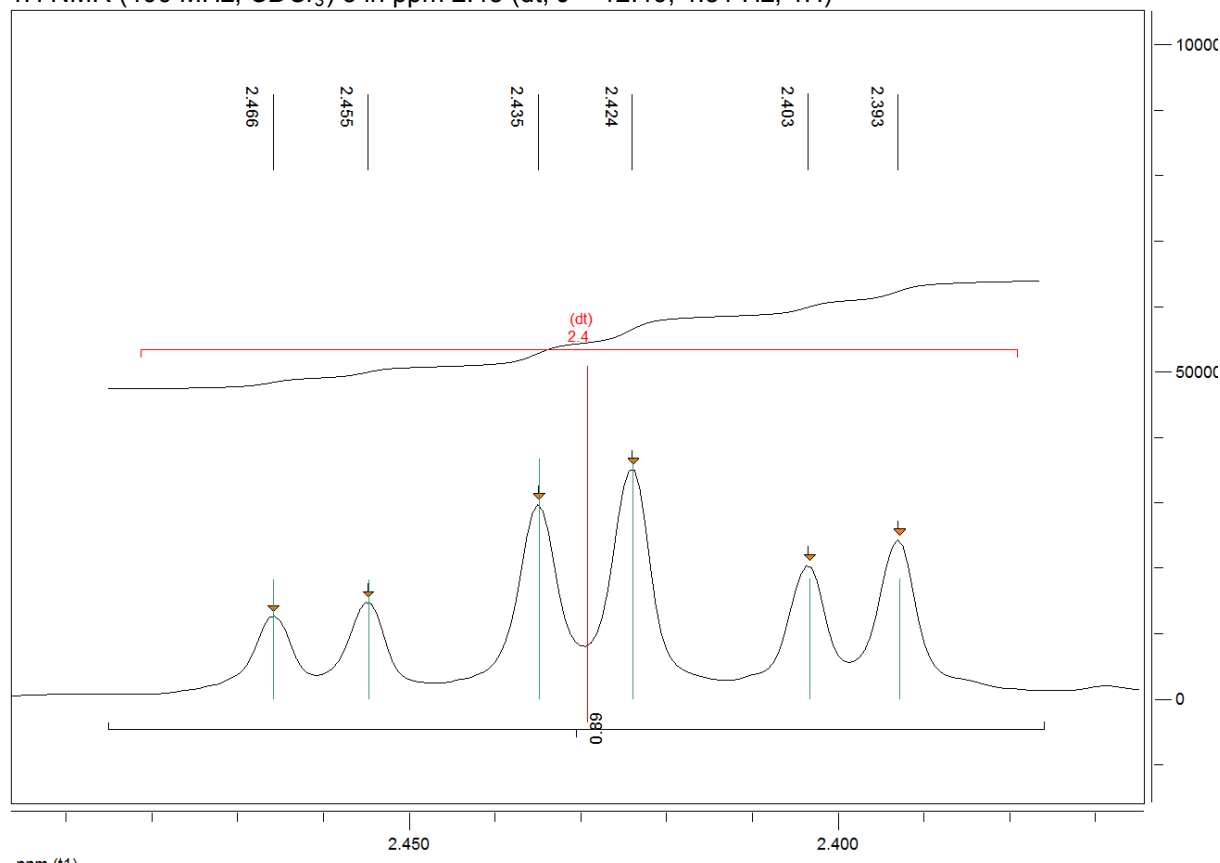


**Fig. 3.41** The  $^1\text{H}$ -NMR fine structure of the H9 $\alpha$  signal at 2.43 ppm.

### 3.2.6 Serratol (21)

Serratol was isolated as colourless viscous oil. The structure is shown in Fig. 3.42. Analysis by TLC (Pentane/ $\text{Et}_2\text{O}$  2:1 and 1 % HOAc) showed a strong green spot after dyeing and heating with anisaldehyde reagent at  $R_f = 0.46$ . Detection by DAD-RP-HPLC was only possible at 210 nm and it eluted at a  $R_t$  value of ca. 28.3 min (co-elution with compound **14** in the RE, if not separated by prior extraction) under standard HPLC conditions (2.3.4.2). Mass spectrometric detection (ESI-MS; low resolution, positive ion mode) delivered the following significant fragmentation pattern:  $m/z$  (%): 291.50  $[\text{M} + \text{H}]^+$  (60); 273.4  $[\text{M} - \text{OH}]^+$  (100). The  $^{13}\text{C}$ -NMR spectrum revealed 20 carbon atom signals. DEPT 90/135 spectra divided these 20 C-atoms into 4 quaternary, 4 CH-, 7  $\text{CH}_2$ - and 5 methyl carbon atoms. The  $^1\text{H}$ -spectrum is shown in Fig. 3.43 and the  $^{13}\text{C}$ -spectrum is shown in Fig. 3.44. Structural elucidation by conventional 2D-NMR techniques (HSQC, COSY, NOESY, and HMBC) is basically presented in Tab. 3.6.

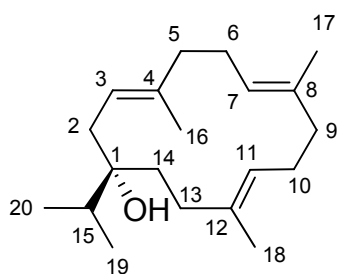


**Fig. 3.42** Structure of serratol (**21**).

## Results and Discussion

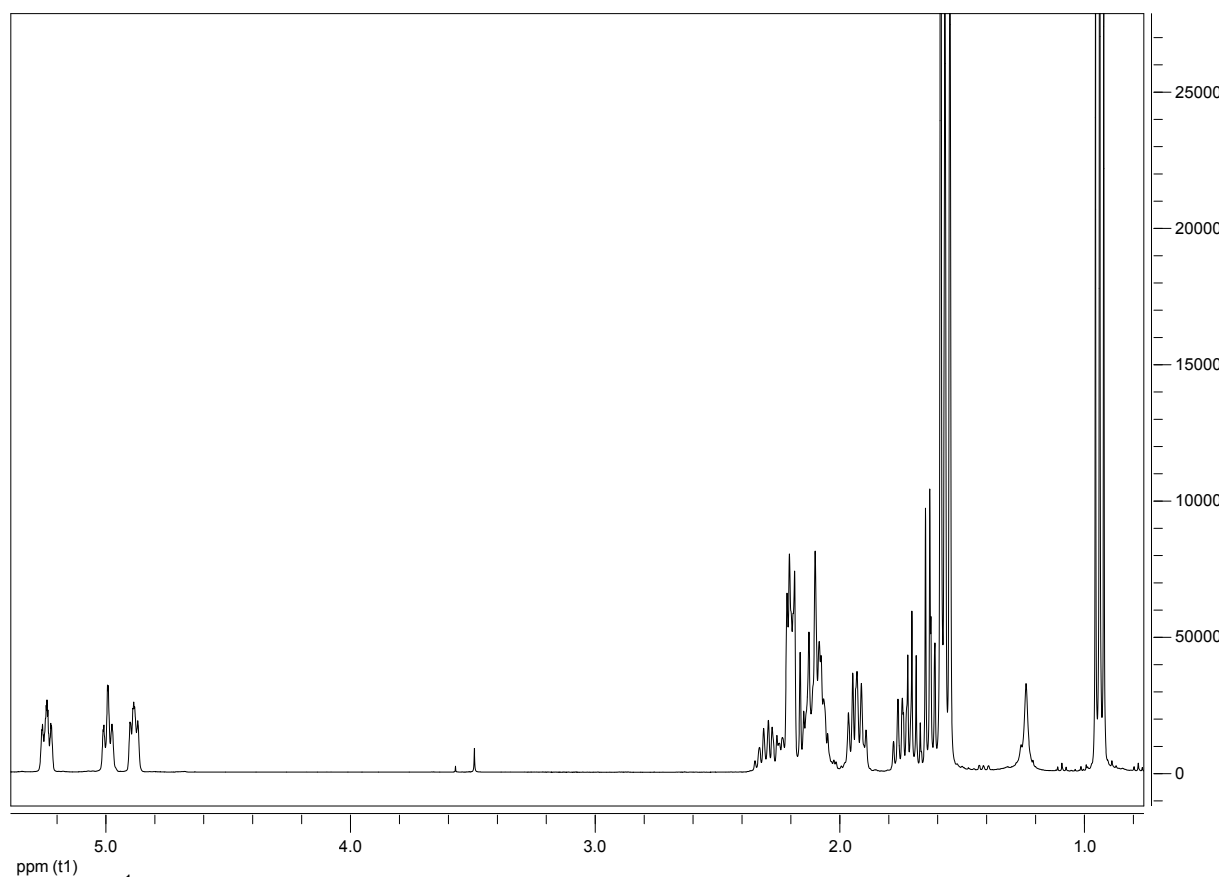


**Fig. 3.43**  $^1\text{H-NMR}$  spectrum serratol (21).

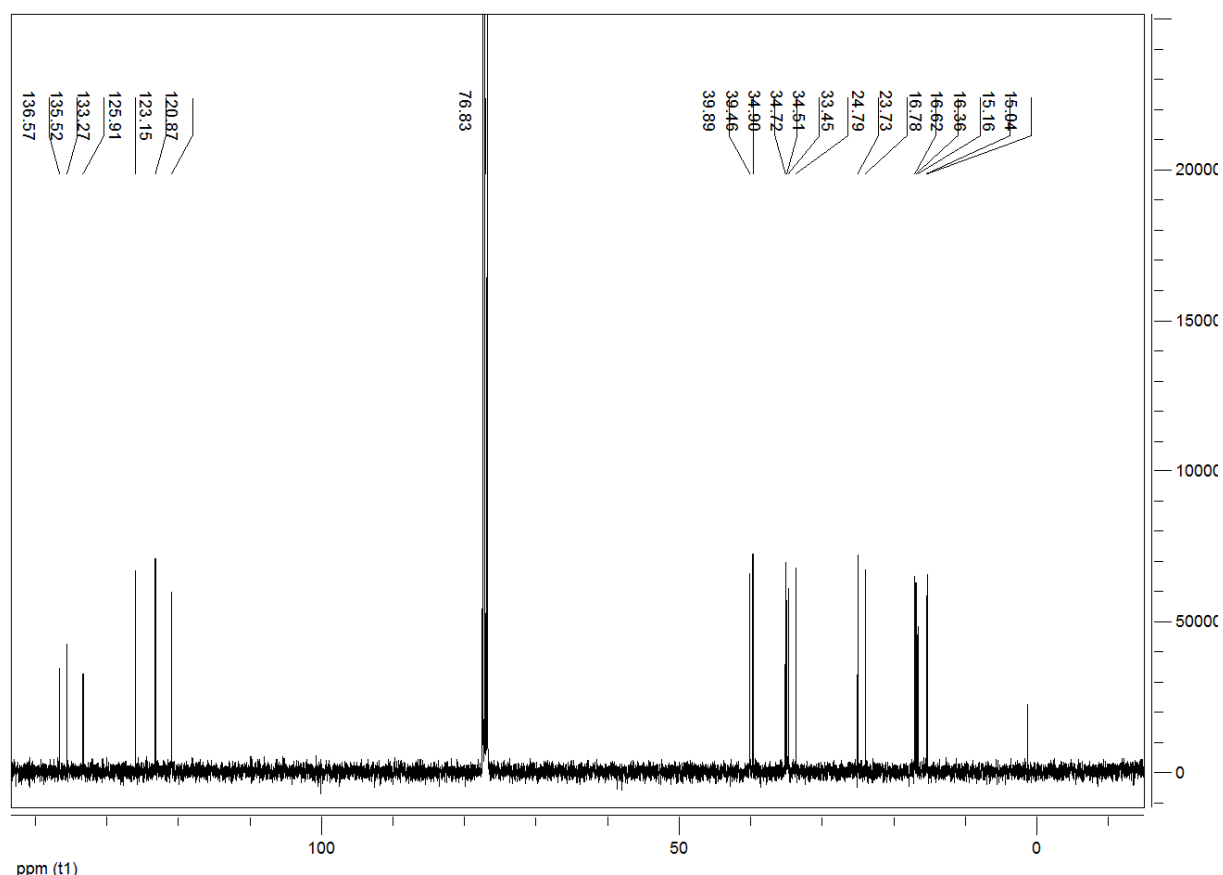


**Fig. 3.44**  $^{13}\text{C-NMR}$  spectrum serratol (21).

## Results and Discussion

Evaluation of the spectral data and comparison with data found in the literature [56,84] confirmed the isolated compound as serratol. The compound itself was firstly described in Bser by Pardhy and Bhattacharyya [83] and in Bcar by Klein and Obermann [82] (both groups in 1978). Seitz [56] isolated this compound also from Bcar and delivered the first 2D NMR data set on serratol. Finally, Schmidt et al. published their complete structural assignment 2D NMR data set of serratol (isolated from Bser) and additionally report on the antiprotozoal activity of this compound [84]. The NMR data delivered here is consistent with the data published by Schmidt et al. [84]. The position of  $\alpha$ - and  $\beta$ -H atoms for secondary carbons ( $\text{CH}_2$ ) is not unambiguously assignable in the NOESY data set. Serratol is a 14 carbons containing monocyclic ring and thus shows a quite high flexibility concerning the possible different conformations of this molecule. This phenomenon can be easily understood if a molecule model is build.

**Tab. 3.6**  $^1\text{H}$  and  $^{13}\text{C}$  NMR assignments (400 MHz) for serratol (**21**).

Atom Nr.	$^{13}\text{C}$ $\delta$ [ppm]	$^1\text{H}$ $\delta$ [ppm], $J$ [Hz]	HMBC ( $^2J$ in Hz)	HMBC ( $^3J$ in Hz)	HH-COSY	NOESY
1	76.83		$2\alpha/\beta$ , $14\alpha/\beta$ , 15	$13\alpha/\beta$ , 19, 20		
2	34.72	2.14 2.20	3	$14\alpha/\beta$		
3	120.87	5.24 (br dd, t) <sup>a</sup>	$2\alpha/\beta$	$5\alpha/\beta$ , 16	$2\alpha/\beta$ , $5\alpha/\beta$ , 16	$2\alpha/\beta$ , 7, 11, $14\alpha/\beta$ , 15
4	136.57		$5\alpha/\beta$ , 16	$2\alpha/\beta$ , $6\alpha/\beta$		
5	39.45	2.21 2.21	$6\alpha/\beta$	3, 16		
6	24.79	2.11 2.30	$5\alpha/\beta$ , 7			
7	125.91	4.88 (br dd, t) <sup>a</sup>	$6\alpha/\beta$	$5\alpha/\beta$ , $9\alpha/\beta$ , 17	$6\alpha/\beta$ , 17	3, $5\alpha/\beta$ , $6\alpha/\beta$ , $9\alpha/\beta$ , 11, $14\alpha/\beta$
8	133.27		$9\alpha/\beta$ , 17	$6\alpha/\beta$		
9	39.89	1.95 2.11	$10\alpha/\beta$	7	$10\alpha/\beta$	
10	23.73	2.09 2.09	$9\alpha/\beta$ , 11		$9\alpha/\beta$	
11	123.15	4.99 (br dd, t) <sup>a</sup>	$10\alpha/\beta$	$9\alpha/\beta$ , $13\alpha/\beta$ , 18	$10\alpha/\beta$ , $13\alpha/\beta$ , 18	3, 7, $10\alpha/\beta$ , $13\alpha/\beta$ , $14\alpha/\beta$
12	135.52		$13\alpha/\beta$ , 18	$10\alpha/\beta$ , $14\alpha/\beta$		
13	33.45	1.93 1.75	$14\alpha/\beta$	11, 18	13( <i>gem.</i> ) $14\alpha/\beta$	
14	34.90	1.65 1.65	$13\alpha/\beta$	$2\alpha/\beta$	$13\alpha/\beta$	
15	34.51	1.71	1, 19, 20		19, 20	
16	15.04	1.54 (br s)	4	3, 5	3	
17	15.16	1.56 (br s)	8	7, 9	7	
18	16.36	1.58 (br s)	12	11, 13	11	
19	16.62 <sup>b</sup>	0.94 (d, $J = 6.8$ )	15	1, 20	1	$2\alpha/\beta$ , $14\alpha/\beta$ , 15
20	16.78 <sup>b</sup>	0.92 (d, $J = 6.8$ )	15	1, 19	1	$2\alpha/\beta$ , $14\alpha/\beta$ , 15

<sup>a</sup> The fine structures show actually a more complex multiplet fine structure within the triplet (dd)

<sup>b</sup> Assignment interchangeable (see also Schmidt et al. [84])

### 3.2.7 Iso-Serratol (20)

Iso-Serratol was isolated as colourless viscous oil. The structure is shown in Fig. 3.45. Analysis by TLC (Pentane/Et<sub>2</sub>O 2:1 and 1 % HOAc) showed a dark blue spot after dyeing and heating with anisaldehyde reagent at  $R_f = 0.30$ . Detection by DAD-RP-HPLC was only possible at 210 nm and the compound eluted at a  $R_t$  value of ca. 27.7 min under standard HPLC conditions (2.3.4.2). Mass spectrometric detection (CI-MS; low resolution) delivered the following significant fragmentation pattern:  $m/z$  (%): 290.24 [M]<sup>+</sup> (3); 273.26 [M – OH]<sup>+</sup> (63); 272.24 [M – H<sub>2</sub>O]<sup>+</sup> (100). High resolution CI-MS gave as  $m/z$  (%): 290.2589 [M]<sup>+</sup> (8), calculated: 290.2610; 273.2594 [M – OH]<sup>+</sup> (100), calculated: 273.2577. Thus, a chemical formula of C<sub>20</sub>H<sub>34</sub>O is given. The <sup>13</sup>C-NMR spectrum revealed 20 carbon atom signals. DEPT 90/135 spectra divided these 20 C-atoms into 4 quaternary, 4 CH-, 7 CH<sub>2</sub>- and 5 methyl carbon atoms. The <sup>1</sup>H-spectrum is shown in Fig. 3.46 and the <sup>13</sup>C- and DEPT 90/135 spectra are shown in Fig. 3.47-3.49. The structural elucidation by conventional 2D-NMR techniques (HSQC, COSY, NOESY, and HMBC) is basically presented in Tab. 3.7.

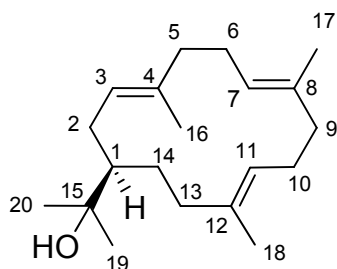


Fig. 3.45 Structure of iso-serratol (20).

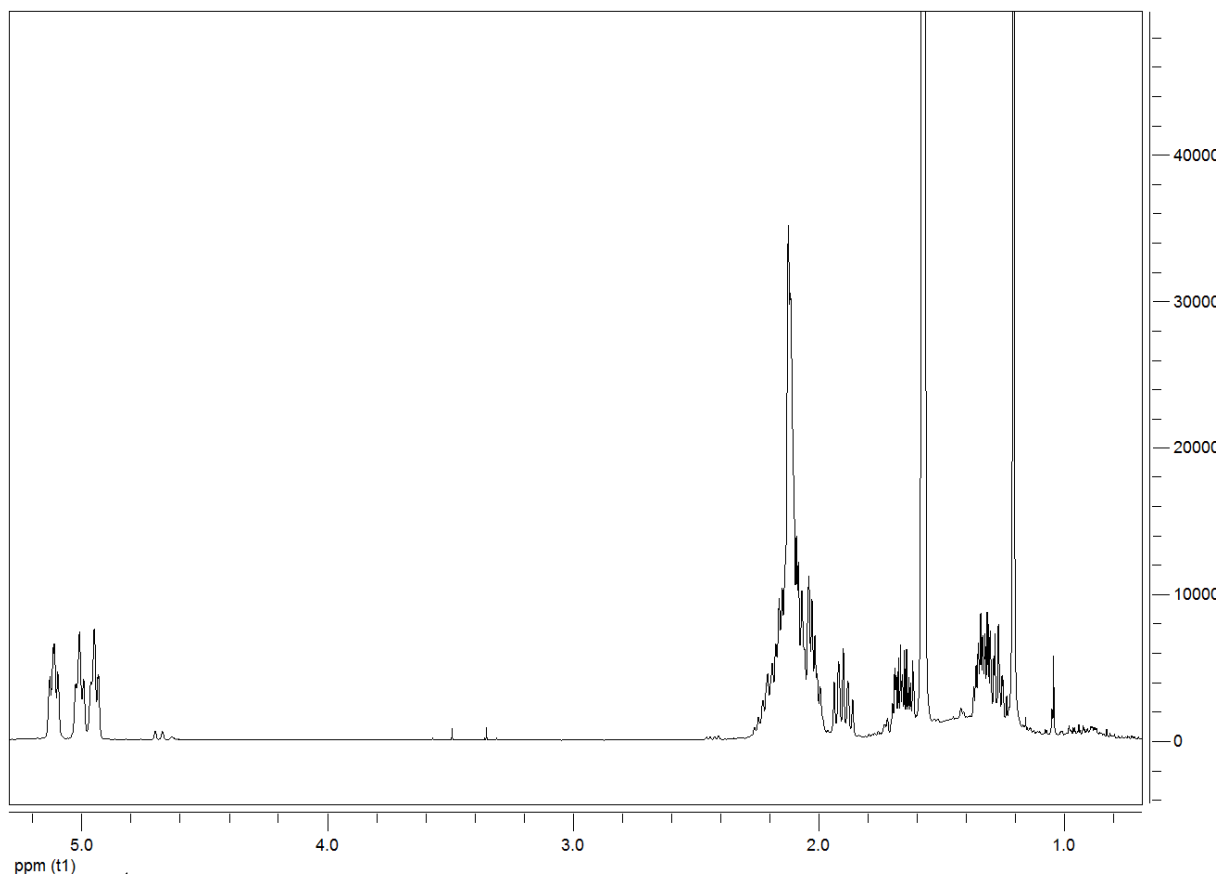
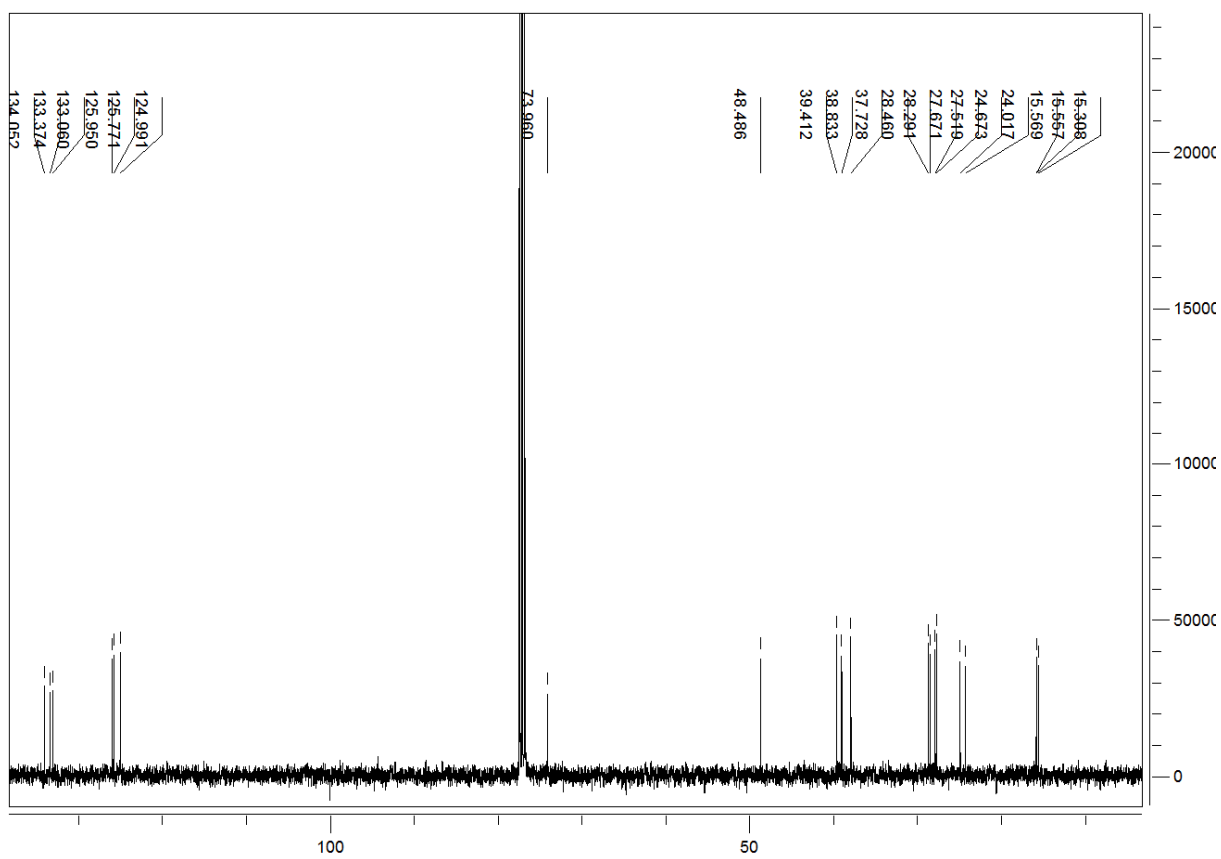
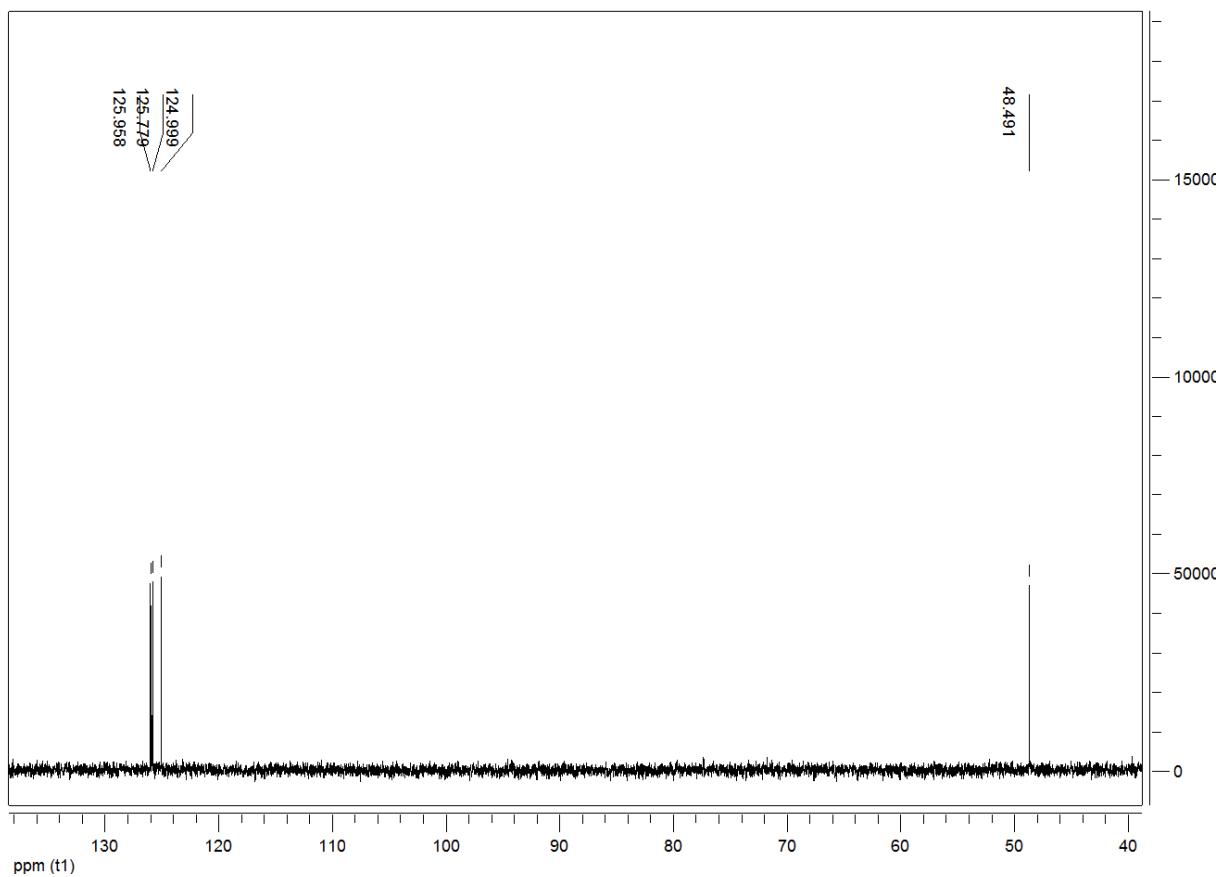


Fig. 3.46 <sup>1</sup>H-NMR spectrum of iso-serratol (20).

## Results and Discussion



ppm (t1)  
**Fig. 3.47**  $^{13}\text{C}$ -NMR spectrum of iso-serratol (**20**).



ppm (t1)  
**Fig. 3.48** DEPT-90 spectrum of iso-serratol (**20**).

## Results and Discussion

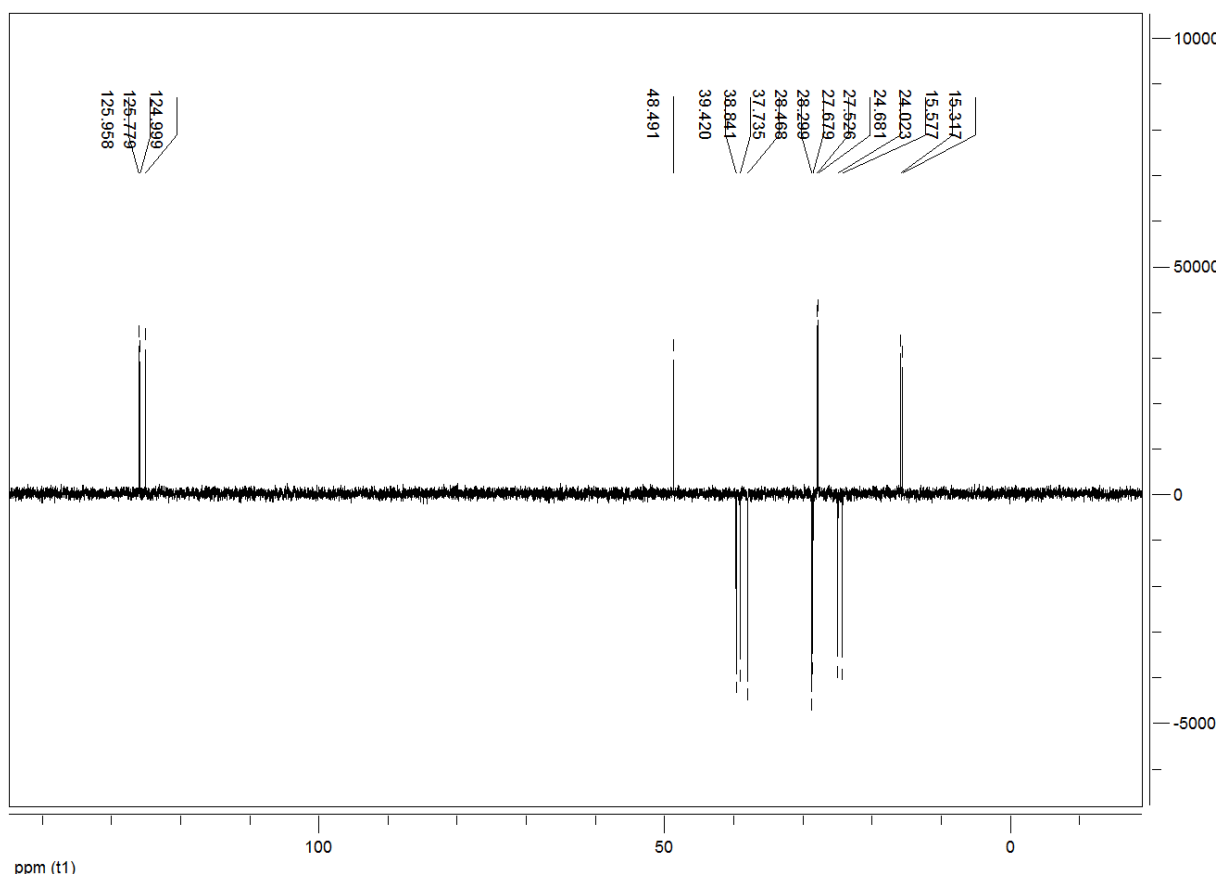


**Fig. 3.49** DEPT-135 spectrum of iso-serratol (**20**).

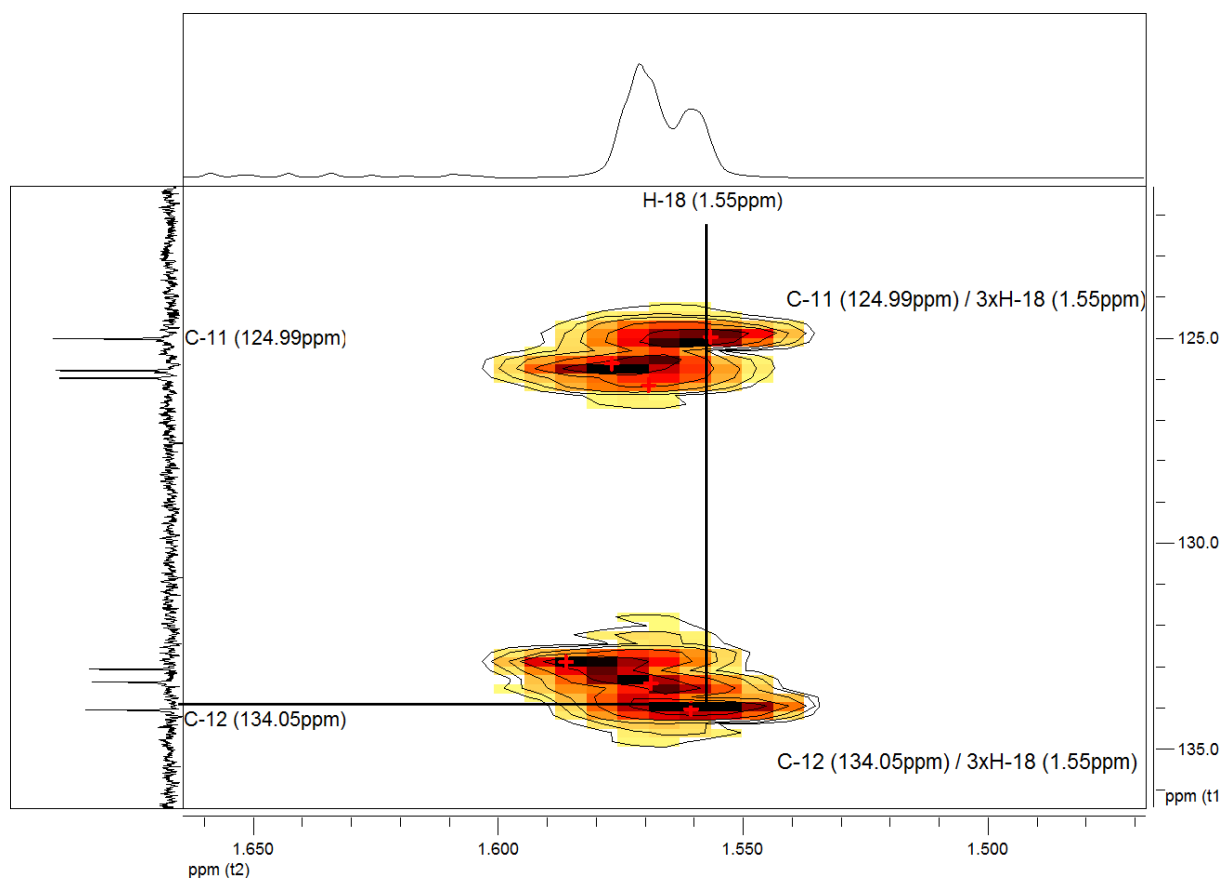


**Fig. 3.50** HMBC spectrum declaring the interaction of C-11 and C-12 with the methyl protons of C-18 in iso-serratol (**20**).

The  $^1\text{H-NMR}$  reveals for iso-serratol, similar as for serratol, three vinyl protons downfield shifted which show the same fine structures as the three vinyl protons from serratol (compare with data from chapter 3.2.6). Chemical shifts for the vinyl protons of C-16, C-17 and C-18 are overlaid to a huge almost unresolved peak signal at 1.55-1.57 ppm. Integration of this signal reveals 9 protons. At 1.20 ppm the two methyl singlets of the isopropyl alcoholic group showing the same chemical shifts and thus giving just one peak (Integration gives 6 protons). Especially the diminishing of the duplet structures at C-19 and C-20 clarifies this fact (compare with data from chapter 3.2.6). Additionally, the three vinyl methyl groups (C-16, C-17 and C-18) must have the same configuration as serratol since they deliver typical  $^{13}\text{C-NMR}$  chemical shifts for cembrene type molecules (see also Gacs-Baitz et al. [81], where (E)-methyl carbons are assigned at approximately 16-17 ppm, while (Z)-methyl signals appear at 22-23 ppm, which basically is the general rule for all cembrene-type molecules discussed here, e.g. incensole and its acetate). Correct assignment of these three methyl carbons (C-16, C-17 and C-18), showing almost identically chemical shifts, was achievable by elucidation of the HMBC spectrum as shown in Fig. 3.50, specifically by unambiguous assignment of the 1.55 ppm proton chemical shift. The position of  $\alpha$ - and  $\beta$ -H atoms for secondary carbons ( $\text{CH}_2$ ) is not unambiguously assignable in the NOESY data set. Iso-serratol, like serratol, is a 14 carbons containing monocyclic ring and thus shows a quite high flexibility concerning the possible different conformations of this molecule. This phenomenon can be easily understood if a molecule model is build.

Thoroughly evaluation of the spectral data confirmed the isolated compound as a derivative of serratol. Hence, it was denoted as iso-serratol since only the position of the hydroxyl function at C-1 is interchanged with the H atom of C-15. This contention can be easily figured out, if both tables for iso-serratol, respectively, serratol are compared at C-1, C-15, C-19 and C-20. The IUPAC nomenclature denotation may be thus (1-*R*)-3E,7E,11E-1-isopropyl-4,8,12-trimethyl-cyclotetradeca-trien-15-ol. The relative configuration at C-1 was not assigned, but seems to be reasonably *R* positioned (see also Fig. 3.51), since it is rather likely the product of the proton catalysed water addition at the double bond of the 1-methylethlyen group in cembrene A. However, with the data delivered here, the relative configuration of iso-serratol at C-1, as already described by Klein and Obermann [82], may be easily ascertainable. Cembrene C is hence probably the pre-cursor diterpene of serratol (see Fig. 3.52). According to the stability of the tertiary carbon cation, the existence of iso-serratol as an analogue of serratol makes sense. Cembrene A and C are ubiquitous natural diterpenes and were reported in Olibanum essential oils before [13,35,74,78]. Thus, it is quite reasonable that these two cembrenes are the pre-cursors of iso-serratol and serratol, respectively. To the best knowledge, this is the first report on a derivative structure of serratol, namely iso-serratol.

## Results and Discussion

**Tab. 3.7**  $^1\text{H}$  and  $^{13}\text{C}$  NMR assignments (400 MHz) for iso-serratol (**20**)

Atom Nr.	$^{13}\text{C}$ $\delta$ [ppm]	$^1\text{H}$ $\delta$ [ppm], $J$ [Hz]	HMBC ( $^2J$ in Hz)	HMBC ( $^3J$ in Hz)	HH-COSY	NOESY
1	48.49	1.33	2 $\alpha/\beta$ , 14 $\alpha/\beta$	13 $\alpha/\beta$ , 19, 20	2 $\alpha/\beta$ , 14 $\alpha/\beta$	3, 7, 11
2	28.46	1.91 2.13	3	14 $\alpha/\beta$	1, 2( <i>gem.</i> ), 3	1, 2( <i>gem.</i> )
3	125.95	5.11 (br dd, t) <sup>a</sup>	2 $\alpha/\beta$	16	2 $\alpha/\beta$ , 5 $\alpha/\beta$ , 16	1, 2 $\alpha/\beta$ , 3, 5 $\alpha/\beta$ , 11
4	133.37		5 $\alpha/\beta$ , 16	2 $\alpha/\beta$ , 6 $\alpha/\beta$		
5	38.83	2.12	6 $\alpha/\beta$	3, 16		
6	24.67	2.20 2.15	7, 5 $\alpha/\beta$			
7	125.77	4.95 (br dd, t) <sup>a</sup>	6 $\alpha/\beta$	9 $\alpha/\beta$ , 17	6 $\alpha/\beta$ , 17	3, 11
8	133.06		9 $\alpha/\beta$ , 17	10 $\alpha/\beta$		
9	39.41	2.02	10 $\alpha/\beta$	11, 17	7	
10	24.02	2.12 2.12	9 $\alpha/\beta$ , 11			
11	124.99	5.00 (br dd, t) <sup>a</sup>	10 $\alpha/\beta$	9 $\alpha/\beta$ , 13 $\alpha/\beta$ , 18	10 $\alpha/\beta$ , 13 $\alpha/\beta$ , 18	3, 7
12	134.05		13 $\alpha/\beta$ , 18	14(1.66)		
13	37.73	2.03 2.10	14 $\alpha/\beta$	1, 11, 18	14 $\alpha/\beta$	
14	28.29	1.26 1.66	1, 13 $\alpha/\beta$	2 $\alpha/\beta$	1, 13 $\alpha/\beta$ , 14( <i>gem.</i> )	
15	73.96		1, 19, 20	2 $\alpha/\beta$ , 14 $\alpha/\beta$		
16	15.56	1.57	4			
17	15.31	1.57	8	7		
18	15.57	1.55	12	11	11	
19	27.52	1.20 (s) <sup>b</sup>	15	1		
20	27.67	1.20 (s) <sup>b</sup>	15	1		

<sup>a</sup> The fine structures show actually a more complex multiplet fine structure within the triplet (dd)

<sup>b</sup> Assignment interchangeable (analogous phenomenon as serratol, see also Schmidt et al. [84])

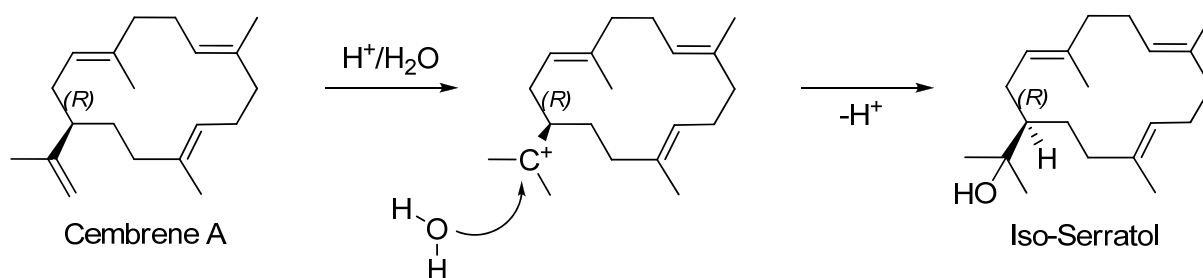


**Fig. 3.51** The proposed reaction scheme for the biosynthesis of iso-serratol, starting from cembrene A via a tertiary carbon cation.

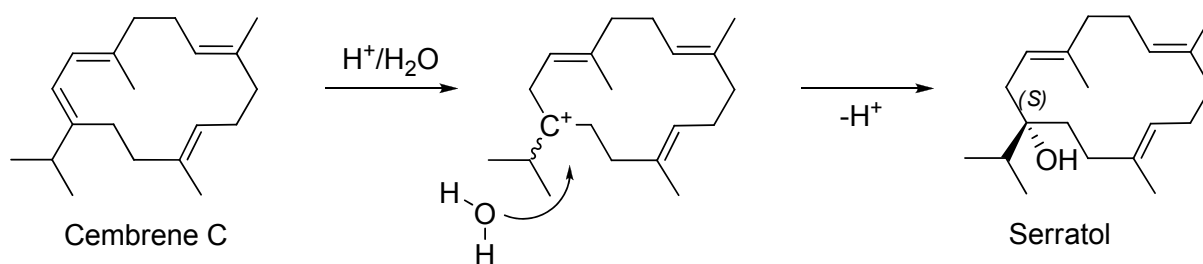


**Fig. 3.52** The proposed reaction scheme for the biosynthesis of serratol, starting from cembrene C via a tertiary carbon cation.

### 3.2.8 $\beta$ -Caryophyllene oxide (**28**)

The compound (**28**) was isolated as colourless viscous oil revealing a weak odour. The structure is shown in Fig. 3.53. Analysis by TLC (Pentane/Et<sub>2</sub>O 2:1 and 1 % HOAc) showed a pink spot after dyeing with anisaldehyde reagent and heating at  $R_f = 0.50$ . The standard HPLC method (2.3.4.2) gave a  $R_t$  value of ca. 21.1 min. Detection by DAD-RP-HPLC was only possible at 210 nm. Mass spectrometric detection (ESI-MS, positive mode; low resolution) delivered two significant peaks with  $m/z$  (%): 203.40  $[M - H_2O]^+$  (100) and 221.09  $[M]^+$  (**28**). The negative ion mode (ESI-MS) delivered a ternary complex of three  $\beta$ -caryophyllene oxide molecules with a base peak of  $m/z$  (%): 666.04 (100), probably due to the high concentration being injected.

However, the structural assignment by 1D and 2D NMR techniques was unequivocal. The <sup>13</sup>C-NMR spectrum revealed 15 carbon atom signals as presented in Fig. 3.54. DEPT 90/135 spectra divided these 15 C-atoms into 3 quaternary, 3 CH-, 6 CH<sub>2</sub>- and 3 methyl carbon atoms. The <sup>1</sup>H-spectrum is shown in Fig. 3.55 and the further structural elucidation by conventional 2D-NMR techniques (HSQC, COSY, NOESY, and HMBC) is basically presented in Tab. 3.8.

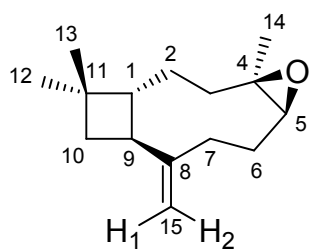


**Fig. 3.53** Structure of  $\beta$ -caryophyllene oxide (**28**).

## Results and Discussion

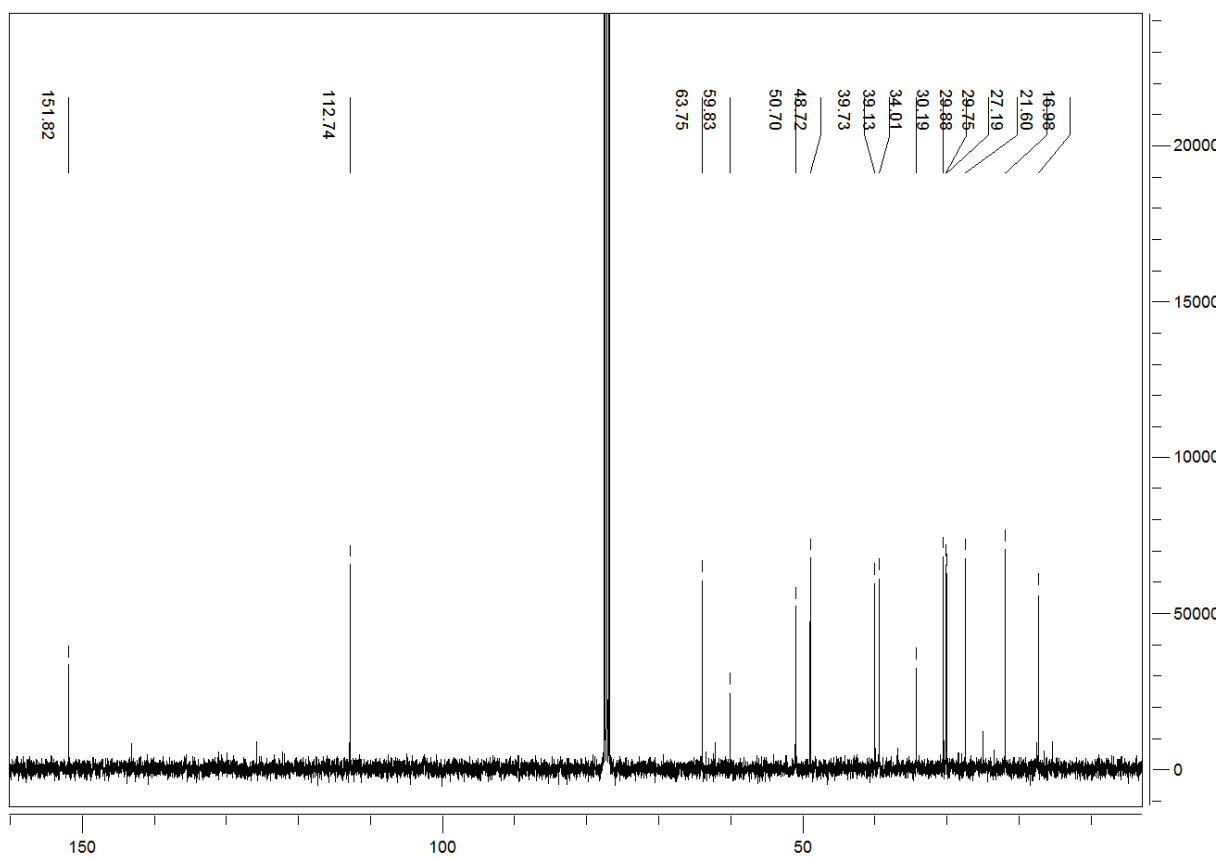


**Fig. 3.54**  $^{13}\text{C}$ -NMR spectrum of  $\beta$ -caryophyllene oxide (**28**).

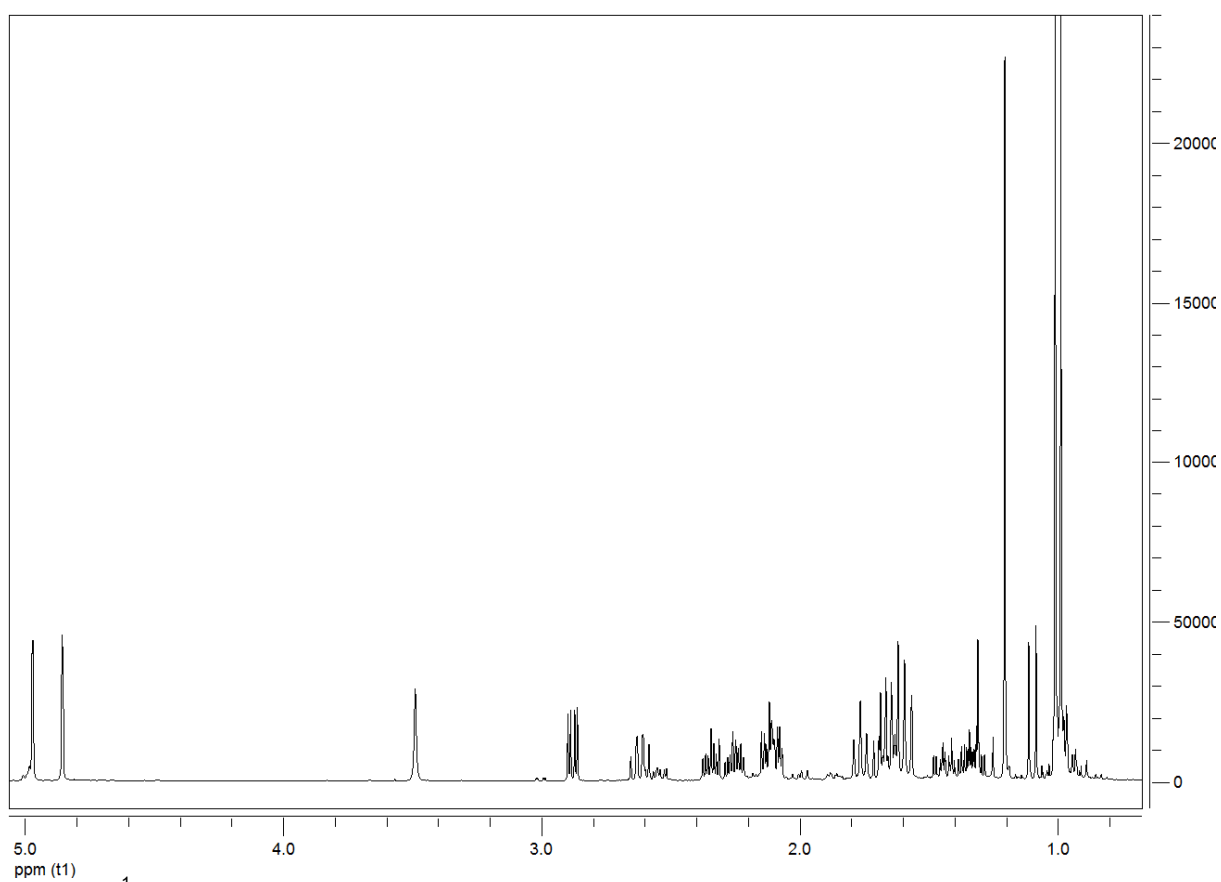


**Fig. 3.55**  $^1\text{H}$ -NMR spectrum of  $\beta$ -caryophyllene oxide (**28**).

## Results and Discussion

**Tab. 3.8**  $^1\text{H}$  and  $^{13}\text{C}$  NMR assignments for  $\beta$ -caryophyllene oxide (**28**).

Atom Nr.	$^{13}\text{C}$ $\delta$ [ppm]	$^1\text{H}$ $\delta$ [ppm], $J$ [Hz]	HMBC ( $^2J$ in Hz)	HMBC ( $^3J$ in Hz)	HH-COSY	NOESY
1	50.70	1.77 (tr, $J = 9.9$ )	9, 2 $\alpha/\beta$	3 $\alpha/\beta$ , 10 $\alpha/\beta$ , 12, 13	2 $\alpha/\beta$	2 $\alpha/\beta$ , 7 $\beta$ , 15H <sub>1</sub>
2	27.19	1.43 ( $\alpha$ ) 1.64 ( $\beta$ )	1, 3 $\alpha/\beta$	9	1, 2( <i>gem.</i> ), 3 $\alpha/\beta$	2( <i>gem.</i> ), 9
3	39.13	0.97 ( $\beta$ ) 2.10 ( $\alpha$ )	2 $\alpha/\beta$	1, 5, 14	2 $\alpha/\beta$ , 3( <i>gem.</i> )	3( <i>gem.</i> ), 6 $\alpha$
4	59.83		3 $\alpha/\beta$ , 5	2 $\alpha/\beta$ , 6 $\alpha/\beta$		
5	63.75	2.88 (dd, $J = 10.6, 4.2$ )	6 $\alpha/\beta$	3 $\alpha/\beta$ , 7 $\alpha/\beta$ , 14	6 $\alpha/\beta$	1, 6 $\alpha/\beta$ , 7 $\alpha/\beta$ , 13, 14
6	30.20	1.32 ( $\alpha$ ) 2.26 ( $\beta$ )	5, 7 $\alpha/\beta$		5, 6( <i>gem.</i> ), 7 $\alpha/\beta$	3 $\alpha$ , 15H <sub>2</sub>
7	29.75	2.11 ( $\alpha$ ) 2.33 ( $\beta$ )	6 $\alpha/\beta$	9	7( <i>gem.</i> ), 6 $\alpha/\beta$ , 15H <sub>2</sub>	15H <sub>2</sub>
8	151.82		7 $\alpha/\beta$ , 9, 15H <sub>1</sub> /H <sub>2</sub>	1, 6 $\alpha/\beta$		
9	48.72	2.62 (dd, $J = 9.6, 8.8$ )	1, 10 $\alpha/\beta$	2 $\alpha/\beta$ , 7 $\alpha/\beta$	1, 10 $\alpha/\beta$ , 15H <sub>1</sub>	7 $\alpha$ , 12, 15H <sub>1</sub>
10	39.73	1.63 ( $\beta$ ) 1.70 ( $\alpha$ )	9	12, 13	9	15H <sub>1</sub>
11	34.01		1, 12, 13	2 $\alpha/\beta$		
12	21.60	1.00 (s)		1, 10 $\alpha/\beta$ , 13		
13	29.88	0.98 (s)		10 $\alpha/\beta$ , 12		15H <sub>1</sub>
14	16.98	1.20 (s)		3 $\alpha/\beta$		2 $\alpha$ , 3 $\alpha$ , 5, 15H <sub>1</sub> /H <sub>2</sub>
15	112.74	4.97 (d, $J = 1.3, H_1$ ) 4.85 (d, $J = 1.6, H_2$ )		7 $\alpha/\beta$ , 9	15( <i>gem.</i> )	15( <i>gem.</i> )

Evaluation of the spectral data and comparison with data found in the literature [176] confirmed the isolated compound as  $\beta$ -caryophyllene oxide. The compound itself has been reported to be the primary air-oxidation product of  $\beta$ -caryophyllene [177,178], which is an ubiquitous compound occurring in several different plant essential oils (e.g. Cannabis: *Cannabis sativa*, oregano: *Origanum vulgare*, black pepper: *Piper nigrum*, etc. [178]).  $\beta$ -caryophyllene oxide is volatile and for example sensed by narcotic detection dogs [178].

In essential oils of *Boswellia* species it was reported by Hamm et al. [13] and Camarda et al. [74] to be specific for the species B<sub>sac</sub> and B<sub>car</sub>. The analytical value of this compound for the classification of B<sub>sac</sub>, respectively, B<sub>car</sub> is discussed in chapter 3.4 and 3.5.

The 2D NMR data set here, compared with the data of Rahman et al. [176], gives a slightly different assignment for the carbon signals. In their paper the carbons at position 2 and 10 are interchanged, compared with the data presented here. Furthermore, the positions of the methyl groups (C-12 and C-13) are again interchanged tabulated. However, the HH-COSY and NOESY data (see Fig. 3.56, respectively, Fig. 3.57) confirm that the structural assignment reported here is correct. The  $J$ -couplings of the protons at C-1, C-5, C-9 and C15 in the  $^1\text{H}$ -NMR data set give same values as reported by Rahman et al. [176] as demonstrated in (Fig. 3.58-3.61).

## Results and Discussion

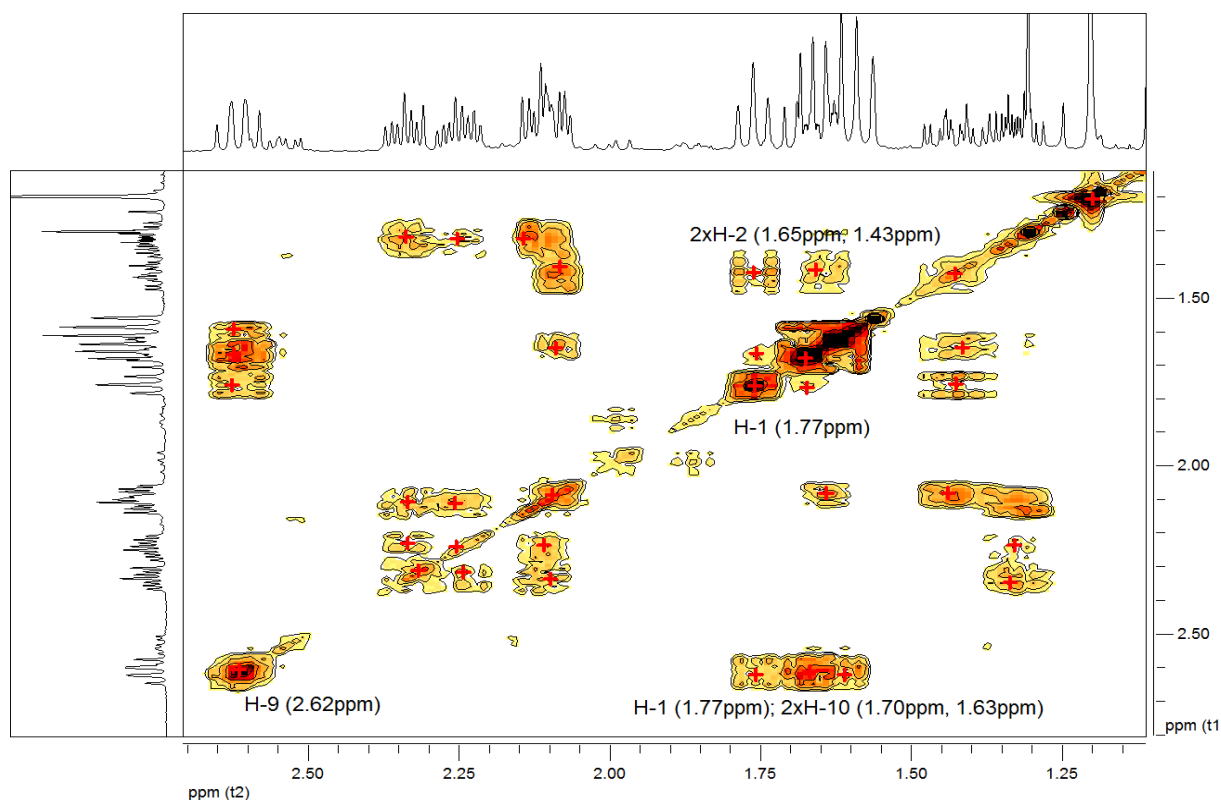


**Fig. 3.56** The HH-COSY spectrum declaring the correlation of H-9 with H-1 and both protons of C-10. See also text for further details.

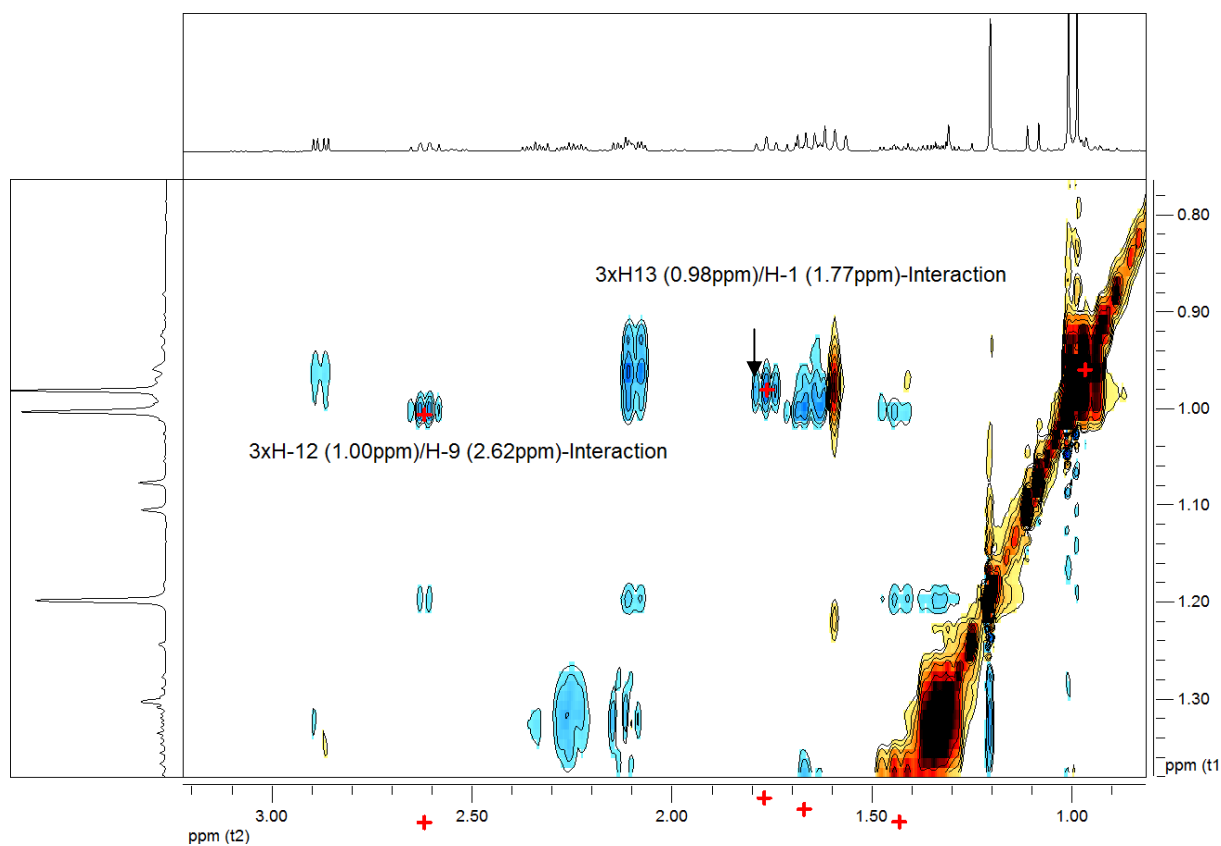
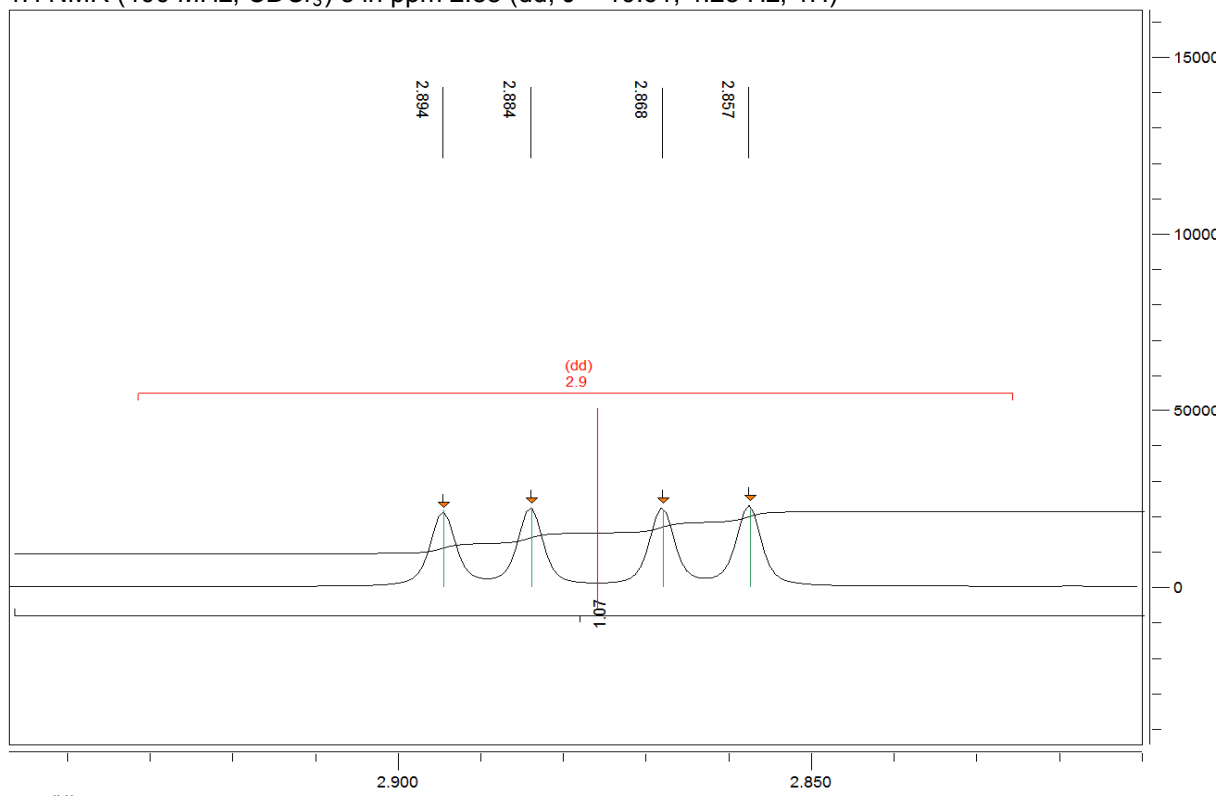


**Fig. 3.57** The NOESY spectrum declaring the relative position of C-12 and C-13, proved by interactions of H-12 with H-9 and H-13 with H-1.

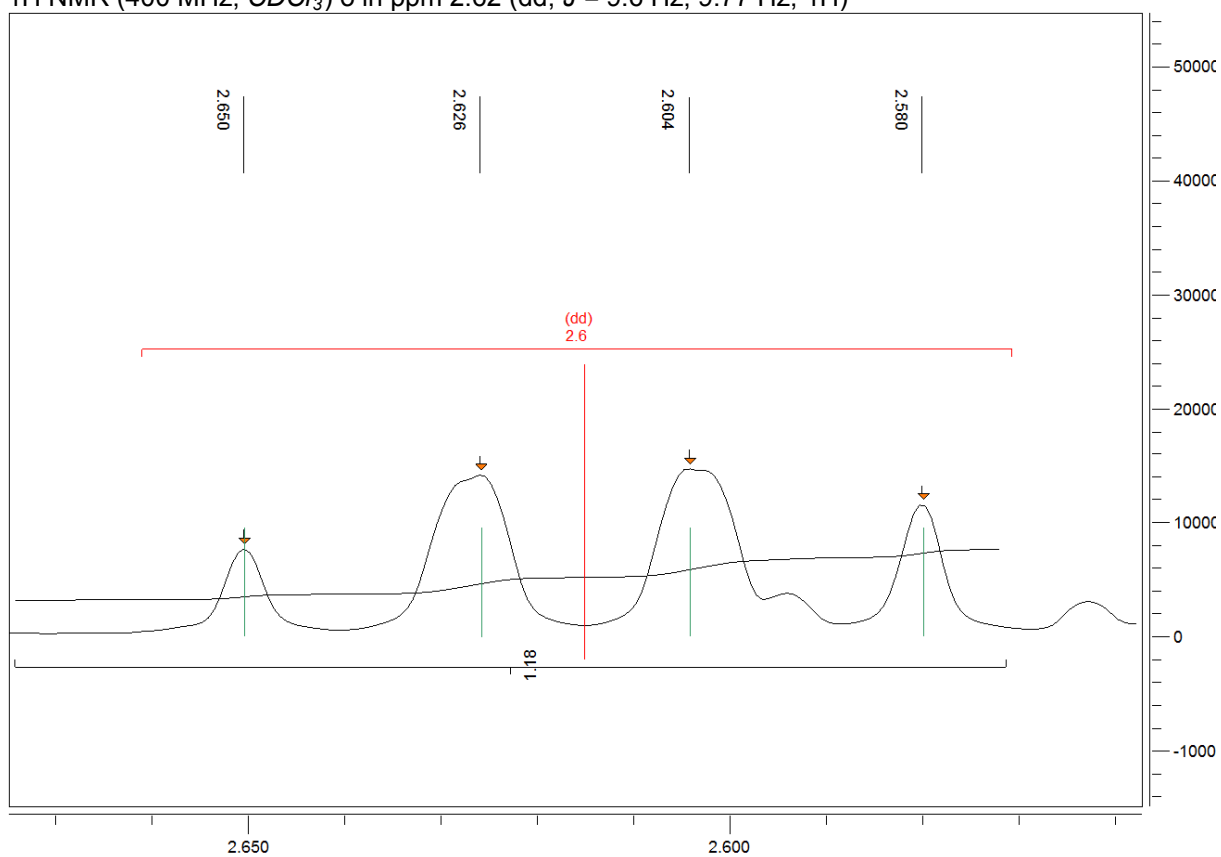
## Results and Discussion

$^1\text{H}$  NMR (400 MHz,  $\text{CDCl}_3$ )  $\delta$  in ppm 2.88 (dd,  $J = 10.61, 4.23$  Hz, 1H)



ppm (t1)  
**Fig. 3.58** The  $^1\text{H}$ -NMR fine structure of H-5 at 2.88 ppm.

$^1\text{H}$  NMR (400 MHz,  $\text{CDCl}_3$ )  $\delta$  in ppm 2.62 (dd,  $J = 9.6$  Hz, 9.77 Hz, 1H)



ppm (t1)  
**Fig. 3.59** The  $^1\text{H}$ -NMR fine structure of H9 at 2.62 ppm.

## Results and Discussion

$^1\text{H}$  NMR (400 MHz,  $\text{CDCl}_3$ )  $\delta$  in ppm 1.77 (t,  $J = 9.90$  Hz, 1H)

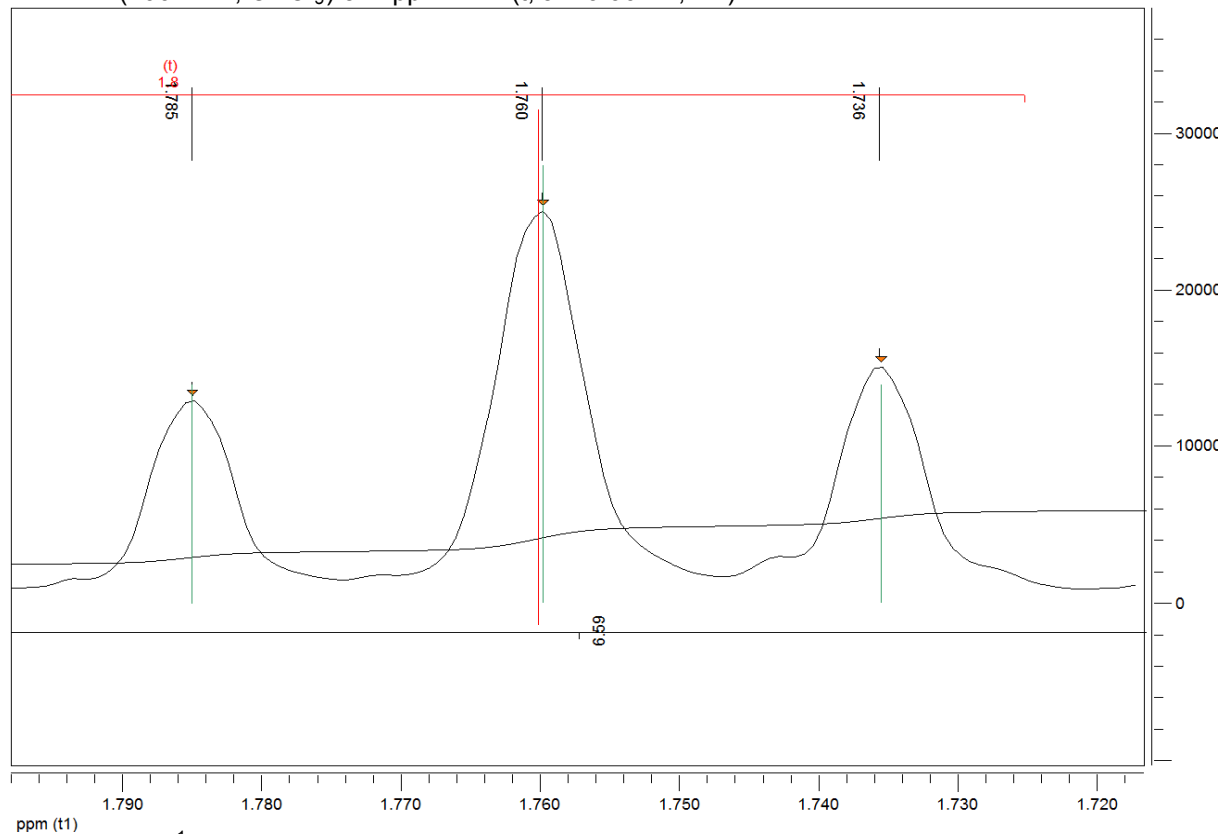


**Fig. 3.60** The  $^1\text{H}$ -NMR fine structure of H-1 at 1.77 ppm.

$^1\text{H}$  NMR (400 MHz,  $\text{CDCl}_3$ )  $\delta$  in ppm 4.97 (d,  $J = 1.28$  Hz, 1H), 4.86 (d,  $J = 1.61$  Hz, 1H)

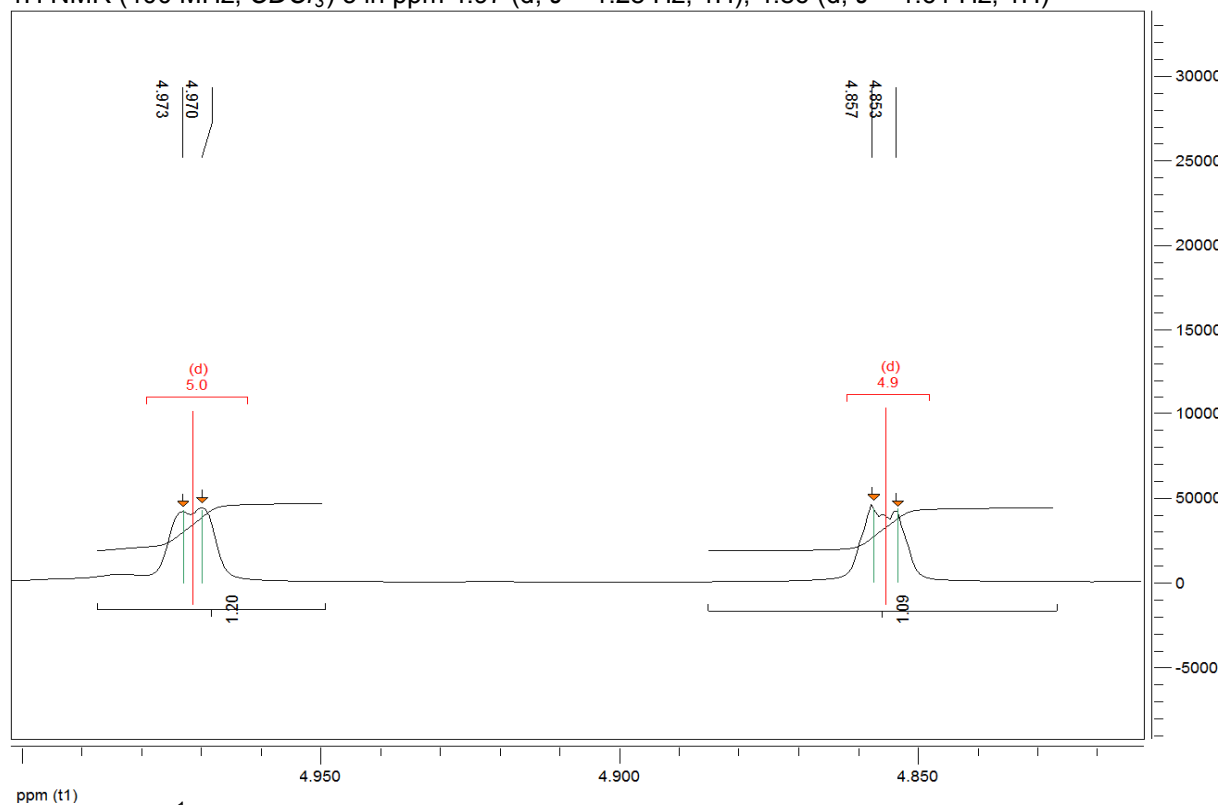


**Fig. 3.61** The  $^1\text{H}$ -NMR fine structure of the vinyl protons at C-15 (declared as H<sub>1</sub>, 4.97 ppm, and H<sub>2</sub>, 4.86 ppm).

### 3.2.9 $\tau$ -Cadinol (25)

The compound (**25**) was isolated as colourless viscous oil. The structure is shown in Fig. 3.62. Analysis by TLC (Pentane/Et<sub>2</sub>O 2:1 and 1 % HOAc) showed a dark blue spot after dyeing and heating with anisaldehyde reagent at  $R_f = 0.35$ . Detection by DAD-RP-HPLC was only possible at 210 nm ( $R_t$  ca. 21.8 min under standard HPLC conditions as described in chapter 2.3.4.2). The <sup>13</sup>C-NMR spectrum revealed 15 carbon atom signals as presented in Fig. 3.63 (minor signals refer to impurities difficult to separate from neutral compounds by liquid preparative chromatography in general). DEPT 90/135 spectra divided these 15 C-atoms into 2 quaternary, 5 CH-, 4 CH<sub>2</sub>- and 4 methyl carbon atoms. The structural elucidation by conventional 2D-NMR techniques (HSQC, COSY, NOESY, and HMBC) is basically presented in Tab. 3.9.

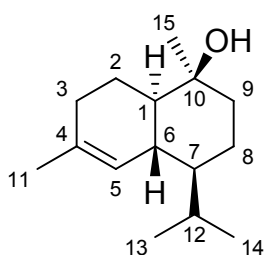


**Fig. 3.62** Structure of  $\tau$ -cadinol (**25**).

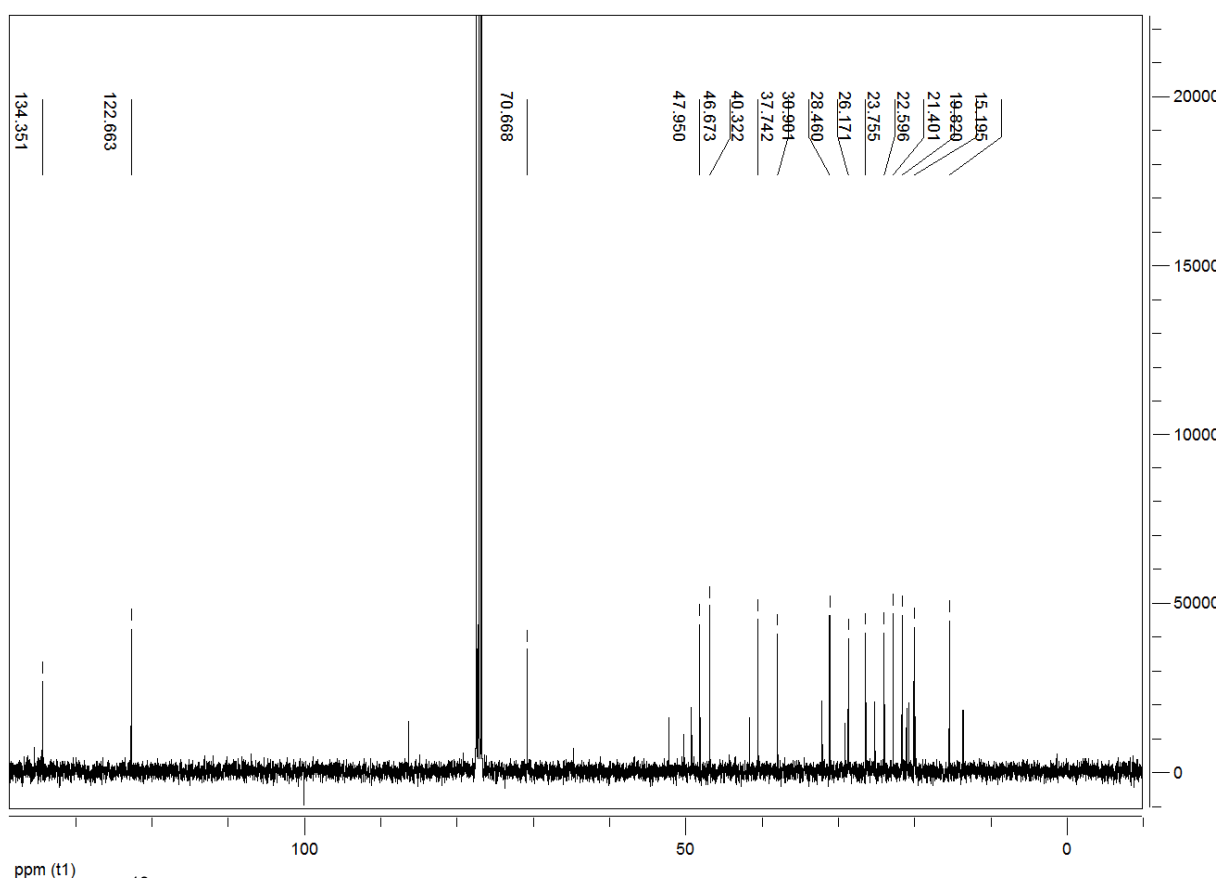


**Fig. 3.63** <sup>13</sup>C-NMR spectrum of  $\tau$ -cadinol (**25**). The minor signals result probably from an isomeric impurity (Note that purification of NB fraction compounds is quite tedious by preparative liquid chromatography).

## Results and Discussion

**Tab. 3.9**  $^1\text{H}$  and  $^{13}\text{C}$  NMR assignments (400 MHz) for  $\tau$ -cadinol (**25**).

Atom Nr.	$^{13}\text{C}$ $\delta$ [ppm]	$^1\text{H}$ $\delta$ [ppm], $J$ [Hz]	HMBC ( $^2J$ in Hz)	HMBC ( $^3J$ in Hz)	HH-COSY	NOESY
1	47.95	1.10 (dd, $J = 10, 2$ )	1, 2 $\alpha/\beta$ , 6	3, 5, 15	2 $\alpha/\beta$	2 $\alpha/\beta$ , 9 $\alpha$ , 7, 15
2	22.60	1.38 ( $\beta$ ) 1.93 ( $\alpha$ )	1		3 $\alpha/\beta$	2( <i>gem.</i> )
3	30.90	1.99 1.99	2 $\alpha/\beta$	1, 5, 11	2 $\alpha/\beta$ , 5, 11(4J)	2 $\beta$ , 11
4	134.35		2 $\alpha$ , 11	3 $\alpha/\beta$		
5	122.66	5.55 (br s)	6	1, 7, 11	3 $\alpha/\beta$ , 6, 11	6, 7, 11, 12, 13
6	37.74	1.97	1, 5	2 $\alpha/\beta$ , 8 $\alpha/\beta$	5	2 $\beta$ , 5, 13
7	46.67	1.00	8 $\alpha/\beta$	5, 9 $\alpha/\beta$ , 13, 14	8 $\alpha/\beta$ , 12	1, 5, 8 $\alpha/\beta$
8	19.82	1.36 ( $\alpha$ ) 1.49 ( $\beta$ )	9 $\alpha/\beta$		9 $\alpha/\beta$	
9	40.32	1.41 ( $\alpha$ ) 1.74 ( $\beta$ )	8 $\alpha/\beta$	15	8 $\alpha/\beta$ , 15(4J)	
10	70.67		9 $\alpha/\beta$ , 15	8 $\alpha/\beta$		
11	23.76	1.67 (br s)	4	3, 5	5	3 $\alpha/\beta$ , 5
12	26.17	2.18 (dsept, $J = 7.0, 3.2$ )	13, 14		7, 13, 14	5, 13, 14
13	15.20	0.79 (d, $J = 7.0$ )	12	14	12	5, 6, 12, 14
14	21.40	0.92 (d, $J = 7.0$ )	12	13	12	8 $\beta$ , 12, 13
15	28.46	1.22 (s)		1, 9		1, 2 $\alpha/\beta$ , 9 $\alpha/\beta$

Evaluation of the spectral data and comparison with data found in the literature [179,180] confirmed the isolated compound as  $\tau$ -cadinol (**25**). It is a ubiquitously occurring sesquiterpenoid (e.g. *Satureja gilliesii*, *Corymbia maculate* etc.).

Interestingly, this compound is, like  $\beta$ -caryophyllene oxide (**28**), reported as a marker for the *Boswellia* species Bcar, respectively, Bsac. Hamm et al. [13] and Camarda et al. [74] report it both, by GC-MS analysis, as a specific terpenoid for these species. They did not observe it in Bpap and Bser. The same conclusions have been deduced in this work (see chapter 3.5 on the GC-FID analysis). In Fig. 3.64-3.66 a few significant  $^1\text{H}$ -NMR fine structures are shown.

## Results and Discussion

$^1\text{H}$  NMR (400 MHz,  $\text{CDCl}_3$ )  $\delta$  in ppm 0.79 (d,  $J = 7.0$  Hz, 3H)

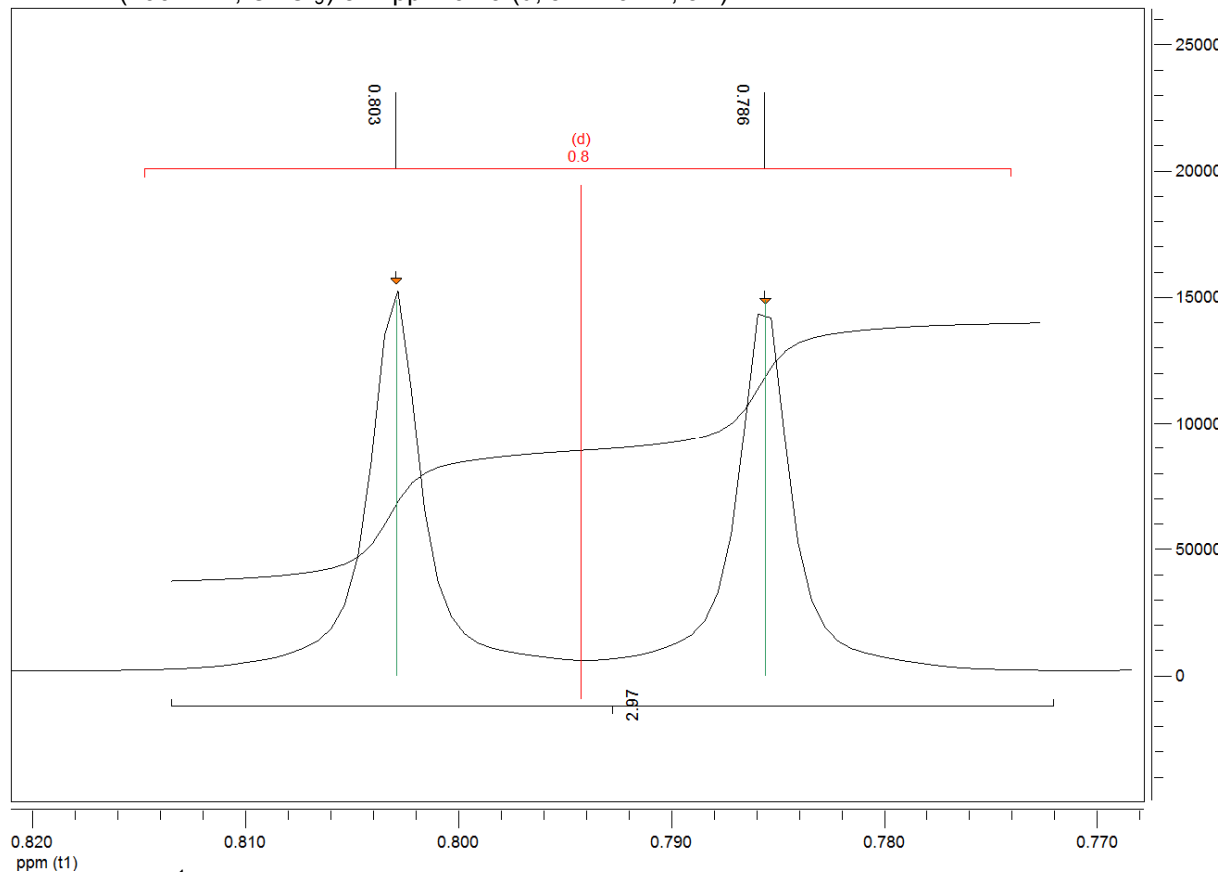


**Fig. 3.64** The  $^1\text{H}$ -NMR fine structure of H-13 (methyl group) at 0.79 ppm.

$^1\text{H}$  NMR (400 MHz,  $\text{CDCl}_3$ )  $\delta$  in ppm 0.92 (d,  $J = 7.0$  Hz, 3H)

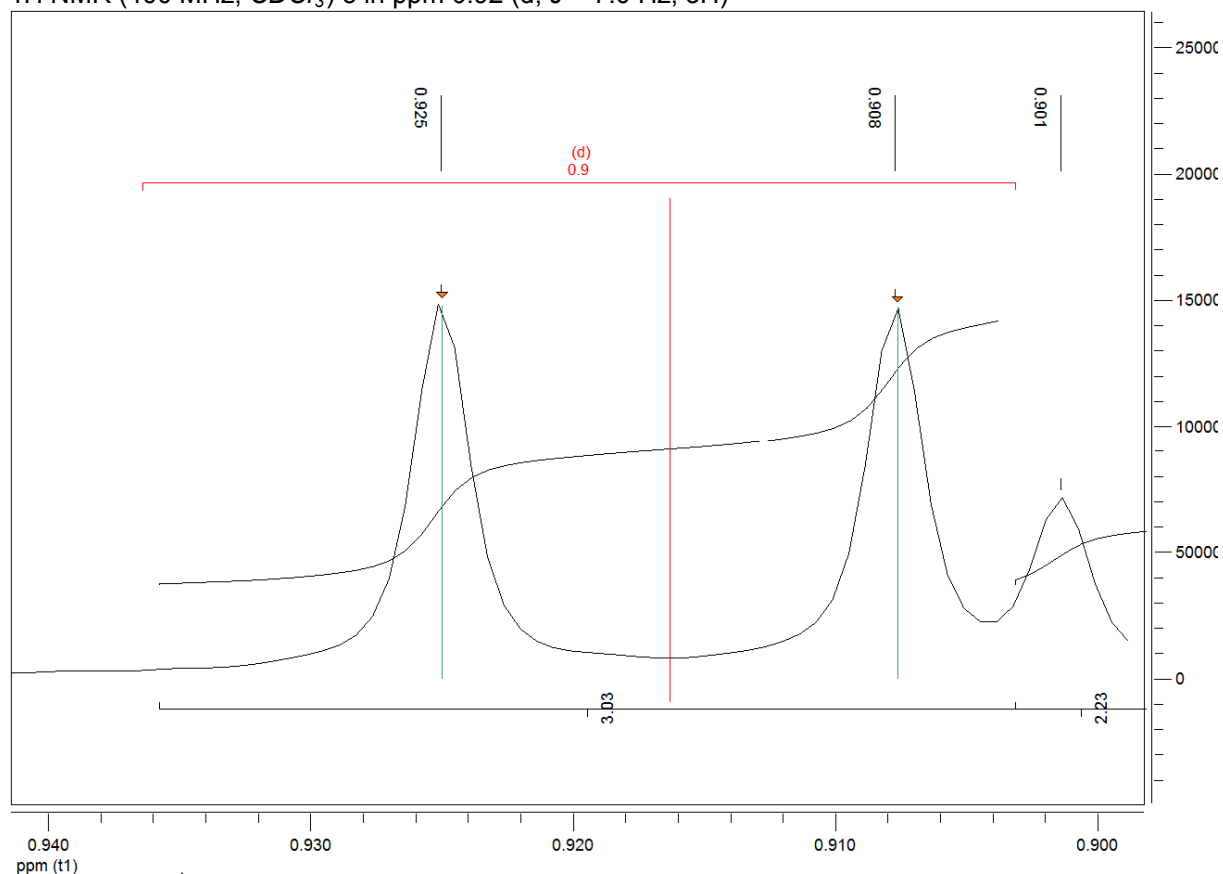


**Fig. 3.65** The  $^1\text{H}$ -NMR fine structure of H-14 (methyl group) at 0.92 ppm.

$^1\text{H-NMR}$  (400 MHz,  $\text{CDCl}_3$ )  $\delta$  in ppm 2.19 (dsept,  $J = 7.0$  Hz, 3.2 Hz, 1H)

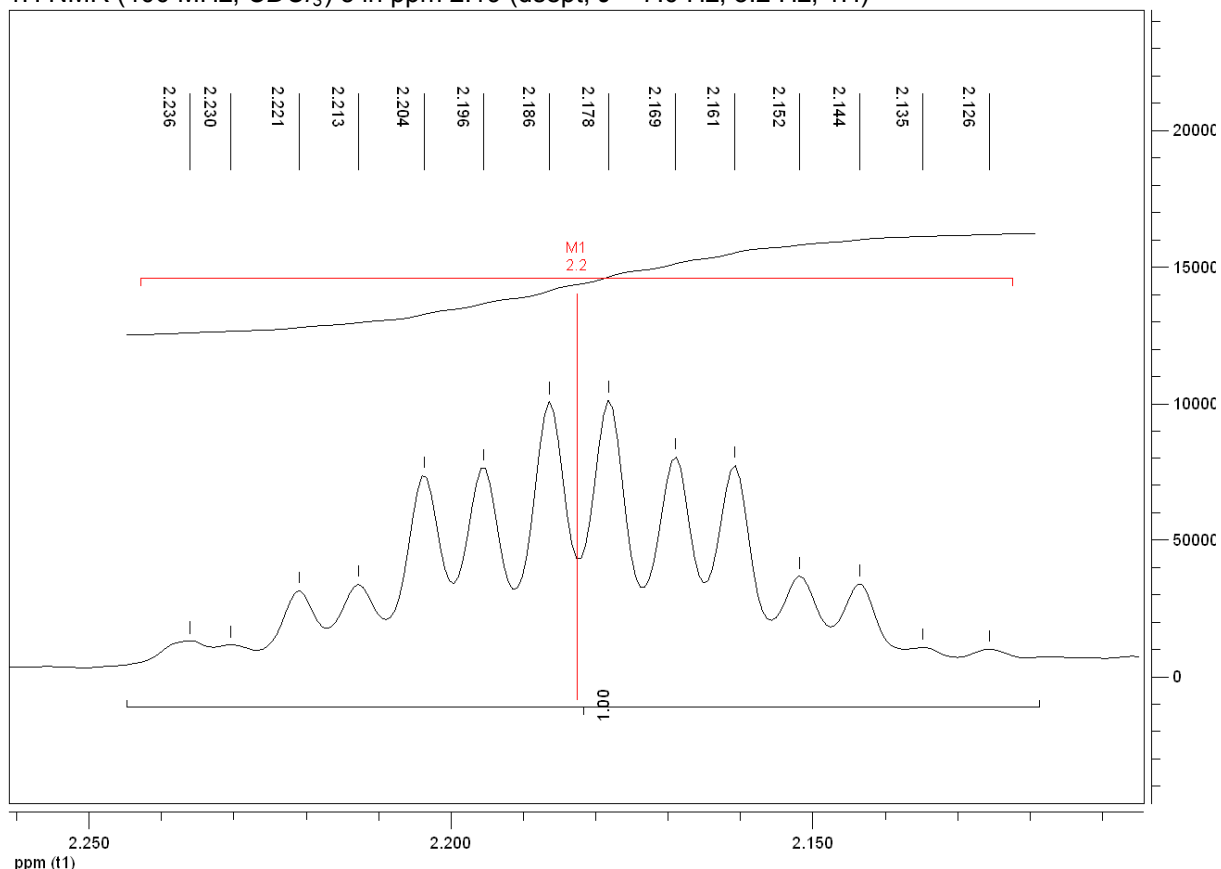


**Fig. 3.66** The  $^1\text{H-NMR}$  fine structure of H-12 at 2.19 ppm.

### 3.2.10 3- $\beta$ -OH-Tirucalol (**29**)

3- $\beta$ -OH-tirucalol was isolated as white solid. The structure is shown in Fig. 3.67. Analysis by TLC (Pentane/ $\text{Et}_2\text{O}$  2:1 and 1 % HOAc) showed a dark blue/violet spot after dyeing and heating with anisaldehyde reagent at  $R_f = 0.26$ . Detection by DAD-RP-HPLC was only possible at 210 nm and the compound eluted at a  $R_t$  value of ca. 57.1 min under standard HPLC conditions (2.3.4.2). The  $^{13}\text{C-NMR}$  spectrum revealed 30 carbon signals. DEPT 90/135 spectra divided them into 7 quaternary, 5  $\text{CH}$ -, 10  $\text{CH}_2$ - and 8 methyl carbon atoms. The  $^1\text{H}$ -spectrum is shown in Fig. 3.68 and the  $^{13}\text{C}$ - and DEPT 90/135 spectra are shown in Fig. 3.69-3.71. Structural elucidation by conventional 2D-NMR techniques (HSQC, COSY, NOESY, and HMBC) is basically presented in Tab. 3.10.

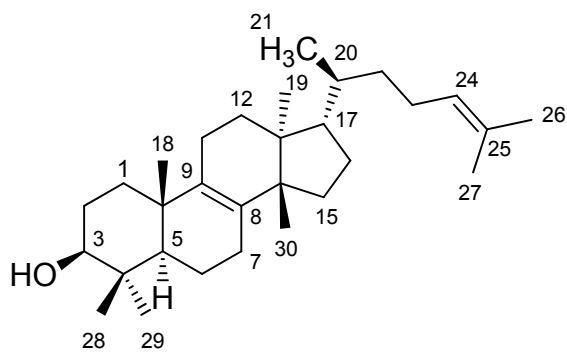


**Fig. 3.67** Structure of 3- $\beta$ -OH-tirucalol (**29**).

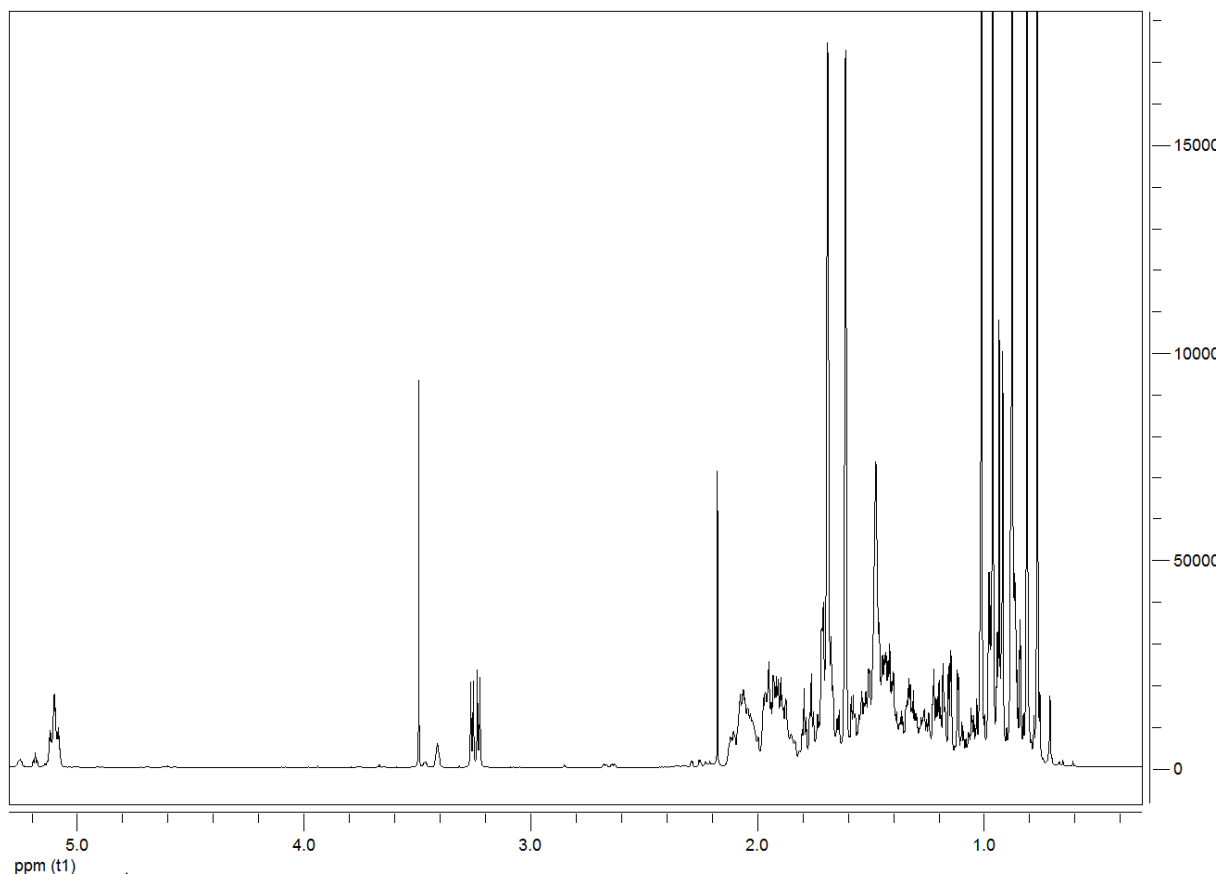


**Fig. 3.68**  $^1\text{H}$ -NMR spectrum of 3- $\beta$ -OH-tirucallol (**29**).

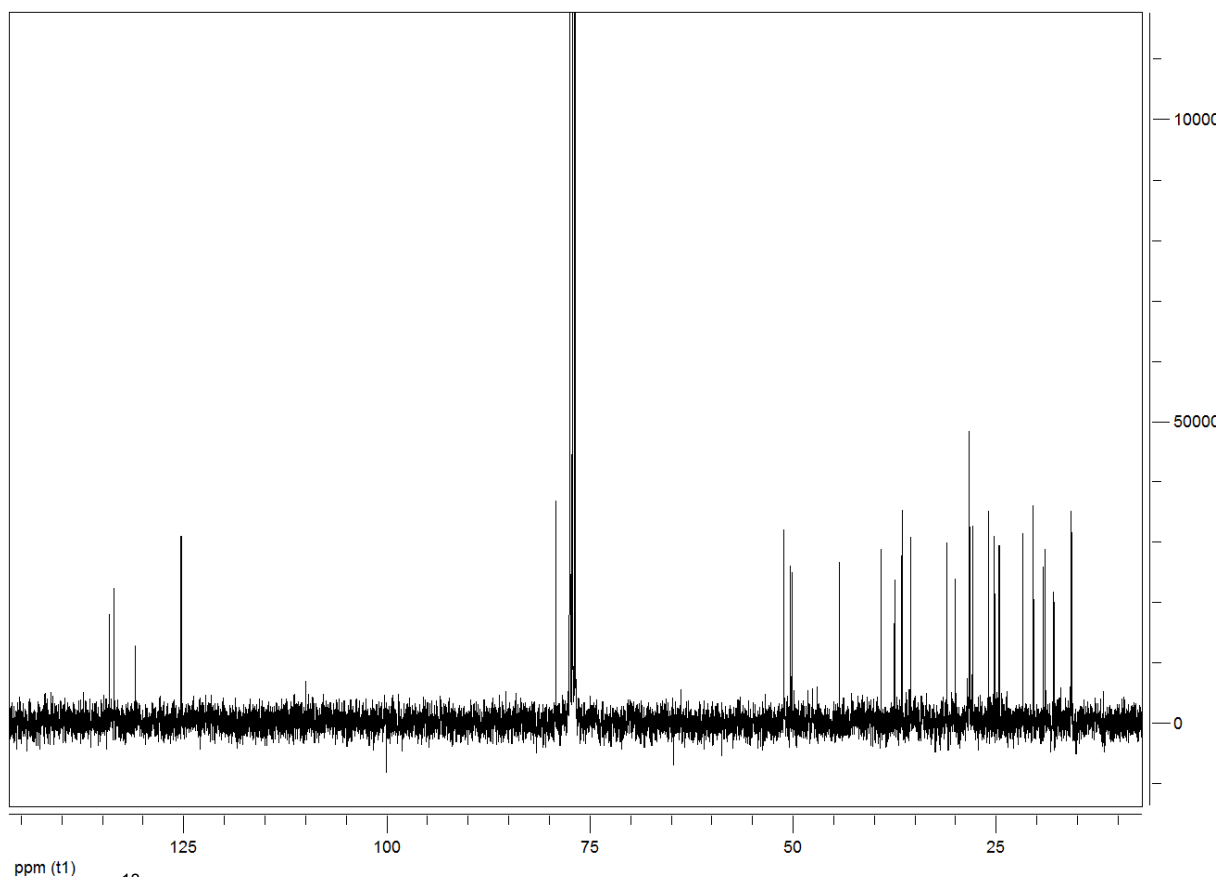


**Fig. 3.69**  $^{13}\text{C}$ -NMR spectrum of 3- $\beta$ -OH-tirucallol (**29**). Signals of C-16 and C-29 are superimposed (view highest peak between 30-25 ppm).

## Results and Discussion

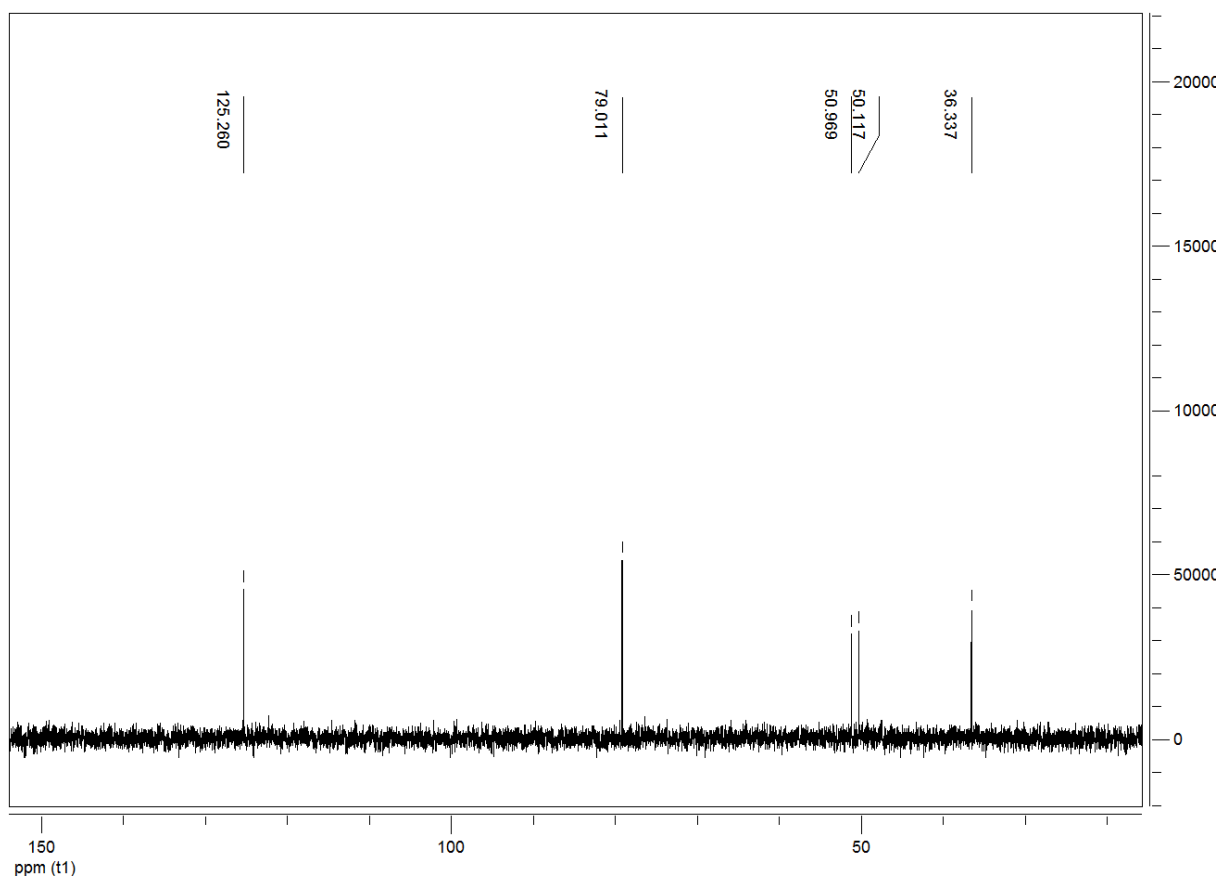


**Fig. 3.70** DEPT-90 spectrum of 3-β-OH-tirucallol (**29**).

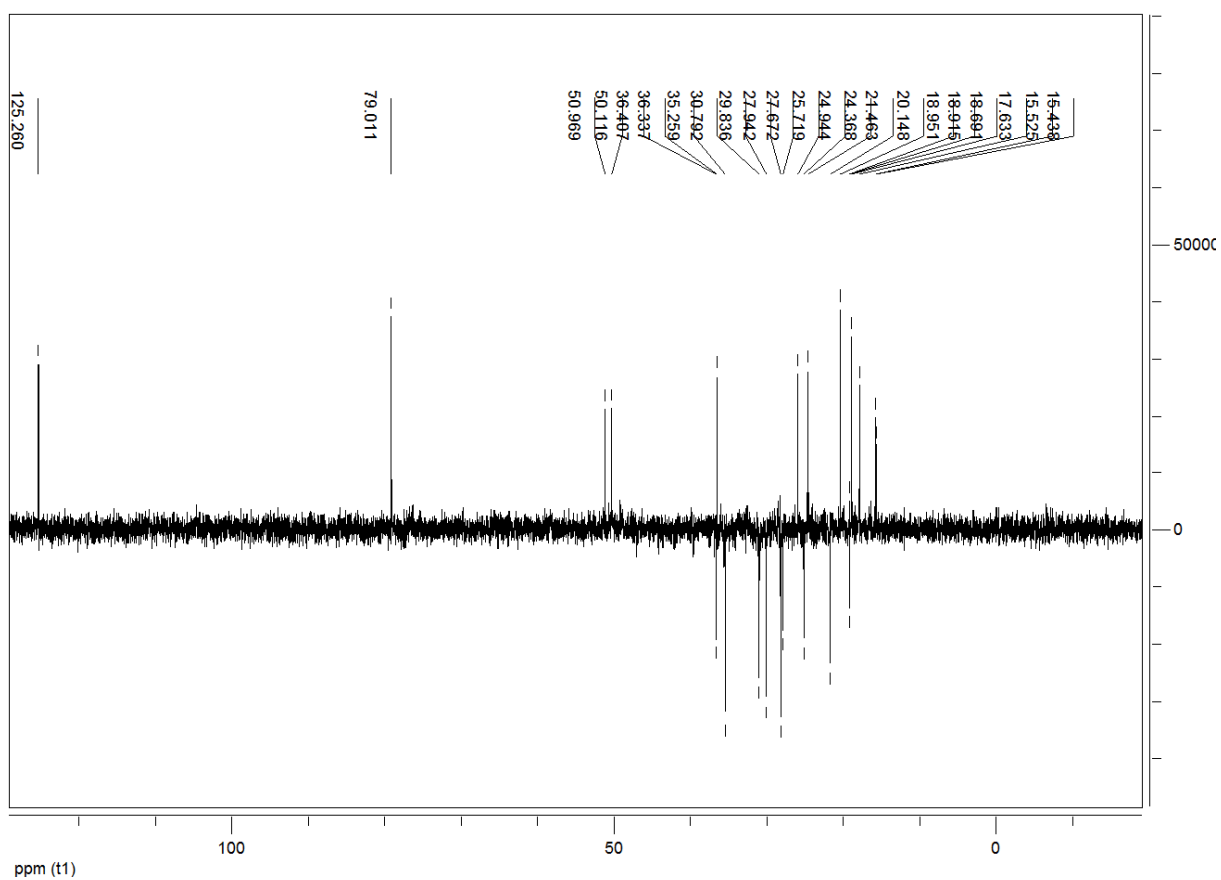


**Fig. 3.71** DEPT-135 spectrum of 3-β-OH-tirucallol (**29**). Signals of C-16 (CH<sub>2</sub>) and C-29 (CH<sub>3</sub>) cancel each other out. Thus, the negative methylene signal and positive methyl signal both disappear.

Evaluation of the spectral data confirmed the isolated compound as 3- $\beta$ -OH-tirucallol [(20S)-(+)-tirucalla-8,24-dien-3 $\beta$ -ol; Trivial: Tirucallol]. These class of compounds (Tirucallanes and Euphanes) is frequently found in plants of the genus *Euphorbiaceae* (e.g. *Euphorbia tirucalli*) [31]. Lanosterol [(+)-lanosta-8,24-dien-3 $\beta$ -ol], one example of compounds with lanostane structure, which also is abundant in Euphorbiaceae [31], differs at positions C-13, C-14, C-17 ( $\alpha$ -H instead of  $\beta$ -H at C-17) and C-20, relatively compared with tirucallol (see Fig. 3.72). Thus, the literature can be sometimes a bit confusing about what kind of triterpene was used for the experimental conditions. For example, Fernandez-Arche et al. [181] report about the topical anti-inflammatory effect of tirucallol isolated from *Euphorbia lactea latex*. However, the paper does not show any chemical structure, neither of tirucallol nor of lanosterol. Only in the experimental part tirucallol was mentioned as lanosta-8,24-dien-3 $\beta$ -ol, which is confusing, since it is not clearly verified, if either tirucallol or lanosterol was used in their experiments. Differentiation of tirucallol and lanosterol is simply possible by NOESY experiments. The data presented here (see Tab. 3.10) confirms the isolated compound as  $\beta$ -tirucallol from the *Boswellia* species Bcar. Interestingly, it seems to be the biosynthetic precursor of  $\beta$ -OH-tirucallic acid (compound **15**; see also [31]). Presumably, the methyl group at C-21 is oxidised by CYP-oxygenase enzymes, since they are ubiquitous on our planet for CH bond activation [19]. The  $\beta$ -configuration of the hydroxyl group at C-3 can be conveniently identified by the strong proton couplings explicitly shown in Fig. 3.73 (dd, Karplus rule [175]; see also Pardhy and Bhattacharyya [66]) and additionally by NOESY experiments.

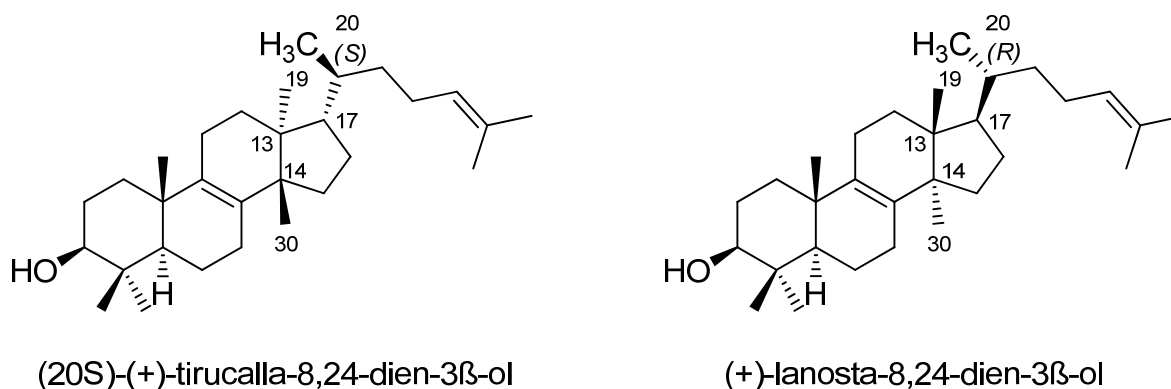


**Fig. 3.72** Structures of tirucallol (on the left) and lanosterol (on the right).

## Results and Discussion

**Tab. 3.10**  $^1\text{H}$  and  $^{13}\text{C}$  NMR assignments (400 MHz) for 3- $\beta$ -OH-tirucallol (**29**).

Atom Nr.	$^{13}\text{C}$ $\delta$ [ppm]	$^1\text{H}$ $\delta$ [ppm], $J$ [Hz]	HMBC ( $^2J$ in Hz)	HMBC ( $^3J$ in Hz)	HH-COSY	NOESY
1	35.25	1.19 ( $\alpha$ ) 1.77 ( $\beta$ )	$2\alpha$	18	$2\alpha/\beta$	
2	27.94	1.59 ( $\beta$ ) 1.68 ( $\alpha$ )	$1\alpha/\beta$		$1\alpha/\beta$ , 3	
3	79.00	3.24 (dd, $J = 11.6, 4.6$ )	$2\alpha/\beta$	$1\alpha/\beta$ , 5, 28, 29	$2\alpha/\beta$	$1\alpha$ , $2\alpha$ , 5, 29
4	38.94		5, 28, 29			
5	50.96	1.13	4, $6\alpha/\beta$	18, 28, 29		29
6	18.94	1.41 ( $\beta$ ) 1.69 ( $\alpha$ )	5		$7\alpha/\beta$	6( <i>gem.</i> )
7	27.66	1.92 ( $\alpha$ ) 2.09 ( $\beta$ )	$6\alpha/\beta$		7( <i>gem.</i> ), $6\alpha/\beta$	7( <i>gem.</i> )
8	133.54		$7\beta$	$6\alpha$ , 30		
9	134.07			$12\beta$ , 18		
10	37.27		$1\alpha/\beta$ , 5, 18	$6\alpha/\beta$		
11	21.45	1.94 ( $\beta$ ) 2.05 ( $\alpha$ )				
12	29.83	1.19 ( $\beta$ ) 1.52 ( $\alpha$ )		19	$11\alpha/\beta$	
13	44.10		$11\beta$ , $12\alpha/\beta$ , 19	$15\alpha/\beta$ , 30		
14	49.95		$15\alpha/\beta$ , 30	$12\alpha/\beta$ , $16\alpha$ , 19		
15	30.79	1.69 ( $\alpha$ ) 1.69 ( $\beta$ )	14	30	$16\alpha/\beta$	
16	28.05 <sup>a</sup>	1.32 ( $\alpha$ ) 1.92 ( $\beta$ )	17		$15\alpha/\beta$ , 16( <i>gem.</i> )	16( <i>gem.</i> ), 19
17	50.11	1.48	$16\alpha$	$15\alpha/\beta$ , $22\alpha/\beta$ , 19, 21		12 $\beta$ , 30
18	20.14	0.95 (s)		$1\beta$ , 5	$1\alpha(4J)$	$1\beta$ , $2\beta$ , $6\beta$ , $11\beta$
19	15.43	0.76 (s)				$11\alpha$ , $12\alpha$ , $15\alpha$ , $16\alpha$ , 20, 21
20	36.33	1.42	$22(1.03)$ , 17, 21	$16\alpha$		19
21	18.68	0.92 (d, $J = 6.4$ )		$22(1.03)$		19
22	36.40	1.03 1.42		17, 21	22( <i>gem.</i> ), $23\alpha/\beta$	22( <i>gem.</i> )
23	24.94	1.88 2.03	$22(1.03)$		23( <i>gem.</i> ), 24, $22\alpha/\beta$	
24	125.20	5.10 (ps tr, $J = 7.1$ ) <sup>b</sup>		$22(1.03)$ , 26, 27	$23\alpha/\beta$ , 26, 27	$22\alpha/\beta$ , $23\alpha/\beta$ , 26
25	130.99		26, 27			
26	25.71	1.68 (s)	25	27		
27	17.62	1.60 (s)	25	26		
28	15.52	0.80 (s)		3, 5, 29	29(4J)	$3\beta$ , $6\beta$ , 18, 29
29	28.05 <sup>a</sup>	1.00 (s)		3, 5, 28	28(4J)	$3\alpha$ , 5, $6\alpha$ , 28
30	24.36	0.87 (s)				$7\beta$ , $11\beta$ , $12\beta$ , $15\beta$ , 17

<sup>a</sup> Signals of C-16 and C-29 are superimposed in the  $^{13}\text{C}$ -NMR spectrum (FID manipulation by apodization resolves the signals)

<sup>b</sup> Actually, the triplet shows a more complex fine structure within its three peaks

$^1\text{H-NMR}$  (400 MHz,  $\text{CDCl}_3$ )  $\delta$  in ppm 3.24 (dd,  $J = 11.62, 4.62$  Hz, 1H)

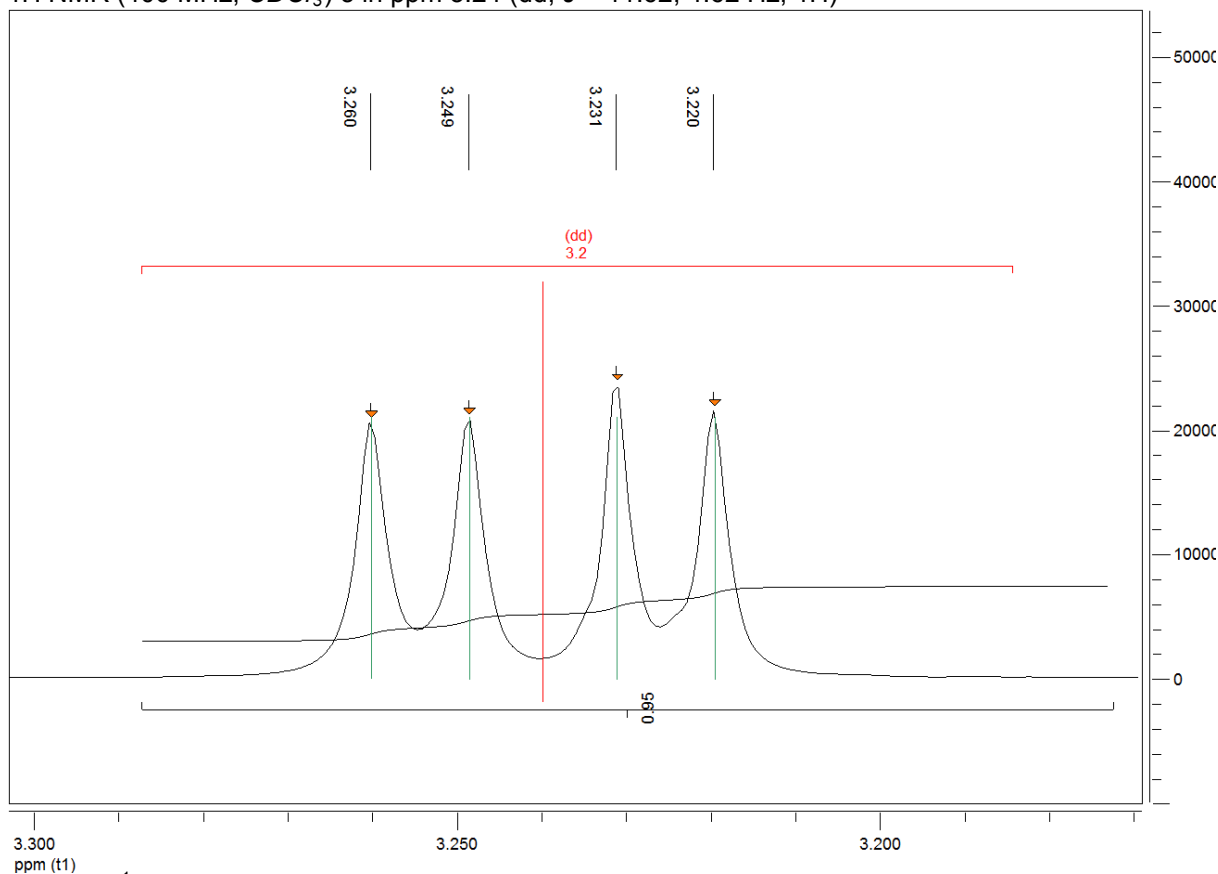


**Fig. 3.73**  $^1\text{H-NMR}$  spectral part of the  $\alpha\text{-H}$  at C-3 (dd) is defining the relative configuration of it.

### 3.2.11 3- $\alpha$ -OH-11-Keto-12-ursen (30)

3- $\alpha$ -OH-11-keto-12-ursen (**30**) was isolated as white solid. The structure is shown in Fig. 3.74. Analysis by TLC (Pentane/ $\text{Et}_2\text{O}$  2:1 and 1 % HOAc) showed a dark blue/violet spot after dyeing and heating with anisaldehyde reagent at  $R_f = 0.25$ . The spot is also visible by UV detection (250 nm). The standard HPLC method (2.3.4.2) gives a  $R_t$  of ca. 32.4 min. Detection by DAD-RP-HPLC was possible at 210 and 250 nm (see also Fig. 3.75). It shows the same absorption maximum as  $\beta$ -KBA and  $\beta$ -AKBA, when the UV spectra are recorded during HPLC elution. The  $^{13}\text{C-NMR}$  spectrum revealed 30 carbon signals. DEPT 90/135 spectra divided them into 7 quaternary, 5  $\text{CH}$ -, 10  $\text{CH}_2$ - and 8 methyl carbon atoms. The  $^1\text{H}$ -spectrum is shown in Fig. 3.76 and the  $^{13}\text{C}$ - and DEPT 90/135 spectra are shown in Fig. 3.77-3.79. Structural elucidation by conventional 2D-NMR techniques (HSQC, COSY, NOESY, and HMBC) is basically presented in Tab. 3.11. The HPLC chromatogram explains the minor impurities found within the  $^1\text{H}$ - and  $^{13}\text{C}$ -NMR spectra. However, the data given here and comparison with the data for 3- $\alpha$ -acetyl-11-keto- $\beta$ -boswellic acid published in the paper of Belsner et al. [53] confirms the structure of 3- $\alpha$ -OH-11-keto-12-ursen, probably the precursor of its acid derivative ( $\beta$ -KBA).

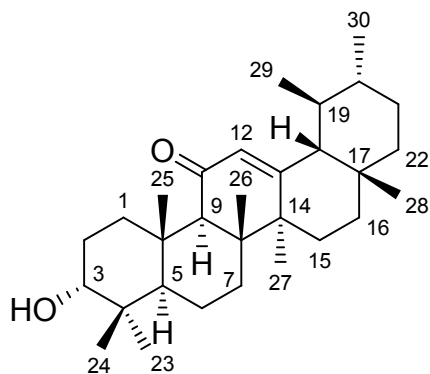


**Fig. 3.74** Structure of 3- $\alpha$ -OH-11-keto-12-ursen (**30**).

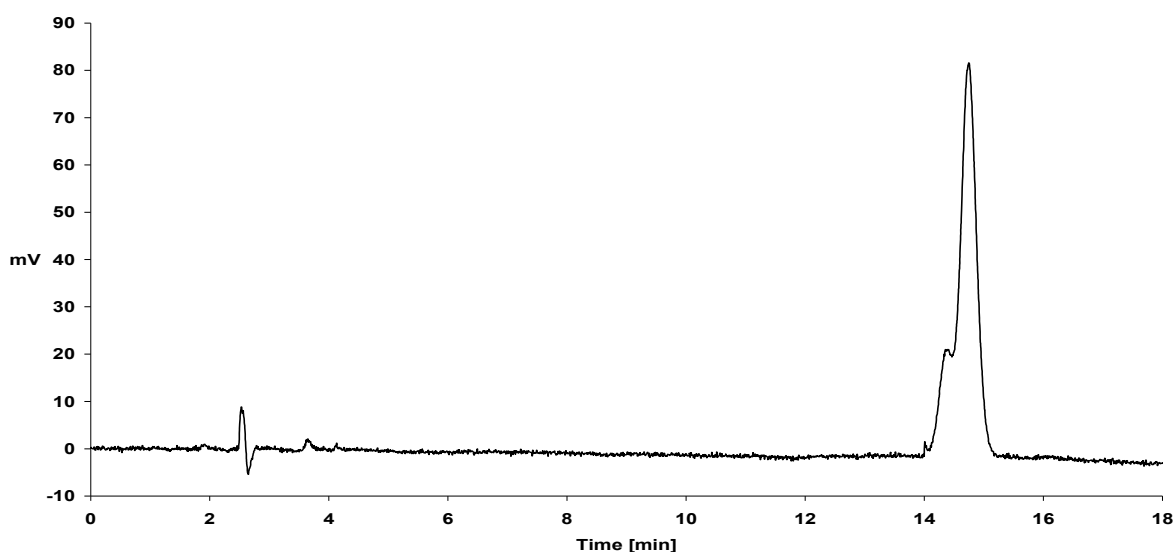


**Fig. 3.75** HPLC chromatogram at 250 nm detection. The impurity at the peak front is visible. HPLC conditions ( $T = 25\text{ }^{\circ}\text{C}$ ;  $u = 1\text{ ml/min}$ ; column = 1 x YMC Pack Pro RS C18 250x4.6 mm ID, 8 nm; isocratic = 98 % MeOH : 2 %  $\text{H}_2\text{O}$  + 0.1 % TFA).

Evaluation of the spectral data confirmed the isolated compound as 3- $\alpha$ -OH-11-keto-12-ursen. The compound itself is probably the precursor of 3- $\alpha$ -OH/acetyl-11-keto- $\beta$ -boswellic acid (**5** and **6**). The impurity almost co-eluting in the HPLC chromatogram (see Fig. 3.75) seems to be the 3- $\alpha$ -OH-11-keto-12-oleanen (same discussion as for  $\beta$ -AKBA and  $\alpha$ -AKBA, see introduction or Büchele et al. [58,134]). Interestingly, by comparison of the NMR data presented here with the data of Belsner et al. [53] the structure of **30** is clarified. Differences are found at C-3 (highfield shift of H-3 for the deacetylated derivative, which is a common phenomenon; compare also C-3 discussions of, for example, ABAs/BAs and Ac-TAs/TAs etc. or see also Seitz [56]). In Fig. 3.80 the fine structure of the  $\beta$ -H atom at C-3 is presented. Rather convincing similarities can be found by comparison of the  $^{13}\text{C}$ -NMR data (also DEPT-90/135 spectra), where all possible chemical shifts are almost equal the data of Belsner et al. [53] for  $\beta$ -KBA, **5**, except the COOH-function at C-24, which is in compound **30** a methyl group instead.

## Results and Discussion

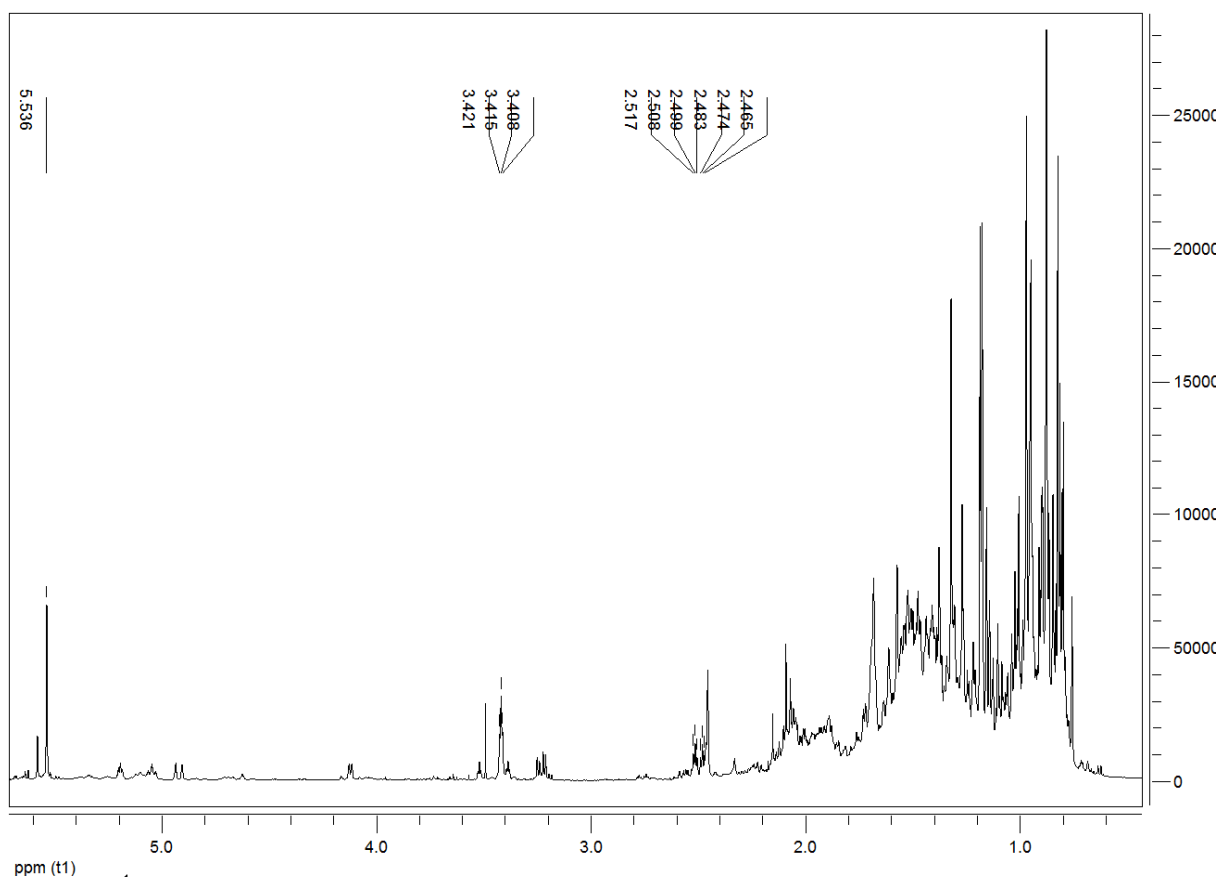


**Fig. 3.76**  $^1\text{H-NMR}$  spectrum of 3- $\alpha$ -OH-11-keto-12-ursen (**30**). For declaration of impurities see Fig. 3.75 and discussion in the text.

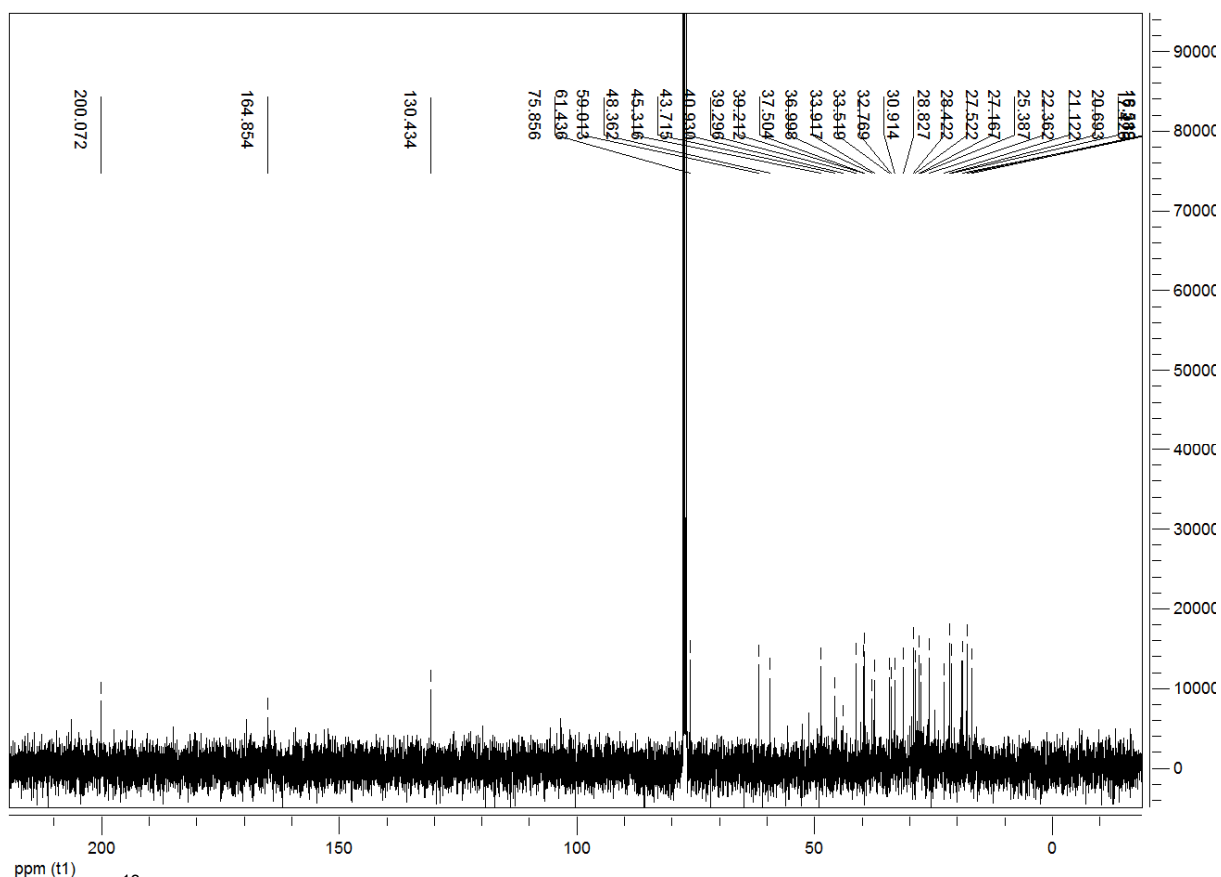


**Fig. 3.77**  $^{13}\text{C-NMR}$  spectrum of 3- $\alpha$ -OH-11-keto-12-ursen (**30**). For declaration of impurities see Fig. 3.75 and discussion in the text.

## Results and Discussion

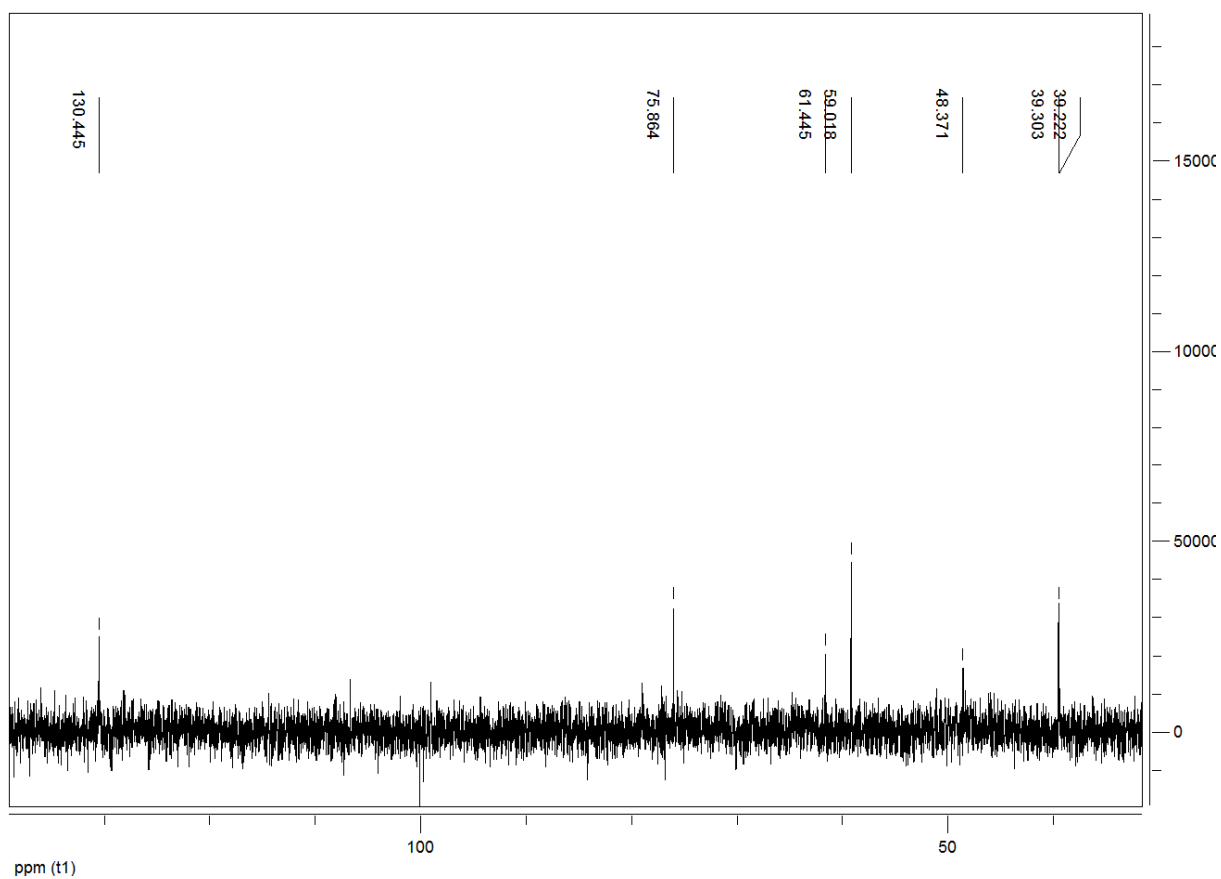


**Fig. 3.78** DEPT-90 spectrum of 3- $\alpha$ -OH-11-keto-12-ursen (**30**).

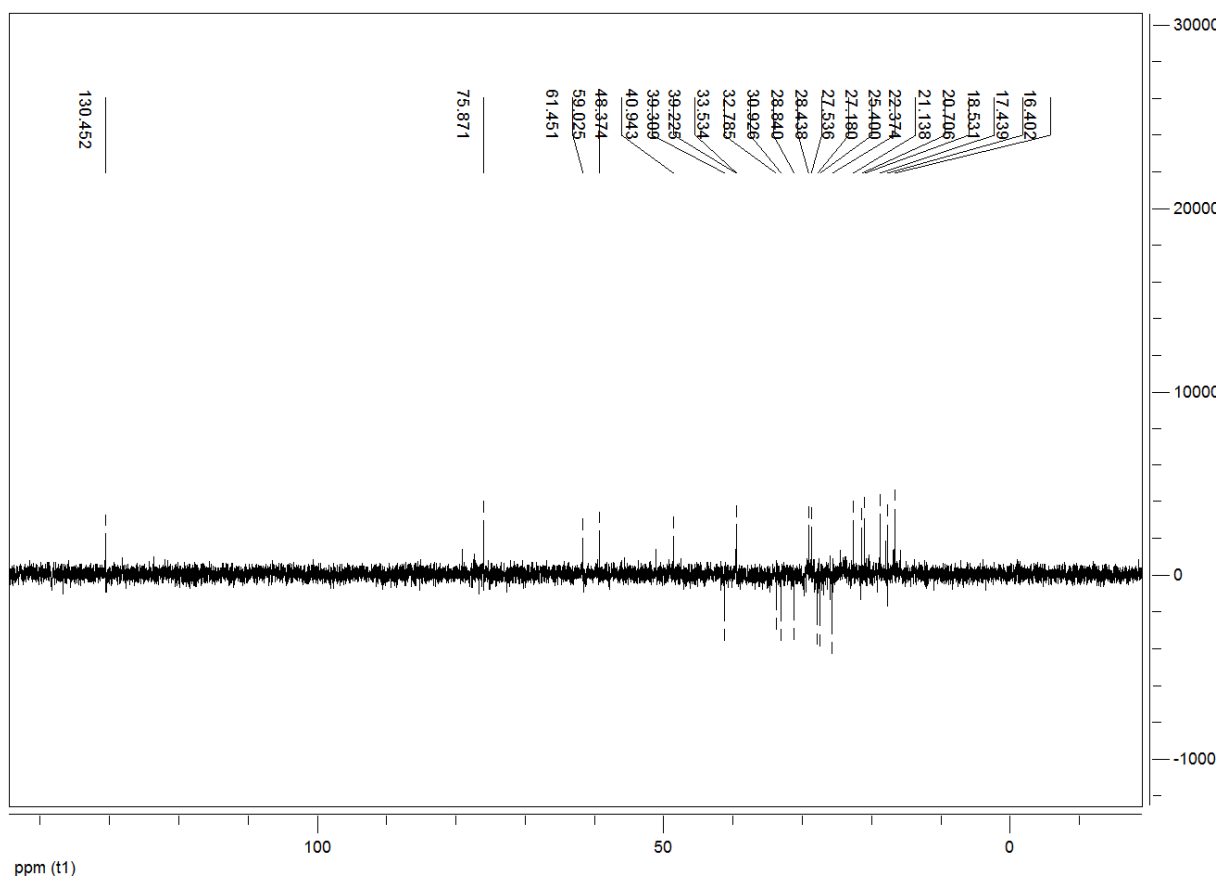


**Fig. 3.79** DEPT-135 spectrum of 3- $\alpha$ -OH-11-keto-12-ursen (**30**).

## Results and Discussion

**Tab. 3.11**  $^1\text{H}$  and  $^{13}\text{C}$  NMR assignments (400 MHz) for 3- $\alpha$ -OH-11-keto-12-ursen (**30**).

Atom Nr.	$^{13}\text{C}$ $\delta$ [ppm]	$^1\text{H}$ $\delta$ [ppm], $J$ [Hz]	HMBC ( $^2J$ in Hz)	HMBC ( $^3J$ in Hz)	HH-COSY	NOESY
1	33.52	1.36 ( $\alpha$ ) 2.49 (dtr, $J = 13.6, 3.6; \beta$ )			2 $\alpha/\beta$	
2	25.39	1.53 ( $\alpha$ ) 2.05 ( $\beta$ )			1 $\alpha/\beta$	
3	75.86	3.42 (tr, $J = 2.7$ )		23, 24		2 $\alpha/\beta$ 23, 24
4	37.50		23, 24			
5	48.36	1.23		23, 24, 25		6 $\alpha$ , 7 $\alpha$ , 24
6	17.45 <sup>a</sup>	1.43 ( $\beta$ ) 1.47 ( $\alpha$ )			7 $\alpha/\beta$	
7	32.77	1.40 ( $\beta$ ) 1.71 ( $\alpha$ )			6 $\alpha/\beta$	
8	45.32		9, 26	27		
9	61.44	2.45	8, 10, 11	14, 25, 26		
10	37.00		9, 25			
11	200.07		9			
12	130.43	5.54 (s)		9, 14, 18	18	18, 19, 26, 29
13	164.85		18	27		
14	43.71		27	9, 26		
15	27.17	1.20 ( $\alpha$ ) 1.89 ( $\beta$ )			16 $\alpha/\beta$	
16	27.52	1.01 ( $\beta$ ) 2.08 ( $\alpha$ )		18, 28	15 $\alpha/\beta$	
17	33.92		16 $\alpha$ , 18, 28			
18	59.01	1.53	13, 17	12, 16 $\beta$ , 20, 28, 29	12	12
19	39.21	1.40		30		12
20	39.30	0.95		29	21 $\alpha/\beta$	
21	30.91	1.29 1.44			20, 22 $\alpha/\beta$	
22	40.93	1.31 ( $\beta$ ) 1.48 ( $\alpha$ )		20, 28	21 $\alpha/\beta$	
23	28.42	0.97 (s)	4	3, 5, 24		6 $\alpha$
24	22.36	0.87 (s)	4	3, 5, 23		
25	16.39	1.18 (s)	10	5, 9		1 $\beta$ , 2 $\beta$
26	18.52	1.17 (s)	8	9, 14		12
27	20.69	1.31 (s)	14	8, 13		6 $\alpha$ , 7 $\alpha$ , 16 $\alpha$
28	28.83	0.81 (s)	17	16 $\alpha/\beta$ , 18, 22		15 $\beta$ , 22 $\beta$
29	17.43 <sup>a</sup>	0.79 (d, $J = 6.5$ )		20	19	12
30	21.12	0.96 <sup>b</sup>		19	20	

<sup>a</sup> Signals superimpose in the  $^{13}\text{C}$ -NMR spectrum

<sup>b</sup> Signal shape not visible owing to complete overlapping with H-20

## Results and Discussion

$^1\text{H}$  NMR (400 MHz,  $\text{CDCl}_3$ )  $\delta$  in ppm 3.41 (t,  $J = 2.72, 2.72$  Hz, 1H)

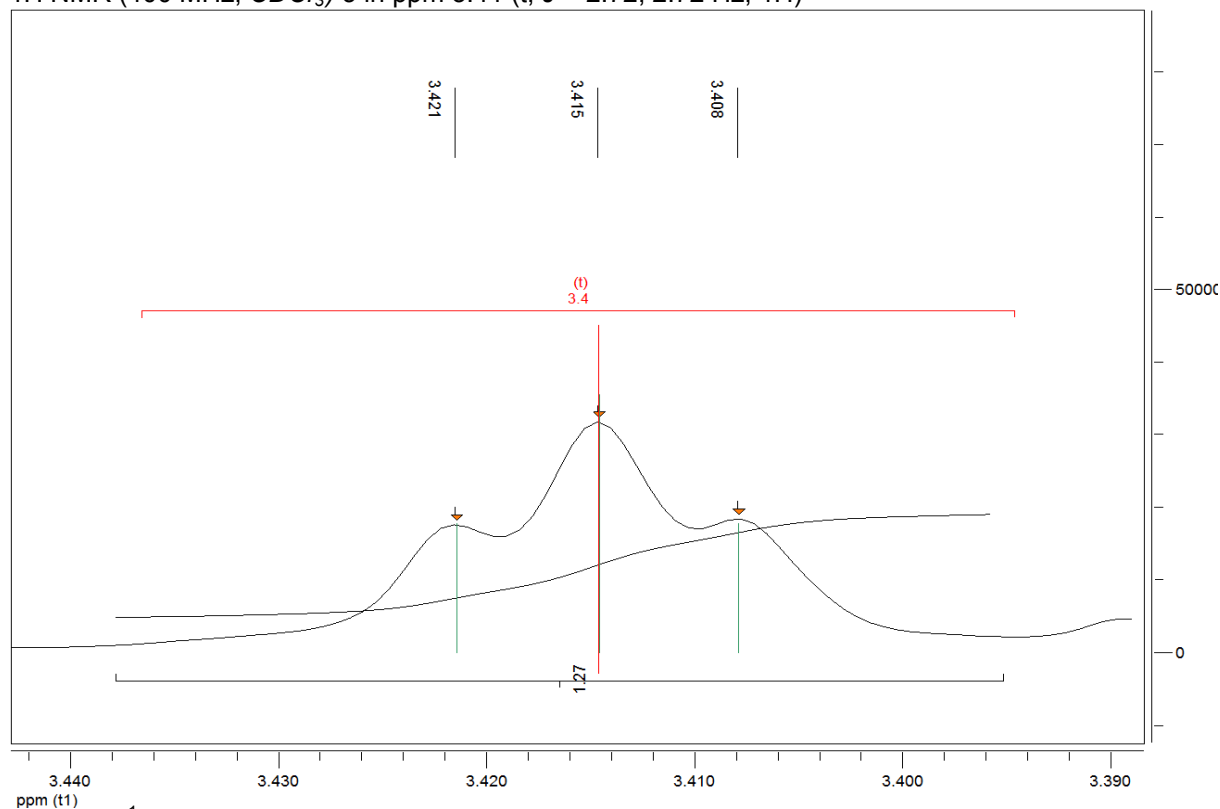


**Fig. 3.80**  $^1\text{H}$ -NMR spectral part of  $\beta$ -H at C-3 (dd) defining the relative configuration as  $\beta$ -configured according to the Karplus rule [175,182].

A general difficulty of neutral compound isolation by liquid RP chromatography, especially the triterpenoids, eluting rather late, is that they can not be resolved sufficiently (see also purity of  $\beta$ -OH-tirucallol, **29**). It is time consuming (late elution, even if 100 % organic phase is used) and quite many compounds (structural isomers) co-elute with another. Thus, structural assignment by GC-MS methods and isolation of them by preparative GC methods is preferable. However, it is still possible, even if the material can not be purified to a high level (> 95 % or better), by comparison of the significant and reasonable signals, to give an unequivocally structural elucidation of the compound in question as presented here.

### 3.3 Extraction and Separation (Acid Fraction and Neutral Fraction)

#### 3.3.1 Analytical Extraction Scale (Bpap, Bser, B<sub>sac</sub>/B<sub>car</sub>)

The discussion here refers only to the analytical extraction scale method (see also chapter 2.2.4). For a discussion of greater extracted amounts see also the paper of Paul et al. [59]. In Fig. 3.81 the values for Bpap and B<sub>sac</sub>/B<sub>car</sub> are presented graphically (for each species three different resin batch samples were extracted). Each triple series was performed on the same day. Thus, the differences in the Loss RE [%] during the separation of NB and RS fractions may additionally be due to the day performance. For a better overview, the Bser extraction results have been separated from the Bpap and B<sub>sac</sub>/B<sub>car</sub> results and are presented in Fig. 3.82.

On average, Bpap gives approximately 64 % RE. The loss during the separation of the acids from the neutral compounds is about 10-15 % (referred to the total weighed resin sample). Thus, about 30 % of the whole resin refers to the acid fraction (RS) and ca. 22 % to the neutral fraction (NB). For B<sub>sac</sub>/B<sub>car</sub> the arithmetic mean for RE = ca. 60 %, for NB = ca. 24 %, for RS = ca. 25 % and the total loss (summation of loss during separation of NB/RS from RE and the not extractable parts) is ca. 50-60 %.

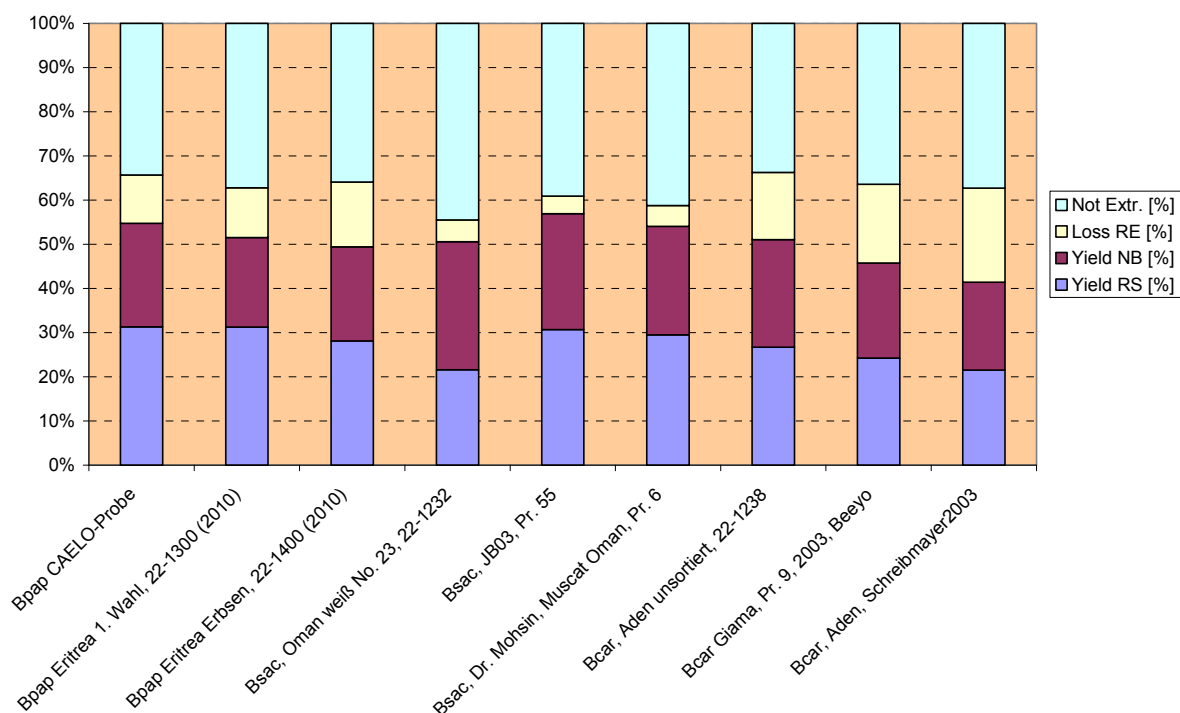


**Fig. 3.81** Stacked column diagram of Bpap (from left to right, columns 1 to 3), of B<sub>sac</sub> (columns 4 to 6) and of B<sub>car</sub> (columns 7 to 9). Not Extr. [%]: Not by Et<sub>2</sub>O extractable material (sugars and polar components); Loss RE [%]: Loss during separation of NB and RS; Yield NB [%]: Yield of neutral compounds; Yield RS [%]: Yield of acid fraction. For further discussions see text.

In Fig. 3.82 the analytical extraction scale results for samples of Bser (pure resin and Gufic Sallaki Tablets® preparation) are presented. The pure resin samples delivered the following arithmetically averaged distribution: RE = ca. 63 %, NB = ca. 25 %, RS = 29 % and a total

## Results and Discussion

loss (Sum: Not Extr. + Loss RE) of ca. 45 %. The Sallaki medicament gives a similar distribution: RE = ca. 55 %, NB = ca. 25 %, RS = ca. 26 % and a total loss (Sum: Not Extr. + Loss RE) of ca. 49 %.

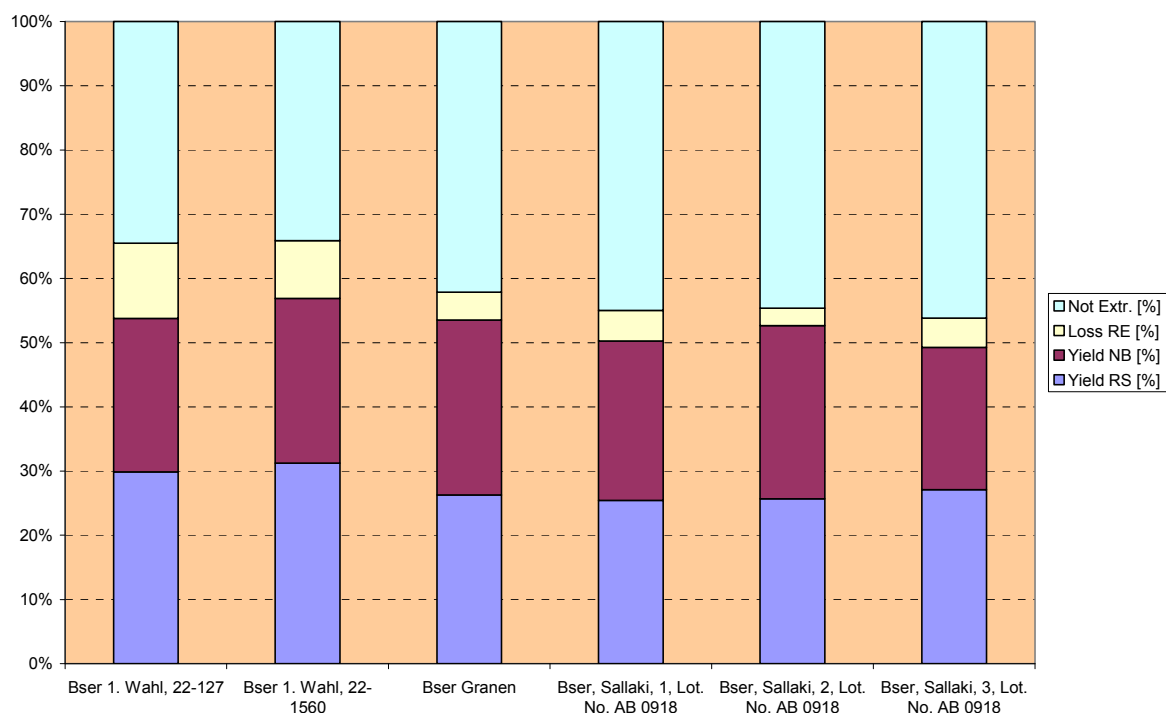


**Fig. 3.82** Stacked column diagram of Bser. The first three rows (from left to right) represent pure resin samples and the last three rows show the extraction samples of the Gufic Sallaki Tablets<sup>®</sup> preparation. Not Extr. [%]: Not by Et<sub>2</sub>O extractable material (sugars and polar components); Loss RE [%]: Loss during separation of NB and RS; Yield NB [%]: Yield of neutral compounds; Yield RS [%]: Yield of acid fraction. For further discussions see text.

The total average, typically obtained for any resin (Bpap, Bser, Gufic Sallaki Tablets<sup>®</sup> from Bser and Bsac/Bcar) extracted by the analytical extraction scale method is presented in Tab. 3.12.

**Tab. 3.12** Total average of all Olibanum samples (Bpap, Bser, Bsac/Bcar) extracted by the analytical extraction scale method. Yield RE (raw extract); Yield RS (acid fraction); Yield NB (neutral fraction); Loss RE (Loss during separation of the RE into RS and NB) and Total Loss (Sum: Not Extr. + Loss RE). Mean: Arithmetic mean; S.D.: Standard deviation; C.V.: Coefficient of variation (S.D / Mean x 100 %).

Yield RE	[%]	Yield RS	[%]	Yield NB	[%]	Loss RE	[%]	Total Loss	[%]
<b>Mean:</b>	60.9	<b>Mean:</b>	27.4	<b>Mean:</b>	24.1	<b>Mean:</b>	15.1	<b>Mean:</b>	48.5
<b>S.D.:</b>	2.3	<b>S.D.:</b>	2.6	<b>S.D.:</b>	2.1	<b>S.D.:</b>	3.5	<b>S.D.:</b>	2.9
<b>C.V.:</b>	4.2	<b>C.V.:</b>	10.9	<b>C.V.:</b>	8.2	<b>C.V.:</b>	23.1	<b>C.V.:</b>	6.4

The table basically demonstrates that, if one of these resins is extracted, approximately 60 % of RE are obtained. The RE then delivers ca. 27 % RS and 24 % NB (referred to the total amount of weighed resin material). The loss during the separation of the RE into the acid

fraction (RS) and neutral fraction (NB) is ca. 15 %. Especially the poor day performance of the NB/RS-separation for the Bcar samples (see Fig. 3.81) led to a worse overall average (Loss RE) and a very strong C.V. of 23 %. This fact should be beard in mind. The value will become narrower when more samples are analysed. Though it could have been treated as an outlier it was nevertheless accepted for the calculation. A further reason for this strong deviation in the Bcar samples (Loss RE) could also have been the poor phase separation (organic/water); as the formation of an emulsion during phase separation was specially observed for samples of B<sub>pac</sub> and B<sub>car</sub>. This seems to be most likely due to the high content of BAs (**1** and **3**) and ABAs (**2** and **4**; see also chapter 3.8).

Eventually, about 50 % of the material had been lost during the extraction of the raw resinous product (Summation of Loss RE and Not Extr.). Extraction differences in detail are due to the nature of the sample itself and the day extraction performance (manual procedure with a separation funnel). The data presented here may give a kind of expectation value for extraction of *Boswellia* resins in general (B<sub>pap</sub>, B<sub>ser</sub>, B<sub>pac</sub>/B<sub>car</sub>) when a questionable resin is analysed by separation of the NB and RS fractions.

### 3.4 TLC data (B<sub>pap</sub>, B<sub>ser</sub>, B<sub>pac</sub>/B<sub>car</sub>)

In this chapter representative TLC chromatograms for the crude resins of the species B<sub>pap</sub>, B<sub>ser</sub> and B<sub>car</sub>/B<sub>pac</sub> are presented. According to the sample population analysed in this work and to critically evaluated data from the literature [13,74,79,82], the TLC method demonstrated in this work provides a simple technique for the unambiguous chemotaxonomic identification of these three species qualitatively. The chromatography techniques are given in chapter 2.3.1. Basically, the data presented here is already published in *Phytochemical Analysis* [11]. In Fig. 3.83 two example chromatograms and a corresponding model chromatogram are shown.

The TLC data ensures the data obtained by HPLC analysis (see chapter 3.7). Furthermore, by combination of both methods, the identity of marker compounds, only by relative methods (TLC: dyeing colour and  $R_f$  value, respectively, in HPLC the  $R_t$  value, when absorption is merely possible at 210 nm detection wavelength), even without more specific detection dimensions (DAD, MS-detection or isolation and NMR), is achievable. Thus, combination of TLC and HPLC can be considered as a multi-dimensional classification approach, when techniques like an additional DAD- or MS-detection dimension are lacking.

Very specific for B<sub>pap</sub> is the existence of a brown spot eluting at  $R_f$  = ca. 0.68, which refers to incensole acetate (compound **23**). Thus far, Inc-Ac has been, in all samples analysed here, only significantly detectable in the species B<sub>pap</sub>. This result is consistent with data published by Obermann, Hamm et al. and Camarda et al. [13,74,79]. Hence, publications reporting the isolation of Inc-Ac (**23**) from B<sub>car</sub> (e.g. Moussaieff et al. [87] and Banno and Akihisa et al. [67,68]) may have been reporting of the resin B<sub>pap</sub> instead. Accordingly, referring to the data population analysed and even found in the literature, this fact seems to be very likely. Furthermore, B<sub>pap</sub> shows, from all species analysed here, the greatest amount of incensole (**22**,  $R_f$  at ca. 0.27; see also chapter 3.8). Another specific marker

compound for Bpap is the strong blue 3-Oxo-TA (**13**) spot at  $R_f = \text{ca. } 0.22$ , which is completely in accordance to the obtained HPLC results (see chapters 3.7 and 3.8).

For Bser a strong green serratol (**21**) spot ( $R_f = \text{ca. } 0.46$ ) is very specific. Similar to Bpap, Bser contains a strong and sharp 3-Oxo-TA (**13**) spot ( $R_f = \text{ca. } 0.22$ ) eluting within  $\alpha/\beta$ -BA (**1** and **3**;  $R_f = \text{ca. } 0.19$ ) and  $\alpha/\beta$ -ABA (**2** and **4**;  $R_f = \text{ca. } 0.25$ ).

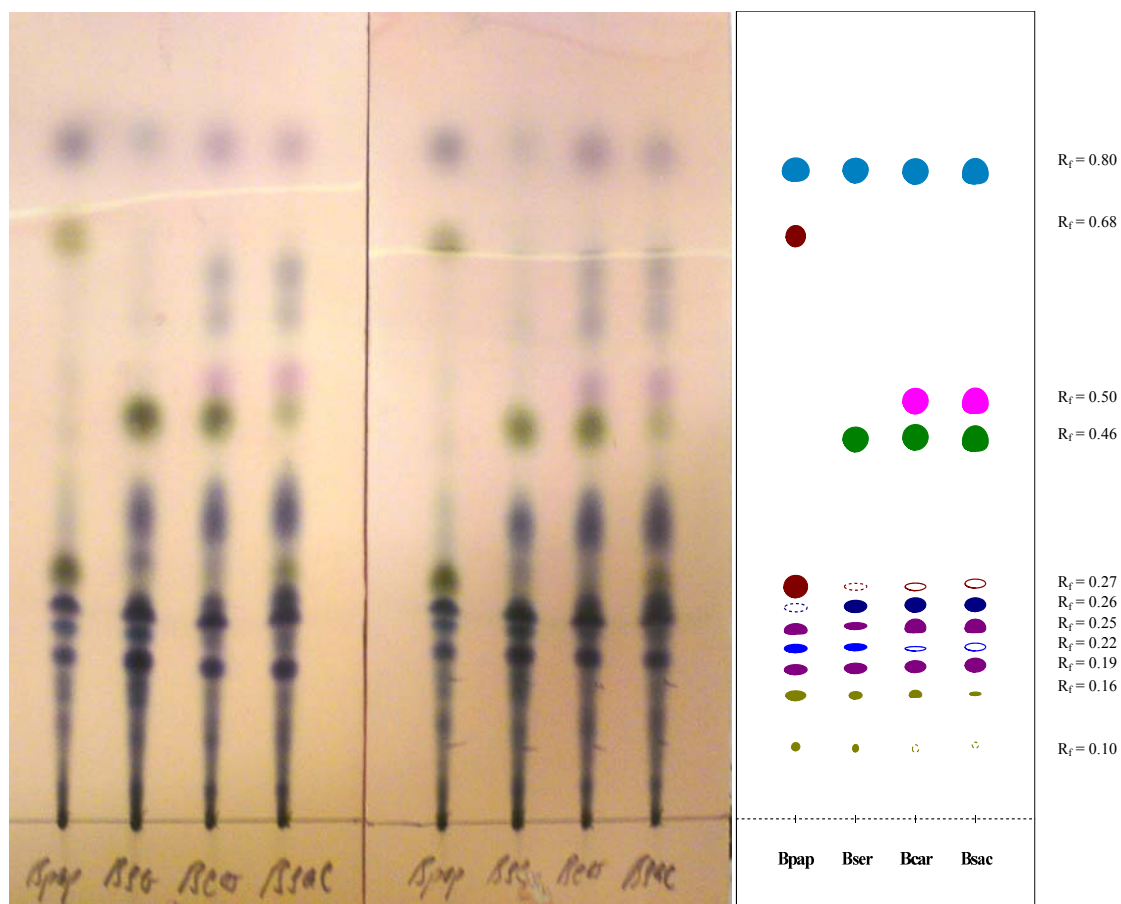


**Fig. 3.83** Real chromatograms of crude resin extracts (left: MeOH extract; middle: Et<sub>2</sub>O extract; after dyeing and ca. 20 min development at room temperature) and the model chromatogram (right) with the corresponding  $R_f$  values. The model presents only the significant spots useful for resin identification. Conditions are as described in chapter 2.3.1 (Eluent: 2 parts of pentane and one part of Et<sub>2</sub>O + 1 % HOAc).  $R_f = \text{ca. } 0.10$  ( $\beta$ -KBA, **5**, UV active);  $R_f = \text{ca. } 0.16$  ( $\beta$ -AKBA, **6**, UV active);  $R_f = \text{ca. } 0.19$  (**1** and **3**, BAs, violet);  $R_f = \text{ca. } 0.22$  (**13**, blue);  $R_f = \text{ca. } 0.25$  (**2** and **4**, ABAs, violet);  $R_f = \text{ca. } 0.26$  (not verified, blue);  $R_f = \text{ca. } 0.27$  (**22**, brown);  $R_f = \text{ca. } 0.46$  (**21**, green);  $R_f = \text{ca. } 0.50$  (**28**, pink);  $R_f = \text{ca. } 0.68$  (**23**, brown);  $R_f = \text{ca. } 0.80$  (most probably terpenes without functional group, e.g. verticillia-4(20),7,11-triene, limonene,  $\beta$ -pinene,  $\alpha$ -humulene,  $\beta$ -caryophyllene etc.; dark blue/violet). Definition of spots in the model chromatogram: Solid spots (good visible), hollow spots (slightly visible), hollow and dashed spots (barely visible). For further discussions see text. *With permission from John Wiley & Sons Ltd., taken from Phytochemical Analysis 2012, 23, page 184-189.*

For Bpap/Bcar (both have the same elution pattern in common) a pink spot at  $R_f = \text{ca. } 0.50$ , referring to  $\beta$ -Car-Ox (compound **28**), is very specific. Hitherto, this spot has been only detected in Bpap/Bcar during this work. In compliance with the results of Camarda et al. [74] and Hamm et al. [13], and the detection of its probable precursor  $\beta$ -caryophyllene (**27**) merely in Bpap/Bcar samples (see also chapter 3.7), it may be an additionally useful

biomarker for species identification, when all pattern pre-conditions for a *Boswellia* species are granted (e.g.  $\beta$ -KBA,  $\beta$ -AKBA, BAs and ABAs). B<sub>sac</sub>/B<sub>car</sub> show also the strong green serratol (**21**) spot ( $R_f = \text{ca. } 0.46$ ). Good support as well is given in the dissertation of Basar [35], where 34 different Olibanum essential oil TLC chromatograms are presented. There, the pink  $\beta$ -Car-Ox (**28**) spot has been specific for almost any Olibanum sample from Somalia (B<sub>car</sub>) and Oman (B<sub>sac</sub>). Hence, this evidence substantiates the statements given here thus far. Incensole (compound **22**) has been also detectable in B<sub>ser</sub> and B<sub>sac</sub>/B<sub>car</sub>, but in quite lower concentrations than for B<sub>pap</sub>. Interestingly, as Ser-OH (compound **21**) is reported as biosynthetic precursor of Inc (**22**) by Klein and Obermann [82], it is remarkable that B<sub>pap</sub> does not reveal a Ser-OH (**21**) spot and a quite huge amount of Inc (**22**), compared with B<sub>ser</sub> and B<sub>sac</sub>/B<sub>car</sub> (see also chapter 3.7). Furthermore, the existence of high quantities of Inc-Ac (**23**) merely in B<sub>pap</sub>, may give proof for a different secondary metabolic pathway expression in this species. It seems that only B<sub>pap</sub> generates a specific enzyme capable of acetylating its precursor incensole (**22**). However, the discussion is just speculative, but reasonable, based on the experimental results so far.



**Fig. 3.84** UV detection of  $\beta$ -AKBA (**6**) and  $\beta$ -KBA (**5**) at 254 nm (from left to right; 1st column: B<sub>pap</sub>, 2nd column: B<sub>ser</sub>, 3rd column: B<sub>car</sub>, 4th column: B<sub>sac</sub>). The two spots per column refer to the extraction method, Et<sub>2</sub>O and MeOH. Note that for the B<sub>car</sub> and B<sub>sac</sub> samples large deviations can be found for the UV detection of  $\beta$ -KBA and  $\beta$ -AKBA (varying concentrations of  $\beta$ -KBA and  $\beta$ -AKBA; see also 3.7 and 3.8). Hence, if only UV detection is used, the species identification may be not unequivocal. For further discussion see text. *With permission from John Wiley & Sons Ltd., taken from Phytochemical Analysis 2012, 23, page 184-189.*

## Results and Discussion

All species discussed here have the classical boswellic acids in common. If only the BAs (**1** and **3**,  $R_f = \text{ca. } 0.19$ ) and the ABAs (**2** and **4**,  $R_f = \text{ca. } 0.25$ ) are considered, no real qualitative species differentiation is achievable. However, for the identification of a questionable resin chunk as species from *Boswellia* the existence of BAs (**1** and **3**) and ABAs (**2** and **4**), respectively,  $\beta$ -KBA (**5**) and  $\beta$ -AKBA (**6**), is mandatory.

In Fig. 3.84 the UV detection of the MeOH and Et<sub>2</sub>O extracts is presented. Expectably, Bpap always delivers a strong UV spot for  $\beta$ -AKBA (**6**) and a weaker one for  $\beta$ -KBA (**5**). Bser, as far as experienced in this work and according to data sceptically inspected in the literature [17,56,57], delivers a weaker spot for  $\beta$ -AKBA (**6**), showing continuously more or less the same absorption as  $\beta$ -KBA (**5**). Normally, samples from Bsac/Bcar reveal UV absorptions for  $\beta$ -AKBA (**6**) similar the concentration levels of  $\beta$ -AKBA in Bser samples.  $\beta$ -KBA (**5**), at this concentration level ( $c = \text{ca. } 5\text{-}10 \text{ mg/ml}$  in TLC analysis; max. 10  $\mu\text{l}$  added), can only be guessed by UV detection. However, samples were analysed revealing in- or decreased  $\beta$ -KBA (**5**) and  $\beta$ -AKBA (**6**) levels for Bsac, respectively, Bcar. Thus, if only the UV detection for TLC analysis is applied, the identification of the species investigated might be ambiguous.

The results of the discussions made in this chapter are summarised in Tab. 3.13. Basically, there are all important points demonstrated concerning the TLC analysis of the sample extracts.

**Tab. 3.13** Marker compound properties referring to the resin species. Full name of marker compound, number (Nr.) and abbreviation (Abbr.), the corresponding  $R_f$  value, the colour after dyeing, UV detection properties and the species (Bpap, Bser, Bsac/Bcar) representative for the characteristic compound (Expressions in parentheses declare, if the spot is strong or faint and thus significant for a certain species). For further discussions see text.

<sup>a</sup> Note that the  $\beta$ -KBA and  $\beta$ -AKBA UV-detection properties for Bsac/Bcar can show strong deviations from the conclusion given here (varying amounts of  $\beta$ -KBA and  $\beta$ -AKBA have been found; see also 3.7 and 3.8).

Compound	Nr. and Abbr.	$R_f$ value	Colour (after dyeing)	UV detection (254 nm)	Species
Incensole	<b>22</b> (Inc)	0.27	brown	-	Bpap (strong), Bser, Bsac/Bcar
Incensole acetate	<b>23</b> (Inc-Ac)	0.68	brown	-	Bpap
3-Oxo-8,24-dien-tirucallic acid	<b>13</b> (3-O-TA)	0.22	blue	-	Bpap, Bser (both strong), Bsac/Bcar
Serratol	<b>21</b> (Ser-OH)	0.46	green	-	Bser, Bsac/Bcar (both strong)
$\beta$ -Caryophyllene oxide	<b>28</b> ( $\beta$ -Car-Ox)	0.50	pink	-	Bsac/Bcar
$\alpha$ - and $\beta$ -Boswellic acid	<b>1</b> and <b>3</b> ( $\alpha/\beta$ -BA)	0.19	violet	-	Bpap, Bser, Bsac/Bcar
$\alpha$ -Acetyl and $\beta$ -Acetyl boswellic acid	<b>2</b> and <b>4</b> ( $\alpha/\beta$ -ABA)	0.25	violet	-	Bpap, Bser, Bsac/Bcar
11-Keto- $\beta$ -boswellic acid	<b>5</b> (KBA)	0.10	yellow golden (if pure spot)	visible	Bpap, Bser, Bsac/Bcar <sup>a</sup>
3-O-Acetyl-11-keto- $\beta$ -boswellic acid	<b>6</b> (AKBA)	0.16	yellow golden (if pure spot)	visible	Bpap (strong), Bser, Bsac/Bcar <sup>a</sup>

### 3.5 GC data (Qualitative Analysis of Essential Oils from Bpap, Bser and Bcar)

In this chapter the GC data of three analysed essential oils (Bpap, Bser and Bcar; Bsac, as showing similar properties as Bcar by TLC and HPLC was not steam distilled) is presented. The oils were won by steam distillation as described in chapter 2.2.5. The here reported results for Bpap, Bser and Bcar were compared with the GC-MS results from Basar, Camarda et al. and Hamm et al. [13,35,74] to verify the conclusions already given by TLC and HPLC analysis. Furthermore, since MS-detection lacked, the Kovats indices (KI) [169], using the van den Dool variant for temperature gradient programs [170], were applied for peak identification of unknown compounds. Therefore, the KI values published by Camarda et al. [74], Hamm et al. [13], the online published terpenoids library list by *Dr. Hochmuth Scientific Consulting* [183] and the GC chromatograms published by Basar [35] were used (Note that for verification of Bpap results, the GC chromatogram of Bcar in the dissertation of Basar, which is unfortunately falsely denoted as Bcar, has been used). For some compounds reference standards were available, which verified the specific indices in question at least by co-injection (limonene,  $\beta$ -pinene,  $\beta$ -caryophyllene,  $\alpha$ -humulene,  $\tau$ -cadinol, methylchavicol, methyleugenol, verticillia-4(20),7,11-triene, incensole, incensole acetate, iso-serratol, serratol and  $\beta$ -caryophyllene oxide). However, the data presented here is solely based on comparison of these Kovats indices. Not verified peak signals were not assigned or a question mark was added in parentheses (correct peak identity strongly evidenced by data from literature).

For Bpap, by steam distillation, ca. 15 mg from 1 g of the NB were extracted (yield: 1.5 %). In Tab. 3.14 the peaks presented in Fig. 3.85 are summarised for the species Bpap.

**Tab. 3.14** Presentation of the GC-data (Bpap) from the chromatogram in Fig. 3.85. The KIs of the significant marker compounds are denoted. For further discussions see text.

Reten. Time [min]	Area [mV.s]	Height [mV]	Area [%]	KI	Compound
2,413	136,23	27,344	8,8		
2,817	3,908	13,571	0,3		
9,413	13,175	21,963	0,9	<b>1033</b>	Limonene
10,2	338,794	27,351	21,9	<b>1074</b>	n-Octanol
10,645	63,852	27,347	4,1	<b>1098</b>	
11,093	62,464	27,342	4	<b>1122</b>	
12,622	275,943	27,359	17,9	<b>1202</b>	n-Octyl acetate
14,322	54,627	27,339	3,5	<b>1283</b>	
31,66	91,069	27,346	5,9	<b>1968</b>	Cembrene A (?)
33,005	117,023	27,345	7,6	<b>2021</b>	Verticillia-4(20),7,11-triene
36,595	177,831	27,347	11,5	<b>2154</b>	Inc-OH
37,452	210,062	27,349	13,6	<b>2186</b>	Inc-Ac
Total	1544,98	309,002	100		

As it is already reported by Camarda et al. [74], Hamm et al. [13] and Basar [35] (Note: Bcar results from Basar refer obviously to Bpap), typical for Bpap essential oils is the existence of strong n-octanol and n-octyl acetate peak signals. Furthermore, as additionally shown by

TLC and HPLC analysis, the existence of verticillia-4(20),7,11-triene (**24**), incensole (**22**) and incensole acetate (**23**) (Peak signals verified by co-injection) is specifically confirming the essential oil as Bpap. The monoterpenes limonene and the diterpene cembrene A seem to be universally occurring molecules in the essential oils of all three species (Bpap, Bser, Bsac/Bcar) [13,35,74,78]. Thus, for the unambiguous identification of the species Bpap the existence of compound **22**, **23** and **24** and huge peak signals of n-octanol and n-octyl acetate may be necessary.

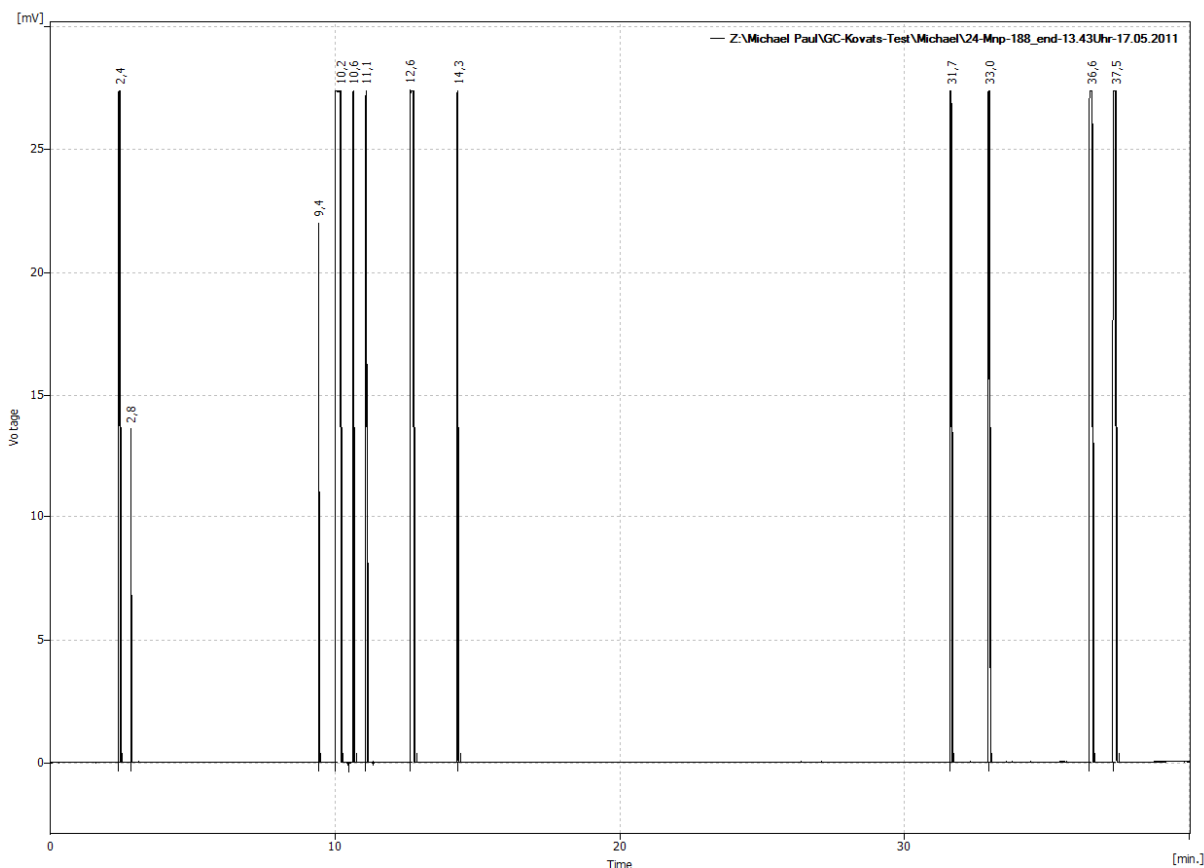


**Fig. 3.85** The GC-FID chromatogram of Bpap. Conditions: 100  $\mu$ L essential oil in 100  $\mu$ L DCM; 0.5  $\mu$ L injection (Split open:  $\frac{1}{2}$  turn; Purge open:  $\frac{1}{4}$ ); gas chromatographic conditions as described in chapter 2.3.10. Peak signals are in detail denoted in Tab. 3.14.

In Tab. 3.15 the GC results for Bser are presented. In Fig. 3.86 the corresponding chromatogram is shown. For Bser, ca. 23 mg from 1 g (NB) were extracted by steam distillation (yield: 2.3 %). In addition to the results reported by Basar [35], Camarda et al. [74] and Hamm et al. [13], typical volatile biomarkers for this species are methylchavicol, methyl eugenol and serratol (peak signals verified by co-injection). Limonene and cembrene A are universally occurring terpenes in *Olibanum* species, at least thus far reported for the species Bpap, Bser, Bsac/Bcar. Hence, Ser-OH (**21**), methylchavicol and methyleugenol seem to be specific biomarkers in the essential oils from the species Bser. Furthermore, Iso-Ser (**20**), which has been described for the first time in this work, is probably co-eluting with Ser-OH (**21**) under these GC-conditions. However, by the HPLC method described here, they (**20** and **21**) are separable (see also chapters 3.7.2 - 3.7.4 for example).

## Results and Discussion

**Tab. 3.15** Presentation of the GC-data (Bser) from the chromatogram in Fig. 3.86. The KIs of the significant marker compounds are denoted. For further discussions see text.

Reten. Time [min]	Area [mV.s]	Height [mV]	Area [%]	KI	Compound
2,483	190,76	190,76	27,37		
9,433	61,429	61,429	27,363	<b>1013</b>	Limonene
9,802	46,652	46,652	27,358	<b>1033</b>	
10,723	61,294	61,294	27,359	<b>1081</b>	
11,003	73,269	73,269	27,36	<b>1096</b>	
11,145	52,523	52,523	27,358	<b>1103</b>	
11,512	85,853	85,853	27,36	<b>1123</b>	
11,62	83,288	83,288	27,361	<b>1128</b>	
12,027	140,44	140,44	27,36	<b>1150</b>	
12,51	117,865	117,865	27,359	<b>1175</b>	
13,74	39,615	39,615	27,353	<b>1236</b>	
16,745	93,631	93,631	27,361	<b>1372</b>	Methyl-Eugenol
17,153	87,613	87,613	27,352	<b>1390</b>	
20,613	36,025	36,025	27,347	<b>1527</b>	
31,865	13,06	13,06	14,11	<b>1960</b>	Cembrene A (?)
37,045	164,276	164,276	27,356	<b>2156</b>	Ser-OH
Total	1347,594	424,485	100		

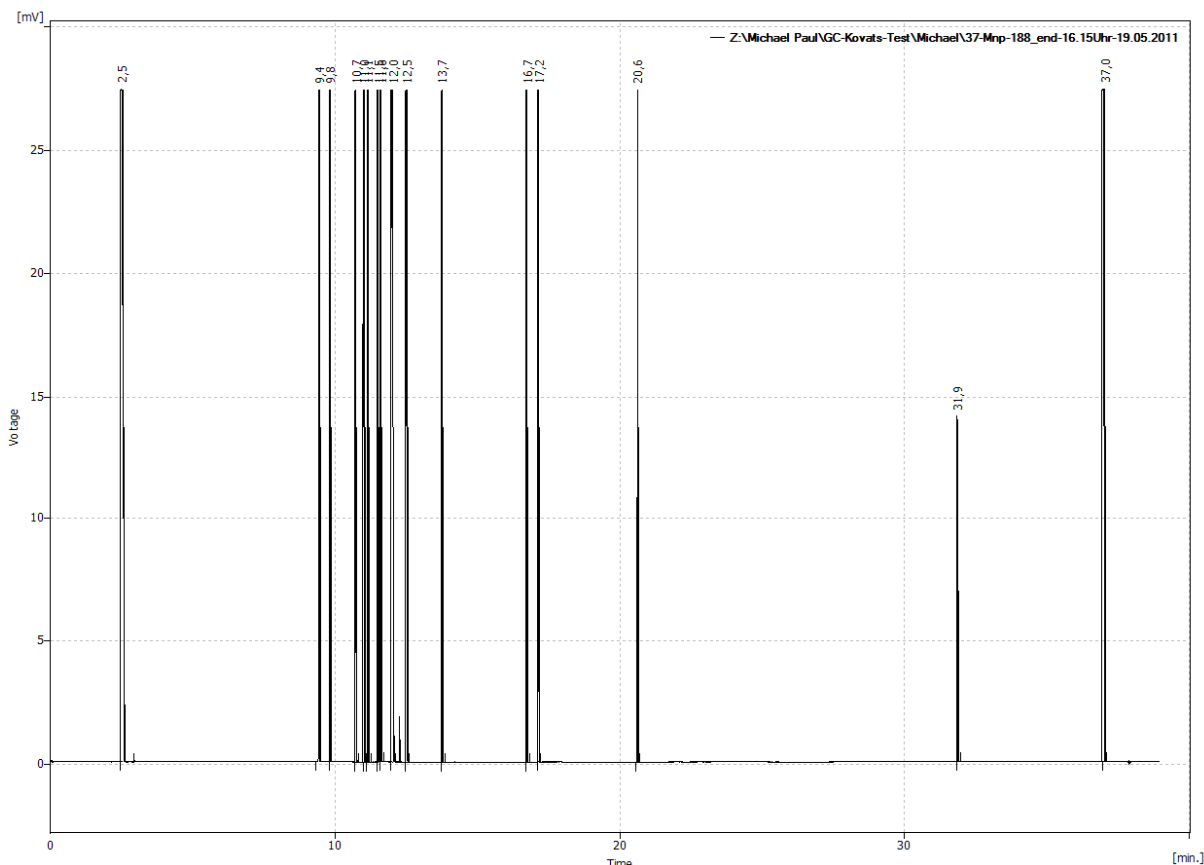


**Fig. 3.86** The GC-FID chromatogram of Bser. Conditions: 100  $\mu$ L essential oil in 100  $\mu$ L DCM; 0.5  $\mu$ L injection (Split:  $\frac{1}{2}$  open; Purge:  $\frac{1}{4}$  open); gas chromatographic conditions as described in chapter 2.3.10. Peaks are explicitly denoted in Tab. 3.15.

The data for Bcar is represented in Tab. 3.16 and in Fig. 3.87 the corresponding chromatogram is demonstrated. For Bcar, by steam distillation, ca. 67 mg from 1g (NB) were

extracted (yield: 6.7 %). Compared to the chromatograms of Bpap and Bser, a more complex pattern is obtained. The reason therefore is a splitless injection to generally show how complex the composition of essential oils still is (Note: Additionally, splitless injection for Bpap and Bser would deliver more complex chromatograms; vice versa, split injection of Bcar delivers a less complex chromatogram compared with the one in Fig. 3.87. Hence, only the major compounds would be detectable. However, to show the differences between split and splitless injection, the splitless injection chromatogram for Bcar is demonstrated). Typical biomarkers in the essential oil of Bcar are  $\beta$ -caryophyllene (**27**) and its oxidised derivative  $\beta$ -caryophyllene-oxide (**28**),  $\tau$ -cadinol (**25**) and serratol (**21**) (verified by co-injection). Probably, iso-serratol (**20**) co-elutes with serratol (**21**) under these GC conditions.

Furthermore,  $\gamma$ -cadinene,  $\delta$ -cadinene and cedrol seem to be typical biomarkers for Bcar, respectively, Bsc. The question mark for  $\gamma$ -cadinene,  $\delta$ -cadinene and cedrol in parentheses denotes that only the KI values were used for biomarker identification.

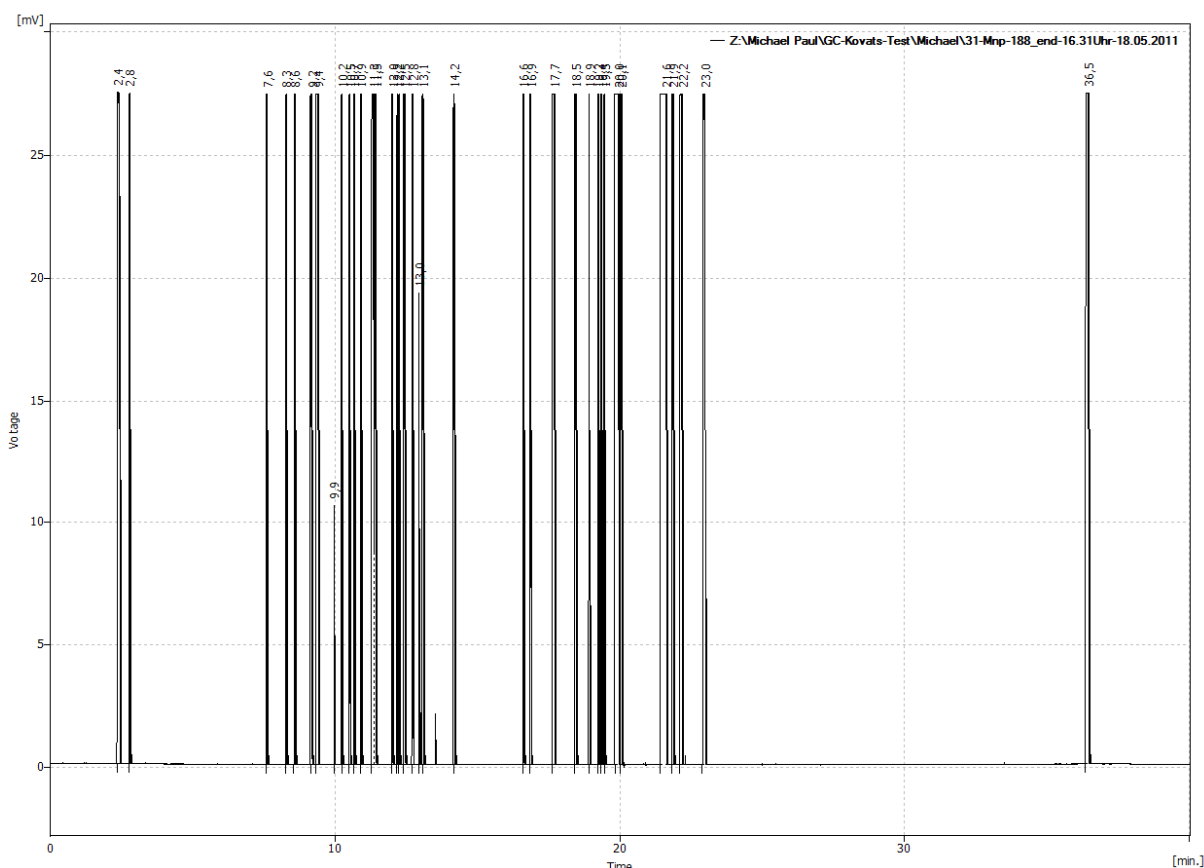


**Fig. 3.87** The GC-FID chromatogram of Bcar. Conditions: 100  $\mu$ L essential oil in 100  $\mu$ L DCM; 0.5  $\mu$ L injection (Split closed; Purge:  $\frac{1}{4}$  open); gas chromatographic conditions as described in chapter 2.3.10. Peaks are explicitly denoted in Tab. 3.16. The closed split delivers a more complex chromatogram.

However, according to the data of Camarda et al. [74] and Hamm et al. [13] these molecules seem to be quite specific for Bcar and hence Bsc samples. Thus, the species Bsc/Bcar seems to biogenetically produce more sesquiterpenes of the cadinane skeleton type ( $\gamma$ -cadinene,  $\delta$ -cadinene and  $\tau$ -cadinol) and even of the cedrane type (cedrol). The work (GC-MS study of Bsc essential oils) of Al Harrasi et al. [184] gives further evidence for the

## Results and Discussion

conclusions deduced from here. Nevertheless, again this is just an assumption, but, according to the literature and the data generated here, this proposal seems to be quite likely.

**Tab. 3.16** Presentation of the GC-data (Bcar) from the chromatogram in Fig. 3.87. The KIs of the significant marker compounds are denoted. Question marks in parentheses declare that only the KI compared with literature results was used for marker identification. For further discussions see text.

Reten. Time [min]	Area [mV.s]	Height [mV]	Area [%]	KI	Compound
2,367	167,445	27,381	4,4		
2,772	28,499	27,353	0,7		
7,617	77,187	27,369	2	<b>939</b>	$\alpha$ -Pinene (?)
8,28	48,071	27,368	1,3	<b>973</b>	$\beta$ -Pinene
8,582	67,396	27,368	1,8	<b>989</b>	$\beta$ -Myrcene (?)
9,187	112,541	27,372	2,9	<b>1021</b>	
9,403	155,898	27,375	4,1	<b>1032</b>	Limonene
9,95	4,281	10,538	0,1	<b>1061</b>	
10,243	39,014	27,362	1	<b>1077</b>	
10,52	62,752	27,368	1,6	<b>1091</b>	
10,683	60,57	27,368	1,6	<b>1100</b>	
10,905	45,344	27,364	1,2	<b>1113</b>	
11,333	126,271	27,37	3,3	<b>1136</b>	
11,455	189,749	27,372	5	<b>1143</b>	
12,02	91,9	27,367	2,4	<b>1172</b>	
12,183	46,259	27,363	1,2	<b>1180</b>	
12,248	50,703	27,365	1,3	<b>1183</b>	
12,457	151,113	27,37	4	<b>1193</b>	
12,757	100,1	27,316	2,6	<b>1209</b>	
12,958	13,399	19,277	0,4	<b>1219</b>	
13,097	70,032	27,367	1,8	<b>1226</b>	
14,197	65,187	27,368	1,7	<b>1278</b>	
16,622	74,341	27,368	1,9	<b>1385</b>	
16,89	92,972	27,369	2,4	<b>1395</b>	
17,712	176,964	27,369	4,6	<b>1428</b>	$\beta$ -Caryophyllene
18,475	106,48	27,37	2,8	<b>1460</b>	$\alpha$ -Humulene
18,925	53,317	27,366	1,4	<b>1478</b>	
19,243	61,714	27,367	1,6	<b>1490</b>	
19,382	83,823	27,37	2,2	<b>1495</b>	
19,487	61,601	27,367	1,6	<b>1499</b>	
19,96	248,43	27,368	6,5	<b>1517</b>	$\gamma$ -Cadinene (?)
20,062	94,952	27,369	2,5	<b>1521</b>	$\delta$ -Cadinene (?)
21,64	401,345	27,375	10,5	<b>1581</b>	$\beta$ -Car-Oxid
21,87	111,425	27,373	2,9	<b>1591</b>	
22,208	150,407	27,37	3,9	<b>1603</b>	Cedrol (?)
22,993	150,795	27,371	3,9	<b>1633</b>	$\tau$ -Cardinol
36,468	180,846	27,37	4,7	<b>2149</b>	Ser-OH
Total	3823,123	987,664	100		

In Tab. 3.17 the KI values for all volatile biomarker compounds discussed here are presented. Since mass spectrometric detection was not available, the retention indices (RI or KI) were used for biomarker ascertainment, when corresponding standards were not

## Results and Discussion

available. Even though, the comparison of all KI values presented in Tab. 3.17 may verify the general correctness of the typical volatile biomarkers for Bpap, Bser and B<sub>ac</sub>/B<sub>car</sub>, there is no absolute guarantee - like obtainable by an unambiguous mass spectrum - for the conclusions made here. However, the retention index C.V.s of ca. maximal 1 % deviation substantiate the general correctness thus far.

**Tab. 3.17** Comparison of all KI values given by Hamm et al., Camarda et al., the Terpenoids Library List and the data generated here (Data Diss. Paul). Mean = Arithmetic Mean (n = 4); S.D. = Standard Deviation (random sample); C.V. = Coefficient of Variation (S.D. / Mean \* 100 %).

Compound	Hamm KI [13]	Camarda KI [74]	Terpenoid KI [183]	Data Diss. Paul KI	Mean	S.D.	C.V.
Methylchavicol	1200	1196	1175	1175	1187	13	1.13
Methyleugenol	1394	1400	1369	1372	1384	16	1.12
n-Octanol	1063	1072	1063	1074	1068	6	0.55
n-Octyl acetate	1220	1213	1188	1202	1206	14	1.16
Verticillia-4(20),7,11-Triene	2004	1999	2040	2021	2016	19	0.92
Incensole	2150	2139	2193	2154	2159	24	1.09
Incensole acetate	2189	2162	2220	2186	2189	24	1.09
Cembrene A	1959	1948	1962	1964	1958	7	0.36
γ-Cadinene	1509	1512	1507	1517	1511	4	0.29
δ-Cadinene	1524	1518	1520	1521	1521	3	0.16
β-Caryophyllene	1426	1414	1421	1428	1422	6	0.44
α-Humulene	1454	1451	1455	1460	1455	4	0.26
β-Caryophyllene oxide	1582	1577	1578	1581	1580	2	0.15
Limonene	1020	1027	1025	1033	1026	5	0.52
β-Pinene	966	973	978	973	973	5	0.51
τ-Cadinol	1634	1638	1633	1633	1635	2	0.15
Serratol	2141 <sup>a</sup>	-	2131	2153	2142	16	0.73
Cedrol	1605 <sup>b</sup>	1599	1603	1603	1603	3	0.16

<sup>a</sup> denoted as unidentified diterpene (according to the KI, it could be Ser-OH, but not verified)

<sup>b</sup> denoted as oxygenated sesquiterpene (according to the KI and mass data, it could be Cedrol, but not verified)

Conclusively, even only by GC experiments the identity of the essential oils from the resins described here is possible. Besides the in plant species universally occurring terpenes (e.g. limonene, β-caryophyllene, β-caryophyllene oxide, etc.), it is mandatory that typical

Olibanum markers are present (e.g. incensole and its acetate or serratol) for an unambiguous species assignment. Quantitative experiments were not carried out.

Iso-incensole and iso-incensole acetate (see Fig. 1.21 in chapter 1.4.5), as reported by Hamm et al. [13], have never been detected in Bcar, respectively, Bsac. Though, these two diterpenes seem to be specific marker compounds for them (Bsac/Bcar). Probably, they may have an almost same KI-value as serratol (**21**) and/or incensole (**22**) and thus co-elute under this peak in the GC chromatograms (see also Hamm et al. [13]). However, even by screening of the neutral fraction of Bcar these compounds (iso-incensole and its acetate) were not detected during the practical part of the work presented here.

### 3.6 Validation Results (1D and 2D HPLC)

#### 3.6.1 Validation Parameters (1D chromatography)

##### Determination of Precision, Selectivity, Peak Homogeneity, Robustness and Accuracy

**Linearity, Precision and Inter-day Precision:** The method was proved to be linear and thus precise for all here quantified analytes ( $R^2 > 0.999$  for all analytes in the first dimension). Inter-day precision was evaluated by generating for each greater quantitation series (Bpap, Bser and Bsac/Bcar) the comprehensive external calibration procedure (see chapter 2.3.4.2). Thus, the complete procedure was carried out three times for each species analysed quantitatively. The detailed discussion is given in chapter 3.6.3.1, where also the arithmetically averaged means of the linear regression functions, including their measurement uncertainty, are given.

**Specificity:** For the determination of compounds detectable at 250 and 280 nm the method is highly specific. Hence, compounds **5** and **6** (at 250 nm) and compounds **9** and **10** (at 280 nm) and even additional signals can be quantified easily. Besides the good resolution of these signals at these detection wavelengths, no significant interfering signals elute in the corresponding retention areas (see chromatograms of RS in chapter 3.7).

**Selectivity:** Selectivity for compounds, merely absorbing at 210 nm, was achieved by generation of resolution values up to  $R = 1.5$  (definition of baseline separation). The smallest resolution was obtained for compound **10** ( $R = 1.1$  at 210 nm). However, as **10** was specifically quantified at 280 nm and showed only low absorption at 210 nm, the adjacent higher peak (compound **2**) was easily resolved, giving negligible integration errors. All other signals gave resolution values from  $R = 1.2 - 7.8$ . A depictive chromatogram and the referring data therefore are presented in Fig. 3.88 and Tab. 3.18.

**Robustness:** Robustness of the method has been granted since resolution and peak areas of target analytes did not vary significantly by changing other parameters slightly (Temperature: +/- 2 °C; flow rate: +/-0.5 ml/min; gradient time: +/- 0.5 min). The elution area of compound **11**, **16**, **9**, **1**, **19**, **3**, **18** and **8** ( $R_t$  ca. 30-35 min) has been most sensitive to these minor changes (data not shown here). However, as for quantitation of compound **1** and **3** (co-elution with compound **18**) in Bser and Bpap a second chromatography dimension was established, this problem had not been of greater concern. Furthermore, for Bsac/Bcar

samples, where compounds **18** and **19** are only in minimal contents present, the 2D chromatography is, as experienced hitherto, unnecessary (see also chapter 3.7.5).

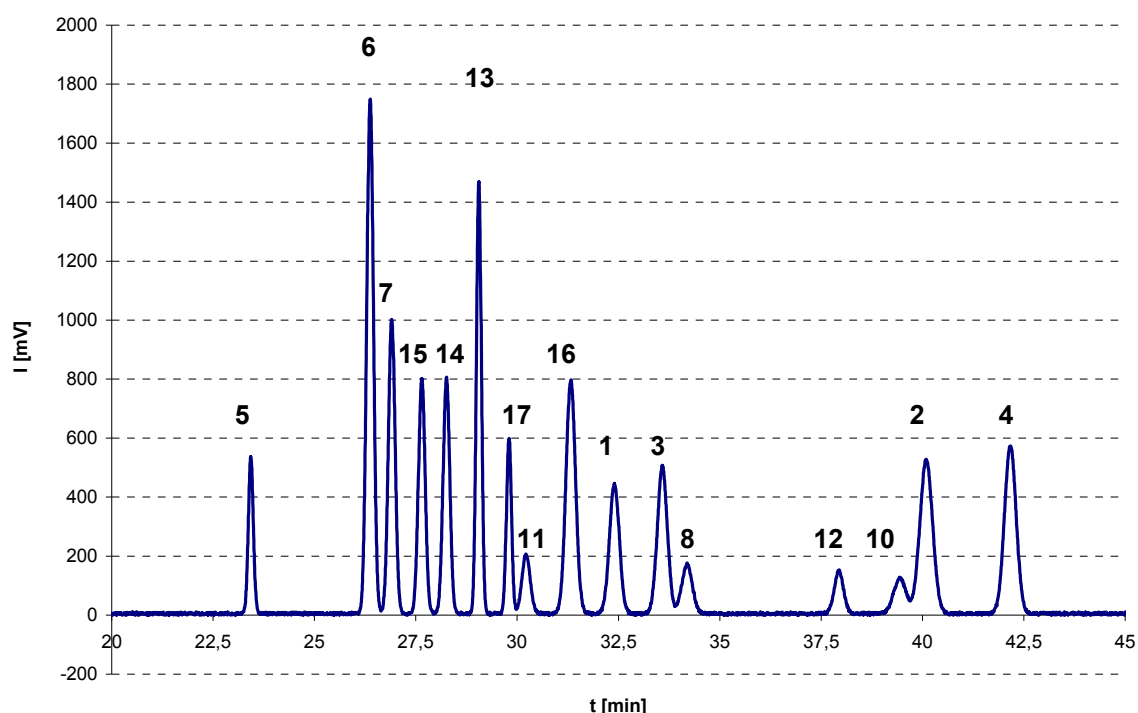


**Fig. 3.88** Depiction of a standard chromatogram at 210 nm detection wavelength, calculated on experimental values, plot of  $\log k'$  results against gradient time [153], with Microsoft Excel<sup>®</sup> 2003 software as described in [162]. Note: Real sample chromatograms contain more minor peak signals. In this “idealised” example the peak heights and areas are fitted to the expectation RS chromatogram ( $c = 5$  mg/ml) for Bpap (see also [59]). Furthermore, compound **17** has not been quantified, and compounds **8** and **10** may not be detectable when no decomposition of compound **7** occurs [55]. In this simulation the peaks of compound **9**, **18** and **19** have not been considered for the calculation. The retention times and resolution values referring to the chromatogram are presented in Tab. 3.18. For details see text.

**Tab. 3.18** Retention times ( $R_t$ ) and resolution values [(calculated on baseline peak width;  $R = 2 \times (t_{r2} - t_{r1}) / (w_1 + w_2)$ ] for each compound as depicted in Fig. 3.88. The worst resolution is given for compounds **17** and **11** ( $R = 1.2$ ) and peak pair **10** and **2** ( $R = 1.1$ ). Compound **17** has not been quantified. Note that  $R$  values depend on the concentrations of target analytes (here  $c = 5$  mg/ml for the RS fraction of Bpap). For details see text.

Compound	Abbr. Nr.	$R_t$ [min]	$R$
$\beta$ -KBA	5	23.43	7.8
$\beta$ -AKBA	6	26.38	1.5
11-OH- $\beta$ -ABA	7	26.91	1.8
$\beta$ -OH-TA	15	27.65	1.4
$\alpha$ -OH-TA	14	28.26	1.9
3-O-TA	13	29.06	1.6
Dien-TA	17	30.00	1.2
LA	11	30.51	2.0
$\alpha$ -Ac-TA	16	31.33	2.2
$\alpha$ -BA	1	32.40	2.5
$\beta$ -BA	3	33.58	1.3

## Results and Discussion

Compound	Abbr. Nr.	R <sub>t</sub> [min]	R
11-OMe-β-ABA	8	34.19	6.8
Ac-LA	12	37.94	2.6
9,11-Dehydro-β-ABA	10	39.44	1.1
α-ABA	2	40.09	3.3
β-ABA	4	42.17	

**Accuracy:** Accuracy was determined by comparison of the method developed here with the HPLC determination method for compound **5** and **6** described in the European Pharmacopoeia 6.0 [20]. The determination of contents for compound **5** and **6** gave similar values for both methods; the pharmacopoeias and the here reported one. Conclusively, the target compounds were almost quantitatively extracted and separated from the neutral fraction compounds (a minor uncertainty can never be excluded). The diterpenes **20**, **21** and **22** have been still detectable in the RS fraction extract. Thus, for them the liquid-liquid extraction procedure has not been optimised. Compound **22** did not co-elute with any target analyte of the RS fraction, whilst compound **20** and **21** did co-elute with compound **14** and **15** in the samples of Bser and Bser/Bcar and therefore falsifying their integration results (see also chapter 3.7 and 3.8). Nevertheless, most of the neutral terpenoids were separated quantitatively as can be noticed by qualitative evaluation (see RS/NB-chromatograms in 3.7).

**Tab. 3.19** Comparison of the two HPLC methods: European Pharmacopoeia 6.0 (without separation of acid- and neutral fraction) and the method developed here (with separation of acid- and neutral fraction). Both determinations are recalculated to the overall amount of processed resin. Injection concentrations for Bpap were 2.5 mg/ml and for Bser samples 5 mg/ml for the standard HPLC method (1D HPLC). The Eur. Pharm. 6.0 conditions were as described in chapter 2.3.9. Recovery value is obtained by division of the contents (1D HPLC / Eur. Pharm. 6.0) and given in percent. Bias is obtained by subtraction of the Recovery value from 100 %. For further discussion see text.

Bpap	Eur. Pharm. 6.0				1D HPLC			
	β-KBA [g/g in %]	β-KBA [g/g in %]	Recovery [%]	Bias [%]	β-AKBA [g/g in %]	β-AKBA [g/g in %]	Recovery [%]	Bias [%]
22-1300	1.22	0.36	29.51	-70.49	4.86	4.94	101.65	1.65
22-1400	0.45	0.30	66.67	-33.33	4.22	4.81	113.98	13.98
22-1400-2010	0.65	0.36	55.38	-44.62	4.26	4.67	109.62	9.62
Mean	0.77	0.34	43.97	-56.03	4.45	4.81	108.10	8.10

Bser	Eur. Pharm. 6.0				1D HPLC			
	β-KBA [g/g in %]	β-KBA [g/g in %]	Recovery [%]	Bias [%]	β-AKBA [g/g in %]	β-AKBA [g/g in %]	Recovery [%]	Bias [%]
22-1560	0.59	0.53	89.83	-10.17	1.01	0.89	88.12	-11.88
Granen	1.04	0.78	75.00	-25.00	1.23	1.18	95.93	-4.07
22-127	0.90	0.86	95.56	-4.44	1.19	0.87	73.11	-26.89
Mean	0.84	0.72	85.77	-14.23	1.14	0.98	85.71	-14.29

For both methods, three samples of each of the two species Bpap (1. Wahl-Nr. 22-1300, Nr. 22-1400 and Nr. 22-1400-2010) and Bser (1. Wahl-Nr. 22-1560, B.Granen and Nr. 22-127)

were compared (all samples were different batches from Gerhard Eggebrecht GmbH, Süderau, Germany). The amount of crude resinous material for each sample preparation was about 2 g (different small resins chunks, randomly picked from the batch, were processed). It should be noted that even within one resin batch, the individual chunks may show a quite strong variation regarding the composition of terpenic acids, even stronger for volatile mono- and diterpens (In general: The greater the sample population of the whole batch, the better the reliability of the determined result). The preparation was implemented as reported in the appropriate chapters (2.2.4 and 2.3.9). The comparison of results from both methods is given in Tab. 3.19.

Approximately, both methods give similar measurement results. The results for the Bser samples show a better fit (Note: The European Pharmacopeia 6.0 method is developed for Indian frankincense, not for any other species). Furthermore, it is striking that the values for  $\beta$ -KBA (**5**) in Bpap, by the standard HPLC method, are, on average, ca. 50 % below the values of the pharmacopoeias method. This could be arbitrary, since for both sample preparations different resin chunks from each batch had been taken. Another point could be that the pharmacopeia method is just a simple one-point calibration, whereas the method reported here is based on a calibration curve with six points. Thus, especially for the  $\beta$ -KBA (**5**) contents in Bpap, which were proved to exceed the one-point calibration peak area by factor 1.5 for sample 22-1400-2010 and by factor 2.3 for sample 22-1300, the values are probably estimated too high. Interestingly, for the  $\beta$ -AKBA (**6**) contents in Bpap both values fit quite well, though the  $\beta$ -AKBA (**6**) peak area is ca. by factor 8.3 bigger as the one-point calibration peak area. Hence, both regression functions cover coincidentally the same range in the case for  $\beta$ -AKBA (**6**) and may differ systematically for  $\beta$ -KBA (**5**) in Bpap.

However, the reason for these results in Bpap was not further evaluated. Probably, if the complete resin population is prepared from one homogenised (electrical mixer or mortar and pestle) sample batch, which then is divided into two sub samples (one for method A and one for method B), expectably the same values may be obtained. Nonetheless, in order to get an overview on the accuracy of results from independent sample populations within the same batch population, this was not done.

Additionally, as it is shown that for Bser and for the  $\beta$ -AKBA (**6**) content of Bpap, comparable results are delivered (Bias < 15 %), both methods may be valid to lead to results almost near the true target analyte concentration. Interestingly, by summation of the  $\beta$ -KBA- and  $\beta$ -AKBA-contents (**5** and **6**) of each sample, the bias is almost within a classical batch to batch measurement uncertainty [Sum of  $\beta$ -KBA and  $\beta$ -AKBA contents for Bpap: 5.15 % (1D HPLC) compared with 5.22 % (Eur. Pharm. 6.0), Bias: -1.34 %; and for Bser: 1.70 % (1D HPLC) with 1.98 % (Eur. Pharm. 6.0), Bias: -14.14 %]. The minor bias difference for the Bpap samples is explainable by the high  $\beta$ -AKBA (**6**) content in this species. Hence, the overall result for Bpap, compared with Bser, is more robust (e.g. fewer errors through integration errors for greater peak areas, etc.), although the  $\beta$ -KBA (**5**) bias is comparably rather strong. Nonetheless, the HPLC method developed in this work could also deliver systematically lower values at low concentration ranges since the concentration values for both, **5** in Bpap and **5** and **6** in Bser, are differing at a content of ca. 1 % (in g/g) about -15 to -50 % from the

results obtained by the Pharmacopeia 6.0 method (see Tab. 3.19). This could be also due to the sample preparation steps (separation of RS and NB, see chapter 2.2.4 and 3.3.1).

### 3.6.2 Validation Parameters (2D chromatography)

#### Determination of Precision, Recovery and Accuracy (compared with 1D results)

**Linearity, Precision and Inter-day Precision:** The second dimension method was proved to be linear. Though the coefficient of correlation was not for all calibration curves greater than the demanded 0.999, it was normally accepted as it included additional sample preparation steps, leading to a greater uncertainty (see also chapter 2.3.4.4). On average, the coefficient of variation, referred to the peak area, for each concentration level was less than 3 %. Inter-day Precision was evaluated by generating for each greater quantitation series (B<sub>pap</sub>, B<sub>ser</sub> and B<sub>sac</sub>/B<sub>car</sub>) the comprehensive external calibration procedure with the fractions collected in the first chromatography dimension (see also chapter 2.3.4.3). Additionally, one RS sample batch was prepared on three different days to test the intermediate-precision. The values therefore are presented in Tab. 3.20. As can be seen there, a quite good laboratory reproducibility is possible (error < 3% for intra-day precision and even better when only the mean values of each day, A-C, are compared; error in this case < 2 %). However, it must be noticed that especially for the B<sub>pap</sub> RS samples at least a concentration of 5 mg/ml should be injected in the first chromatography dimension to obtain a sufficient signal to noise ratio (S/N) and thus a minor integration error in the second dimension. As evaluated, the species B<sub>pap</sub> contains the lowest contents of BAs (**1** and **3**) compared with B<sub>ser</sub> and B<sub>sac</sub>/B<sub>car</sub> (see also chapter 3.8). Thus, based on the approximate equation  $[C.V. \approx 50/(S/N)]$  from [153], the uncertainty can be predicted (e.g. peak height for compound **1**,  $S \approx 70$  mV divided by  $N \approx 3$  mV gives a C.V. of ca. 2.14 %; peak height for compound **3**,  $S \approx 80$  mV divided by  $N \approx 3$  mV gives a C.V. of ca. 1.88 %; both estimated C.V.s lay within the experimental obtained C.V. as demonstrated in Tab. 3.20).

**Tab. 3.20** Inter-day precision for the determination of compound **1** (first row) and **3** (second row) by the 2D chromatography method, obtained by three injections for each day ( $c = 5$  mg/ml, sample B<sub>pap</sub> RS fraction). Mean (referring to the Peak Area); Standard Deviation (S.D.) and the Coefficient of Variation (C.V. in %; S.D. divided through Mean and multiplied with 100 %). Overall represents the arithmetic mean and referring S.D. of all three measurements (Inter-Day precision of the means A, B and C).

A:Intra-Day 2D			B:Intra-Day 2D			C:Intra-Day 2D			Overall: Inter-Day		
Mean [PeakArea]	S.D	C.V. [%]									
193277 ( <b>1</b> )	2844	1.47	195683 ( <b>1</b> )	5235	2.68	197567 ( <b>1</b> )	2843	1.44	195509 ( <b>1</b> )	2151	1.10
403638 ( <b>3</b> )	6788	1.68	395430 ( <b>3</b> )	5564	1.41	399794 ( <b>3</b> )	5020	1.26	399620 ( <b>3</b> )	4107	1.03

Therefore, the peak height should be as high as possible. Otherwise the results lose a lot of precision and a different approach may be needed for method validation (e.g. peak heights

## Results and Discussion

or plausibility consideration via relative percentages of peak areas obtained in the second dimension for compounds **1**, **3** and **18**).

**Tab. 3.21** Retention times ( $R_t$ ) and resolution values [calculated on baseline peak width;  $R = 2 \cdot (t_{r2} - t_{r1}) / (w_1 + w_2)$ ] for each compound as depicted in Fig. 3.89. All target compounds are well resolved. Note that  $R$  values depend on the concentrations of target analytes (here  $c = 5$  mg/ml for the prepared RS fraction of Bpap). For details see text.

Compound	Abbr. Nr.	$R_t$ [min]	$R$
$\beta$ -Ac-8,24-dien-TA	19	9.692	0.6
$\alpha$ -Ac-7,24-dien-TA	18	9.967	1.8
$\alpha$ -BA	1	10.967	2.0
$\beta$ -BA	3	12.083	2.0
11-OMe- $\beta$ -ABA	8	13.05	

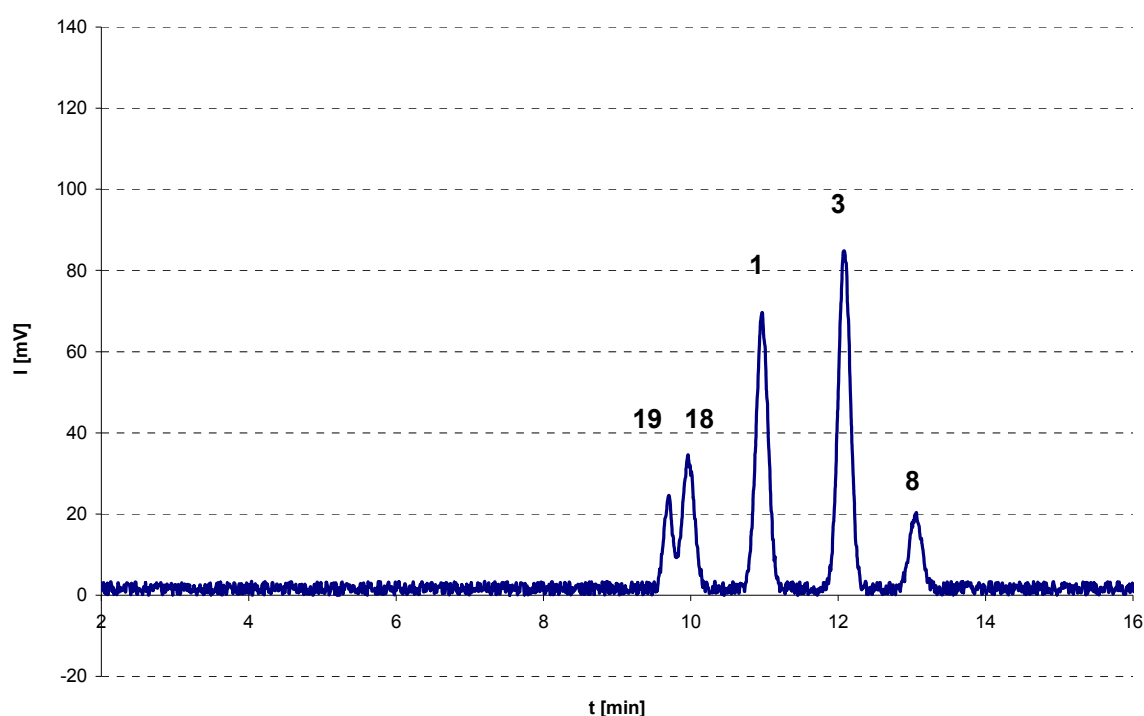


**Fig. 3.89** Depiction of a 2D chromatogram at 210 nm detection wavelength (calculated on experimental values with Microsoft Excel<sup>®</sup> 2003 software as described in [162]). The chromatogram is based on a typical expectation value for Bpap samples, prepared from an injection concentration of 5 mg/ml RS fraction (minimum required RS concentration for a quite reliable integration result). Note: Peak **8** is mostly not observable in real sample chromatograms (see also [59]). For further details see text.

**Selectivity:** Selectivity is granted as resolution values greater than 1.5 were generated for compound **1**, **3** and **8**. The co-eluting compounds **18** and **19** in the first dimension are well resolved from the target analytes. A typical expectation chromatogram of a prepared Bpap RS sample ( $c = 5$  mg/ml) is presented in Fig. 3.89 and in Tab. 3.21 the corresponding data is shown.

**Recovery:** The quantitative control value of  $\pm 5\%$  had been evaluated on empirical results and normally lay within the theoretically estimated error propagation of the system (Theory:

+/-1 % error during the slight N<sub>2</sub>/Air-drying of the fraction; +/- 2 % error by resolving in 100 µl MeOH; +/- 2 % error by injection and integration; see also the review of Meyer on measurement uncertainty [163]). Generally, the recovery values are better the greater the concentrations of compound **1** and **3** in the sample are. Furthermore, the error of +/-5 % according to the second dimension became more precise, the more samples had been analysed. Normally, in this work, an error less than 3 % was obtained. For each analyte, dependent on the concentration level, the regression model was chosen which showed a better fit to the real experimental data (see also discussions in chapter 3.6.3). The calibration data is show in Tab. 3.23 and 3.24 in chapter 3.6.3.1.

### 3.6.2.1 General Remarks on the 2D Method Sample Preparation

The crucial steps to obtain reproducible results are reported here. Firstly, it is important to use a very slight N<sub>2</sub>-stream to definitely concentrate the sample at the bottom of the pointed 10 ml flask. If this is not done appropriately, the white sample film will be covered over a great surface within the flask, which makes dissolution in 100 µl MeOH inaccurate (danger of evaporation!) and can lead to an insufficient sample recovery. Additionally, using a 250 µl Hamilton injection syringe for sample resolving with 100 µl MeOH delivers better results than with an automatic 100 µl pipette (empirical experience made in this work and also plausible as the sample gets better dissolved by a better variable solvent distribution, possible through the more flexible Hamilton syringes). The calibration of the 250 µl syringe is shown in Tab. 3.22 and proves that a good precision is granted. Finally, after the sample is dissolved again, it must be immediately injected (evaporation danger!). If all these steps are carried out carefully, it is possible to obtain quite precise results for the 2D chromatography. However, the greater the sample amount collected in the 1D chromatography, the more accurate and precise will be the result in the second dimension. The minimum concentration, as already discussed, should be 5 mg/ml to obtain precisely reproducible results. This is especially important for samples of the species Bpap since the RS fractions show expectably the lowest contents for compound **1** and **3**.

**Tab. 3.22** Hamilton Syringe calibration for the 2D chromatography sample preparation, according to [155] (MeOH was used instead of water). Mean: Arithmetic mean of 10 immediately repeated steps (10 x 100 µl with a 250 µl syringe); S.D.: Standard Deviation and the C.V.: Coefficient of Variation in percent.

100 µL MeOH	Nr.	Weight [mg]	Nr.	Weight [mg]
	1	0.07790	6	0.07780
	2	0.07733	7	0.07727
	3	0.07797	8	0.07732
	4	0.07790	9	0.07780
	5	0.07731	10	0.07771
Mean:		0.07763		
S.D.:		0.00027		
C.V. [%]		0.35		

For Bser and B<sub>sa</sub>c/B<sub>ca</sub>r, which contain normally higher amounts of BAs, the C.V.s can be even better at this concentration level (c = 5 mg/ml). Anyway, the second dimension is not necessary for samples of B<sub>sa</sub>c/B<sub>ca</sub>r, since compounds **18** and **19** are only minimally

expressed (see chapter 3.7.5). Hence, the integration inaccuracy in the first chromatography dimension lay within the error of repeatability. For samples of Bser, which contain the greatest amounts of BAs (**1** and **3**), the integration error is smaller in the first dimension compared with samples of Bpap. Furthermore, if it is known that compound **18** co-elutes within a certain expectation interval with compound **3**, the second dimension may be unnecessary when the confidence interval is widened or the value for compound **3** is corrected (on average by a factor which represents the differences in the estimated integration). Thus, someone may of course doubt if the huge effort for the second dimension is justified, when after a great analysed sample population a trustfully corrected value may be predictable.

### **3.6.3 General Discussion and Statistical Evaluation of the HPLC Calibration**

#### **3.6.3.1 HPLC Calibration Data**

In this chapter the data generated by external calibration is discussed thoroughly. It should be beard in mind that the whole method development was firstly evaluated for the species Bpap [59]. For the species Bser and Bsac, respectively, Bcar, there occur a few other characteristics, based on the here analysed sample population. Generally, prior to each quantitation series (Bpap quantitation, Bser quantitation and Bsac/Bcar quantitation) the corresponding calibration (6 standard concentrations with three injections each) was carried out. The same was done for the second chromatography dimension for the determination of compound **1** and **3**. According to the evaluated differences between these species, the corresponding linearity range was extended for Bser and Bsac/Bcar, when a RS fraction concentration of 5 mg/ml was kept constant. Hence, for evaluation of Bser and Bsac/Bcar samples the linearity range for the compounds **1**, **2**, **3**, **4** (BAs and ABAs) and for compounds **11** and **12** (LAs) was expanded. The preliminary tests revealed for these species expectably greater amounts concerning the mentioned boswellic and lupeolic acids (e.g. for Bsac/Bcar great quantities of BAs, ABAs and LAs can be found, and for Bser the BAs showed a significant higher content level compared with Bpap). Certainly, another solution would have been to inject RS fraction concentrations lower than 5 mg/ml to bring the analytes in the expected concentration range. However, especially for accurate integration results in the 2D chromatography a sample concentration of at least 5 mg/ml RS fraction had been normally necessary. Thus, for the samples of Bser and Bsac/Bcar the linearity range was adjusted. The summarised calibration data is shown in Tab. 3.23. The data set represents the arithmetically averaged calibration curves obtained by three independent determinations. Besides the standard deviation, the overall measurement uncertainty is given [162]. For BAs, ABAs and LAs the linearity ranges were extended as mentioned above, which is indicated by superscripts. The extended operating ranges are demonstrated in Tab. 3.24. All 1D chromatography calibrations led to an acceptable precision ( $R^2 > 0.999$ ). Furthermore, the ordinate intercept has been negligible, since it is basically just a product of coincidence, and even the straight line through the origin gave for all references an adequate precision. The 2D chromatography expectably revealed, as it is a product of further sample preparation steps, a weaker linearity (especially for compound **1**). The very good linearity value for

## Results and Discussion

compound **3** may be just a matter of coincidence in this case. However, the main purpose for the second dimension was to resolve compound **3** from compound **18** and **19** in order to generate more accurate quantitation results for it. The method gave significant differences in the integration results when these compounds (**18** and **19**) co-eluted with **3** in the first dimension, while compound **1** (in all samples eluting as homogenous peak in the first dimension) delivered integration results within the predicted interval for a certain concentration. The strong MU value for compound **11** is explained by the great operating range and is similar to the values presented in Tab. 3.24 (compound **11** was analogue prepared as compound **12** in order to cover their greater contents in B<sub>ser</sub>/B<sub>car</sub>). If the linearity range for this compound is minimised (e.g. 8-250 µg/ml, as for compound **12**), the MU will be expectably decreased.

**Tab. 3.23** RS-fraction calibration data for the 15 quantified compounds. Linear regression ( $y =$  unit of peak area;  $x =$  weighed sample in mg/ml; plus/minus the ordinate intercept); the arithmetically averaged Measurement Uncertainty (MU; calculated according to [162]) given in % (Note that for each standard concentration the MU varies; high values for low concentration levels and lower values for higher concentration levels); Correlation Coefficient (Corr. Coeff.,  $R^2$ ); Limit of Quantitation (LOQ) and the Operating Range. The Limit of Detection,  $LOD = LOQ / 3.33$ ; LOD was determined by multiplication of the noise-standard deviation by factor 3; LOQ was determined by multiplication of the noise-standard-deviation by factor 10 and accepted when integration errors were negligible at this stage. For further details see text.

<sup>a</sup> Operating Range extended for B<sub>ser</sub> (for RS-c = 5 mg/ml), see also Tab. 3.24.

<sup>b</sup> Operating Range extended for B<sub>ser</sub>/B<sub>car</sub> (for RS-c = 5 mg/ml), see also Tab. 3.24.

<sup>c</sup> Great Operating Range for LA leads to a rather high MU at low concentrations (see also discussions about Ac-LA in chapter 3.6.3.2). The high uncertainty for low concentrations was taken into account.

Compound	Detection at	Weighted Linear Regression (+/- stand. dev.)	Averaged MU [%]	Ordinate Intercept (+/- stand. dev.)	Corr. Coeff. $R^2$	LOQ [µg/ml]	Operating Range [µg/ml]
<b>1<sup>a, b</sup></b>	210 nm	7.92E+06 (+/- 7.07E+04)	6	7.43E+03 (+/-1.59E+04)	0.99982	15	15 – 480
<b>1(2D)<sup>a, b</sup></b>	210 nm	1.32E+06 (+/- 1.53E+04)	5	7.50E+03 (+/- 4.35E+03)	0.99880	60	60 – 480
<b>2<sup>b</sup></b>	210 nm	8.15E+06 (+/- 6.25E+04)	7	-1.05E+04 (+/- 3.03E+04)	0.99979	13	13 – 514
<b>3<sup>a, b</sup></b>	210 nm	7.50E+07 (+/- 4.72E+04)	6	-1.49E+04 (+/- 1.09E+04)	0.99991	15	15 – 490
<b>3(2D)<sup>a, b</sup></b>	210 nm	1.31E+07 (+/- 1.35E+04)	4	6.09E+03 (+/- 6.37E+03)	0.99975	60	60 - 490
<b>4<sup>b</sup></b>	210 nm	6.26E+06 (+/- 6.96E+04)	9	-2.59E+03 (+/- 3.75E+04)	0.99977	15	15 – 575
<b>5</b>	250 nm	5.20E+07 (+/- 5.49E+05)	5	-1.30E+04 (+/- 2.83E+05)	0.99973	0.5	0.5 - 275
<b>6</b>	250 nm	4.98E+07 (+/- 4.64E+05)	11	5.75E+04 (+/- 2.27E+05)	0.99984	0.7	0.7 - 260
<b>7</b>	210 nm	1.23E+07 (+/- 1.40E+05)	10	2.84E+04 (+/- 3.51E+04)	0.99969	9	9 - 540
<b>8</b>	210 nm	1.93E+07 (+/- 3.40E+05)	12	-3.97E+02 (+/- 2.27E+04)	0.99968	8	8 - 150

## Results and Discussion

Compound	Detection at	Weighted Linear Regression (+/- stand. dev.)	Averaged MU [%]	Ordinate Intercept (+/- stand. dev.)	Corr. Coeff. $R^2$	LOQ [ $\mu\text{g/ml}$ ]	Operating Range [ $\mu\text{g/ml}$ ]
<b>10</b>	280 nm	3.70E+07 (+/- 6.34E+05)	9	-5.10E+04 (+/- 3.59E+04)	0.99966	2	2 - 120
<b>11<sup>c</sup></b>	210 nm	8.48E+06 (+/- 8.81E+04)	20	1.42E+05 (+/- 2.14E+05)	0.99922	8	8 – 1530
<b>12<sup>b</sup></b>	210 nm	7.34E+06 (+/- 7.47E+04)	7	-5.00E+02 (+/- 8.64E+03)	0.99971	8	8 – 250
<b>13</b>	210 nm	1.47E+06 (+/- 3.69E+05)	9	4.21E+03 (+/- 1.14E+05)	0.99915	8	8 – 650
<b>14</b>	210 nm	1.85E+07 (+/- 1.39E+05)	4	4.06E+04 (+/- 3.41E+04)	0.99989	6	6 - 520
<b>15</b>	210 nm	1.42E+07 (+/- 1.12E+05)	4	2.57E+04 (+/- 5.26E+04)	0.99965	7	7 – 680
<b>16</b>	210 nm	1.77E+07 (+/- 1.30E+05)	6	3.88E+04 (+/- 3.32E+04)	0.99987	7	8 - 540

**Tab. 3.24** Extended Operating Range. Definitions and Abbreviations are the same as in Tab. 3.23. Since higher concentrations of BAs in Bser and BAs, ABAs, LA and Ac-LA in B<sub>ser</sub>/B<sub>car</sub> are found, when RS-samples with  $c = 5 \text{ mg/ml}$  are measured, the working range was extended. For further discussions see text.

Compound	Detection at	Weighted Linear Regression (+/- stand. dev.)	Averaged MU [%]	Ordinate Intercept (+/- stand. dev.)	Corr. Coeff. $R^2$	LOQ [ $\mu\text{g/ml}$ ]	Operating Range [ $\mu\text{g/ml}$ ]
<b>1</b>	210 nm	8.66E+06 (+/- 1.96E+05)	15	-1.05E+04 (+/- 1.12E+05)	0.99929	15	15 – 1300
<b>1(2D)</b>	210 nm	1.60E+06 (+/- 3.04E+04)	12	-4.65E+03 (+/- 1.26E+04)	0.99909	60	60 – 900
<b>2</b>	210 nm	1.01E+07 (+/- 4.34E+05)	26	-1.01E+05 (+/- 3.69E+05)	0.99900	13	13 – 1500
<b>3</b>	210 nm	8.06E+06 (+/- 1.69E+05)	12	-2.81E+04 (+/- 1.12E+05)	0.99932	15	15 – 1500
<b>3(2D)</b>	210 nm	1.39E+06 (+/- 2.68E+04)	12	4.19E+03 (+/- 1.32E+04)	0.99855	60	60 - 1010
<b>4</b>	210 nm	8.70E+06 (+/- 3.70E+05)	27	-1.31E+05 (+/- 3.19E+05)	0.99908	15	15 – 1500
<b>12</b>	210 nm	8.30E+06 (+/- 2.37E+05)	17	-1.09E+04 (+/- 1.35E+05)	0.99952	8	8-1450

In Tab. 3.24 the extended operation ranges are presented. There, as explicitly discussed for compound **12** in chapter 3.6.3.2, the MU values encompass a quite great interval and thus a lower precision. The reason for this phenomenon can be explained by the greater scattering of values along the greater interval and hence an entirely weaker coefficient of correlation compared with the smaller operating ranges presented in Tab. 3.23.

Since the extension of the operating range for compounds **1**, **2**, **3**, **4** and **12** was implemented to cover the higher contents of these compounds in B<sub>ser</sub>, respectively, B<sub>ser</sub>/B<sub>car</sub>, their error is not as great as someone could assume by the data presented in there. If only the high concentration levels are regarded, the MU value is more precise. This

is explicitly explained in chapter 3.6.3.2, where the two linearity ranges of compound **12** are discussed. The conclusion made there can be referred to all standards for which the operating range was extended.

In Tab. 3.25 the external calibration data for the neutral compounds **20**, **21**, **22** and **23** is shown. All compounds are merely quantifiable at 210 nm detection wavelength. However, due to the fact that compounds **20** and **21** contain three double-bond systems, their absorption coefficients are higher than for **22** and **23** (only two double-bond systems). This led to a polynomial S-shaped calibration function over a rather minimal concentration range (for our system: 0 – 0.5 mg/ml); or to two different linearity ranges (linearity range No. 1: ca. 0 – 0.18 mg/ml, and linearity range No. 2: ca. 0.18 – ca. 0.45 mg/ml). Since for a polynomial calibration curve (order two or three) much more calibration data points are necessary to verify the accuracy of the function [156], it was decided to chose the minimum linearity range (from 0 – 0.18 mg /ml) to quantify Ser-OH (**20**) and Iso-Ser (**21**). Although, this approach needed in some cases two trial injections with real samples of NB to find the adequate working range of the function. Calibration curves for Inc (**22**) and Inc-Ac (**23**) were linear within a wide range (up to 600 µg/ml).

**Tab. 3.25** HPLC calibration data for iso-serratol (**20**), serratol (**21**), incensole (**22**) and its acetate (**23**). Linear regression ( $y = \text{unit of peak area}$ ;  $x = \text{the weighted sample in mg/ml}$ ; plus/minus the ordinate intercept); correlation coefficient ( $R^2$ ); limit of detection (LOD) and the operating range (LOD was determined by multiplication of the noise-standard-deviation by factor = 3; limit of quantitation, LOQ, was determined by multiplication of the noise-standard-deviation by factor = 10; Operating range results from the maximum concentration levels, within the values were linear). The measurement uncertainty (MU) was calculated as described in [162]. For further details see text.

Compound	Detection at	Weighted Linear Regression (+/- stand. dev.)	Averaged MU [%]	Ordinate Intercept (+/- stand. dev.)	Corr. Coeff. $R^2$	LOQ [ $\mu\text{g/ml}$ ]	Operating Range [ $\mu\text{g/ml}$ ]
<b>20</b>	210 nm	5.03E+07 (+/- 4.01E+05)	6	-5.18E+04 (+/- 5.83E+04)	0.99965	5	5 - 180
<b>21</b>	210 nm	5.18E+07 (+/- 4.24E+05)	8	- 9.06E+04 (+/- 7.73E+04)	0.99945	5	5 - 180
<b>22</b>	210 nm	1.93E+07 (+/- 6.74E+05)	19	-2.92E+04 (+/-1.68E+05)	0.99966	7	7-530
<b>23</b>	210 nm	1.70E+07 (+/- 3.94E+04)	15	-1.77E+04 (+/- 1.09E+05)	0.99929	15	15-590

### 3.6.3.2 General Calibration Issue (Example of Compound **12**, AcLA)

Normally, the increase of the operating range increases the slope of the calibration curve to keep the summation of least squares minimal. This expectation was verified in the here given example of the linearity range extension for AcLA (compound **12**; see Fig. 3.90). Basically, when great operating ranges, even with an acceptable correlation coefficient ( $> 0.999$ ), are given, the values for low concentration levels tend to be more inaccurate.

A good example for this problem is reported in the paper of Johnson et al. [185]. Thus, for high operating ranges revealing a strong variance inhomogeneity (ascertainable via the F-

test, see also [159,162]), the weighted linear regression model is recommended. Figuratively, like on a classical scale, the weighing of measuring points at the one end will lead to a difference in coordinates on the other end of the calibration curve. This model takes into account the relevance of the relative deviation of measuring points, whereas a conventional linear regression model just minimises the sum of least squares. An easily understandable and exemplary explanation on weighted least squares is given in the book by R. de Levie [186].

Here, two linearity ranges, generated by both models, are compared to show how difficult and delusive the simple and blind trust on linear models can be, without proving analytical results by common sense.

A reliable linearity range for Ac-LA (**12**), referring to the RS fraction of B<sub>pap</sub> and B<sub>ser</sub>, was finally realised to be operable within the concentration range of 8 µg – 250 µg/ml. This concentration range is, as far as here experienced, sufficient for quantitative experiments with the species B<sub>pap</sub>, respectively, B<sub>ser</sub> (expectation value for B<sub>pap</sub> and B<sub>ser</sub> in the real sample acid fraction with c = 5 mg/ml is ca. 0.05-0.12 mg/ml). Both calibration models were applied, the unweighted and the weighted. Since it was realised that the B<sub>sac</sub>/B<sub>car</sub> samples contain often LA/AcLA contents above this range, the linearity range was extended to give a function sufficiently for all samples (B<sub>pap</sub>, B<sub>ser</sub> and B<sub>sac</sub>/B<sub>car</sub>). Furthermore, this was necessary to keep the overall injection concentration for acid fractions constant (c = 5 mg/ml; minimum RS content for the 2D chromatography, as lower RS concentrations deliver greater integration errors in the second dimension, see also chapter 3.6.2). Therefore, as for analytical measurement systems a broad linearity range is generally desirable, it was extended to 1.45 mg/ml and still showed a good linearity within this great interval (> 0.999). However, for the greater linearity range a greater overall error is given.

The results of both regression models (weighted and unweighted) are presented in Fig. 3.90. There, as expected for both concentration ranges, the VVK for the weighted regression model delivered a better value. Additionally, the confidence and prediction interval is wider for the greater operating range (measurement uncertainty: from 20 % for low concentration to 15 % for high concentrations) and, vice versa, narrower for the smaller range (measurement uncertainty: from 10 % for low concentrations to 4 % for high concentrations).

Obviously, the narrower linearity range will deliver more accurate results compared with the extended version. However, to “really” clarify which of the regression models suits the concentration range best, a more profound evaluation may be necessary, in order to obtain a better knowledge on the calibration model. In Tab. 3.26 this approach is demonstrated.

## Results and Discussion

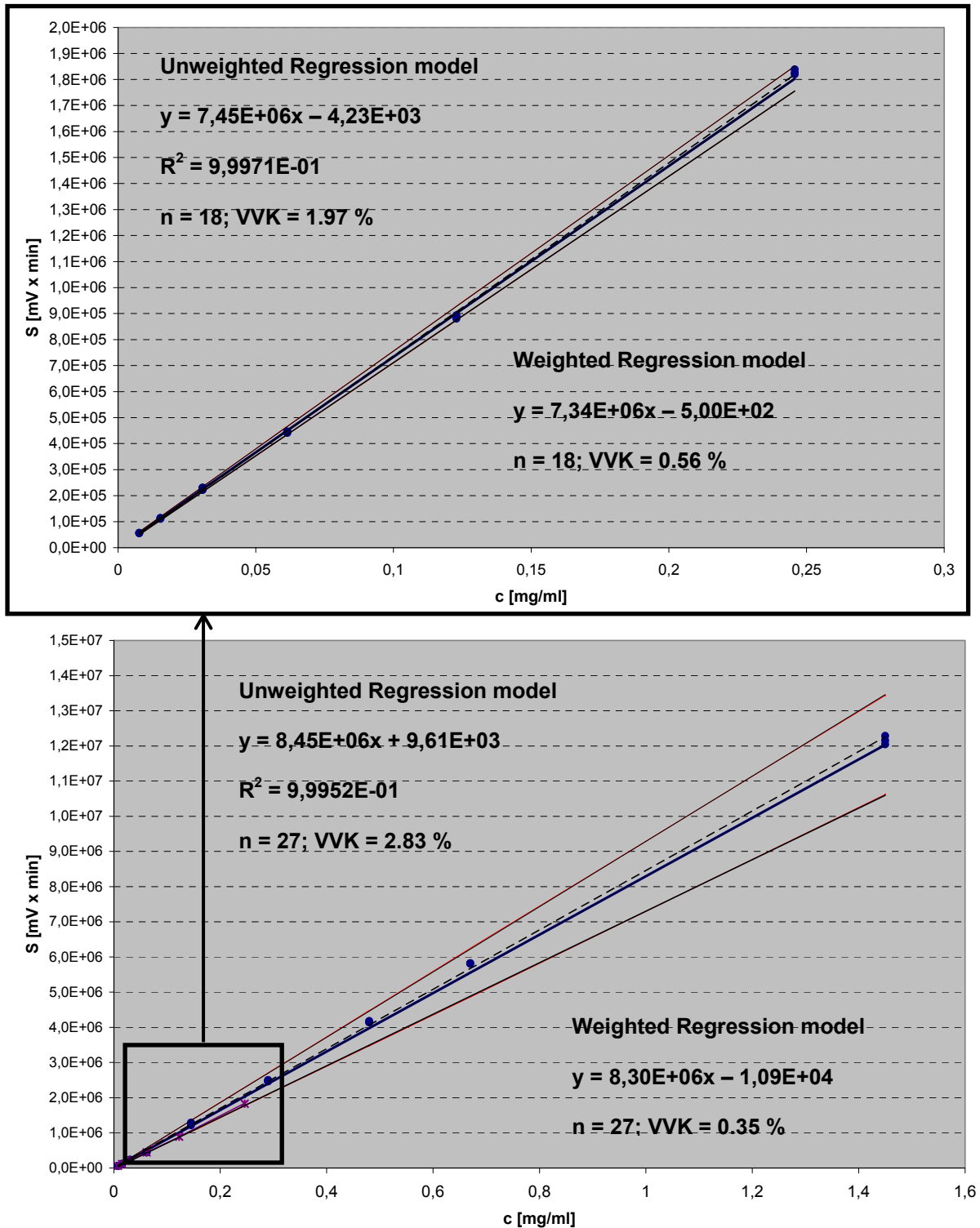


**Fig. 3.90** Comparison of the two different regression ranges for compound **12**. Upper diagram: 8-250  $\mu\text{g/ml}$ . Lower diagram: 8-1450  $\mu\text{g/ml}$ . The weighted regression models were obtained with the excel working sheet reported on in [162]. Both unweighted regression models were proved to be linear ( $R^2 = 0.99971$  and  $0.99952$ ). The VVK (Coefficient of Variation, referred to the mean value of the linearity range) had been for the weighted linear regression model always better. The difference in the slopes is about 10 % between the lower and higher linearity range. The scale differences are clarified by the rectangles and the arrow, which indicate the enlargement of the minor linearity range. The two outer straight lines represent the measurement uncertainty interval (calculated according to [162]). For further details see text.

## Results and Discussion

**Tab. 3.26** Comparison of the two linearity ranges (denoted as A and B) by weighted and unweighted linear regression. Nominal [mg/ml]: The expected analyte concentration of the weighed (balance) and diluted (volume) sample. Calculated [mg/ml]: Calculated value, based on the respective regression model. Bias [+/- %]: Deviation of the calculated from the nominal value in percent (Significant deviations are highlighted by red colours). Sum Bias<sup>2</sup>: The summation of the squared single bias values (The percent value between refers to the percentage of the minor value relative to the major value). The ordinate intercept was not within calculated as the failure is random and negligible (for all models << 0.5 %). For further details see text.

A: Linearity Range (8-250 µg/ml)					B: Linearity Range (8-1450 µg/ml)				
Weighted			Unweighted		Weighted			Unweighted	
Nominal [mg/ml]	Calculated [mg/ml]	Bias [+/- %]	Calculated [mg/ml]	Bias [+/- %]	Nominal [mg/ml]	Calculated [mg/ml]	Bias [+/- %]	Calculated [mg/ml]	Bias [+/- %]
0,0077	0,0075	-1,7	0,0075	-2,9	0,0077	0,0067	-13,1	0,0066	-14,6
0,0077	0,0076	-1,2	0,0075	-2,3	0,0077	0,0067	-12,6	0,0066	-14,1
0,0077	0,0077	0,9	0,0077	-0,3	0,0077	0,0069	-10,8	0,0067	-12,3
0,0154	0,0155	1,1	0,0153	-0,1	0,0154	0,0137	-10,7	0,0135	-12,2
0,0154	0,0153	-0,1	0,0152	-1,3	0,0154	0,0136	-11,7	0,0133	-13,2
0,0154	0,0150	-2,2	0,0148	-3,3	0,0154	0,0133	-13,5	0,0131	-15,0
0,0307	0,0302	-1,8	0,0298	-3,0	0,0307	0,0267	-13,2	0,0262	-14,7
0,0307	0,0313	1,9	0,0310	0,8	0,0307	0,0277	-9,9	0,0272	-11,4
0,0307	0,0314	2,3	0,0311	1,1	0,0307	0,0278	-9,6	0,0273	-11,1
0,0614	0,0607	-1,2	0,0600	-2,4	0,0614	0,0536	-12,7	0,0527	-14,2
0,0614	0,0609	-1,0	0,0601	-2,1	0,0614	0,0538	-12,4	0,0529	-13,9
0,0614	0,0601	-2,2	0,0594	-3,3	0,0614	0,0531	-13,5	0,0522	-15,0
0,1229	0,1200	-2,4	0,1186	-3,5	0,1450	0,1462	0,8	0,1437	-0,9
0,1229	0,1217	-1,0	0,1203	-2,1	0,1450	0,1500	3,4	0,1474	1,7
0,1229	0,1211	-1,4	0,1197	-2,6	0,1450	0,1556	7,3	0,1529	5,4
0,2458	0,2505	1,9	0,2476	0,8	0,2900	0,2979	2,7	0,2928	1,0
0,2458	0,2489	1,3	0,2461	0,1	0,2900	0,3014	3,9	0,2962	2,2
0,2458	0,2479	0,9	0,2451	-0,3	0,2900	0,2960	2,1	0,2909	0,3
<div style="border: 1px solid black; padding: 5px;"> <p><b>A(8-250µg/ml):</b> The weighted model is evaluated to be superior for this linearity range. However, both models fit approximately well.</p> <p><b>B(8-1450µg/ml):</b> Here, also the weighted model is evaluated to be superior. However, for low concentration levels the errors for both are huge, and for higher concentrations the unweighted model is actually better.</p> </div>					0,4800	0,4994	4,0	0,4908	2,3
					0,4800	0,5032	4,8	0,4946	3,0
					0,4800	0,4982	3,8	0,4897	2,0
					0,6700	0,6994	4,4	0,6875	2,6
					0,6700	0,7011	4,6	0,6891	2,9
					0,6700	0,7005	4,5	0,6885	2,8
					1,4500	1,4637	0,9	1,4387	-0,8
					1,4500	1,4504	0,0	1,4256	-1,7
					1,4500	1,4799	2,1	1,4546	0,3
		<b>Sum Bias<sup>2</sup></b>		<b>Sum Bias<sup>2</sup>.</b>			<b>Sum Bias<sup>2</sup></b>		<b>Sum Bias<sup>2</sup>.</b>
		35	(= 4.9 % of)	712			8900	(= 46.2 % of)	19284

The two linearity ranges were split into two columns (A and B) comparing both regression models with the nominal value (value obtained by weighing the reference material on a balance and dilution by a pipette or a volumetric flask). The calculated values are based on the corresponding regression equations. As it is demonstrated, the weighted linear regression model gives for Range A (8-250 µg/ml), as expected, a better fit. The squared summation of the bias leads to only 4.9 % ( $35/712 * 100$  %) deviation compared with the unweighted model. Nevertheless, the unweighted model is still quite precise and not even much more error-prone for some concentrations levels.

By thorough evaluation of both linear regression models for Range B (8-1450 µg/ml), it is quite astonishing that both models deliver for the lower concentration range ( $c = 0.008-0.06$  mg/ml) strong biases from the nominal values (errors of up to 15 % below the nominal value, indicated by the red colours). A probable reason therefore could be a systematic pipette failure leading to constantly lower values. However, since all nine calibration points were proved to be linear ( $> 0.999$ ), the calibration model was accepted. The difference in the sum of squared biases is not as significant as obtained for Range A, only 46.2 % ( $8900/19284 * 100$  %). Hence, again the weighted model is expectably delivering on average a better accuracy. Anyhow, for the concentration range from 0.145-1450 µg/ml the unweighted model delivers more accurate values (compare bias-errors from 0.145-1450 µg/ml, which gives lower deviations for the unweighted model), while at low concentrations both models are quite equally insufficient. The great deviation at lower concentrations should be taken into account, if values within this concentration range are obtained.

In general, the wider working range in this case leads to a quite great uncertainty at low concentration levels for both regressions (0.008-0.061 mg/ml) and becomes more certain at higher concentrations (0.145-1450 µg/ml).

The expectation value for AcLA (**12**) in B<sub>sac</sub>/B<sub>car</sub> RS samples ( $c = 5$  mg/ml) was within 0.18-0.35 mg/ml. Thus, an operating range of up to 0.70 mg/ml would have been sufficient for these samples and would quite likely lead to a better overall fit of the model (theory: the narrower the range, the more precise the results). Nevertheless, the expectation value for B<sub>sac</sub>/B<sub>car</sub> samples had been within the more precise concentration range of the calibration. At least, the most important is to know the measurement uncertainty at each concentration level; and, if it may be insufficient for a certain purpose, to eliminate the cause of failure (in this example, probably a systematic volumetric error). However, as in this work the primary goal was not emphasised on the HPLC method optimisation and as additionally the time therefore was not given, the calibration model was accepted. Furthermore, if the calibration will be carried out several times, the random uncertainties will cancel each other and the regression model will become more precise. If not, then a systematic error can be derived and the reason therefore must be determined; in this case a pipette volume error may be the plausible reason for the strong deviations at low concentrations in Range B.

Basically, this example shall just clarify that a blind trust on criterions such as VVK values or coefficients of correlations fulfilling the requirement for linearity ( $> 0.999$ ) may be encountered with caution. A profound calculation as presented in Tab. 3.26 will serve the analyst a more thorough assurance of his calibration model and may help making decisions easier on which regression model should be preferred. The evaluation of calibration models

for all target analytes quantified in this work (see Tab. 3.23 - 3.25 in chapter 3.6.3.1) was carried out in a similar way as explicitly explained in this chapter for Ac-LA (**12**).

Finally, to obtain precise and accurate results, it is most important to keep the sample expectation value of the target analyte in the centre of the operating range and thus the calibration curve. The model will lead to a greater certainty as shown for Range A. Nonetheless, it is quite difficult for natural products, growing under not controlled conditions, to generally make a correct estimation for an analyte of interest. This fact became clear by the difficulty of estimating the value for  $\beta$ -AKBA (**6**) in B<sub>ac</sub>/B<sub>car</sub> samples (see also chapter 3.8) where quite high deviations from the expectation value had been observable.

### 3.7 HPLC Analysis (Qualitative Consideration)

In the following chapters representative overview chromatograms of the raw extract (RE), the neutral extract (NB) and the acid fraction extract (RS) of the species B<sub>pap</sub>, B<sub>ser</sub> and B<sub>ac</sub>/B<sub>car</sub> are shown. Each chromatogram series (RE, NB, and RS) represents two different sample batches. The chromatograms show typically expected fingerprints of the species being discussed. The standard gradient DAD-HPLC method (two columns in series) described in chapter 2.3.4.2 was used. Note that only significant and structurally ascertained peak signals are discussed. The corresponding quantitative data is reported in chapter 3.8.

#### 3.7.1 *Boswellia papyrifera* (RE, NB, RS)

In Fig. 3.91-3.93 the chromatograms of the RE-, NB- and the RS-extracts are presented (two different extractions samples, discontinuous extraction, Et<sub>2</sub>O, Soxhlet). It is shown that the RE chromatogram still reveals a quite complex elution pattern with co-elution of neutral terpenic compounds with acidic triterpenoids (Fig. 3.91). For example, Inc-Ac (**23**) elutes between compound **1** and **3** and thus co-elutes with compound **19**. Inc (**22**) elutes between  $\beta$ -KBA (**5**) and  $\beta$ -AKBA (**6**). Furthermore, there are several minor peak signals eluting between 20 and 30 min. These belong probably to all sorts of saturated mono-terpenes (e.g. limonene,  $\beta$ -pinene; verified by co-injection of standards; data not shown) and semi-polar diterpenes. Thus, co-elution of them with target analytes (e.g. TAs) within the range of ca. 20-30 min is ascertainable.  $\beta$ -KBA (**5**) and  $\beta$ -AKBA (**6**) can be easily determined, even without separation of NB- and RS-fractions, since they are specifically detectable at 250 nm. By separation of NB- and RS-fractions it is possible to obtain more meaningful fingerprint chromatograms, especially referring to the detection wavelength of 210 nm. In Fig. 3.92 the NB overview chromatograms are shown. There, as most significant peak signals, compound **22**, **23** and **24** (verticillia-4(20),7,11-triene) can be ascertained. Interestingly, compound **24** has been reported by Basar et al. [85] as isolated from the species B<sub>car</sub>. This fact is probably wrong, and the compound is a specific biomarker for the species B<sub>pap</sub> instead. Compound **22** and **23** have been quantified (see chapter 3.6.3.1 and 3.8) and are the main diterpenic molecular entities in the NB fraction of B<sub>pap</sub>. Hence, these three diterpenic compounds seem to be specific biomarkers for this species as already reported on by Hamm et al. [13] and Camarda et al. [74]. In Fig. 3.93 the RS fraction chromatograms are presented.

## Results and Discussion

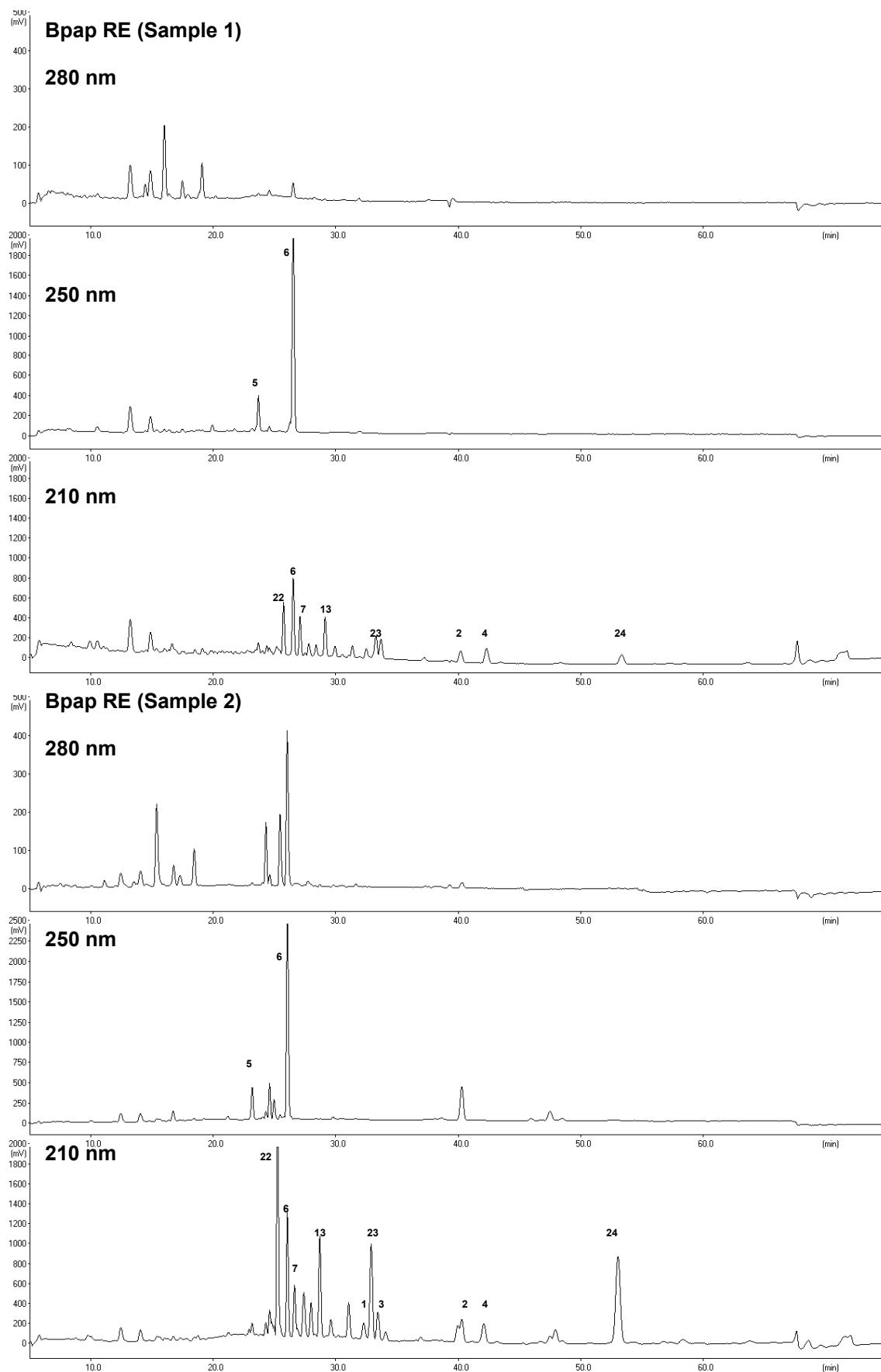


**Fig. 3.91** Two examples of RE chromatograms at three different wavelengths (Extraction: Et<sub>2</sub>O, Soxhlet). Injection concentration: 5 mg/ml. For further discussions see text.

## Results and Discussion

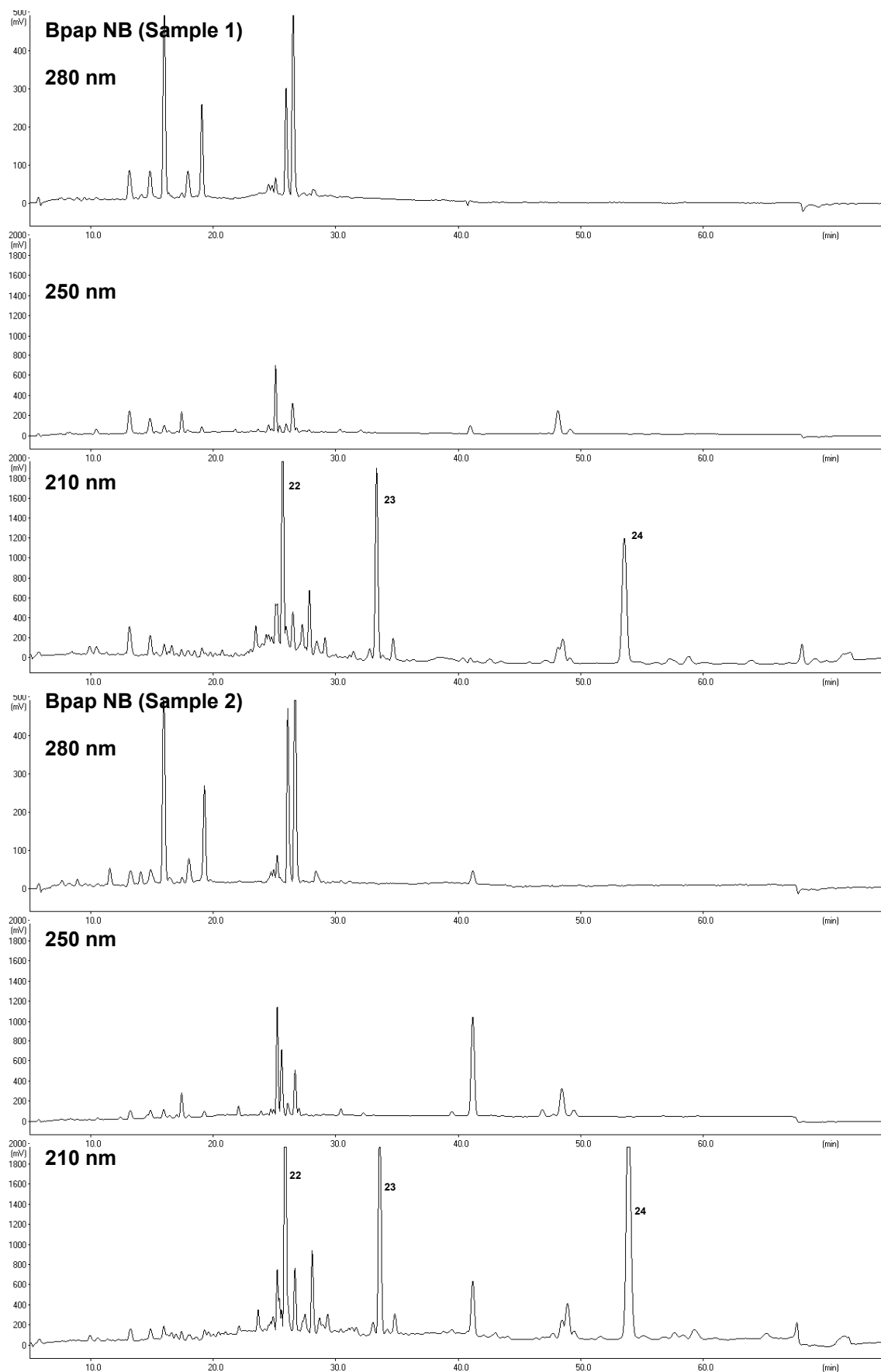


**Fig. 3.92** Two examples of NB chromatograms at three different wavelengths (Extraction: Et<sub>2</sub>O, Soxhlet). Injection concentration: 5 mg/ml. For further discussions see text.

## Results and Discussion

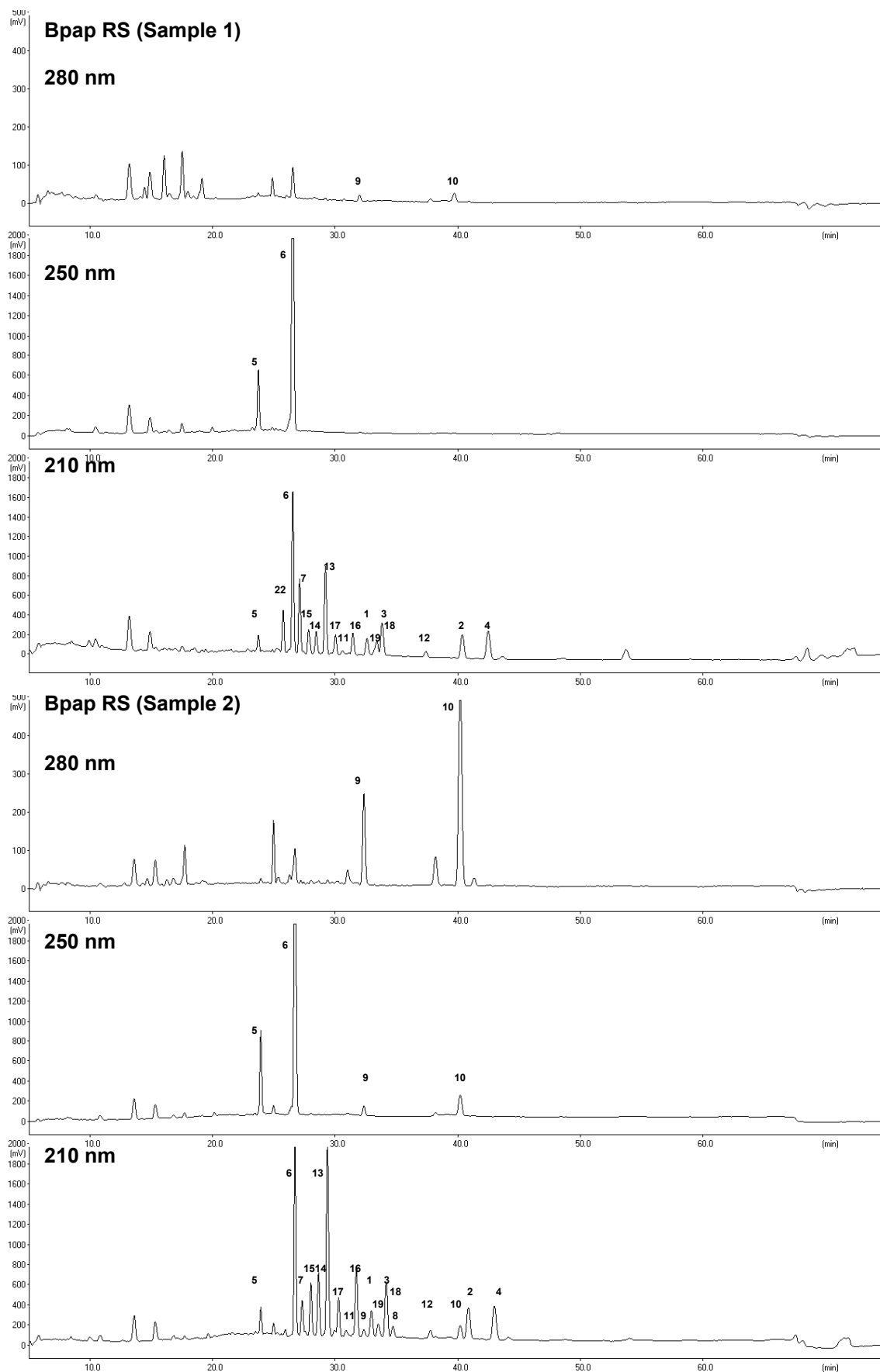


**Fig. 3.93** Two examples of RS chromatograms at three different wavelengths (Extraction: Et<sub>2</sub>O, Soxhlet). Injection concentration: 5 mg/ml. For further discussions see text.

Typically for Bpap RS extracts are normally a high amount of  $\beta$ -AKBA (**6**) and a strong 3-O-TA (**13**) peak. Furthermore, as already reported in [59],  $\beta$ -BA (**3**) co-elutes with compound **18** (see also chapter 3.7.5). Also, the decomposition of 11-OH- $\beta$ -ABA (**7**) into compound **10** can be noticed (Bpap RS, Sample 2) [55,59].

### 3.7.2 *Boswellia serrata* (RE, NB, RS)

In Fig. 3.94-3.96 the chromatograms of the RE-, NB- and the RS-extracts for Bser are presented (two different extractions samples, discontinuous extraction, Et<sub>2</sub>O, Soxhlet). Additionally, as shown for Bpap, the RE chromatograms still reveal a quite complex elution pattern with co-elution of neutral terpenic compounds with acidic triterpenoids (Fig. 3.94). However, a different overview RE-chromatogram compared with Bpap-RE is obtained, which is, as far as experienced in this work, very specific for Bser. At 210 nm detection wavelength, the here called “Triplet-Peak” between 25 and 30 min is highly conspicuous. This is a result of co-elution from  $\beta$ -TA (**15**) with Iso-Ser (**20**; first minor peak), from  $\alpha$ -TA (**14**) with Ser-OH (**21**; second main peak) and from 3-O-TA (**13**; third peak, eluting homogenous). The pattern was always obtained when the RE extract of Bser was analysed and can be hence used for species identification. At 250 nm, the peaks of  $\beta$ -KBA (**5**) and  $\beta$ -AKBA (**6**) are easily detectable, even without further separation of NB and RS fractions, and reveal the approximately typical 1:1 peak height ratio (significant for Bser, compared with Bpap and Bsac/Bcar; see also publication of Büchele et al. [57] which gives the same conclusions).

Separation of the RE fraction into neutral and acid fraction gives more meaningful chromatograms. In Fig. 3.95 the NB overview chromatograms are presented. Specific for Bser is the existence of Iso-Ser (**20**) and Ser-OH (**21**) at 210 nm. Inc (**22**) is also detectable at 210 nm, but to a lesser amount compared with the NB fraction from Bpap. Inc-Ac (**23**) is not significantly detectable (peak heights too low in the appropriate elution area for an unambiguous statement and also never has been visible in the TLC experiments, see also chapter 3.4).

The RS fraction overview chromatograms are shown in Fig. 3.96. As already discussed, the  $\beta$ -KBA (**5**) and  $\beta$ -AKBA (**6**) ratio of about 1:1 is very specific for Bser. Furthermore, Bser contains a relatively huge amount of 3-O-TA (**13**, similar to Bpap) and on average the highest amounts of  $\alpha$ -BA (**1**) and  $\beta$ -BA (**3**), compared with Bpap and Bsac/Bcar. The quantitation of  $\beta$ -TA (**15**) and  $\alpha$ -TA (**14**) delivers, compared with Bpap, greater peak areas for these two compounds. This fact can be explained since the separation of NB and RS fractions is not optimised for the species Bser. Thus, the RS extract still contains the quite semi-polar diterpenes Iso-Ser (**20**) and Ser-OH (**21**), which both co-elute with  $\beta$ -TA (**15**), respectively,  $\alpha$ -TA (**14**). In addition, compound **18** also co-elutes with  $\beta$ -BA (**3**) as yet demonstrated for Bpap samples. However, the amount of compound **18** relative to the normally higher amount of  $\beta$ -BA (**3**) in Bser gives a lower integration error for Bser samples compared with Bpap samples (see also chapter 3.7.5). In Fig. 3.96 the chromatogram of Bser sample 2 also reveals the decomposition of 11-OH- $\beta$ -ABA (**7**) into its dehydro-derivative (**10**) [55,59].

## Results and Discussion

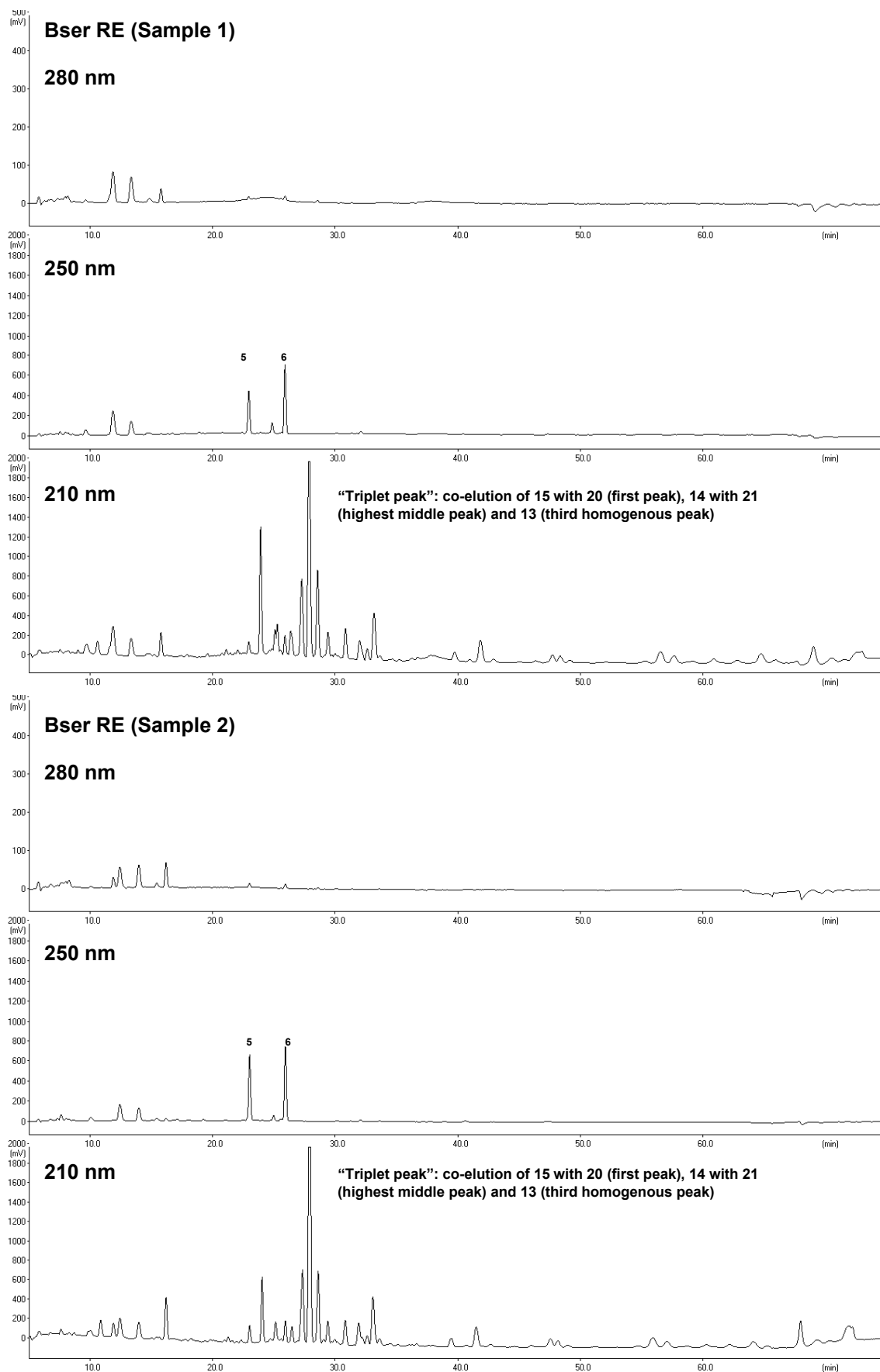


**Fig. 3.94** Two examples of RE chromatograms at three different wavelengths (Extraction: Et<sub>2</sub>O, Soxhlet). Injection concentration: 5 mg/ml. For further discussions see text.

## Results and Discussion

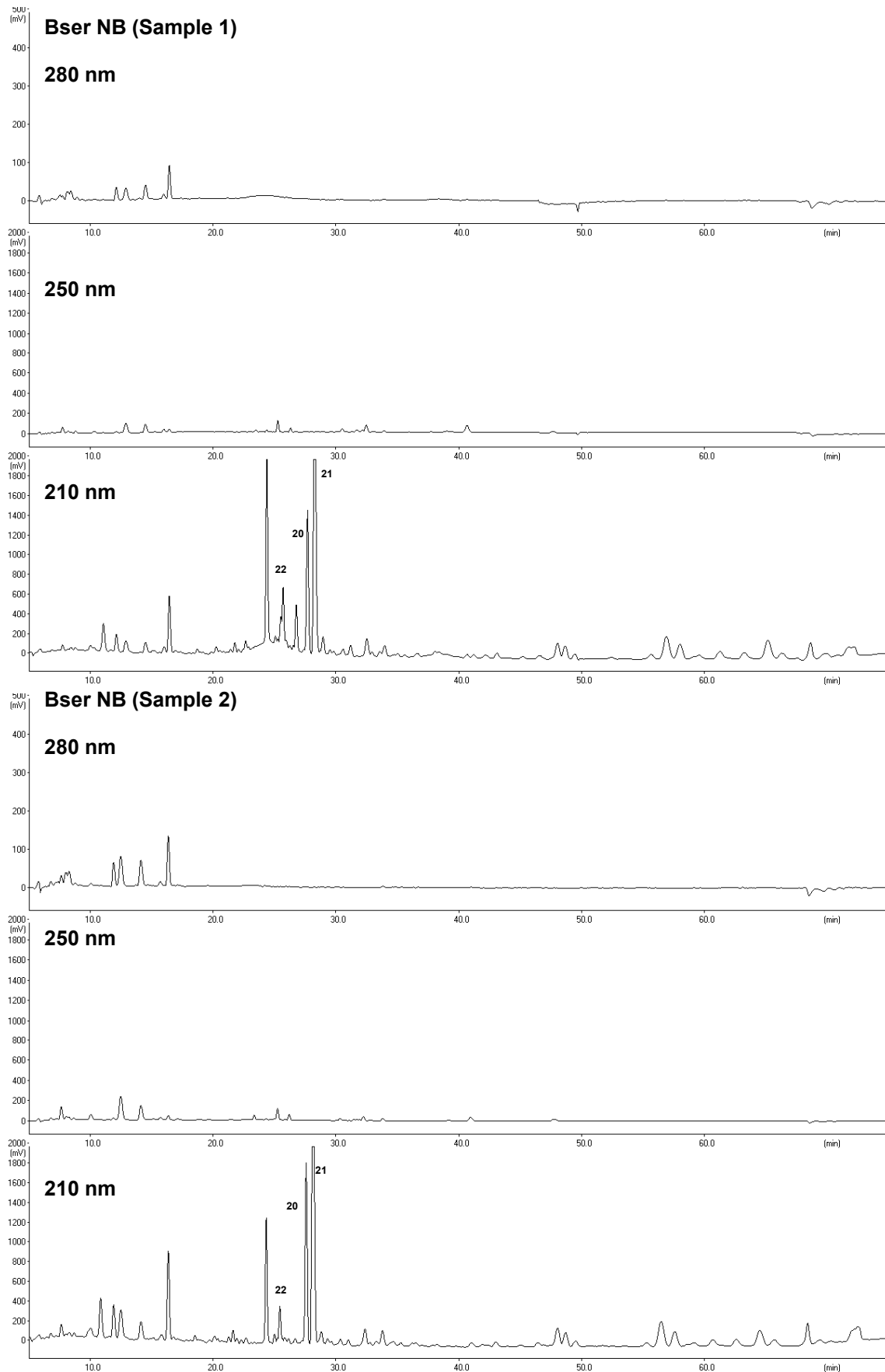


**Fig. 3.95** Two examples of NB chromatograms at three different wavelengths (Extraction: Et<sub>2</sub>O, Soxhlet). Injection concentration: 5 mg/ml. For further discussions see text.

## Results and Discussion

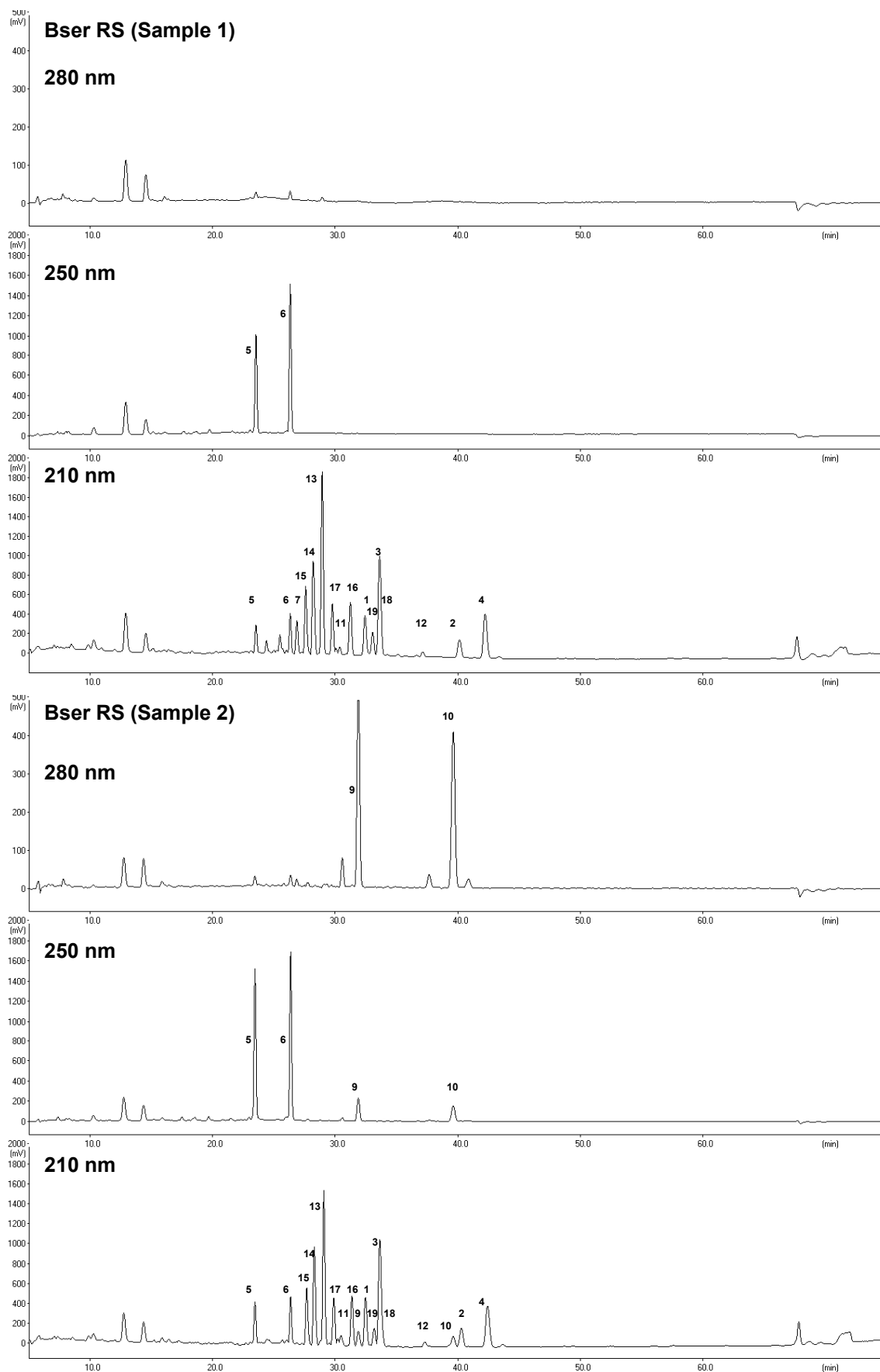


**Fig. 3.96** Two examples of RS chromatograms at three different wavelengths (Extraction: Et<sub>2</sub>O, Soxhlet). Injection concentration: 5 mg/ml. For further discussions see text.

### 3.7.3 *Boswellia sacra* (RE, NB, RS)

In Fig. 3.97-3.99 the chromatograms of the RE-, NB- and the RS-extracts are presented (two different extractions samples, discontinuous extraction, Et<sub>2</sub>O, Soxhlet). Similar to Bpap and Bser, the RE chromatograms still reveal a quite complex elution pattern with co-elution of neutral terpenic compounds with acidic triterpenoids (Fig. 3.97). The overview RE-chromatogram is different from the RE chromatograms of Bpap and Bser, and as far as experienced in this work, very specific for Bsac. It reveals also the existence of Inc (**22**) in minor concentrations (see also chapter 3.4 or [11]), Iso-Ser (**20**) and Ser-OH (**21**). Further on, the  $\beta$ -caryophyllene (**27**) elution peak can be detected (elutes shortly after **3**). The retention area within 55 and 60 min reveals another here called "Triplet-Peak", of which the biggest middle peak refers to 3- $\beta$ -OH-tirucallol (**29**). Normally, the  $\beta$ -AKBA (**6**) signal is always greater than the  $\beta$ -KBA (**5**) signal in Bsac, but compared with Bpap, the amounts of both,  $\beta$ -KBA and  $\beta$ -AKBA, deliver a lower content for this species. However, there are always exceptions from the general expectation, since it was found in another sample of Bsac that the amount of  $\beta$ -AKBA can be tremendously huge or contrary low (the same is valid for  $\beta$ -KBA). This phenomenon seems due to the fact that these resins are not standardised natural products, and the composition of their secondary metabolites may depend on different environmental influences [3]. However, the species can be still identified unambiguously thus far, even for samples with great deviations for certain biomarkers (e.g.  $\beta$ -AKBA and  $\beta$ -KBA), if all important chemotaxonomic parameters are considered (see also chapter 3.8). In Fig. 3.98 the NB overview chromatograms are presented. Bsac delivers a somehow similar NB overview chromatogram as Bser. Differences can be noticed in the elution area of 30 to 35 min, where  $\alpha$ -humulene (**26**) and  $\beta$ -caryophyllene (**27**) are detectable in Bsac (verified by co-injection). Additionally specific for Bsac is the existence of Iso-Ser (**20**) and Ser-OH (**21**) at 210 nm. Inc (**22**) is also detectable at 210 nm, but reveals a lower content compared with the NB of Bpap. Inc-Ac (**23**) is not significantly detectable (same discussion as for Bser and Bcar). In Fig. 3.99 the RS overview chromatograms are presented. Typical is the ratio of  $\beta$ -KBA (**5**) and  $\beta$ -AKBA (**6**) of which **5** usually gives the smallest peak area of all species discussed here. The  $\beta$ -AKBA peak is on average always higher than the  $\beta$ -KBA peak, though great deviations from the expectation value have been observed. Interestingly, the tirucallic acids occur in quite minimal amounts (relative to Bpap and Bser), which is thus far always specific for Bsac. The BA and the ABA peak signals are normally always higher than the tirucallic acid peak signals (compare with the RS chromatograms of Bpap and Bser). The  $\beta$ -BA peak (**3**) elutes as homogenous peak, which is clarified by the 2D chromatography (see chapter 3.7.5). It seems that the tirucallic acids are only minimally genetically expressed in the species of Bsac (compounds **18** and **19** are merely in traces detectable). On the contrary, Bsac reveals quite huge amounts of BAs and ABAs compared with Bser and Bpap; but also the largest deviations for some biomarker contents (see also chapter 3.8). Another interesting point is that Bsac contains the greatest amounts of LA (**11**) and Ac-LA (**12**) compared with Bpap and Bser. Conclusively, Bsac seems to have a biogenetically stronger pathway directed to boswellic acids, as lupeolic acids are reported to be probably the biogenetic precursors of boswellic acids (see also chapter 3.13 and [31]).

## Results and Discussion

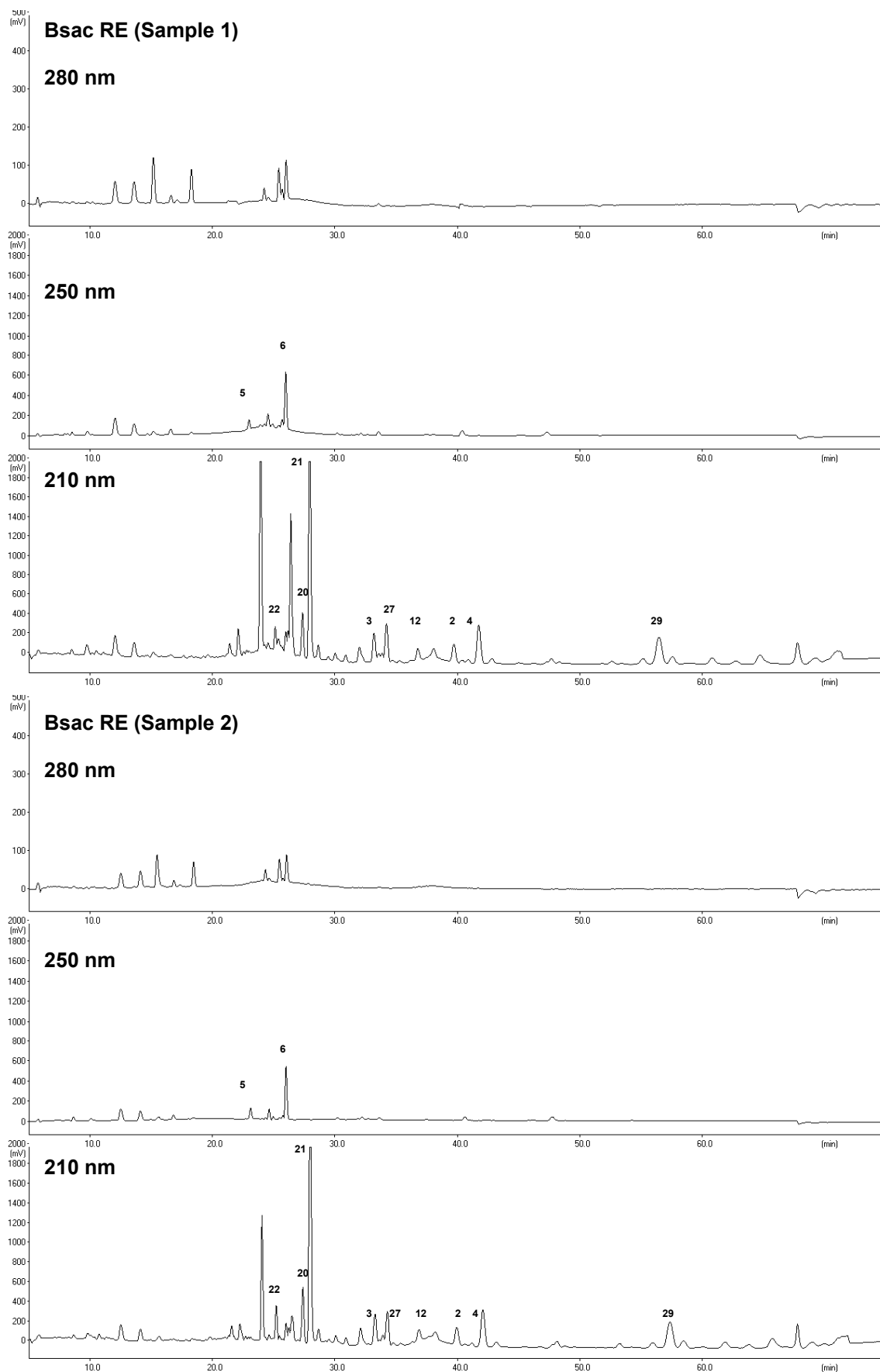


**Fig. 3.97** Two examples of RE chromatograms at three different wavelengths (Extraction: Et<sub>2</sub>O, Soxhlet). Injection concentration: 5 mg/ml. For further discussions see text.

## Results and Discussion

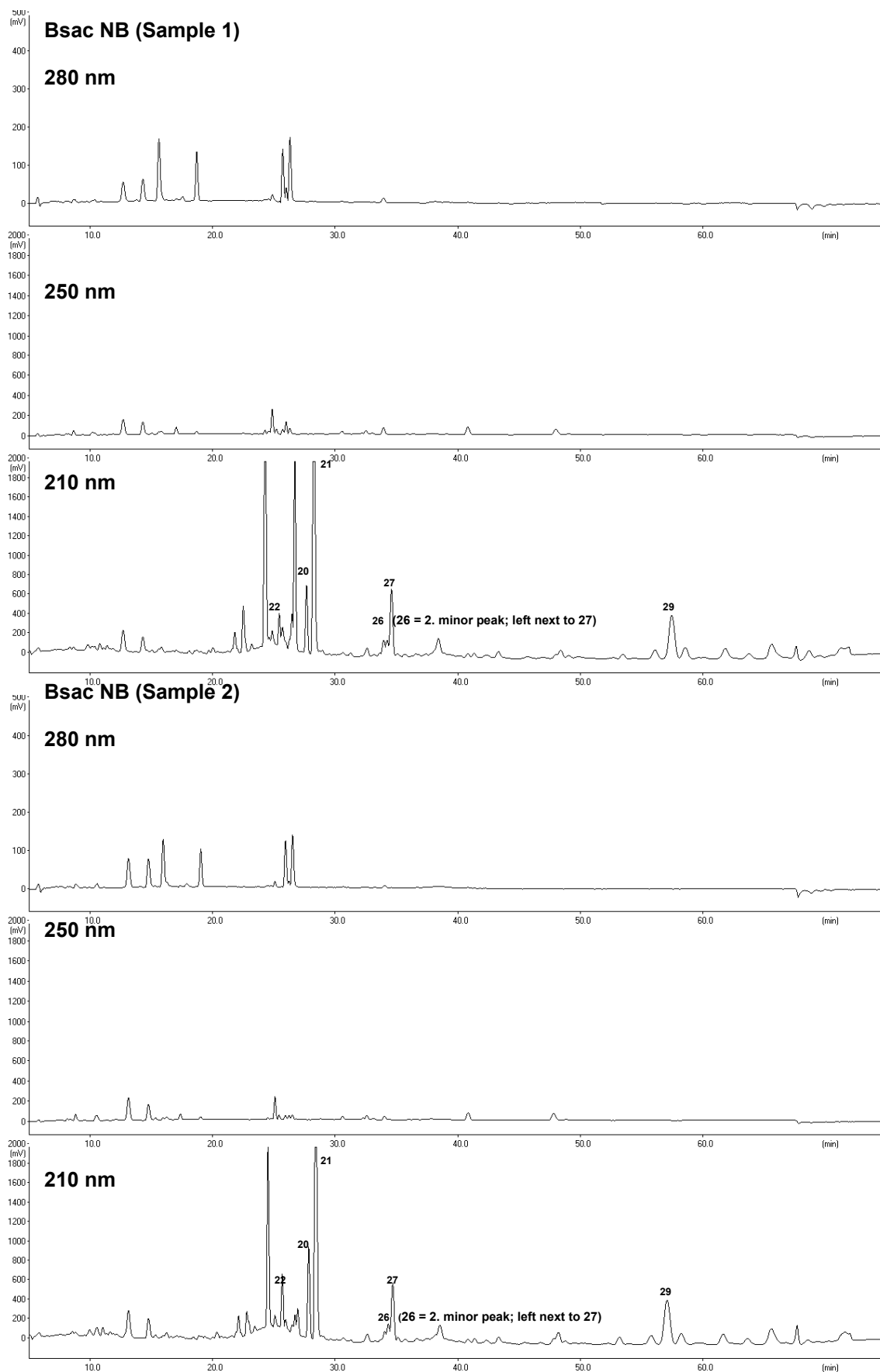


**Fig. 3.98** Two examples of NB chromatograms at three different wavelengths (Extraction: Et<sub>2</sub>O, Soxhlet). Injection concentration: 5 mg/ml. For further discussions see text.

## Results and Discussion

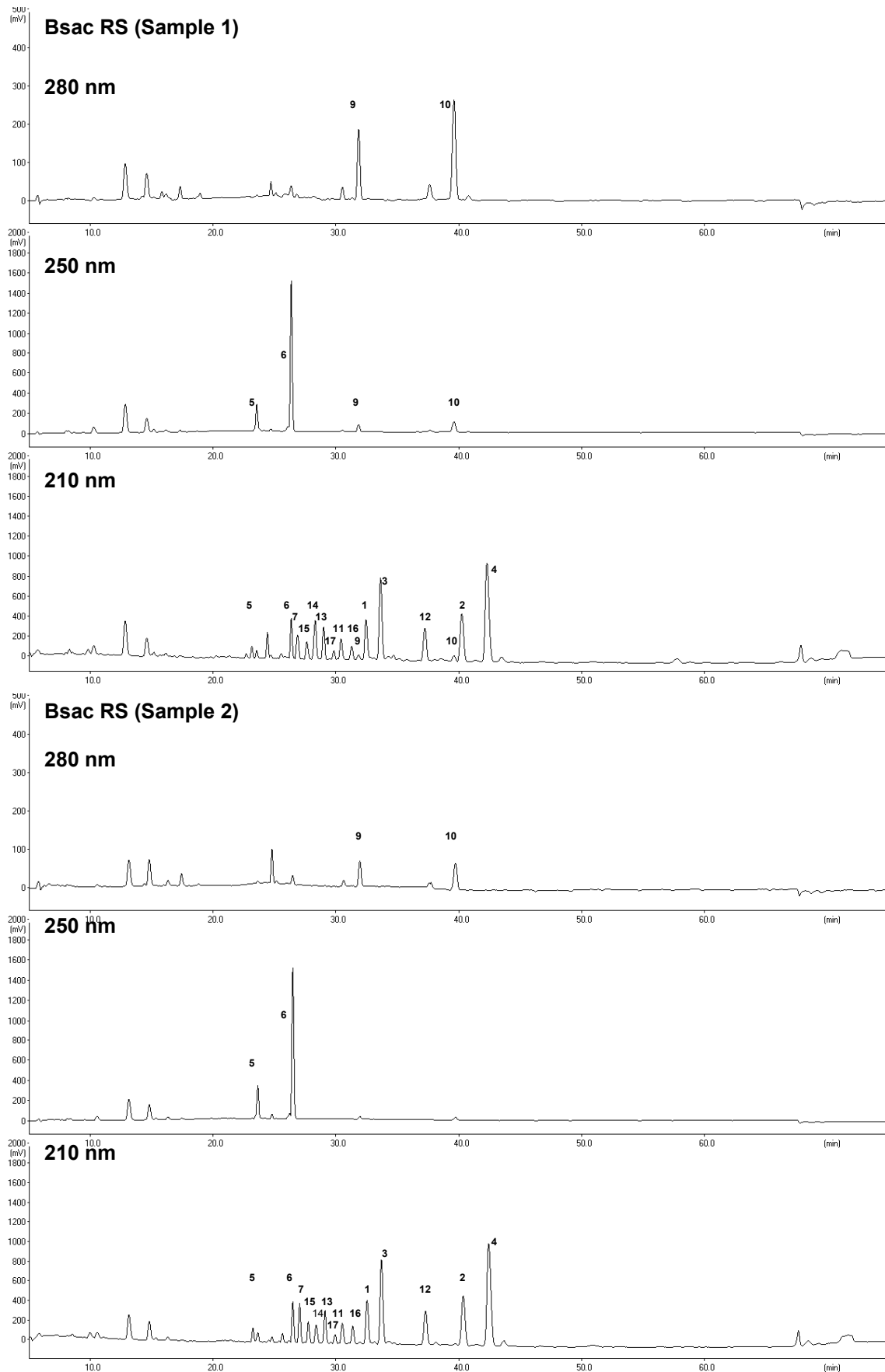


**Fig. 3.99** Two examples of RS chromatograms at three different wavelengths (Extraction: Et<sub>2</sub>O, Soxhlet). Injection concentration: 5 mg/ml. For further discussions see text.

### 3.7.4 *Boswellia carterii* (RE, NB, RS)

In Fig. 3.100-3.102 the chromatograms of the RE-, NB- and the RS-extracts are presented (two different extractions samples, discontinuous extraction, Et<sub>2</sub>O, Soxhlet). Basically, the Bcar chromatograms reveal the same information as already given in chapter 3.7.3 for Bsac. Thus, the species must be regarded as identical, at least on a biological and chemotaxonomic point of view (Thulin & Warfa [12], Mathe et al. [73], Hamm et al. [13] and Paul et al. [11]).

The RE overview chromatogram in Fig. 3.100 also reveals Inc (**22**), Iso-Ser (**20**), Ser-OH (**21**) and the here called "Triplet-peak" eluting within 55 and 60 min of which the biggest middle peak refers to 3- $\beta$ -OH-tirucallol (**29**). The NB overview chromatograms in Fig. 3.101 show the growing peak signals of Inc (**22**), Iso-Ser (**20**), Ser-OH (**21**), 3- $\beta$ -OH-tirucallol (**29**) and the  $\alpha$ -Hum (**26**) and  $\beta$ -Car (**27**) peaks. Thus, a similar elution pattern as already presented for Bsac is obtained. In Fig. 3.102 the RS overview chromatograms of Bcar are demonstrated. Again, these chromatograms lead to the same conclusions as made for Bsac. The smallest amount for  $\beta$ -KBA (**5**, compared with Bpap and Bser), which, compared to  $\beta$ -AKBA (**6**), mostly has been the minor peak in Bcar/Bsac. However, especially for the  $\beta$ -AKBA and  $\beta$ -KBA contents in the species Bsac/Bcar differing compositions have been detected. This is explicitly shown in Fig. 3.103 for a sample from Bsac (Bergmann [17], JB03 Probe 55) where a differing quantitative pattern is presented. There, the  $\beta$ -AKBA (**6**) and 11-OH- $\beta$ -ABA (**7**) peak signals are quite strong and corresponding to this matter of fact the BA (**1**, **3**) and ABA (**2**, **4**) peak signals are rather low. Thus, they seem to be biosynthetically correlated (higher expression of  $\beta$ -KBA and  $\beta$ -AKBA may lead to a weaker expression of BAs and ABAs; see also chapter 3.13 and 3.14). In addition, the tirucallic acids are present in significantly less contents (compared with Bpap and Bser), and the 2D chromatography (see chapter 3.7.5) again verifies the elution of  $\beta$ -BA (**3**) in the first dimension as homogenous peak signal. For Bsac the same deductions have been made (compounds **18** and **19** are only in traces detectable). Thus, if peak **19** (eluting between **1** and **3**) is not detectable in the first chromatography dimension, the second chromatography dimension may be redundant; as in all samples analysed so far compounds **18** and **19** seem to be directly correlated (low amount of **19** = low amount of **18** and vice versa). This fact may have a biogenetic reason. The BA (**1** and **3**) and ABA (**2** and **4**) peak signals are always bigger than the tirucallic acid signals and are present in great quantities in Bcar, respectively, Bsac. Additionally, Bcar samples show the same high deviation within its biomarker composition as it is discussed for Bsac, especially concerning the BAs, ABAs and keto-boswellic acids (**5** and **6**). The greater peak heights of LA (**11**) and Ac-LA (**12**), compared with Bpap and Bser, are similar to the results obtained for Bsac, and again give evidence that for the species Bcar (*Olibanum Somalia*) and Bsac (*Olibanum Yemen, Oman*) the biological pathway for the production of boswellic acids may be stronger expressed (relative to Bpap and Bser). For further discussions clarifying these contents see chapter 3.13, 3.14 and [31]. Perceivably, the quite high signal for compound **29** and, on the contrary, the rather low content levels of the TAs (**13-19**) in Bcar and Bsac samples, strongly indicate that they are biosynthetically correlated (see also chapters 3.13 and 3.14).

## Results and Discussion

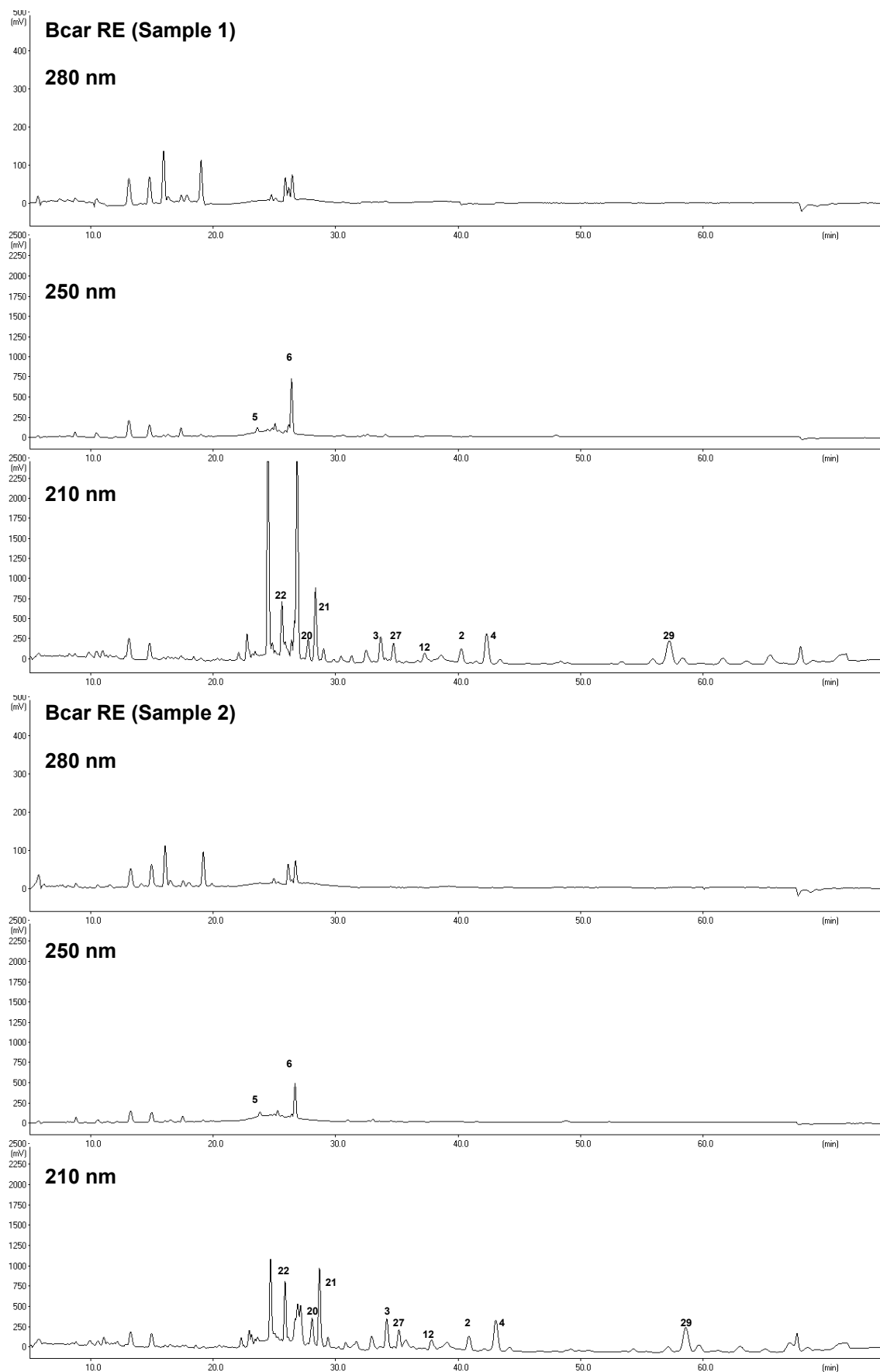


**Fig. 3.100** Two examples of RE chromatograms at three different wavelengths (Extraction: Et<sub>2</sub>O, Soxhlet). Injection concentration: 5 mg/ml. For further discussions see text.

## Results and Discussion

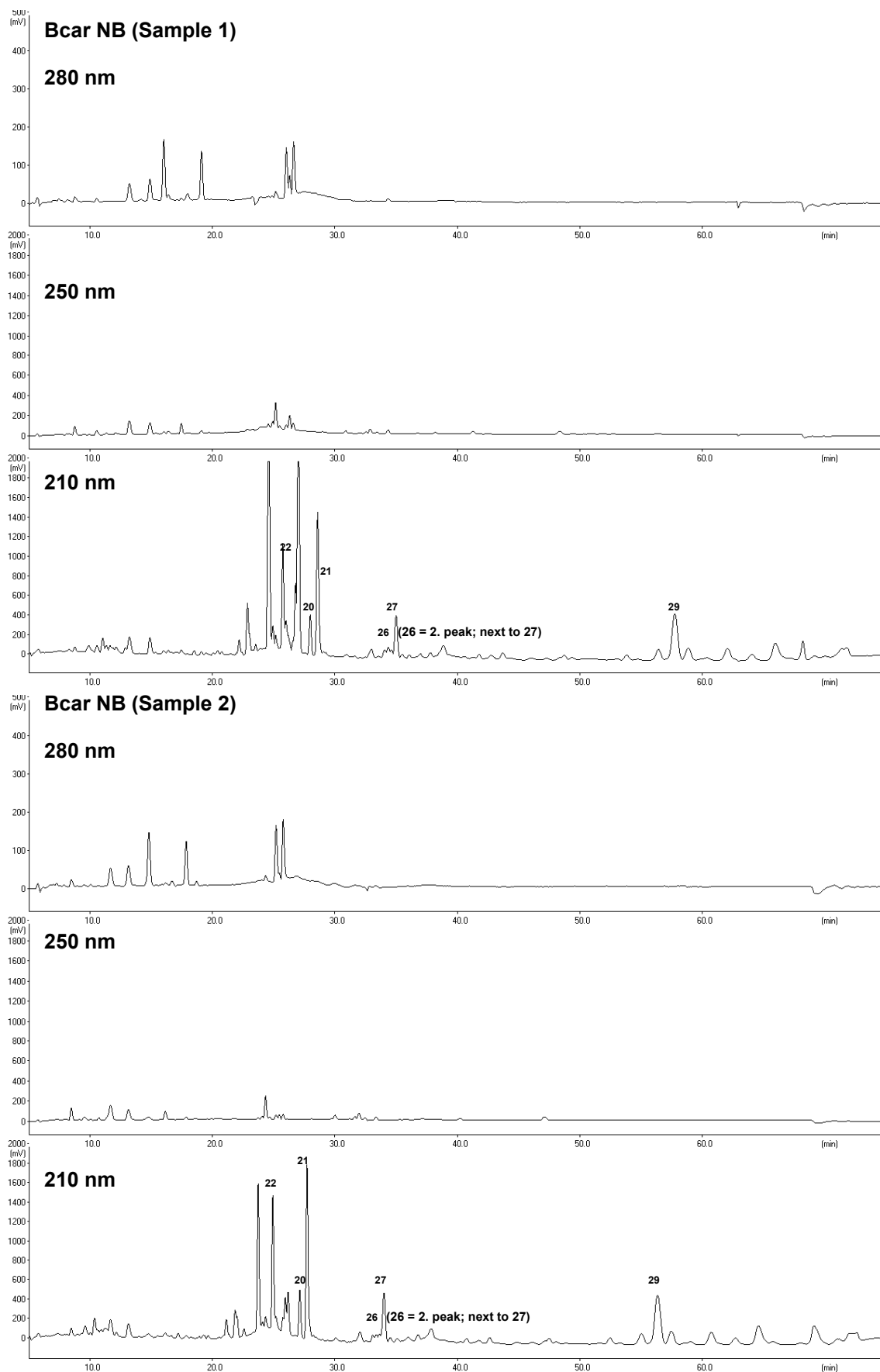


**Fig. 3.101** Two examples of NB chromatograms at three different wavelengths (Extraction: Et<sub>2</sub>O, Soxhlet). Injection concentration: 5 mg/ml. For further discussions see text.

## Results and Discussion

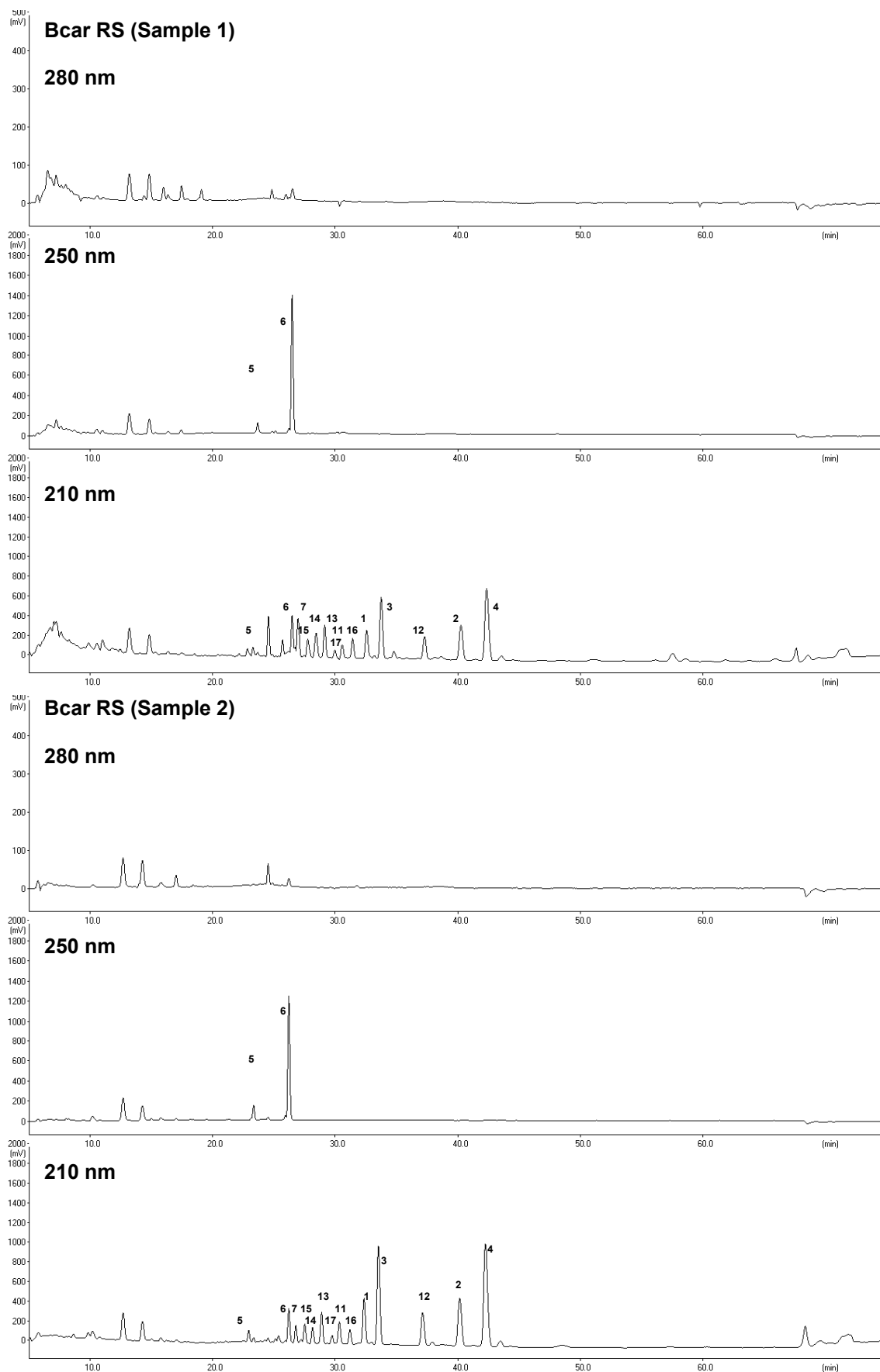


**Fig. 3.102** Two examples of RS chromatograms at three different wavelengths (Extraction: Et<sub>2</sub>O, Soxhlet). Injection concentration: 5 mg/ml. For further discussions see text.

It seems that the secondary metabolite synthesis of TAs (in B<sub>sa</sub>c and B<sub>ca</sub>r) is restricted and leads to an enrichment of compound **29**. For the species B<sub>pa</sub>p and B<sub>se</sub>r, which both reveal quite high TA levels, compound **29** is depleted and thus not significantly detectable.

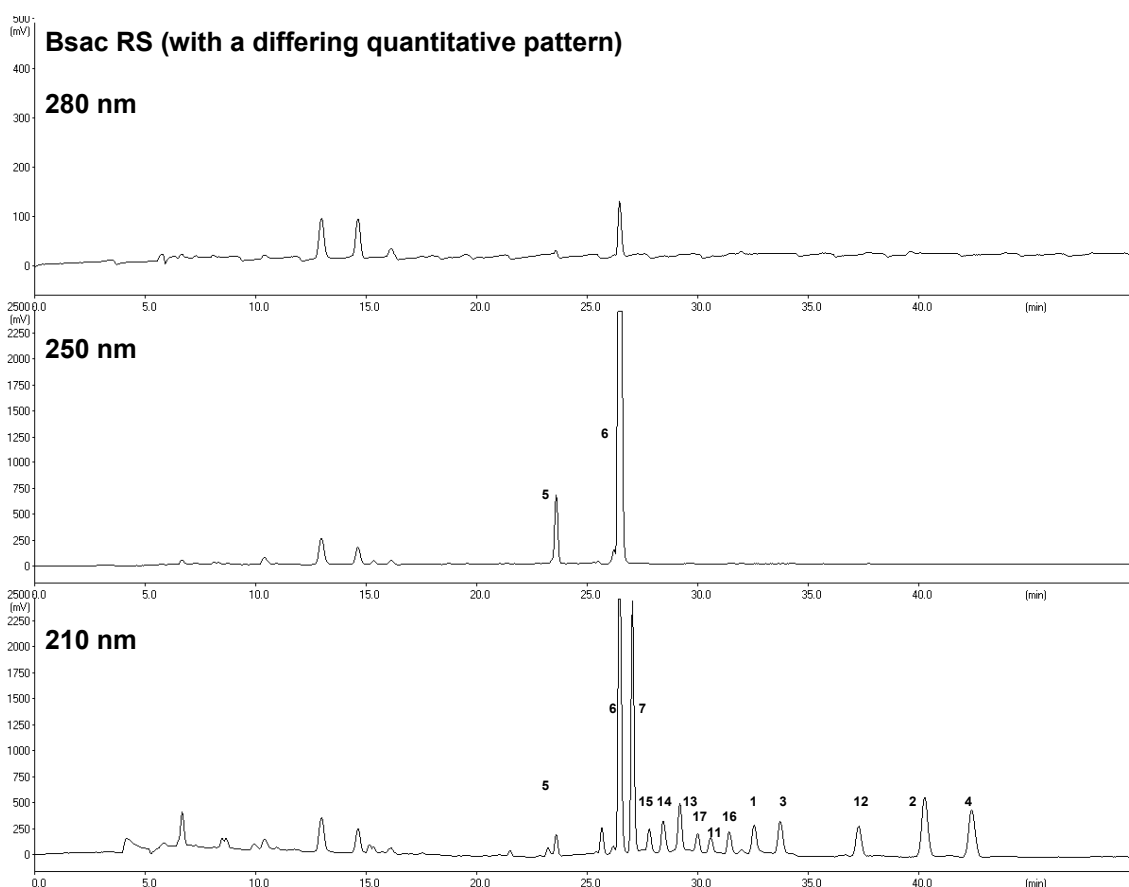


**Fig. 3.103** RS chromatogram of a B<sub>sa</sub>c sample from J. Bergmann [17] (JB 03, Probe 55) with differing expectation values concerning the  $\beta$ -KBA (**5**),  $\beta$ -AKBA (**6**), BA (**1** and **3**) and ABA (**2** and **4**) contents. As noticeable, if the  $\beta$ -AKBA (**6**) and 11-OH- $\beta$ -ABA (**7**) contents are high, the BA and ABA levels are rather low. According to the chromatogram, the sample could be mistaken as the species B<sub>pa</sub>p, especially if merely the  $\beta$ -KBA and  $\beta$ -AKBA levels are considered. However, the comparably great LA/Ac-LA (**11** and **12**) contents and even the other data (e.g. 2D chromatography with a lack of compounds **18** and **19**, and NB-fraction with a lack of Inc-Ac, **23**; see also TLC analysis in chapter 3.4) declare this sample as the species B<sub>sa</sub>c, respectively, B<sub>ca</sub>r (see also chapter 3.14). For further discussions see text.

### 3.7.5 Qualitative Comparison 2D HPLC Data

In this chapter representative 2D chromatograms are shown. The technical discussion is given in chapter 2.3.4.4. Every chromatogram presented here had been obtained from the corresponding collected fractions of the RS samples ( $c = 5$  mg/ml).

The 2D chromatograms for B<sub>pa</sub>p and B<sub>se</sub>r are given in Fig. 3.104. As can be seen there, the application of the second chromatography dimension delivers more correct integration results for compound **3** ( $\beta$ -BA) for these two species as they are finally resolved. Compound **19** (3 $\beta$ -OAc-8,24-dien-TA) eluted between compound **1** ( $\alpha$ -BA) and **3** ( $\beta$ -BA), and compound **18** (3 $\alpha$ -

OAc-7,24-dien-TA) co-eluted with compound **3** in the first dimension. Thus, the co-elution of **18** with **3** led to wrong peak areas for compound **3**.

However, the integration error in the first dimension has been more significant for Bpap, since it revealed on average the least amount of  $\beta$ -BA compared with Bser and Bsac/Bcar. Bser had approximately the highest amount of  $\beta$ -BA (especially compared with Bpap). Thus, the co-elution of compound **18** in the first chromatographic dimension has been giving a lower integration error. Hitherto, these results are specific for Bpap and Bser, as for these two species an expectably higher expression of tirucallic acids has been observed, relatively compared with Bsac/Bcar (see also chapter 3.8).

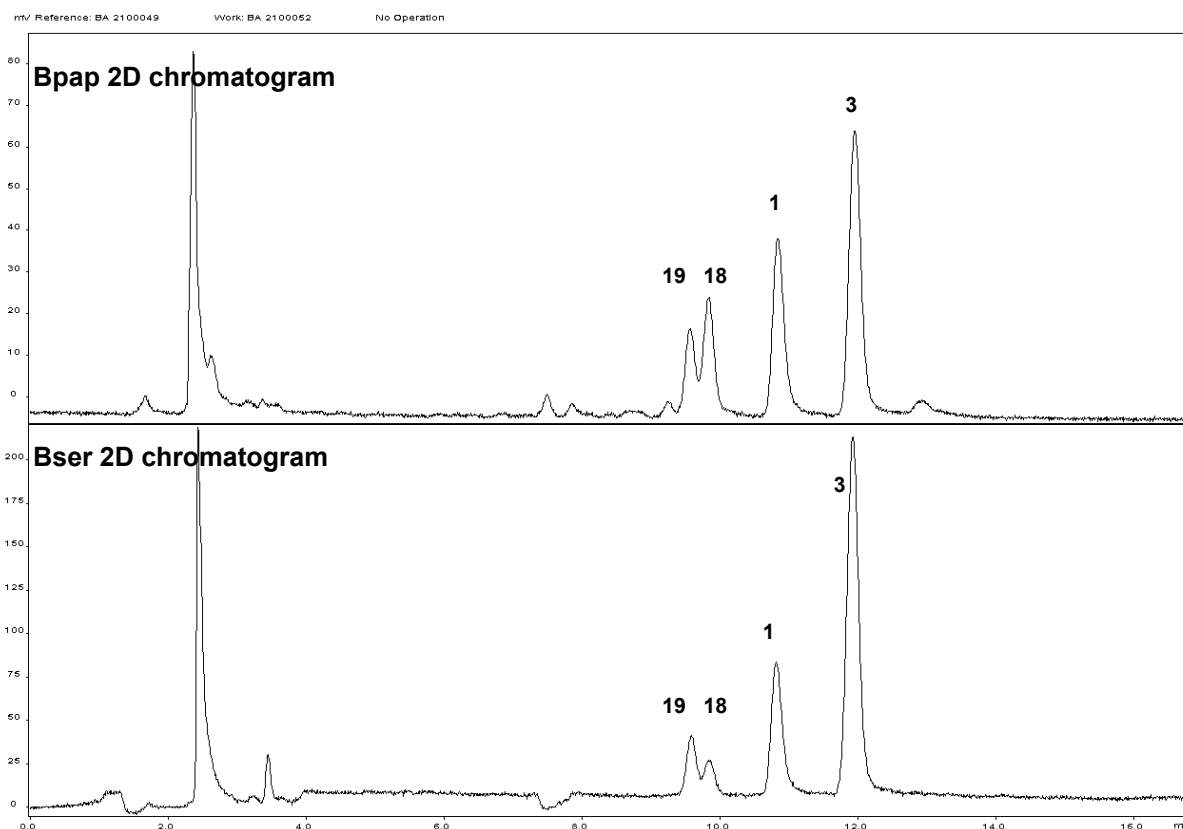


**Fig. 3.104** 2D chromatograms of prepared Bpap and Bser samples at 210 nm detection ( $c = 5$  mg/ml).

In Fig. 3.105 the comparison of 2D chromatograms from Bsac and Bcar is shown. The two chromatograms do not reveal significant impurity signals. The peak signals of  $3\beta$ -OAc-8,24-dien-TA (**19**) and  $3\alpha$ -OAc-7,24-dien-TA (**18**) are only in traces detectable. This result is due to the minor expression of tirucallic acids in these two olibanum species (see chapter 3.8 and chromatograms of Bsac and Bcar in chapters 3.7.3, respectively, 3.7.4). Furthermore, the comparison of 1D and 2D integration results delivered similar results (integration errors lay within the defined  $\pm 5\%$  limits and even better), which expectably makes the application of the second chromatography dimension for Bsac and Bcar samples unnecessary, at least among the sample population analysed in this work (see also 3.8).

Generally, a low occurrence of chromatographically well resolved TAs (e.g. compound **13**, **14**, **15**, **16** and **17**) and, vice versa, relatively greater peak heights for the LAs (**11** and **12**) may already indicate that the RS sample in question is almost free from compounds **18** and

**19**, and thus may strongly indicate that the questionable resin refers to the species Bsac, respectively, Bcar.

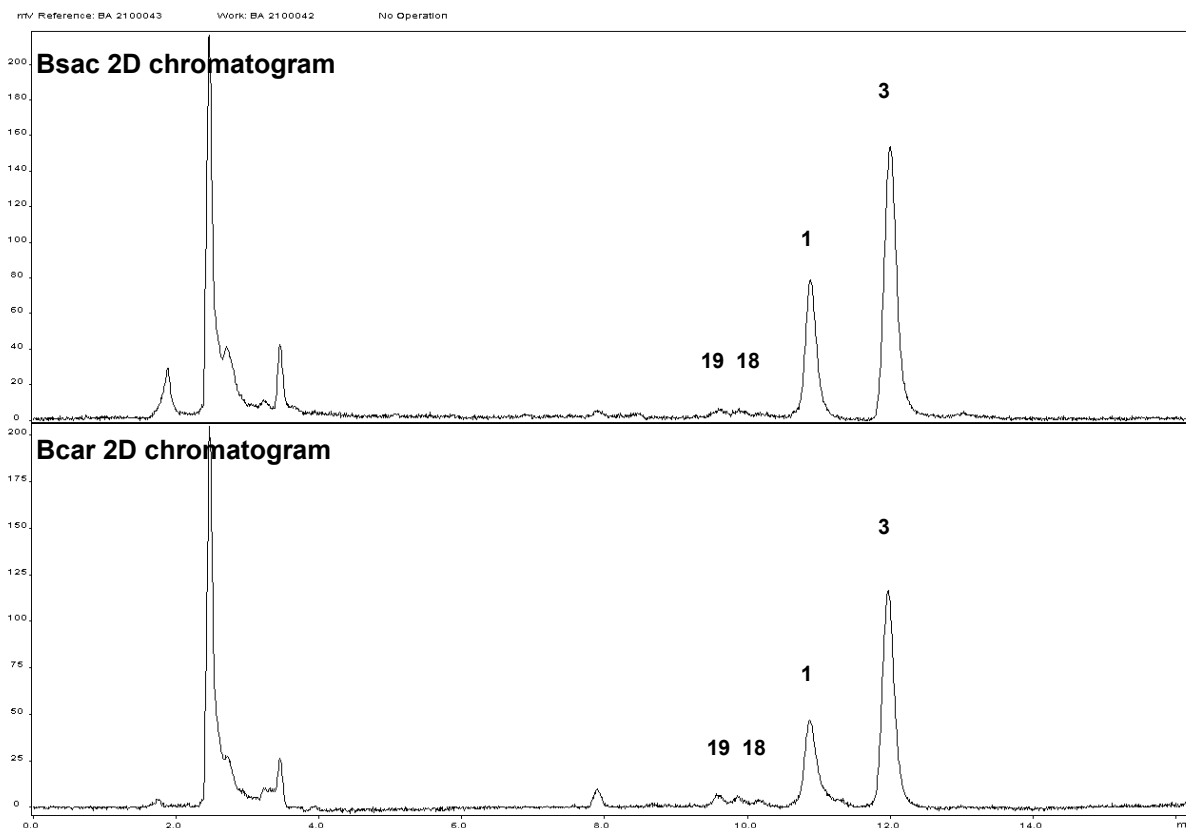


**Fig. 3.105** 2D chromatograms of prepared Bsac and Bcar samples at 210 nm ( $c = 5$  mg/ml).

The quantitative data is explicitly discussed in chapter 3.6.2 and additionally in chapter 3.8. The depictions here shall just clarify the discussions already given. Interestingly, if the method was firstly developed for the species Bsac, respectively, Bcar, instead, there would not have been any need for the second chromatography dimension. Furthermore, in samples of Bser, where the  $\alpha/\beta$ -BA (**1** and **3**) contents are rather high, the peaks would have been perhaps additionally regarded as homogeneous signals, not giving any clue about any potentially co-eluting compound (Note that the integration error would have been only up to 10 % in Bser; compared with Bpap, where it had been up to 25-30 %). Thus, merely the choice of Bpap for the HPLC method development revealed this fairly interesting matter of fact (Note that this species was firstly chosen since it had been in the focus of the research interests of the *AureliaSan GmbH*, Bisingen, and the pharmacologists at the University of Tübingen; working group, Prof. Dr. Oliver Werz, now Professor at the University of Jena, Germany).

### 3.7.6 Comparison of Specific Wavelengths for Bpap, Bser and Bsac/Bcar

In this chapter, chromatograms of the first dimension of all three species (Bpap, Bser and Bsac/Bcar) are directly compared to give a better qualitative view and understanding on the differences and commonalities of these frankincense samples.

In Fig. 3.106 the comparison of all species chromatograms at 250 nm detection wavelength is shown (standard HPLC method, see chapter 2.3.4.2). As already discussed, for Bpap a high  $\beta$ -AKBA (**6**) signal is significant and usually always greater than the  $\beta$ -KBA (**5**) signal. Bser exhibits a similar peak height, respectively, area ratio for  $\beta$ -KBA and  $\beta$ -AKBA (approximately 1:1). Bsac, respectively, Bcar, reveal a similar ratio as reported for Bpap, but expectably a much lower content for the  $\beta$ -AKBA peak signal. Additionally, the  $\beta$ -KBA signal shows for these species the lowest peak signal (compared with the  $\beta$ -KBA signals from Bpap and Bser). However, especially for Bsac/Bcar samples, greater content intervals had been already reported in the dissertation of Bergmann [17] and have been also found in this work. Thus, the  $\beta$ -KBA and  $\beta$ -AKBA ratio should be carefully used for species differentiation (see also chapter 3.7.4, Fig. 3.103).

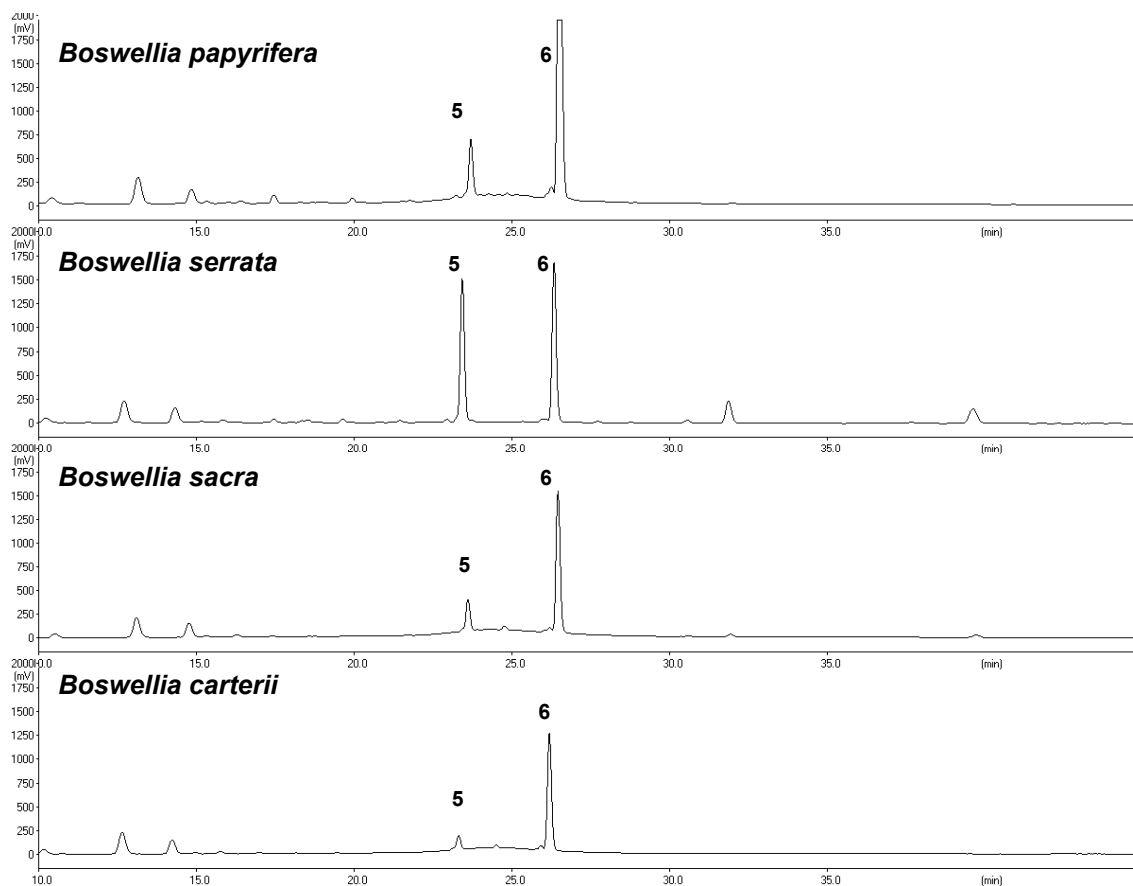


**Fig. 3.106** Comparison of the RS-extract chromatograms from Bpap, Bser and Bsac/Bcar at 250 nm ( $c = 5$  mg/ml).

In Fig. 3.107 the three species are compared at 210 nm detection wavelength. There it can be noticed that Bpap and Bser contain higher tirucallic acid contents (TAs, **13-19**) than Bsac/Bcar. Especially striking is the high 3-O-TA (**13**) peak signal for Bpap and Bser (marked

by the black arrows for a better overview), which is comparable with the TLC results obtained (see chapter 3.4).

For Bsac/Bcar the overall tirucallic acid (**13-19**) amount is rather low, when compared with Bpap and Bser. Furthermore, the amount of LA (**11**) and Ac-LA (**12**) has been throughout greater in samples of Bsac/Bcar (marked by the grey arrows for a better overview).

This phenomenon has been significant for all thus far analysed samples: Higher amounts of LA and Ac-LA (**11** and **12**) for Bsac/Bcar compared with Bpap and Bser; and higher amounts of 3-O-TA (and tirucallic acids in general, **13-19**) for Bpap and Bser compared with Bsac/Bcar. Also, on average, Bsac/Bcar reveals the greatest amounts of ABAs (**2** and **4**). The BA (**1** and **3**) contents are quite high for Bser and Bsac/Bcar, whereas Bpap reveals the lowest amounts of BAs on average (see also Tab. 3.27 in chapter 3.8 for a quantitative discussion).

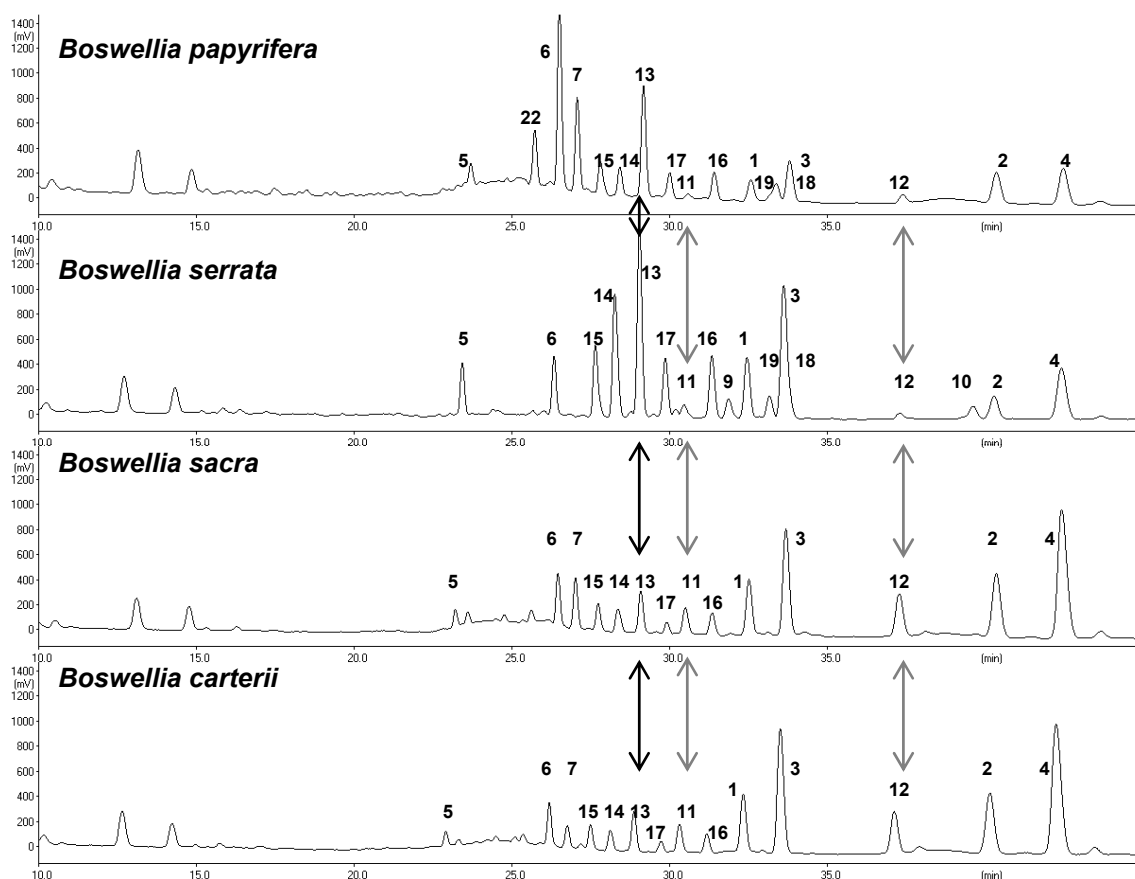


**Fig. 3.107** Comparison of the RS-extract chromatograms from Bpap, Bser and Bsac/Bcar at 210 nm ( $c = 5$  mg/ml).

The comparison of NB chromatograms from all three species at 210 nm is presented in Fig. 3.108. The significant differences are easily perceivable. Bpap shows three major peaks, referring to Inc (**22**) and its acetate (**23**) and to verticillia-4(20),7,11-triene (**24**). Bser reveals significant Iso-Ser (**20**) and Ser-OH (**21**) signals (Inc, **22**, is just a minor compound in the Bser NB extract). For Bsac/Bcar the Iso-Ser (**20**) and Ser-OH (**21**) signals are also significantly present. Additionally interesting is the existence of the  $\alpha$ -humulene (**26**) and  $\beta$ -caryophyllene (**27**) peak and the triplet combination with  $3\beta$ -OH-tirucallosol (**29**) as middle main

peak (B<sub>ser</sub>/B<sub>car</sub>) in the elution range from 55 to 60 min. Note that for B<sub>ser</sub> occur similar peak signals in that elution range. Compound **29** was isolated from B<sub>car</sub> and thus it is actually not verified for B<sub>ser</sub>. However, the existence of compound **29** in B<sub>ser</sub> can not be excluded. On the contrary and according to the general commonalities of *Boswellia* species it may also occur in all species producing tirucallic compounds (See also chapter 3.13 on biosynthesis hypothesis). The signals from  $\beta$ -caryophyllene oxide (**28**) and  $\tau$ -cadinol (**25**) are minimally detectable at 210 nm for the species B<sub>ser</sub>/B<sub>car</sub> (verified by co-injection). These are more conveniently detected by GC (chapter 3.5) or TLC methods (chapter 3.4).

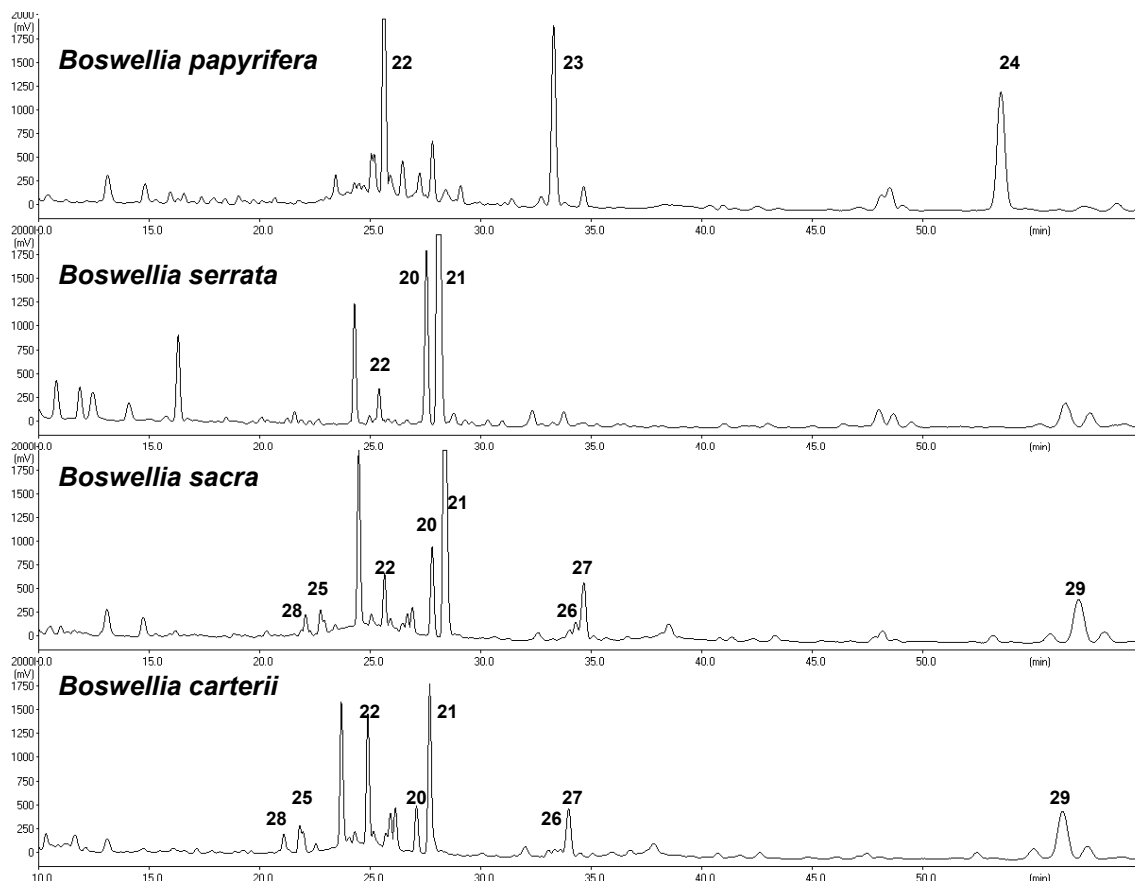


**Fig. 3.108** Comparison of the NB-extract chromatograms from B<sub>pap</sub>, B<sub>ser</sub> and B<sub>ser</sub>/B<sub>car</sub> at 210 nm ( $c = 5 \text{ mg/ml}$ ).

In Fig. 3.109 the RE extract overview chromatograms for all three species are shown. The differentiation among the RE chromatograms is also possible. For B<sub>ser</sub> the here called “Triplet peak”, eluting between 25 and 30 min, is specific (co-elution of  $\beta$ -TA and Iso-Ser,  $\alpha$ -TA and Ser-OH and the 3-O-TA peak; see also chapter 3.7.2 about B<sub>ser</sub>). B<sub>ser</sub>/B<sub>car</sub> reveals only the Iso-Ser (**20**) and Ser-OH (**21**) peak, whereas B<sub>pap</sub> does not show any significant signals within this elution area, except the minor peak areas of  $\beta$ -TA (**15**),  $\alpha$ -TA (**14**) and 3-O-TA (**13**). In some cases the existence of a minor peak for Ac-LA (**12**) may already ascertain an unknown resin sample as B<sub>ser</sub>/B<sub>car</sub>, since for B<sub>pap</sub> and B<sub>ser</sub> no significant peak signal is detectable within this elution range. Additionally, high peak signals for  $\alpha$ -ABA (**2**) and  $\beta$ -ABA (**4**) may identify an unknown resin sample already as B<sub>ser</sub>/B<sub>car</sub>, as they expectably occur in greater amounts there. Furthermore, for B<sub>ser</sub>/B<sub>car</sub> the existence of the broad triplet peak

eluting within 55 and 60 min seems to be also remarkable. Thus, even if only the RE chromatograms of all three species are considered, it may be still possible to figure out the identity, if an unknown resin is analysed.

However, the data generated hitherto is based on a few samples which attempt to represent a whole population of resin samples. The data may be correct and further analysis of more and more samples will quite likely deliver the same information as given here. Nevertheless, as experienced also in this work, there are, concerning a few biomarkers (e.g.  $\beta$ -KBA and  $\beta$ -AKBA in B<sub>sa</sub>c/B<sub>ca</sub>r), always differences from the rule of thumb.

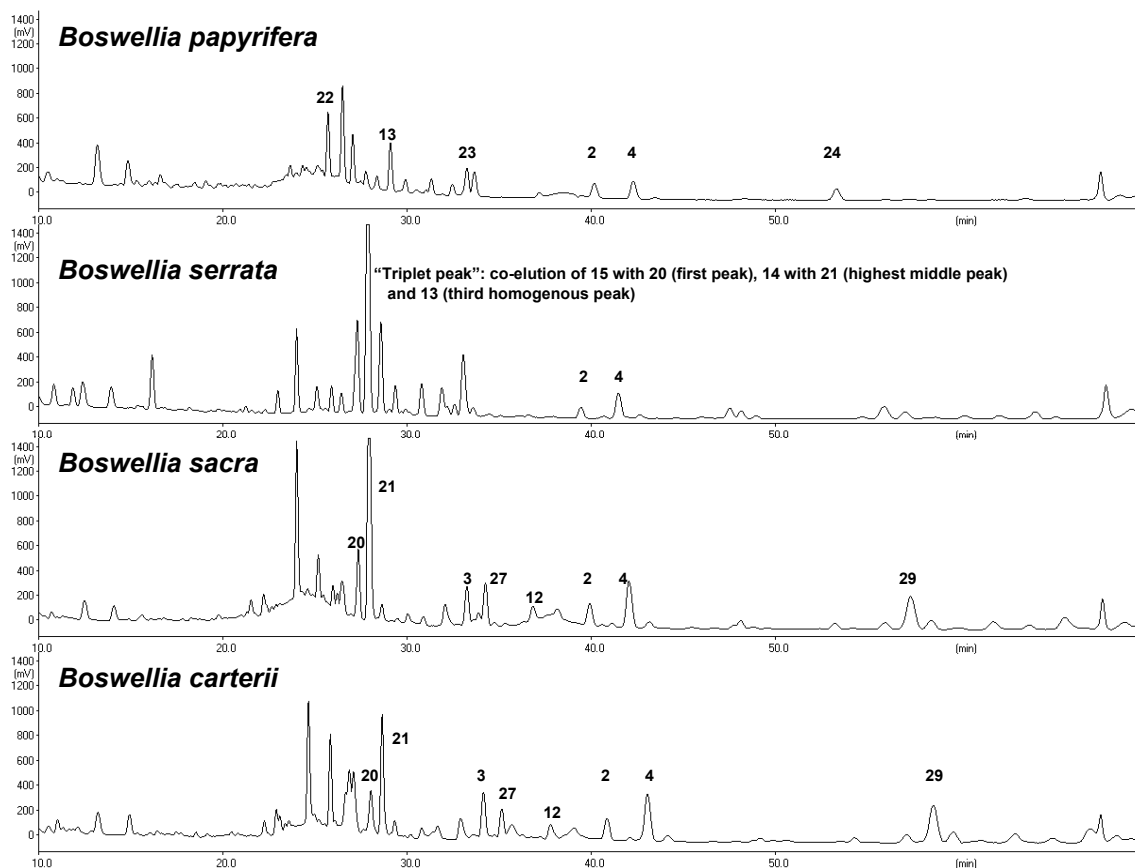


**Fig. 3.109** Comparison of the RE-extract chromatograms from B<sub>pap</sub>, B<sub>ser</sub> and B<sub>sa</sub>c/B<sub>ca</sub>r at 210 nm (c = 5 mg/ml).

### 3.8 HPLC Data (Quantitative Consideration)

To summarise the qualitative discussions given in the chapter before, the quantitative data is presented in this chapter. For details concerning the technical aspects view chapter 2.3.4. Tab. 3.27 presents the arithmetically averaged data of all analysed samples (total of 15 compounds) during this work concerning the RS acid fraction (Note that the arithmetic average was preferred, although the number of samples would suggest a median data set distribution, see also [159]). However, in the author's opinion the arithmetic average gives a better overview and a better feeling for expectation values. Significant standard deviations

## Results and Discussion

are explicitly discussed). The single values of each sample are given in Tab. 3.37 in chapter 3.14, where the matrix calculation by principal component analysis is presented.

For some values quite great standard deviations are obtained (e.g. compound **7** and **10**, due to the fact of a random decomposition of **7** during the extraction, see also [55,59]; 3-O-TA, **13**, for Bpap;  $\beta$ -AKBA, **6**,  $\alpha$ -BA, **1**,  $\beta$ -BA, **3**,  $\alpha$ -ABA, **2** and  $\beta$ -ABA, **4**, for B<sub>ser</sub>/B<sub>car</sub>). The great standard deviations for  $\beta$ -AKBA,  $\alpha$ -BA,  $\beta$ -BA,  $\alpha$ -ABA and  $\beta$ -ABA in B<sub>ser</sub>/B<sub>car</sub> are due to the many different samples analysed (even older samples from J. Bergmann [17] were evaluated) and is quite interesting, since there may be always an exception from the general expectation value. However, the identity of B<sub>ser</sub>/B<sub>car</sub> is normally granted, since the values for LA (**11**) and Ac-LA (**12**) always delivered significant higher results compared with Bpap and B<sub>ser</sub>. Another significant fact is that B<sub>ser</sub>/B<sub>car</sub> did quantitatively reveal fairly low contents for the tirucallic acids (**13-19**), whereas the amounts of boswellic and acetylated boswellic acids have been comparably high (**1-4**). Additionally, for every B<sub>ser</sub>/B<sub>car</sub> sample the typical  $\beta$ -Car-Ox (**28**) spot (see also chapter 3.4) was detectable. Thus, even if there was a differing peak pattern for B<sub>ser</sub>/B<sub>car</sub> and a significantly deviating  $\beta$ -KBA/ $\beta$ -AKBA content from the given mean values in Tab. 3.27, the identity of this species has been normally always guaranteed (e.g. extreme values for  $\beta$ -AKBA have been 0.1 % and 20 % g/g in the RS fraction). The strong standard deviation for 3-O-TA (**13**) in Bpap is a result of wide limiting values (e.g. 5 % and 16 %, which seems to be a normal batch to batch difference).

**Tab. 3.27** The arithmetically averaged measurement results for the RS acid fraction (S.D. = standard deviation, random sample; n = numbers of different resin batches analysed; #NV = not detectable). Since B<sub>car</sub> and B<sub>ser</sub> can be considered the same species, their data was combined to B<sub>ser</sub>/B<sub>car</sub>.

Compound	Nr.	n = 6		n = 4		n = 10		n = 14		n = 10	
		B <sub>car</sub>	S.D.	B <sub>ser</sub>	S.D.	Bpap	S.D.	B <sub>ser</sub>	S.D.	B <sub>ser</sub> /B <sub>car</sub>	S.D.
		[g/g in %]				[g/g in %]		[g/g in %]		[g/g in %]	
$\beta$ -KBA	<b>5</b>	0.48	0.25	0.64	0.43	1.22	0.30	3.16	0.52	0.56	0.34
$\beta$ -AKBA	<b>6</b>	5.38	5.09	8.03	8.88	14.33	1.98	3.28	0.43	6.70	6.98
11-OH- $\beta$ -ABA	<b>7</b>	3.60	1.70	6.22	6.44	4.41	3.04	2.37	0.70	4.91	4.07
$\beta$ -OH-TA	<b>15</b>	1.20	0.28	1.20	0.43	2.98	0.77	4.44 <sup>a</sup>	0.63	1.20 <sup>a</sup>	0.35
$\alpha$ -OH-TA	<b>14</b>	1.33	0.91	1.45	0.75	2.47	0.89	5.77 <sup>a</sup>	1.18	1.39 <sup>a</sup>	0.83
3-O-TA	<b>13</b>	1.73	0.51	1.64	1.05	11.66	5.31	11.64	2.23	1.68	0.78
$\alpha$ -Ac-TA	<b>16</b>	0.75	0.33	0.71	0.52	3.21	1.25	3.13	1.00	0.73	0.43
$\alpha$ -BA	<b>1</b>	7.78	2.60	6.45	3.00	3.72	0.76	8.32	0.91	7.11	2.80
$\alpha$ -BA (2D)	<b>1</b>	7.64	2.52	6.40	3.01	3.73	0.77	8.12	1.10	7.02	2.76
$\beta$ -BA	<b>3</b>	15.94	3.83	12.19	7.27	9.21	1.66	19.45	1.48	14.07	5.55
$\beta$ -BA(2D)	<b>3</b>	15.92	4.00	12.15	7.25	7.01	1.37	17.43	1.55	14.04	5.62
11-Ome- $\beta$ -ABA	<b>8</b>	#NV	#NV	#NV	#NV	#NV	#NV	#NV	#NV	#NV	#NV
LA	<b>11</b>	2.78	0.75	2.51	1.33	0.68	0.26	1.41	0.18	2.64	1.04
Ac-LA	<b>12</b>	4.89	1.13	5.04	2.04	1.81	0.27	1.07	0.31	4.97	1.58
9,11-Dehydro- $\beta$ -ABA	<b>10</b>	0.02	0.02	0.35	0.52	1.57	1.96	0.21	0.77	0.18	0.27
$\alpha$ -ABA	<b>2</b>	10.25	2.49	10.60	3.32	6.73	0.88	4.21	0.25	10.43	2.91
$\beta$ -ABA	<b>4</b>	20.08	5.59	17.18	7.84	11.13	2.11	13.83	0.89	18.63	6.72
Sum <sup>b</sup> :		76.21		74.20		72.94		77.33		75.21	
Unknown Rest:		23.79		25.80		27.06		22.67		24.79	

<sup>a</sup> Values of **14** and **15** in B<sub>ser</sub> and B<sub>ser</sub>/B<sub>car</sub> are actually too high (Co-elution with **21** and **20**, see also 3.7.2 – 3.7.4).

<sup>b</sup> The 2D contents of  $\beta$ -BA have been used for summation.

The standard deviation of 11-OH- $\beta$ -ABA (**7**) can be explained by the decomposition of this compound into its 9,11-dehydro-derivative, vice versa for 9,11-dehydro- $\beta$ -ABA (**10**) [55,59].

The averaged sum shows that approximately 75 % of the acid fraction can be determined by this method for all species investigated. However, it should be noted that even samples with a much lower or higher overall content were analysed (e.g. ca. 50-80 % for Bpap; ca. 60-95 % for Bser and ca. 40-90 % for Bsac/Bcar). Furthermore, one very critical batch of Bsac revealed only 22 %. This batch was not used for the arithmetic mean as it could be determined as an outlier referring to the analysed sample population, though it may be actually part of the overall population. Furthermore, it already gave a rather low amount of RE extract by the extraction methods described in chapter 2.2.4 for example. A great negative deviation from the expectation extraction values presented in chapter 3.3.1 may already declare the poor quality of a resin sample.

Hence, it is still a quite difficult undertaking to give an absolutely correct overall marker compound distribution for these natural resins. Interestingly, the almost similar overall amounts of resinous acids (ca. 70-75 %) in any species may declare that every species has approximately the same carbon material available, which is then transformed via the different biosynthetic pathways. However, this is merely a presumption and thus far not proved by real scientific evidence. Also the environmental influences may certainly have an enormous impact on the secondary metabolism of these plants [3]. An easily understandable example, which explains the natural product dependency on environmental influences clearly, is given in chapter 3 in the book of Cseke et al. [19], where the production of the secondary metabolite camptothecin in *Camptotheca accuminata*, depending on light and shading cycles, is reported. The experiments described there may be generally valid for any kind of plant species on this planet.

The values in Tab. 3.27 are shown as graphic in Fig. 3.110. This graphic may help clarifying the values given in Tab. 3.27. For every species (Bpap, Bser and Bsac/Bcar) the content in percent (g/g) of the RS acid fraction is plotted against the corresponding marker compound. The given confidence interval for each compound was set to +/- 20 %, referring to the corresponding mean value presented in Tab. 3.27. Thus, a quite good certainty of the mean value is given. However, the standard deviations are for some samples still greater than 20 %, but would be confusing for the graphical depiction.

On average, the  $\beta$ -KBA content is rather low for the species Bpap and Bsac/Bcar compared with the  $\beta$ -AKBA content. However, Bsac/Bcar samples show a very strong deviation concerning the  $\beta$ -KBA/ $\beta$ -AKBA contents (see S.D. in Tab. 3.27). For Bser the  $\beta$ -KBA/ $\beta$ -AKBA ratio is balanced (expectation value = ca. 1:1 ratio). Expectably, Bpap samples produce the most  $\beta$ -AKBA, followed by Bsac/Bcar (strong S.D.). Compounds 11-OH- $\beta$ -ABA and 9,11-dehydro- $\beta$ -ABA values vary heavily for all species. The reason therefore is the known decomposition reaction of these compounds [55,59]. For Bser and Bpap significantly higher values for 3-O-TA are obtained (compared with Bsac/Bcar). Furthermore, the values for  $\beta$ -TA and  $\alpha$ -TA in Bpap and Bser are normally higher than in Bsac/Bcar (Note that for Bser the  $\beta$ -TA and  $\alpha$ -TA peaks still co-elute with Iso-Ser and Ser-OH, since these two semi-polar diterpenes are not absolutely separable by the extraction method developed here, and

thus the peak areas in the RS fraction of Bser are estimated too high; see also chapter 3.7.2 about Bser).

Bser contains on average the greatest amounts of  $\alpha$ -BA and  $\beta$ -BA. B<sub>ser</sub>/B<sub>car</sub> reveal  $\alpha$ -BA and  $\beta$ -BA in differing quantities, but expectably always higher than in B<sub>pap</sub> and almost likely high the values of B<sub>ser</sub> (Note that depending on the single resin sample even higher values for B<sub>ser</sub>/B<sub>car</sub>, than found in B<sub>ser</sub>, had been obtained). The LA and Ac-LA amounts have been in every B<sub>ser</sub>/B<sub>car</sub> sample greater than in B<sub>pap</sub> and B<sub>ser</sub>, which seems to be very significant for Olibanum Somalia and Oman, respectively, Yemen. Furthermore, the maximum  $\alpha$ -ABA and  $\beta$ -ABA contents can be found in B<sub>ser</sub>/B<sub>car</sub>. For B<sub>pap</sub> and B<sub>ser</sub> the ABA values are almost similar and occur in lower contents compared with B<sub>ser</sub>/B<sub>car</sub>.

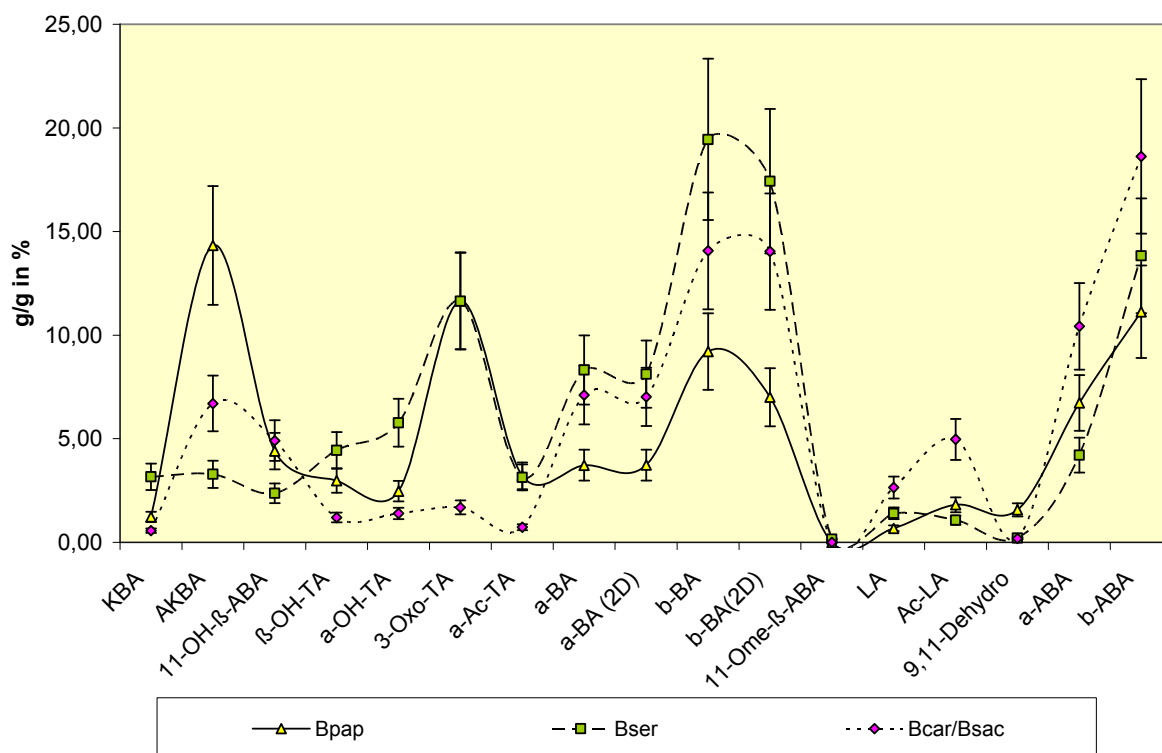


**Fig. 3.110** Graphical depiction of the arithmetic mean values presented in Tab. 3.27. The confidence interval is set to 20 % of the mean value in Tab. 3.27. The scheme here shall clarify Tab. 3.27 and may be useful for species identification, since for each biomarker compound analysed here an expectation value is given. Throughout significant levels have been obtained for the tirucallic acids (TAs) and lupeolic acids (LAs). For further discussions see text.

Interestingly, the 2D measurement results verify the general correctness of the peak homogeneities in the first, respectively, the second chromatography dimension. As reported in the corresponding chapters (3.6.2 and 3.7.5), the second dimension is not necessary for samples from B<sub>ser</sub>/B<sub>car</sub> (similar values for compound **1** and **3** in both dimensions within the estimated  $\pm 5\%$  confidence interval). For samples of B<sub>ser</sub>, the averaged error in the first dimension is about 10 %, meaning that on average the content for compound **3** is ca. 10 % lower than actually determined (1D chromatography), because of co-elution with compound **18**. Samples of B<sub>pap</sub> reveal a greater error for the determination of compound **3** in the first

dimension. The reason therefore is the quite low content of **3** in samples of Bpap. Thus, a greater integration error is given (up to 30 %).

As already mentioned in chapter 3.6.2, if a great sample population will be analysed, the error may be within a certain confidence interval predictable and hence may make the application of the second chromatography dimension redundant. Furthermore, for Bsac/Bcar samples the second dimension is thus far not necessary, and for samples of Bser it may be acceptable to calculate an averaged uncertainty of +/- 10 % within the real content of  $\beta$ -BA (**3**). Furthermore, the techniques nowadays provided (UHPLC and MS-detection) can overcome such difficulties easily (e.g. easier achievable resolution of peaks with UHPLC columns and systems and/or application of the additional MS detection dimension for co-eluting compounds with differing molecular masses and/or differing fragmentation patterns, as far as no ion-suppression takes place; therefore, see also chapter 8 in the book of Dolan and Snyder [153] for the discussion of MS as detection tool in liquid chromatography, and, for example, the paper of Wu et al. on the advantages of ultra-high performance liquid chromatography, UHPLC, [187]).

In Tab. 3.28 the quantitative HPLC results for the neutral fractions of Bpap, Bser and Bsac/Bcar are given. Only significant signals were quantified. In cases where the suspected peak signal was too small and/or additionally not good enough resolved the compound had been set not detectable (= 0).

As noticeable, Bpap distinguishes itself from the other species by the highest amounts of incensole (**22**) and incensole acetate (**23**). Almost 30-40 % of the neutral fraction consist thus of incensole and its acetate. Interestingly, Inc-Ac (**23**) had been only detected in samples of Bpap. On the other hand, Bser and Bsac, respectively, Bcar, contain serratol (**21**) and its isomeric derivative iso-serratol (**20**). These two, **20** and **21**, have never been significantly detectable in samples of Bpap. Thus, there seem to be remarkable differences in the biogenesis. Representative NB-chromatograms can be found in chapter 3.7. The corresponding single values of each analysed sample are presented in Tab. 3.37 in chapter 3.14 where the matrix calculation by principal component analysis is presented.

**Tab. 3.28** The arithmetically averaged measurement results for the NB neutral fractions (S.D. = standard deviation, random sample; n = numbers of different resin batches analysed; 0 = not detectable). Since Bcar and Bsac can be considered the same species, their data was combined to Bsac/Bcar.

Compound	Nr.	n = 10		n = 14		n = 10	
		Bpap	S.D.	Bser	S.D.	Bsac/Bcar	S.D.
		[g/g in %]		[g/g in %]		[g/g in %]	
Inc	<b>22</b>	20.99	3.45	1.41	1.27	3.39	3.46
Inc-Ac	<b>23</b>	15.17	2.62	0	0	0	0
Ser-OH	<b>20</b>	0	0	8.60	5.46	7.59	7.39
Iso-Ser	<b>21</b>	0	0	1.73	0.99	1.16	0.99

### 3.9 Comparison with Literature Results (HPLC)

In this chapter the quantitative HPLC data obtained here is compared with quantitative results from the literature. The work of Ganzera et al. [188] and of Büchele et al. [57] were chosen therefore. In these two papers the complex extracts of Olibanum gums were analysed by HPLC. In another work of Ganzera et al. [189] even quantitation by capillary electro chromatography (CEC) was achieved. However, since this paper just delivers similar quantitative conclusions as already given in [188] it was not further regarded. The comparison of these results with the data obtained here is demonstrated in Tab. 3.29. As can be noticed, on average, the overall amounts of all three methods are comparable. Especially the overall amount for the Indian frankincense (Bser) fits quite well. The difference for African frankincense is greater. Though Bsac can be classified as Bcar, this species, as originated from the Arabian Peninsula was not explicitly tabulated (generally the same composition as Bcar, see also Tab. 3.27). If the single compounds are regarded, stronger deviations are deducible. This may be arbitrary, but is also due to the expectable naturally occurring differences (e.g. highly fluctuating deviations for  $\beta$ -AKBA, **6**, and  $\beta$ -KBA, **5**, in Bcar).

Additionally, the values in the columns Paul-Bpap, -Bcar and -Bser were arithmetically averaged. Nevertheless, compounds **2** ( $\alpha$ -ABA), **4** ( $\beta$ -ABA), **6** ( $\beta$ -AKBA), **11** (LA) and **12** (Ac-LA) fit quite well for Bpap with the results of Büchele et al. for African frankincense. The high deviation for compound **10** (9,11-dehydro- $\beta$ -ABA) can be explained by the randomly occurring decomposition probability of compound **7** (11-OH- $\beta$ -ABA) (see also [55,59]). The overall difference of 3-4 % for Bcar, respectively, Bpap lies within a certain accuracy compared with the results of Büchele. Particularly, when regarding the contents of compound **5**, **6**, **2**, **4**, **11** and **12**, the African frankincense species may be indeed the species Bpap. However, this is only based on the quantitative similarities and because of the fact that Bcar samples showed, in all samples analysed in this work, a significant greater content for the lupeolic acids (**11** and **12**), relatively compared with Bpap (see Tab. 3.27).

The values for Bser give an even better overall comparability. Quite good in accordance to the results of Büchele et al. are the determined amounts for the BAs (compound **1** and **3**). There, a recovery of 110 % ( $5.05 / 4.60 \times 100$  %) for compound **3** ( $\beta$ -BA) and a recovery of even 98 % ( $2.41 / 2.45 \times 100$  %) for compound **1** ( $\alpha$ -BA) are deducible. The recovery of the LAs (compound **11** and **12**) is also lying within the value of expectation, as these compounds typically occur in lower amounts in Bser, respectively, Bpap (see also Tab. 3.27).

The determination results by Ganzera et al. for Bser would lead to the assumption that the sample analysed was actually the species Bpap instead, since the corresponding quantities fit best with this species (quite remarkable is the high  $\beta$ -AKBA-value, **6**, which was never found as similar high in the species Bser during this work). However, it should be still beard in mind the possibility of stronger quantitative deviations otherwise than stated here. Thus, for every general expectation there might be still an exception and uncertainty.

Hitherto, the requirements how these species generate special biomarkers under certain environmental conditions have not been evaluated or at least have not been published by other research groups. There should be further scientific evaluation conducted, especially concerning those questions (e.g. specific genes encoding specific enzymes and experiments

## Results and Discussion

with whole plants under certain different conditions like light- and shading cycles, soil quality, humidity etc. as it is described in the book of Cseke et al. [19]).

**Tab. 3.29** Comparison of the quantitative HPLC results generated in this work with the results of Büchele et al. [57] and of Ganzera et al. [188]. All values are given in percent (g/g [%]). The values for Paul-Bpap, -Bser and -Bcar were adjusted to the overall resin (RS results in Tab. 3.27 divided by ca. factor 3) to be comparable. For compound **3** the 2D chromatography result is presented. Bpap and Bcar, as African frankincense (African-Fr.), were compared with the results of African frankincense from Büchele; and Bser (Indian-Fr.) was compared with the results of Büchele and Ganzera for Indian frankincense. Overall: The sum of the same compounds quantified in both columns to give a comparable overall amount. Overall + Rest: The sum of all compounds quantified in the work reported here (e.g. + TAs, **13-16**, and **7** compared with Büchele; +TAs and +LAs, **11-16**, and **7** and **10** compared with Ganzera). #NV: not detectable. For further details see text.

Compound (Nr.)	Paul-Bpap	Büchele African-Fr.	Paul-Bcar	Büchele African-Fr.	Paul-Bser	Büchele-Indian-Fr.	Ganzera HPLC-Ind-Fr.
<b>5</b>	0.36	1.01	0.12	1.01	0.92	2.02	1.38
<b>6</b>	4.51	4.70	1.29	4.70	0.95	1.43	5.40
<b>7</b>	1.61		0.86		0.69		
<b>15</b>	0.86		0.29		1.29		
<b>14</b>	0.69		0.32		1.67		
<b>13</b>	3.12		0.42		3.38		
<b>16</b>	0.95		0.18		0.91		
<b>1</b>	1.13	2.69	1.87	2.69	2.41	2.45	1.34
<b>3(2D)</b>	2.07	3.72	3.82	3.72	5.05	4.60	1.42
<b>11</b>	0.19	0.23	0.67	0.23	0.41	0.32	
<b>12</b>	0.52	0.78	1.17	0.78	0.31	0.35	
<b>10</b>	0.28	0.028	0.00	0.028	0.06	0.018	
<b>2</b>	2.09	2.11	2.46	2.11	1.22	0.47	2.52
<b>4</b>	3.57	3.98	4.82	3.98	4.01	2.54	3.34
<b>Overall</b>	14.72	19.25	16.22	19.25	15.34	14.29	15.40
<b>Overall +Rest</b>	21,95 <sup>a</sup>		18.29 <sup>a</sup>		23.28 <sup>a,b</sup>		

<sup>a</sup> **Overall + Rest** (for Büchele) = + results for compounds **7** and **13-16**

<sup>b</sup> **Overall + Rest** (for Ganzera) = + results for compounds **7** and **10-16**

### 3.10 Summary (Analytics)

Here, the generated qualitative and quantitative data is summarised in Tab. 3.30. This table may serve as an overview checklist for the identification of an Olibanum resin in question. The data presented is based on the results from chapters 3.4, 3.7 and 3.8.

**Tab. 3.30** Systematic overview table presenting the main differences and communalities of the three species Bpap, Bser, Bsac/Bcar.

<sup>a</sup> Comparable with a typical orange scent (high contents of octyl acetate, which has an orange fragrance); quite specific for Bpap.

<sup>b</sup> Probably due to the high content of apolar triterpenic compounds (see also chapter 3.7.6, Fig. 109)

<sup>c</sup> Expectation value; deviations from this rule of thumb have been observed (varying  $\beta$ -KBA/ $\beta$ -AKBA contents, see also for example chapters 3.7.4, 3.8 or 3.14).

	Bpap	Bser	Bcar	Bsac
Odour	Sweetish <sup>a</sup>	Frankincense-like	Frankincense-like	Frankincense-like
Solubility of the Et <sub>2</sub> O extract in MeOH	Clear solution	Milky blur <sup>b</sup>	Milky blur <sup>b</sup>	Milky blur <sup>b</sup>
AKBA-UV (TLC at 254 nm; c = 5 mg/ml)	Significant	Faint	Faint <sup>c</sup>	Faint <sup>c</sup>
KBA-UV (TLC at 254 nm; c = 5 mg/mL)	Faint	Faint	Faint <sup>c</sup>	Faint <sup>c</sup>
In-Spot (TLC after dyeing)	Strong brown	Faint brown	Faint brown	Faint brown
In-Ac-Spot (TLC after dyeing)	Brown	Not detectable	Not detectable	Not detectable
$\beta$ -Car-Oxid-Spot (TLC after dyeing)	Not detectable	Not detectable	Faint pink	Faint pink
Serratol-Spot (TLC after dyeing)	Not detectable	Strong green	Strong green	Strong green
3-O-TA-Spot (TLC after dyeing)	Strong blue	Strong blue	Faint blue	Fain blue
KBA/AKBA-Ratio (HPLC, 250 nm)	ca. 1:10	ca. 1:1	ca. 1:5 <sup>c</sup>	ca. 1:5 <sup>c</sup>
AKBA-Content (HPLC, referred to Acid Fraction)	> 10 % (n = 10)	ca. 2-4% (n = 14)	ca. 2-13 % (n = 6)	ca. 0.1-20 % (n = 4)
Sum: $\alpha$ -BA/ $\beta$ -BA-Content (HPLC, referred to Acid Fraction)	ca. 11 % (n = 10)	ca. 20-30 % (n = 14)	ca. 15-30 % (n = 6)	ca. 10-30 % (n = 4)
Sum: $\alpha$ -ABA/ $\beta$ -ABA-Content (HPLC, referred to Acid Fraction)	ca. 18 % (n = 10)	ca. 15 - 18 % (n = 14)	ca. 20 - 35 % (n = 6)	ca. 20 - 35 % (n = 4)
3-O-TA-Content (HPLC, referred to Acid Fraction)	ca. 5 - 15 % (n = 10)	ca. 8 - 17 % (n = 14)	< 3 % (n = 6)	< 3 % (n = 4)
Sum: LA/Ac-LA-Content (HPLC, referred to Acid Fraction)	ca. 2 - 3 % (n = 10)	ca. 2 - 3 % (n = 14)	> 5 % (n = 6)	> 5 % (n = 4)

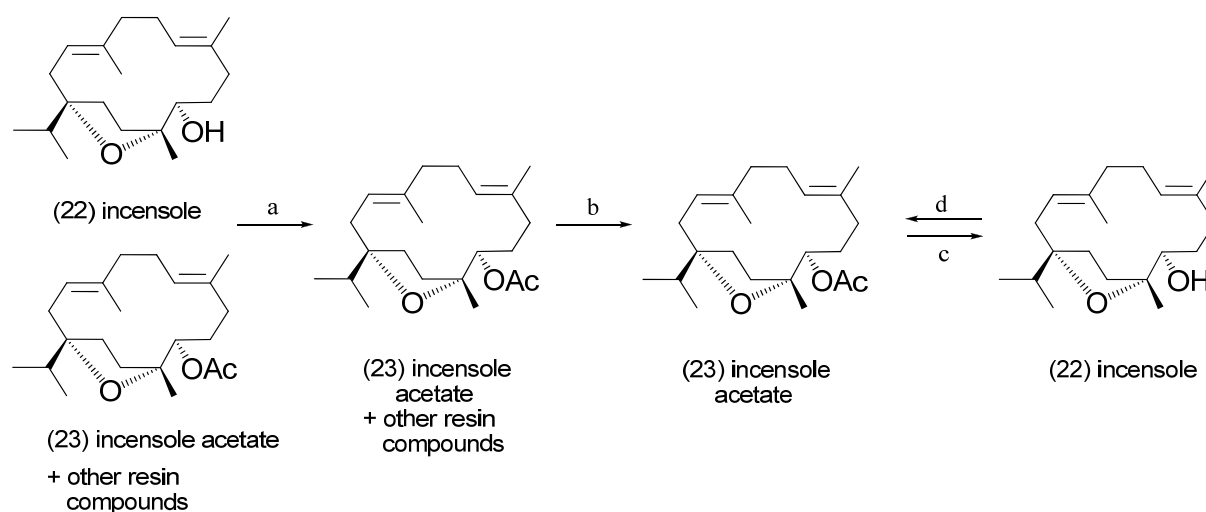
### 3.11 Experiments with Incensole and its Acetate

#### 3.11.1 Semisynthesis of Inc-Ac (NB-fraction of Bpap)

In this chapter the semi synthetic approach for the production of Inc-Ac (**23**) in high quantities is reported. Besides, the here presented preparation method has been already published in *Natural Product Communications* [154]. As the chromatographic analysis (TLC and HPLC) only revealed for the NB fraction of Bpap the existence of Inc (**22**) and its acetate (**23**) in good quantities (see chapter 3.8), this resin was used. The experimental procedure is described in chapter 2.7.2.

Moussaieff et al. showed that incensole (**22**) and its acetate (**23**), as novel anti-inflammatory diterpenes, may contribute to the overall pharmacological action of frankincense gum preparations by inhibition of the Nuclear Factor- $\kappa$ B activation [87]. It is further reported by Moussaieff et al. that incensole acetate elicits neuronal activity in mice by activating the transient receptor potential cation channel 3 (TRPV3) in the brain [145]. A recent publication by Moussaieff et al. additionally revealed protective effects of incensole acetate on cerebral ischemic injury in mice models [147].

Hence, great amounts of these two diterpenic compounds may be desirable for further investigations proving their pharmaceutical potential.



**Sch. 3.1** "Focussing" approach to large-scale synthesis of incensole acetate; **a:**  $\text{Ac}_2\text{O}$ /pyridine/DMAP, DCM, gentle reflux, 4 h; **b:** flash chromatography with silica gel, pentane/diethyl ether (6:1), purity of incensole acetate (> 80 %); preparative RP-HPLC, isocratic: methanol (100 %), purity of incensole acetate (> 99 %); yield of incensole acetate = 4 g of 25 g (16 %, referring to the not acetylated neutral compounds). Conversion reactions of **22** and **23**. **c:** 1 N KOH in *i*PrOH, gentle reflux, 3 h, yield: > 90 %, purity > 98 %, optional: Column or instrumental chromatography for guaranteed purity; **d:**  $\text{Ac}_2\text{O}$ /pyridine/DMAP, DCM, gently reflux, 4 h, yield: > 90 %, purity > 99 %, optional: Column or instrumental chromatography for guaranteed purity.

Therefore, a simple method for the isolation of incensole and its acetate from *Boswellia papyrifera*, which contains these two diterpenes in relatively high amounts, was developed. Since Jauch and Bergmann developed a method for the large scale preparation of 3-O-acetyl-11-oxo- $\beta$ -boswellic acid ( $\beta$ -AKBA, **6**) [190] from various frankincense resins, it was

## Results and Discussion

presumed that using a similar strategy, it should also be possible to obtain **23** in large amounts by acetylating the neutral fraction. The synthesis route is shown in Scheme 3.1. The acetylation process can be easily followed by TLC and after 4 hours **22** is completely converted into **23**. Fig. 3.111 shows the comparison of chromatograms before and after acetylation.

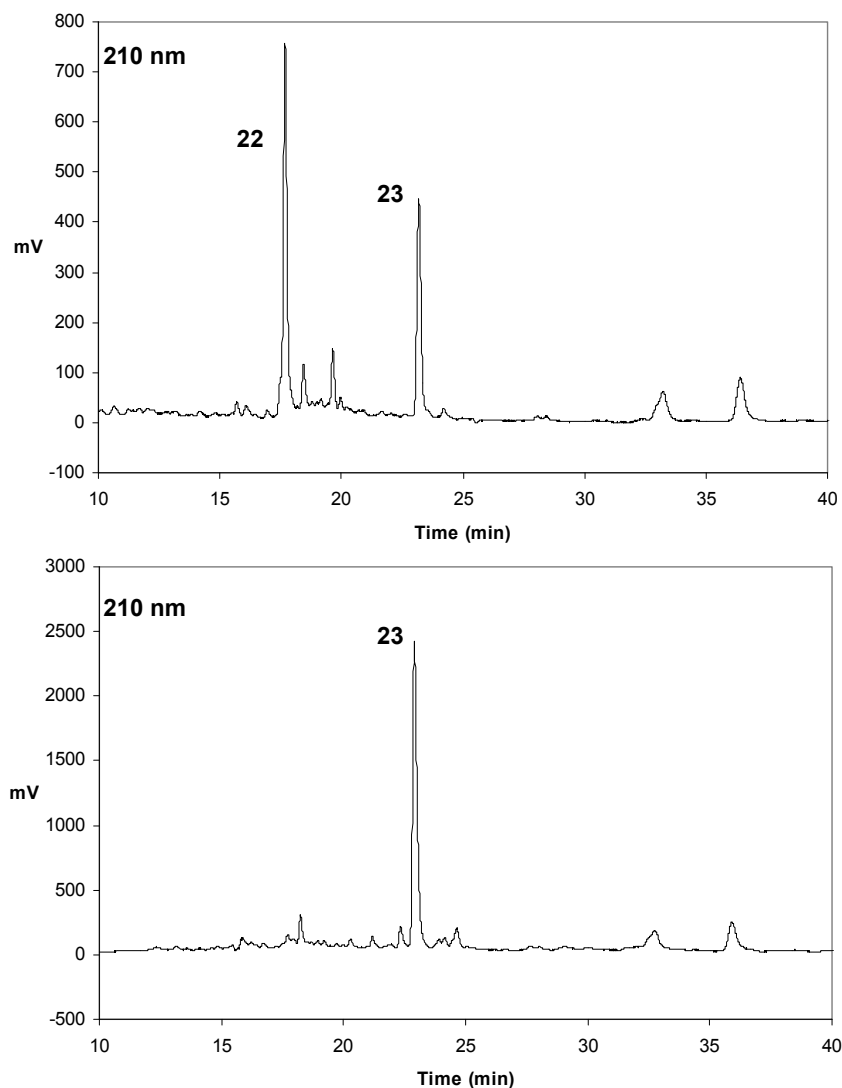


**Fig. 3.111** The comparison of the chromatograms of the neutral fraction before acetylation (chromatogram above) and after the acetylation experiment (chromatogram below). The incensole signal (**22**) disappeared. Control chromatogram conditions: 1 x Grom (guard column) and 1 x YMC (250x4.6 mm I.D, S-5 $\mu$ m, 8nm); T = 30 °C; u = 0.85 ml/min; detection: 210 nm; Gradient profile (A: MeOH; B: H<sub>2</sub>O + 0.1 % TFA): Isocratic from 0-1 min 85 % A, gradient from minute 1-13 to 100 % A, minute 13 to 45 isocratic at 100 % A, isocratic from 45-60 min at 85 % A for equilibration. For further details see text.

By application of conventional flash column chromatography [151] the acetylated mixture was fractionated and 14 fractions were obtained. Note that the column was overloaded with material: 29 g of the acetylated mixture were separated in a 10 cm diameter column. A better separation may be achieved if less material (< 20 g) is separated in this dimension. However, a good compromise in attainable quantity and purity of incensole acetate was attained.

## Results and Discussion

Fraction 2, 3 and 4 contained the whole amount of **23** in differing purities. Fraction 3 had the greatest quantity and purity (6.9 g, 85 % by HPLC control; see also Fig. 3.112) Through application of preparative HPLC this fraction was purified (>99 %) and a yield of 62 % was obtained (1.28 g from 2.07 g of fraction 3; Note: To achieve a purity >99% some of the incensole acetate gets lost, since the peak signal was fractionated generously, see also Fig. 3.113). Approximately calculated, a total yield of 3.84 g from 6.9 g (62 %, purity > 99 %) could be obtained, if fraction 3 would have been purified completely. Thus, leading to a total yield of 5 % referred to the overall weighed amount of resin. Calculations for the purification of incensole acetate are shown in Tab. 3.31. The detailed preparative chromatographic procedure is explained in the experimental section (chapter 2.7.2).

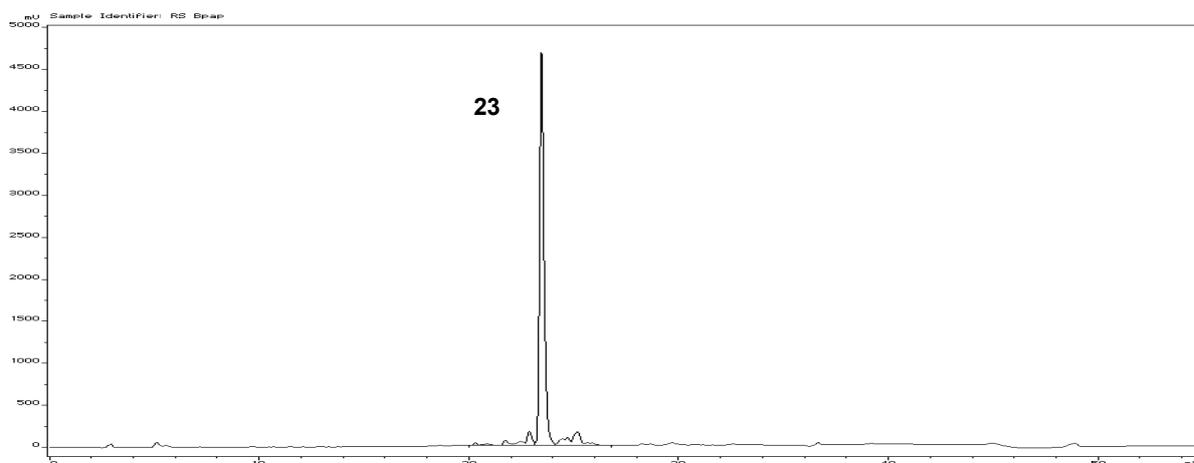


**Fig. 3.112** Incensole acetate in Fraction 3 after separation (flash column chromatography) of the acetylated neutral fraction of *Boswellia papyrifera*. Same chromatographic conditions as presented in Fig. 3.111. The fraction was further purified by preparative HPLC. For details see text.

Incensole acetate and incensole can be easily converted into their counterparts as it is presented in Scheme 3.1. The detailed synthesis procedures are described in the experimental section (chapter 2.7.2).

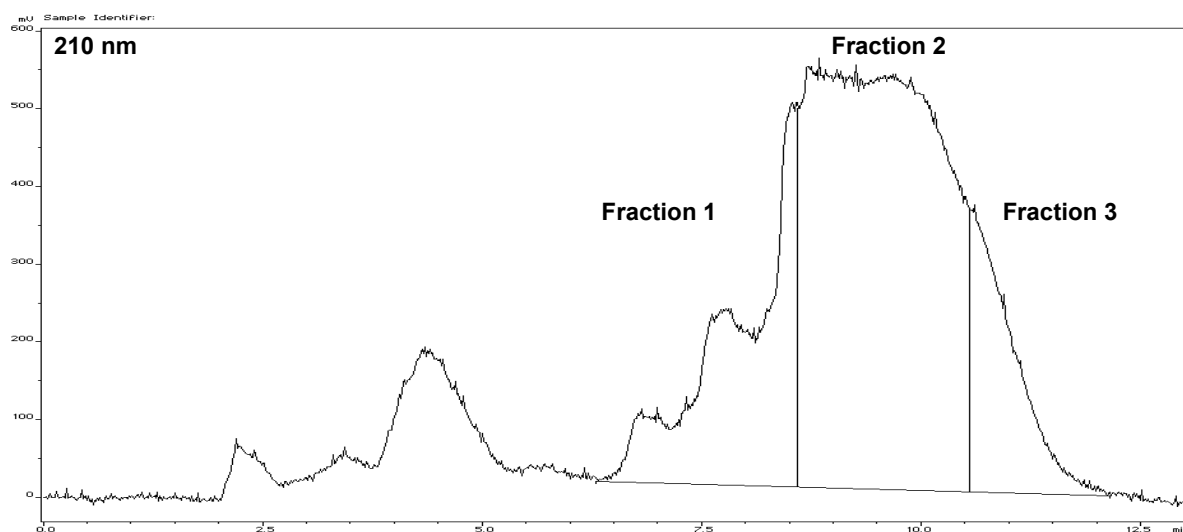


**Fig. 3.113** The purification of Fraction 3 via preparative HPLC. The peak was portioned in three further fractions. Yield of incensole acetate > 99 % (Fraction 2). For details see text.

## Results and Discussion

**Tab. 3.31** The calculated yield of the semi-synthetic production of compound **23** (Inc-Ac). The data presented here is based on the experimental results obtained and projected to a greater quantity for the prepared Bpap resin sample. For further details see text.

<sup>a</sup> Contents for incensole and incensole acetate in the NB fraction of Bpap were determined by the HPLC method described in chapter 2.3.4.2.

	Mass [g]	Percentage [%]
<b>Crude resin</b>	<b>84</b>	<b>100</b>
<b>Yield of neutral fraction</b>	<b>25</b>	<b>30</b>
Incensole <sup>a</sup>	5	6
Incensole acetate <sup>a</sup>	4	5
<b>Acetylated neutral fraction</b>	<b>29</b>	<b>30</b>
Incensole	-	-
Incensole acetate	10	12
<b>Column chromatography isolation (purity &gt; 80 %)</b>		
Incensole acetate	7	8
<b>Preparative HPLC isolation (purity &gt; 99 %)</b>		
Incensole acetate	4	5

In summary, the method described here allows the semi-preparative synthesis of incensole acetate from the neutral fraction of the frankincense species *Boswellia papyrifera* in large quantities. This is simply achieved by acetylation of incensole in the crude neutral fraction and thus gives a convenient method for the isolation of these two chemical entities. By conventional deacetylation and acetylation reactions, both diterpenes can be converted into one another.

### 3.11.2 Decomposition Results for Incensole Acetate

In this chapter the decomposition results are presented. Interestingly, as it was figured out that the presumably expected inhibitory activity of Inc-Ac (**23**), respectively, Inc (**22**) had been due to a decomposition of the molecules itself, tests were performed to check if these decomposition effects are repeatable. The chromatograms of an intact Inc-Ac batch compared with the first batch, which coincidentally was decomposed, are depicted in Fig. 3.114. As can be noticed, the decomposed sample shows numerous peak signals, which may be in combination with Inc-Ac responsible for the inhibitory action. Several different batches of intact Inc-Ac, respectively, Inc were tested and no inhibitory effect could be observed anymore. Thus, the inhibitory effect has been due to an uncountable combination of decomposed “daughter molecules” from Inc-Ac, respectively, Inc. This statement was proved as the repetition of the decomposition experiments delivered similar results and similar inhibitory effects, at least in the cell free mPGES-1-assay (see chapter 3.12.1).

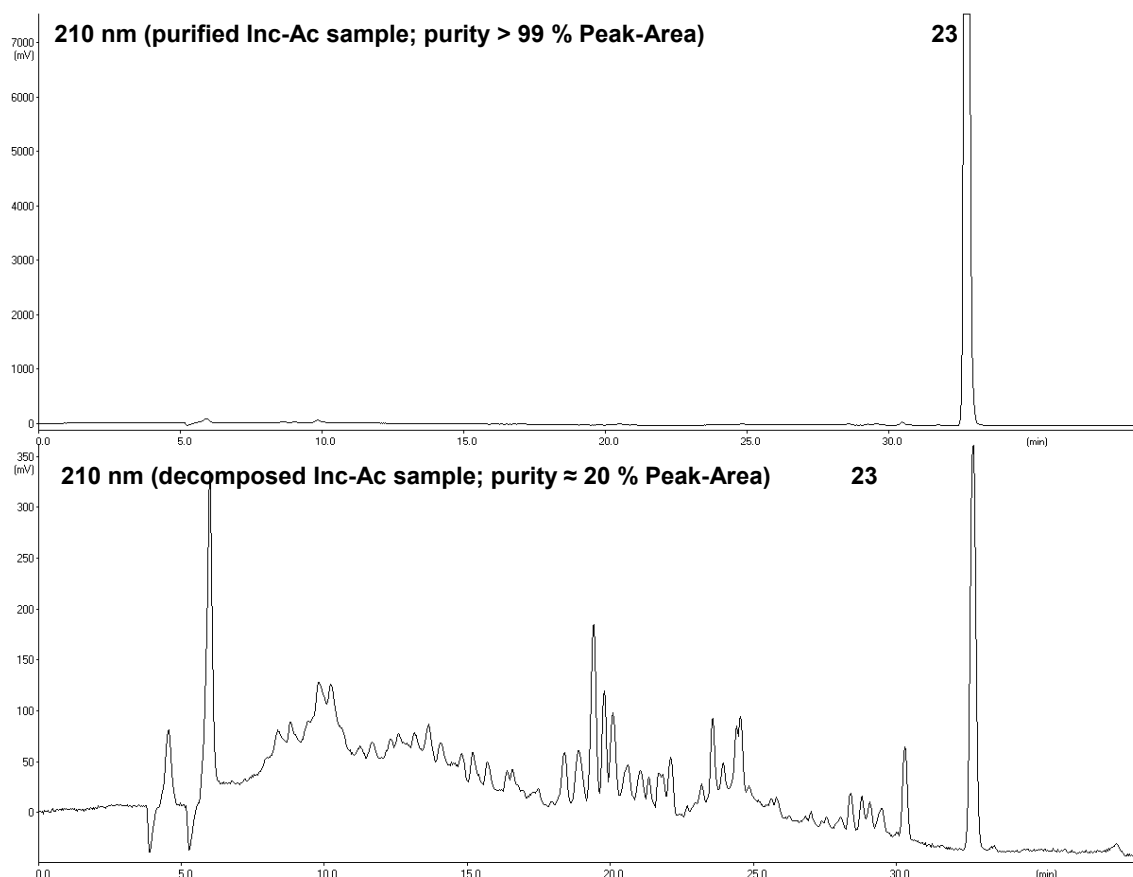


**Fig. 3.114** Comparison of an intact Inc-Ac (**23**) compound (upper chromatogram) with an “inhibitory active”, decomposed sample of Inc-Ac (lower chromatogram). Standard-Gradient (2 x YMC columns, see chapter 2.3.4.2). The determined amount for Inc-Ac in the decomposed sample refers to ca. 6.4 % (g/g); thus, the 2.5 mg of the sample batch consisted of 0.16 mg Inc-Ac. The peaks eluting in front are most likely to be oxidation products from Inc-Ac. For further details see text.

In Fig. 3.114 the comparison of two chromatograms at 210 nm detection wavelength is presented. The upper chromatogram refers to a purified (prep. HPLC) sample of Inc-Ac. The lower chromatogram refers to a decomposed sample of Inc-Ac. This sample was firstly isolated and determined to be pure as the sample shown above. Somehow, probably during the transport to the lab of the University of Tübingen, the pure sample got decomposed and finally revealed a huge “forest” of undeterminable signals (ca. 50 peak signals were integrated). Interestingly, these signals all elute in front of the peak of compound **23**. Most likely, these are oxidation products from Inc-Ac and thus are smaller molecules and/or more polar substances (see also TLC results in chapter 3.11.4). Furthermore, since the intact Inc and Inc-Ac samples did not show any inhibitory actions in the mPGES1 assay, it was finally realised that only decomposed Inc-Ac, respectively, Inc samples are responsible for the inhibition (see also chapter 3.12.1).

The analytical HPLC chromatograms for the artificial decomposition tests at 60 °C are shown in the upcoming figures. The experimental basics are described in chapter 2.6.1. Test 1 (storage for 7 days at room temperature) did not reveal any significant decomposition. Hence, the sample is stable within a certain time at room temperature and the air caused decomposition is kinetically inhibited. The chromatogram after Test 2 (storage under air exposure for 16 h at 60 °C) is demonstrated in Fig. 3.115. It is noticeable that first

decomposition reactions took place at 60 °C. Hence, the decomposition of Inc-Ac is at room temperature, as assumed, kinetically inhibited.

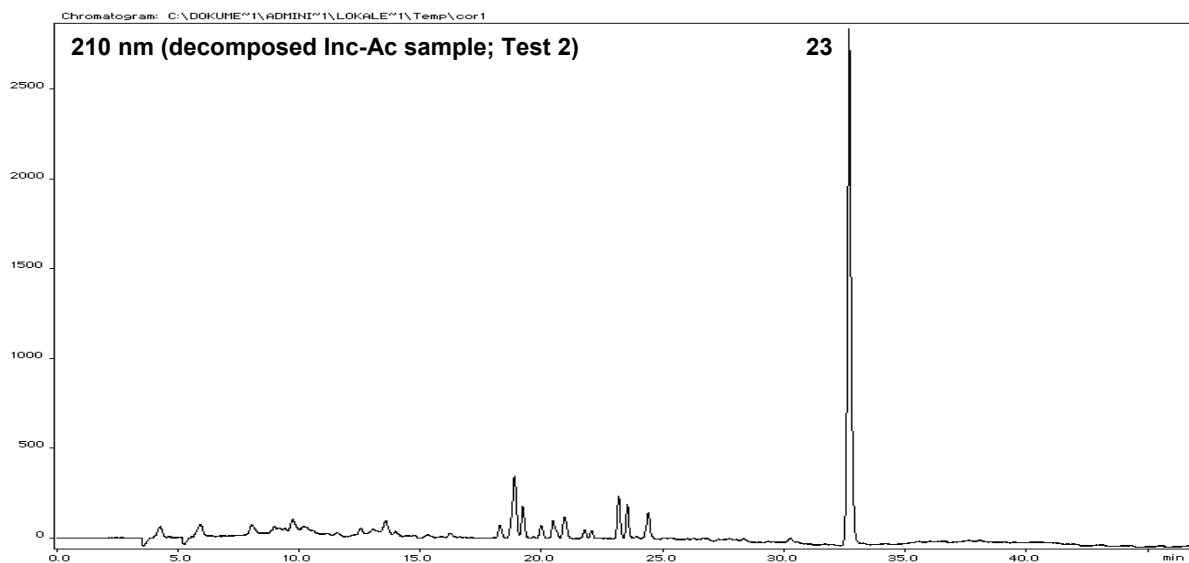


**Fig. 3.115** Test 2: The chromatogram of the Inc-Ac sample after 16 h at 60 °C in the compartment drier. The compound, which had previously a purity of > 99 %, now just revealed a purity of 55.7 %. Thus, the effective concentration in the sample was finally 0.92 mg from 2.3 mg (40 % g/g). For further details see text.

In Fig. 3.116 the chromatogram obtained after further 15 h (Test 3) is presented. As expected, the decomposition process continuous. After a total amount of 31 h at 60 °C (15h + 16 h from Test 2) only 6.7 % (g/g) of compound **23** are left in the sample. At last, after further 16 h at 60 °C (Test 4) none of the Inc-Ac can be detected anymore. This is depicted in the chromatogram in Fig. 3.117.

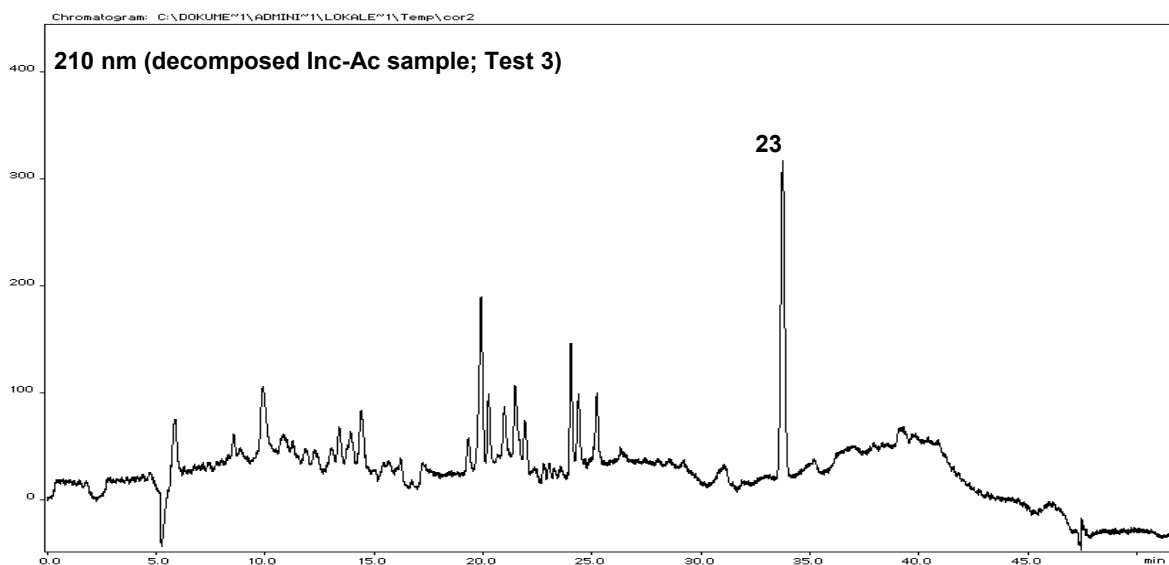


**Fig. 3.116** Test 3: The chromatogram of the Inc-Ac sample after in total ca. 31 h (15 h + 16 h from Test 2) at 60 °C in the compartment drier. The compound, which had previously a purity of 55.7 % (after Test 2), now just revealed a purity of 15.0 %. Thus, the effective concentration in the sample was finally 0.08 mg from 1.2 mg (6.7 % g/g). For further details see text.

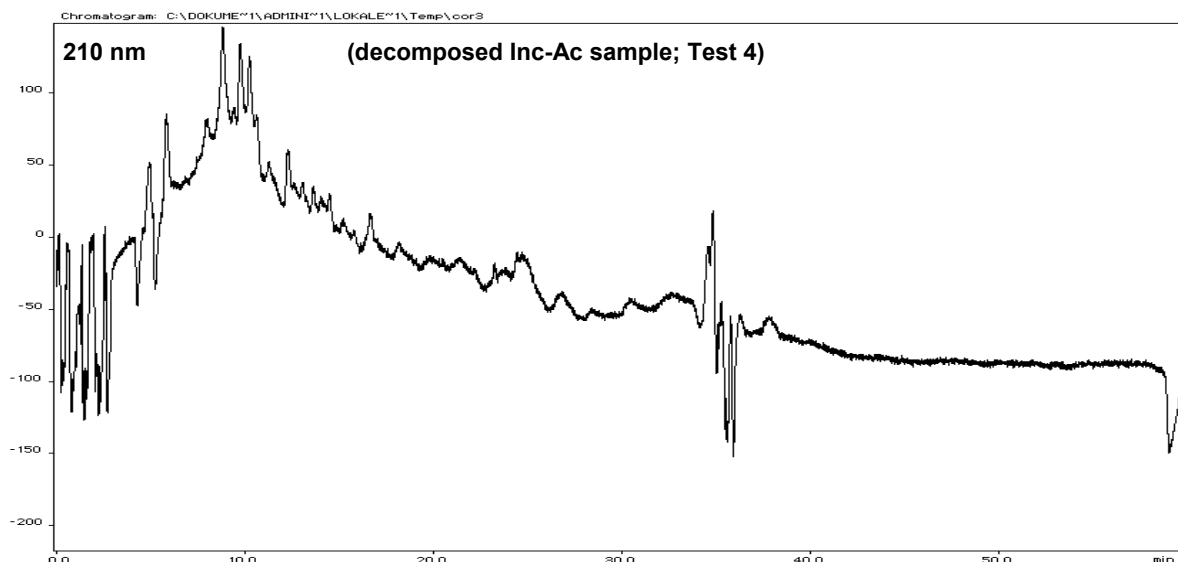


**Fig. 3.117** Test 4: The chromatogram of the Inc-Ac sample after in total ca. 47 h (15 h + 16 h + 16 h) at 60 °C in the compartment drier. The compound, which had previously a purity of 6.7 % (after Test 3) did not reveal any Inc-Ac peak anymore. Hence, it was completely decomposed after Test 4 (merely a huge garbage peak with a few signals is visible). Note that the strong baseline noise and the randomly occurring spikes were due to the old age of the D2 lamp. The lamp was during this analysis only used for qualitative control samples, not for important quantitative evaluations anymore. Even the strong spike in the Inc-Ac elution area is not assignable to a peak signal. This was further verified by TLC analysis (see chapter 3.11.4). For further details see text.

### 3.11.3 Reaction Kinetic Model for the Decomposition of Incensole Acetate

In Fig 3.118 a diagram is given, which shows the decomposition of compound **23** (Inc-Ac) dependent on the time at  $T = 60\text{ °C}$  (Time dependent concentration levels were determined with the samples from the decomposition tests, see chapter 3.11.2). The decomposition follows a negative slope e-function and thus may be due to a first order reaction kinetic (see chapter 2.6.2 or literature, e.g. [173,174]). As rather probable, the only reaction partner may be oxygen (and/or perhaps Inc-Ac reactions with its own entity or derived decomposed entities catalysed by oxygen) due to the fact that oxygen is under normal conditions in excess available (ca. 20 % in the air). Hence, this assumption is reasonable.

Since the experiment primarily served to obtain the decomposition of Inc-Ac for a further pharmacological testing, no “real” kinetic study was implemented. Furthermore, the data presented here is only based on 4 experiments (Start concentration, two time dependent decomposed concentrations and no concentration, according to the chromatograms in Fig. 3.114-3.117) without any repetition and measurement in duplicate. For a more accurately kinetic study, the experiment should be repeated and developed more precisely. Additionally, the discontinuous time dependent concentration determination (HPLC-measurement and stop of the experiment for each measurement) is not optimal and thus may have been leading to some falsifications. However, since the data may be interesting for other scientists and research groups working in the field of chemical reaction velocities, the obtained data values are briefly discussed.

## Results and Discussion

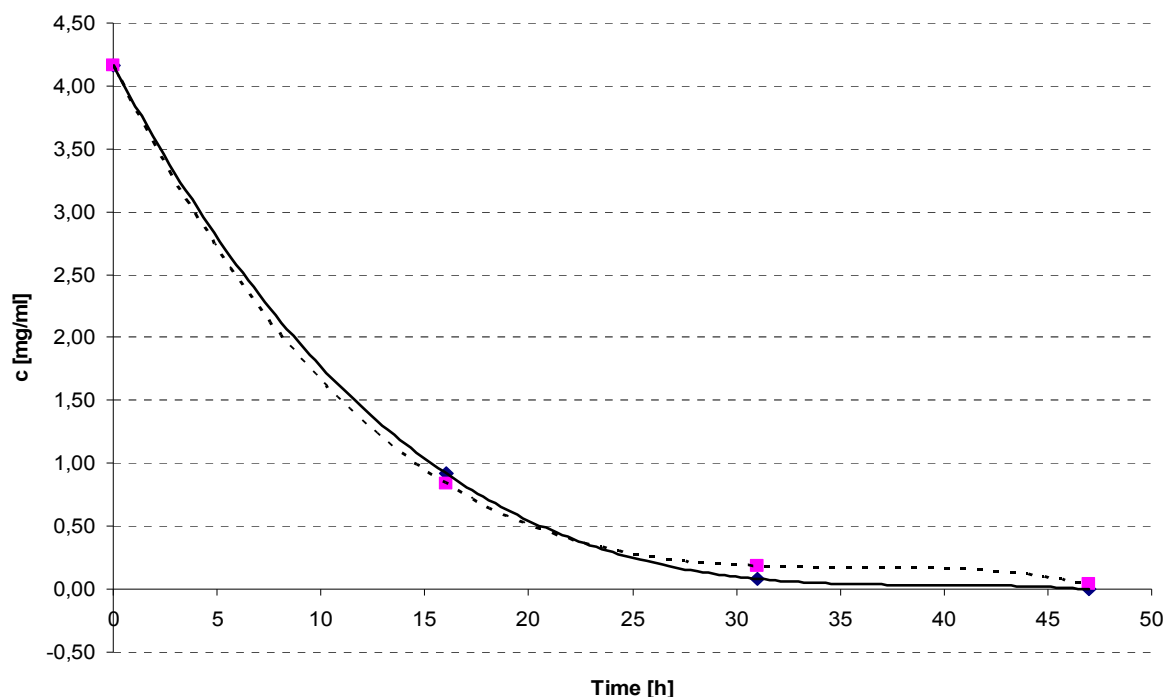


**Fig. 3.118** The experimental and theoretical calculated data points for the time dependent decomposition of compound **23** at  $T = 60\text{ }^{\circ}\text{C}$ . The rhombuses ( $\blacklozenge$ ) represent the measured data points (e-function drawn as straight line). The squares ( $\blacksquare$ ) represent the data points obtained by the equation  $c(A) = c_0(A) \times e^{-kt}$  (e-function drawn as dashed line, with  $k = 0.1$ ). As can be noticed, both data sets fit quite well. Thus, the assumption (first order kinetics) may be acceptable. For further details see text.

The corresponding linear model of the e-function from Fig. 3.118 is presented in Fig. 3.119. As noticeable, the theoretical assumption of a first order reaction kinetic seems to be fulfilled as the measured and calculated data points fit almost well. The great imprecision of the results is due to the fact that only two calculable measuring points were generated giving only two experimental values for the rate constant  $k$  ( $c = 0.92\text{ mg/ml}$  at  $t = 16\text{ h}$  and  $c = 0.08\text{ mg/ml}$  at  $t = 31\text{ h}$ , giving  $k = 0.09$ , respectively,  $k = 0.13$ ). For calculations with these two differing values of  $k$ , they have been set to one significant digit ( $k \approx 0.1$ ).

**Tab. 3.32** The numeric data for the time dependent decomposition of Inc-Ac at  $T = 60\text{ }^{\circ}\text{C}$  according to the first time law described in chapter 2.6.2. The data has been obtained by the HPLC quantitation results given in Fig. 3.114-3.117 in chapter 3.11.2. The obtained reaction constant  $k$  is rounded to one significant digit ( $k = 0.1$ ), since the precision of the experiment carried out has not been very exact.

Experimental Data				
Peak Area (HPLC)	70846560	15664266	1423398	0
$c$ [mg/ml] $\blacklozenge$	4.17	0.92	0.08	0
$t$ [h]	0	16	31	47
$\ln c$	1.43	-0.08	-2.49	
Calculated Data				
e-fkt $\blacksquare$	4.17	0.84	0.19	0.04
$t$ [h]	0	16	31	47
$\ln c$ (calculated with $k \approx 0.1$ )	1.43	-0.17	-1.67	-3.27
$k$ constant [1/h]		0.09 ( $\approx 0.1$ )	0.13 ( $\approx 0.1$ )	

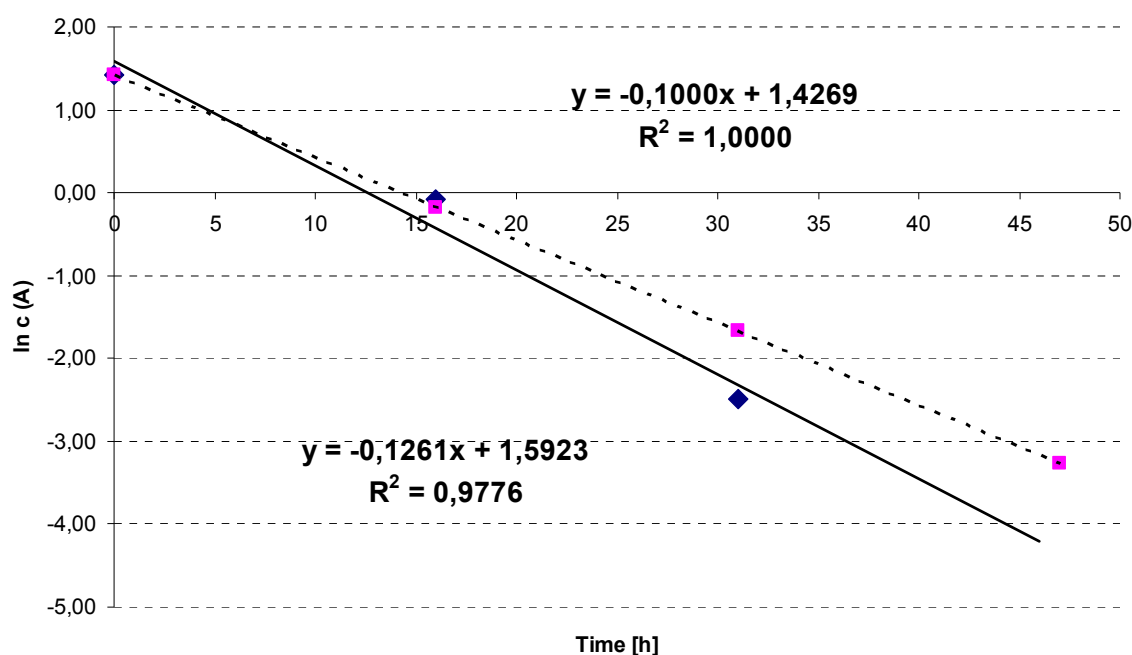


**Fig. 3.119** The linear regression model for the decomposition experiments of compound **23** (Inc-Ac) at  $T = 60\text{ }^{\circ}\text{C}$ . The rhombuses ( $\blacklozenge$ ) refer to the measured data ( $y = -0.1261x + 1.5923$ ; straight line) and the squares ( $\blacksquare$ ) refer to the theoretical calculated values with  $k = 0.1$  ( $y = -0.1x + 1.4269$ ). The data points follow approximately ( $R^2 = 0.98$ ) the theoretical presumed equation model,  $\ln c(A) = -k \times t + \ln c_0(A)$ . Though the experimental values are quite imprecise, the model fulfils within a defined precision the equation specification of a first order kinetic time rate. For further details see text.

According to the linear regression models given in Fig. 3.119, this approximation may be within a reliable accuracy. Though the value of  $k$ , referring to the experimental data, is more probable greater than 0.1 (see equation in Fig. 3.119 with  $k = -0.1261$ , giving a better fit to the real data set). At last and as discussed before, the experimental data set is too small for an unambiguous verification of the reaction kinetic model, but is most likely, based on the theoretical presumption (decomposition by oxygen, which is present in excess) and the approximately good fit, the model of choice (“pseudo”-first order).

#### 3.11.4 Qualitative TLC Analysis of the Decomposition Products

The quantitative discussion about decomposition of Inc-Ac (**23**) can be also made qualitatively by TLC analysis. For evaluation, the standard NP-TLC method has been used as described in chapter 2.3.1. The corresponding TLC results are declared in Fig 3.120. Each row there is explained and must be only compared with the corresponding chromatograms in Fig. 3.114-3.117 in chapter 3.11.2. As shown in the NP-TLC chromatograms, any decomposition product has a smaller  $R_f$ -value than Inc-Ac (**23**). Hence, every decomposition product is conclusively more polar than compound **23** and most likely an oxidation product originating from it. Further evidence for this assumption may be given, if hyphenated LC-MS and/or GC-MS experiments are conducted with these decomposed samples.

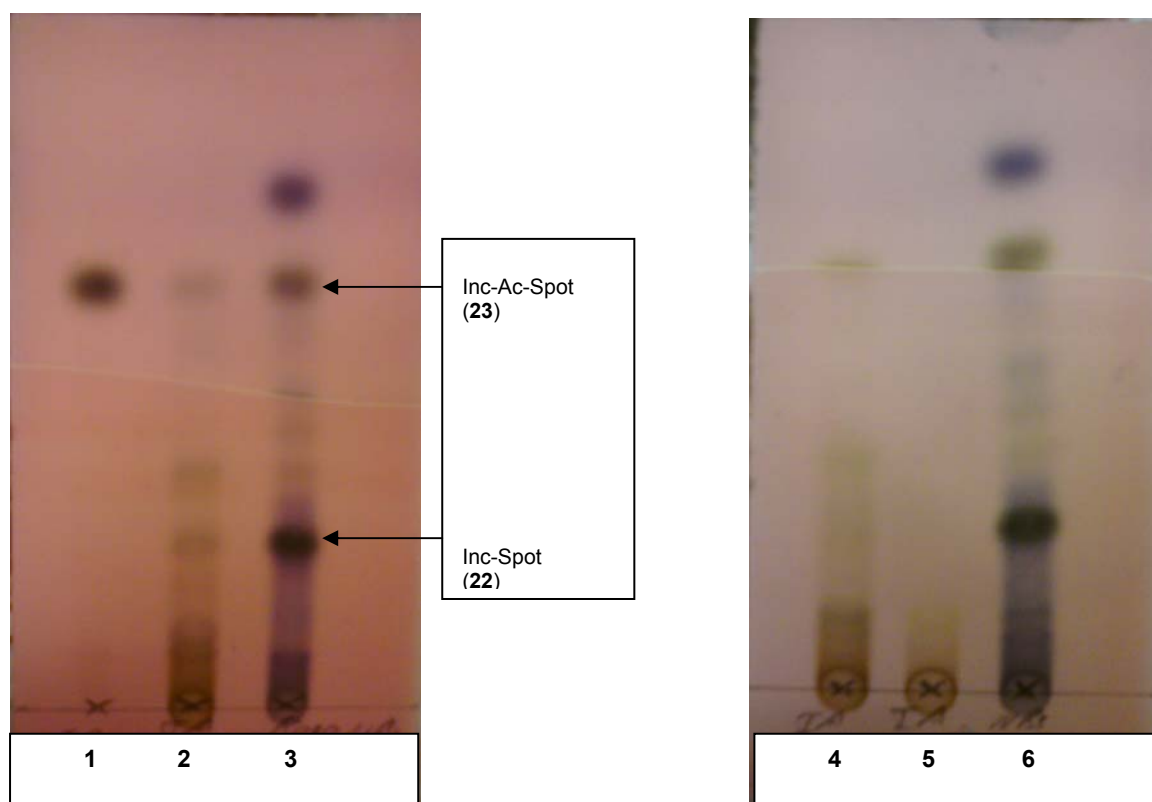


**Fig. 3.120** Two different TLC chromatograms (NP). From left to right: 1 = pure Inc-Ac (strong brown spot > 99 % by HPLC; compare with Fig. 3.114); 2 = decomposed Inc-Ac (Inc-Ac  $\approx$  20 %; compare with Fig. 3.114); 3 = NB fraction of Bpap (for comparison of  $R_f$ -values); 4 = decomposed Inc-Ac (Inc-Ac  $\approx$  15 %; compare with Fig. 3.115); 5 = completely decomposed Inc-Ac (compare with Fig. 3.117); 6 = NB fraction of Bpap. For further details see text.

### 3.12 Pharmacological Results

In this chapter the pharmacological results for the mPGES1-Assay (cell-free) are presented. The data shown here is representative for Inc-Ac (**23**), respectively, its decomposition products which have been basically responsible for the inhibition activity. Additionally, the data for the three isolated compounds from Fr. 9 (see chapter 3.1.1.3) and two of their single compounds (**18** and **19**) in differing concentration combinations are shown. According to the theory of synergy [149,150] the results presented here may be quite interesting.

#### 3.12.1 mPGES-1-Results for Incensole Acetate and its Decomposition Products

The data for the cell free assay from Inc-Ac (**23**) is explicitly discussed here. The crucial step for the investigation of the decomposed Inc-Ac fractions (see chapter 3.11.2) had been the fact that only the first evaluated batch of Inc-Ac showed an inhibitory effect on the mPGES-1 enzyme. The following tested batches from Inc-Ac paradoxically did not reveal anymore any inhibitory activity. Thus, the first active batch was re-analysed by HPLC (see chapter 3.11.2) and NMR ( $^1\text{H}$  and  $^{13}\text{C}$ ; data not shown) and exhibited a decomposed mixture of several unknown compounds originating from Inc-Ac. Hence, the previously purified and intact Inc-Ac batch was probably decomposed during the transport. The reason for the decomposition of

## Results and Discussion

this first batch could not be determined anymore. Subsequently, compound **23** was artificially decomposed as it is described in chapter 3.11.2, and the decomposed fractions were compared with another intact batch from compound **23** in order to evaluate their pharmacological activity again. The results are presented in Tab. 3.33 and in Fig. 3.121. Interestingly, if the first analysed batch (compound **23**) was still intact, the results with the decomposed mixtures probably would not have been recognised. Note that the discussion given here for compound **23** is also valid for compound **22** (incensole). For compound **22** a similar behaviour was observed (data not explicitly shown here). Only the decomposed batches revealed inhibitory effects.

**Tab. 3.33** The inhibition of mPGES-1 activity in microsomal preparations of IL-1 $\beta$ -stimulated A549 cells (see chapter 2.5) for each tested sample. **EC1**: First active batch, decomposed (during transport to Tübingen), with 6.4 % (g/g) Inc-Ac; **EC2**: Totally decomposed sample with 0 % (g/g) Inc-Ac; **EC-16h**: Decomposed sample (after 16 h at 60 °C) with 40 % (g/g) Inc-Ac; **Inc-Ac pure**: intact sample of Inc-Ac (purity > 99 %). See also chapter 3.11.2 for the corresponding chromatograms. Concentration levels: 0, 1, 10 and 30  $\mu$ M, respectively,  $\mu$ g/ml. Remaining activity is given in %. For further details see text.

Nominal c (HPLC)	6.4 % (g/g)	0 % (g/g)	40 % (g/g)	99% (g/g)
	<b>EC1 [<math>\mu</math>M]</b>	<b>EC2 [<math>\mu</math>g/ml]</b>	<b>EC-16h [<math>\mu</math>g/ml]</b>	<b>Inc-Ac pure [<math>\mu</math>M]</b>
<b>Concentration</b>	<b>remaining activity</b>	<b>remaining activity</b>	<b>remaining activity</b>	<b>remaining activity</b>
	<b>[%]</b>	<b>[%]</b>	<b>[%]</b>	<b>[%]</b>
<b>0</b>	100.00	100.00	100.00	100.00
<b>1</b>	86.62	92.60	60.39	99.03
<b>10</b>	22.52	24.12	12.71	100.81
<b>30</b>	9.87	11.41	8.04	103.68

As noticeable, the intact Inc-Ac sample does not inhibit the enzyme at any concentration level. In contrast, the decomposed samples EC1 (6.4 % Inc-Ac), EC2 (40 % Inc-Ac) and even the total decomposed sample EC2 (0 % Inc-Ac) did show a significant inhibition in the mPGES-1-Assay. These findings prove that Inc-Ac has been definitely not responsible for the observed bioactivity. Unfortunately, it could not be determined if there is a single chemical entity responsible for the inhibition, since every decomposed sample revealed an uncountable amount of peak signals. These signals seem to literally knock out the enzyme activity without any specific inhibition mechanism. However, to exactly detect how the inhibition works under these circumstances, it would be necessary to isolate every molecular compound from the complex mixture. Hitherto, this seems to be an impossible task. Additionally, there is nothing known about the stability of the decomposition products, since they are generated randomly and no specific degradation product or route has been observed. Perhaps by HPLC-SPE-NMR hyphenation techniques and/or by additional mass spectrometric detection further evidence on the molecular composition may be achievable. However, it is questionable if this is worth the huge effort which may be necessary to clarify these elusive findings.

The discussion here should at least declare that every result should be treated with great caution, as compound **23** was before, after testing of the first batch (EC1), held for an

mPGES-1 bioactive entity, and further tests with complete cell-systems etc. had been already carried out. The results of a few other cell-assays with the decomposed products from Inc-Ac are presented in Tab. 3.34. Based on these results it was finally concluded that Inc-Ac (**23**) itself does not show any inhibitory action in any of these evaluated assays.

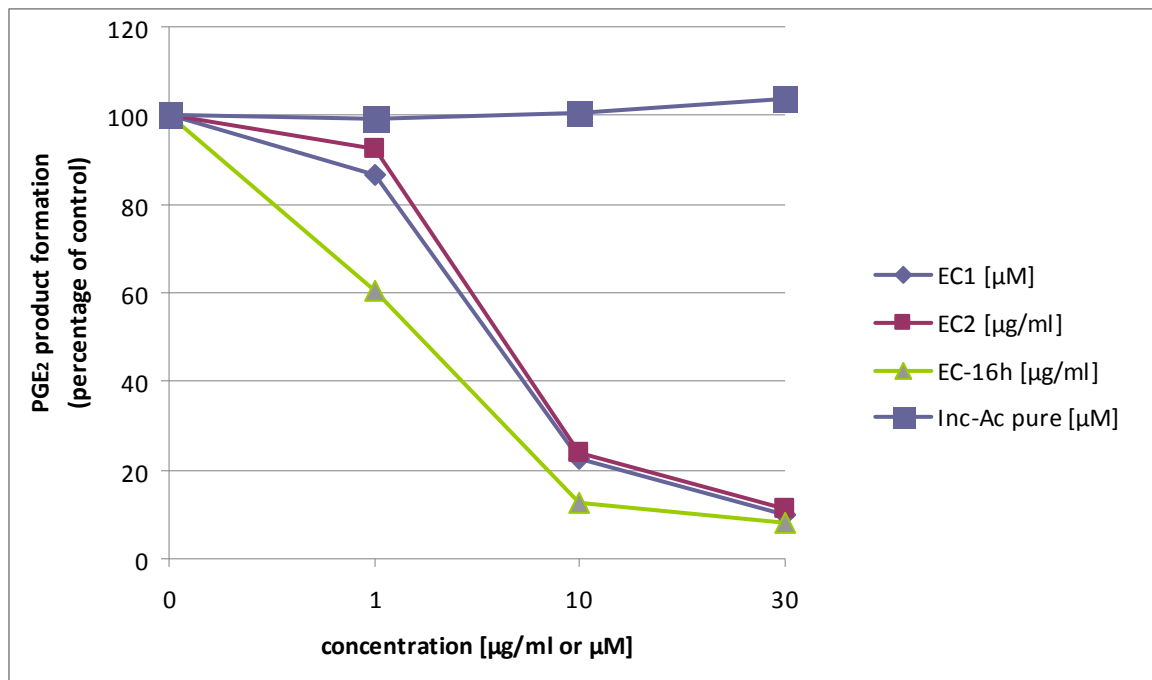


**Fig. 3.121** The graphic referring to Table 3.33. As discussed, the pure and intact Inc-Ac sample does not reveal any inhibitive activity in the cell-free mPGES-1-Assay. Only the decomposed samples affect the enzyme inhibitive. For further details see text.

If this is further proof on synergistic effects, as reported by Berenbaum [149] or Wagner and Ulrich-Merzenich [150] can not be verified by the results given here. There occur definitely too many molecular entities in the samples to reasonably substantiate this theory. Nevertheless, tests applied with cellular systems (LPS-stimulated monocytes and IL-1 $\beta$ -stimulated A549 cells etc.) did show some inhibitory actions for the decomposition products of Inc-Ac and Inc as presented in Tab. 3.34.

## Results and Discussion

**Tab. 3.34** The results ( $IC_{50}$ ) for further other biological assays with the decomposed samples from Inc-Ac (**23**) and Inc (**22**). The data is obtained from the working group of Oliver Werz in Tübingen, Germany [172] and is only valid for the decomposed Inc-Ac, respectively, Inc samples. For further details see text. For clarification see also chapter 1.5 on pharmacology.

<b>mPGES-1 activity in LPS stimulated monocytes</b>		
Inc-Ac <sup>decomposed</sup>	no effect	
Inc <sup>decomposed</sup>	no effect	
<b>5-Lipoxygenase cell-free (purified from E. coli)</b>		
Inc-Ac <sup>decomposed</sup>	23 $\mu$ M	
Inc <sup>decomposed</sup>	58 $\mu$ M	
<b>5-LO activity; PMNL; stimulated with AA [20 <math>\mu</math>M] + A23187 [2,5<math>\mu</math>M]</b>		
Inc-Ac <sup>decomposed</sup>	24 $\mu$ M	
Inc <sup>decomposed</sup>	33 $\mu$ M	
<b>5-LO activity; PMNL; stimulated with A23187 [2,5<math>\mu</math>M]</b>		
Inc-Ac <sup>decomposed</sup>	> 50 $\mu$ M	
Inc <sup>decomposed</sup>	23 $\mu$ M	
<b>COX-1 in human platelets</b>		
Inc-Ac <sup>decomposed</sup>	100 $\mu$ M	
Inc <sup>decomposed</sup>	> 100 $\mu$ M	
<b>COX-2 in A549 cells</b>		
Inc-Ac <sup>decomposed</sup>	22 $\mu$ M	
Inc <sup>decomposed</sup>	no effect	
<b>Phospholipase-A2 (cPLA2); cell-free</b>		
Inc-Ac <sup>decomposed</sup>	no effect	
Inc <sup>decomposed</sup>	no effect	
<b>whole blood (5h)</b>		
Inc-Ac <sup>decomposed</sup>	no effect	Note: Assay is vulnerable to errors. Even the controls did not reveal any inhibitory effect [172].
Inc <sup>decomposed</sup>	no effect	

In addition to the results of Moussaieff et al. [87,145-147], who revealed for Inc (**22**) and Inc-Ac (**23**) a few biological activities, these may be some interesting findings. The question may be thus, if perhaps their results are also merely based on the decomposition of Inc (**22**) and Inc-Ac (**23**). In the review by Moussaieff and Mechoulam in 2009 they report on the inhibition of COX-2 with a significant effect at 60  $\mu$ M (denoted as unpublished data in their publication) [108]. Additionally, in the paper of cerebral ischemic injury protection in mice by Inc-Ac (**23**) [147], it is stated that the Inc-Ac (**23**) plasma levels were analogously measured with LC-MS as reported by Gerbeth et al. [144]. However, Gerbeth et al. only measured the plasma levels of compounds **1-6** ( $\beta$ -KBA,  $\beta$ -AKBA,  $\alpha/\beta$ -BA and  $\alpha/\beta$ -ABA) in the ESI-negative mode (due to the COOH-function) and nothing is said about the detection of Inc-Ac (**23**) by LC-MS in their paper. In the positive mode merely  $\beta$ -KBA and  $\beta$ -AKBA seem to be able to catch a proton (unpublished data [191], or see also the LC-MS/MS paper by Reising et al. [192]).

Consequently, a paper on the LC-MS quantification and ionization probabilities of Inc (**22**) and Inc-Ac (**23**) is still lacking thus far.

As a consequence, further tests should be carried out to evaluate the real potential of Inc (**22**) and Inc-Ac (**23**), since according to the findings given here merely their decomposed mixtures were bioactive.

### 3.12.2 mPGES-1-Results for Compound 18 and 19 in Differing Compositions

The data for the cell free mPGES-1-assay from the isolated fraction E2h 6.6 (see also chapter 3.1.1.3), including compound **18**, **19** and a further yet not known compound (1 isomer; 16 % HPLC), is demonstrated in Tab. 3.35 and graphically depicted in Fig. 3.122. Interestingly, the inhibitory efficiency decreased the purer compound **18** became (Note: relative peak areas in % are given in parentheses behind each compound, see Tab. 3.35).

**Tab. 3.35** Comparison of the inhibition of mPGES-1 in microsomal preparations of IL-1 $\beta$  stimulated A549 cells (see chapter 2.5) for different compound combinations of the isolated peak group from fraction E2h 6.6. The samples were purified by prep. HPLC and hence leading to the randomly different rel. peak area percentages (shown in parentheses). Inhibition concentrations are given in  $\mu\text{g/ml}$ , the arithmetic mean of the remaining activity in %, the standard deviation (S.D., also in %) with three measurements for each concentration ( $n = 3$ ) and the Standard-Error in %. For further details see text.

Sample	Conc. [ $\mu\text{g/ml}$ ]	Remaining activity [%] ( $n = 3$ )	S.D.	Standard-Error
$\alpha$ -Ac-7,24-dien-TA	10	20.56	4.64	2.68
(96 % HPLC) +	3	31.77	4.56	2.63
$\beta$ -Ac-8,24-dien-TA	1	41.46	5.78	3.33
(4 % HPLC)	0.3	64.61	7.25	4.18
	0.1	81.11	4.88	2.81

Sample	Conc. [ $\mu\text{g/ml}$ ]	Remaining activity [%] ( $n = 3$ )	S.D.	Standard-Error
$\alpha$ -Ac-7,24-dien-TA (76 % HPLC)	10	25.22	8.01	4.63
+ $\beta$ -Ac-8,24-dien-TA (24 % HPLC)	1	41.09	4.52	2.61

Sample	Conc. [ $\mu\text{g/ml}$ ]	Remaining activity [%] ( $n = 3$ )	S.D.	Standard-Error
E2h Fraction 6.6	10	15.82	6.28	3.63
$\alpha$ -Ac-7,24-dien-TA (46 % HPLC) +	3	13.73	3.18	1.84
$\beta$ -Ac-8,24-dien-TA (32 % HPLC) +	1	13.38	3.89	2.25
1 Isomers	0.3	32.11	6.20	3.58
(16 % HPLC)	0.1	75.03	11.17	5.59
	0.03	97.30	11.60	6.70

The most potent results were obtained with the E2h Fraction 6.6, which consisted of a mixture of compound **18** and **19** and the hitherto unknown compound with a probably similar structure (perhaps also an acetylated tirucallic acid?).

## Results and Discussion

Thus, these results seem to confirm the theory on synergy effects stated by Berenbaum [149] and highly debated by Wagner and Ulrich-Merzenich [150]. In both articles it is discussed how different chemical entities in combination may enhance or, vice versa, diminish the bioactivity of a certain compound. According to the discussions there, the inhibition of mPGES-1 is enhanced in the example given here, at least in the cell-free assay. However, the data presented just delivers results with the almost purified enzymes. In whole cell systems completely different results could be obtained. Several reasons therefore are known (Cell permeability, other target enzymes, etc.). Furthermore, in animal or human models the hepatic metabolism of compounds has to be taken into account and even if single cells get inhibited, these results can generally not be extrapolated to more complex organisms [94]. The pharmacological results reported in this work may just clarify the complexity of inhibition mechanisms, not to mention how complex an Olibanum extract may affect several targets in the human body when used as oral administration form. At last, the results reported here may encourage other research groups for further examinations of such phenomena.

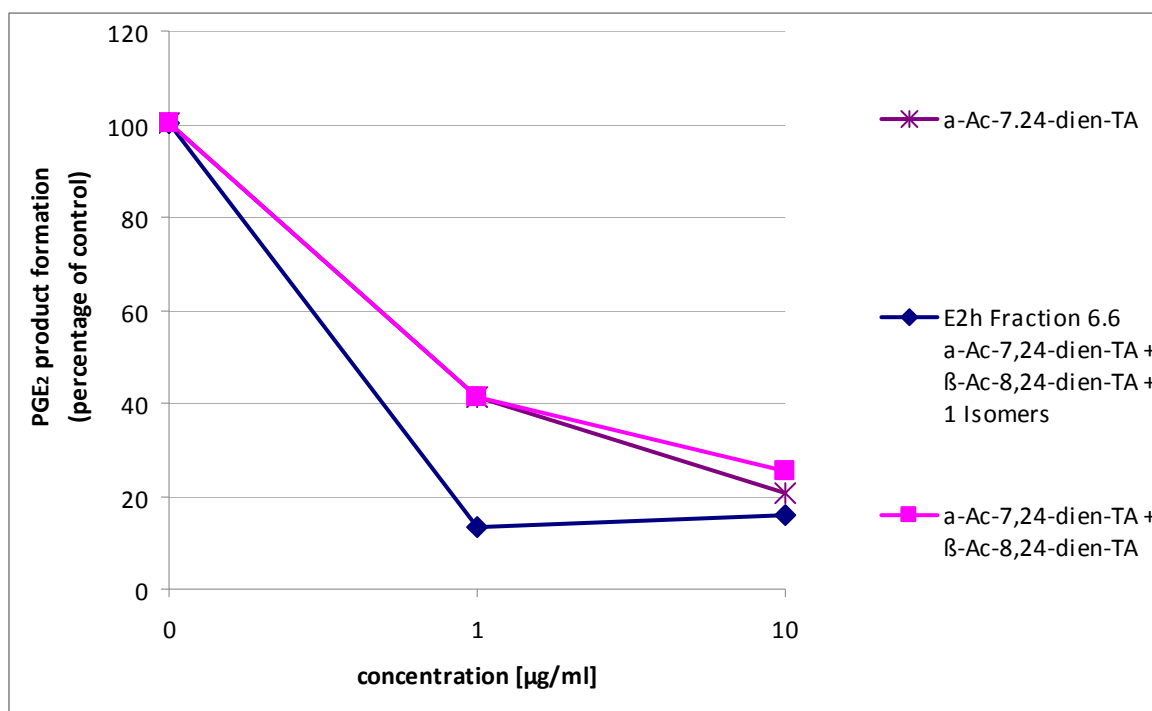


**Fig. 3.122** The graphical depiction of the results in Tab. 3.34 for the concentration levels of 1 and 10 µg/ml. Very interesting is the strong inhibition activity for E2h Fraction 6.6 (α-Ac-7,24-dien-TA + β-Ac-8,24-dien-TA + 1 isomer) at  $c = 1$  µg/ml (ca. 13 % remaining activity of the enzyme), while at this conc.-level (1 µg/ml) the other two combinations still deliver a remaining activity of ca. 40 %. At  $c = 10$  µg/ml the values converge again. For further details see text.

### 3.13 Biosynthetic Pathway Proposal

According to the obtained HPLC quantitation data (see chapter 3.8) and qualitative TLC data (see chapter 3.4) a hypothesis on the different particularities of the biosynthetic pathways for the three species Bpap, Bser and Bsac, respectively, Bcar is given here. Generally, specific pentacyclic biomarkers for Olibanum species are definitely the boswellic acids, at least verified for Bpap, Bser and Bsac/Bcar where they are detectable in huge quantities. Besides, there occur the tirucallic acids in great quantities and the lupeolic acids in minor quantities compared with the other biomarkers (BAs and TAs). The data is qualitatively summarised in Tab. 3.36 to present an overview on the characteristic amounts determined in the corresponding species.

Interestingly, the great quantities of BAs and ABAs found in Bsac/Bcar in combination with always greater amounts of LAs (LA and Ac-LA), compared with Bpap and Bser, lead to the conclusion for Bsac/Bcar that this biological pathway is strongly expressed. Another interesting fact is that simultaneously the TA contents are rather low compared with Bpap and Bser, which both instead revealed always quite high tirucallic acid contents. As both pentacyclic acids, the BAs and TAs, are probably derived from two different cyclisation reaction directions of 2,3-epoxysqualene [31,193], it seems that these two ways are differently expressed in the species Bsac/Bcar and, respectively, Bpap and Bser. Thus, the production of TAs is probably stronger expressed in the species Bpap and Bser, while for Bsac/Bcar the synthesis of LAs and hence BAs seems to be superior, holding the synthesis of TAs in this species on a quite low level. This fact is additionally substantiated as for Bsac/Bcar the second chromatography dimension is unnecessary for the quantitation of compound **3** ( $\beta$ -BA), since the two acetylated TAs, compound **18** and **19**, are only minimally detectable (see also chapter 3.7.5).

**Tab. 3.36** Comparison of the quantities (HPLC) of some specific biomarkers in the species Bpap, Bser and Bsac/Bcar. Boswellic acids (BAs and ABAs); Tirucallic acids (All TAs); Lupeolic Acids (LA and Ac-LA).  $\beta$ -KBA and  $\beta$ -AKBA are not taken into account in the table here. For further details see text.

+++ : Great quantity; ++ : Average quantity; + : detectable; - : not detectable.

	Specific Triterpenes			Specific Diterpenes			Sesquiterpenes	
	Boswellic Acids	Tirucallic Acids	Lupeolic Acids	Inc	Inc-Ac	Serratol	$\alpha$ -Humulene	$\beta$ -Caryophyllene
Bpap	++	++	+	+++	++	-	-	-
Bser	+++	++	+	+	-	++	-	-
Bsac	+++	+	++	+	-	++	+	+
Bcar	+++	+	++	+	-	++	+	+

The synthesis of specific diterpenes such as serratol is probably given for all species. Quite interesting is that Bser and Bsac/Bcar reveal relatively great quantities of serratol and to a lesser amount incensole, which has been additionally detectable as it is reported to be derived from serratol [82]. For Bpap, serratol has not been significantly detectable. Instead,

Bpap revealed the greatest quantities of incensole (see chapter 3.8). Furthermore, incensole acetate, as the product molecule of incensole, has been only detectable in the species Bpap during this work. The other species, Bser and Bsac/Bcar, did not reveal incensole acetate, at least not in easily detectable quantities (HPLC-UV or TLC). Thus, it seems that only the species Bpap possesses a highly active specific enzyme expression for the acetylation of incensole.

The existence of  $\alpha$ -humulene and especially  $\beta$ -caryophyllene in the species Bsac/Bcar, give evidence on a higher regulated expression of enzymes for the biosynthesis of these ubiquitous sesquiterpenes in *Olibanum Somalia* and *Oman/Yemen*. These two sesquiterpenes are quite probably very specific for Bsac and Bcar samples as similar conclusions have been already reported in the literature [13,74,184].

### 3.13.1 Proposal of the Specific Biosynthesis Pathways

In the following the probable biogenetic synthesis pathways of some of the specific biomarker molecules in Bpap, Bser and Bsac/Bcar are described. Since there is nothing about the isolation and structural elucidation of specific enzymes from boswellic species published hitherto, the pathways presented here are merely based on the determination of their quantities (HPLC), and thus are only hypothetical. For an unambiguous clarification of the hypothesis given here, experiments with the plants itself may be implemented. However, since only the air-dried gum exudates and not the plants itself were accessible, the theory given in this work may be confirmed or disproved by experiments with the plants and biological extracts thereof. Therefore, the parts of the plants (e.g. the bark), where those specific enzymes are supposed to be located, must be extracted and biological tests may be implemented proving the occurrence and/or existence of a specific enzyme by investigations with specific precursor molecules (e.g. for an acetyl-transferase, acetyl-CoA and unacetylated precursors may be added, such as LA, incensole or  $\alpha$ - and  $\beta$ -BA).

A good example of this approach is given in the publication of Schmidt et al. [194] where two highly specific enantioselective germacren-D-synthases have been detected by adding specific precursor molecules to subsequently purified plant extract fractions.

However, since there was no real frankincense plant material for further investigations available, the pathways presented here are based on the experimental data obtained during this work and a hitherto merely a presumption.

#### 3.13.1.1 Sesquiterpenes

As depicted in Fig. 3.123, the ring closure of C-1 and C-11 of farnesane produces the 11 membered skeleton of a class of monocyclic sesquiterpenes called humulanes. The further C-2 and C-10 closure leads to an additional cyclobutane ring and gives the caryophyllane type skeletons [31]. This probably universal pathway seems to be highly expressed in the *Boswellia* species Bsac and Bcar, respectively. In the species Bpap and Bser they were not detectable in similar quantities (see also HPLC chromatograms in chapter 3.7).

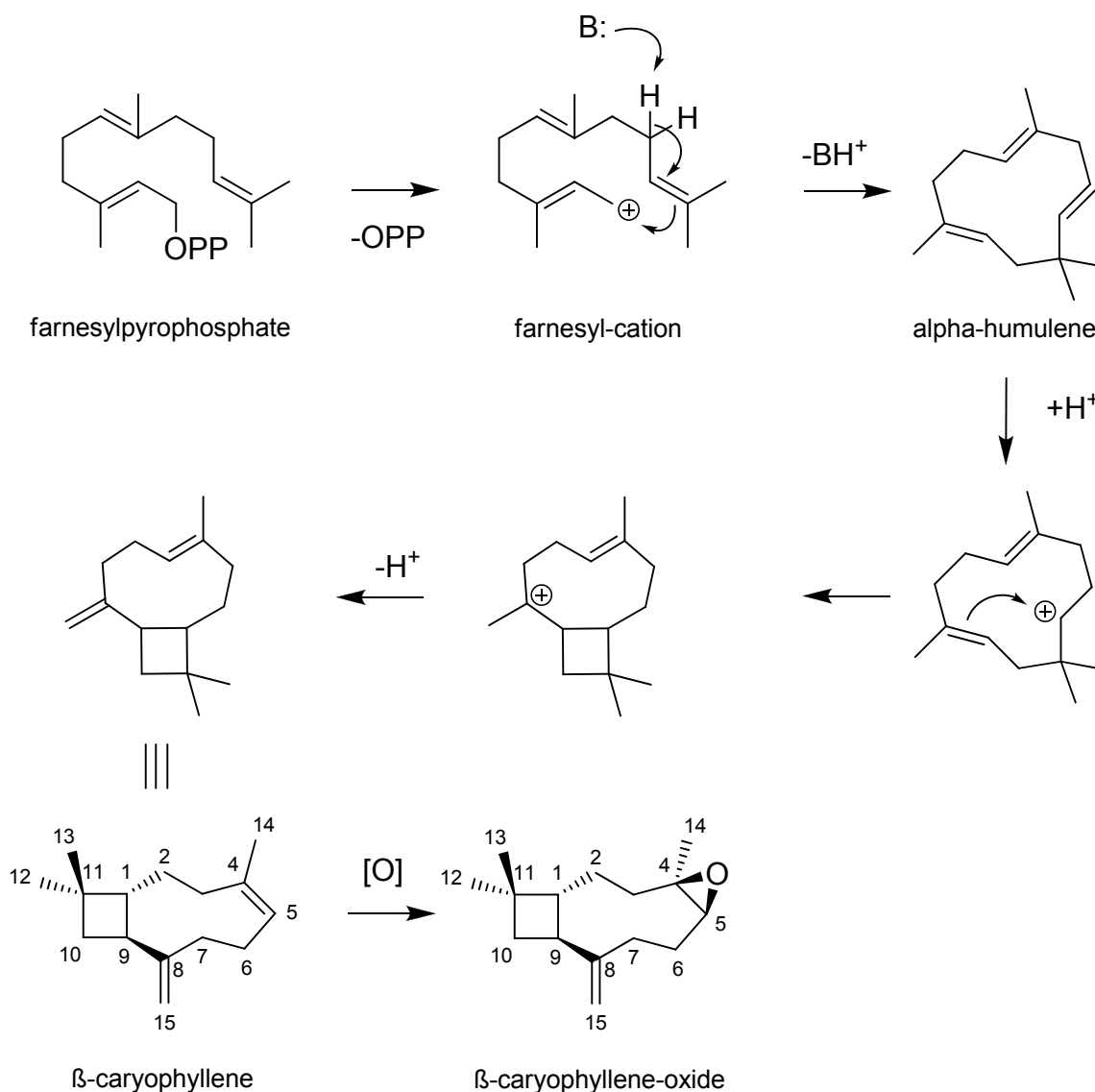


**Fig. 3.123** Biosynthesis route for  $\alpha$ -humulene and  $\beta$ -caryophyllene.  $\beta$ -caryophyllene-oxide is probably the product of the air caused oxidation of  $\beta$ -caryophyllene [177]. For further details see text.

### 3.13.1.2 Diterpenes

The 1,14-cyclisation of geranylgeranylpyrophosphate via an allylic cation intermediate state leads to the biosynthesis of the 14-membered skeleton of 3,7,11,15-cembratetraene, also known as cembrene A [31]. Cembrene A, respectively, cembrene C, are thus probably the precursors of iso-serratol and serratol. Serratol, as reported by Klein and Obermann [82], is the precursor of incensole and thus its acetate. The basic biogenesis route is shown in Fig. 3.124. Though incensole has been also detectable in samples from Bser and Bsac/Bcar, its acetate was merely detectable in samples from Bpap. Furthermore, serratol and iso-serratol, which were easily detected in samples of Bser and Bsac/Bcar, have not been detectable in Bpap (see also HPLC chromatograms in chapter 3.7 and TLC chromatograms in chapter 3.4). Quite astonishing has been the fact that samples of Bpap contain incensole and incensole acetate in quite high quantities. Approximately 30-40 % of the neutral fraction

mass refers to them (**22** and **23**; see also chapter 3.8). On the other hand, samples of Bser and Bsac/Bcar reveal rather great amounts of neutral tetra- and pentacyclic triterpenes, which is especially deducible if the chromatograms in chapter 3.7 are considered. There, neutral extract samples of Bser and Bsac/Bcar showed more lately eluting peak signals than samples of Bpap. This could also explain their solution properties already reported [11]. An Et<sub>2</sub>O-extract of Bpap was easily dissolvable in MeOH, whereas the Et<sub>2</sub>O extracts of Bser and Bsac/Bcar gave a white dim and colloidal solution when dissolved in MeOH again.

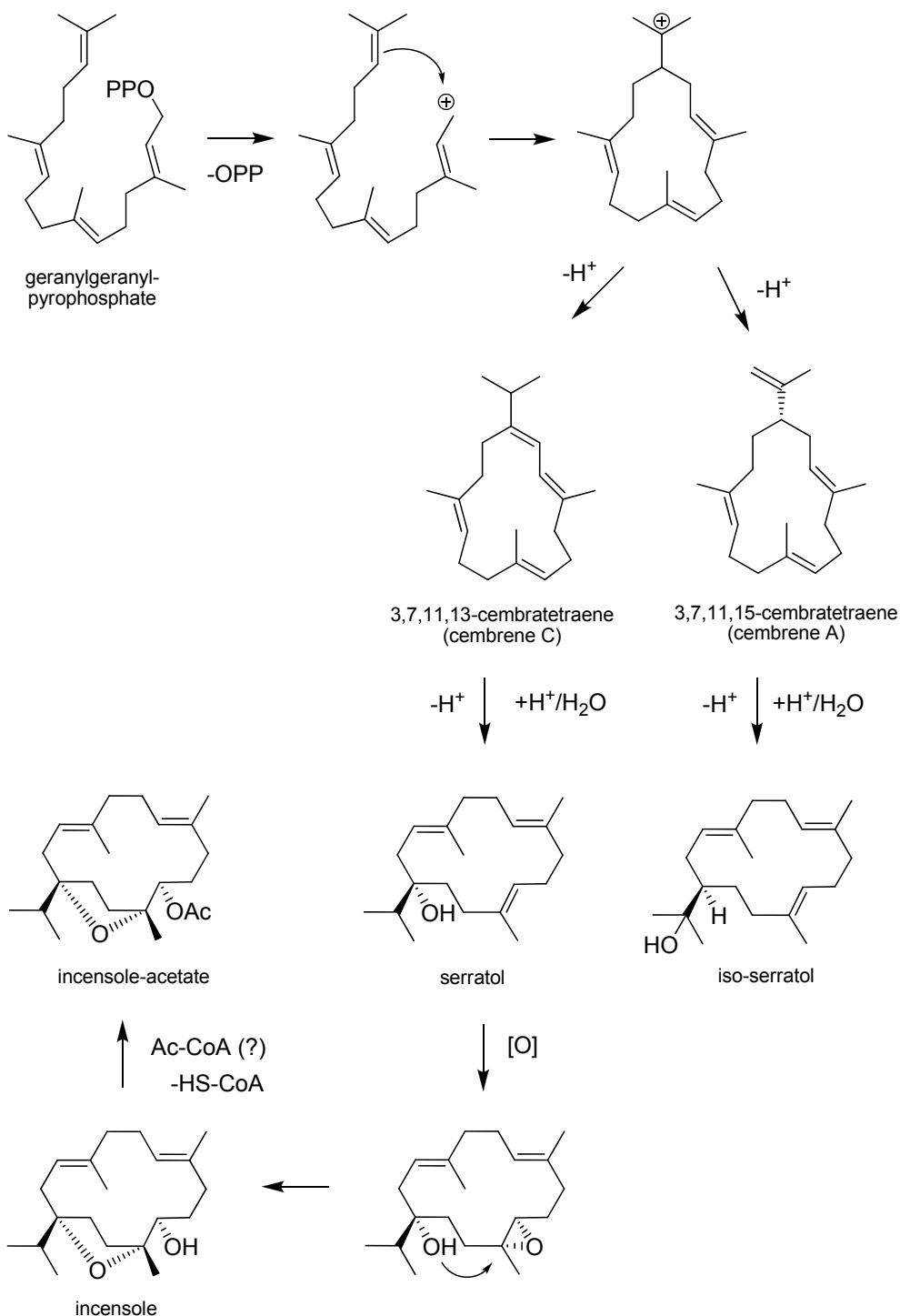


**Fig. 3.124** Biosynthesis route for serratol, iso-serratol, incensole and incensole acetate. For further details see text.

### 3.13.1.3 Tetra- and Pentacyclic Triterpenes

The biosynthetic precursor of tetracyclic triterpenes of the gonane type is 2,3-epoxysqualene leading via synthesis of dammarane type molecules to the synthesis of tirucallane type molecules, most likely the precursors of the tirucallic acids.

Production of pentacyclic triterpenes from the bacharane type is also based on another cyclisation of 2,3-epoxysqualene, which leads to the synthesis of baccharane type molecules, the precursor of the lupanes and thus most probably of the oleanane and the ursane type molecules [31,193]. Finally, these represent the lupeolic and boswellic acids in the *boswellia* species.

Interestingly, each species, beginning from 2,3-epoxysqualene reveals different priorities for the synthesis of their specific biological compound composition. As mentioned, Bpap and Bser reveal great quantities of TAs (compounds **13-19**), whereas Bsac/Bcar shows huge amounts of BAs (compounds **1-4**) and additionally the LAs (compounds **11** and **12**). The existence of, on average, the greatest quantities of  $\beta$ -AKBA (compound **6**) and 11-OH- $\beta$ -ABA (**7**) in Bpap and in the same time, the lowest amounts of BAs (**1-4**), may declare that  $\beta$ -AKBA is the final product of this enzyme reaction cascade.

Furthermore, when high levels of BAs (**1-4**) have been found in Bsac/Bcar, the levels of  $\beta$ -KBA and  $\beta$ -AKBA (**5** and **6**) were comparably low (as shown in the chromatograms of the HPLC quantitation in chapter 3.7.4, compare Fig. 3.102 with 3.103). Contrary, when the  $\beta$ -AKBA or  $\beta$ -KBA and even 11-OH- $\beta$ -ABA contents (**5**, **6** and **7**) in Bsac/Bcar were greater as expected, the amounts of BAs (**1-4**) were rather low (see also discussion on HPLC results in chapter 3.7.4). Thus, probably depending on the environmental conditions, the pathways are differently expressed. The highest amounts of  $\alpha$ -BA and  $\beta$ -BA (**1** and **3**) in the species Bser may be explainable through the low biosynthesis levels of  $\beta$ -KBA and  $\beta$ -AKBA (**5** and **6**), as for this species the levels of these two most likely biosynthesis end products (**5** and **6**) are rather low. The hypothetical biosynthesis pathways are given in Fig. 3.125 for the tirucallic acid synthesis and in Fig. 3.126, respectively, Fig. 3.127, for the lupeolic and boswellic acid synthesis.

As can be seen in Fig. 3.125 the biosynthesis of the tirucallic acids may begin with the protonation of an 2,3-epoxysqualene. After cyclisation of 2,3-epoxysqualene to the corresponding dammarane (a;  $3\alpha$  or  $3\beta$ ), it converts probably into an apotirucallane by a concerted migration of the hydrid (C-17 to C20) and of the methyl group C-18 from C-14 to C13 (b). The methyl-shift (C-30 methyl from C-8 to C14), consequently followed by elimination of the proton at C-9, giving the double bond (C-8 with C-9), converts it into tirucallane (step c). This step may be catalysed enzymatically (base = B:, which abstracts the proton at C-9, giving B<sup>+</sup>-H, as depicted in Fig. 3.125). The final steps for the biosynthesis of  $3\beta$ -OH-8,24-dien-tirucallic acid may be then the C-H activation at C-21, probably by in plants universally occurring Cytochrome P450 enzymes [19] and further oxidation to a COOH-function (step d). The same reaction pathway may be valid for the biosynthesis of  $3\alpha$ -OH-8,24-dien-tirucallic acid. There, only the conformation of the epoxysqualene cation is different, which leads to an  $\alpha$ -configured hydroxyl function. By another oxidation the secondary alcohol function of both 8,24-dien-tirucallic acids at C-3 is probably converted into 3-oxo-8,24-dien-tirucallic acid (step e). However, the pathway presented here is merely a

## Results and Discussion

hypothetical model based on the publication of Cotterell et al. [62], the book of Breitmaier [31] and the review by Ikuro Abe [193].

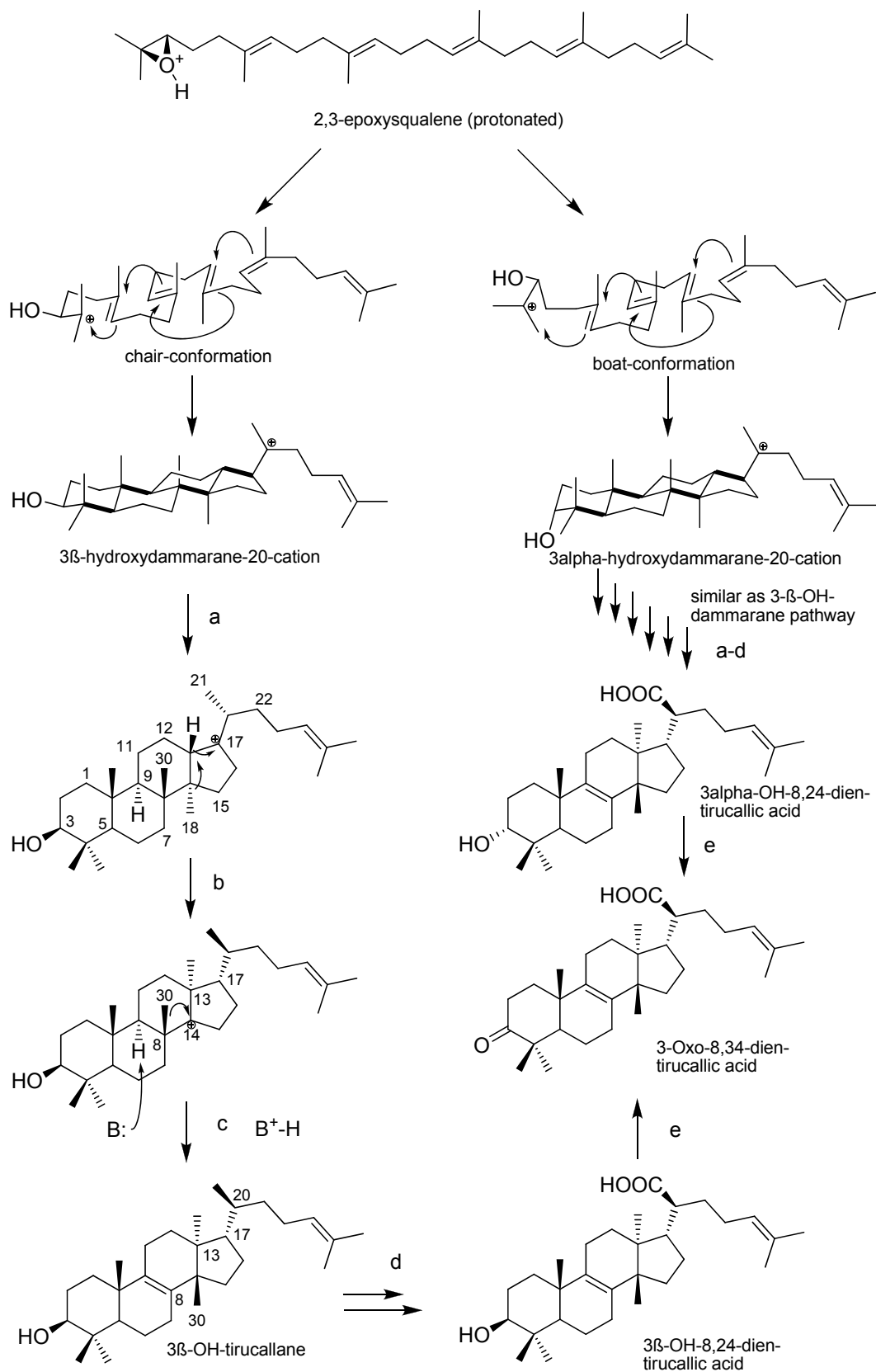


**Fig. 3.125** Hypothetical biogenesis pathway for  $\alpha$ -TA,  $\beta$ -TA and 3-Oxo-TA. For further details see text.

## Results and Discussion

The acetylated derivatives (compounds **16** and **19**) and also the isomers, respectively, the acetylated isomers with a C7-C8 double-bond (compounds **17** and **18**), may follow a similar way as shown in Fig. 3.125, but just with differences in the hydrogen elimination (C-7 and C-8, instead of C-8 and C-9), leading to the different double-bond positions, and an additional acetylating reaction for each of the compounds (probably via Ac-CoA and corresponding acetyl-transferases).

The starting reaction for the probable biosynthesis pathway of the LAs (**11** and **12**) and the BAs (**1-7**) is shown in Fig. 3.126.

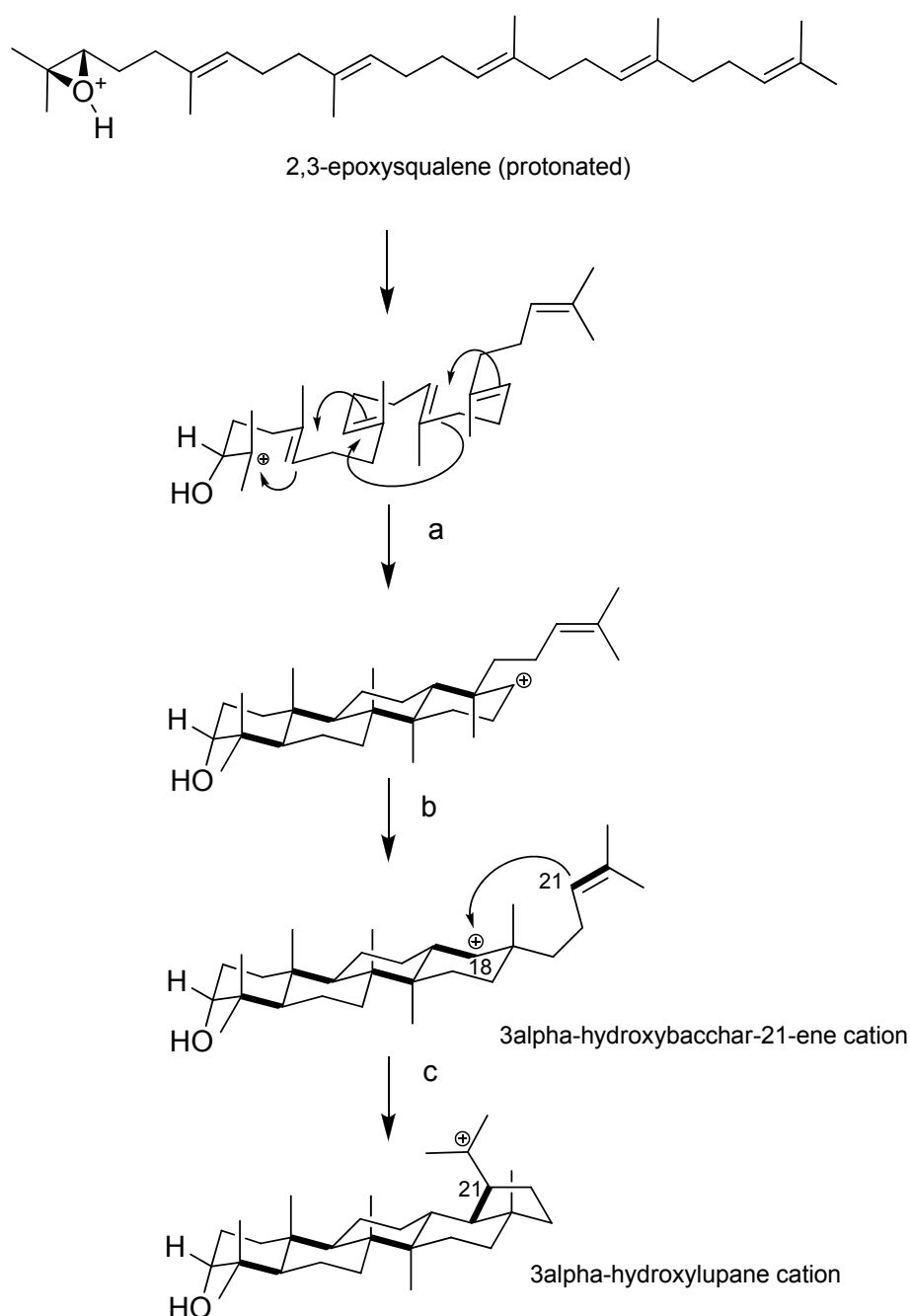


**Fig. 3.126** The probable starting reactions for the biosynthesis of the LAs (**11** and **12**) and BAs (**1-7**). For details see text.

On the contrary to the synthesis of the tirucallane compounds shown in Fig. 3.125, the cyclisation of the 2,3-epoxysqualene leads to the six-membered ring *D* (a).

The following Wagner-Meerwein rearrangement (b) leads to the intermediate cation of the tetracyclic triterpene 3 $\alpha$ -OH-bachar-21-ene (furthermore, the 3 $\beta$ -OH-bacchar-21-ene may be also built, similar to as shown in Fig. 3.125 for the  $\alpha/\beta$ -dammarane skeletons). Finally, the ring is closed and the pentacyclic 3 $\alpha$ -OH-lupanium cation is built (c). This product then reacts into the LAs and BAs as described in Fig. 3.127. For further information see the book of Breitmaier [31] or the review of Ikuro Abe [193].

The further hypothetical reaction steps for the bisynthesis of the LAs (compounds **11** and **12**) and the BAs (compounds **1-7**) are presented in Fig. 3.127. The connection of a bond from C-18 to C-21 of baccharane leads to the five-membered ring *E* of the pentacyclic lupanes as already shown in Fig. 3.126. The double bond C-20-C-29 may be built by enzymatically catalysed elimination ( $B: + H-CH_2-R \rightarrow B^+-H CH_2=C-R$ ) of the proton (methyl at C-29). Between the steps of d and f, the C-H activation (via Cytochrome P450 enzymes [19]) of C-24 may occur, giving first the alcohol and finally the COOH-function. By acetylation, probably via Ac-CoA and an acetyl-transferase, Ac-LA (**12**) is then obtained (f).

The expansion of the cyclopentane ring *E* in lupanes to the six-membered ring *E* by shifting carbon atom C-21 from C-19 to C-20 leads to the oleanane skeleton ( $\beta$ -amyrine). This may be achieved by concerted hydride shifts from C-18 to C-19 and C-13 to C-18 (g), respectively, followed by elimination ( $B: + H-CH-R \rightarrow B^+-H CH=C-R$ ) of the proton at C-12 (h), giving the double bond (C-12-C13). Finally, C-H activation and oxidation at C-24 (i) leads to  $\alpha$ -BA (probably by Cytochrome P450 enzymes [19]). A further acetylation reaction (j) gives thus  $\alpha$ -ABA (probably via Ac-CoA and an acetyl-transferase).

Further reaction steps may lead to the 11 $\alpha$ -hydroxy- $\alpha$ -BA (k) and finally the 3- $\alpha$ -OH-11-keto- $\alpha$ -BA-derivatives (l and m), though they definitely may be only expressed in infinitesimal quantities (Note that these two compounds have been predicted in olibanum species, see also [57,59], and were already partial-synthesised by Büchele et al. [58,134]).

For the biosynthesis of  $\beta$ -BAs (compound **2**, **4**, **5** and **6**) the oleanane skeleton formally may undergo methyl shifts to a variety of other pentacyclic triterpene intermediates leading to the ursane skeleton (step n-u). Hence, the C-29-methyl group may migrate from C-20 to C-19 giving the positive tertiary carbo-cation at C-20 (n). The following hydride shifts from C-19, C-18 and C-13 may concertedly build the tertiary carbo-cation at C-13 (o), which thus may give the  $\alpha$ -amyrine skeleton by enzymatically catalysed ( $B: + H-CH-R \rightarrow B^+-H CH=C-R$ ) proton elimination of C-12 (p). Similar to as described for the synthesis of  $\alpha$ -BA (steps i-m), the COOH function at C-24 may be built (q) and further acetylation may lead to  $\beta$ -ABA (r). Oxidation at C-11 thus may lead to 11-OH- $\beta$ -BA (not detected yet, but proposed [57]) and 11-OH- $\beta$ -ABA (**7**) (step s) and finally to  $\beta$ -KBA (**5**) and  $\beta$ -AKBA (**6**) (steps t and u).

In which sequence the specific reactions are operated is not known hitherto. Thus, all the pathways presented here are merely hypothetical presumptions and are not based on real experimental proof. To achieve this, further biochemical experiments, especially with real frankincense plants, must be conducted to elucidate the correct secondary metabolism routes of frankincense plants.

## Results and Discussion

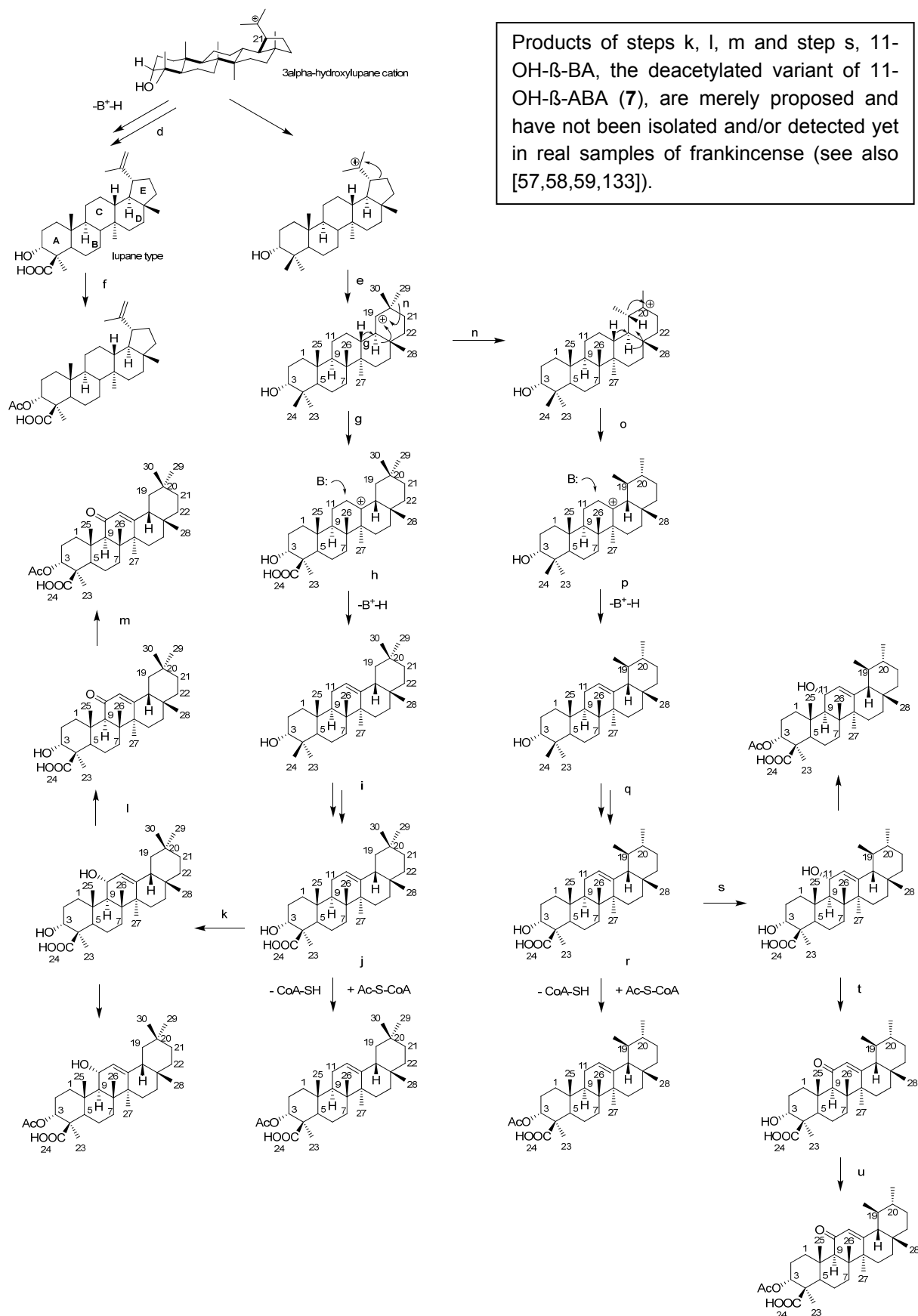


**Fig. 3.127** Scheme for the biosynthesis of LAs (11 and 12) and BAs (1-7) beginning from the 3 $\alpha$ -hydroxylupane cation as probable precursor. For details see text.

### 3.14 Validation of Biosynthesis Hypothesis by PCA

The in chapter 3.13 discussed specific biosynthesis hypothesis for each species has been substantiated by principal component analysis (PCA) in this chapter. In table 3.37 the PCA matrix is presented. The calculation details are described in chapter 2.3.8. For Bpap, 10 different resin batch samples were analysed (three different distributor sources). Bser samples consisted of 14 different samples (three different distributor sources). Bcar consisted of 6 (three different distributor sources) and Bsac of 4 (three different distributor sources) samples.

**Table 3.37** The raw data matrix for the PCA. Note that for  $\beta$ -Car-Ox, compound **28**, (only TLC) and Vert-4(20),7,11-triene, compound **24**, (not quantified) a different encoding system was used (0 = not detectable; 1 = detectable). The other data is based on HPLC quantitation results (chapter 3.8). For further details see text.

Compound	5	6	15	14	13	16	1 (2D)	3 (2D)	11	12	2	4	22	23	21	20	24	28
Bpap-Seitz	1,0	13,1	2,1	1,8	7,3	2,7	3,5	4,2	0,4	1,6	6,0	10,7	24,9	18,5	0,0	0,0	1	0
Bpap-MP-0409	2,0	13,1	3,5	2,6	8,8	3,5	3,3	5,4	0,7	1,6	6,1	10,6	23,0	16,7	0,0	0,0	1	0
Bpap-AS-070509-A2b	1,4	15,3	2,5	2,1	9,1	2,3	3,5	5,7	1,0	1,8	6,9	8,5	19,6	15,2	0,0	0,0	1	0
Bpap-AS-260309-A1c	1,0	14,8	1,8	1,1	5,5	1,3	2,3	5,2	0,4	1,2	5,5	9,1	18,8	14,0	0,0	0,0	1	0
Bpap-AS-090610-F1a	1,2	16,3	3,3	3,1	12,8	4,7	4,2	7,4	1,2	1,5	6,7	10,2	22,9	16,2	0,0	0,0	1	0
Bpap-AS-060910-F1a	1,3	11,6	3,6	3,3	22,7	4,7	4,5	8,0	0,7	1,7	7,4	11,4	23,1	18,6	0,0	0,0	1	0
Bpap-AS-220509-A1c	1,0	11,0	2,1	1,3	6,2	1,4	2,8	5,1	0,4	1,2	5,6	9,3	25,0	16,6	0,0	0,0	1	0
Bpap-Caelo-Pr	1,2	15,6	4,0	3,3	15,8	3,7	4,6	11,0	0,7	1,8	7,4	13,6	15,3	10,9	0,0	0,0	1	0
Bpap-22-1300	1,2	16,5	3,5	3,6	14,2	4,0	4,5	8,9	0,7	1,8	7,6	13,0	21,3	13,2	0,0	0,0	1	0
Bpap-22-1400	1,0	16,0	3,4	2,8	14,2	3,9	4,2	9,2	0,6	2,0	8,1	15,0	16,1	11,9	0,0	0,0	1	0
Bser-AS-240309-A3c	1,6	2,5	4,3	3,8	10,5	3,5	5,3	14,3	1,1	1,0	4,0	13,6	2,5	0,0	16,8	3,1	0	0
Bser-AS-190409-A3b	1,8	2,9	4,3	4,4	10,5	3,9	6,8	15,0	1,1	1,5	4,4	14,9	0,9	0,0	5,3	0,9	0	0
Bser-AS-110809-A3c	1,5	2,5	4,9	5,9	11,5	3,6	6,8	16,1	1,0	1,0	4,2	14,2	2,2	0,0	14,2	2,6	0	0
Bser-AS-060910-F3a	2,4	2,9	4,2	5,8	9,7	3,2	7,2	17,5	1,5	0,3	4,1	13,6	2,4	0,0	4,1	0,7	0	0
Bser-AS-060810-F3b-RS	2,2	2,9	4,3	5,5	11,7	4,1	8,4	18,3	1,3	1,0	4,5	15,1	1,6	0,0	11,2	2,2	0	0
Bser-siccum 96 % EtOH-a	2,4	2,9	4,4	5,1	11,5	3,5	8,0	17,1	1,4	1,1	4,3	14,5	2,0	0,0	3,0	0,6	0	0
Bser-siccum 96 % EtOH-b	2,4	2,9	4,3	5,1	11,7	3,3	8,1	17,1	1,3	1,2	4,5	14,7	2,2	0,0	2,0	0,8	0	0
Bser-siccum 96 % EtOH-c	3,0	3,4	3,2	2,9	7,7	0,6	8,6	18,7	1,3	1,1	4,6	15,2	2,1	0,0	2,3	1,4	0	0
Bser-Art. No. 22.127	3,0	3,0	4,0	5,4	10,8	3,0	8,5	18,8	1,5	0,9	3,9	12,4	4,0	0,0	9,1	1,7	0	0
Bser Granen	2,7	4,1	3,2	3,8	8,4	2,5	8,0	16,0	1,4	1,5	4,5	13,4	0,0	0,0	6,0	1,0	0	0
Bser-No. 22-1560	1,8	3,1	5,3	7,1	16,3	4,2	7,6	17,6	1,3	1,2	4,6	15,0	0,0	0,0	5,1	0,4	0	0
Bser-Gufic, AB0918	6,7	4,6	5,7	9,1	17,2	3,3	10,7	20,9	1,8	1,0	4,2	13,3	0,0	0,0	15,7	3,1	0	0
Bser-Gufic, AB0919	7,1	4,4	5,8	10,4	15,6	3,0	10,6	19,6	2,0	1,4	3,8	12,7	0,0	0,0	15,9	3,1	0	0
Bser-Gufic, AB0920	5,7	4,1	4,4	6,7	9,9	2,3	9,1	17,1	1,7	0,9	3,5	11,4	0,0	0,0	9,1	1,7	0	0
Bcar-RS (AK Jauch)	0,9	2,2	1,5	3,0	1,4	0,7	7,5	13,7	2,8	3,8	7,2	13,6	0,0	0,0	1,0	0,3	0	1
Bcar-AS-050910-A11c	0,2	2,3	1,1	1,7	2,1	1,2	4,6	10,4	2,2	4,0	7,9	16,7	5,2	0,0	2,6	0,7	0	1
Bcar-AS-040910-F11a	0,3	2,1	1,3	0,9	2,0	0,9	6,9	16,3	2,9	6,1	11,2	23,7	5,8	0,0	2,9	0,8	0	1
Bcar-22-1238	0,5	11,1	1,3	1,1	2,3	0,9	8,4	17,0	2,1	6,1	14,1	27,9	11,4	0,0	4,5	0,8	0	1
Bcar-Giama	0,5	12,7	0,7	0,5	0,9	0,2	12,1	22,5	4,2	3,9	11,1	15,6	5,6	0,0	3,6	0,4	0	1
Bcar-Aden, Schreibmayer	0,6	1,8	1,2	0,9	1,7	0,7	6,4	15,6	2,6	5,6	10,1	23,1	1,2	0,0	1,9	0,0	0	1
Bsac-AS-040910-A10a	0,5	2,5	1,5	1,1	2,0	1,1	7,3	14,3	2,8	6,7	11,5	23,5	2,7	0,0	10,3	1,3	0	1
Bsac-22-1232	0,1	0,1	0,5	1,5	0,2	0,1	10,8	22,6	4,4	5,6	12,8	22,8	1,9	0,0	8,8	3,0	0	1
Bsac-JB03 Pr 55	1,1	20,0	1,5	1,8	2,9	1,3	4,5	5,1	1,8	5,4	13,2	10,5	0,0	0,0	0,5	0,0	0	1
Bsac-Dr. Mohsin Pr. 6	1,1	15,0	1,2	0,4	1,0	0,3	2,8	5,4	0,8	1,5	4,9	6,9	0,0	0,0	14,0	1,6	0	1

## Results and Discussion

As usual in PCA, the matrix was built up by the objects (samples; Bpap, Bser, Bsac and Bcar) row-wise and the loadings (variables; compounds **1-6**, **11-16**, **20-24** and **28**) column-wise. Thus, a total matrix of 34 objects with 18 variables (loadings) was built.

For the loadings, only robust biomarkers were chosen. Unstable biomarkers were not taken into account (Compounds **7** and **10**; see also [55,59] or chapter 3.7). The 2D HPLC quantitation results of the BAs (**1** and **3**) have been used (see also chapter 3.7.5 and 3.8) for the PCA described here. Furthermore, the second chromatography dimension data for qualitative description of compounds **18** and **19** was not considered, although the data could be used analogously as the TLC data for example (0 = only traces of compounds; 1 = detectable). The biomarker  $\beta$ -Car-Ox (**28**), as it is not really detectable by HPLC-analysis, but significantly by TLC (pink spot) has been used as a nominal control in the PCA (0 = not detectable; 1 = detectable). The same counts for Vert-4(20),7,11-triene (**24**), which is basically quantifiable, but since we did not quantify it accurately by external calibration, this load, as a significant compound for Bpap, had been used the same way (0 = not detectable, 1 = detectable). For all other compounds (**1-6**, **11-16** and **20-23**) the HPLC quantitation results were used (% in g/g for the acid fraction and neutral fraction results, respectively). The final principal component plot, including the scores (samples of Bpap, Bser and Bsac/Bcar) and the loadings (variables; compounds **1-6**, **11-16**, **20-24** and **28**) is shown in Figure 3.128. Note that even only the HPLC results (acid and neutral fractions), without the nominal data (compound **24** and **28**, 0 or 1), give an unambiguous principal component plot for species identification (data not shown here).

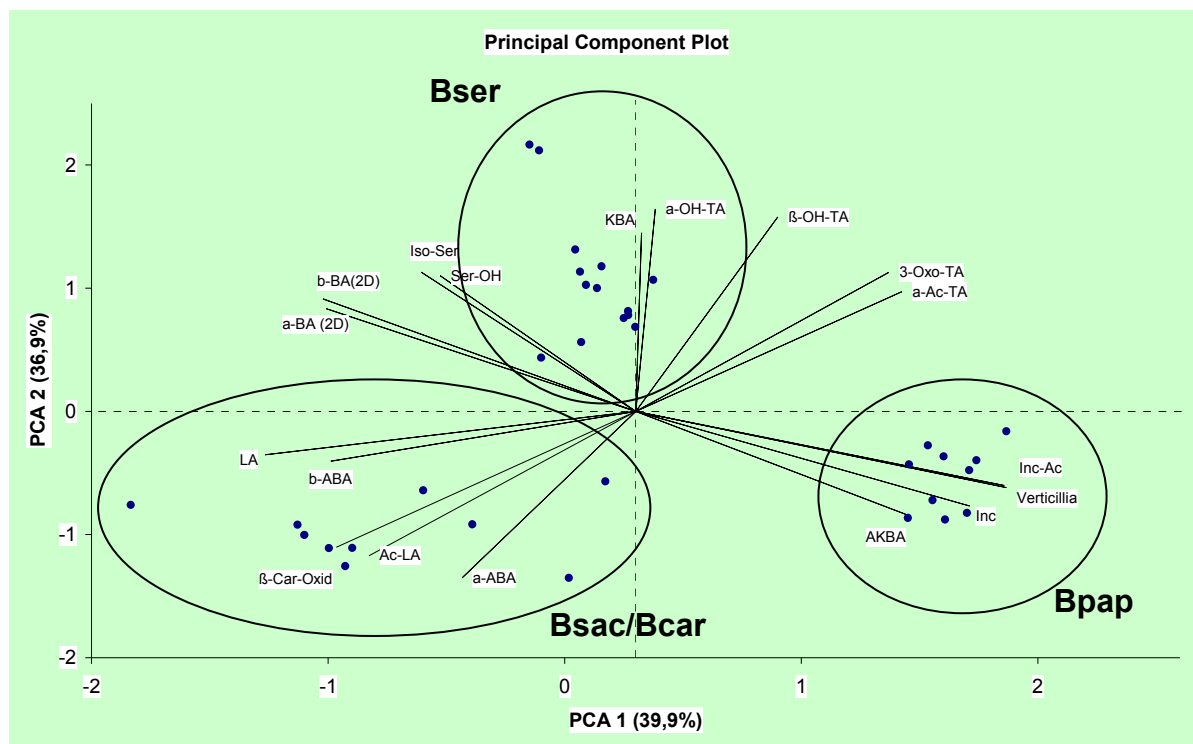


**Fig. 3.128** Principal components plot. The first two principal components (PCA 1 and PCA 2) were sufficient to describe the differences between Bpap, Bser and Bsac/Bcar. The vectors (e.g. AKBA, Ac-LA, 3-Oxo-TA, etc.) determine the position of each object (sample) in the plot. For further details see text.

Basically, sample spots near each other have similar properties, whereas samples revealing a greater distance are described by other attributes. In this case, for every species investigated, a typical expectation area can be given. This may be useful for future predictions on other incense resin samples, since expectably same samples give a similar cluster.

Though PC1 (39.9 %) and PC2 (36.9 %) just cover approximately 77 % of the total variance (Kaiser-criterion = every principal component Eigenvalue greater 1 is important, see also [165] or Fig. 3.131), both components are already sufficient to describe these “three” resins unambiguously. The scores plot is depicted in Fig. 3.129 and the loadings plot is shown in Fig. 3.130. As shown in the mixed scores and loadings plot in Fig. 3.128, Bpap is completely described by the vectors of  $\beta$ -AKBA (**6**), Inc (**22**), Inc-Ac (**23**) and Vert-4(20),7,11-triene (**24**). Furthermore, the Bpap scores are influenced by the high amounts of tirucallic acids, especially 3-Oxo-TA (**13**).

Bser distinguishes itself from the others by the on average highest amount of  $\beta$ -KBA (**5**) and by high quantities of tirucallic acids (**13-16**), Ser-OH (**21**), Iso-Ser (**20**), and the on average highest amounts of BAs (**1** and **3**).

The samples of B<sub>sac</sub> and B<sub>car</sub> are clustering around the same area. They are mainly described by the highest levels of lupeolic acids (**11** and **12**) and the on average highest quantities of ABAs (**2** and **4**). Furthermore, the positive qualitative detection of  $\beta$ -Car-Ox (**28**) in every sample of them, gives a strong vector classifying both to be identical. However, some precautions must be met when B<sub>sac</sub> and B<sub>car</sub> are analysed. Since, for example, two samples of B<sub>sac</sub> (see Table 3.37, samples JB03-Pr.55 and Dr.MohsinPr.6) revealed rather high quantities of  $\beta$ -AKBA (**6**), concluding that every single observed biomarker concentration must be treated with the uttermost carefulness. If merely the acid fraction, without any neutral fraction compounds, is processed by PCA, the two samples (JB03-Pr.55 and Dr.MohsinPr.6) would lead to the conclusion that it could be Bpap instead, which always constantly showed quite high  $\beta$ -AKBA (**6**) levels. However, since these samples could be additionally distinguished by the other parameters (e.g. LAs, **11** and **12**, low levels of tirucallic acids, **13-16**, the existence of  $\beta$ -Car-Ox, **28**, and Ser-OH, **21**, and the absence of Inc-Ac, **23**), the identification has been still unequivocal.

Interestingly, as the correlation between the serratols (**20** and **21**) and incensoles (**22** and **23**) is negative (compare their positions in Fig. 3.128 or 3.130), the here performed PCA gives also the evidence that detection of high levels of incensoles (**22** and **23**) reveal very low levels of serratols (**20** and **21**), vice versa. The same almost negative correlations can be deduced from the BAs (**1** and **3**) and  $\beta$ -AKBA (**6**), and additionally for the TAs (**13-16**) and LAs (**11** and **12**). Here, especially AcLA (**11**) and 3-O-TA (**13**) are striking. As already discussed, high levels of LAs lead to low levels of TAs. And high  $\beta$ -AKBA levels always delivered lower BA-levels, vice versa. However, the conclusions deduced here are merely based on the in this work analysed sample population. Thus, every single result should be still regarded carefully.

## Results and Discussion

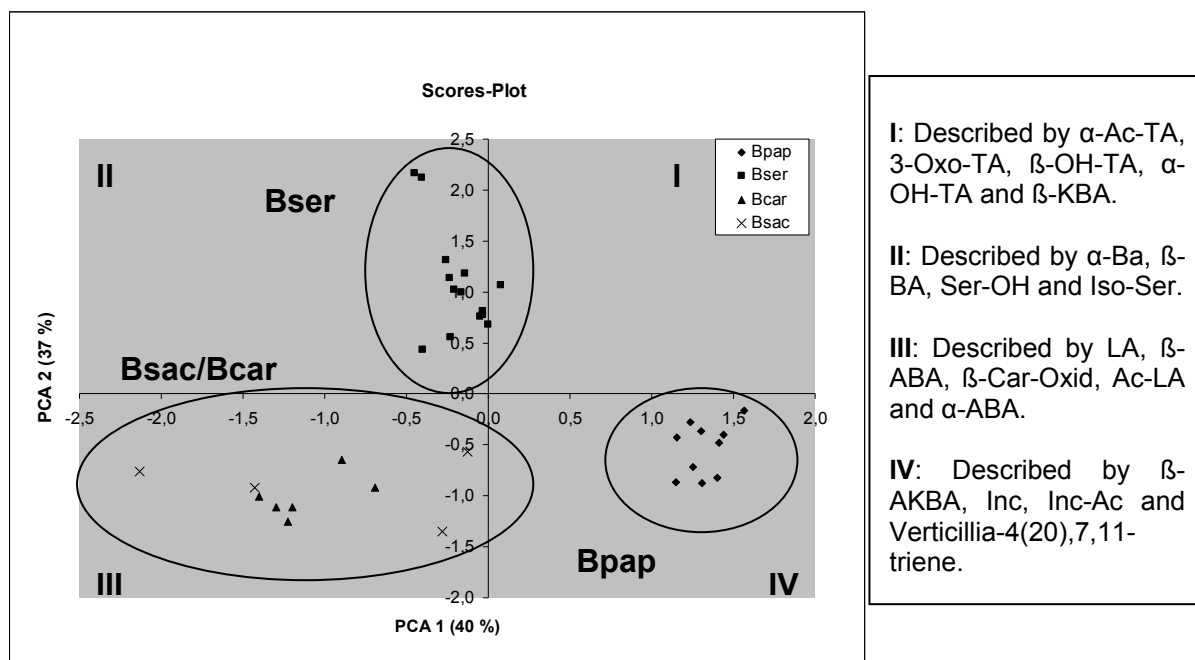


**Fig. 3.129** The scores plot of all here analysed samples. Every sample can be classified by the principal component analysis applied here. Samples of Bsac and Bcar show the strongest deviation in general. For further details see text.

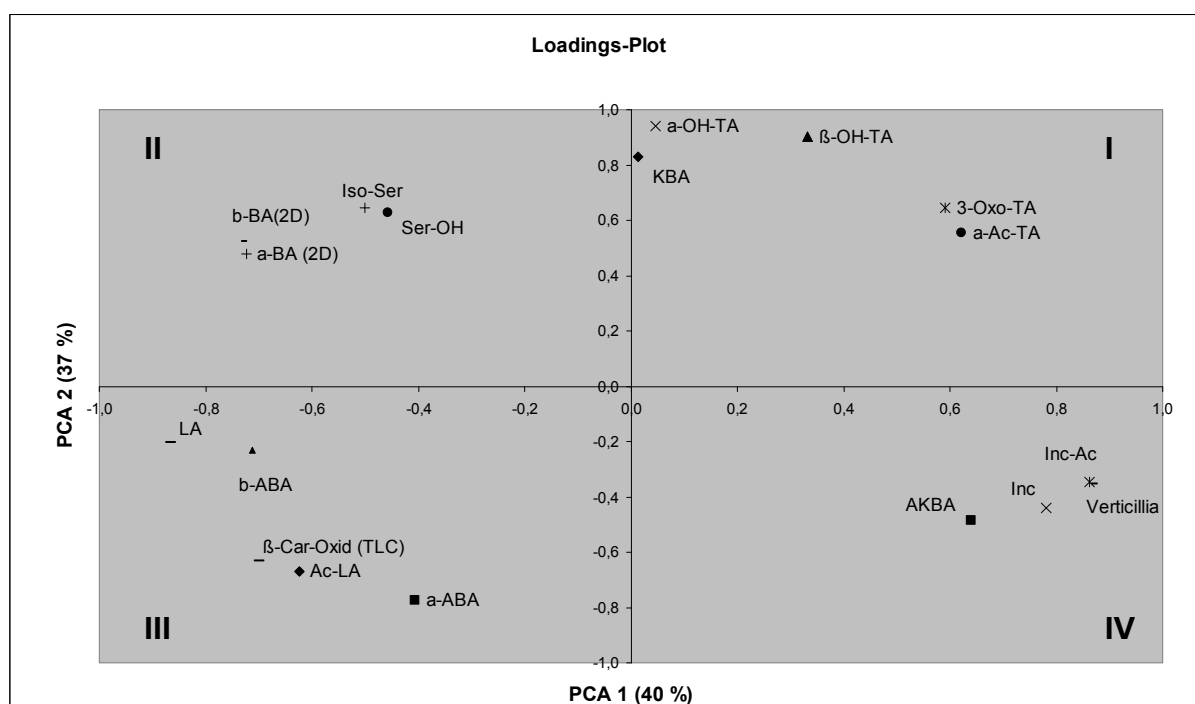
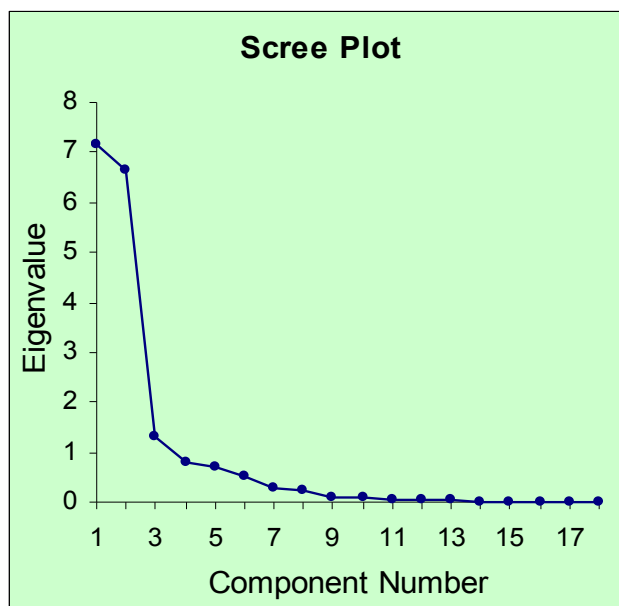


**Fig. 3.130** The loadings plot of all variables. Samples of Bser are mainly described by the vectors of the BAs (1 and 3,  $\beta$ -BA and  $\alpha$ -BA), Iso-Ser (20), Ser-OH (21),  $\beta$ -KBA (5) and the tirucallic acids. Bpap samples distinguish themselves by high quantities of Inc (22) and Inc-Ac (23),  $\beta$ -AKBA (6) and the existence of verticillia-4(20),7,11-triene (24). The samples of Bsac and Bcar are classified by the highest LA-levels (LA and Ac-LA, 11 and 12), high ABA-levels (2 and 4,  $\beta$ -ABA and  $\alpha$ -ABA), very low TA-levels and the detection of  $\beta$ -Car-Ox (28). For further details see text.

## Results and Discussion

Casewise PCA Scores		
Case	PCA 1	PCA 2
Bpap-Seitz	1,401	-0,826
Bpap-MP-0409	1,410	-0,478
Bpap-AS-070509-A2b	1,255	-0,721
Bpap-AS-260309-A1c	1,151	-0,865
Bpap-AS-090610-F1a	1,440	-0,397
Bpap-AS-060910-F1a	1,566	-0,161
Bpap-AS-220509-A1c	1,308	-0,878
Bpap-Caelo-Pr	1,235	-0,277
Bpap-22-1300	1,301	-0,366
Bpap-22-1400	1,155	-0,430
Bser-AS-240309-A3c	-0,163	1,001
Bser-AS-190409-A3b	-0,002	0,685
Bser-AS-110809-A3c	-0,144	1,178
Bser-AS-060910-F3a	-0,032	0,814
Bser-AS-060810-F3b-RS	-0,235	1,134
Bser-siccum 96 % EtOH-a	-0,032	0,781
Bser-siccum 96 % EtOH-b	-0,051	0,757
Bser-siccum 96 % EtOH-c	-0,399	0,436
Bser-Art. No. 22.127	-0,210	1,027
Bser Granen	-0,230	0,562
Bser-No. 22-1560	0,074	1,067
Bser-Gufic, AB0918	-0,408	2,118
Bser-Gufic, AB0919	-0,449	2,165
Bser-Gufic, AB0920	-0,256	1,314
Bcar-RS (AK Jauch)	-0,898	-0,642
Bcar-AS-050910-A11c	-0,691	-0,917
Bcar-AS-040910-F11a	-1,296	-1,110
Bcar-22-1238	-1,228	-1,257
Bcar-Giama	-1,400	-1,004
Bcar-Aden, Schreibmayer	-1,198	-1,109
Bsac-AS-040910-A10a	-1,429	-0,921
Bsac-22-1232	-2,134	-0,760
Bsac-JB03 Pr 55	-0,282	-1,352
Bsac-Dr. Mohsin Pr. 6	-0,128	-0,569



Explained Variance (Eigenvalues)										
Value	PC 1	PC 2	PC 3	PC 4	PC 5	PC 6	PC 7	PC 8	PC 9	PC 10
Eigenvalue	7,18	6,64	1,32	0,80	0,69	0,52	0,30	0,22	0,08	0,08
% of Var.	39,90	36,88	7,34	4,46	3,84	2,90	1,67	1,23	0,46	0,42
Cum. %	39,90	76,78	84,12	88,57	92,42	95,32	96,99	98,22	98,68	99,11

**Fig. 3.131** The metric data of the casewise scores for the principal components 1 and 2 (these describe the position of each sample in the plot of Fig. 3.129), the scree-plot (Eigenvalue plotted against PC1, PC2, etc.) and the calculated eigenvalues, explaining the variance. The first ten principal components cover more than 99 % of the variance (PC11 – PC18 are not shown). Though, PC3 has an eigenvalue > 1 (Kaiser-Criterion) it was not used for clarification. PC1 and PC2 have been sufficient for species classification. For further details see text.

The statistical raw data, given in Figure 3.131, contains the calculated results of the casewise scores for every sample (position of every sample in Fig. 3.128 and 3.129), the

## Results and Discussion

scree-plot (graphical depiction of the eigenvalues against PC1, PC2, PC3, etc; *Kaiser criterion* > 1) and the calculated eigenvalues (explained variances). Furthermore, in Tab. 3.38 the descriptive statistics for all here analysed samples are given. Especially this table may be useful as an expectation value for classifying any resin being questioned as a resin of the genus *Boswellia* (Bpap, Bser and Bsac/Bcar).

**Tab. 3.38** The descriptive statistics for all 34 observations from Table 3.37. Basically, the arithmetic average of all quantitative HPLC measurements for every resin (Bpap, Bser and Bsac/Bcar) made in this work (except  $\beta$ -Car-Ox and Verticillia). For further details see text.

Descriptive Statistics				
Variable	Mean	Std Dev.	Std Err	N
KBA (254nm)	1,829	1,674	0,287	34
AKBA (254nm)	7,622	6,042	1,036	34
$\beta$ -OH-TA	3,052	1,523	0,261	34
a-OH-TA	3,482	2,450	0,420	34
3-Oxo-TA	8,709	5,689	0,976	34
a-Ac-TA	2,449	1,442	0,247	34
a-BA (2D)	6,540	2,594	0,445	34
b-BA(2D)	13,439	5,661	0,971	34
LA	1,554	0,979	0,168	34
Ac-LA	2,343	1,864	0,320	34
a-ABA	6,768	3,048	0,523	34
b-ABA	14,388	4,745	0,814	34
Inc	7,750	9,135	1,567	34
Inc-Ac	4,462	7,149	1,226	34
Ser-OH	4,996	5,449	0,935	34
Iso-Ser	0,940	1,046	0,179	34

The here described classification by PCA may give a useful tool for quality control. Due to the expected confidence region, an incense resin being questioned may be found within a defined PCA area (see Fig. 3.128 and Fig. 3.129). Additionally, more results could be used for the PCA presented here, if quantitative GC-results, instead of TLC-results, are applied. Thus, there are still other possibilities for a different design by PCA.

However, due to the fact that these resins are naturally occurring products from different harvesting sides, there occur generally great deviations concerning their biomarker compositions. These differences could be caused by environmental influences (soil, rain, sun, etc.) but also could be the product of genetically variations, where maybe one tree does not have a specific enzyme for the synthesis of a specific product. Thus, the general correctness of this model still has to be proved in the future by additional analytical evidence.

### Conclusion and Outlook

The aim of the study has been the unambiguous chemotaxonomic classification of resins from the frankincense species *Boswellia papyrifera*, *Boswellia serrata* and *Boswellia sacra*, respectively, *Boswellia carterii* by conventional chromatographic methods (TLC, HPLC and GC). All three methods enable the identification by means of typical biomarker compounds (e.g. TLC-analysis [11]). Additionally, the results were compared with reliable data from literature [13,15,74,79,184] and samples of certified origin [17].

Besides, a HPLC method (external standard calibration with 2D-Offline option, if necessary) has been developed, capable of quantifying up to 17 and even possibly 19 compounds in the acid fraction matrix of all three species [59]. In total, 15 compounds (**1-8** and **10-16**) were quantified in this work. Particularly, the class of tirucallic acids has been firstly separated in the acid fraction matrix by reversed-phase liquid chromatography. Four compounds of the separated five were quantified (compounds **13-16**, without **17**).

In case of the species *Boswellia papyrifera* and *Boswellia serrata*, where the  $\beta$ -BA (**3**) peak co-eluted with two compounds (**18** and **19**), a second chromatography dimension was added [160] in order to quantify this compound (**3**) less error-prone and more accurate. This method, which is hitherto quite time-consuming and assumedly not very robust (additional manual preparation steps), gives evidently more correct results than a simple perpendicular drop [162] of the poorly resolved peaks (**3**, **18** and **19**) does.

Furthermore, it was revealed that the second chromatography dimension is not necessary for the species *Boswellia sacra* and *Boswellia carterii*, since the compounds 3 $\alpha$ -O-acetyl-7,24-dien-tirucallic acid (**18**) and 3 $\beta$ -O-acetyl-8,24-dien-tirucallic acid (**19**) occur there in only minimal traces. Thus, the integration error, caused by co-elution of **18** and **19** with  $\beta$ -BA (**3**), has been negligible (see chapter 3.7.5).

Approximately, ca. 75 % of the total acids have been determined (see chapter 3.8). All of the three species approach this value independent from the quantities of the single components (e.g. high TA-contents, therefore a low BA/ABA and/or KBA/AKBA content and vice versa). When the quality of the resin being analysed is sufficient, this mean value is obtainable by comparable extraction procedures. However, samples of inferior quality were analysed revealing an extreme bias from the expectation value. This means principally that there exists a specific fingerprint-pattern for every species, but it must not be fulfilled mandatorily (see also chapter 3.8). These resins are more or less naturally grown products with their quality depending on environmental influences. Furthermore, it is important to measure a great overall population of the sample resin as even within one batch great quantitative variations can be found (e.g. to grind 10 g is safer than to grind 1 g, even though the consumption may be immense then).

Unequivocal biomarkers for the species *Boswellia papyrifera* (Eritrea, Ethiopia and Sudan) are incensole (**22**), incensole acetate (**23**) and verticillia-4(20),7,11-triene (**24**). *Boswellia papyrifera* is identifiable by all three methods (TLC, HPLC and GC). Hitherto, this species has been often mistaken in the literature with the species *Boswellia carterii* (Somalia), though there have been already sufficient publications (e.g. Obermann in 1978 [79] and Hamm et al.

in 2005 [13]) giving similar conclusions as stated in the work presented here. Additionally, the species *Boswellia papyrifera* distinguishes itself through the highest  $\beta$ -AKBA (**6**) content on average, and a rather high overall content of tirucallic acids (chapter 3.8). Another interesting fact is that in all relevant publications on this topic [13,74,79], as well as in all analysed samples during this work, the compound incensole acetate (**23**) had been merely detected in *Boswellia papyrifera*. The compounds incensole (**22**) and incensole acetate (**23**) have been firstly quantified by HPLC (external standard calibration) and are the main components in the neutral fraction of the species *Boswellia papyrifera* (contents from 30 to over 40 % were detected; see also chapter 3.8). The quantitative HPLC results had been verified by isolation experiments with incensole (**22**) and its acetate (**23**) (see chapter 3.11.1). Through enrichment of the incensole acetate (**23**) content by partial-synthesis in the neutral fraction of *Boswellia papyrifera* (acetylation of the neutral fraction) and the following chromatographic isolation, this compound has been isolated in great quantities (chapter 3.11.1). With the species *Boswellia serrata* and *Boswellia sacra/Boswellia carterii* this would not have been possible, as they show significantly lower contents of incensole (**22**), and the biosynthesis seems to be focused on serratol (**21**) instead, the precursor of incensole (**22**) (see chapter 3.13.1.2 or [11]). The two compounds (**22** and **23**) could be conveniently transformed into one another by simple deacetylation and acetylation experiments.

For the species *Boswellia serrata* (India) the compounds serratol (**21**), the here firstly described iso-serratol (**20**; see chapter 3.2.7) and a quite high overall content of tirucallic acids are typical (chapter 3.8). Apparently, the ubiquitous occurring compounds methylchavicol and methyleugenol, which were determined in the steam-distillate by means of their GC-retention-indices, seem to be also specific for *Boswellia serrata* [13,35,74]. The species is further characterised by an approximately equal  $\beta$ -KBA/ $\beta$ -AKBA-content and the highest BA-contents ( $\alpha$ -BA, **1** and  $\beta$ -BA, **3**) on average. With regard to bio-availability, where  $\beta$ -BA (**3**) revealed the throughout highest blood-plasma levels [125,126,144], this species seems to be the most promising, as long as it is standardised on  $\beta$ -BA (**3**).

For *Boswellia sacra* (Oman, Yemen) and *Boswellia carterii* (Somalia), which can be regarded as identical species so far [11-13,73], same biomarkers have been identified by the chromatographic methods implemented here (TLC, HPLC and GC). Specifically is therefore the occurrence of  $\beta$ -caryophyllene (**27**) and its mono-oxidation product (**28**). Compound **27** has been detectable by HPLC (chapter 3.7.3 and 3.7.4) and **28** significantly by TLC (see chapter 3.4). This result had been verified by the GC-tests and by reliable results from literature [13,74,184] (chapter 3.5). The compounds serratol (**21**) and iso-serratol (**20**) were also detected in these species. Both compounds, **20** and **21**, have been firstly quantified in the neutral fraction of Bsac/Bcar, and additionally in Bser, by the HPLC method described here (see chapters 3.7 and 3.8). Their acid fractions reveal great quantities of BAs (**1** and **3**) and ABAs (**2** and **4**). Furthermore, they showed throughout significantly greater lupeolic acid contents (**11** and **12**), relatively compared with *Boswellia papyrifera* and *Boswellia serrata* (chapter 3.7.6 and 3.8). This is probably due to different characteristics of the specific biosynthesis pathways. The contents of  $\beta$ -KBA (**5**) and  $\beta$ -AKBA (**6**) varied considerably for the species *Boswellia carterii* and *Boswellia sacra* (chapter 3.8). Therefore, the  $\beta$ -KBA/ $\beta$ -AKBA-ratio should be regarded with the uttermost caution if used for species identification.

Expectably, the  $\beta$ -AKBA (**6**) peak is greater than the peak of  $\beta$ -KBA (**5**). However, this must not always be the case since differing signal-ratios were detected. On average, these species revealed the smallest  $\beta$ -KBA (**5**) content, compared with *Boswellia papyrifera* and *Boswellia serrata*. The great variation of biomarker concentrations found in samples of *Boswellia carterii* and *Boswellia sacra* may also be due to the many different distributor sources where these resin samples were purchased from. Basically, the same deductions have been already made by Bergmann [17]. Nevertheless, in all here analysed samples the overall tirucallic acid content has been significantly smaller than for *Boswellia papyrifera* and *Boswellia serrata* (chapter 3.8). This fact is again most probably due to the differences in the biosynthesis pathways with a focus on lupeolic (**11** and **12**) and boswellic acids (**1-4**) for *Boswellia sacra*, respectively, *Boswellia carterii* (see also chapter 3.13).

Eleven compounds in total were isolated from the resins of *Boswellia papyrifera* (**18**, **19**, **22**, **23** and **24**) and *Boswellia carterii* (**20**, **21**, **22**, **25**, **28**, **29** and **30**) and their structures were assigned by 1D and 2D NMR experiments. Iso-serratol (**20**), a derivate of the known compound serratol (**21**), has been firstly isolated from the resin of *Boswellia carterii*. Furthermore, the isolation of 3- $\beta$ -OH-tirucalol (**29**) and of 3- $\alpha$ -OH-11-keto-ursen (**30**) from the neutral fraction of *Boswellia carterii* has not been described in detail before. These two compounds, **29** and **30**, are most likely biosynthetic precursors of the corresponding tirucallic and 11-keto-boswellic acids.

The two acetylated tirucallic acid derivates **18** and **19**, isolated from *Boswellia papyrifera*, have been comprehensively described for the first time in this work. Though Estrada et al. reported their isolation from a resin of the species *Boswellia carterii*, there is no explicit data (isolation details) published in literature by this working group [57,70]. Additionally, *Boswellia carterii* produces **18** and **19** in only minimal amounts (see especially chapter 3.7.5 on 2D-HPLC). Hence, the species has been more likely *Boswellia papyrifera* instead, or a partial-synthetic method was used, as it is described for the semi-synthesis of **18** starting from **17** by Banno et al. [68] and Akihisa et al. [67]. In the publications of Banno and Akihisa et al. the origin of **18** is also addressed to *Boswellia carterii*. However, the reported compounds, specifically the isolation of incensole acetate (**23**), lead also to the assumption that the resin has been *Boswellia papyrifera* instead. Particularly, the difficulty of the separation of these two compounds, **18** and **19**, as well as the generally rather low content in frankincense resins, seems to substantiate this conjecture (see also chapter 3.1.1.3 and 3.7.5). Thus, this work describes the first chromatographic and spectroscopic “coordinates” for these two, pharmacologically interesting, compounds (**18** and **19**). In connection with the term “coordinates” it may be mentioned that they are synthesised in greater quantities by the species *Boswellia papyrifera* and *Boswellia serrata* and that additionally their HPLC retention times are denoted for the first time. The species *Boswellia sacra*, respectively, *Boswellia carterii* revealed continuously lower tirucallic acid contents. Hence, also the two compounds, **18** and **19**, were merely detected in traces (chapter 3.7.5).

## Conclusion and Outlook

---

The compounds for the quantitative HPLC tests (**1-8**, **10-16**) have been also isolated and purified from the species *Boswellia papyrifera* as already stated in the dissertation of Seitz [56,59].

Another interesting fact has been that purified incensole (**22**) and its acetate (**23**) are quite unstable, if exposed to air over a longer period of time (chapter 3.11.3). Thus, their firstly presumed pharmacological activity has been repatriated to their decomposition products (see chapter 3.12.1). This assumption was confirmed by reaction kinetic experiments with incensole acetate (**23**) (chapter 3.11.2-3.11.4). It may be mentioned here that the working group of Moussaieff has published these compounds, especially incensole acetate (**23**), with promising pharmacological properties [87,145-147]. Though, in the work presented here, merely the decomposed fractions of incensole (**22**) and its acetate (**23**) did reveal pharmacological activity (chapter 3.12.1). The question may be thus, if the results by Moussaieff et al. have been based on the same decomposition phenomena as they were “accidentally” discovered here.

Concerning synergy effects the fraction containing compounds **18** and **19** as well as another unidentified compound (presumably another isomer similar to **18** and **19**) revealed an interesting pharmacological potential (see chapter 3.1.1.3 for isolation and 3.12.2 for pharmacology). Unfortunately, the unknown compound of this fraction could not be isolated hitherto. In the cell-free mPGES-1 assay the complex mixture (unknown compound, **18** and **19**) gave more efficient inhibitory concentrations than the subsequently purified single compounds. This could be evidence on a synergistic effect. Though it is not absolutely compelling as in other biological systems they could react in a completely different manner [150] which is a general problem for the evaluation of active agents [94]. However, these results may perhaps encourage other research groups to conduct further tests. But most likely, these findings conclude that the tirucallic acids, as essential parts of the acid fraction of frankincense resins, have not negligible pharmacological effects.

Furthermore, the quantitative HPLC results are not completely validated thus far (chapter 3.8). Up to here there is no real data on the inter-laboratory-reproducibility generated (e.g. another lab, other equipment, other staff, etc.; see also [156]), as the quantitation by this method has been firstly described in the thesis presented here. Nevertheless, accuracy has been confirmed by comparison of this method with a robust HPLC method from the literature [20,21], needing less preparation steps (selective quantitation of  $\beta$ -KBA and  $\beta$ -AKBA; see chapter 2.3.9 and 3.6.1). The results, dependent on the way of proceeding, are similar for both methods. Besides, comparison of the quantitation results from this work with results from other publications substantiates the general correctness thus far (see chapter 3.9). However, an absolute certainty will be only achieved, if the methodology is repeated several times – additionally in other laboratories – to lastly obtain a statistically sufficient and reliable overall population [159]. This concerns both, the number of measured samples representative for *Boswellia papyrifera*, *Boswellia serrata* and *Boswellia sacra*, respectively, *Boswellia carterii*, and the procedure characteristics which will be revealed by several

repetitions of the methodology [156]. From this point of view, the quantitative data generated in this work has to be regarded merely as a first estimation of reality. It still has to be proven by further investigations in the future.

To summarise again, the data generated in this work may enable the determination of the origin of resins from the incense species *Boswellia papyrifera*, *Boswellia serrata* and *Boswellia sacra*, respectively, *Boswellia carterii*, by means of their specific chemotaxonomic markers, unambiguously. Even every single method (TLC, HPLC or GC) for itself may be able to achieve this. Whereby the TLC procedure, due to its convenient handling and significance, may be most convincing (chapter 3.4 and [11]).

The GC method requires the steam-distillation of the resins, respectively, their neutral fractions, as a prior preparation step, and delivers ubiquitous mono- and incense specific diterpenes (e.g. compound **21**, **22**, **23** and **24**; see also chapter 3.5).

Certainly, the HPLC procedure requires the most effort, as for an unambiguous quantitative determination the acid fraction has to be separated from the neutral part of the resin (chapter 2.2.4 and 2.3.4). However, this preparation step is necessary since the results would be falsified by other mono- and diterpenes co-eluting in the range of boswellic and tirucallic acids (e.g. **20**, **21**, **22** and **23**). The method has been validated for the acid fraction of *Boswellia papyrifera*, which does not reveal any significant traces of serratol (**21**) and iso-serratol (**20**). Thus, the quantitative results for  $\alpha$ -TA (**14**) and  $\beta$ -TA (**15**) are quite accurate. For the other species, which contain serratol (**21**) and iso-serratol (**20**) in greater quantities, the values for  $\alpha$ -TA (**14**) and  $\beta$ -TA (**15**) are afflicted with uncertainties. These two compounds co-elute with iso-serratol (**20**; with **15** =  $\beta$ -TA) and serratol (**21**; with **14** =  $\alpha$ -TA) in the unprepared raw extract (see especially the so-called “Triplet-Peak” in the Bser raw extract in chapter 3.7.2, but also chapter 3.7.3 and 3.7.4 for *Boswellia sacra*, respectively, *Boswellia carterii*). Even after separation of the acid fraction and neutral fraction by liquid-liquid-extraction (chapter 2.2.4) there are still traces of serratol (**21**) and iso-serratol (**20**) in the acid fraction detectable (TLC analysis) co-eluting with the corresponding tirucallic acids. Thus, the contents of **14** and **15** appear bigger than they actually are. This experimental result has been already stated in the dissertation of Seitz, who also isolated serratol (**21**) from the acid fraction of *Boswellia carterii* [56]. For *Boswellia papyrifera*, which does not reveal any quantities of serratol (**21**) and iso-serratol (**20**), therefore incensole (**22**) and its acetate (**23**) in greater amounts, this problem does not exist. Incensole (**22**) is merely in traces detectable in the acid fraction extract of *Boswellia papyrifera* but does not co-elute with any of the target analytes ( $R_t$  = between  $\beta$ -KBA and  $\beta$ -AKBA).

In addition, the quantitative HPLC results and even the qualitative HPLC fingerprints deliver some evidence on the preferred biosynthesis pathways of the single species (chapter 3.13). This evidence was substantiated by application of principal component analysis (PCA) (chapter 3.14).

*Boswellia papyrifera* seems to synthesise  $\beta$ -AKBA (**6**), incensole (**22**) and its acetate (**23**) in relatively great amounts. Furthermore, the content of tirucallic acids is rather high and the

## Conclusion and Outlook

---

lupeolic acid (**11**, **12**) and boswellic acid content (**1-4**) is rather low instead. Incensole acetate (**23**) has been detected only in this species (see chapter 3.7.1 and 3.7.6).

*Boswellia serrata* reveals quite low  $\beta$ -AKBA (**6**) contents, but therefore rather great BA (**1**, **3**) contents and also great tirucallic acid contents (**13-19**) instead. The  $\beta$ -KBA (**5**) and  $\beta$ -AKBA (**6**) peak-ratio is almost the factor 1, which is in good agreement with the results from literature [57,195]. The existence of serratol (**21**) and iso-serratol (**20**) and the absence of incensole acetate (**23**) are also characteristic for this species (see chapter 3.7.2 and 3.7.6).

The species *Boswellia sacra*, respectively, *Boswellia carterii*, which both revealed the strongest content deviations, seem to accommodate a distinct pathway for the biosynthesis of  $\beta$ -caryophyllene (**27**). Its oxide,  $\beta$ -caryophyllene-oxide (**28**), is specifically detectable by TLC (chapter 3.4). Furthermore, they revealed significantly high BA (**1**, **3**) contents and on average the greatest ABA (**2**, **4**) contents. The lupeolic acid contents (**11**, **12**) are additionally the greatest in these species, if compared with *Boswellia papyrifera* and *Boswellia serrata*. Interestingly, the tirucallic acid content (**13-19**) has been for all samples of *Boswellia sacra* and *Boswellia carterii* significantly lower (see chapter 3.7.3, 3.7.4 and 3.7.6). The two acetylated tirucallic acids, **18** and **19**, are merely in traces detectable. Therefore, the second chromatography dimension is actually obsolete for these species (chapter 3.7.5). This result could be explained by the fact that the lupeolic acids (**11** and **12**) or lupeolic cations can be regarded as the biosynthetic precursors of the boswellic acids (chapter 3.13 or the book of Breitmaier on Terpenes [31]). Hence, the lupeolic acids (**11** and **12**) and boswellic acids, especially **1-4**, are in greater quantities detectable in the resins of *Boswellia sacra* and *Boswellia carterii*. And as the synthesis of tirucallic acids (**13-19**) is probably proceeding via another biosynthetic step, they are only in minimal quantities produced (chapter 3.13).

On the contrary, *Boswellia papyrifera* and *Boswellia serrata* reveal rather great amounts of tirucallic acids (**13-19**) and significantly lower values for the lupeolic acids (**11** and **12**). This leads to the conclusion that they differ in their biosynthesis pathways in detail (chapter 3.8 and 3.13). Hitherto, these statements are merely speculations based on the quantitative HPLC results (chapter 3.8). There are definitely further biochemical experiments necessary to substantiate this proposal. To achieve this, access to trees or fresh *Boswellia* material must be ensured. Within this work it was unfortunately not possible to do this.

Of further interest could be also still the systematic evaluation of the different incense resin ingredients with regard to their synergistic and/or antagonistic properties in pharmacological test systems [150]. Since the data presented here, but also the data previously generated by Bergmann [17] and Seitz [56], give essential information on the analytics, the identification, the isolation and even the quantitation of incense resin ingredients, it should be possible for other research groups to isolate the compounds necessary for further pharmacological investigations.

Furthermore, the here developed HPLC method is still capable of improvement. It surely enables the certain quantitation of some tirucallic acids in the acid fraction matrix of *Boswellia papyrifera*, but is for the other species still with greater uncertainties combined

(keyword: Co-elution). Through hyphenation techniques like LC-MS/MS-coupling, it may be also finally achievable to determine blood-plasma concentration levels of the tirucallic acids. A mass selective detector could also overcome the co-elution problem of  $\beta$ -BA (**3**, M = 456.70 g/mol) with  $\alpha$ -Ac-7,24-dien-TA (**18**, M = 498.73 g/mol), if no ion suppression phenomenon occurs. Some experiments on the *in vitro* and *in vivo* application of LC-MS, respectively, LC-MS/MS-couplings with incense resin ingredients have been already carried out [143,144,192,195]. In the long-term, the here described HPLC methodology should make it possible to even determine the biologically active class of tirucallic acids in complex matrices (e.g. blood plasma).

The characteristic chemotaxonomy of the three species *Boswellia papyrifera*, *Boswellia serrata* und *Boswellia sacra*, respectively, *Boswellia carterii*, may be also finally clarified with publication of this work. Thus, it should not happen anymore that the species *Boswellia carterii* and *Boswellia papyrifera* are confused with each another as it occurred unfortunately several times before in the literature [35,67,68,85-88,146].

Questionable is also, if the species *Boswellia papyrifera*, which accommodates the significantly greatest quantities of incensole (**22**) and incensole acetate (**23**), will be one day extinct. According to the matrix-based model of Groenendijk et al. [26] this species is going to consist of only 10 % of the present population within the next 50 years, if there are no immediate precautions met. The yield of resin from this species could be already in the next 15 years merely 50 % of the present supply. Thus, this material, whether useful for the Catholic Church or the Pharmacological Research, may be rather rare and hence expensive.

In general, the results reported here are properly speaking merely valid for the in this work analysed sample population. However, the congruency with a few literature results substantiates the general correctness thus far. Further investigations in the future will have to finally prove the statements given here.

### Zusammenfassung und Ausblick

Zielsetzung dieser Arbeit war eine eindeutige chemotaxonomische Klassifizierung der Harze der Weihrauchspezies *Boswellia papyrifera*, *Boswellia serrata* und *Boswellia sacra*, respektive, *Boswellia carterii*, mittels gängiger chromatographischer Methoden (DC, HPLC und GC). Alle drei Methoden erlauben eine eindeutige Identifizierung anhand typischer Biomarker (z. Bsp. DC-Analytik [11]). Zusätzlich wurden die Ergebnisse mit verlässlichen Literaturresultaten [13,15,74,79,184] verglichen und anhand von zertifizierten Referenzmustern abgesichert [17]. Außerdem wurde eine HPLC-Methode (Methode des externen Standards mit 2D-Offline-Option, falls notwendig) entwickelt, die bis zu 17 eventuell sogar 19 Verbindungen in der Rohsäurefraktion aller drei Spezies identifizieren bzw. quantifizieren kann [59]. Insgesamt sind 15 dieser Verbindungen (**1-8** und **10-16**) in dieser Arbeit quantifiziert worden. Erstmals wurden einige Tirucallensäuren in der Rohsäurematrix chromatographisch aufgetrennt. Vier der fünf aufgelösten TA-Peaksignale sind schließlich quantifiziert worden (Verbindung **13-16**, ohne **17**).

Da für die Spezies *Boswellia papyrifera* und *Boswellia serrata* der  $\beta$ -BA-(**3**)-Peak mit koeludierenden Verbindungen (**18** und **19**) überlagerte, wurde eine zweite Chromatographiedimension hinzugefügt [160], um diese Verbindung relativ fehlerfrei quantifizieren zu können. Diese Methode ist zwar bis dato noch sehr aufwendig und vermutlich auch nicht sehr robust (manuelle Zwischenpräparationsschritte), liefert allerdings nachweislich richtigere Ergebnisse als eine einfache Löffällung [162] der schlecht aufgelösten Peaks (**3**, **18** und **19**).

Weiterhin stellte sich heraus, dass die zweite Chromatographiedimension für die Spezies *Boswellia sacra* und *Boswellia carterii* nicht notwendig ist, da hier die Verbindungen 3 $\alpha$ -O-Acetyl-7,24-dien-tirucallensäure (**18**) und 3 $\beta$ -O-Acetyl-8,24-dien-tirucallensäure (**19**) in so geringen Mengen vorkommen, dass der Integrationsfehler durch Koelution mit  $\beta$ -BA (**3**) vernachlässigbar war (siehe Kapitel 3.7.5).

Interessanterweise sind für alle drei Spezies durchschnittlich vergleichbare Gesamtgehalte im Rohsäureharz wiedergefunden worden, die sich zwar aus den verschiedenen unterschiedlichen Einzelkomponenten (BAs, ABAs, KBAs, TAs, LAs etc.) zusammensetzen, aber auf einen einheitlichen Kohlenstoff-Gesamtmetabolismus schließen lassen. Approximativ sind ca. 75 % der Gesamtrohsäuren determiniert worden (siehe Kapitel 3.8). Alle drei Spezies nähern sich diesem Wert an, unabhängig von den Quantitäten ihrer einzelnen Komponenten (z. Bsp. hoher TA-Gehalt, dafür niedrigerer BA/ABA und/oder KBA/AKBA-Gehalt und umgekehrt). Bei guter Harzqualität ist dieser Mittelwert mit vergleichbaren Extraktionsmethoden zu erreichen. Jedoch sind auch Proben analysiert worden, die definitiv von minderwertiger Qualität waren, was sich extrem auf den Erwartungswert auswirkte. Das bedeutet prinzipiell, dass es zwar ein typisches Fingerprint-Muster für jede Spezies gibt, dieses allerdings nicht immer zwingend erfüllt sein muss (siehe ebenfalls Kapitel 3.8). Bei den Harzen handelt es sich mehr oder weniger um ein wildwachsendes Naturprodukt, dessen Qualität auch von Umwelteinflüssen abhängt. Weiterhin ist es wichtig eine große Gesamtpopulation des Probeharzes zu vermessen, da es bereits innerhalb einer Charge recht große Schwankungen geben kann (z. Bsp. 10 g zu vermahlen ist sicherer als 1 g, auch wenn der Verbrauch natürlich dann immens ist).

Eindeutige Biomarker für die Spezies *Boswellia papyrifera* (Eritrea, Äthiopien und Sudan) sind Incensol (**22**), Incensol-Acetat (**23**) und das Verticillia-4(20),7,11-trien (**24**). *Boswellia papyrifera* kann mit allen drei Methoden (DC, HPLC und GC) identifiziert werden. Die Spezies wurde in der Literatur bis dato oft mit der Spezies *Boswellia carterii* (Somalia) verwechselt, obwohl bereits genügend Arbeiten vorlagen (z. Bsp. Obermann [79], 1978, und Hamm et al. [13], 2005), die zu gleichen Schlussfolgerungen gelangten wie sie in dieser Dissertation publiziert sind. Weiterhin zeichnet sich diese Spezies durch den durchschnittlich höchsten  $\beta$ -AKBA-Gehalt und einen recht hohen Gesamtgehalt an Tirucallensäuren aus (Kapitel 3.8). Interessant ist ebenso, dass in allen relevanten Publikationen zum Thema [13,74,79] sowie in allen in dieser Arbeit untersuchten Proben die Verbindung Incensol-Acetat (**23**) nur in der Sorte *Boswellia papyrifera* nachgewiesen wurde. Die Verbindungen Incensol (**22**) und Incensol-Acetat (**23**) sind in dieser Arbeit ebenfalls erstmalig mittels HPLC quantifiziert worden (Methode des externen Standards) und stellen die Hauptkomponenten der Neutralbestandteile der Spezies *Boswellia papyrifera* dar (Gehalt von 30 bis über 40 % in den öligen Neutralbestandteilen; siehe auch Kapitel 3.8). Die HPLC-Ergebnisse wurden durch Isolierungsexperimente von Incensol (**22**) und seinem Acetat (**23**) bestätigt (siehe Kapitel 3.11.1). Durch Anreicherung des Incensol-Acetat-Gehaltes (**23**) in den Neutralbestandteilen von *Boswellia papyrifera* mittels Partial-Synthese (Acetylierung der Neutralbestandteile) sowie der anschließenden chromatographischen Isolierung, konnte diese Verbindung in sehr hohen Ausbeuten gewonnen werden (Kapitel 3.11.1). Mit den Spezies *Boswellia serrata* und *Boswellia sacra*/*Boswellia carterii* wäre dies nicht möglich gewesen, da diese signifikant geringere Incensol-(**22**)-Gehalte aufweisen und die Biosynthese auf der Stufe des Serratols (**21**) bereits zu stagnieren scheint (siehe Kapitel 3.13.1.2 oder auch [11]). Mittels einfacher Deacetylierungs- und Acetylierungsexperimente konnten diese beiden Verbindungen (**22** und **23**) wieder ineinander umgewandelt werden. Für die Spezies *Boswellia serrata* (Indien) sind Serratol (**21**), die erstmalig beschriebene Verbindung Iso-Serratol (**20**; siehe Kapitel 3.2.7) und auch ein recht hoher Gesamtgehalt an Tirucallensäuren typisch (Kapitel 3.8). Scheinbar sind ebenfalls die ubiquitär vorkommenden Verbindungen Methyl-Chavicol und Methyl-Eugenol, die im Wasserdampfdestillat anhand ihrer GC-Retention-Indizes bestimmt wurden, für *Boswellia serrata* spezifisch [13,35,74]. Außerdem zeichnet sich diese Spezies durch einen relativ gleich großen  $\beta$ -KBA/ $\beta$ -AKBA-Gehalt und den durchschnittlich höchsten BA-Gehalt ( $\alpha$ -BA, **1** und  $\beta$ -BA, **3**) aus. Dieses Ergebnis stimmt mit den Ergebnissen von Büchele et al. überein [57]. In Hinblick auf die Bioverfügbarkeit, wo  $\beta$ -BA (**3**) die höchsten Blutplasmakonzentrationen aufwies [125,126,144], scheint diese Spezies, sofern auf  $\beta$ -BA (**3**) standardisiert, die vielversprechendste zu sein.

Für die Spezies *Boswellia sacra* (Oman, Jemen) und *Boswellia carterii* (Somalia), die bis dato als identische Spezies zu betrachten sind [11-13,73], wurden auch in dieser Arbeit identische Biomarker mit allen drei chromatographischen Methoden gefunden (DC, HPLC und GC). Spezifisch sind hierfür speziell das Vorhandensein von  $\beta$ -Caryophyllen (**27**) und seinem Monooxidationsprodukt (**28**), wobei **27** mittels HPLC (Kapitel 3.7.3 und 3.7.4) nachweisbar war, und **28** sehr signifikant mittels DC (siehe Kapitel 3.4). Diese Resultate wurden durch die GC-Experimente sowie auch durch Literaturresultate [13,74,184] bestätigt

(Kapitel 3.5). Weiterhin sind auch für diese beiden Spezies Serratol (**21**) und das Iso-Serratol (**20**) wiedergefunden worden. Beide Verbindungen, **20** und **21**, wurden in den Neutralbestandteilen von Bsac/Bcar, aber auch Bser, mittels HPLC erstmalig quantifiziert (siehe Kapitel 3.7 und 3.8). Die Rohsäuren dieser Spezies zeichnen sich durch relativ große Gehalte an BAs (**1** und **3**) und ABAs (**2** und **4**) aus. Ebenfalls zeigten sie durchgehend signifikant größere Lupansäuregehalte (**11** und **12**), verglichen mit *Boswellia papyrifera* und *Boswellia serrata* (Kapitel 3.7.6 und 3.8). Dies lässt auf eine unterschiedliche Ausprägung der Biosynthesewege schließen. Der Gehalt von  $\beta$ -KBA (**5**) und  $\beta$ -AKBA (**6**) variierte stark in den Spezies *Boswellia carterii* und *Boswellia sacra* (Kapitel 3.8 und 3.14). Von daher ist das  $\beta$ -KBA/ $\beta$ -AKBA-Verhältnis zur Speziesidentifizierung mit äußerster Vorsicht zu betrachten. Erwartungsgemäß ist der  $\beta$ -AKBA-Peak (**6**) größer als der  $\beta$ -KBA-Peak (**5**); das ist jedoch nicht zwingend, da auch stark differierende Signalverhältnisse und Gehalte gemessen wurden. Im Durchschnitt offenbarten diese Spezies jedoch den geringsten  $\beta$ -KBA-Gehalt (**5**) im Harz, verglichen mit *Boswellia papyrifera* und *Boswellia serrata*. Die Tirucallensäuregehalte waren in allen hier analysierten Proben für beide Spezies signifikant geringer als für *Boswellia papyrifera* und *Boswellia serrata* ermittelt (Kapitel 3.8 und 3.14). Diese Tatsache lässt erneut auf eine bevorzugte Biosynthese der Boswelliasäuren in *Boswellia sacra* und *carterii* schließen (siehe auch Kapitel 3.13).

Insgesamt wurden elf Verbindungen aus den Harzen von *Boswellia papyrifera* (**18**, **19**, **22**, **23**, **24**) und *Boswellia carterii* (**20**, **21**, **22**, **25**, **28**, **29**, **30**) isoliert und deren Struktur mittels 1D- und 2D-NMR-Experimenten aufgeklärt. Erstmals im Harz von *Boswellia carterii* wurde die Verbindung Iso-Serratol (**20**) gefunden, einem Derivat vom literaturbekannten Serratol (**21**). Weiterhin ist die Isolierung von 3- $\beta$ -OH-Tirucallol (**29**) und auch von 3- $\alpha$ -OH-11-Keto-12-ursen (**30**) aus der Neutralfraktion von *Boswellia carterii* noch nicht detailliert beschrieben worden. Diese Verbindungen stellen mit hoher Wahrscheinlichkeit biosynthetische Zwischenstufen auf dem Weg zu den bekannten Tirucallen- und 11-Ketoboswelliasäuren dar.

In der Rohsäurefraktion von *Boswellia papyrifera* wurden erstmalig die beiden acetylierten Tirucallensäure-Derivate **18** und **19** ausführlich beschrieben. Zwar wurde von Estrada et al. berichtet, dass diese beiden Verbindungen aus dem Harz der Spezies *Boswellia carterii* isoliert worden sind, jedoch sind keine expliziten Daten hierzu von dieser Arbeitsgruppe veröffentlicht [57,70]. Weiterhin scheint *Boswellia carterii* diese beiden Verbindungen, **18** und **19**, nur in minimalen Mengen zu synthetisieren (siehe speziell 2D-HPLC in Kapitel 3.7.5), so dass es sich eher um die Spezies *Boswellia papyrifera* oder eine partialsynthetische Methode gehandelt haben muss, wie es in den Veröffentlichungen von Banno et al. [68] und Akihisa et al. [67] für die Semisynthese von **18**, ausgehend von **17**, beschrieben wurde. Auch in den Publikationen von Banno und Akihisa et al. ist von der Spezies *Boswellia carterii* die Rede. Jedoch, die isolierten Verbindungen, insbesondere die Isolierung des Incensol-Acetats (**23**), legen auch hier die Vermutung nahe, dass es sich um das Harz der Sorte *Boswellia papyrifera* handelte. Speziell die Schwierigkeit der Trennung dieser beiden Verbindungen, **18** und **19**, sowie das relativ geringe Vorkommen dieser im Weihrauchharz, scheinen diese Annahme zu bekräftigen (siehe Kapitel 3.1.1.3 und 3.7.5). Folglich liefert diese Arbeit erste

chromatographische und spektroskopische „Koordinaten“ zu diesen beiden, ebenfalls pharmakologisch interessanten Verbindungen (**18** und **19**). Im Zusammenhang mit Koordinaten sei angemerkt, dass die Spezies *Boswellia papyrifera* und *Boswellia serrata* diese in größerer Menge synthetisieren, und auch erstmalig HPLC-Retentionsdaten für diese mit angegeben wurden. Die Spezies *Boswellia sacra* bzw. *Boswellia carterii* zeichneten sich durchgehend durch einen relativ geringen Tirucallensäure-Gehalt aus. Die beiden Verbindungen, **18** und **19**, wurden dort nur in Spuren nachgewiesen (Kapitel 3.7.5).

Die Verbindungen für die HPLC-Quantifizierung (**1-8**, **10-16**) wurden ebenfalls alle aus dem Harz der Spezies *Boswellia papyrifera* isoliert, so wie bereits in der Dissertation von Stefanie Seitz beschrieben [56,59].

Eine weitere interessante Feststellung war die Tatsache, dass Incensol (**22**) und sein Acetat (**23**) relativ instabil sind, wenn sie über einen längeren Zeitraum in Reinform der Luft ausgesetzt werden (Kapitel 3.11.3). So wurden die ursprünglich gefundenen pharmakologischen Werte auf Zersetzungsprodukte dieser zurückgeführt (siehe Kapitel 3.12.1). Durch reaktionskinetische Tests mit Incensol-Acetat (**23**) wurde diese Annahme bestätigt (Kapitel 3.11.2-3.11.4). Hier sei angemerkt, dass auch die Arbeitsgruppe um Moussaieff diese Verbindungen, speziell Incensol-Acetat (**23**), mit vielversprechenden pharmakologischen Eigenschaften publizierte [87,145-147]. In der hier publizierten Arbeit konnten jedoch sämtliche pharmakologische Wirkungen nur auf die Zersetzungsprodukte von Incensol (**22**) und seinem Acetat (**23**) zurückgeführt werden (Kapitel 3.11.3 und 3.12.1). Von daher stellt sich die prinzipielle Frage, ob diese Verbindungen in unzersetzter Reinform überhaupt wirklich bioaktiv sind. Weitere Arbeiten zu diesem Thema sollten aufklären helfen.

In punkto Synergiewirkung wurde nur die Fraktion, die auch Verbindung **18** und **19** sowie eine nicht weiter identifizierte Verbindung (vermutlich auch eine isomere Verbindung von **18** und **19**) enthält, untersucht (siehe Kapitel 3.1.1.3 zur Isolierung und 3.12.2 zur Pharmakologie). Diese unbekannte Verbindung konnte leider noch nicht isoliert werden. Interessanterweise konnten hier für die komplexe Mischung, im zellfreien mPGES-1-Test, effektivere Hemmwerte als für die schrittweise gereinigten Verbindungen festgestellt werden. Dies könnte ein Hinweis auf Synergie sein, muss es jedoch nicht zwingend, da sich diese Verbindungen in anderen Systemen wieder komplett anders verhalten könnten [150]. Das ist ein generelles Problem der Wirkstoffevaluierung [94]. Doch sollten diese Ergebnisse vielleicht andere Forschergruppen zu weiteren Experimenten motivieren.

Interessanterweise lässt sich dadurch aber auch schlussfolgern, dass die Tirucallensäuren, als wesentlicher Bestandteil der Rohsäurefraktion von Weihrauchharzen, bestimmt einen pharmakologischen Effekt haben.

Weiterhin sind die quantitativen HPLC-Ergebnisse sicherlich noch mit Fehlern behaftet (Kapitel 3.8). Bisher liegen noch keine Daten auf Reproduzierbarkeit vor (z. Bsp. anderes Labor, andere Ausrüstung, andere Mitarbeiter etc.; siehe auch [156]), da die Quantifizierung mit dieser Methode in dieser Arbeit erstmalig beschrieben wurde. Gewisse Sicherheiten

konnten erlangt werden, indem die Methode mit einer robusten literaturbekannten HPLC-Methode [20,21], die weniger Probenpräparationsschritte benötigt, verglichen wurde (selektive Quantifizierung von  $\beta$ -KBA und  $\beta$ -AKBA; siehe Kapitel 2.3.9 und 3.6.1). Die Ergebnisse, abhängig von der Vorgehensweise, sind ähnlich. Ein Vergleich der Quantifizierungsergebnisse dieser Arbeit mit weiteren Quantifizierungsergebnissen aus der Literatur untermauert jedoch die generelle Richtigkeit der Daten soweit (siehe Kapitel 3.9). Dennoch, absolute Sicherheit wird erst durch vermehrte Wiederholungen dieser Messmethodik - auch in anderen Laboren - erreicht werden, um letztlich eine statistisch ausreichende und vertrauenswürdige Gesamtpopulation vorliegen zu haben [159]. Dies betrifft sowohl die Anzahl der gemessenen Proben, repräsentativ für *Boswellia papyrifera*, *Boswellia serrata* und *Boswellia sacra* bzw. *Boswellia carterii*, als auch die durch mehrfache Wiederholung der Messmethodik ermittelten Verfahrenskennzahlen [156]. Von diesem Standpunkt her gesehen, sind die quantitativen Daten dieser Arbeit als eine erste Schätzung bzw. Stichprobe der Tatsächlichkeit zu betrachten.

Abschließend sei noch einmal festgehalten, dass durch diese Arbeit die Spezies der Weihrauchharze von *Boswellia papyrifera*, *Boswellia serrata* und *Boswellia sacra* bzw. *Boswellia carterii*, anhand chemotaxonomischer Marker, eindeutig bestimmt werden kann. Selbst jede Methode (DC, HPLC, GC) für sich genommen, dürfte dies bereits eindeutig belegen können. Wobei die DC-Methode, wegen ihrer einfachen Handhabung, aber dafür recht signifikanten Aussagekraft, am meisten überzeugen sollte (Kapitel 3.4 und [11]).

Die GC-Methode benötigt als Probenaufarbeitungsschritt die Wasserdampfdestillation der Harze bzw. der Neutralbestandteile dieser, und liefert ubiquitäre Mono- und auch weihrauchspezifische Diterpene (z. Bsp. Verbindungen **21**, **22**, **23** und **24**; siehe auch Kapitel 3.5).

Die HPLC benötigt definitiv, durch Trennung der Rohsäuren von Neutralbestandteilen, den meisten Arbeitsaufwand (Kapitel 2.2.4 und 2.3.4). Jedoch scheint dies noch notwendig zu sein, da die Ergebnisse sonst zu sehr verfälscht würden, weil auch verschiedene Mono- und Diterpene im Bereich der Boswellia- und Tirucallensäuren eluieren (z. Bsp. **20**, **21**, **22** und **23**). Die Methode wurde anhand der Rohsäure von *Boswellia papyrifera* evaluiert, die keine signifikanten Spuren von Serratol (**21**) und Iso-Serratol (**20**) enthält. Folglich sind die quantitativen Angaben für  $\alpha$ -TA (**14**) und  $\beta$ -TA (**15**) relativ sicher. Für die anderen Spezies, die sich durch das Vorkommen von Serratol (**21**) und Iso-Serratol (**20**) auszeichnen, sind die Quantitäten für  $\alpha$ -TA (**14**) und  $\beta$ -TA (**15**) noch mit Ungenauigkeiten behaftet. Diese beiden Verbindungen koeluieren mit Iso-Serratol (**20**; mit **15** =  $\beta$ -TA) und Serratol (**21**; mit **14** =  $\alpha$ -TA) im unbehandelten Rohextrakt (siehe speziell auch den sogenannten „Triplett-Peak“ für den Bser-Rohextrakt in Kapitel 3.7.2, aber auch die Kapitel 3.7.3 und 3.7.4 für *Boswellia sacra*, respektive, *Boswellia carterii*). Auch nach Trennung der Rohsäuren von den Neutralbestandteilen mittels Flüssig-flüssig-Extraktion (Kapitel 2.2.4) lassen sich noch Spuren von Serratol (**21**) und Iso-Serratol (**20**) in der Rohsäure finden (DC-Analytik), die mit den entsprechenden Tirucallensäuren koeluieren und somit die Gehalte dieser, **14** und **15**, höher erscheinen lassen als sie es in Wirklichkeit sind. Dieser experimentelle Befund wurde

bereits in der Dissertation von Seitz bestätigt, die Serratol (**21**) ebenfalls aus der Rohsäurefraktion von *Boswellia carterii* isolierte [56].

Für *Boswellia papyrifera*, die kaum bzw. nicht nachweisbar Serratol (**21**) und Iso-Serratol (**20**) enthält, dafür allerdings Incensol (**22**) und sein Acetat (**23**) in größeren Mengen, stellt sich dieses Problem nicht. Incensol (**22**) kann zwar in Spuren noch im Rohsäureextrakt von *Boswellia papyrifera* wiedergefunden werden, koeluiert aber mit keiner Zielkomponente ( $R_f$  = zwischen  $\beta$ -KBA und  $\beta$ -AKBA).

Die quantitativen HPLC-Gehaltsangaben und auch die qualitativen HPLC-Fingerprints liefern Hinweise auf die bevorzugten Biosynthesewege der einzelnen Spezies (Kapitel 3.13). Dies wurde durch Anwendung der Hauptkomponentenanalyse (Principal Component Analysis, PCA) untermauert (Kapitel 3.14).

*Boswellia papyrifera* scheint  $\beta$ -AKBA (**6**), Incensol (**22**) und sein Acetat (**23**) in relativ großen Mengen zu synthetisieren. Weiterhin sind die Tirucallensäuregehalte (**13-19**) sehr hoch, und die Lupansäure-(**11**, **12**) und Boswelliasäure-(**1-4**)-gehalte mit die geringsten. Incensol-Acetat (**23**) wurde nur in dieser Spezies gefunden (siehe Kapitel 3.7.1 und 3.7.6).

*Boswellia serrata* zeichnet sich durch geringere  $\beta$ -AKBA-(**6**)-Gehalte, dafür aber durch sehr große BA-(**1**, **3**)- sowie Tirucallensäuregehalte (**13-19**) aus. Das Verhältnis der  $\beta$ -AKBA-(**6**)- und  $\beta$ -KBA-(**5**)-Peaksignale ist annähernd dem Faktor 1, was der Literatur entspricht [57,195]. Das Auftreten von Serratol (**21**) und Iso-Serratol (**20**) bei gleichzeitiger Abwesenheit von Incensol-Acetat (**23**) ist ebenfalls typisch für diese Spezies (siehe Kapitel 3.7.2 und 3.7.6).

Die Spezies *Boswellia sacra* bzw. *Boswellia carterii*, die beide das am stärksten variierende Gehaltsmuster aufwiesen, scheinen sich durch eine recht ausgeprägte Biosynthese von  $\beta$ -Caryophyllen (**27**) auszuzeichnen, was sich als sein Oxid (**28**), speziell in der DC-Analytik (Kapitel 3.4), bemerkbar macht. Außerdem besitzen sie mitunter signifikant hohe BA-(**1**, **3**)- und auch die durchschnittlich größten ABA-(**2**, **4**)-Werte. Die Lupansäuregehalte (**11**, **12**) sind in diesen Spezies ebenfalls durchgehend am größten, relativ verglichen mit *Boswellia papyrifera* und *Boswellia serrata*. Währenddessen die Tirucallensäuregehalte (**13-19**) in allen Proben von *Boswellia sacra* und *Boswellia carterii* signifikant niedriger waren (siehe Kapitel 3.7.3, 3.7.4 und 3.7.6). Die beiden acetylierten Tirucallensäuren, **18** und **19**, sind sogar nur noch in Spuren nachweisbar, wodurch die zweite Chromatographiedimension für diese Spezies eigentlich obsolet ist (Kapitel 3.7.5). Dieser Befund könnte dadurch erklärt werden, dass die Lupansäuren (**11** und **12**) als biosynthetische Vorstufen zu den Boswelliasäuren betrachtet werden können (siehe Kapitel 3.13 oder auch das Buch von Breitmaier über Terpene [31]). Folglich sind die Lupansäuren (**11** und **12**) und Boswelliasäuren, speziell **1-4**, in den Spezies *Boswellia sacra* bzw. *Boswellia carterii* in größerer Quantität vorhanden. Da die Tirucallensäuren (**13-19**) wahrscheinlich über einen anderen Biosyntheseweg ablaufen (Kapitel 3.13) sind sie in nur geringen Mengen nachweisbar.

Im Gegensatz dazu sind für *Boswellia papyrifera* und *Boswellia serrata* recht hohe Gehalte an Tirucallensäuren (**13-19**) sowie signifikant niedrigere Werte für die Lupansäuren (**11** und **12**) wiedergefunden worden. Das lässt ebenfalls auf unterschiedlich exprimierte Biosynthesewege schließen (Kapitel 3.8 und 3.13). Bis dato sind diese Aussagen aber nur

reine Spekulation. Weitere Tests, speziell biochemischer und/oder molekularbiologischer Natur, sind notwendig. Hierfür müsste Zugang zu den Bäumen bzw. frischem *Boswellia*-Material selbst gewährleistet sein, was aber im Rahmen dieser Arbeit nicht möglich bzw. auch nicht das Ziel war.

Ebenfalls von weiterem Interesse könnte sein, wie die verschiedenen Weihrauchharzinhaltsstoffe in pharmakologischen Testsystemen zusammen- bzw. entgegenwirken. Dies in Hinblick auf synergistische bzw. antagonistische Effekte [150]. Da durch diese Arbeit, aber auch bereits durch die Dissertationen von Jochen Bergmann [17] und Stefanie Seitz [56], wesentliche Grundsteine zur Analytik, Identifizierung, Isolierung und Quantifizierung von Weihrauchharzen gelegt wurden, sollte es weiteren Forschergruppen gewährleistet sein, die für diese pharmakologischen Untersuchungen notwendigen Verbindungen zu gewinnen.

Des Weiteren ist die hier entwickelte HPLC-Methode noch ausbaufähig. Sie ermöglicht zwar die relative sichere Quantifizierung einiger Tirucallensäuren in der Rohsäurematrix für die Spezies *Boswellia papyrifera*, ist aber für die anderen Spezies noch mit größeren Unsicherheiten behaftet (Stichwort: Koelution). Weiterhin könnten durch entsprechende LC-MS/MS-Kopplungen dann vermutlich auch die Blutplasma-Konzentrationen der Tirucallensäuren bestimmt werden. Ein massenselektiver Detektor würde auch die Problematik der Koelution von  $\beta$ -BA (**3**, M = 456,70 g/mol) mit  $\alpha$ -Ac-7,24-dien-TA (**18**, M = 498,73 g/mol) umgehen können, nicht stattfindende Ionen-Suppression vorausgesetzt. Einige Experimente zur *in vitro* und *in vivo* Anwendung der LC-MS bzw. MS/MS-Kopplung auf Weihrauchinhaltsstoffe wurden bereits publiziert [143,144,192,195]. Durch die hier beschriebene HPLC-Methodik sollte es auch langfristig gesehen möglich sein, die biologisch aktiven Tirucallensäuren in komplexen Matrices (z. Bsp. Blutplasma) zu bestimmen.

Die spezifische Chemotaxonomie der drei Spezies *Boswellia papyrifera*, *Boswellia serrata* und *Boswellia sacra* bzw. *Boswellia carterii* dürfte mit Veröffentlichung dieser Arbeit nun endgültig geklärt sein. Folglich sollten auch die Spezies *Boswellia carterii* und *Boswellia papyrifera* nicht mehr verwechselt werden können, was, wie in dieser Arbeit ausführlich geschildert, unglücklicherweise öfter geschehen ist [35,67,68,85-88,146].

Fraglich ist jedoch auch, ob die Spezies *Boswellia papyrifera*, die die größten Quantitäten an Incensol (**22**) und Incensol-Acetat (**23**) enthält, nicht eines Tages ausgestorben sein wird. Dem matrixbasierten Modell von Groenendijk et al. [26] nach, dürfte diese Sorte nämlich innerhalb der nächsten 50 Jahre – sofern keine sofortigen Gegenmaßnahmen eingeleitet werden - auf ca. 10 % ihres heutigen Bestandes zurückgegangen sein. Die Harzausbeute dieser Spezies könnte bereits innerhalb der nächsten 15 Jahre um ca. 50 % geringer ausfallen, was dieses Material, ob nun für die Kirchen oder die Pharmakologie, entsprechend rar und somit wertvoll bzw. teuer machte.

Allgemein festzustellen ist, dass die Ergebnisse strenggenommen nur für dieses Datenmaterial gültig sind. Jedoch scheint die Kongruenz mit einigen Literaturdaten, die generelle Richtigkeit der hier getroffenen Aussagen bisher zu bestätigen. Zukünftige Untersuchungen werden das letztendlich beweisen.

### Bibliography

- [1]Duke JA, Duke PA, duCellier JL. 2008. Duke's Handbook of Medicinal Plants of the Bible. CRC Press Taylor & Francis Group: Boca Raton, FL, USA.
- [2]Thieret JW. 1996. Frankincense and Myrrh. *Lloydiana* **1**(4):6-9.
- [3]Martinetz D, Lohs K, Janzen J, editors. 1988. Weihrauch und Myrrhe, Kulturgeschichte und wirtschaftliche Bedeutung. 1. Edition ed. Stuttgart: Wissenschaftliche Verlagsgesellschaft mbH.
- [4]Tucker AO. 1986. Frankincense and Myrrh. *Economic Botany* **40**(4):425-433.
- [5]Safayhi H, Mack T, Sabieraj J, Anazodo MI, Subramanian LR, Ammon HP. 1992. Boswellic acids: novel, specific, nonredox inhibitors of 5-lipoxygenase. *J Pharmacol Exp Ther* **261**(3):1143-1146.
- [6]Ernst E. 2008. Frankincense: systematic review. *BMJ* **337**:a2813.
- [7]Schlager N, Lauer J. 2001. Science and its Times Understanding the Social Significance of Scientific Discovery - Volume 1 (2000 B.C. to A.D. 699). The Gale Group: Farmington Hills, MI, USA.
- [8]Ammon HP. 2006. Boswellic acids in chronic inflammatory diseases. *Planta Med* **72**(12):1100-1116.
- [9]Shah BA, Qazi GN, Taneja SC. 2009. Boswellic acids: a group of medicinally important compounds. *Nat Prod Rep* **26**(1):72-89.
- [10]Rawer D. 2007. Synthese von Boswelliasäuren [Diploma]. Saarbrücken, Germany: Saarland University.
- [11]Paul M, Bruning G, Bergmann J, Jauch J. 2012. A Thin-layer Chromatography Method for the Identification of Three Different Olibanum Resins (*Boswellia serrata*, *Boswellia papyrifera* and *Boswellia carterii*, respectively, *Boswellia sacra*). *Phytochem Anal* **23**:184-189.
- [12]Thulin M, Warfa AM. 1987. The frankincense tree (*Boswellia* spp., Burseraceae) of northern Somalia and southern Arabia. *Kew Bull.* **42**:487-493.
- [13]Hamm S, Bleton J, Connan J, Tchaplal A. 2005. A chemical investigation by headspace SPME and GC-MS of volatile and semi-volatile terpenes in various olibanum samples. *Phytochemistry* **66**(12):1499-1514.
- [14]Sunnichan VG, Mohan Ram HJ, Shivanna KR. 2005. Reproductive biology of *Boswellia serrata*, the source of salai guggal, an important gum-resin. *J Linn Soc London, Bot* **147**:73-82.
- [15]Melese A. 2007. Phytochemical Investigation of the Resins of *Boswellia* Species Collected from Kebele Area in Agew-Awi (Gojjam) [Master]. Addis-Ababa, Ethiopia: Addis Ababa University.
- [16]Ogbazghi W, Rijkers T, Wessel M, Bongers F. 2006. Distribution of the frankincense tree *Boswellia papyrifera* in Eritrea: the role of environment and land use. *J Biogeogr* **33**:524-535.
- [17]Bergmann J. 2004. Untersuchungen zum Harz des Weihrauchbaums (*Boswellia* spp.) unter besonderer Berücksichtigung der Säurefraktion [Dissertation]. Munich, Germany: TU München.
- [18]Nelson D, Cox M. 2005. Lehninger Biochemie. Springer-Verlag: Berlin Heidelberg.
- [19]Cseke L, Kirakosyan A, Kaufman P, Warber S, Duke J, Brielmann H. 2006. Natural Products from Plants. Taylor & Francis: Boca Raton, FL, USA.
- [20]Indian Frankincense, *Olibanum indicum*. *EUROPEAN PHARMACOPOEIA 6.0*:2128-2129.

## Bibliography

---

- [21] Indian Frankincense, *Olibanum indicum*. EUROPEAN PHARMACOPOEIA 7.0.1152.
- [22] OLIBANUM INDICUM, Indian Frankincense. *ESCOP MONOGRAPHS 2. Edition* (Supplement 2009):184-197.
- [23] Pfeifer M. 2008. *Der Weihrauch Geschichte Verwendung Bedeutung*. Verlag Friedrich Pustet: Regensburg, Germany.
- [24] Asmuth T. 2010. Erst kauen - Der Jemen gilt als neue Basis des Terrornetzwerks al-Quaida. Aber die Menschen haben noch ein ganz anderes Problem. Ihr Land trocknet aus. Der Grund: die Droge Kat. *Fluter - Magazin der Bundeszentrale für politische Bildung* Nr. 37:37-39.
- [25] Gresh A, Radvanyi J, Rekecwicz P, Samary C, Vidal D. 2009. Unstaaten am Horn von Afrika. *Le Monde diplomatique (Atlas der Globalisierung)*:154-155.
- [26] Groenendijk P, Eshete A, Sterck FJ, Zuidema PA, Bongers F. 2011. Limitations to sustainable frankincense production: blocked regeneration, high adult mortality and declining populations. *Journal of Applied Ecology Online-First* (Downloaded 13.01.2012).
- [27] Bhat SV, Nagasampagi BA, Sivakumar N. 2005. *Chemistry of Natural Products*. Springer: Berlin-Heidelberg.
- [28] Wallach O. 1887. Zur Kenntnis der Terpene und der Ätherischen Öle. *Liebig's Ann. Chem* **239**:1-45.
- [29] Ruzicka L. 1932. The Life and Work of Otto Wallach. *J. Chem. Soc.* **1582**.
- [30] Ruzicka L. 1963. In *Perspektiven der Biogenese und Chemie der Terpene*. IUPAC:493-523.
- [31] Breitmaier E. 2008. *Terpenes - Flavors, Fragrances, Pharmaca, Pheromones*. WILEY-VCH Verlag: Weinheim, Germany.
- [32] Lynen F. 1964. The pathway from "activated acetic acid" to the terpenes and fatty acids. *Nobel Lecture December the 11th, 1964*.
- [33] Bloch K. 1964. The biological synthesis of cholesterol. *Nobel Lecture December the 11th, 1964*.
- [34] Barkovich R, Liao JC. 2001. Metabolic engineering of isoprenoids. *Metab Eng* **3**(1):27-39.
- [35] Basar S. 2005. *Phytochemical investigations on Boswellia species [Dissertation]*. Hamburg, Germany: University of Hamburg.
- [36] Rohmer M, Knani M, Simonin P, Sutter B, Sahn H. 1993. Isoprenoid biosynthesis in bacteria: a novel pathway for the early steps leading to isopentenyl diphosphate. *Biochem. J.* **295**:517-524.
- [37] Steinbacher S, Kaiser J, Eisenreich W, Huber R, Bacher A, Rohdich F. 2003. Structural basis of fosmidomycin action revealed by the complex with 2-C-methyl-D-erythritol 4-phosphate synthase (IspC). Implications for the catalytic mechanism and anti-malaria drug development. *J Biol Chem* **278**(20):18401-18407.
- [38] Rücker G. 1973. Sesquiterpene. *Angew. Chem.* **20**:895-907.
- [39] Tschirch A. 1900. *Die Harze und die Harzbehälter*. Bornträger: Leipzig, Germany.
- [40] Tschirch A, Halbey O. 1898. Untersuchungen über die Sekrete. *Arch Pharm* **236**:487-503.
- [41] Halbey O. 1898. *Über das Olibanum*. Bern, Switzerland: Universität Bern.
- [42] Winterstein A, Stein G. 1932. Untersuchungen in der Saponinreihe X. Zur Kenntnis der Mono-oxytriterpenesäuren. *Z. physiol. Chem.* **208**:9-25.
- [43] Simpson JCE. 1937. Structure of  $\beta$ -boswellinic acid. *Nature* **140**:467.

## Bibliography

---

- [44]Ruzicka L, Wirz W. 1939. Zur Kenntnis der Triterpene (50. Mitteilung). Umwandlung der  $\beta$ -Boswellinsäure in  $\alpha$ -Amyrin. *Helv. Chim. Acta* **22**:948-951.
- [45]Ruzicka L, Wirz W. 1940. Zur Kenntnis der Triterpene (52. Mitteilung). Umwandlung der  $\alpha$ -Boswellinsäure in  $\beta$ -Amyrin. *Helv. Chim. Acta* **23**:132-135.
- [46]Beton JL, Halsall TG, Jones ERH. 1956. The Chemistry of Triterpenes and Related Compounds. Part XXVIII.  $\beta$ -Boswellic Acid. *J. Chem. Soc.*:2904-2909.
- [47]Budzikiewicz H, Wilson JM, Djerassi C. 1963. Mass Spectrometry in Structural and Stereochemical Problems. XXXII. Pentacyclic Triterpenes. *J. Am. Chem. Soc* **85**:3688-3699.
- [48]Pardhy RS, Bhattacharyya SC. 1978.  $\beta$ -Boswellic acid, Acetyl- $\beta$ -boswellic acid, Acetyl-11-keto- $\beta$ -boswellic acid and 11-Keto- $\beta$ -boswellic acid, four pentacyclic triterpene acids from the resin *Boswellia serrata* Roxb. *Indian J Chem* **16B**:176-178.
- [49]Snatzke G, Vertesy L. 1966. Über die Neutralen Sesqui- und Triterpene des Weihrauchs. *Mh. Chem.* **98**:121-132.
- [50]Schweizer S, Eichele K, Ammon HP, Safayhi H. 2000. 3-Acetoxy group of genuine AKBA (acetyl-11-keto-beta-boswellic acid) is  $\alpha$ -configured. *Planta Med* **66**(8):781-782.
- [51]Rajnikant, Gupta VK, Rangar VD, Bapat SR, Agarwal RB, Gupta R. 2001. Crystallographic analysis of acetyl  $\beta$ -boswellic acid. *Crystal Research and Technology* **36**:93-100.
- [52]Culioli G, Mathe C, Archier P, Vieillescazes C. 2003. A lupane triterpene from frankincense (*Boswellia* sp., Burseraceae). *Phytochemistry* **62**:537-541.
- [53]Belsner K, Büchele B, Werz U, Syrovets T, Simmet T. 2003. Structural analysis of pentacyclic triterpenes from the gum resin of *Boswellia serrata* by NMR spectroscopy. *Magn. Reson. Chem.* **41**:115-122.
- [54]Corsano S, Iavarone C. 1964. Isolamento dall'incenso dell'acido 3-acetil-11-ossi- $\beta$ -bosvellico. *Gazz Chim Ital* **94**:328-339.
- [55]Schweizer S, von Brocke AF, Boden SE, Bayer E, Ammon HP, Safayhi H. 2000. Workup-dependent formation of 5-lipoxygenase inhibitory boswellic acid analogues. *J Nat Prod* **63**(8):1058-1061.
- [56]Seitz S. 2008. Isolierung und Strukturaufklärung von entzündungshemmenden Inhaltsstoffen aus Weihrauchharz [Dissertation]. Saarbrücken, Germany: Saarland University.
- [57]Büchele B, Zugmaier W, Simmet T. 2003. Analysis of pentacyclic triterpenic acids from frankincense gum resins and related phytopharmaceuticals by high-performance liquid chromatography. Identification of lupeolic acid, a novel pentacyclic triterpene. *J Chromatogr B* **791**(1-2):21-30.
- [58]Büchele B, Zugmaier W, Genze F, Simmet T. 2005. High-performance liquid chromatographic determination of acetyl-11-keto- $\alpha$ -boswellic acid, a novel pentacyclic triterpenoid, in plasma using a fluorinated stationary phase and photodiode array detection: application in pharmacokinetic studies. *J Chromatogr B Analyt Technol Biomed Life Sci* **829**(1-2):144-148.
- [59]Paul M, Brüning G, Wehrather J, Jauch J. 2011. Qualitative and Quantitative Analysis of 17 different Types of Tetra- and Pentacyclic Triterpenic Acids in *Boswellia papyrifera* by a Semi-Automatic Homomodal 2D HPLC Method. *Chromatographia* **74**:29-40.

## Bibliography

---

- [60]Belsner K, Büchele B, Werz U, Simmet T. 2003. Structural analysis of 3- $\alpha$ -acetyl-20(29)-lupene-24-oic acid, a novel triterpene isolated from the gum resin of *Boswellia serrata*, by NMR spectroscopy. *Magn. Reson. Chem.* **41**:629-632.
- [61]Atta ur Rahman, Naz H, Fadimatou, Makhmoor T, Yasin A, Fatima N, Ngounou FN, Kimbu SF, Sondengam BL, Choudhary MI. 2005. Bioactive constituents from *Boswellia papyrifera*. *J Nat Prod* **68**(2):189-193.
- [62]Cotterrell GP, Halsall TG, Wriglesworth MJ. 1970. The Chemistry of Triterpenes and Related Compounds. Part XLVII. Clarification of the Nature of the Tetracyclic Triterpene Acids of Elemi Resin. *J. Chem. Soc. (C)*:739-743.
- [63]Sawadogo M, Vidal-Tessier AM, Delaveau P. 1985. [The oleoresin of *Canarium schweinfurthii* Engl]. *Ann Pharm Fr* **43**(1):89-96.
- [64]Marques DD, Graebner IB, de Lemos TL, Machado LL, Assuncao JC, Monte FJ. 2010. Triterpenes from *Protium hebetatum* resin. *Nat Prod Commun* **5**(8):1181-1182.
- [65]Corsano S, Picconi G. 1962. Isolamento del racido elemadienonico dall'incenso. *Ann Chim* **52**:802-808.
- [66]Pardhy RS, Bhattacharyya SC. 1978. Tetracyclic Triterpene Acids from the Resin of *Boswellia serrata* Roxb. *Indian J Chem* **16B**:174-175.
- [67]Akihisa T, Tabata K, Banno N, Tokuda H, Nishimura R, Nakamura Y, Kimura Y, Yasukawa K, Suzuki T. 2006. Cancer chemopreventive effects and cytotoxic activities of the triterpene acids from the resin of *Boswellia carteri*. *Biol Pharm Bull* **29**(9):1976-1979.
- [68]Banno N, Akihisa T, Yasukawa K, Tokuda H, Tabata K, Nakamura Y, Nishimura R, Kimura Y, Suzuki T. 2006. Anti-inflammatory activities of the triterpene acids from the resin of *Boswellia carteri*. *J Ethnopharmacol* **107**(2):249-253.
- [69]Mora AJ, Delgado G, Diaz de Delgado G, Usubillaga A, Khouri N, Bahsas A. 2001. 3- $\alpha$ -Hydroxytirucalla-7,24-dien-21-oic acid: a triterpene from *Protium crenatum* Sandwith. *Acta Cryst.* **C57**:638-640.
- [70]Estrada AC, Syrovets T, Pitterle K, Lunov O, Buchele B, Schimana-Pfeifer J, Schmidt T, Morad SA, Simmet T. 2010. Tirucallic acids are novel pleckstrin homology domain-dependent Akt inhibitors inducing apoptosis in prostate cancer cells. *Mol Pharmacol* **77**(3):378-387.
- [71]Jong T, Chen C. 1994. Roburic acid, a triterpene 3,4-seco acid. *Acta Cryst.* **C50**:1326-1328.
- [72]Fattorusso E, Santacroce C, Xaasan C. 1983. 4(23)-Dihydroroburic acid from the resin (incense) of *Boswellia carterii*. *Phytochemistry* **22**:2868-2869.
- [73]Mathe C, Culioli G, Archier P, Vieillescazes C. 2004. High-performance liquid chromatographic analysis of triterpenoids in commercial frankincense. *Chromatographia* **60**:493-499.
- [74]Camarda L, Dayton T, Di Stefano V, Pitonzo R, Schillaci D. 2007. Chemical composition and antimicrobial activity of some oleogum resin essential oils from *Boswellia* spp. (Burseraceae). *Ann Chim* **97**(9):837-844.
- [75]Corsano S, Nicoletti R. 1967. The structure of incensole. *Tetrahedron* **23**:1977-1984.
- [76]Forcellese ML, Nicoletti R, Petrossi U. 1972. The Structure of Iso-Incensole-Oxide. *Tetrahedron* **28**:325-331.

## Bibliography

---

- [77]Forcellese ML, Nicoletti R, Santarelli C. 1973. The Revised Structure of Iso-Incense-Oxide. *Tetrahedron Letters* **39**:3783-3786.
- [78]Hamm S, Lesellier E, Bleton J, Tchaplal A. 2003. Optimization of headspace solid phase microextraction for gas chromatography/mass spectrometry analysis of widely different volatility and polarity terpenoids in olibanum. *J Chromatogr A* **1018**(1):73-83.
- [79]Obermann H. 1977. Die chemischen und geruchlichen Unterschiede von Weihrauchharzen. *Dragoco Rep.* **24**:260-265.
- [80]Ertelt J, (Pharmacist H-A, Bisingen, Germany). 2010. Personal Communication.
- [81]Gacs-Baitz E, Radics L, Fardella G, Corsano S. 1978. <sup>13</sup>C NMR study of some 14-membered macrocyclic diterpenes. *J. Chem. Research (M)*:1701-1713.
- [82]Klein E, Obermann H. 1978. (S)-1-Isopropyl-4,8,12-trimethyl-cyclotetradeca-3E, 7E, 11 E-trien-1-ol, ein neues Cembrenol aus dem ätherischen Öl von Olibanum. *Tetrahedron Letters* **4**:349-353.
- [83]Pardhy RS, Bhattacharyya SC. 1978. Structure of serratol, a new diterpene cembranoid alcohol from *Boswellia serrata* roxb. *Indian J. Chem.* **16B**:171-173.
- [84]Schmidt TJ, Kaiser M, Brun R. 2011. Complete structural assignment of serratol, a cembrane-type diterpene from *Boswellia serrata*, and evaluation of its antiprotozoal activity. *Planta Med* **77**(8):849-850.
- [85]Basar S, Koch A, König WA. 2001. A verticillane-type diterpene from *Boswellia carterii* essential oil. *Flavour Fragr. J.* **16**:315-318.
- [86]Vernin M, Boniface, C., Metzger, J., Maire, Y., Rakotorijaona, Fraisse, D., Parkanyi, C. 1989. GC-MS data bank analysis of the essential oils from *Boswellia frereana* Birdw and *Boswellia carterii* Birdw *Flavors and Off-Flavors*:511-542.
- [87]Moussaieff A, Shohami E, Kashman Y, Fridé E, Schmitz ML, Renner F, Fiebich BL, Munoz E, Ben-Neriah Y, Mechoulam R. 2007. Incense acetate, a novel anti-inflammatory compound isolated from *Boswellia* resin, inhibits nuclear factor-kappa B activation. *Mol Pharmacol* **72**(6):1657-1664.
- [88]Hanus LO, Moussaieff A, Rezanka T, Abu-Lafi S, Dembitsky VM. 2007. Phytochemical analysis and comparison for differentiation of *Boswellia carterii* and *B. serrata*. *Nat. Prod. Com.* **2**(2):139-142.
- [89]Yoshikawa M, Morikawa T, Oominami H, Matsuda H. 2009. Absolute stereostructures of olibanumols A, B, C, H, I, and J from olibanum, gum-resin of *Boswellia carterii*, and inhibitors of nitric oxide production in lipopolysaccharide-activated mouse peritoneal macrophages. *Chem Pharm Bull (Tokyo)* **57**(9):957-964.
- [90]Morikawa T, Oominami H, Matsuda H, Yoshikawa M. 2010. Four new ursane-type triterpenes, olibanumols K, L, M, and N, from traditional egyptian medicine olibanum, the gum-resin of *Boswellia carterii*. *Chem Pharm Bull (Tokyo)* **58**(11):1541-1544.
- [91]Morikawa T, Oominami H, Matsuda H, Yoshikawa M. 2011. New terpenoids, olibanumols D-G, from traditional Egyptian medicine olibanum, the gum-resin of *Boswellia carterii*. *J Nat Med* **65**(1):129-134.

## Bibliography

---

- [92]Goddemeier C. 2006. Alexander Fleming (1881–1955): Penicillin. *Dtsch Arztebl* **103**(36):A-2286 / B-1984 / C-1915.
- [93]Kuhnert N. 1999. Hundert Jahre Aspirin. *Chemie in unserer Zeit* **33**(4):213-220.
- [94]Aktories K, Förstermann U, Hofmann FB, Starke K. 2009. Allgemeine und spezielle Pharmakologie und Toxikologie - Begründet von W. Forth, D. Henschler, W. Rummel Urban & Fischer Verlag/Elsevier GmbH: München, Germany.
- [95]D'Costa VM, McGrann KM, Hughes DW, Wright GD. 2006. Sampling the antibiotic resistome. *Science* **311**(5759):374-377.
- [96]Kather N. 2007. Synthese und Struktur-Wirkungs-Beziehungen von Boswelliasäuren und deren Derivaten [Dissertation]. Saarbrücken, Germany: Saarland University.
- [97]Ammon HP, Mack T, Singh GB, Safayhi H. 1991. Inhibition of leukotriene B4 formation in rat peritoneal neutrophils by an ethanolic extract of the gum resin exudate of *Boswellia serrata*. *Planta Med* **57**(3):203-207.
- [98]Koeberle A, Werz O. 2009. Inhibitors of the microsomal prostaglandin E(2) synthase-1 as alternative to non steroidal anti-inflammatory drugs (NSAIDs)--a critical review. *Curr Med Chem* **16**(32):4274-4296.
- [99]Simmons DL, Botting RM, Hla T. 2004. Cyclooxygenase isozymes: the biology of prostaglandin synthesis and inhibition. *Pharmacol Rev* **56**(3):387-437.
- [100]Funk CD. 2001. Prostaglandins and leukotrienes: advances in eicosanoid biology. *Science* **294**(5548):1871-1875.
- [101]Park JY, Pillinger MH, Abramson SB. 2006. Prostaglandin E2 synthesis and secretion: the role of PGE2 synthases. *Clin Immunol* **119**(3):229-240.
- [102]Koeberle A, Siemoneit U, Buhning U, Northoff H, Laufer S, Albrecht W, Werz O. 2008. Licofelone suppresses prostaglandin E2 formation by interference with the inducible microsomal prostaglandin E2 synthase-1. *J Pharmacol Exp Ther* **326**(3):975-982.
- [103]Koeberle A, Haberl EM, Rossi A, Pergola C, Dehm F, Northoff H, Troschuetz R, Sautebin L, Werz O. 2009. Discovery of benzo[g]indol-3-carboxylates as potent inhibitors of microsomal prostaglandin E(2) synthase-1. *Bioorg Med Chem* **17**(23):7924-7932.
- [104]Siemoneit U, Koeberle A, Rossi A, Dehm F, Verhoff M, Reckel S, Maier TJ, Jauch J, Northoff H, Bernhard F, Doetsch V, Sautebin L, Werz O. 2011. Inhibition of microsomal prostaglandin E2 synthase-1 as a molecular basis for the anti-inflammatory actions of boswellic acids from frankincense. *Br J Pharmacol* **162**(1):147-162.
- [105]Sailer ER, Subramanian LR, Rall B, Hoernlein RF, Ammon HP, Safayhi H. 1996. Acetyl-11-keto-beta-boswellic acid (AKBA): structure requirements for binding and 5-lipoxygenase inhibitory activity. *Br J Pharmacol* **117**(4):615-618.
- [106]Sailer ER, Schweizer S, Boden SE, Ammon HP, Safayhi H. 1998. Characterization of an acetyl-11-keto-beta-boswellic acid and arachidonate-binding regulatory site of 5-lipoxygenase using photoaffinity labeling. *Eur J Biochem* **256**(2):364-368.
- [107]Young RN. 1999. Inhibitors of 5-lipoxygenase: a therapeutic potential yet to be fully realized. *Eur. J. Med. Chem.* **34**:671-685.

## Bibliography

---

- [108]Moussaieff A, Mechoulam R. 2009. Boswellia resin: from religious ceremonies to medical uses; a review of in-vitro, in-vivo and clinical trials. *J Pharm Pharmacol* **61**(10):1281-1293.
- [109]Weber P, ebi-pharm-ag, Kirchlindach, Switzerland. 2012. Personal Communication.
- [110]Singh GB, Atal CK. 1986. Pharmacology of an extract of salai guggal ex-Boswellia serrata, a new non-steroidal anti-inflammatory agent. *Agents Actions* **18**(3-4):407-412.
- [111]Gupta I, Gupta V, Parihar A, Gupta S, Ludtke R, Safayhi H, Ammon HP. 1998. Effects of Boswellia serrata gum resin in patients with bronchial asthma: results of a double-blind, placebo-controlled, 6-week clinical study. *Eur J Med Res* **3**(11):511-514.
- [112]Sander O, Herborn G, Rau R. 1998. [Is H15 (resin extract of Boswellia serrata, "incense") a useful supplement to established drug therapy of chronic polyarthritis? Results of a double-blind pilot study]. *Z Rheumatol* **57**(1):11-16.
- [113]Gerhardt H, Seifert F, Buvari P, Vogelsang H, Regges R. 2001. [Therapy of active Crohn disease with Boswellia serrata extract H 15]. *Z Gastroenterol* **39**(1):11-17.
- [114]Kimmatkar N, Thawani V, Hingorani L, Khiyani R. 2003. Efficacy and tolerability of Boswellia serrata extract in treatment of osteoarthritis of knee--a randomized double blind placebo controlled trial. *Phytomedicine* **10**(1):3-7.
- [115]Madisch A, Miehlke S, Eichele O, Mrwa J, Bethke B, Kuhlisch E, Bastlein E, Wilhelms G, Morgner A, Wigglinghaus B, Stolte M. 2007. Boswellia serrata extract for the treatment of collagenous colitis. A double-blind, randomized, placebo-controlled, multicenter trial. *Int J Colorectal Dis* **22**(12):1445-1451.
- [116]Sontakke S, Thawani V, Pimpalkhute P, Kabra P, Babhulkar S, Hingorani H. 2007. Open, randomized, controlled clinical trial of *Boswellia serrata* extract as compared to valdecoxib in osteoarthritis of knee. *Indian J Pharmacol* **39**:27-29.
- [117]Sengupta K, Alluri KV, Satish AR, Mishra S, Golakoti T, Sarma KV, Dey D, Raychaudhuri SP. 2008. A double blind, randomized, placebo controlled study of the efficacy and safety of 5-Loxin for treatment of osteoarthritis of the knee. *Arthritis Res Ther* **10**(4):R85.
- [118]Heidemeier A. 2006. Entwicklung und Anwendung von Methoden zur pharmakokinetischen Untersuchung von Boswelliasäuren [Dissertation]. Giessen, Germany: Justus-Liebig-Universität Giessen.
- [119]Michie CA, Cooper E. 1991. Frankincense and myrrh as remedies in children. *J R Soc Med* **84**(10):602-605.
- [120]Sailer ER, Hoernlein RF, Lakshminarayanapuram RS, Safayhi H, Ammon HP. 1996. Preparation of Novel Analogues of the Nonredox-Type Non-Competitive Leukotriene Biosynthesis Inhibitor AKBA. *Arch. Pharm. Med. Chem.* **329**:54-56.
- [121]Safayhi H, Sailer ER, Ammon HP. 1995. Mechanism of 5-lipoxygenase inhibition by acetyl-11-keto-beta-boswellic acid. *Mol Pharmacol* **47**(6):1212-1216.
- [122]Werz O, Szellas D, Henseler M, Steinhilber D. 1998. Nonredox 5-lipoxygenase inhibitors require glutathione peroxidase for efficient inhibition of 5-lipoxygenase activity. *Mol Pharmacol* **54**(2):445-451.

## Bibliography

---

- [123]Altmann A, Poeckel D, Fischer L, Schubert-Zsilavecz M, Steinhilber D, Werz O. 2004. Coupling of boswellic acid-induced Ca<sup>2+</sup> mobilisation and MAPK activation to lipid metabolism and peroxide formation in human leucocytes. *Br J Pharmacol* **141**(2):223-232.
- [124]Safayhi H, Boden SE, Schweizer S, Ammon HP. 2000. Concentration-dependent potentiating and inhibitory effects of *Boswellia* extracts on 5-lipoxygenase product formation in stimulated PMNL. *Planta Med* **66**(2):110-113.
- [125]Sterk V, Buchele B, Simmet T. 2004. Effect of food intake on the bioavailability of boswellic acids from a herbal preparation in healthy volunteers. *Planta Med* **70**(12):1155-1160.
- [126]Büchle B, Simmet T. 2003. Analysis of 12 different pentacyclic triterpenic acids from frankincense in human plasma by high-performance liquid chromatography and photodiode array detection. *J Chromatogr B Analyt Technol Biomed Life Sci* **795**(2):355-362.
- [127]Abdel Tawab M, Kaunzinger A, Bahr U, Karas M, Wurglics M, Schubert-Zsilavecz M. 2001. Development of a high-performance liquid chromatographic method for the determination of 11-keto- $\beta$ -boswellic acid in human plasma. *J. Chromatogr. B* **761**:221-227.
- [128]Poeckel D, Werz O. 2006. Boswellic acids: biological actions and molecular targets. *Curr Med Chem* **13**(28):3359-3369.
- [129]Simoneit U, Hoffmann B, Kather N, Lamkemeyer T, Madlung J, Franke L, Scheider G, Jauch J, Poeckel D, Werz O. 2008. Identification and functional analysis of cyclooxygenase-1 as a molecular target of boswellic acids. *Biochem. Pharmacol.* **75**:503-513.
- [130]Ammon HP, Safayhi H, Mack T, Sabieraj J. 1993. Mechanism of antiinflammatory actions of curcumine and boswellic acids. *J Ethnopharmacol* **38**(2-3):113-119.
- [131]Kaunzinger A, Baumeister A, Cuda K, Haring N, Schug B, Blume HH, Raddatz K, Fischer G, Schubert-Zsilavecz M. 2002. Determination of 11-keto-boswellic acid in human plasma. *J Pharm Biomed Anal* **28**(3-4):729-739.
- [132]Tausch L, Henkel A, Siemoneit U, Poeckel D, Kather N, Franke L, Hofmann B, Schneider G, Angioni C, Geisslinger G, Skarke C, Holtmeier W, Beckhaus T, Karas M, Jauch J, Werz O. 2009. Identification of human cathepsin G as a functional target of boswellic acids from the anti-inflammatory remedy frankincense. *J Immunol* **183**(5):3433-3442.
- [133]Boden SE, Schweizer S, Bertsche T, Dufer M, Drews G, Safayhi H. 2001. Stimulation of leukotriene synthesis in intact polymorphonuclear cells by the 5-lipoxygenase inhibitor 3-oxo-tirucallic acid. *Mol Pharmacol* **60**(2):267-273.
- [134]Büchle B, Zugmaier W, Estrada A, Genze F, Syrovets T, Paetz C, Schneider B, Simmet T. 2006. Characterization of 3 $\alpha$ -acetyl-11-keto- $\alpha$ -boswellic acid, a pentacyclic triterpenoid inducing apoptosis in vitro and in vivo. *Planta Med* **72**(14):1285-1289.
- [135]Hoernlein RF, Orlikowsky T, Zehrer C, Niethammer D, Sailer ER, Simmet T, Dannecker GE, Ammon HP. 1999. Acetyl-11-keto- $\beta$ -boswellic acid induces apoptosis in HL-60 and CCRF-CEM cells and inhibits topoisomerase I. *J Pharmacol Exp Ther* **288**(2):613-619.
- [136]Syrovets T, Buchele B, Gedig E, Slupsky JR, Simmet T. 2000. Acetyl-boswellic acids are novel catalytic inhibitors of human topoisomerases I and II $\alpha$ . *Mol Pharmacol* **58**(1):71-81.

## Bibliography

---

- [137]Shao Y, Ho CT, Chin CK, Badmaev V, Ma W, Huang MT. 1998. Inhibitory activity of boswellic acids from *Boswellia serrata* against human leukemia HL-60 cells in culture. *Planta Med* **64**(4):328-331.
- [138]Hostanska K, Daum G, Saller R. 2002. Cytostatic and apoptosis-inducing activity of boswellic acids toward malignant cell lines in vitro. *Anticancer Res* **22**(5):2853-2862.
- [139]Liu JJ, Nilsson A, Oredsson S, Badmaev V, Duan RD. 2002. Keto- and acetyl-keto-boswellic acids inhibit proliferation and induce apoptosis in Hep G2 cells via a caspase-8 dependent pathway. *Int J Mol Med* **10**(4):501-505.
- [140]Dahmen U, Gu YL, Dirsch O, Fan LM, Li J, Shen K, Broelsch CE. 2001. Boswellic acid, a potent antiinflammatory drug, inhibits rejection to the same extent as high dose steroids. *Transplant Proc* **33**(1-2):539-541.
- [141]Safayhi H, Rall B, Sailer ER, Ammon HP. 1997. Inhibition by boswellic acids of human leukocyte elastase. *J Pharmacol Exp Ther* **281**(1):460-463.
- [142]Winking M, Sarikaya S, Rahmanian A, Jodicke A, Boker DK. 2000. Boswellic acids inhibit glioma growth: a new treatment option? *J Neurooncol* **46**(2):97-103.
- [143]Kruger P, Daneshfar R, Eckert GP, Klein J, Volmer DA, Bahr U, Muller WE, Karas M, Schubert-Zsilavecz M, Abdel-Tawab M. 2008. Metabolism of boswellic acids in vitro and in vivo. *Drug Metab Dispos* **36**(6):1135-1142.
- [144]Gerbeth K, Meins J, Kirste S, Momm F, Schubert-Zsilavecz M, Abdel-Tawab M. 2011. Determination of major boswellic acids in plasma by high-pressure liquid chromatography/mass spectrometry. *J Pharm Biomed Anal* **56**(5):998-1005.
- [145]Moussaieff A, Rimmerman N, Bregman T, Straiker A, Felder CC, Shoham S, Kashman Y, Huang SM, Lee H, Shohami E, Mackie K, Caterina MJ, Walker JM, Fride E, Mechoulam R. 2008. Incensole acetate, an incense component, elicits psychoactivity by activating TRPV3 channels in the brain. *FASEB J* **22**(8):3024-3034.
- [146]Moussaieff A, Shein NA, Tsenter J, Grigoriadis S, Simeonidou C, Alexandrovich AG, Trembovler V, Ben-Neriah Y, Schmitz ML, Fiebich BL, Munoz E, Mechoulam R, Shohmi E. 2008. Incensole acetate: a novel neuroprotective agent isolated from *Boswellia carterii*. *Journal of Cerebral Blood Flow & Metabolism* **28**:1341-1352.
- [147]Moussaieff A, Yu J, Zhu H, Gattoni-Celli S, Shohami E, Kindy MS. 2012. Protective effects of incensole acetate on cerebral ischemic injury. *Brain Res.* **1443**:89-97.
- [148]NCBI PubMed Online Library, (Key-word: boswellia OR boswellic acid), 300 articles found. Date: 20.01.2012. <http://www.ncbi.nlm.nih.gov/pubmed?term=boswellia+OR+boswellic%20acid>.
- [149]Berenbaum MC. 1989. What is synergy? *Pharmacol Rev* **41**(2):93-141.
- [150]Wagner H, Ulrich-Merzenich G. 2009. Synergy research: approaching a new generation of phytopharmaceuticals. *Phytomedicine* **16**(2-3):97-110.
- [151]Still C, Kahn M, Mitra A. 1978. Rapid chromatographic technique for preparative separations with moderate resolution. *J. Org. Chem.* **43**:2923-2925.
- [152]Meyer V. 2004. Praxis der Hochleistungs-Flüssigchromatographie. WILEY-VCH Verlag: Weinheim, Germany.

## Bibliography

---

- [153] Snyder L, Dolan J. 2007. High-Performance Gradient Elution The Practical Application of the Linear-Solvent-Strength Model. John Wiley & Sons: Hoboken, New Jersey, USA.
- [154] Paul M, Jauch J. 2012. Efficient Preparation of Incensole and Incensole Acetate, and Quantification of These Bioactive Diterpenes in *Boswellia papyrifera* by a RP-DAD-HPLC Method. *Nat. Prod. Com.* **7**(3):283-288.
- [155] Hamilton\_Bonaduz\_AG. 2011. White Paper: Determining the Performance of Hamilton Syringes; Access Date: 14. Oct. 2011.
- [156] Kromidas S. 2011. Validierung in der Analytik. WILEY-VCH Verlag: Weinheim, Germany.
- [157] Ebel S. 1986. Validierung und Kalibrierung in der HPLC. *Chromatographia* **22**:373-378.
- [158] Ellison S, Rosslein M, Williams A. 2000. Quantifying Uncertainty in Analytical Measurement. 2. Edition ed: EURACHME/CITAC Guide CG4.
- [159] Sachs L, Hedderich J. 2009. Angewandte Statistik - Methodensammlung mit R. Springer Dordrecht: Heidelberg London New York.
- [160] Mondello L, Lewis A, Bartle K. 2002. Multidimensional Chromatography. John Wiley & Sons: Chichester, West Sussex, UK.
- [161] Werz O. 2010. Personal Communication. Department of Biopharmaceutical Analytics, University of Tübingen, Germany (now Professor at the University of Jena, Germany).
- [162] Kromidas S, Kuss H. 2008. Chromatogramme richtig integrieren und bewerten. WILEY-VCH Verlag: Weinheim, Germany.
- [163] Meyer VR. 2007. Measurement uncertainty. *J Chromatogr A* **1158**(1-2):15-24.
- [164] Kramer R. 1998. Chemometric Techniques for Quantitative Analysis. Marcel Dekker, Inc.: New York, Basel.
- [165] Danzer K, Hobert H, Fischbacher C, Jagemann K-U. 2001. Chemometrik - Grundlagen und Anwendungen. Springer: Berlin Heidelberg New York.
- [166] Backhaus K, Erichson B, Plinke W, Weiber R. 2011. Multivariate Analysemethoden Eine anwendungsorientierte Einführung. Springer: Berlin Heidelberg New York.
- [167] Chen J, Zhao X, Fritsche J, Yin P, Schmitt-Kopplin P, Wang W, Lu X, Haring HU, Schleicher ED, Lehmann R, Xu G. 2008. Practical approach for the identification and isomer elucidation of biomarkers detected in a metabonomic study for the discovery of individuals at risk for diabetes by integrating the chromatographic and mass spectrometric information. *Anal Chem* **80**(4):1280-1289.
- [168] Euerby MR, Petersson P. 2003. Chromatographic classification and comparison of commercially available reversed-phase liquid chromatographic columns using principal component analysis. *J Chromatogr A* **994**(1-2):13-36.
- [169] Kovats E. 1958. Gas-chromatographische Charakterisierung organischer Verbindungen; Teil 1: Retentionsindices aliphatischer Halogenide, Alkohole, Aldehyde und Ketone. *Helv. Chim. Acta* **XLI**:1915-1932.
- [170] van den Dool H, Kratz P. 1963. A Generalization of the Retention Index System Including Linear Temperature Programmed Gas-Liquid Partition Chromatography. *J. Chromatogr.* **II**:463-471.
- [171] Bradford MM. 1976. A rapid and sensitive method for the quantitation of microgram quantities of protein utilizing the principle of protein-dye binding. *Anal Biochem* **72**:248-254.

## Bibliography

---

- [172]Müller D., Verhoff M. 2010. Personal Communication. Department of Biopharmaceutical Analytics (Prof. Dr. O. Werz), University of Tübingen, Germany.
- [173]Atkins PW, de Paula J. 2006. Physikalische Chemie. WILEY-VCH Verlag: Weinheim, Germany.
- [174]Mortimer CE. 2001. Chemie - Das Basiswissen der Chemie. Georg Thieme Verlag: Stuttgart, Germany.
- [175]Friebolin H. 2004. Basic One- and Two-Dimensional NMR Spectroscopy. WILEY-VCH Verlag: Weinheim, Germany.
- [176]Rahman MM, Khondkar P, Gray AI. 2005. Terpenoids from *Atylosia scarabaeoides* and their antimicrobial activity. *J. Pharm. Sci.* **4(2)**:141-144.
- [177]Skold M, Karlberg AT, Matura M, Borje A. 2006. The fragrance chemical beta-caryophyllene-air oxidation and skin sensitization. *Food Chem Toxicol* **44(4)**:538-545.
- [178]Gertsch J, Leonti M, Raduner S, Racz I, Chen JZ, Xie XQ, Altmann KH, Karsak M, Zimmer A. 2008. Beta-caryophyllene is a dietary cannabinoid. *Proc Natl Acad Sci U S A* **105(26)**:9099-9104.
- [179]Cornwell CP, Reddy N, Leach DN, Grant Wyllie S. 2001. Germacradienols in the essential oils of the Myrtaceae. *Flavour Fragr. J.* **16**:263-273.
- [180]Labbe C, Castillo M, Connolly JD. 1993. Mono and Sesquiterpenoids from *Satureja Gilliesii*. *Phytochemistry* **34 (No.2)**:441-444.
- [181]Fernandez-Arche A, Saenz MT, Arroyo M, de la Puerta R, Garcia MD. 2010. Topical anti-inflammatory effect of tirucallol, a triterpene isolated from *Euphorbia lactea* latex. *Phytomedicine* **17(2)**:146-148.
- [182]Hesse M, Meier H, Zeeh B. 2005. Spektroskopische Methoden in der organischen Chemie. Georg Thieme Verlag: Stuttgart, Germany.
- [183]Hochmuth D, (Dr\_Hochmuth\_Scientific\_Consulting). 2011. Terpenoids Library List ([http://massfinder.com/wiki/Terpenoids\\_Library\\_List](http://massfinder.com/wiki/Terpenoids_Library_List)): Access Date: 11. Nov. 2011.
- [184]Al-Harrasi A, Al-Saidi S. 2008. Phytochemical Analysis of the Essential Oil from Botanically Certified Oleogum Resin of *Boswellia sacra* (Omani Luban). *Molecules* **13**:2181-2189.
- [185]Johnson EL, Reynolds DL, Wright DS, Pachla LA. 1988. Biological sample preparation and data reduction concepts in pharmaceutical analysis. *J Chromatogr Sci* **26(8)**:372-379.
- [186]de Levie R. 2004. How to Use Excel in Analytical Chemistry and in General Scientific Data Analysis. Cambridge, UK: Cambridge University Press.
- [187]Wu T, Wang C, Wan X, Xiao H, Ma Q, Zhang Q. 2008. Comparison UPLC and HPLC for Analysis of 12 Phthalates. *Chromatographia* **68**.
- [188]Ganzera M, Khan IA. 2001. A reversed phase high performance liquid chromatography method for the analysis of boswellic acids in *Boswellia serrata*. *Planta Med* **67(8)**:778-780.
- [189]Ganzera M, Stöggli WM, Bonn GK, Khan IA, Stuppner H. 2003. Capillary electrochromatography of boswellic acids in *Boswellia serrata* Roxb. *J. Sep. Sci.* **26**:1383-1388.
- [190]Jauch J, Bergmann J. 2003. An efficient method for the large-scale preparation of 3-O-acetyl-11-oxo- $\beta$ -boswellic acid and other Boswellic acids. *Eur. J. Org. Chem.*:4752-4756.
- [191]Deeg M, (LC-MS/MS-Analytik, Universität Tübingen, Germany). 2010. Personal Communication.

## Bibliography

---

- [192]Reising K, Meins J, Bastian B, Eckert G, Mueller W, Schubert-Zsilavec M, Abdel-Tawab M. 2005. Determination of Boswellic Acids in Brain and Plasma by High-Performance Liquid Chromatography/Tandem Mass Spectrometry. *Anal. Chem.* **77**:6640-6645.
- [193]Abe I. 2007. Enzymatic synthesis of cyclic triterpenes. *Nat. Prod. Rep.* **24**:1311-1331.
- [194]Schmidt CO, Bouwmeester HJ, de Kraker JW, König WA. 1998. Biosynthese von (+)- und (-)-Germacren D in *Solidago canadensis*: Isolierung und Charakterisierung zweier enantioselektiver Germacren-D-Synthasen. *Angew. Chem.* **110**(10):1479-1481.
- [195]Frank A, Unger M. 2006. Analysis of frankincense from various *Boswellia* species with inhibitory activity on human drug metabolising cytochrome P450 enzymes using liquid chromatography mass spectrometry after automated on-line extraction. *J Chromatogr A* **1112**(1-2):255-262.

